

ASSESSING DEBRIS FLOW HAZARDS ON ALLUVIAL FANS IN DAVIS COUNTY, UTAH

by

*Jeffrey R. Keaton, Loren R. Anderson,
and Christopher C. Mathewson*

CONTRACT REPORT 91-11 JULY 1991
UTAH GEOLOGICAL SURVEY
a division of
UTAH DEPARTMENT OF NATURAL RESOURCES

**THE PUBLICATION OF THIS PAPER
IS MADE POSSIBLE WITH MINERAL LEASE FUNDS**

A primary mission of the UGS is to provide geologic information of Utah through publications. This Contract Report represents material that has not undergone policy, technical, or editorial review required for other UGS publications. It provides information that, in part, may be interpretive or incomplete and readers are to exercise some degree of caution in the use of the data. The UGS makes no warranty as to the accuracy of the information contained in this publication.

ASSESSING DEBRIS FLOW HAZARDS ON ALLUVIAL FANS IN DAVIS COUNTY, UTAH

by

Jeffrey R. Keaton

Adjunct Associate Professor, Department of Civil and Environmental Engineering,
Utah State University, Logan, Utah 84322-4110; alternative address:
Senior Engineering Geologist, Sergeant, Hauskins & Beckwith,
4030 S. 500 W., Suite 90, Salt Lake City, Utah 84123

Loren R. Anderson

Professor, Department of Civil and Environmental Engineering, and
Associate Dean, College of Engineering, Utah State University,
Logan, Utah 84322-4100

and

Christopher C. Mathewson

Professor, Department of Geology, and
Director, Center for Engineering Geosciences, Texas A&M University,
College Station, Texas 77843-3115

September 1988

ASSESSING DEBRIS FLOW HAZARDS ON ALLUVIAL FANS IN DAVIS COUNTY, UTAH

ABSTRACT

Debris flows have caused damage to developments on alluvial fans in Davis County, Utah, intermittently since the county was settled in 1847. The most recent damage occurred in the spring of 1983 in response to rapid snowmelt; earlier damage resulted from cloudburst thunderstorms. The objective of this research was to develop a probabilistic model for evaluating debris flow hazards. The principal goal of any hazard model should be quantification of the hazard in meaningful terms which can be used for actuarial purposes, investment decisions, and engineering design. The model developed for alluvial fans in Davis County, Utah, begins with historic records to document the number of historic events. If specific records are available, the volumes of the events are estimated directly; alternatively, they are estimated by volumetric proportion from those fans where records are available. The total volume of the fan is estimated from topographic maps and the volume of prehistoric sedimentation is estimated by subtracting the historic volume. The number of prehistoric events is estimated from stratigraphy and geomorphology or volumetric proportion. Magnitude-frequency relationships are developed from the historic and prehistoric sedimentation event data. Exceedance probabilities are calculated for exposure times of interest.

Sedimentation hazards are evaluated by comparing the volumes of probabilistic events to the cross section area of the principal channel at the apex of the fan and the middle fan and the volume of any existing debris basin or catchment area. The average sediment yield rate is compared to the time since and the volume of the last historic sedimentation event. Proximal fan hazard is considered high if the apex fan channel is smaller than the peak discharge associated with the 50 percent, 100-year event; it is moderate if the apex fan channel is smaller than the 10 percent, 50-year event; it is low if the channel is smaller than the 10 percent, 100-year event; and it is very low if the channel is larger than the 10 percent, 100-year event. Similar comparisons are made between mid-fan channel areas and probabilistic event discharges for assessment of medial fan hazards. Similar comparisons are made between debris basin volumes and probabilistic event volumes for assessment of distal fan hazards. The time since and volume of the last historic sedimentation event is compared to the Holocene sedimentation rate for assessment of the historic fan hazard. This last term is based on the observation that most of the sediment delivered to the fans in the 1983 and 1984 events was derived from the channels; time will be required for additional sediment to accumulate in the channels before the next event of the approximate size of the last event can occur. The overall fan hazard rating is the arithmetic mean of the four hazard terms, using ordinal rankings of 1 for very low, 2 for low, 3 for moderate, and 4 for high. Fans with arithmetic means > 3 were classified as high hazard fans; means between 2 and 3 were classified as moderate hazard fans; means between 1.25 and 2 were classified as low hazard fans; and means ≤ 1.25 were classified as very low hazard fans.

In 1983, a USGS study of the potential for debris flows and debris floods from the canyons in Davis County indicated that most canyons had high to very high potential for sediment delivery to the fans. The results of the model described above suggests that the hazard on these fans is generally moderate, and in some cases low. Some fans with high hazard were identified by the model. It is important to note that clear water flooding is not treated by this model; however, the probabilistic sedimentation hazard analysis can be combined with the quantitative flood hazard analysis for a combined hazard assessment. Other quantifiable hazards (e.g., earthquake shaking) can be integrated with these results for an assessment of multiple hazards.

ACKNOWLEDGMENTS

This research was sponsored by the U.S. Geological Survey Landslide Hazard Reduction Program Agreement Number 14-08-0001-A0507 (Utah Geological and Mineral Survey Contract No. 88-0886 with Utah State University); financial support is gratefully acknowledged. This report represents a significant amount of the senior author's Ph.D. thesis at Texas A&M University.

Discussions with numerous individuals, particularly Gerald F. Wieczorek, Elliott W. Lips, Donald R. Currey, Thomas C. Pierson, John E. Costa, Bruce C. Vandre, Earl P. Olson, Robert C. Rasely, Genevieve Atwood, Robert W. Fleming, and Russell H. Campbell, regarding sedimentation processes and hazards contributed to the quality of this paper. Discussions with local residents provided excellent insight into matters which otherwise would have been unknown, particularly Bill Rigby, Rulon Ford, Wesley Ford, Carma Jenkins, Leo and Lavon Worsley of Centerville, Jeff Warburton, Joyce Miller, Leonard and Dorothy Blackner of Layton, and Cammon Arrington of Farmington. Mr. Rulon Ford kindly granted permission for excavation of test pits on his property at Ricks Creek. Mr. Lee M. Gunnerson, Manager, Real Property, Real Estate Division, Church of Jesus Christ of Latter-Day Saints kindly granted permission for the excavation of test pits on Church-owned property at Ricks Creek.

Paul M. Santi, graduate student in engineering geology at Texas A&M University, and Sara Monteith, graduate student in geotechnical engineering at Utah State University, provided able assistance in creating exposures of the alluvial-fan stratigraphy and engaging in stimulating discussions about the stratigraphy. Donald R. Currey provided valuable interpretation about Lake Bonneville stratigraphy underlying the alluvial-fan deposits. Robert C. Rasely provided information and guidance regarding the PSIAC method of estimating annual sediment yield.

TABLE OF CONTENTS

	<u>PAGE</u>
ABSTRACT	ii
ACKNOWLEDGEMENTS	iii
LIST OF TABLES	vii
LIST OF FIGURES	ix
LIST OF SYMBOLS	xiii
INTRODUCTION	1
Scope of Research	4
Related Studies	6
SEDIMENTATION CHARACTER	8
Range of Processes	8
Sources of Water	9
Intense Rainstorms	9
Rapid Snowmelt	10
Bedrock Groundwater	10
Grain Support Mechanisms	11
Character of Flow	13
Eyewitness Accounts	15
Summary of Published Accounts	15
Davis County Accounts	17
STRATIGRAPHY	24
Davis County Sample Descriptions	24
Criteria for Differentiation	28
Field Observation	30
Laboratory Testing	30
Sediment Gradation	30
Atterberg Limits	32
Slurry Experiments	33
Calculated and Derived Parameters	34
Sediment Concentration	35
Ungraded Deposits	39
Matrix-Supported Deposits	39
Clast-Supported Deposits	39
Intermediate Deposits	39
Graded Deposits	46
Fining Upward Deposits	46
Coarsening Upward Deposits	46
Ideal Stratigraphic Sequence	46
Predictive Model	49

GEOMORPHOLOGY	53
Davis County Landform Hierarchy	53
Mountain Front Characteristics	54
Drainage Basins	55
Channels	57
Alluvial Fans	57
Morphometric Correlations	57
Levees and Boulder Fronts	66
Progressive Fan Development	67
Historic Sedimentation Events	75
Prehistoric Sedimentation Events	83
Ricks Creek Fan	84
Rudd Creek Fan	93
Lightning Canyon Fan	99
Other Fans	99
HAZARD EVALUATION	105
Hazard versus Risk	105
Hazard Variability	106
Damage	107
Temporal Variations	107
Spatial Variations	108
Locations	110
Frequencies	110
Magnitudes	112
Rates	112
Durations	112
Forecastabilities	113
Effects	114
Hazard Model	115
Variations on a Specific Fan	116
Variations between Fans	121
Magnitude-Frequency Relationships	122
Probabilistic Hazard Evaluation	122
Hazard Classifications	123
HAZARD RESPONSE ALTERNATIVES	143
Introduction	143
Alternatives	144
Ignore the Hazard	147
Continue Current Practices	147
Modify the Hazard	147
Sediment Catch Basins	148

Channel Improvements	148
Sediment Source Modifications	149
Modify What is at Risk	149
Modify Procedural and/or Operational Aspects	150
Life Safety Issues	150
Economic Loss Issues	151
Avoid the Hazard	152
SUMMARY AND CONCLUSIONS	153
REFERENCES	157
APPENDIX A: REPORTED MAJOR CLOUDBURST AND SNOWMELT FLOODS IN DAVIS COUNTY, UTAH, SINCE 1848	A-1
APPENDIX B: STRATIGRAPHIC SECTIONS	B-1
APPENDIX C: SUMMARY OF EXPERIMENTAL DATA	C-1
APPENDIX D: SUMMARY OF SELECTED GEOMORPHIC PARAMETERS	D-1
APPENDIX E: SUMMARY OF MAGNITUDE-FREQUENCY RELATIONSHIPS	E-1
APPENDIX F: SUMMARY OF EXCEEDANCE PROBABILITY CALCULATIONS	F-1
APPENDIX G: COMPUTER PROGRAMS	G-1

LIST OF TABLES

Table		Page
1	Classification of sediment gravity flows.	12
2	Major types of mass transport processes, behaviors, and clast support mechanisms.	13
3	Sediment concentrations and selected parameters for the range of flow behaviors of sedimentation evdnts on alluvial fans in Davis County.	38
4	Parameters considered as independent variables in a multivariate statistical analysis.	50
5	Summary of <i>a priori</i> ordinal ranking and computed factors of clast support mechanism.	51
6	Summary of statistical analysis of computed factors of clast supprt mechanism.	52
7	Hierarchical spatial ordering of landforms in Davis County.	53
8	Selected morphometric data for alluvial fans in Davis County.	58
9	Correlation matrix of morphometric parameters of drainage basins and alluvial fans in Davis County.	59
10	Correlation matrix of logarithmic transformations of morphometric parameters of drainage basins and alluvial fans in Davis County.	60
11	Selected data regarding relationships of alluvial-fan area and drainage basin area.	62
12	Selected data regarding relationships of alluvial-fan slope and drainage basin area.	65
13	PSIAC sediment yield factors and ratings for Davis County conditions.	69
14	Summary of alluvial-fan areas, thicknesses, and volumes.	72
15	Pertinent age data regarding alluvial fans in Davis County.	74
16	Summary of average erosion and deposition rates in Davis County.	76
17	Average annual sediment volumes for drainage basins and alluvial fans in Davis County.	77

Table		Page
18	Summary of historic flood events in Davis County from 1847 to 1987.	81
19	Description of soil formed on the Ricks Creek fan surface.	86
20	Geomorphic parameters of the Death Hollow channel used in the diffusion-equation model.	91
21	Results of palynologic evaluation of a sample from the 1984 Lightning Canyon sedimentation event.	100
22	Summary of estimated prehistoric sedimentation event data.	101
23	Intensity scale for alluvial-fan sedimentation event damage.	107
24	Summary of probabilistic evaluation of sedimentation hazards on alluvial fans in Davis County.	135
25	Summary of fan-head trench areas, middle fan channel areas, and debris basin volumes.	137
26	Overall fan hazard classifications for average hazard rating values.	141
27	Comparison of fan hazard classifications from this study with potential for debris flow and debris flood from Wieczorek and others (1983).	142
28	Some techniques for reducing natural hazards.	143

LIST OF FIGURES

Figure		Page
1	Vicinity map of research area.	5
2	Conceptual range of processes and sediment concentrations for sediment-water mixtures.	11
3	Photograph of debris flow damage in Farmington, Utah, in 1983. ..	21
4	Photograph of transitional flow and hyperconcentrated sediment flow damage in Farmington, Utah, in 1983.	22
5	Photograph of sedimentation damage in Layton, Utah, in 1984.	23
6	Map showing sample locations and selected features on the Lightning Canyon fan.	25
7	Map showing sample locations and selected features on the Rudd Creek fan.	26
8	Map showing sample locations and selected features on the Ricks Creek fan.	27
9	Stratigraphic discrimination model.	31
10	Theoretical relationship between water content and sediment-water mixture volume.	33
11	Theoretical relationship between sediment concentration by weight and by volume.	36
12	Photograph of matrix-supported debris flow deposit.	40
13	Photograph of clast-supported hyperconcentrated sediment flow deposit.	41
14	Photograph of matrix- to clast-supported transitional flow deposit. .	42
15	Photograph of an isolated megaclast.	43
16	Photograph of an uneroded basal contact.	44
17	Photograph of an eroded basal contact.	45
18	Photograph of a graded, fining upward streamflow deposit.	47
19	Ideal alluvial-fan stratigraphic sequence showing features of the characteristic depositional units.	48
20	Comparison of <i>a priori</i> ordinal ranking with calculated values.	52

Figure	Page
21	Plot of alluvial-fan area versus drainage basin area. 61
22	Plot of alluvial-fan slope versus drainage basin area. 64
23	Schematic diagram showing components of alluvial-fan geometry used to compute fan volumes. 73
24	Temporal distribution of historic flood events in Davis County. 79
25	Cumulative number of historic flood events in Davis County. 79
26	Cumulative departure from mean precipitation at Salt Lake City from 1875 to 1985. 80
27	Deviation of summer solar irradiation from 1950 value at 40° North Latitude. 84
28	Geomorphic map of the Ricks Creek fan 85
29	Profiles of Death Hollow channel slopes. 89
30	Relationships between maximum slope angle and slope height. 90
31	Distribution of prehistoric sedimentation events at the Rudd Creek fan. 96
32	Area covered by the 1983 sedimentation event at the Rudd Creek fan. 97
33	Photograph of debris basin constructed at Rudd Creek, Farmington, Utah in 1983. 98
34	Risk-based method for assessing hazards and responses. 106
35	Attenuation of sedimentation event damage with distance. 109
36	Alluvial fan flow events as a function of the thickness of the weathered layer in the mountains. 111
37	A model for hazards related to sedimentation processes on alluvial fans in Davis County, Utah. 117
38	Representative exceedance probability curves for sedimentation events on the Corbett Creek fan. 124
39	Representative exceedance probability curves for sedimentation events on the Hobbs Canyon fan. 124
40	Representative exceedance probability curves for sedimentation events on the Lightning Canyon fan. 125

Figure	Page
41	Representative exceedance probability curves for sedimentation events on the Kays Creek (Middle Fork) fan. 125
42	Representative exceedance probability curves for sedimentation events on the Kays Creek (South Fork) fan. 126
43	Representative exceedance probability curves for sedimentation events on the Snow Creek fan. 126
44	Representative exceedance probability curves for sedimentation events on the Adams Canyon fan. 127
45	Representative exceedance probability curves for sedimentation events on the Webb Canyon fan. 127
46	Representative exceedance probability curves for sedimentation events on the Baer Creek fan. 128
47	Representative exceedance probability curves for sedimentation events on the Half Canyon fan. 128
48	Representative exceedance probability curves for sedimentation events on the Shepard Creek fan. 129
49	Representative exceedance probability curves for sedimentation events on the Farmington Canyon fan. 129
50	Representative exceedance probability curves for sedimentation events on the Rudd Creek fan. 130
51	Representative exceedance probability curves for sedimentation events on the Steed Canyon fan. 130
52	Representative exceedance probability curves for sedimentation events on the Davis Creek fan. 131
53	Representative exceedance probability curves for sedimentation events on the Halfway Canyon fan. 131
54	Representative exceedance probability curves for sedimentation events on the Ricks Creek fan. 132
55	Representative exceedance probability curves for sedimentation events on the Barnard Creek fan. 132
56	Representative exceedance probability curves for sedimentation events on the Parrish Creek fan. 133
57	Representative exceedance probability curves for sedimentation events on the Centerville Canyon fan. 133

Figure		Page
58	Representative exceedance probability curves for sedimentation events on the Buckland Creek fan.	134
59	Representative exceedance probability curves for sedimentation events on the Ward Canyon fan.	134
60	Flow diagram for program HAZ.MOD.	136
61	Peak discharge as a function of sedimentation event magnitude.	138
62	Relationship among the time since the last sedimentation event, the volume of the last event, and the average annual sediment yield.	140
63	A model for hazard and risk management.	145
64	A model for hazard response alternatives.	146

LIST OF SYMBOLS

- a = Intercept coefficient in regression equations
- A = Ratio of reduced extreme-value standard deviation to sample standard deviation
- A_b = Basin area
- A_e = Area over which erosion occurs
- A_f = Fan area
- AF = Annual frequency
- AFP = Predicted alluvial fan process ordinal ranking
- A_g = Age of Lake Bonneville regression
- A_i = Incremental area
- A_t = Age of Lake Bonneville transgression
- b = Slope coefficient in regression equations
- B = Number of taps required to close a standard groove in a pat of sediment-water mixture in a liquid limit test
- C = Total risk cost
- $C(P_i)$ = Partial risk cost for the i th pathway in an event tree
- c = Diffusivity
- c^* = Modified diffusivity
- c^*_{NW} = Modified diffusivity for northwest-facing slopes
- c^*_{SE} = Modified diffusivity for southeast-facing slopes
- C_c = Coefficient of curvature
- CI = Contour interval
- C_u = Coefficient of uniformity
- C_v = Sediment concentration by volume
- C_w = Sediment concentration by weight
- D = Debris flow
- d = Grain size in mm

D_a = Distance from apex of active fan

d_o = Unit grain size

D_b = Nominal basin dimension

E_b = Basin elongation

eb = Basin eccentricity

E_g = Elevation of Lake Bonneville during regression

E_r = Erosion rate

erf = Error function

erf^{-1} = Inverse error function

E_{r_h} = Erosion rate for hills

E_{r_m} = Erosion rate for mountains

$E_{r_{pl}}$ = Erosion rate for plains

E_t = Elevation of Lake Bonneville during transgression

F = Percent passing Number 200 sieve; also ratio of population variances

FA = Fines activity

FA' = Normalized fines activity

FD = Fractal dimension

FF = Fines flow index

FF' = Normalized fines flow index

FI = Flow index

F_o = Basin form factor

G = Specific gravity

h = Thickness of flowing debris

H = Hyperconcentrated flow

H_i = Incremental height

H_s = Slope height

I = Intensity of sedimentation event damage

I_r = Rainfall intensity

K = Lemniscate factor

K_G = Graphic kurtosis

K_G' = Normalized graphic kurtosis

L = Length

L_b = Basin length

L_d = Length to principal divide

L_e = Possible economic loss

L_h = Hill land type

L_i = Incremental length

LL = Liquid limit

Ll = Magnitude of life loss

L_m = Mountain land type

L_{mf} = Mountain front length

L_p = Length from a contour to its projection along the axis of maximum fan convexity

L_{pl} = Plain land type

L_r = Length ratio

L_{sl} = Straight line length

L_t = Land type ordinal rank

M = Percent passing Number 40 sieve, and magnitude of sedimentation events

\bar{M} = Mean value of magnitude of sedimentation events

MA = Matrix activity

MA' = Normalized matrix activity

MF = Matrix flow index

MF' = Normalized matrix flow index

m_s = weathered layer maximum thickness

M_z = Mean grain size

N = Number of increments

N_{PR} = Cumulative frequency normalized to a period of record of PR years

PAR = Population at risk

$P(E)$ = Probability that event E will occur

$P(R|E)$ = Conditional probability that response R will occur given event E

$P(O|R)$ = Conditional probability that outcome O will occur given response R

$P(L|O)$ = Conditional probability that that life loss L will occur given outcome O

$P(e \geq M, t)$ = Exceedance probability

PL = Plastic limit

PR = Period of record

R = Rainfall duration

R_e = Sedimentation event rank

r = Rate of accumulation; also coefficient of correlation

r^2 = Coefficient of determination

R_b = Basin relief

R_e = Event rank

RF = Rating factor

$RI_{PR,M}$ = Average recurrence interval of events of magnitude M in period of record PR

R_r = Relief ratio

R_u = Basin ruggedness

S_e = Standard error of regression

S_f = Fan slope

S_f = Slope along axis of maximum fan convexity

Sk_I = Inclusive graphic skewness

Sm_f = Mountain front sinuosity

S_{MM} = Sum of squares about the mean value of magnitude

SY = Sediment yield

T = Transitional flow

t = Time; also Student's parameter

T_e = Time during which erosion occurs

T_f = Maximum fan thickness

T_{fm} = Mean fan thickness

TL = Total length

U = Parameter in extreme-value probability distribution

UR_{LH} = Late Holocene uplift rate

UR_{MH} = Mid-Holocene uplift rate

V = Total volume

V_a = Volume of air

V_c = Coarse fraction volume

V_e = Eroded volume

V_f = Fine fraction volume

V_s = Volume of solids

V_w = Volume of water

W = Total weight

w = Water content

W_b = Basin width

W_s = Weight of solids

W_w = Weight of water

x = Position in diffusion-equation model

y = Elevation in diffusion-equation model

y_s = Weathered layer thickness

α = Angle at which diffusion processes begin, also probability function for Student's t parameter

β = Error function argument

γ = Rate of shear strain

ϕ = Grain size in phi units

η = rate-of-weathering constant

μ_G = Mean value of reduced extreme-value distribution

μ_M = Mean magnitude of sample

θ = Maximum slope angle

ρ_C = Coarse fraction density

ρ_D = Debris flow density

ρ_H = Hyperconcentrated flow density

ρ_S = Laboratory slurry density and debris flow density

ρ_T = Transitional flow density

σ_G = Graphic standard deviation, also standard deviation of reduced extreme-value distribution

σ_I = Inclusive graphic standard deviation

σ_S = Standard deviation of sample

τ_C = Yield strength

τ_O = Applied shear stress

ASSESSING DEBRIS FLOW HAZARDS ON ALLUVIAL FANS IN DAVIS COUNTY, UTAH

by

Jeffrey R. Keaton¹, Loren R. Anderson², and Christopher C. Mathewson³

INTRODUCTION

Historically unprecedented late spring snowfall in 1983 followed by a rapid and sustained warming trend over much of the western United States resulted in widespread snowmelt flooding and numerous slope failures. Particularly extensive damage occurred in Davis County, Utah, from sedimentation processes caused by mobilization of failed slope material and stream channel sediments into debris flows and debris floods which traveled down steep canyons and into communities situated on alluvial fans at canyon mouths (Anderson and others, 1984). The basis for community response to the damage caused by the sedimentation processes apparently was the assumption that what happened in 1983 was likely to happen again soon, even though over 50 years had passed since the last major damaging sedimentation events in most of Davis County.

Seventy-seven flood events, with 56 being major or damaging, have been reported in Davis County since initial settlement in 1847 (Woolley, 1946; Croft, 1962, 1967, 1981; Butler and Marsell, 1972; Marsell, 1972; Wieczorek and others, 1983; Anderson and others, 1984; Olson, 1985; Mathewson and Santi, 1987). Fourty of the damaging flood events were caused by summer cloudburst rainstorms, with the most severe occurring in 1923 and 1930, while 16 were caused by snowmelt in 1983 and 1984. Snowmelt floods also occurred in 1922 and 1952 along the Wasatch Front (the urbanized area at the western base of the of the Wasatch Range) (Marsell, 1972; Anderson and others, 1984), but Davis County communities experienced very minor damage.

The community response following the sedimentation events of 1930 consisted of construction of sediment catch basins and diversions on the alluvial fans and contour terracing of hillsides near the crest of the Wasatch Range. The mountain land was acquired by the Federal Government under the jurisdiction of the U.S. Forest Service to control land use practices considered to be a major contributing factor to the high volume of sediment which was deposited on the alluvial fans at the canyon mouths (Bailey and others, 1934). The land on which the sediment catch basins were constructed, however, remained in private ownership. Complacency on the part of the citizens resulted from an apparent amelioration of the sedimentation problems in Davis County and, without having a public agency responsible for maintenance, the catch basins fell into states of disrepair or alternative uses (in one case, a home was constructed inside a catch basin). The community response following damaging sedimentation events of 1983 consisted of acquiring into public ownership the land on which the sediment catch basins had been

¹ Adjunct Associate Professor, Department of Civil and Environmental Engineering, Utah State University, Logan, Utah 84322-4110; alternative address: Sergeant, Hauskins & Beckwith, 4030 South 500 West, Suite 90, Salt Lake City, Utah 84123.

² Associate Dean, College of Engineering, Utah State University, Logan, Utah 84322-4100.

³ Director, Center for Engineering Geosciences, Department of Geology, Texas A&M University, College Station, Texas 77843-3115.

constructed earlier, repairing the basins and surface drainage devices, and constructing new sediment catch basins.

A major factor in the design of catch basins is the volume of sediment which should be trapped to provide a desired level of community protection. A reconnaissance-level evaluation of the potential for major sedimentation events (debris flows and debris floods) from canyons along the northern Wasatch Front was conducted by the U.S. Geological Survey (Wieczorek and others, 1983). They estimated the volume of sediment which could be anticipated to reach the canyon mouths and recommended measures to mitigate potential damage. They considered the sedimentation events of 1983 to represent "only one episode in a long history of similar phenomena" and the presence of young alluvial-fan deposits at canyon mouths to indicate a high potential for future sedimentation events (Wieczorek and others, 1983, p. 2). Bailey and others (1934, p. 10) noted that the alluvial fans deposited in Davis County since Lake Bonneville receded below the elevation of the canyon mouths were very small in comparison with the alluvial fans deposited farther north where, unlike Davis County, the watersheds almost entirely consisted of steep, bare rock surfaces virtually devoid of soil and vegetation. They observed that the quantity of sediment added to the alluvial fans in central Davis County by the floods of 1923 and 1930 was considerably out of proportion to the amount brought down through the previous thousands of years of post-Bonneville history (Bailey and others, 1934, p. 10-11). They concluded that damage to the watersheds caused by overgrazing and fire permitted accelerated erosion which resulted in sedimentation "far in excess of the previous normal rate..." (Bailey and others, 1934, p. 20).

Damage caused by sedimentation events on alluvial fans in Davis County included collapse of structures, translation of structures off of foundations, floodlike inundation of structures, and clogging of surface drainage devices with resultant diversion of surface water. Damage reported in published accounts of sedimentation events elsewhere (chiefly called mudslides, mud flows, mud floods, debris flows, or debris floods) is similar in character to the Davis County events. Inundation- and/or impact-related damage due to sedimentation events has been reported or shown by photographs from California (Campbell, 1975), Colorado (Mears, 1977), Virginia (Williams and Guy, 1973), western Canada (VanDine, 1985), and other places outside the United States (Schuster and Fleming, 1986).

The damage caused by the sedimentation events resulted in public awareness of the hazardous process. Varnes (1984) reports that the most common first action in natural hazard assessment is delineation of areas of hazard and degrees of risk. A common second action is dissemination of information to governing bodies and the public, along with education and warnings. Once the hazards are identified, actions can include enacting land-use regulation and building ordinances, acquisition of land in high risk areas, and emergency response in the event the hazard occurs. Incentives for developing in "safe" areas and disincentives for developing in unsafe areas can be accomplished by tax-assessment practices and financing policies. In some cases, hazards can be removed and facilities at risk can be protected with control works.

The possible actions described by Varnes (1984) collectively can be viewed as natural hazard risk management. The ultimate objective of managing risks is reduce risks to acceptable levels at minimum costs. These costs are capital expenditures and maintenance burdens as well as social and environmental costs related to alternative, and sometimes conflicting, land uses (e.g., homes versus debris basins). The principal elements of natural hazard risk management, once a hazard has been recognized, are evaluation of the hazard and evaluation of what is at risk. An optimum response alternative can be selected once a decision has been made regarding the acceptable level of risk

associated with the particular hazard. Periodic review of hazards and risks is needed to assess possible changes in the hazard, the risk, or the perception of risk. Evaluation of the hazard must focus on the probability of the occurrence of the hazard at intensities sufficient to cause damage; evaluation of the risk must focus on the population and facilities exposed to injury or damage and the consequences of the occurrence of the hazard at damaging intensities. Natural hazards currently being evaluated in this manner are floods and earthquakes. Sedimentation events are still being evaluated in a deterministic way in the sense that the potential for a major sediment delivery event (e.g., a debris flow) is taken as a representation of the hazard regardless of the probability of an event of a damaging intensity.

A natural hazard which serves to illustrate the limitations of the deterministic approach is meteorite impact. Anyone who has seen Meteor Crater in north-central Arizona is impressed at the destructive power that the impact must have had. Intuitively, a similar meteorite could collide with the earth at virtually any point. Thus, if the potential for meteorite impact were taken to represent the meteorite impact hazard, then the entire surface of the earth would be rated as high hazard. However, intuitively, the probability of a meteorite impact is exceedingly small -- so small that meteorite impact hazards are dismissed and never considered in the siting or design of any facilities, not even critical facilities (e.g., hospitals, nuclear power plants).

Sedimentation events caused by cloudburst rainstorms or rapid snowmelt are nearly always associated with other types of flood damage. The Committee on Methodologies for Predicting Mudflow Areas (1982) recognized the continuous spectrum from clear water floods (0 percent sediment) to dry landslides (100 percent sediment) and subdivided it into clear water floods, mud floods, mud flows, and other landslides. They further noted that the National Flood Insurance Program intended to cover damage from the first three classes only. They concluded that areas susceptible to mud flows could be mapped by adapting existing methods for mapping landslide susceptibility and that areas susceptible to mud floods probably could be mapped by adapting standardized methods of flooding (Committee on Methodologies for Predicting Mudflow Areas, 1982, p. 30).

Identification of areas susceptible to potentially damaging processes represents only one aspect of hazard evaluation. Hazards are naturally occurring or man-induced processes which have the potential to cause damage or injury. A complete hazard evaluation of potentially damaging processes consists of identifying 1) their locations, 2) their frequencies, 3) their magnitudes, 4) the rates at which they occur, 5) their durations, 6) the certainty with which they can be forecasted, and 7) possible effects. Risk is exposure of something of value to potential damage or individuals to potential injury as a result of the occurrence of hazardous processes. Risk reduction must be based on 1) a complete hazard evaluation, 2) an inventory of potentially exposed facilities and population, 3) an estimate of the probability of damage or injury given the occurrence of the hazard, and 4) an understanding of available options to mitigate the hazards.

The objective of this research is to develop a probabilistic model for evaluating hazards related to sedimentation processes on alluvial fans. Using the geologic record to quantify the probability of occurrence of damaging intensities of natural processes is an application of geologic principles to a problem in which mankind is directly involved; thus, this research is engineering geology. The probability of an event of a damaging intensity can be calculated from an understanding of the frequency of occurrence of events of sufficient magnitude to cause damage. Estimating the relationship between sedimentation event magnitude and frequency is an application of geologic principles to the interpretation of the geologic record contained in the alluvial-fan deposits (historic and prehistoric records). Interpreting the geology recorded in alluvial fans requires an understanding of

the geologic phenomena of alluvial-fan processes, such as hydrodynamics and sedimentology.

SCOPE OF RESEARCH

Alluvial fans are cone-shaped landforms created by streams emerging from mountains. In the context of this dissertation, sedimentation processes are taken to mean transportation and deposition of sediment carried by flowing sediment-water mixtures. Sedimentation processes on alluvial fans range from debris flows to normal streamflows and vary with the ratio of sediment to water. Flow behavior ranges from plastic to fluid and from laminar to turbulent. Hazards associated with the range of processes can be related to impact, burial, inundation, and erosion.

This research comprises an engineering geologic evaluation based on a corollary to the Law of Uniformitarianism: The recent past is the key to the near future. A combination of field, laboratory, theoretical, and analytical investigations were used to achieve the objectives of this research. Eyewitness accounts of major sedimentation events were combined with observations of the stratigraphy and geomorphology of post-Lake Bonneville prehistoric deposits to develop an understanding of the distribution, frequency, and magnitude of the variety of sedimentation processes on alluvial fans in Davis County (Figure 1). Davis County was selected for field investigation because 1) damaging major sedimentation events occurred in 1923, 1930, and 1983 due to cloudburst rainstorms and rapid snowmelt (Woolley, 1946; Butler and Marsell, 1972; Anderson and others, 1984), 2) a hazard evaluation was conducted (Wieczorek and others, 1983) and served as the basis for community response decisions, 3) a difference of opinion exists regarding the frequency and magnitude of major sedimentation events (Bailey and others, 1934; Wieczorek and others, 1983), 4) the stratigraphy of Lake Bonneville is well known and provides a lower bound on the age of the post-Bonneville alluvial-fan deposits (Currey and Oviatt, 1985), and 5) the results of this research may have tangible benefits to many residents in urban centers along Utah's heavily populated Wasatch Front who may be exposed to the risk of damage resulting from future sedimentation events.

Field investigations consisted of mapping and describing exposures of prehistoric alluvial-fan deposits and collecting samples for subsequent laboratory analyses. Mapping was done on both reconnaissance and detailed levels. Detailed mapping was done at two locations where alluvial-fan deposits are preserved in accessible, unurbanized conditions (Rudd Creek fan and Ricks Creek fan, numbers 13 and 17 on Figure 1). Reconnaissance mapping was done along the base of the Wasatch Range in Davis County with the aid of stereoscopic aerial photographs taken in 1946, 1980-81, 1983, and 1984 at scales ranging from 1:20,000 to 1:6,000. The stereoscopic aerial photos were supplemented by orthotopographic maps prepared by Aero-Graphics, Inc. for the Davis County Planning Commission in 1982 at a scale of 1:2,400. Relative dating techniques (Burke and Birkeland, 1979), degree of soil development (Birkeland, 1984), and slope degradation by diffusion (Pierce and Colman, 1986) were used in estimating the ages of alluvial-fan deposits.

Laboratory investigations consisted of determination of grain size distributions, Atterberg limits, specific gravity of gravel clasts, and experimentations with reconstituted sediment-water slurries at water contents representing the threshold of mobility. Parameters derived from the laboratory test results were computed for use in statistical analyses of alluvial fan deposits.

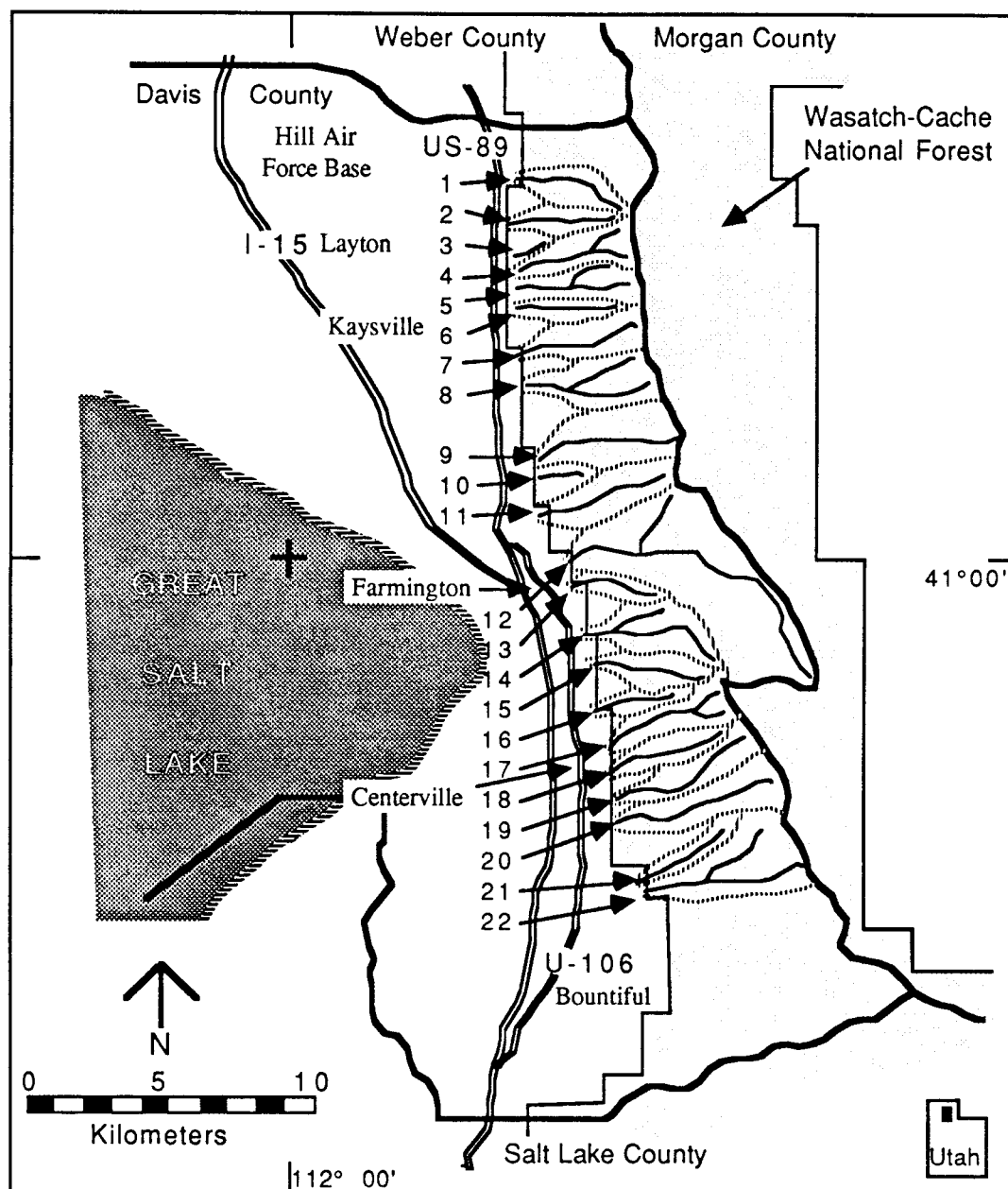


Figure 1. Vicinity map of research area. Selected drainage basins are designated by number as follows:

1, Corbett Creek;	3, Lightning Canyon;	4, Kays Creek (Middle Fork);
2, Hobbs Canyon;	6, Snow Creek;	7, Adams Canyon;
5, Kays Creek (South Fork);	9, Baer Creek;	10, Half Canyon;
8, Webb Canyon;	12, Farmington Canyon;	13, Rudd Creek;
11, Shepard Creek;	15, Davis Creek;	16, Halfway Canyon;
14, Steed Canyon;	18, Barnard Creek;	19, Parrish Creek;
17, Ricks Creek;	21, Buckland Creek;	22, Ward Canyon.
20, Centerville Canyon;		

Theoretical and analytical investigations consisted of interpretations of erosion and sedimentation histories at the sites of detailed mapping; characterization of sedimentation processes by direct observation of deposits and results of laboratory testing; analysis and interpretation of erosion and sedimentation at sites of reconnaissance mapping; and correlation of results from Davis County with understanding of stratigraphic and geomorphic features from other pertinent research.

The observed stratigraphic features (clast support mechanisms, stratification, gradation character, condition of basal contact, presence or absence of megaclasts) were given ordinal ranking so that they could be combined with results of laboratory tests and derived parameters and analyzed with use of multivariate statistical techniques to produce an empirical model for classification of sedimentation processes responsible for deposit character.

The results of field, laboratory, and theoretical investigations were synthesized into a complete hazard evaluation including location, frequency, magnitude, rate, duration, forecastability, and effects of the various sedimentation processes. This hazard evaluation based on the features present at the canyon mouths was compared to the evaluation prepared by Wieczorek and others (1983) based chiefly on features present within the drainage basins. Recommended hazard response alternatives are summarized and provide a perspective for risk reduction decisions. Conclusions are made regarding general characteristics of hazards related to alluvial fan sedimentation, the appropriateness of the community responses to the sedimentation events of 1983, alternatives to provide protection from future events, and opportunities for further research on this topic.

RELATED STUDIES

The Association of State Floodplain Managers held a symposium entitled "Western State High Risk Flood Areas" at their annual meeting in Las Vegas, Nevada, in March, 1986. Workshops at this symposium focused on mapping and modeling alluvial fan flooding and sedimentation, among other issues. The general consensus regarding clear water flooding was that available hydrologic models provided an adequate basis for hazard identification for those drainage basins with substantial records. The general consensus regarding what they termed "mudflows and mudfloods" was that hydrologic models were grossly inadequate. Only in southern California have major sedimentation events occurred with sufficient frequency to permit an empirical approach to evaluating the hazard.

Identification of landslide susceptibility is not standardized and evaluations of hazards are presently restricted to deterministic approaches for the most part. Current approaches to landslide hazard evaluation are summarized in Hansen (1984), Varnes (1984), and Crozier (1986). Kockelman (1986) summarizes some techniques for reducing landslide hazards. Innovative approaches to landslide susceptibility using multivariate statistical analyses (Pack, 1985) and multispectral remote sensing data (Jadkowski, 1987) have been developed recently.

Methods of differentiating between debris flows and debris floods, or hyperconcentrated sediment flows (Beverage and Culbertson, 1964), have been developed only recently. Pierson and Costa (1987) have formulated a rheological classification of subaerial sediment-water flows which advances earlier research by Smith (1986), Pierson and Scott (1985), Obrien and Julien (1985), Pierson (1985a), Lawson (1982), Takahashi (1981), and Lowe (1979). During a sedimentation event in Utah in June, 1983, Pierson (1985b) differentiated debris flow, hyperconcentrated sediment flow, and normal stream

flow on the basis of observed behavior, sediment concentration, and textural characteristics of the flowing mass.

Stratigraphic and geomorphic aspects of alluvial fans and debris flow-dominated sedimentation processes have been the subject of several reports. Collections of articles have been published in volumes edited by Koster and Steel (1984) and Nilsen (1985). General treatments of alluvial fans have been published by Bull (1977), Rachocki (1981), and Nilsen (1982). General treatments of debris flows have been published by Takahashi (1981), Innes (1983), Costa (1984), and Johnson and Rodine (1984). Discussions of stratigraphic features associated with alluvial fan sedimentation are included in reports by Heward (1978), Larsen and Steel (1978), Lowe (1982), and Nemec and Steel (1984). Stratigraphic and sedimentologic aspects of major sedimentation processes from volcanic terrain (lahars) have been published by Smith (1986), Scott (1985), and Pierson and Scott (1985).

Published reports regarding sedimentation processes on alluvial fans have focused on sedimentologic, stratigraphic, and geomorphic aspects. Thus far, systematic assessment of alluvial-fan sedimentation processes to permit elucidation of the variety of associated hazards has not been conducted; therefore, this research represents a worthwhile scientific contribution as well as a useful advancement for hazard evaluation and risk reduction.

SEDIMENTATION CHARACTER

RANGE OF PROCESSES

Alluvial fans have been the subject of several general reports (Blissenbach, 1954; Beatty, 1963; Denny, 1967; Bull, 1972; Spearing, 1974; Bull, 1977; Rachocki, 1981; Nilsen, 1982; and Schumm and others, 1987). The general features which have been discussed in these reports include fan shape, relation of fan area to drainage basin area, downfan trends in grain size and bed thickness, and some factors affecting sediment deposition.

Alluvial fans are named for the shape they make in plan view on topographic maps. Streams emerging from mountains deposit sediments in the general form of a segment of a cone (Nilsen, 1982, p. 49). The cone-shaped landform generally has three segments which can be distinguished in radial profiles; each of the three segments exhibits a linear elevation profile with the segment closest to the apex of the fan (proximal) having the steepest gradient and the segment farthest from the apex (distal) having the flattest gradient (Bull, 1977, p. 255). Thus, the radial profile is concave upward and the segments have been termed the upper, middle and lower fan segments. Cross-fan profiles are convex upward providing the conical shape. Consequently, alluvial fan morphologies are inherently unstable, causing streams to diverge, forming the characteristic fan shape and inhibiting establishment of long-term equilibrium.

The areas of alluvial fans have been related to the areas of the drainage basins responsible for producing them (Bull, 1977, p. 246). Values of fan area versus drainage basin area for suites of fans in specific arid and semiarid localities are approximately parallel on log-log plots (Bull, 1977, p. 246), suggesting that drainage basin processes and sediment yields may be comparable. However, differences in numerous factors can contribute to differences in fan area, fan thickness, and fan volume. Character of local base level (Lustig, 1965, p. 134), tectonic activity (Hooke, 1972), and climate (Kochel and Johnson, 1984, p. 111) have been suggested as reasons that observed fan-drainage basin areas deviate from the log-log relationships. In Davis County, the alluvial fans are very small (Bailey and others, 1934, p. 10) and younger than Lake Bonneville ($< \pm 11$ ka). The drainage basins in Davis County apparently formed during rapid uplift of the Wasatch Range over the past 10 ma (Naeser and others, 1983, p. 35); thus, the drainage basins are approximately three orders of magnitude older than the alluvial fans and relationships between fan area and drainage basin area may be quite different in Davis County than in other semiarid or arid locations.

Downfan trends in grain size and bed thickness have also been recognized as elements which are characteristic of alluvial fans (Sharp and Nobles, 1953; Blissenbach, 1954; Bluck, 1964). All researchers studying fans have concluded that, in general, grain sizes and bed thicknesses decrease in a downfan direction.

A number of factors have been recognized as important in affecting deposition of sediment on alluvial fans. These factors, therefore, affect the development of all aspects of alluvial fans. The importance of tectonic activity on local base level has already been mentioned. Base-level changes (mountain channel down-cutting or basin lowering) can promote entrenchment of the stream channel into the apex of the fan which tends to shift the main deposition zone in a downfan direction. Uplift of the mountain block can counteract the entrenchment of the fan apex if the uplift rate exceeds the rate of channel down-cutting

or base level sedimentation (Bull, 1977, p. 250). Thus, in tectonically active areas, the location of active fan sedimentation should be situated adjacent to fault scarps at the bases of the mountains, while in tectonically stable areas, fanhead entrenchment should have shifted the location of active fan sedimentation in a downfan direction. The point on the fan where an entrenched channel emerges onto the surface on the fan has been called the intersection point (Hooke, 1967, p. 450).

Laboratory and controlled field models of alluvial fans have provided insight into alluvial fan processes. Hooke (1967) presented results of a laboratory model which indicated clearly that a combination of water-dominated and sediment-dominated deposition events were required to produce the characteristic fan shape. He found that steeper fans were produced when debris flows were the dominant process and flatter fans were produced when fluvial processes dominated. Rachocki (1981) used a gravel pit to generate a small fan in an area where survey control points had been established so that fan development could be monitored in a precise manner. A comparative evaluation of parameters of alluvial fans from four climatic environments was prepared by Kochel and Johnson (1984, p. 120). Their evaluation pertains to arid, humid-glacial, humid-tropical, and humid-temperate fans.

The discussion of general aspects of alluvial fan processes presented above indicates that sedimentation on alluvial fans should have some general trends, but wide variability should be a dominant characteristic. Sources of water, grain support mechanisms, and character of flowing sediment-water mixtures contribute to or are governed by sedimentation processes on alluvial fans.

Sources of Water

Sedimentation on alluvial fans has been caused by intense rainstorms, rapid snowmelt, and possibly by high pressure in groundwater in fractured bedrock. Water released during volcanic eruptions (e.g., the 1980 eruption of Mount St. Helens, Washington; Scott, 1985) and water displaced from lakes or reservoirs by landslides (e.g., the 1983 rock avalanche and debris flow at Ophir Creek, Nevada; Glancy, 1985) could also cause sedimentation events; however, sources such as these are not present in Davis County and are not considered further.

Intense Rainstorms

Rainstorms can contribute to sedimentation processes in two fundamentally different ways. First, shallow slope materials can become saturated during a series of rainstorms and then a more intense rainstorm causes slope failures to occur which subsequently results in sedimentation on alluvial fans. Second, cloudburst rainstorms can result in surficial erosion of slope and/or stream channel materials.

Seasonal antecedent rainfall of about 255 mm was found to be a prerequisite for shallow slope failures in the Los Angeles, California, area which occurred during rainstorms exceeding an intensity of about 6.4 mm/hr (Campbell, 1975). The higher intensity rainstorms resulted in surface water infiltration into thin surficial deposits which exceeded deeper percolation into bedrock, permitting pore-water pressures to accumulate in the surficial deposits promoting slope failures. The material involved in the slope failures rapidly disintegrated into debris flows which flowed out onto alluvial fans. Intensity and duration data for rainstorms associated with slope failures leading to sedimentation events

were collected by Caine (1980) who found the following relationship for world-wide locations:

$$I_r = 14.82 R^{-0.39} \quad (1)$$

where I_r is rainfall intensity in mm/hr and R is rainfall duration in hr.

The term "cloudburst" has been used to describe high-intensity, short-duration rainstorms (Woolley, 1946; Butler and Marsell, 1972). Such rainstorms are relatively common in arid and semiarid areas and can cause substantial erosion of slope and stream channel materials. Beaty (1974, p. 40) found that approximately 85 to 90 percent by volume of the sediment contributed to alluvial fans on the west side of the White Mountains, California, was due to debris flows caused by summer thunderstorms while only 10 to 15 percent of the sediment was contributed by "so-called 'normal' stream processes."

Rapid Snowmelt

Rapid melting of snowpack can contribute water to slope systems in a manner similar to seasonal rainfall. The amount of water in the snowpack and the rate of melting are important factors. Repeated sedimentation events have occurred at Wrightwood, California, due to melting of snow in a landslide area (Sharp and Nobles, 1953; Johnson, 1970; Morton and Campbell, 1974; Morton and others, 1979).

Rapid melting of an unprecedented heavy snowpack in Utah was the major factor contributing to landslides, debris flows, and flooding in 1983 (Anderson and others, 1984). Marsell (1972, p. N13) noted seven conditions which promoted snowmelt flooding: 1) A heavy winter snowpack; 2) saturated soil mantle at the start of the winter due to heavy, late autumn rains; 3) abnormally low temperatures during late winter and early spring; 4) sustained high temperatures once melting starts; 5) additional precipitation, especially warm rain, to increase the rate of melting; 6) streams reaching peak discharge simultaneously; and 7) lack of adequate storage reservoirs in the watersheds to regulate discharge. These conditions existed in Utah in 1922, 1952, and 1983 (except the melting was not exacerbated in 1983 by warm rainfall). No major sedimentation events were associated with the snowmelt flooding in 1922 or 1952, but major and widespread sedimentation occurred in 1983.

Bedrock Groundwater

Discharge of groundwater has been suggested to be an important process in initiating sedimentation on alluvial fans in Davis County (Mathewson and Santi, 1987). In their model, pressures in groundwater in fractured bedrock are permitted to accumulate by recharge due to snowmelt or rainfall and confinement by surficial deposits of relatively low hydraulic conductivity. At such time as the pressure in the groundwater reduces the effective stress of the shallow slope system to zero, slope failures occur. The displacement of a mass of surficial material exposes the fractured bedrock and permits sustained discharge of groundwater. Sediment can be incorporated into flowing water from the material involved in the initial slope failure and/or from the material mobilized from the bed and banks of the stream channel below the failure area (Santi and Mathewson, 1988; Santi, 1988).

Grain Support Mechanisms

Geomorphic and sedimentologic features of sedimentation processes on alluvial fans should be sufficiently unique to provide unequivocal means of classifying the deposits on the basis of dominant process (Costa and Jarrett, 1981, p. 312 ff). Debris flows are generally considered to be a mass-wasting process intermediate between landslides and normal streamflows (Figure 2), and distinguished on the basis of Newtonian versus non-Newtonian behavior (Wieczorek, 1986, p. 220). At low water contents, hence, high sediment concentrations, debris flows have relatively high shear strength, but the strength is very sensitive to additional water (Costa, 1984, p. 290). The shear strength of a debris flow can be reduced by a factor of two or more with the addition of as little as two or three weight-percent water. Clear water floods have generally low shear strength which increases slowly with increasing sediment load and can be described by conventional hydraulic formulas based on Newtonian fluid behavior. Up to fluid densities of about 1.5 to 1.8 g/cm³, flood flows transport sediment by turbulence, shear, lift and drag forces (Costa, 1984, p. 291). At some critical sediment concentration, hence fluid density, shear strength increases rapidly and is accompanied by an apparently irreversible entrainment of sediment (Pierson and Scott, 1985, p. 1512).

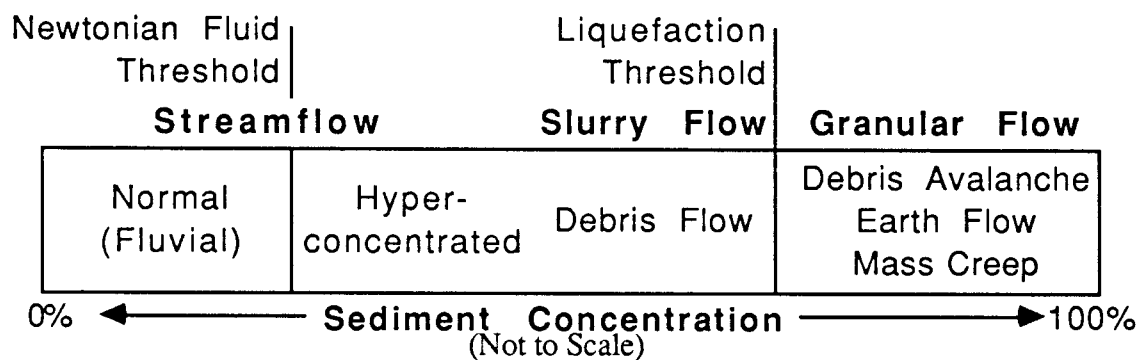


Figure 2. Conceptual range of processes and sediment concentrations for sediment-water mixtures. Modified from Wieczorek (1986, p. 220).

Additional clarification of grain support mechanisms has recently been developed by Pierson and Costa (1987) and is based on flow behavior as a function of deformation rates (flow velocity). At low flow velocities and in clay-rich mixtures, velocity-independent frictional and viscous forces dominate. At higher velocities and in coarser grained mixtures, velocity-dependent inertial forces dominate. Bouyancy, cohesion, and structural support are low-velocity grain-support mechanisms while turbulence, dispersive stress, and fluidization are higher velocity mechanisms.

Lowe (1982, p. 280) has suggested a classification of sediment gravity flows based on flow rheology and particle support mechanism (Table 1). Flow behavior in Lowe's classification is either *fluid* or *plastic* and the flow character is either *laminar* or *turbulent*. As indicated in Table 1, turbidity currents are *fluidal flows* in which flow turbulence is the primary mechanism maintaining the larger sedimentary grains above the bed. Large grains are fully supported by escaping pore fluid in *fluidized flows* but only partially supported by

Table 1. Classification of sediment gravity flows. Modified from Lowe (1982, p. 280-281).

Flow Behavior		Flow Type		Clast Support Mechanism	Depositional Process
Fluid	Turbulent	Fluidal Flow	Turbidity Current	Fluid Turbulence	Suspension Sedimentation
			Fluidized Flow	Escaping Pore Fluid (Full Support)	
			Liquefied Flow	Escaping Pore Fluid (Partial Support)	
Plastic	Laminar	Debris Flow	Grain Flow	Dispersive Pressure	Frictional Freezing
			Mudflow or Cohesive Debris Flow	Matrix Strength and Density	Cohesive Freezing

escaping pore fluid in *liquefied flows*. *Grain flows* are associated with large grain support by dispersive pressure generated by particle collisions and large grains in *cohesive flows* are supported by a cohesive matrix.

Lowe (1982, p. 281-282) notes that sediment is deposited by decelerating sediment gravity flows by two different mechanisms which he designates as *sedimentation* and *freezing*. Sediment deposition from fluidal flows is on an individual grain basis from the base upward from bed load or suspended load. These modes of deposition are called *traction sedimentation* and *suspension sedimentation*, respectively. Sediment deposition from debris flows is related to a threshold ratio of the yield strength of the moving sediment-water mixture to the applied shear stress which is related to density, depth, and hydraulic gradient of the flow (Hooke, 1967, p. 452). Lowe (1982, p. 282) notes that debris flows exhibit a strain-dependent "freezing" in which the flows solidify en masse or from the surfaces inward. The grain flow types of debris flow solidify as a consequence of frictional grain resistance and Lowe (1982, p. 282) describes this process as *frictional freezing*. Cohesive debris flows solidify as a consequence of cohesive grain interactions which Lowe calls *cohesive freezing*.

Nardin and others (1979, p. 64) summarized mass transport processes ranging from rockfalls to turbidity currents by mechanical behaviors, and grain support and transport mechanisms (Table 2). They further identified sedimentary structure assemblages which they believed to be characteristic of the mechanical behavior and transport processes.

Table 2. Major types of mass transport processes, behaviors, clast support mechanisms. From Nardin and others (1979, p. 64).

Mass Transport Processes			Mechanical Behavior	Transport and Sediment Support Mechanism
Rock Fall			Elastic	Freefall and subordinate rolling of individual blocks or clasts along steep slopes
Slide	Glide			Shear failure along discrete shear planes with little internal deformation or rotation
	Slump			Shear failure accompanied by rotation along discrete surfaces with little internal deformation
Sediment Gravity Flow	Mass Flow	Debris Flow	Plastic Limit	Shear distributed throughout the sediment mass. Strength is principally from cohesion due to clay content. Additional matrix support may come from bouyancy.
		Mud Flow		
	Fluidal Flow	Grain Flow	Liquid Limit	Cohesionless sediment supported by dispersive pressure. Flow may be in inertial (high concentration) or viscous (low concentration) regime. Usually requires steep slopes.
		Inertial Viscous		
		Liquefied Flow	Viscous Fluid	Cohesionless sediment supported by upward displacement of fluid (dilatance) as loosely packed structure collapses, settling into a more tightly packed framework. Requires slopes > 3°.
		Fluidized Flow		Cohesionless sediment supported by the forced upward motion of escaping pore fluid. Thin (<10 cm) and short-lived.
		Turbidity Current		Supported by fluid turbulence

Character of Flow

Alluvial fan deposits traditionally have been subdivided into two classifications: Streamflow (or water-laid) and debris flow (or mudflow) and related processes (Nilsen, 1985, p.2). A third classification, transitional between water-laid and debris flow, has been included by some workers (Bull, 1977, p. 233 ff; Rachocki, 1981, p. 20-22; Nilsen, 1982, p. 59-60). Some researchers prefer to call the dominant processes by terms like streamflood, sheetflood, mud flood, hyperconcentrated flow, streamflow, mass flow, grain flow, density flow, sediment gravity flow, slurry flow, or lahar (Lowe, 1982; Nemec and Steel, 1984; Costa, 1984; Pierson and Costa, 1987). Alternative evaluations of alluvial fan sediments have incorporated rheological properties of moving sediment-water mixtures (Pierson, 1980; Costa, 1984; Johnson and Rodine, 1984; Nemec and Steel, 1984; Pierson and Costa, 1987; Wiczorek, 1986). The expected character of sedimentary deposits due to a range of rheological properties has been considered by Lowe (1982) and by Nemec and Steel (1984).

Streamflow processes result in sediment transportation in suspension, saltation, and traction by channelized or nonchannelized flowing water (Nilsen, 1985, p. 2). Streamflows exhibit Newtonian behavior and have strength characteristics which are dependent on the velocity (strain rate) of flowing water. Thus, swift water has greater competence than slow water, and as water velocity slows, the largest particles are deposited first, creating clast-supported, stratified, graded (fining upward) bedding.

Debris flow processes result in sediment transportation which is related to matrix material composed of sediment-water mixtures (slurries). The specific gravity of the slurry tends to support large clasts and accounts for the ability of debris flows to transport huge boulders (Rodine and Johnson, 1976; Hampton, 1979). Debris flows exhibit non-Newtonian behavior and have strength characteristics which are independent of the velocity of the flow. Plastic deformation is dominant in slower-moving flows while visco-plastic deformation is dominant in faster-moving flows. Thus, debris-flow deposits commonly are ungraded, unsorted, unstratified sediment accumulations (diamictons) which are matrix-supported.

Processes transitional between streamflow and debris flow should be expected because the ratio of sediment to water (sediment concentration) should be a continuum from 0.0 to 1.0. At some threshold of the sediment-to-water ratio (0.72 by weight according to O'Brien and Julien, 1985, p. 264), deformation processes change from debris flow (at lower ratios) to landslides (at higher ratios). Sediment concentrations as high as 0.88 by weight in debris flows have been measured by Morton and Campbell (1974, p. 383) in California and by Pierson (1985b, p. 144) in Utah. The transition from debris flow processes to extreme concentrations of sediment in flowing water has been assigned to sediment concentrations ranging from 0.8 to 0.4 by weight by Beverage and Culbertson (1964, p. 146) and has been called hyperconcentrated flow.

Pierson (1985b, p. 139 ff) observed a relatively minor sedimentation event at Rudd Creek which occurred at 10:30 a.m. on June 5, 1983, six days after major debris flows damaged 12 residential structures built on the alluvial fan. His point of observation was above the channel of Rudd Creek about 55 m upstream from the apex of the alluvial fan where sediment samples were collected for laboratory analysis. He observed completely laminar flow at sediment concentrations exceeding 0.8 by weight. The slurry at this sediment concentration had a viscous appearance and carried cobble- to boulder-size clasts in suspension. He observed minor turbulence developing as sediment concentrations dropped below 0.8 by weight. The surface of the slurry began to appear shiny and wet and turbulence was increasing but some pebbles were still in suspension at sediment concentrations of about 0.75 by weight.

Pierson (1985b, p. 139 ff) observed behavior transitional between typical debris flows and hyperconcentrated streamflows at sediment concentrations between about 0.75 and 0.7 by weight. Turbulence was present over the entire flow surface at sediment concentrations of about 0.74 by weight and vigorous splashing occurred in places with only very fine pebbles in suspension. Turbulence was well developed over the entire flow surface at sediment concentrations of about 0.71 by weight and rounded wave crests indicated that the slurry was considerably more viscous than water but only coarse sand and fine particles remained in suspension. At sediment concentrations below 0.7 by weight, the flow surface acquired an agitated, choppy appearance which Pierson (1985b, p. 142) interpreted to represent hyperconcentrated sediment flow.

EYEWITNESS ACCOUNTS

Summary of Published Accounts

Depositional processes on alluvial fans have been witnessed by a number of individuals, scientists and non-scientist alike. One of the early eye witness descriptions of debris flow processes was by Pack (1923) in Utah. He observed three phases of alluvial fan flooding: first, a short period of gradually increasing stream volume; second, a longer period of cataclysmic intensity; and third, a still longer period of normal flooding characterized by highly swollen streams at the beginning which gradually decreased to their ordinary size. He notes that the second phase consisted of two impulses. The first impulse included vast quantities of woody material first derived from collapse of what he called "temporary dams along the channel" (p. 353). It appears that this material moved relatively slowly, had no free water associated with it at its toe, left steep-sided, heterogeneous deposits, and moved by shoving rather than rolling. The second impulse consisted of "tremendous quantities of rock-waste [which] shot from narrow canyons into open vallies with suddenness that almost challenges belief" (p. 353). The first impulse almost certainly represents plastic deformation of a debris flow, but the second impulse might represent a transition to a hyperconcentrated sediment flow.

Blackwelder (1928) provides descriptions of several debris production events and references McGee's (1897) account in Arizona and northern Mexico with the first use of the term "mudflow." Blackwelder observed a debris flow at Morgan, Utah in 1909 and the deposits created by the events described by Pack (1923). Blackwelder (1928, p. 470) interviewed a resident in the southern San Joaquin Valley of California who witnessed a debris flow in 1905(?). The resident noted that the noise of the flow moving down the canyon could be heard before the flow was visible at the canyon mouth. The flow was accompanied by a cloud of dust created by incorporation of dry soil from the banks of the channel as the flow descended. The first wave came to a complete stop about one half mile from the canyon mouth and was succeeded in a few minutes by another wave, larger and swifter than the first. No dust came from waves other than the first one. Immense masses of rock were dancing along on the surface of the flow. The second wave extended about a half mile further down the canyon than the first wave when it came to a stop. In a few minutes another wave swept by, followed by others at intervals of a few minutes, each succeeding wave getting thinner and traveling with greater velocity than the preceding one, until, in about half an hour, the mass was no longer mud, but a steady rush of yellow, foaming water. The water flow gradually reduced in width and increased in depth and velocity as it cut into the previously deposited muddy debris.

Similar features were observed by Jahns (1949) near Parker, Arizona, resulting from a cloudburst rainstorm in January 1943. The first phase of a debris flow at the mouth of a canyon moved slowly, had a steep front about 35 feet high, and included boulders more than 30 feet in maximum dimension. Dust clouds were created by collapse of dry material from the walls of the canyon. Boulders and tree trunks floated along in the upper surface of the flow, buoyed by the density of the fluid. Jahns noted that the rock "masses were very buoyant in the heavy, sludge-like "liquid" of water and ill-sorted debris, and were held up also by the almost solid mosaic of rock fragments between them and the bed of the wash" (p. 13). Waves more than eight feet high traveled slightly faster than the initial wave and succeeded each other at frequent intervals. The part of the flow that succeeded the initial wave became progressively richer in water and behaved more like ordinary stream flow. The snout of the deposit of the initial wave had been breached at several places by later flows of more liquid material. Free water was not observed at any place examined by Jahns (1949, p. 13).

Debris flows caused by snowmelt runoff have been observed at Wrightwood, California, by Sharp and Nobles (1953), Morton and Campbell (1974), and Morton and others (1979). The period over which flows occurred during debris flow activity in 1941 was "a week to 10 days" (Sharp and Nobles, 1953, p. 551), and the period of flow activity in 1969 was 40 days (Morton and Campbell, 1974, p. 378). Sharp and Nobles (1953, p. 551) noted that debris came in waves or surges beginning daily at about 9:00 in the morning and reached peak frequency in early afternoon. Fluidity was greatest at midday. Bumping boulders and splashing fluid mud made characteristic noises likened to a concrete mixer. The fronts of advancing fluid surges at the height of activity "slithered and slopped along much like the front of a rapidly flowing tongue of water or the swash from breakers on a beach." Boulders were pushed along by the finer matrix without rolling or turbulent action. As the material became more viscous in late afternoon, velocities decreased and bouldery fronts became more massive, steeper, and higher.

Morton and Campbell (1974) observed generally the same features as Sharp and Nobles (1953) on debris flows in 1969 coming from the same source area and related to the same source of water as those in 1941. Morton and Campbell (1974, p. 383; also Morton and others, 1979, p. 16 - 17) determined specific gravities and estimated sediment concentrations by collecting samples of the moving debris at two sites, an upper site and a lower site. Gravelly mud at the upper site had a range of sediment concentration by weight from 0.835 to 0.882 while sandy mud at the upper site ranged from 0.295 to 0.79. At the lower site, gravelly mud ranged in sediment concentration by weight from 0.673 to 0.835 while sandy mud ranged from 0.554 to 0.752. More fluid material was also measured at both sites and found to range in sediment concentration from 0.123 to 0.61. One fluid sample was found to have a sediment concentration of 0.807 but was discounted as having some bed load sediment inadvertently included. Temporal sequence data pertaining to these sediment concentration values is not included in the report, but based on accounts of debris flows at other locations, a reasonable sequence would consist of gravelly material succeeded by sandy material succeeded by fluid material.

An account of alluvial fan depositional processes from events in 1952 in the northern White Mountains of California is presented by Beaty (1963). Debris flow and flood features from three alluvial fans were sketched by Beaty (1963, p. 520 - 521) and provide additional important information about distribution of alluvial fan sedimentation. The general downfan decrease in grain size is supported by the distribution of debris-flow (bouldery) deposits in the proximal fan areas, mudflow (sandy and gravelly) deposits in the mid-fan areas, and water and silt in the distal fan areas.

The most recent observations of alluvial fan sedimentation are from the snowmelt debris flows of May and June, 1983, in Utah. Pierson (1985b) observed and sampled a surging, channelized debris flow on June 5, 1983, at Farmington, Utah. The results of his observations and measurements provide insight regarding temporal changes at a point in a channel 55 m above the apex of the fan at Rudd Creek. He collected samples at 1- to 10-minute intervals during a 45-minute long surge beginning at 10:30 in the morning on June 5. Pierson (1985b, p. 144) classified the samples as debris flow, transitional, hyper-concentrated, and normal stream flow on the basis of sediment concentration as defined by Beverage and Culbertson (1964). Pierson (1985b, p. 150) found that the highest flow velocities corresponded to sediment concentrations greater than 0.8 by weight which is contradictory to observations of debris flows described above. One possible explanation for this contradiction is that the velocity measurements were made where the debris was channelized 55 m above the apex of the fan. Such lateral confinement could contribute to higher velocities than suggested by earlier observations made on fan surfaces where no such confinement existed.

Davis County Accounts

The earliest reported alluvial fan flooding in Davis County occurred at Farmington on July 23, 1878 (Woolley, 1946, p. 89). Fifty-six major events of alluvial fan flooding have been reported in Davis County; 40 were caused by cloudburst rainstorms while 16 were caused by rapid snowmelt (Woolley, 1946; Croft, 1967; Butler and Marsell, 1972; Anderson and others, 1984; Lindskov, 1984). A summary of reported flood events in Davis County is presented in Appendix A. The most severe and damaging sedimentation events in Davis County occurred in 1923, 1930, and 1983.

The earliest scientific discussion of sedimentation events in Davis County was prepared by Pack (1923), who described the flowing debris and deposits from the events of the 1923 floods. Paul and Baker (1925) also discussed the floods of 1923, but focused more on the source of sediment in the mountains. Blackwelder (1928) also referenced the 1923 sedimentation events in his classic report on the importance of "mudflows" as geologic agents.

Paul and Baker (1925, p. 14) comment on the contribution of overgrazing and "an extensive burn" on sediment yield from steep slopes in Steed Canyon southeast of Farmington. They also noted that Rudd Canyon, adjacent to the north side of Steed Canyon, was exposed to the same rainfall as Steed Canyon and Farmington Canyon; however, the canyon was protected by brush and erosion from it was insignificant (p. 17).

Four separate damaging sedimentation events occurred in Davis County and elsewhere in northern Utah during the summer of 1930 (July 10, August 11, August 13, and September 4) (Woolley, 1946, p. 111-114). On September 9, 1930, Utah Governor George H. Dern appointed a special commission to evaluate the extent and cause of the flooding problems in northern Utah. Eighteen individuals were appointed to the commission with Sylvester Q. Cannon, the former City Engineer of Salt Lake City, as Chairman. The report of the commission was submitted to Governor Dern on December 31, 1930 and published in January, 1931, as Utah State Agricultural College Agricultural Experiment Station Circular 92 (Cannon and others, 1931).

The commission concluded that the causes of the 1930 flood damage were:

1. Uncommonly heavy rainfall.
2. Steep topography and geological conditions conducive to sudden run-off and to a large quantity of flood debris.
3. Scant vegetation on portions of the watersheds of the canyons which flooded, due in some cases to the natural barrenness or semi-barrenness of the land, but in many cases such as those in Davis County, to the depletion of the natural plant growth, by overgrazing, by fire and to a small extent by over-cutting of timber. (Cannon and others, 1931, p. 16).

The commission also compared the deposits of 1923 and 1930 in Davis County to the alluvial fans at the mouths of the canyons and noted that the floods of 1923 and 1930

"mark a distinct increase increase from the normal rate of erosion and deposition of the thousands of years since Lake Bonneville receded to the present level of Great Salt Lake. In depth of cutting, in quantity of material and size of the boulders carried, these floods far exceed the normal occurrence since the recession of Lake Bonneville. The post-Bonneville alluvial deposits are small, and the quantity of material brought down and added to them by the

1923 and 1930 floods is all out of proportion to the amount brought down through the thousands of years of post-Bonneville history.... If floods had occurred at intervals of one-half century for the 30,000 or more years since the recession of Lake Bonneville, the alluvial structures would be found extending far out into the lake." (Cannon and others, 1931, p. 17).

Crawford and Thackwell (1931) observed prehistoric debris-flow deposits exposed in the eroded channel of at the mouth of Ricks Creek. They acknowledged the importance placed by earlier workers on overgrazing and fire on sediment production and flooding, but argued that these factors had been "over-stressed and that the primary factors lie in other unbalanced conditions in nature, and that these other conditions are of sufficient importance to cause intermittent floods even if the contributing causes of over grazing [sic] and forest fires did not exist" (Crawford and Thackwell, 1931, p. 100). The "unbalanced conditions" relate to uplift of the Wasatch Range along the Wasatch fault, and absence of large alluvial fans along the fault in Davis County was used by Davis (1925) as "evidence of recent, if not active, displacement along the Wasatch fault" (Crawford and Thackwell, 1931, p. 100). Woolley (1946) thought that the influence of man-induced watershed degradation may have been overstated and that, at the time of his investigation, "the relationship between physiographic and geologic features and the meteorologic phenomena involved in the storms" had not been adequately evaluated in a scientific manner (p. 5).

Several long-time residents of Davis County were interviewed as part of the present research. Mr. Bill Rigby (verbal communication, 1986 and 1987) described the sedimentation event of 1923 at Ricks Creek as a pulse of thick rocky mud that spread out from the canyon mouth and covered what is now Main Street (Utah Highway 106) in Centerville. The debris eroded the channel of Ricks Creek a few feet and destroyed an irrigation canal. The canal was replaced with a suspended pipe. That pipe was destroyed by a much larger debris flow in 1930, at which time the channel of Ricks Creek was eroded about 20 m. The erosion occurred in lacustrine sand which was flushed out of the canyon mouth as a relatively thin slurry for a distance of about 1.5 km. Mr. Rigby's home, on the north side of Ricks Creek, is underlain by lacustrine deposits, but the land on the south side of the creek contains numerous boulders which clearly were deposited as debris flows on an alluvial fan.

Mr. Rulon Ford (verbal communication, 1987) described the sediment accumulation in 1923 at the mouth of Ricks Creek as being 1.5 to 3 m high and 15 to 30 m wide where it crossed Highway 106. The channel of Ricks Creek where a wier diverted water into canals for irrigation (approximately 1 km east of Mr. Ford's house) was eroded no more than 3 m. The flood events of 1930 resulted in down cutting of the channel by 15 m or more at the position of a water diversion. Before 1923, the water was diverted by a wier in the creek into two canals. The flood of 1923 destroyed the wier and caused sufficient erosion that a pipe was required for conveying the water across the creek. The pipe was placed by men standing on the eroded channel and reaching over their heads. The floods of 1930 destroyed the pipe and caused enough erosion that the replacement pipe had to be suspended by elaborate means. The diversion pipe was not damaged in the flood events of 1983. A considerable amount of sediment that was flushed across the highway at Ricks Creek in 1930 was sand derived from erosion of the channel after the flood water had left the mountain; the 1930 sedimentation events were different from the 1923 event because the 1923 sediment contained a considerable amount of large fragments of bedrock.

Mr. Rulon Ford (verbal communication, 1987) remembered that each sedimentation event lasted approximately one-half to three-quarters of an hour. The State of Utah removed the sediment from the highway and adjacent properties following the 1923 event but following the 1930 events, it was left in place and a new highway was constructed on

the sediment. The wall in front of Mr. Ford's home was "chest high" (about 1.3 m) before 1930, but today it appears as if it were a curb (about 4 cm high) because the sediment which accumulated in 1930 was never cleared away.

Mr. Rulon Ford (verbal communication, 1987) herded cattle in the Wasatch Range from Farmington Canyon to Parrish Creek. Sheep herding in the mountains was also common. The sheep herders were known to cut brush and burn the watersheds to protect the wool on the sheep and to promote the growth of grass. Mr. Bill Rigby (verbal communication, 1986) also remembered the burning for livestock range and recalled that the City of Centerville owned nearly all of Centerville Canyon and prohibited burning or cutting in it. Damaging sedimentation events did not occur in Centerville Canyon in either 1923 or 1930.

Mr. Wesley Ford (verbal communication, 1987) recalled the flood of 1923 and four events in 1930. The 1923 sedimentation event spread "boulders and sand" 1.8 to 2.5 m thick over about half of a 0.18-km² farm on the west side of the Highway 106. The sedimentation events were very brief and moved so slowly that a man could out walk them. Only one sediment flow occurred during each event.

Mrs. Carma Jenkins (written communication, 1987) compiled excerpts from a hand-written account by LaVon Duncan of the July 1930 flood at Parrish Creek in Centerville. A threatening cloud settled above Parrish Creek and a roar could be heard coming from the canyon.

"The force of the water pushing the hugh boulders was a sight that was very frightening. Our cherry trees were washed downhill in a standing position about as fast as a pony could run. As the large boulders would hit a house or another boulder, it would cause a 10- or 15-foot wave and when it cleared, the house was gone. The houses that weren't hit by boulders filled with mud. Three homes on Parrish Lane were completely washed away leaving only the footings of the buildings. The basement of the Worsley home and the Fuller home were filled with mud which, when dry, was hard to remove." (Account by LaVon Duncan excerpted by Mrs. Carma Jenkins, 1987).

Mr. and Mrs. Leo Worsley (verbal communication, 1987) recalled the flood of 1930 at Parrish Creek in Centerville. They could hear a roaring sound coming from the canyon just before a wall of mud entered the community and filled their basement about one-quarter full of mud with out large rocks. Approximately 30 minutes to one hour elapsed from the time they first heard the roaring sound to the time sediment stopped flowing in the creek. The stream flow returned to normal within 8 to 12 hours. They commented that the events of the 1983 flood at Parrish Creek were insignificant compared to those of the 1930 flood.

Sedimentation from Rudd Creek in 1983 caused damage in Farmington (Anderson and others, 1984). A major debris flow occurred at about 6:30 p.m. on May 30, 1983, and several smaller sedimentation events occurred during the following eight days. A landslide occurred in the Rudd Creek drainage and contributed approximately 12,230 to 15,290 m³ of sediment and an unknown amount of water into the channel (Vandre, 1983, p. 2). Approximately 49,700 to 57,340 m² of sediment was deposited as a debris fan in Farmington and an additional 5,350 to 10,700 m² was deposited in a thin (< 0.3-m thick) veneer beyond the toe of the debris fan (Vandre, 1983, p. 8). The volume of sediment deposited in Farmington exceeding the volume contributed by the landslide was derived

from erosion of the channel bed and banks. The channel of Rudd Creek was eroded to bedrock (Anderson and others, 1984, p. 65).

The initial pulse of sediment in Farmington plugged the small channel of the creek on the fan and diverted subsequent pulses to the south. Four or five homes were completely destroyed, one home was pushed off of its foundation and carried approximately 30 m, and numerous homes were partially inundated with sediment (Anderson and others, 1984, p. 63). Typical views of the sedimentation in Farmington are shown in Figures 3 and 4.

Mr. Cammon Arrington (verbal communication, 1987) described the channel of Rudd Creek adjacent to his home in Farmington as being eroded to bedrock (at least 3 m) in 1983 and partially filled by less energetic sedimentation events in 1984. Several large boulders created a dam in the channel near his home which trapped smaller rocks and sediment.

A sedimentation event occurred east of Layton on May 14, 1984 in a small canyon informally named Lightning Canyon by Mr. and Mrs. Leonard Blackner (verbal communication, 1986). Aspects of this event have been described by Olson (1985), Mathewson and Santi (1987), Santi and Mathewson (1988), and Santi (1988). A very small landslide with a volume of approximately 780 m^3 occurred in a small drainage basin with an area of about 0.55 km^2 (Olson, 1985, p. 9). Erosion of the channel to bedrock provided the bulk of the sediment deposited on the alluvial fan, which has been estimated by Olson (1985, p. 18) to be approximately $8,770 \text{ m}^3$. Olson (1985, p. 18) further estimates that the total volume of mobilized sediment is about $13,880 \text{ m}^3$ with approximately 37 percent being deposited as levees or a veneer in the channel between the landslide and the alluvial fan.

Mathewson and Santi (1987, p. 256) summarize the sequence of sedimentation events as determined from interviews with local residents approximately one month after they occurred. Three pulses of sediment followed by normal streamflow comprise the sedimentation events. The initial pulse of sediment was dark brown in color because of the abundance of organic material. This pulse moved slowly once it emerged onto the alluvial fan from the confinement of the canyon, was laminar, and carried large boulders (some exceeding 3 m in maximum dimension) and an abundance of oak branches. Shortly after the first pulse stopped moving, the second pulse began. The second pulse was lighter brown, moved more quickly, was intermediate between laminar flow and turbulent flow, and did not contain large boulders or oak branches. The third pulse began shortly after the second pulse ended. It was considerably more fluid than the first two pulses; it was lighter brown, moved more quickly, was sufficiently turbulent that it splashed mud onto the walls and roofs of the structures that it passed. The quantity of sediment carried by the water gradually diminished to the point of being normal streamflow. The conditions on the Lightning Canyon fan in June, 1984, about one month after the damaging sedimentation event, are shown on Figure 5.

Prior to the sedimentation event of 1984, Lightning Canyon discharged small quantities of water only following substantial rainstorms or snowmelt. However, following the sedimentation event, the creek issuing from the canyon discharged significant quantities of water for nearly two years (Mathewson and Santi, 1987, p. 264).



Figure 3. Photograph of debris flow damage in Farmington, Utah, in 1983.



Figure 4. Photograph of transitional flow and hyperconcentrated sediment flow damage in Farmington, Utah, in 1983.



Figure 5. Photograph of sedimentation damage in Layton, Utah, in 1984.

STRATIGRAPHY

DAVIS COUNTY SAMPLE DESCRIPTIONS

Samples were collected from three alluvial fan areas in Davis County for subsequent laboratory testing. These fan areas are associated with Lightning Canyon, Rudd Creek, and Ricks Creek (Figure 1). Surface samples only were collected from the Lightning Canyon fan. These samples are identified as Lightning 1, Lightning 2, and Lightning 3. The Lightning Canyon samples were obtained from sediment deposited by an alluvial-fan flooding event in May 1984 at locations shown on Figure 6.

Samples collected at Rudd Creek were obtained from stream-bank exposures, man-made cut slopes, and hand-dug pits at locations shown on Figure 7. These samples are identified as Rudd 1 through Rudd 27 and Rudd TP-1 and TP-2. Multiple samples were collected at several Rudd Creek sample locations; these multiple samples are identified with hyphenated numbers and letters (e.g., Rudd 4-3 and Rudd 4-4a). Stratigraphic sections of the Rudd Creek sample locations are presented in Appendix B.

Samples collected at Ricks Creek were obtained from stream-bank exposures, man-made cut slopes, hand-dug pits, and test pits excavated by a hydraulic backhoe at locations shown on Figure 8. These samples are identified as Ricks 1 through Ricks 15 and Ricks TP-1 through Ricks TP-8. Multiple samples were collected at several Ricks Creek sample locations; these multiple samples are identified with hyphenated numbers. Stratigraphic sections of the Ricks Creek sample locations are presented in Appendix B.

Laboratory test results for samples collected from all three fans are presented in Appendix C.

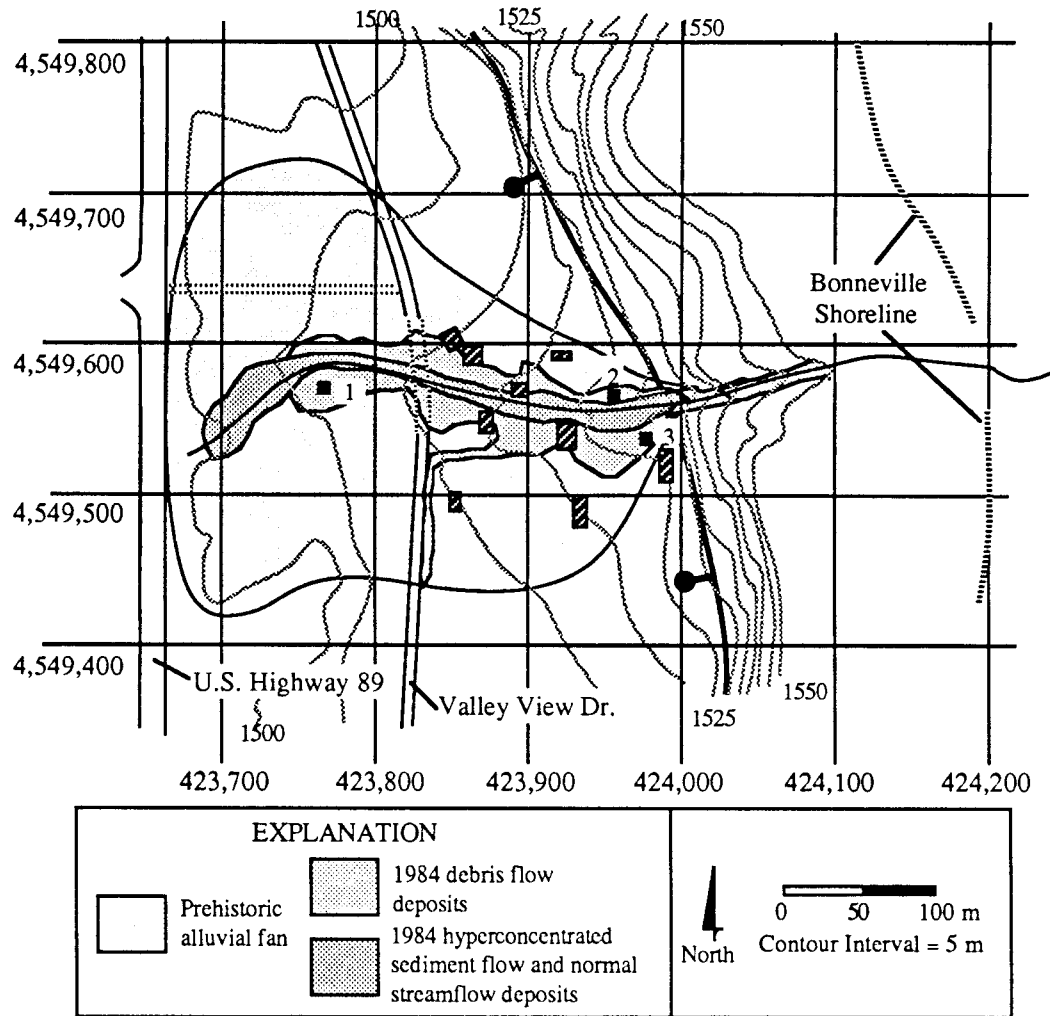


Figure 6. Map showing sample locations and selected features on the Lightning Canyon fan. Base map modified from Davis County orthotopographic map of Sec. 12, T. 4 N., R. 1 W. prepared in 1982. Sample locations are numbered squares; hachured rectangles are structures. Solid heavy line is the approximate location of the Wasatch fault. Coordinates are the Universal Transverse Mercator (UTM) zone 12 grid in meters.

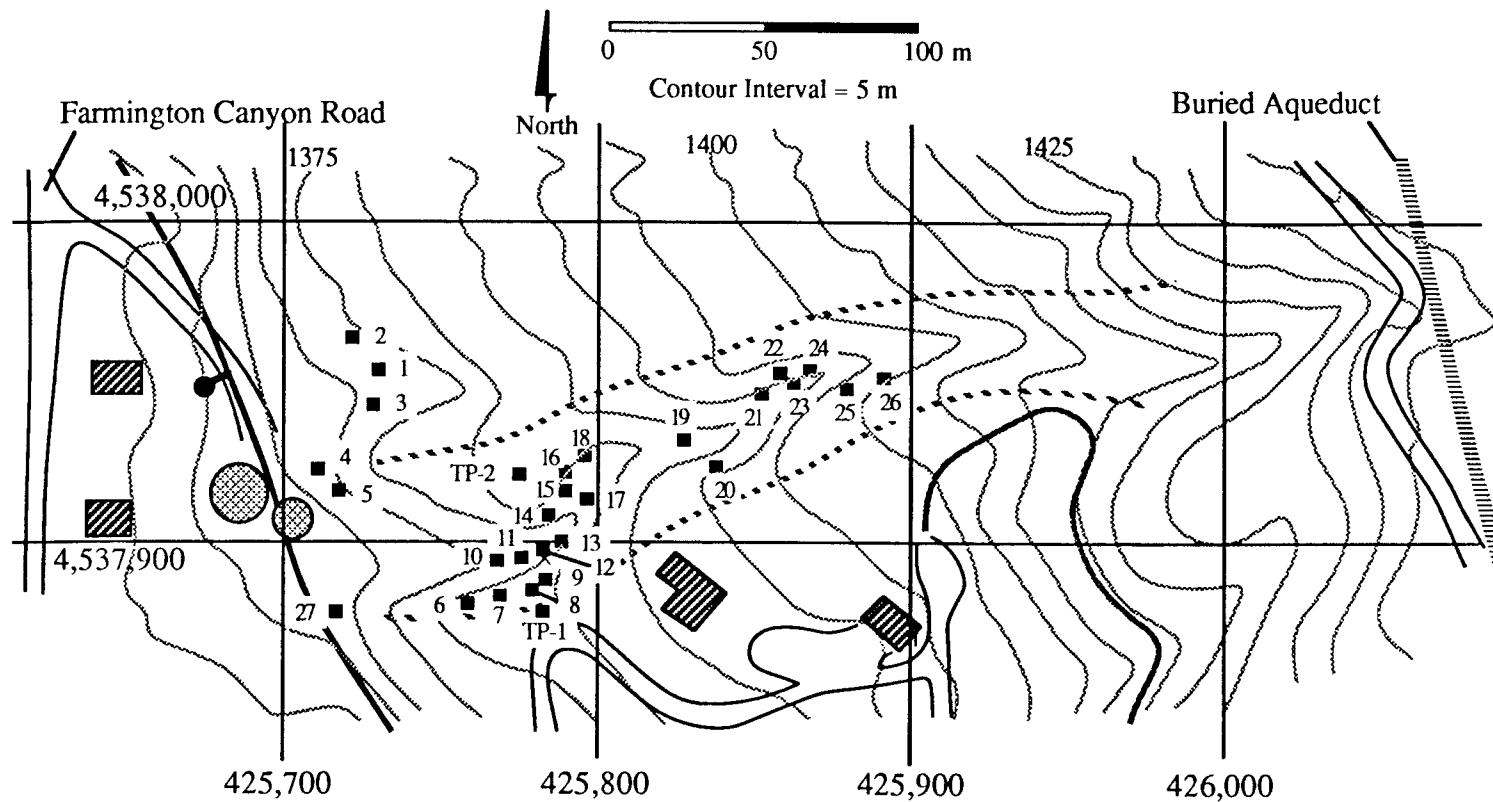


Figure 7. Map showing sample locations and selected features on the Rudd Creek fan. Base map modified from Davis County orthotopographic map of Sec. 18, T. 3 N., R. 1 E. prepared in 1982. Sample locations are numbered squares; hachured rectangles are structures; cross-hatched circles are water tanks. Crests of prehistoric debris flow levees are shown by dotted lines parallel to Rudd Creek. Solid heavy line is the approximate location of the Wasatch fault. Coordinates are the Universal Transverse Mercator (UTM) zone 12 grid in meters.

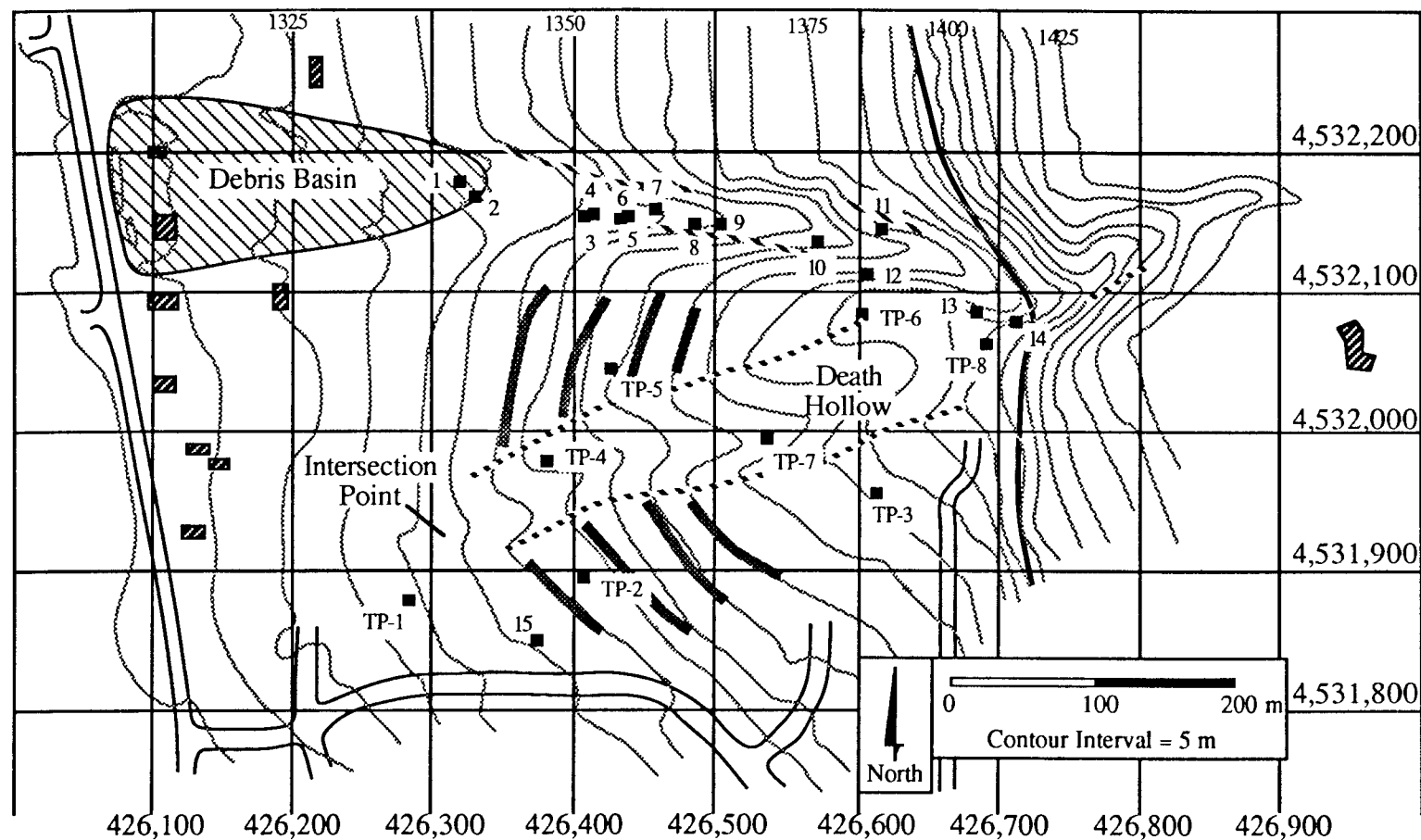


Figure 8. Map showing sample locations and selected features on the Ricks Creek fan. Base map modified from Davis County orthotopographic map of Sec. 5 and 6, T. 2 N., R. 1 E. prepared in 1982. Sample locations are numbered squares; hachured rectangles are structures. Crests of debris flow levees are shown by dotted lines parallel to Ricks Creek and Death Hollow. Shaded heavy lines are boulder fronts. Solid heavy line is the approximate location of the Wasatch fault. Coordinates are the Universal Transverse Mercator (UTM) zone 12 grid in meters.

CRITERIA FOR DIFFERENTIATION

A generalized model of alluvial fan sedimentation was developed by Spearing (1974) utilizing radial and cross-fan sections to illustrate the discontinuous and relatively chaotic nature of the streamflow and debris-flow deposits comprising a typical alluvial fan. Streamflows and debris flows are sediment-water mixtures which are components in a continuous spectrum from 100 percent sediment to 100 percent water (Figure 2). The primary basis for differentiating sediment-water mixtures traditionally has been relative, qualitative differences in style and rate of movement and on morphology and sedimentology of deposits. Pierson and Costa (1987) proposed a more quantitative classification based on mean velocity and sediment concentration of flowing sediment-water mixtures. They define the ability of the mixture to liquefy as the threshold between granular flow, in which grain support is provided by grain-to-grain contact, and slurry flow, in which grain support is provided by excess pore fluid pressure. An abrupt decrease in yield strength is the threshold between slurry flow and hyperconcentrated streamflow, in which grain support is provided by dispersive pressure. Acquisition of yield strength is the threshold between hyperconcentrated streamflow and normal (Newtonian) streamflow, in which grain support is provided by turbulence (Pierson and Costa, 1987). Pierson and Costa (1987) note that "morphology and sedimentology of flow deposits commonly can be used to deduce rheologic behavior, but caution needs to be exercised in inferring processes from deposits."

Nemec and Steel (1984) prepared a general report on alluvial and coastal conglomerates and identified some typical features of subaerial mass-flow deposits. For the condition of debris-flow material overlain by stream deposits, the basal contact of the debris flow is sharp and unchanneled indicating that it was non-erosive. A shear zone with inverse grading created by basal shearing during flow deformation may be present in the debris-flow material at the basal contact. The bulk of the debris-flow deposit is clast- to matrix-supported and ungraded with disorganized fabric and some vertical clasts. Some large clasts may protrude above the upper surface of the debris-flow deposit due to the buoyancy effect of the dense fluid. Stream deposits may bury the upper surface of the debris-flow deposits and show graded bedding created by decreasing energy of traction current.

Crude bedding may be present between deposits of individual surges of surging debris flows, and basal contacts are generally sharp and can be non-erosive to erosive, according to Nemec and Steel, 1984, p. 15). Gradational contacts may reflect waning and waxing flow energy. Such deposits may be clast- to matrix-supported. Signs of tractive current transport may be visible in between deposits of individual surges or at the top of packages of surges.

Fluidal sediment flows or turbulent streamfloods, in the terminology of Nemec and Steel (1984, p. 15), may have channelized basal contacts, sometimes with large flutes. The deposits are commonly clast-supported and exhibit crude imbrication, and crude, thick, irregular cross-stratification. The upper part of such deposits may be stratified and finer grained indicating waning flow energy.

Nemec and Steel (1984, p. 15) also consider interbedded deposits of several debris flows and stream flows. The lowest deposit in their sedimentary package is a debris flow with a basal shear zone and a non-eroded base. The basal shear zone may give the appearance of a laminated or inversely graded condition. The deposit may be matrix-supported, contain isolated megaclasts, and exhibit subhorizontal clast fabric. A non-

erosive contact separates the lower debris-flow deposit from the upper one. The upper deposit is matrix-supported and does not include megaclasts. An erosive contact separates the upper debris-flow deposit from stream flow deposits.

Four methods have been used to describe sedimentologic factors which can provide a means for distinguishing debris-flow deposits from streamflow (fluvial) deposits. These methods involve relationships between the coarsest particle size and the median particle size, between the median grain size and the quartile deviation, between the maximum particle size and bed thickness, and between the mean grain size and the sorting coefficient.

Bull (1962) used a relationship (the CM relationship) between the coarsest one percentile (d_{99}) and the median particle size (d_{50}) to distinguish debris-flow (mudflow) deposits from fluvial (stream channel) deposits. Pe and Piper (1975) modified the CM relationship to compare median grain size (M_d or D_{50}) and the quartile deviation (QDa or $[d_{75} - d_{25}] / 2$). They argued that M_d - QDa plots were of greater value than CM plots when only small samples were available because unrepresentative sampling has a substantially greater effect on the coarsest percentile value than on the quartile deviation.

Larsen and Steel (1978) expanded on Blissenbach's (1954, p. 182) and Bluck's (1967, p. 142) original observation that particle size and bed thickness decrease in a downfan direction. They compared maximum particle size (MPS) to bed thickness (BTh) and found trends that they could use to differentiate positions on fans (proximal, intermediate, distal). They defined the maximum particle size to be the arithmetic mean of the ten largest clast diameters. Subsequent work by Gloppen and Steel (1981) and Nemec and Steel (1984) indicates that subaerial and subaqueous mass-flow deposits could be distinguished by linear MPS-BTh relationships. They could find no similar linear correlation on MPS-BTh plots for deposits of fluvial origin; therefore, they suggested that linear MPS-BTh trends can be used to support the interpretation of mass-flow origins for such deposits.

Distinctions among actively moving debris flows, hyperconcentrated streamflows, normal streamflows, and flows transitional between debris flow and hyperconcentrated streamflow have been demonstrated by Pierson (1985b, p. 145) on the basis of relationships between graphic mean grain size (M_z) and graphic standard deviation (σ_G). In this application, M_z and σ_G are from Folk (1980, p. 41 and 42) and defined as:

$$M_z = (\phi_{16} + \phi_{50} + \phi_{84}) / 3 \quad (2)$$

$$\sigma_G = (\phi_{84} - \phi_{16}) / 2 \quad (3)$$

where ϕ_{16} is the size, in phi units, which 16 percent of the grains comprising the sample exceed in nominal diameter. Similarly, ϕ_{50} and ϕ_{84} are the sizes which 50 and 84 percent of the grains in a sample exceed in diameter. The phi size was defined by Krumbein (1938) as:

$$\phi = -\log_2 d \quad (4)$$

where d is grain diameter in mm. McManus (1963) redefined the phi size as

$$\phi = -\log_2 (d/d_0) \quad (5)$$

where d_0 is the unit diameter in mm. This revised definition clarifies the dimensionless aspect of phi values. The relationship between ϕ and d is presented graphically in Appendix C, along with the descriptive names of the grain size classes commonly used in

geology (the Wentworth grade scale) and in engineering (the Unified Soil Classification System).

The references pertaining to grain support and transport mechanisms, rheologic classifications, and typical features of subaerial mass-flow deposits described above (Nardin and others, 1979; Pierson and Costa, 1987; and Nemec and Steel, 1984) suggest that unique features suggestive of depositional process should be preserved in alluvial fan deposits. Key features used in Davis County to distinguish alluvial-fan deposits on the basis of stratigraphy consisted of 1) presence of graded bedding, 2) presence of grain-to-grain support for coarse clasts, 3) presence of partial matrix support for coarse clasts, 4) presence of full matrix support for coarse clasts, 5) eroded basal contact of deposit, and 6) presence of isolated megaclasts. A flow chart showing the relationships among the principal elements in a stratigraphic discrimination model is presented on Figure 9.

An ordinal *a priori* ranking was assigned to each classification (Figure 9) for use in a multivariate statistical analysis described in a subsequent section this chapter. The *a priori* ranking was found to be useful, as described below, but the understanding of general stratigraphic features of individual units was greatly enhanced by observation of the relationship with adjacent units. Geomorphic features and relationships are discussed below, but, in general, were found to provide confidence for the interpretation developed on the basis of the stratigraphy.

Field Observation

A significant field observation which was made systematically at Rudd Creek and Ricks Creek, as described below, was the nominal dimension of clasts exceeding 50 mm. Samples representative of the fraction of the sample smaller than 50 mm were collected for subsequent laboratory testing. Sample sizes ranged from about 0.8 kg for well-sorted sediments to nearly 3 kg for poorly-sorted sediments.

Laboratory Testing

Laboratory testing consisted of sieve analyses, hydrometer analyses, Atterberg Limits determinations, and experimentations with reconstituted sediment-water slurries. The results of the laboratory testing are presented in Appendix C.

Sediment Gradation

Sieve analyses were performed on virtually all samples collected from alluvial-fan deposits. Non-standard dry sieve procedures were used to develop grain size distributions because of the coarse nature of the sediments. The samples collected in the field were representative of the stratigraphic unit sampled. Rather than split the samples to obtain a representative sample of about 100 g, as described in standardized sieve procedures, all of each sample was sieved. Most samples required mechanical disaggregation of small clods; this was achieved by grinding the clods in a mortar with a pestal until only individual grains could be observed on the sieves. Standard U.S. sieves were used and subjected to a minimum of 10 minutes of mechanical sieve shaking utilizing a Soiltest sieve shaker. All but three samples had less than 5 percent finer than the #200 sieve (opening of 75 μm , 3.737 ϕ). Hydrometer analyses were performed on the three samples with more than 5 percent finer than the #200 sieve, all of which were surface samples from the 1984 sedimentation event at Lightning Canyon in Layton.

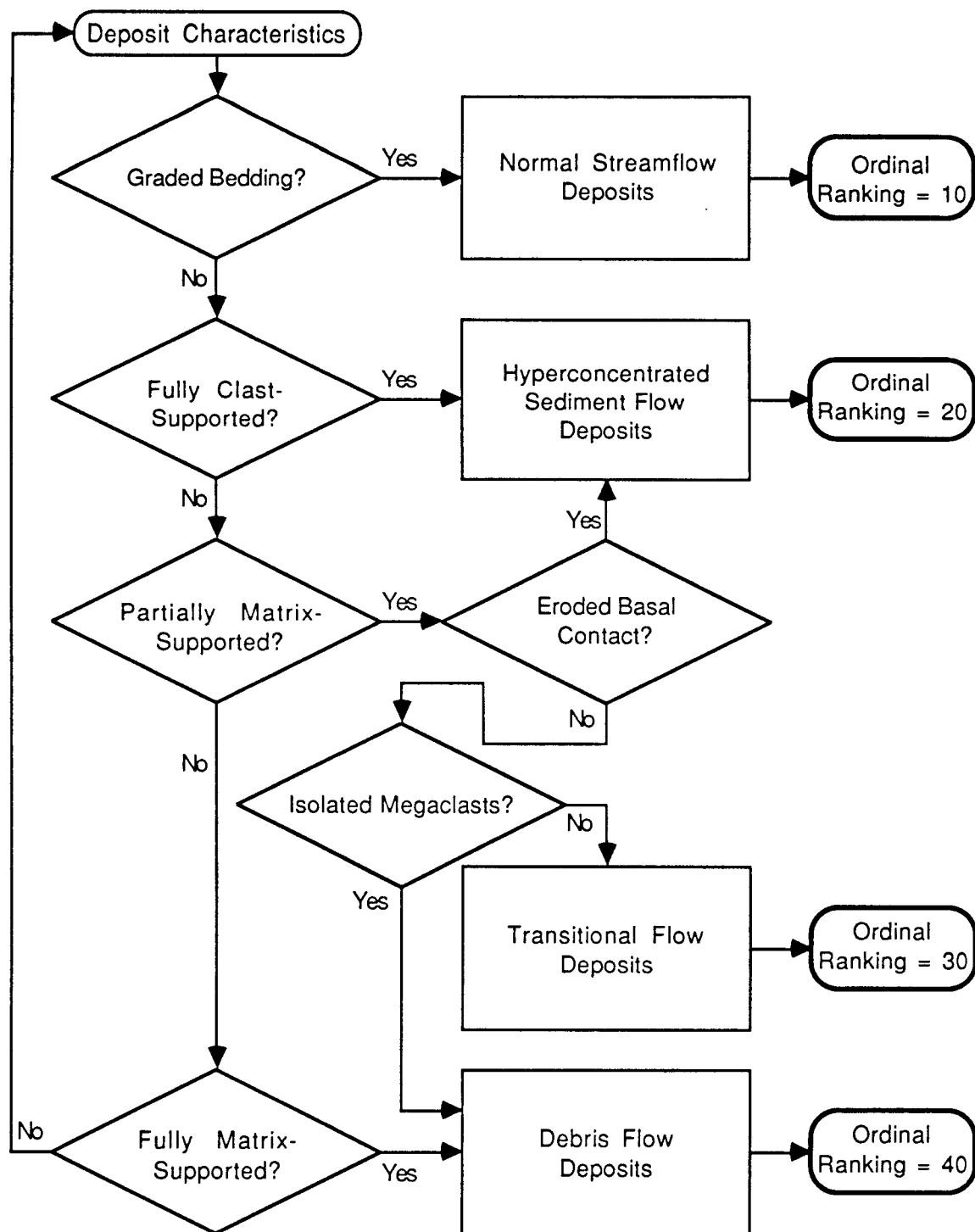


Figure 9. Stratigraphic discrimination model.

Most of the deposits of significance in this research contained clasts which exceeded 50 mm in nominal diameter; therefore, the results of laboratory sieve analyses had to be combined with field observations to develop accurate representations of the gradation of stratigraphic units. Kellerhals and Bray (1971) determined that the number-percentage of surface grains is equal to the weight percentage of a three dimensional sample if the grain sizes are randomly distributed. Williams and Guy (1973) combined pebble-count (number) percentages and sieve analysis (weight) percentages into continuous frequency distributions based on relative proportions of pebbles exceeding about 16 mm and finer sediment collected at regular spacing along a tape laid across flood-deposited sediments. At each predetermined tape station, they either measured the intermediate dimension of clasts exceeding 16 mm or collected a small amount of sediment. The clast measurements were subdivided into size classes and percentages were calculated on the basis on the total number of clasts. The small individual sediment samples were combined, blended, and split into a representative sample for sieve analysis. The percentages within subgroups were combined by multiplying each size class percentage by the ratio of the number of clasts in the size class to the total number of observations or by the ratio of the number of sediment samples to the total number of observations.

The procedure developed by Williams and Guy (1973) was modified for this research by measuring nominal areas of clasts exceeding 50 mm in a representative area of a stratigraphic unit and proportioning the clasts by the ratio of the clast area to the total representative area. A representative sample of material smaller than 50 mm was collected from within the representative area for conventional weight-percentage analysis. Combined frequency distributions were based on a two-dimensional representation of the concept of Kellerhals and Bray (1971) that the area percentage of surface grains is proportional to the weight percentage of grains in a randomly distributed three-dimensional sample if all grains have the same specific gravity.

The value of specific gravity used in all analyses is 2.65. Volumetric displacement analyses using Archimedes' principle were conducted on pebbles from 5 samples. Details of the analyses are presented in Appendix C. The results of statistical analysis of the data indicate that insufficient evidence exists to conclude that the mean values of specific gravity determined for each of the five samples differ significantly from 2.65. Therefore, a value of 2.65 was accepted as the specific gravity for all samples.

Grain size distribution curves for all samples analyzed are presented in Appendix C. These distributions show both laboratory sieve analysis data and data corrected for clasts > 50 mm based on field observations. It is clear that the shift from laboratory data to field-laboratory data is significant and can change the median grain size, for example, by several phi classes. All derived parameters used in this research which are based on grain size distributions are developed from the combined field-laboratory curves.

Atterberg Limits

The Atterberg limits consist of three values of water content of cohesive sediment-water mixtures which separate behaviors described as solid, semi-solid, plastic, and liquid. The names given to these values of water content are 1) the shrinkage limit, 2) the plastic limit, and 3) the liquid limit. These limits typically are used in the engineering classification of soils with guidelines established by the Unified Soil Classification System (American Society for Testing and Materials, 1984). The theoretical relationship between water content and sediment-water mixture volume is presented on Figure 10. The Atterberg limits separating the four behavior states are also indicated on Figure 10.

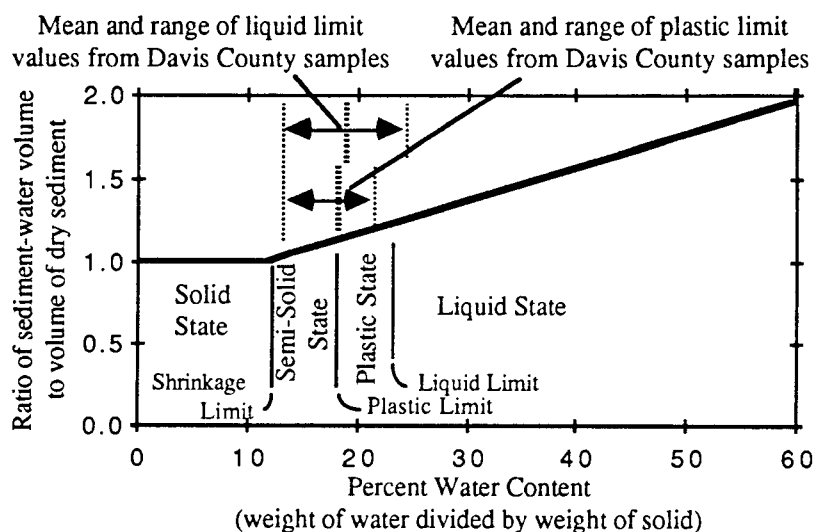


Figure 10. Theoretical relationship between water content and sediment-water mixture volume. The relationship shown is for sediment with a dry unit weight of 19.61 kN/m^3 and an initial void ratio, e_0 , of 0.325. The water content values separating the behavior states are the Atterberg Limits. Mean values and ranges are indicated for liquid limits and plastic limits determined for samples collected from Davis County.

The plastic and liquid behavior states defined by the Atterberg limits are the states of interest in differentiating debris flows from hyperconcentrated sediment flows. Consequently, these Atterberg limits were determined for most alluvial-fan samples. The results of the Atterberg limits determinations are presented in Appendix C. Standardized test procedures were followed but the liquid limit was determined even if the sediment was found to be nonplastic.

The mean values and the ranges of the plastic limit and liquid limit for the Davis County samples are plotted on the graph relating water content and sediment-water volume (Figure 10). This graph indicates that the alluvial fan sediments have a very small range of plastic behavior and that liquid behavior can occur at low values of water content. The results of a statistical analysis of the liquid limit and the plastic limit data indicate that the mean values of the two limits do not differ significantly from each other.

Slurry Experiments

Samples of alluvial-fan deposits collected at Rudd Creek and Ricks Creek were reconstituted in the laboratory after grain size distributions and Atterberg limits were determined. The procedure described by Johnson and Rodine (1984, p. 291- 292) was followed with one significant exception. Their procedure begins with sampling a representative volume of a debris-flow deposit and separating the coarse material ($> 20 \text{ mm}$) from the fine material ($< 20 \text{ mm}$). The coarse material is used to determine the

average density of the coarse clasts (2.65 g/cm^3 for the clasts from Davis County fans). Water is added to the fine material until it becomes mobile and a known volume is weighed to calculate the average density of the slurry. The equation for determining the density of a debris flow including coarse clasts was derived by Johnson and Rodine (1984, p. 292) and is:

$$\rho_d = \rho_s + [V_c/(V_c + V_f)] \cdot (\rho_c - \rho_s) \quad (6)$$

where ρ_d is the density of the flowing debris, ρ_s is the density of the slurry reconstituted in the laboratory, V_c and V_f are the volumes of coarse and fine material, respectively, and ρ_c is the density of the coarse clasts.

The procedure used in this research is based on a representative sample for which a grain size distribution has been corrected for large material ($> 50 \text{ mm}$). The sample is separated into coarse material ($> 19 \text{ mm}$, the opening size of the standard $3/4"$ sieve) and fine material ($\leq 19 \text{ mm}$). Water is mixed with the fine material until it becomes mobile and a known volume is weighed to calculate the average density of the slurry (ρ_s). The density of the coarse clasts (ρ_c) was taken to be 2.65 g/cm^3 , as described above. The value of $V_c/(V_c + V_f)$ is taken to be the weight percentage of the deposit coarser than -4.25ϕ (19 mm). Use of the weight percentage of the coarse fraction of the deposit is an appropriate representation of the volume percentage because the specific gravity was taken to be the same for both coarse and fine fractions.

The results of the slurry experiments are presented in Appendix C. A typical example of the debris-flow density calculation is shown below for a sample with a slurry density (ρ_s) of 2.074 and 57 percent coarser than -4.25ϕ :

$$\rho_d = 2.074 + [0.57] \cdot (2.65 - 2.074) = 2.402 \text{ g/cm}^3 \quad (7)$$

The results of a statistical analysis of the slurry density data indicate that the densities determined from slurries reconstituted from debris-flow deposits and transition deposits cannot be distinguished from each other but the densities determined from hyperconcentrated sediment-flow deposits differ significantly from the other two types.

Calculated and Derived Parameters

The results of laboratory tests described above were used to derive eleven parameters for consideration in a multivariate statistical analysis. Five parameters are evaluated in terms of phi classes and are based on values of cumulative percent coarser than the size indicated. In all cases, field-corrected grain size distributions were used as the bases for the derived parameters. Folk (1980, p. 41) argues that those parameters incorporating the greatest amount of the grain size distribution curve provide the best measures of the sample. For this reason, Folk (1980) suggests that the Trask sorting coefficient (S_o) and the phi quartile deviation ($QD\phi$) should no longer be used since they use only the middle 50 percent of the grain size curve. Folk (1980) has developed alternative parameters which better represent poorly sorted, coarse sediment. These parameters are mean grain size, graphic standard deviation, inclusive standard deviation, inclusive skewness, and normalized graphic kurtosis. Mean grain size and graphic standard deviation are defined by Folk (1980) and were defined in equations (2) and (3). The expression for phi in terms of grain size in mm is given in equation (4). Equations for the other parameters are given in Appendix C.

Four index parameters were derived during this research to aid in classification of the sediment. Because these parameters can range widely in value, they have been normalized by dividing the parameter by the parameter plus unity to give a theoretical range from zero to unity. Fines activity (FA) is defined as:

$$FA = LL / F \quad (8)$$

where LL is the liquid limit and F is the percentage of sediment passing the No. 200 sieve (0.075 mm). The No. 200 sieve represents the size separating coarse-grained and fine-grained soils in engineering usage (American Society for Testing and Materials, 1984) and is used in this research as fine-grained sediment. Normalized fines activity (FA') is defined as:

$$FA' = FA / (FA + 1) \quad (9)$$

Matrix activity is defined as:

$$MA = LL / M \quad (10)$$

where M is the percentage of sediment passing the No. 40 sieve (0.425 mm). The No. 40 sieve is the limit of coarse sediment used in the Atterberg limits test; therefore, it was used in this research to represent matrix sediment. This usage is reasonable because the No. 40 sieve can be related to the results of the Atterberg limits tests and probably represents a reasonable approximation of matrix in many sedimentation events on alluvial fans. Normalized matrix activity (MA') is defined as:

$$MA' = MA / (MA + 1) \quad (11)$$

The fines flow index (FF) is defined as:

$$FF = F / FI \quad (12)$$

where FI is the flow index from the Atterberg limits test (Spangler and Handy, 1982, p. 298). Normalized fines flow index (FF') is defined as:

$$FF' = FF / (FF + 1) \quad (13)$$

The matrix flow index (MF) is defined as:

$$MF = M / FI \quad (14)$$

where the terms have been described above. Normalized matrix flow index (MF') is defined as:

$$MF' = MF / (MF + 1) \quad (15)$$

The parameters described above are tabulated in Appendix C and provide comparable numerical values for use in a multivariate statistical analysis for classification of alluvial-fan deposits. The statistical analysis is described below.

Sediment Concentration

Sedimentation events on alluvial fans range from nearly 100 percent sediment (debris flow) to nearly 100 percent water (normal streamflow). Marked differences in flow behavior are associated with variations in the ratio of sediment to water (Pierson and Costa, 1987). Sediment concentration can be expressed in terms of weight (Cw) or volume (Cv):

$$Cw = Ws / W \quad (16)$$

$$= Ws / (Ws + Ww) \quad (17)$$

$$= Ws / (Ws + w Ws) \quad (18)$$

$$= 1 / (1 + w) \quad (19)$$

$$Cv = Vs / V \quad (20)$$

$$= Vs / (Vs + Vw + Va) \quad (21)$$

$$= (Ws/G) / ((Ws/G) + w Ws + Va) \quad (22)$$

where W_s is the weight of solids, W is the total weight, W_w is the weight of water, w is the gravimetric water content ($w = W_w/W_s$), V_s is the volume of solids, V is the total volume, V_w is the volume of water, V_a is the volume of air, and G is the specific gravity of solids.

Both C_w and C_v may be calculated for a range of values of w using equations (19) and (22) for given values of G and V_a , and assuming a unit total volume, V . Relationships of sediment concentration by weight and by volume are shown on Figure 11 for a specific gravity of 2.65 and 0, 5, and 10 volume percent air. Morris (1986, p. 36 - 37) reports that the transition from Newtonian water flows to non-Newtonian "debris floods" (hyperconcentrated sediment flows) occurs from $C_v < 0.04$ ($C_w < 0.11$) for flows containing highly active clays (e.g., smectite) to $C_v \geq 0.25$ ($C_w \geq 0.47$) for clay-free flows. The clay minerals in the sediments derived from the gneiss and schist comprising the Wasatch Range in Davis County are probably kaolinite derived from plagioclase and orthoclase. Furthermore, the sediments are clay-poor, with a maximum clay ($< 2 \mu\text{m}$) content of about 3 percent (Lightning Canyon debris flow samples in Appendix C). Therefore, in Davis County, the transition from Newtonian to non-Newtonian behavior should be in the higher range of reported C_v or C_w values. However, Pierson (1985b, p. 144) reports 8 percent clay (defined as $< 4 \mu\text{m}$) for a 5 June 1983 hyperconcentrated

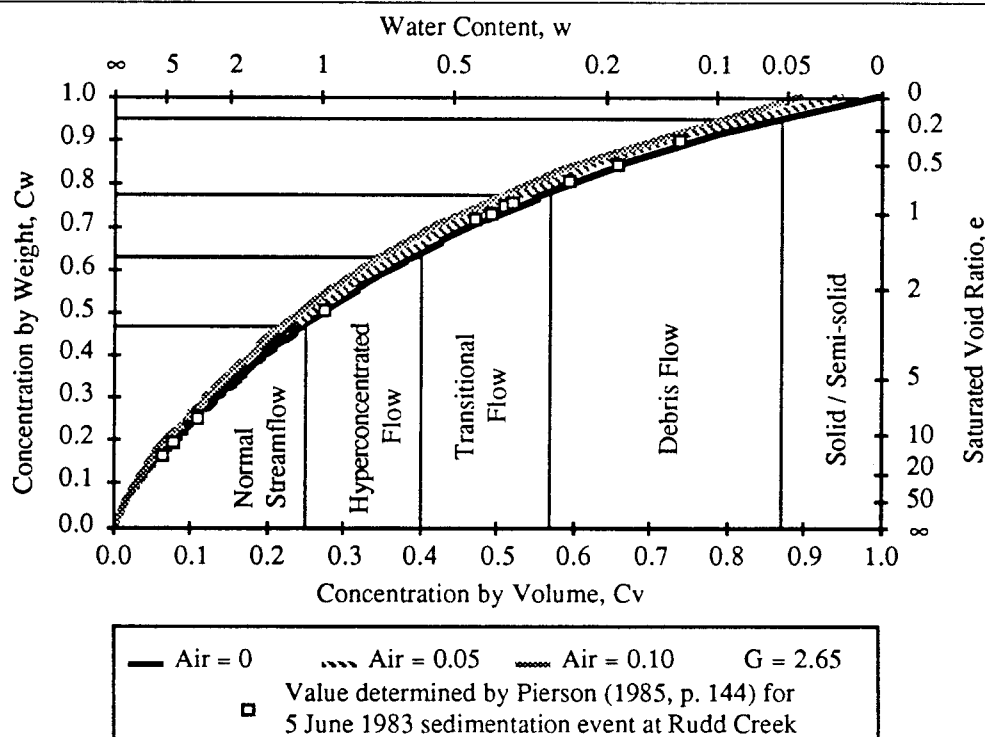


Figure 11. Theoretical relationship between sediment concentration by weight and by volume. The relationships shown are for sediment with a specific gravity of 2.65 and volumetric air contents of 0, 0.05, and 0.10. Also shown are void ratio at saturation (air content of 0) and water content. Data presented by Pierson (1985b, p. 144) for the 5 June 1983 sedimentation event at Rudd Creek are plotted within fields corresponding to observed behavior.

sediment flow at Rudd Creek and 11 to 18 percent clay for normal streamflow during the same event. Pierson's (1985b, p. 136) samples were collected by reaching out from the edge of the Rudd Creek channel and dipping 3.6-L, 95-mm wide plastic jars into flowing slurry. Pierson acknowledges the sampling bias against clasts larger than about 9 cm but argues that, except for the bouldery debris flow front and peak flow discharge, the coarsest particles were finer than 9 cm (1985b, p. 136).

Pierson (1985b, p. 144) measured sediment concentrations for normal streamflows and found that C_w ranged from 0.18 to 0.22. By specifying a unit volume and manipulating equation (19),

$$w = (1 - C_w) / C_w \quad (23)$$

$$V = 1 = V_s + V_w + V_a \quad (24)$$

$$1 - V_a = W_s / G + w W_s \quad (25)$$

Solving equation (25) for W_s :

$$W_s = G (1 - V_a) / (1 + w G) \quad (26)$$

$$C_v = W_s / G \quad (27)$$

Therefore, if Pierson sampled a saturated flow ($V_a = 0$), corresponding C_v values would range from 0.08 to 0.10. Pierson (1985, p. 144) also sampled a hyperconcentrated sediment flow at Rudd Creek and found $C_w = 0.52$ which corresponds to $C_v = 0.29$ for a saturated flow. These values are compatible with the range reported by Morris (1986, p. 37) for the transition from normal streamflow to hyperconcentrated sediment flow.

Morris (1986, p. 42) reports sediment concentrations at the transition from "debris flood" to debris flow to range from $C_v = 0.34$ ($C_w = 0.59$) to $C_v = 0.57$ ($C_w = 0.78$). Pierson (1985, p. 144) reports a range of clay ($< 4 \mu\text{m}$) from 6 to 8 percent for flow behavior at Rudd Creek which was transitional between hyperconcentrated sediment flow and debris flow. Pierson called this behavior "transitional flow" and measured C_w values ranging from 0.70 to 0.75 which correspond to C_v values ranging from 0.47 to 0.53 for a saturated flow. Pierson (1985, p. 144) reports a range of clay ($< 4 \mu\text{m}$) from 4 to 7 percent for a debris flow at Rudd Creek and measured C_w values ranging from 0.80 to 0.88 which correspond to C_v values ranging from 0.60 to 0.73. These sediment concentration values for Rudd Creek are compatible with the range of values reported by Morris (1986, p. 42) for the transition to debris flow, as shown on Figure 11. Therefore, alluvial fan sedimentation events in Davis County appear to conform in general with sediment concentration patterns exhibited in other areas. Furthermore, the clay content of samples of debris flow collected by Pierson (1985, p. 144) more closely agrees with the highest clay contents measured at Lightning Canyon (about 4 percent $< 4 \mu\text{m}$; see Appendix C).

Morris (1986, p. 47) reported sediment concentration values corresponding to a transition in behavior from debris flow to semi-solid deformation. He reports C_v values ranging from 0.66 to 0.87 corresponding to C_w values ranging from 0.84 to 0.95. Sediment concentrations were calculated from density values measured during slurry experiments reported above. The computed values are presented in Appendix C and summarized here. Air volumes ranged from 0 to 7.4 percent in reconstituted slurries consisting of particles of 19-mm maximum size, although no systematic technique was employed to control the entrained air. Johnson (1965, p. 171 - 172) measured parameters of reconstituted fine-grained debris and found air volumes ranging from 0.05 to 5.81

percent. Most calculations involving sediment concentrations described below are based on an assumed saturated condition ($V_a = 0$) which maximizes unit weight estimates.

Based on the range of sediment concentrations reported by Morris (1986) for different flow behaviors and on the sediment concentrations measured by Pierson (1985) at Rudd Creek, a suite of sediment concentration values have been identified as boundaries separating flow behaviors of sedimentation events on alluvial fans in Davis County. These boundaries are plotted on Figure 11 and summarized in Table 3. Additional selected parameters summarized in Table 3 were calculated on the basis of an assumed unit volume, saturated conditions ($V_a = 0$), and a specific gravity of 2.65. Laboratory-determined sediment concentrations calculated using the technique developed by Johnson and Rodine (1984) as described in equations (6) and (7) all fell within the range $0.66 \leq C_v \leq 0.75$ ($0.85 \leq C_w \leq 0.90$), which is within the range of debris flow samples measured by Pierson (1985b). This clustering suggests that the technique is appropriate for debris flow material only. The water contents for transitional flow, hyperconcentrated flow, and normal streamflow sediments appear to be approximately factors of 2, 4, and 8, respectively, higher than for debris flow sediments.

Table 3. Sediment concentrations and selected parameters for the range of flow behaviors of sedimentation events on alluvial fans in Davis County. C_v is sediment concentration by volume. Unit volume, saturated conditions, and a specific gravity of 2.65 were assumed for calculation of the parameters.

PARAMETER	$C_v = 1.00$	$C_v = 0.87$	$C_v = 0.57$	$C_v = 0.40$	$C_v = 0.25$	$C_v = 0$
Water Content (W_w/W_s)	0	0.056	0.285	0.566	1.132	∞
Weight of Solids (W_s) (g)	2.650	2.308	1.510	1.060	0.663	0
Weight of Water (W_w) (g)	0	0.129	0.430	0.600	0.750	1.000
Total Unit Weight (g/cm^3)	2.650	2.437	1.940	1.660	1.413	1.000
(kN/m^3)	25.98	23.89	19.02	16.28	13.85	9.805
Behavior	Semi-solid	Debris Flow	Transitional Flow	Hyperconcentrated Flow	Normal Stream Flow	

UNGRADED DEPOSITS

Ungraded deposits described in published literature relating to alluvial fans (e.g., Nemec and Steel, 1984; Lowe, 1982) and those observed in Davis County can be differentiated on the basis of clast support mechanism. Ungraded deposits can have clasts supported by the matrix of the deposit or by other clasts. In some cases, a deposit may have clasts supported by both matrix and other clasts.

Matrix-Supported Deposits

Matrix-supported deposits in this research are defined as those in which clasts 4 mm or larger are supported by smaller grain sizes. Commonly, matrix-supported deposits consist of clasts larger than 50 mm supported by a matrix of silty sand. An example of a matrix-supported deposit from Ricks Creek is shown on Figure 12. As shown on Figure 9, matrix-supported deposits were interpreted to be debris-flow sediments deposited by frictional freezing. Cohesive freezing apparently is not a significant sedimentation mechanism in Davis County because of the generally small percentage of clay-sized ($< 2 \mu\text{m}$) particles (see Appendix C).

Isolated megaclasts commonly are present in matrix-supported deposits. A megaclast in this research is defined as a clast which is larger than about 256 mm (boulder size). Isolated megaclasts are easily recognizable in a deposit because they are generally more than an order of magnitude larger than any other clasts within 2.5 clast diameters. Identification of megaclasts is subjective in the sense that it is scale-dependant; megaclasts in one deposit can be matrix in another deposit. Alluvial-fan deposits dominated by clay, such as those described by Bull (1964), might have clasts in the range of 20 mm considered to be megaclasts.

Clast-Supported Deposits

Clast-supported deposits in this research are defined as those deposits in which clasts 4 mm or larger in diameter are supported by other clasts 4 mm or larger. An example of a clast-supported deposit from Ricks Creek is shown on Figure 13. Isolated megaclasts can be present in clast-supported deposits. As shown on Figure 9, clast-supported deposits are interpreted to be hyperconcentrated sediment-flow sediments deposited by frictional freezing.

Intermediate Deposits

In many cases in Davis County, a deposit contains pockets in which the clasts are clast-supported surrounded by material which is matrix-supported. An example of such an intermediate deposit is shown on Figure 14. As indicated on Figure 9, these deposits were interpreted to be debris-flow deposits if isolated megaclasts were present (Figure 15), but they were interpreted to be transitional deposits if isolated megaclasts were absent and the basal contact was uneroded (Figure 16). Alternatively, these deposits were interpreted to be hyperconcentrated sediment-flow deposits if the basal contact was eroded (Figure 17).



Figure 12. Photograph of matrix-supported debris flow deposit.

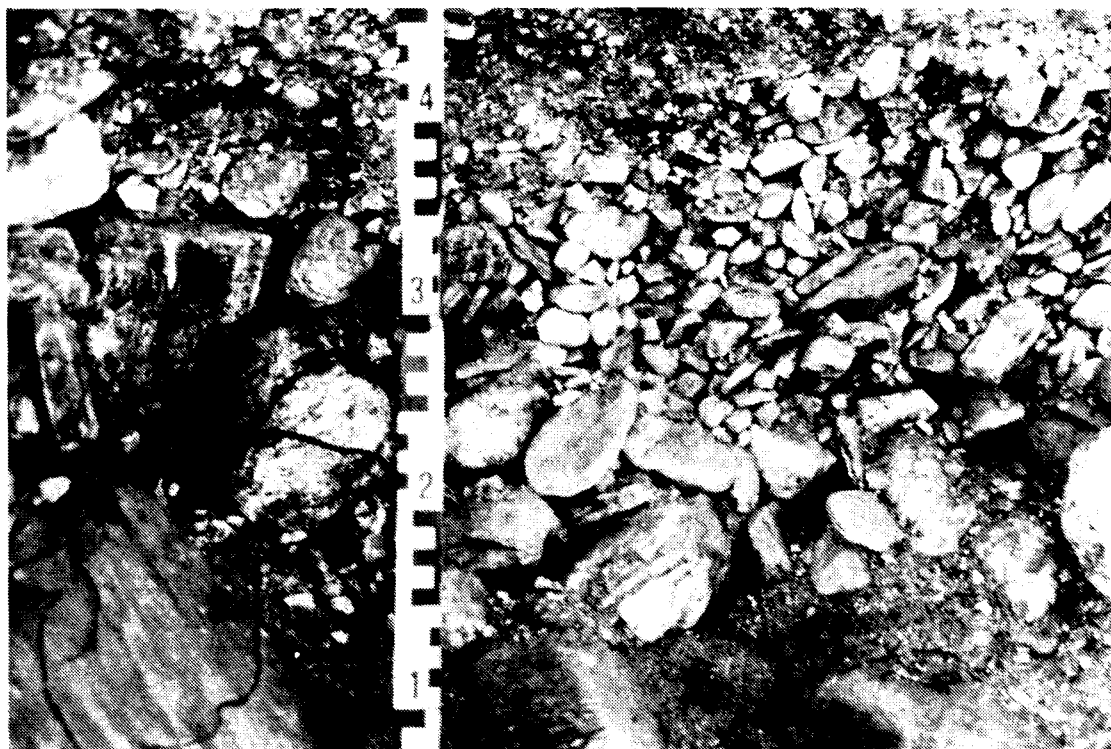


Figure 13. Photograph of clast-supported hyperconcentrated sediment flow deposit.

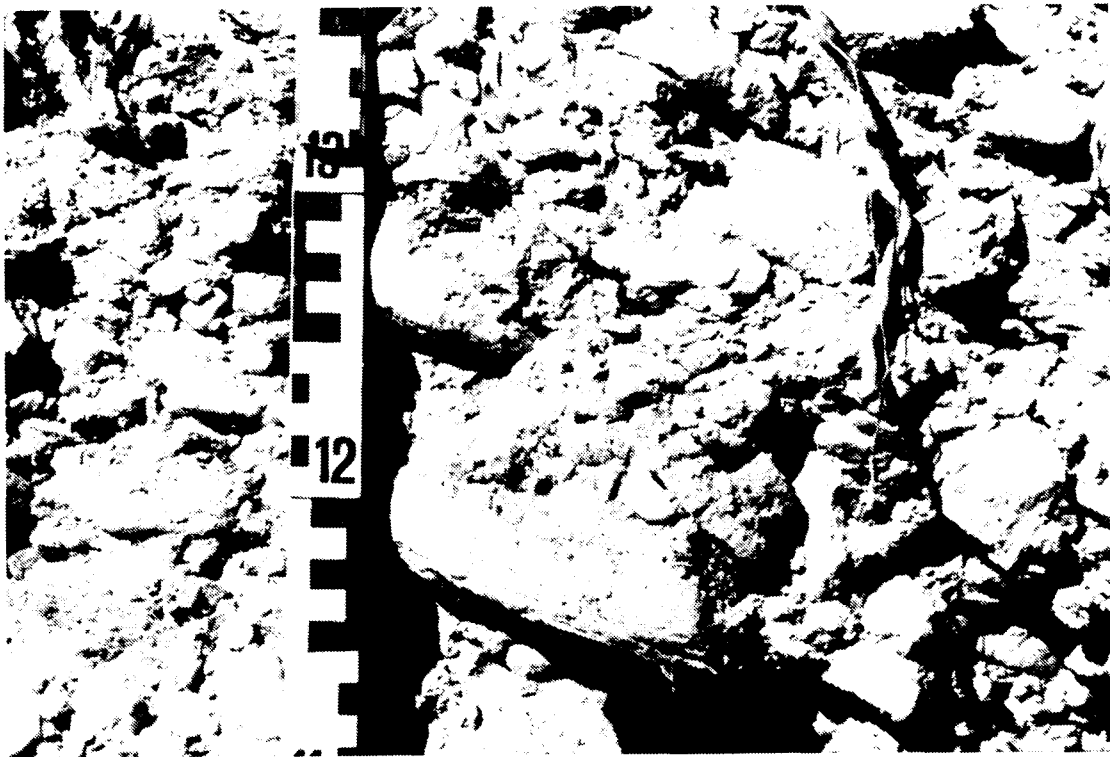


Figure 14. Photograph of matrix- to clast-supported transitional flow deposit.

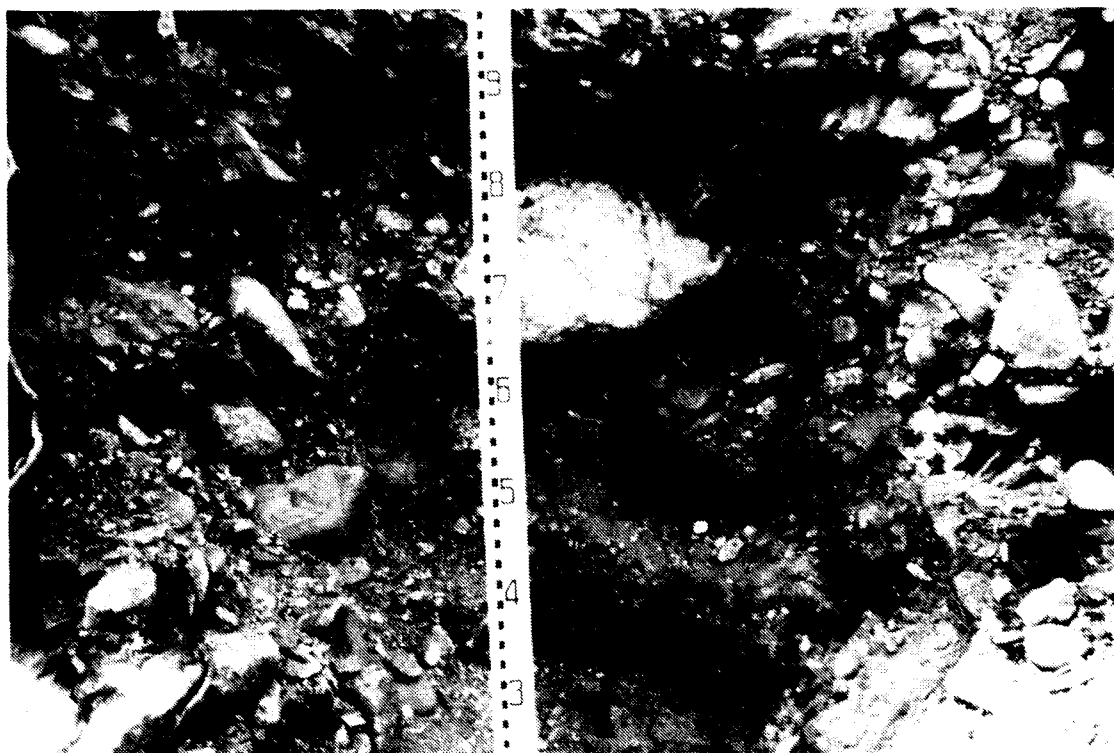


Figure 15. Photograph of an isolated megacryst.



Figure 16. Photograph of an uneroded basal contact.

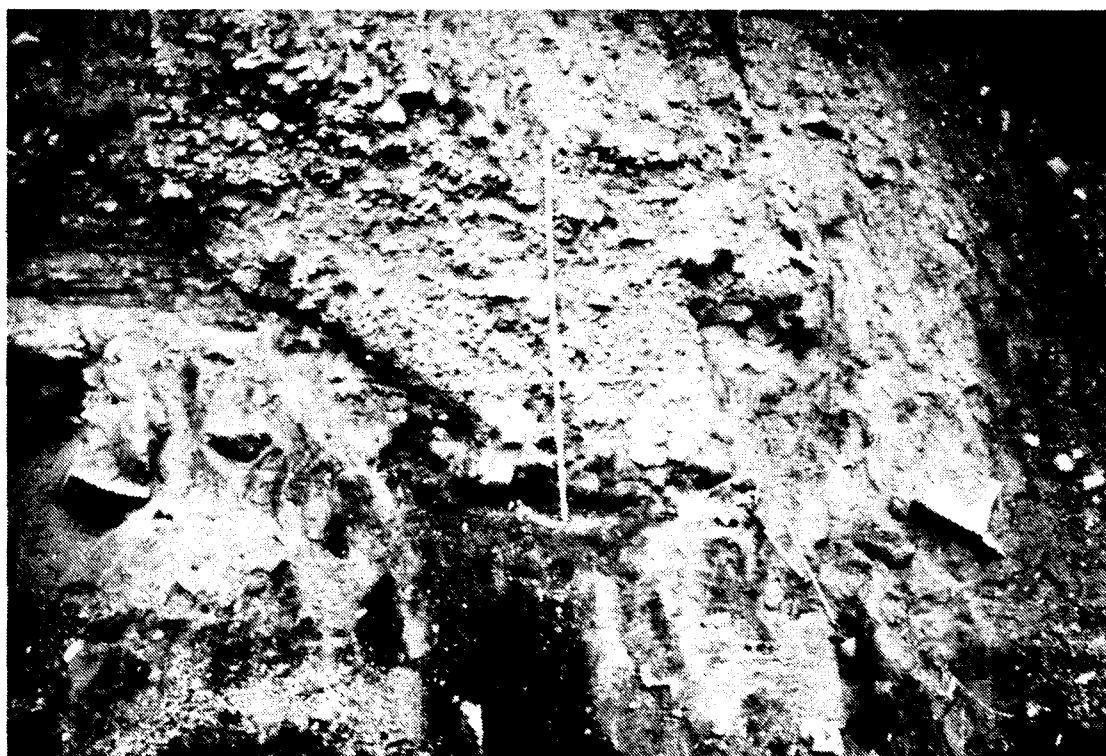


Figure 17. Photograph of an eroded basal contact.

GRADED DEPOSITS

Graded deposits described in published literature on alluvial fans (e.g., Heward, 1978; Lowe, 1982) can have progressively finer grain sizes higher in the deposit (fining upward) or progressively coarser sizes higher in the deposit (coarsening upward). Deposits exhibiting a fining upward character and those exhibiting a coarsening upward character were observed in Davis County.

Fining Upward Deposits

Fining upward deposits observed in Davis County appeared to be confined to channels cut into ungraded alluvial-fan deposits or underlying lacustrine deposits. An example of a fining upward deposit is shown on Figure 18. As indicated on Figure 9, fining upward deposits were interpreted to be fluvial or normal streamflow sediments deposited by traction or suspension sedimentation. Fining upward lacustrine deposits appeared to be restricted to thin zones within beach facies.

Coarsening Upward Deposits

Coarsening upward deposits observed in Davis County appeared to be confined to isolated, minor locations within otherwise ungraded alluvial-fan deposits or underlying lacustrine deposits. These deposits chiefly represent delta front sediments deposited in Lake Bonneville. These deposits are significant only on the scale of entire alluvial fans. As alluvial fans build out from mountain fronts, relatively coarse-grained sediments bury finer sediments. Initially, the alluvial-fan deposits bury lake-bottom sediments of Lake Bonneville. Subsequently, coarser, proximal alluvial-fan deposits bury finer, distal alluvial-fan deposits in a manner described by Heward (1978, p. 685 - 687).

IDEAL STRATIGRAPHIC SEQUENCE

The model of ideal alluvial-fan stratigraphy presented below is based on published eyewitness accounts of alluvial-fan processes and deposits described above. The ideal stratigraphic sequence on alluvial fans can be compared to the traditional ideal Bouma turbidite sequence consisting of five facies (Figure 19). Berg (1986, p. 403 -405) demonstrates that the commonly observed turbidite sequences are incomplete at any particular location and can be used to identify position on submarine fans by recognizing which facies are present or absent and by their relative thicknesses. Similarly, all facies of the ideal alluvial-fan sequence need not be present at any particular location.

The ideal alluvial-fan stratigraphic sequence consists of four units which are comparable with observed temporal sequences of alluvial fan sedimentation described above and typical features of mass-flow deposits described by Nemec and Steel (1984, p. 15). The ideal temporal sequence begins with an initial plastic debris flow (Unit 1), followed by a viscous flow transitional between debris flow and hyperconcentrated sediment flow (Unit 2), followed by a liquid hyperconcentrated sediment flow (Unit 3), and completed by a fluid streamflow with a decreasing sediment load (Unit 4). These four facies are shown diagrammatically on Figure 19. Unit 1 deposits are matrix-supported, ungraded, unsorted, with disorganized fabric and isolated megaclasts. Unit 2 deposits are matrix- to clast-supported and may exhibit crude depositional fabric. Unit 3 deposits are clast-supported and exhibit crude imbrication and may have irregular cross-stratification.

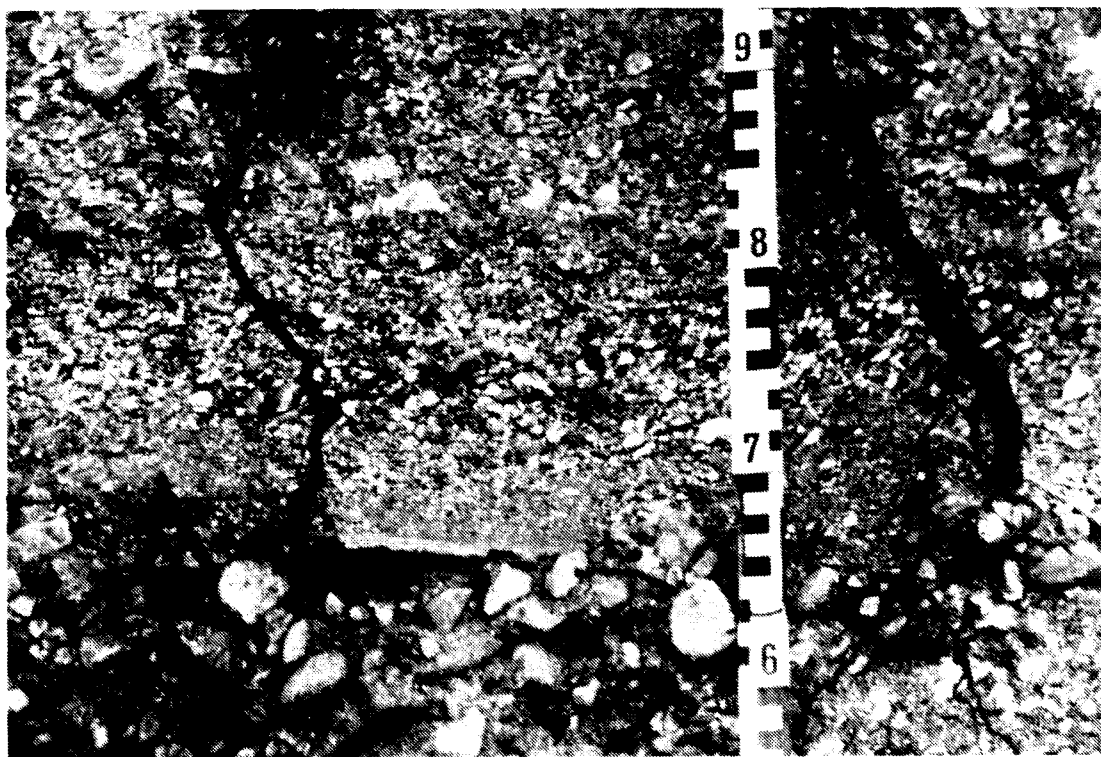


Figure 18. Photograph of a graded, fining upward streamflow deposit.

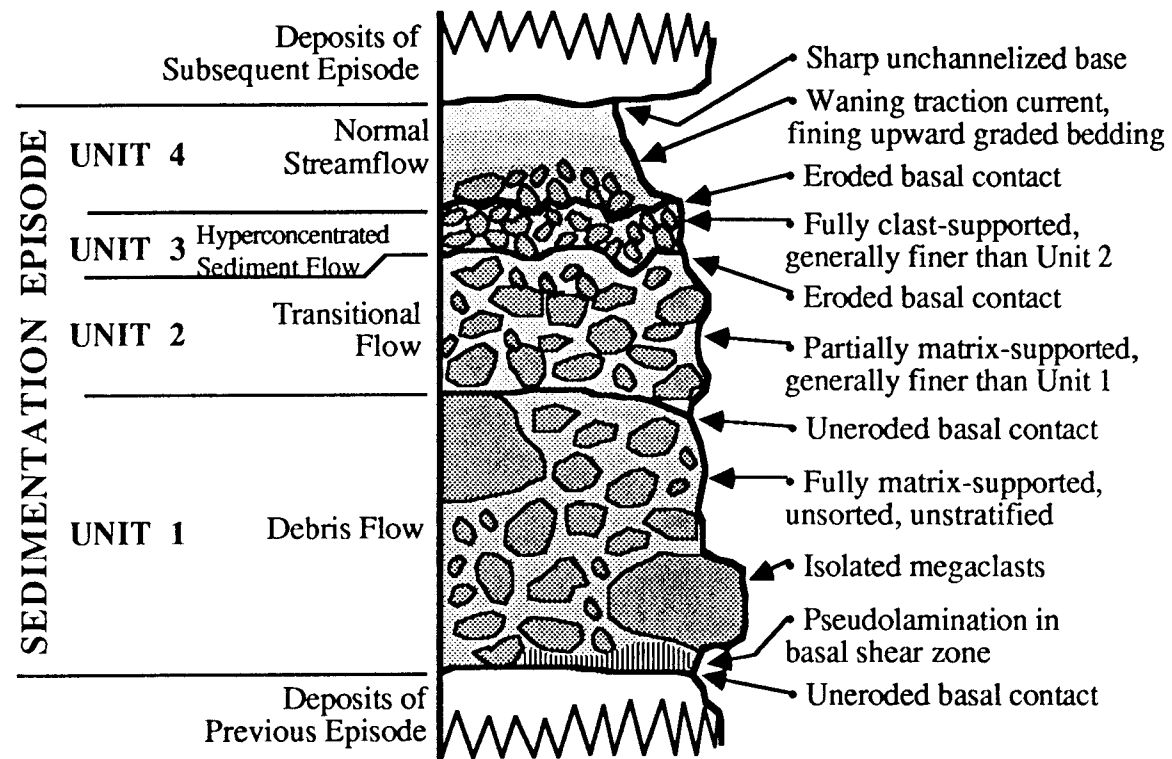


Figure 19. Ideal alluvial - fan stratigraphic sequence showing features of the characteristic depositional units.

Unit 4 deposits are normal streamflow deposits which are clast-supported and exhibit graded bedding.

The basal contact of a Unit 1 deposit is uneroded because the deposit behaves as a non-Newtonian plastic and sediment concentrations are so high that the flowing unchanneled debris cannot entrain additional sediment. Unit 2 deposits are transitional between debris flows and hyperconcentrated sediment flows and can have uneroded or eroded basal contacts. Unit 3 deposits have eroded basal contacts because the material has sufficient velocity to scour into the previously deposited debris and sediment concentrations are low enough that additional sediment can be entrained. Unit 4 deposits can be originally deposited sediment or reworked from Units 1, 2, and/or 3.

Not all units need be present in an individual sedimentary package at any particular site, and extrinsic factors affecting fan sedimentation (e.g., tectonic adjustments, climate) contribute to overall fining upward or coarsening upward megasequences. Episodes of sedimentation under ideal conditions comprise individual flow events which begin with Unit 1, change gradationally, and end with Unit 4. Unit 4 processes probably persist for the longest periods of any of the processes contributing to ideal fan stratigraphy. Normal streamflow may dominate alluvial fan environments for a number of years, decades, or longer, between major sedimentation events which include deposition of Unit 1, 2, and/or 3 sediments.

PREDICTIVE MODEL

Deterministic approaches to predictive modeling are based on the premise that knowledge of physical laws controlling natural systems allows prediction of exact system behavior (Knighton, 1984, p. 5). Natural systems are so complex that deterministic explanations are unattainable even if individual components comprising the systems may be explained in deterministic terms. Furthermore, all systems inevitably are parts of larger systems from which they cannot be separated (Shreve, 1975, p. 529). A number of researchers have claimed that randomness is an inherent property of natural systems (e.g., Leopold and Maddock, 1953; Langbein and Leopold, 1964). Probabilistic approaches to predictive modeling incorporate apparent randomness of natural systems and allow prediction of approximate system behavior and "reflect the world as it is, not as we would like it to be" (Shreve, 1975, p. 529).

Consequently, a probabilistic approach was attempted as part of this research. Parameters determined from laboratory testing and derived from test results were analyzed with a multivariate statistical method using a commercial program (StatView by BrainPower, Inc.) on a Macintosh 512K personal computer. The *a priori* ordinal ranking values were taken as the dependent variable; parameters considered as independent variables are listed in Table 4. Those samples ranked with the greatest confidence were used to develop the predictive equation. Fourteen samples were chosen: Six Unit 1 samples, four Unit 2 samples, two Unit 3 samples, and two Unit 4 samples. The best predictive equation was considered to be the one with the highest coefficient of determination and lowest standard error and was developed with six of the independent variables listed in Table 4:

$$\text{AFP} = 31.70 - 2.53 M_Z + 6.22 \sigma_I - 38.11 K_G' - 31.42 (Sk_I)^2 + 53.98 FF' - 42.46 MF', (r^2 = 0.997, n = 14) \quad (28)$$

where AFP is predicted alluvial fan process in terms of *a priori* ordinal ranking and the other terms are identified in Table 4. The coefficient of determination (r^2) indicates that

99.7 percent of the variability in AFP is explained by the variability in the six independent variables. All samples were classified using equation (28) and compared to the *a priori* ordinal ranking, as shown in Table 5 and on Figure 20. The APF values of 29 of the 35 samples (83 percent) were classified within ± 5 of their *a priori* values and were considered to be classified correctly. The remaining 6 samples (17 percent) were misclassified. The results of the comparison of APF and *a priori* ordinal ranking values suggest that samples of alluvial-fan deposits can be classified with reasonable confidence on the basis of relatively simple laboratory testing. Knowledge of dominant process is a necessary part of hazard evaluation.

The *a priori* and computed values of clast support mechanism were evaluated statistically with a commercially available program (StatView by BrainPower) on a Macintosh SE personal computer. The summary of this statistical analysis (Table 6) indicates that the probability that mean value of the *a priori* ordinal rankings and the mean value of the computed values is in the 75 to 80 percent range. Reasonable probabilities are also indicated that the computed values are equal to the *a priori* values for ordinal rankings of 40, 30, and 10. The analysis for an ordinal ranking of 20 has the poorest probability that the computed value mean is equal to 20.

Table 4. Parameters considered as independent variables in a multivariate statistical analysis. The purpose of the analysis was to predict alluvial fan process identified by *a priori* ordinal ranking values.

Parameter Name	Symbol	Parameter Type	Reference
Mean Grain Size	M_Z	Derived	Folk (1980)
Graphic Standard Deviation	σ_G	Derived	Folk (1980)
Inclusive Standard Deviation	σ_I	Derived	Folk (1980)
Inclusive Graphic Skewness	Sk_I	Derived	Folk (1980)
Normalized Graphic Kurtosis	K_G'	Derived	Folk (1980)
Coefficient of Uniformity	C_U	Derived	ASTM (1984) ¹
Coefficient of Curvature	C_C	Derived	ASTM (1984) ¹
Liquid Limit	LL	Measured	ASTM (1984) ¹
Plastic Limit	PL	Measured	ASTM (1984) ¹
Percent Passing No. 200 Sieve	F	Measured	ASTM (1984) ¹
Normalized Fines Activity	FA'	Derived	This Report
Normalized Matrix Activity	MA'	Derived	This Report
Normalized Fines Flow Index	FF'	Derived	This Report
Normalized Matrix Flow Index	MF'	Derived	This Report

¹ American Society for Testing and Materials (1984)

Table 5. Summary of *a priori* ranking and computed factors of clast support mechanism.

Sample Identification	<i>A Prori</i> Ranking	Computed Value Rounded to Integer	Sample Used To Develop Regression Equation	Classified Within ± 5
<u>Lightning Canyon:</u>				
Sample 1	40	40	Yes	Yes
Sample 2	40	41	No	Yes
Sample 3	40	37	No	Yes
<u>Rudd Creek:</u>				
Sample 1-1	0 (a)	-1	No	-- (b)
Sample 1-3	0 (a)	16	No	-- (b)
Sample 1-4	0 (a)	5	No	-- (b)
Sample 1-5	40	45	No	Yes
Sample 1-6	30	30	No	Yes
Sample 1-7	30	21	No	No
Sample 3-1	20	20	No	Yes
Sample 3-2	10	11	Yes	Yes
Sample 3-3	20	23	No	Yes
Sample 3-4	40	13	No	No
Sample 4-1	0 (a)	-5	No	-- (b)
Sample 4-2	30	28	No	Yes
Sample 4-3	40	40	Yes	Yes
Sample 4-4A	20	20	Yes	Yes
Sample 4-4B	20	25	No	Yes
Sample 4-5	10	12	No	Yes
Sample 4-6	30	36	No	No
Sample 4-7	10	23	No	No
Sample 4-8	40	39	Yes	Yes
Sample 6-1	0 (a)	14	No	-- (b)
Sample 6-2	40	40	Yes	Yes
Sample 17	30	31	Yes	Yes
Sample 18	30	30	Yes	Yes
Sample 20	40	40	Yes	Yes
Sample 22-1	10	9	Yes	Yes
Sample 22-2	30	32	No	Yes
Sample 23	40	40	Yes	Yes
Sample 25	20	21	No	Yes
<u>Ricks Creek:</u>				
Sample 6	30	28	No	Yes
Sample 7-1	30	34	No	Yes
Sample 7-2	30	15	No	No
Sample 10-1	30	29	Yes	Yes
Sample 10-2	20	20	Yes	Yes
Sample 12	40	37	No	Yes
Sample 13	30	25	No	Yes
Sample 14	30	29	Yes	Yes
Sample 15	20	23	No	Yes
Samples used/evaluated with regression = 35				Correct = 30 (85.7%)
Samples used to develop regression = 14				Incorrect = 5 (14.3%)
Samples not used to develop regression = 21				

(a) Ordinal ranking of 0 was used to designate samples of lacustrine deposits.

(b) Lacustrine samples were not used to evaluate the success of the regression equation prediction.

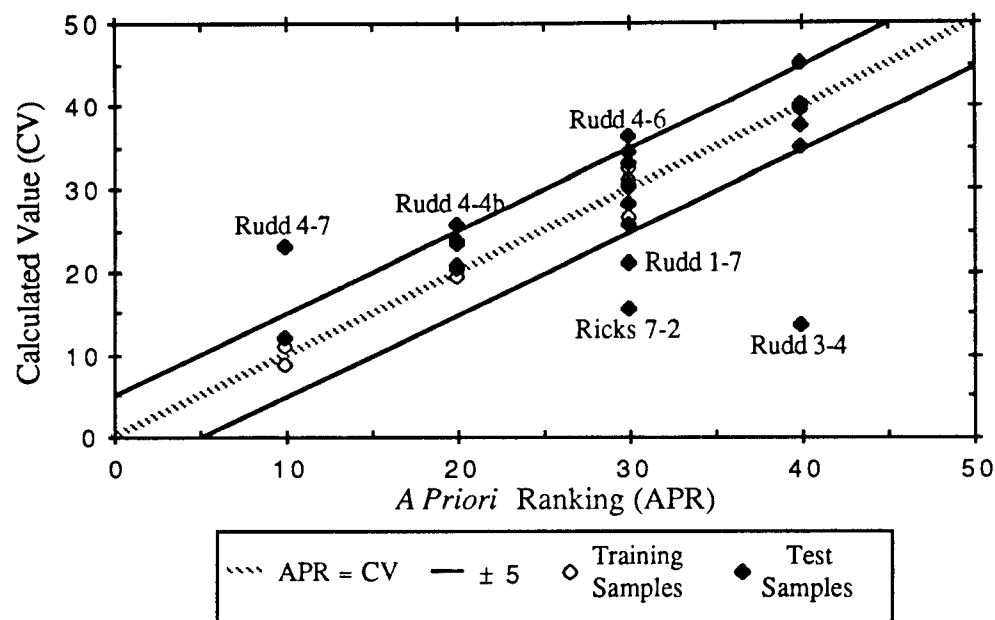


Figure 20. Comparison of *a priori* ordinal ranking with calculated values. Values were calculated using equation (28). Samples indicated exhibit calculated values which deviate by 5 or more from the *a priori* value.

Table 6. Summary of statistical analysis of computed factors of clast support mechanism.

Parameter	<i>A Priori</i> All Samples	Computed All Samples	<i>A Priori</i> 40	<i>A Priori</i> 30	<i>A Priori</i> 20	<i>A Priori</i> 10
Mean	28.857	28.200	37.454	28.301	21.714	13.750
Standard Deviation	9.932	9.818	8.383	5.483	1.976	6.291
Number	35	35	11	13	7	4
Null Hypothesis	Test Statistic		Degrees of Freedom		Probability Null Hypothesis is True	
<i>A Priori</i> mean = Computed mean	t = 0.278		68		0.75 < p ≤ 0.80	
Computed mean for <i>A Priori</i> 40 = 40	t = -1.007		10		0.20 < p ≤ 0.75	
Computed mean for <i>A Priori</i> 30 = 30	t = -1.113		12		0.20 < p ≤ 0.75	
Computed mean for <i>A Priori</i> 20 = 20	t = 2.295		6		0.05 < p ≤ 0.10	
Computed mean for <i>A Priori</i> 10 = 10	t = 1.192		3		0.20 < p ≤ 0.75	

GEOMORPHOLOGY

DAVIS COUNTY LANDFORM HIERARCHY

The geomorphology of the Davis County area is dominated by the north-trending ridge of the Wasatch Range, benches eroded into the mountain front by Lake Bonneville, and topographic scarps created by traces of the Wasatch fault zone. Chorley and others (1984, p. 15) suggested a taxonomic approach to landform evaluation based on a systematic ten-fold spatial ordering of geomorphic phenomena. They acknowledge that both morphogenetic and morphometric phenomena are combined in their hierarchical ordering, but suggest that systematic classification tends to generate the best information. The hierarchical spatial ordering of landforms in Davis County is presented in Table 7. Morphologic features of Orders 5 through 10 are the focus of this dissertation. The stratigraphic and sedimentologic aspects (Orders 9 and 10) were presented in the preceding section of this chapter.

Geomorphic systems consist of processes and landforms which function individually and interact jointly (Chorley and others, 1984, p. 5). The development of geomorphic systems is a function of the mass and energy entering, transferring, and leaving the system. Schumm (1977) developed this concept in the context of an ideal

Table 7. Hierarchical spatial ordering of landforms in Davis County. This ordering is based on the classification system of Chorley and others (1984, p. 15).

Order	Geomorphic Features
1	West-central part of the North American Continent; west-central part of the North American lithospheric plate (Strahler and Strahler, 1984, p. 231).
2	Straddles the Wasatch fault zone, which is the boundary separating the Basin and Range Physiographic Province on the west from the Middle Rocky Mountains Physiographic Province on the east (Dohrenwend, 1987, p. 304; Madole and others, 1987, p. 212). Davis County is situated on the western base of the Wasatch Range and near the eastern limit of the Bonneville Basin (Dohrenwend, 1987, p. 304).
3	Davis County segment of the Wasatch Range; Weber segment of the Wasatch fault zone (Machette and others, 1987, p. A15); terrain comprised of rocks of the Precambrian Farmington Canyon metamorphic complex (Bryant, 1984).
4	Shorelines of Lake Bonneville (Currey and Oviatt, 1985); scarps of the Weber segment of the Wasatch fault zone (Machette and others, 1987).
5	22 individual drainage basins; 22 alluvial fans.
6	Nested alluvial fans; fan-head trenches; 2nd- to 5th-order streams in basins.
7	Individual hillslopes and channels eroded into alluvial fans and lake deposits.
8	Levees and boulder fronts on individual alluvial fans; exposures in stream cuts.
9	Individual boulders on levees and boulder fronts; stratigraphy of exposures.
10	Relief on individual boulders; sedimentology of morphostratigraphic units.

fluvial system. The components of Schumm's fluvial system consist of Zone 1, the drainage basin, where energy enters the system and sediment is produced; Zone 2, the stream channel, where sediment is transferred and potential energy is converted to kinetic energy; Zone 3, the piedmont, where sediment is deposited and potential energy is depleted. In Davis County, the drainage basins are sufficiently close to the local base level that the geomorphic system chiefly is composed of drainage basins (Zone 1) and alluvial fans (Zone 3) with very little stream channel (Zone 2) between.

MOUNTAIN FRONT CHARACTERISTICS

The western base of the Wasatch Range in Davis County is relatively linear, indicating that tectonic uplift is exceeding the rate at which stream erosion is destroying the straightness of the mountain front. Mountain front sinuosity, as a geomorphic index of tectonic activity, was developed by Bull and McFadden (1977). They defined mountain front sinuosity, S_{mf} , as

$$S_{mf} = L_{mf} / L_{sl} \quad (29)$$

where L_{mf} is the length of the mountain front, including all deviations created by streams, and L_{sl} is the straight line length of the same segment of mountain front. The 1600-m contour taken from the 1:100,000 topographic quadrangles was selected as representative of the mountain front because it is about 15 m above the Bonneville Shoreline of Lake Bonneville; hence minor deviations of the contour would not be buried by youthful sediments. Using the 1:100,000-scale maps, and incorporating all crenulations of the 1600-m contour, a length of 31.9 km was obtained across the study area. The straight line distance for this segment of the mountain front is 25.5 km, resulting in a sinuosity factor of 1.251.

The length of an irregular line, such as a topographic contour line, is scale-dependent, as demonstrated by Mandelbrot (1967) in his answer to the question, "How long is the coast of Britain?" Mandelbrot discovered that the length of a line was a function of the increments in which it was measured; few, long increments and many, short increments were required to measure a line. Mandelbrot further discovered that the relationship was a power function in the form

$$TL = N \cdot L^{FD} \quad (30)$$

where TL is the total length of the line, L is the increment length, N is the number of increments, and FD is an exponent. This function can be normalized by setting $TL = 1$, thus

$$N = L^{-FD} \quad (31)$$

Mandelbrot defined FD as the fractal dimension of a line. A perfectly straight line will have a fractal dimension of 1.000, while a line so irregular that it fills a two-dimensional area will have a fractal dimension of 2.000.

The Davis County mountain front, represented by the 1600-m contour at a scale of 1:100,000, was measured in increments ranging from 0.1 to 25 km. Linear regression analysis of these data using $\log N$ as the dependent variable and $\log L$ as the independent variable yields

$$N = 27.39 L^{-1.069}, (r^2 = 0.998, n = 7) \quad (32)$$

Hence, the fractal dimension of the Davis County mountain front is 1.069.

Another measure of the linearity is the coefficient of determination (r^2) calculated from linear regression analysis of the geographic coordinates of the mountain front. The linear regression of the 1600-m contour data was developed by measuring the easting of the

1600-m contour in Universal Transverse Mercator (UTM) coordinate values in km for each 1-km increment in a north direction. The regression equation obtained was

$$\text{East} = 1274.941 - 0.187 \text{ North}, (r^2 = 0.912, n = 26) \quad (33)$$

where East is easting and North is northing, both in UTM coordinates expressed as km. The coefficient of determination indicates that 91.2 percent of the variability in the easting is explained by the variability in the northing. The slope coefficient in the regression equation indicates a mountain-front trend of $\tan^{-1} (-0.187) \approx N 10.6^\circ W$.

DRAINAGE BASINS

The study area comprises 22 drainage basins, as shown on Figure 1; selected morphometric data and parameters regarding these basins are presented in Appendix D. These traditional geomorphic parameters were developed for the drainage basins in the study area to provide a means for comparing the study area to other areas where aspects of sedimentation have been published. The drainage basins range in order from 2 to 5, as shown in Appendix D. The stream order system developed by Strahler (1952) was used to classify the basins in Davis County. Basin area, A_b , was determined by planimetry of basin outlines on conventional U.S. Geological Survey topographic quadrangles at a scale of 1:24,000; measurements were made using a Numonics Corp. Model 1224 Electronics Graphic Calculator.

Basin length, L_b , was measured on topographic quadrangles as the horizontal distance from the basin mouth to the most distant point on the basin divide; in most cases, the most distant point was also the highest point. The basin length ratio, L_r , is a dimensionless parameter defined as

$$L_r = L_b / L_d \quad (34)$$

where L_b is the basin length and L_d is the length from the basin mouth to the principal divide of the Wasatch Range measured in the same direction as basin length. Those basins which do not extend to the principal divide were called "half canyons" by Wieczorek and others (1983, p. 10). Wieczorek and others (1983, Plate 1) applied the informal names of "Half" and "Halfway" for the basins between Baer and Shepard and between Davis and Ricks, respectively, which were unnamed on the topographic quadrangles. These names have been used in this report; however, it should be noted that Halfway Canyon is also the name of one of the tributaries in Farmington Canyon (Croft, 1981) and is shown on the Peterson Quadrangle, Utah (7.5-minute series).

Basin relief, R_b , is the difference in elevation from the highest point in the basin to the mouth. The elevations were determined from 1:24,000-scale topographic quadrangles and converted from feet to meters. Basin relief for the research area was found to correlate moderately well in a power function with basin area as

$$R_b = 950.6 A_b^{0.184}, (r^2 = 0.617, n = 22) \quad (35)$$

The relief ratio, R_r , is a dimensionless parameter equivalent to the nominal basin slope and is defined as

$$R_r = R_b / L_b \quad (36)$$

where R_b is the basin relief in m and L_b is the basin length in m.

The basin ruggedness factor, R_u , is a dimensionless parameter developed by Melton (1965, p. 23) and defined as

$$R_u = R_b / (A_b)^{0.5} \quad (37)$$

where R_b is the basin relief in m and A_b is the basin area in m^2 . An R_u factor of 1.0 indicates that the basin relief and the nominal basin dimension are equal. The nominal basin dimension, D_b , is

$$D_b = (A_b)^{0.5} \quad (38)$$

$$= (L_b + W_b) / 2 \quad (39)$$

and $W_b = A_b / L_b \quad (40)$

where A_b is basin area in m^2 , L_b is basin length in m, and W_b is nominal basin width in m.

The basin form factor, F_o , was developed by Horton (1932) and defined as

$$F_o = A_b / (L_b)^2 \quad (41)$$

where A_b is basin area in m^2 and L_b is basin length in m. An F_o factor of 1.0 would correspond to a square basin while an F_o factor of $\pi/4$ ($= 0.785$) would indicate a circular basin. Elliptical basins would have F_o factors of $e_b \pi/4$ where the eccentricity, e_b , is defined as

$$e_b = W_b / L_b \quad (42)$$

where W_b is the basin width in m and L_b is the basin length in m.

The basin elongation factor, E_b , was developed by Schumm (1956) and is a comparison of the basin length to the diameter of a circle with the same area as the basin. The factor E_b is defined as

$$E_b = 2 (A_b/\pi)^{0.5} / L_b \quad (43)$$

where A_b is the basin area in m and L_b is the basin length in m. A basin elongation factor of 1.0 indicates a circular basin.

The lemniscate factor, K , was developed by Chorley and others (1957) and defined as

$$K = L_b^2 / 4 A_b \quad (44)$$

where L_b is the basin length in m and A_b is the basin area in m^2 . The lemniscate factor reported in Appendix D is a modification of the factor developed by Chorley and others (1957). The equation of a lemniscate in polar coordinates is

$$r = L \cos(kt) \quad (45)$$

where L is the length of the long axis and k is a measure of the elongation (Scheidegger, 1961, p. 275). The area of a lemniscate is

$$A = \pi L^2 / 4 k \quad (46)$$

Therefore, the elongation of a lemniscate of length L_b required to approximate the area of a drainage basin, A_b , can be expressed as

$$K = \pi L_b^2 / 4 A_b \quad (47)$$

Thus, the lemniscate factor, K , reported in Appendix D is π times the factor developed by Chorley and others (1957). Circular basins have lemniscate factors of 1.0; long, thin basins have lemniscate elongation factors > 1 while short, wide basins have factors < 1 . Goudie (1981, p. 44) notes that the lemniscate elongation (equation 47) corresponds to the ellipticity index of Tinkler (1971) and the reciprocal of Horton's (1932) form factor (equation 41) as modified by Haggett (1965) and the squared reciprocal of Schumm's (1956) elongation factor (equation 43).

The drainage basin parameters summarized in Appendix D demonstrate the degree of variability among the basins and permit comparison of the basins in Davis County with basins elsewhere. No further analysis of the drainage basin parameters is presented in this

report because the focus is on sedimentation events on the alluvial fans. However, integration of slope failure susceptibility studies (e.g., Pack, 1985; Brooks, 1986; Jankowski, 1987) with the results of the hazard model presented in a subsequent section will be facilitated by an ability to compare the drainage basins which generate the sediment delivered to the fans.

CHANNELS

Channels, as separate geomorphic elements between basins and fans, are minor features in Davis County. Chiefly, the channels which represent Schumm's (1977) Zone 2 are restricted to the terrain below the Bonneville Shoreline at approximately elevation 1585 m and above the apexes of the alluvial fans, some of which are as low as elevation 1400 m. In most cases, stream channels have entrenched the Bonneville Alloformation deposits and are confined until they reach the intersection points of the alluvial fans. The highest order channels in the Davis County basins are relatively straight, as can be seen on the figures in Appendix D.

ALLUVIAL FANS

The study area comprises 22 alluvial fans, as shown on Figure 1. Selected morphometric data pertaining to these fans are presented in Table 8. The fans range in area from 0.29 to 1.356 km², with slopes ranging from 0.04 to 0.154, if estimated from topographic maps at a scale of 1:24,000, to 0.067 to 0.20, if estimated from maps of 1:2,400-scale.

Morphometric Correlations

Correlations among basin and fan variables listed in Appendix D and Table 8 are summarized in Tables 9 and 10. Table 9 is a correlation matrix computed with the variables as listed in Appendix D and Table 8; Table 10 is a correlation matrix computed with logarithmic transformations of the variables. Significant correlations exist among all parameters except the fan slope determined from 1:2,400-scale topographic maps. The logarithmic correlation matrix displays the same trend as the linear correlation matrix.

A number of morphometric parameters regarding alluvial fans have been developed since Bull's pioneering studies in 1964. Many parameters are represented as power functions in the form

$$A_f = m A_b^n \quad (48)$$

where A_f is the fan area, A_b is the basin area, and m and n are regression coefficients. Most relationships developed before about 1980 in the United States expressed areas in mi². These relationships were converted to the metric system for presentation in this report by recognizing that the coefficient m represents the value of the fan area corresponding to a basin area of 1 mi², or

$$m = A_f | A_b = 1 \text{ mi}^2 \quad (49)$$

Consequently,

$$m \text{ mi}^2 (2.589 \text{ km}^2 / \text{mi}^2) = k (2.589 \text{ km}^2)^n \quad (50)$$

where k is the coefficient for the metric equivalent of m and the power n remains constant provided that the units of the abscissa and ordinate remain the same. Solving equation 50 for k ,

Table 8. Selected morphometric data for alluvial fans in Davis County.

Basin	Area (km ²) Af	Slope (a) Sf	Slope (b) Sfd
Corbett	0.130	0.100	0.125
Hobbs	0.069	0.154	0.114
Lightning	0.080	0.120	0.100
Kays (Middle)	0.146	0.105	0.125
Kays (South)	0.118	0.109	0.077
Snow	0.256	0.091	0.125
Adams	0.162	0.100	0.091
Webb	0.168	0.100	0.125
Baer	0.254	0.086	0.125
Half	0.029	0.140	0.091
Shepard	0.518	0.105	0.125
Farmington	1.356	0.075	0.067
Rudd	0.197	0.073	0.200
Steed	0.382	0.081	0.167
Davis	0.264	0.075	0.125
Halfway	0.056	0.123	0.125
Ricks	0.556	0.090	0.111
Barnard	0.406	0.067	0.125
Parrish	0.280	0.076	0.100
Centerville	0.852	0.064	0.100
Buckland	0.072	0.114	0.091
Ward	0.896	0.040	0.100
Mean	0.329	0.095	0.115
Standard Deviation	0.332	0.026	0.029

(a) Slope measured from 1:24,000-scale topographic maps.

(b) Slope measured from 1:2,400-scale ortho-topographic maps.

$$k = 2.589 \text{ m} / (2.589)^n \quad (51)$$

$$= \text{m} (2.589)^{1-n} \quad (52)$$

Thus, the metric equivalent of equation 48 is

$$\text{Af} = \text{m} (2.589)^{1-n} \text{Ab}^n \quad (53)$$

where Af and Ab are expressed in km².

The relationships of alluvial fan area to drainage basin area from a number of studies are summarized on Figure 21. The regression equations, fan locations, Köppen-Geiger climate classifications, and references corresponding to letter designations on Figure 21 are presented in Table 11. The relationship for Davis County (designation O) indicates that fan areas generally are considerable smaller for drainage basins of the same size in California, but the fan areas increase with increasing basin areas at about the same rate as in California. The dry climate prevalent in most areas of alluvial fan studies in California is

Table 9. Correlation matrix of morphometric parameters of drainage basins and alluvial fans. Symbols used in this table are described in Appendix D and Table 8. All correlations are based on $n = 22$ (20 degrees of freedom). $|r| \geq 0.28$ correspond to $p \leq 0.20$ or 80 percent confidence; $|r| \geq 0.36$ corresponds to $p \leq 0.1$ or 90 percent confidence; $|r| \geq 0.42$ corresponds to $p \leq 0.05$ or 95 percent confidence (probabilities from the t-distribution table in Ott, 1984, p. 697).

PARAMETERS	O	Ab	Lb	Lr	Rb	Rr	Ru	Fo	Eb	K	Af	Sf	Sfd
O	1.00												
Ab	0.49	1.00											
Lb	0.65	0.92	1.00										
Lr	0.79	0.48	0.66	1.00									
Rb	0.74	0.47	0.62	0.90	1.00								
Rr	-0.55	-0.73	-0.87	-0.48	-0.30	1.00							
Ru	-0.71	-0.80	-0.87	-0.71	-0.53	0.87	1.00						
Fo	0.58	0.58	0.46	0.60	0.56	-0.24	-0.68	1.00					
Eb	0.56	0.57	0.45	0.61	0.57	-0.22	-0.66	1.00	1.00				
K	-0.51	-0.53	-0.40	-0.61	-0.59	0.13	0.60	-0.97	-0.98	1.00			
Af	0.45	0.88	0.86	0.44	0.41	-0.73	-0.73	0.44	0.44	-0.41	1.00		
Sf	-0.65	-0.45	-0.59	-0.47	-0.50	0.52	0.48	-0.25	-0.23	0.20	-0.65	1.00	
Sfd	-0.05	-0.37	-0.34	-0.05	0.10	0.41	0.35	-0.07	-0.07	0.07	-0.26	-0.17	1.00

Table 10. Correlation matrix of logarithmic transformations of morphometric parameters of drainage basins and alluvial fans. Symbols used in this table are described in Appendix D and Table 8. All correlations are based on $n = 22$ (20 degrees of freedom). $|r| \geq 0.28$ correspond to $p \leq 0.20$ or 80 percent confidence; $|r| \geq 0.36$ corresponds to $p \leq 0.1$ or 90 percent confidence; $|r| \geq 0.42$ corresponds to $p \leq 0.05$ or 95 percent confidence (probabilities from the t-distribution table in Ott, 1984, p. 697).

PARAMETERS	O	Ab	Lb	Lr	Rb	Rr	Ru	Fo	Eb	K	Af	Sf	Sfd
O	1.00												
Ab	0.82	1.00											
Lb	0.81	0.95	1.00										
Lr	0.85	0.85	0.82	1.00									
Rb	0.79	0.79	0.75	0.91	1.00								
Rr	-0.50	-0.72	-0.82	-0.42	-0.24	1.00							
Ru	-0.65	-0.91	-0.87	-0.60	-0.45	0.88	1.00						
Fo	0.51	0.70	0.45	0.56	0.56	-0.18	-0.63	1.00					
Eb	0.51	0.70	0.44	0.56	0.56	-0.18	-0.63	1.00	1.00				
K	-0.51	-0.70	-0.44	-0.56	-0.56	0.18	0.63	-1.00	-1.00	1.00			
Af	0.64	0.79	0.80	0.63	0.63	-0.63	-0.71	0.45	0.45	-0.45	1.00		
Sf	-0.63	-0.56	-0.60	-0.42	-0.42	0.51	0.52	-0.25	-0.25	0.25	-0.80	1.00	
Sfd	-0.01	-0.24	-0.26	0.01	0.12	0.48	0.43	-0.09	-0.09	0.09	-0.03	-0.10	1.00

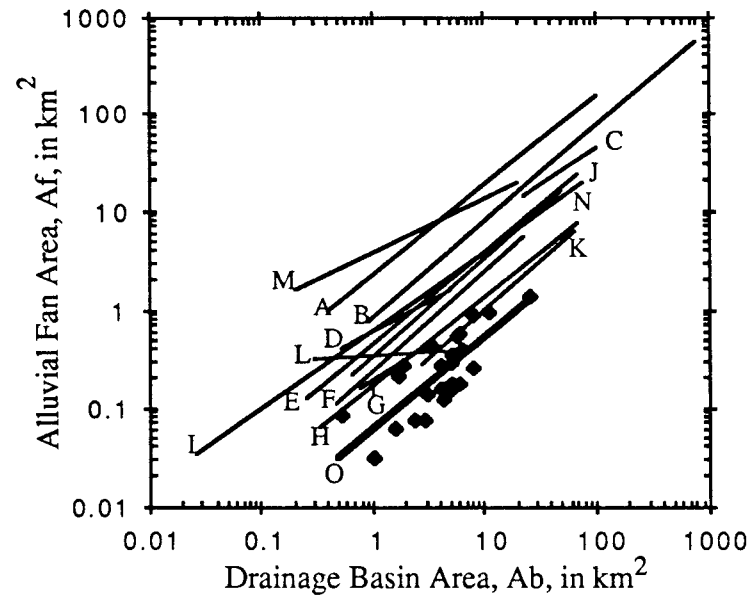


Figure 21. Plot of alluvial-fan area versus drainage basin area. Letters represent individual fan-basin relationships which are summarized in Table 11. Data points are for Davis County; heavy line designated "O" is the regression of the Davis County data.

Table 11. Selected data regarding relationships of alluvial-fan area and drainage basin area.

Designation	Regression ^(a) Equation	Location	Köppen-Geiger ^(b) Climate Class	Reference
A	$Af = 2.29 Ab^{0.91}$	Fresno Co., CA	Csb	Bull, 1964, p.95 modified by Hooke, 1968, p. 612
B	$Af = 0.81 Ab^{0.98}$	Fresno Co. CA	Csb	Bull, 1964, p. 95 modified by Hooke, 1968, p. 612
C	$Af = 1.32 Ab^{0.76}$	Death Valley, CA, west side	BWk	Hooke, 1968, p. 612
D	$Af = 0.63 Ab^{0.62}$	Deep Springs, CA	BWk	Hooke, 1968, p. 612
E	$Af = 0.44 Ab^{0.94}$	Owens Valley, CA	BWk	Hooke, 1968, p. 612
F	$Af = 0.24 Ab^{1.01}$	Cactus Flats, CA	BWk	Hooke, 1968, p. 612
G	$Af = 0.20 Ab^{0.75}$	Deep Springs, CA	BWk	Hooke, 1968, p. 612
H	$Af = 0.16 Ab^{0.90}$	Death Valley, CA, east side	BWk	Hooke, 1968, p. 612
I	$Af = 0.60 Ab^{0.80}$	Amargosa and Death Valley, CA	BWk	Denny, 1965, p. 15
J	$Af = 0.33 Ab^{1.00}$	Shadow Mtn, CA	BWk	Denny, 1965, p. 15
K	$Af = 0.10 Ab^{1.00}$	Death Valley, CA, east side	BWk	Denny, 1965, p. 15
L	$Af = 0.34 Ab^{0.08}$	Nelson Co., VA	Cfa	Kochel and Johnson, 1984, p. 111
M	$Af = 3.84 Ab^{0.55}$	Ventura Co., CA high uplift rate	Csb	Rockwell and others, 1985, p. 198
N	$Af = 0.59 Ab^{0.80}$	Ventura Co., CA low uplift rate	Csb	Rockwell and others, 1985, p. 198
O	$Af = 0.059 Ab^{0.918}$ $r^2 = 0.622, n = 22$	Davis Co., UT	BSk	This study

(a) Af is alluvial fan area in km²; Ab is drainage basin area in km².

(b) Köppen-Geiger climate classification from Strahler and Strahler (1984, p. 160)

similar to the climate of Davis County. Consequently, differences in slope of the regression equations relating fan area and basin area should correspond to the rate of formation of the fans, erodibility of rocks in the basins, degree of tectonic activity, and age of fans.

The rocks in the Davis County basins are exclusively gneiss and schist of the Precambrian Farmington Canyon Complex (Bryant, 1984). These rocks are generally hard, but extensively fractured. Bedrock exposures constitute only about 10 percent of the mountain block in the study area, and colluvial deposits up to 12.2 m thick have been

found at elevations as high as 2440 m (Brooks, 1986). Rock types in areas of other alluvial fan studies have been sedimentary or meta-sedimentary rocks of Paleozoic (Denny, 1965; Hooke, 1968), Mesozoic (Bull, 1964), and Cenozoic (Rockwell and others, 1985) ages, and crystalline rock of Precambrian age (Kochel and Johnson, 1984). Bull (1964) found that fans in Fresno Co., CA, derived from basins underlain by shale and mudstone (designation A on Figure 21) are about twice the size of fans derived from comparable size basins underlain by less erodible sandstone (designation B). The fan area-basin area relationship developed by Kochel and Johnson (1984, p. 111) for Precambrian crystalline rock types in Virginia (designation L) shows little variation in fan size with increasing basin size. They note that coalescence of fans on the piedmont slopes contributed to difficulty in determining areal extent of individual fans. For basins exceeding about 10 km² in area, fans in Davis Co., UT (designation O), are larger than corresponding fans in Nelson Co., VA (designation L), according to the regression relations summarized on Figure 21.

Rockwell and others (1985) and Hooke (1972) indicate that tectonic activity affects the fan area-basin area relationship. Rockwell and others (1985) found that fans developed in areas of high uplift rate (designation M on Figure 21) are significantly larger than fans developed in areas of low uplift rate (designation N). Hooke (1972) found that eastward tilting of Death Valley contributed to development of large fans on the west side, where fanhead entrenchment caused progressive down-fan deposition, and small fans on the east side, where down-dropping of the valley caused continual fanhead deposition. The degree of tectonic activity is significantly less in the Nelson Co., VA, area (designation L) than all other areas reported in Table 11 and summarized on Figure 21, and the slope of the line defining the relation is the gentlest of those shown. However, the slope of the regression line for low uplift rate in Ventura Co., CA (designation N) is steeper than that for the high uplift rate (designation M).

The alluvial fans below about elevation 1585 m (the Bonneville shoreline) in Davis County are younger than about 14.5 ka, and those below about elevation 1463 m (the Provo shoreline) are younger than about 12 ka (Currey and Oviatt, 1985, p. 1091). Therefore, small fans could be explained in Davis County by erosion and/or burial of older alluvial-fan deposits by Lake Bonneville. Similar processes have occurred in Death Valley, where Lake Manley existed in mid-Pleistocene time (Currey, 1987, oral communication). In addition to erosion of alluvial-fan deposits in Death Valley, playa deposition on the east side of the valley, which has been relatively continuous since the retreat of Lake Manley, has been burying the distal parts of the fans, leaving the younger, upper parts exposed.

Relationships among alluvial fan slope and drainage basin area parameters have been developed by Bull (1962; 1964; 1977), Denny (1965), Melton (1965), Ryder (1971), Hooke (1972), Mills (1982), Harvey (1984), and Rockwell and others (1985). Those power functions between drainage basin area and fan slope are summarized on Figure 22. The regression equations, fan locations, Köppen-Geiger climate classifications, and references corresponding to letter designations on Figure 22 are presented in Table 12. The relationship for Davis County (designation K on Figure 22) indicates that fan slopes generally are steeper for drainage basins of the same size elsewhere, but the fan slopes decrease with increasing basin areas at about the same rate as elsewhere. Studies by Bull (1964; 1977) and Hooke (1972) suggested that fan slopes were a function of lithology of source area, particle size of the fan sediments, drainage basin area and discharge. Steeper fans generally are associated with coarser sediments and smaller drainage basins. These concepts were supported by observations in Ventura Co., CA (Rockwell and others, 1985, p. 200), and in Spain (Harvey, 1984, p. 131). Harvey (1984, p. 131) also suggests that relative abundance of deposition by debris flows contributes not only coarse sediment, but the debris-flow process inherently produces steeper deposition slopes than do fluvial

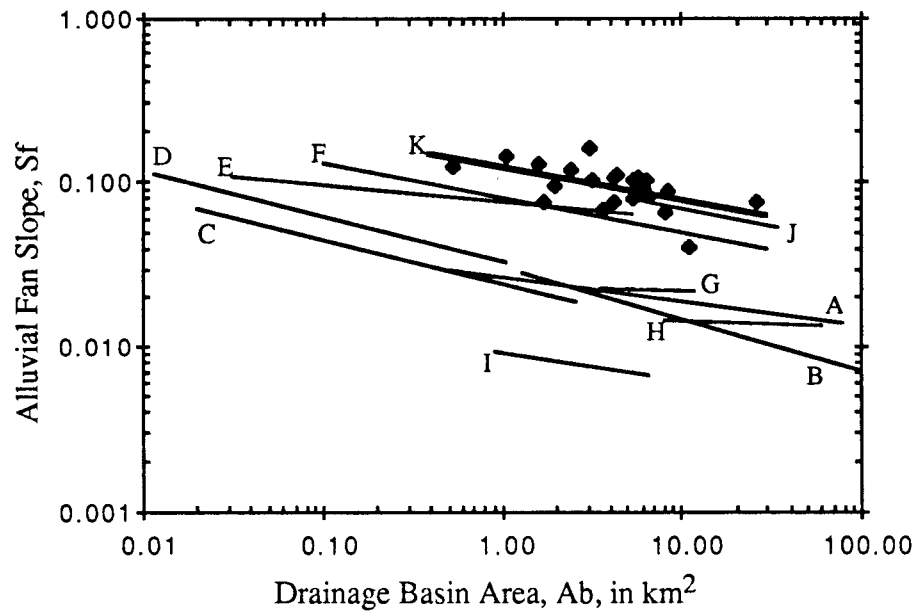


Figure 22. Plot of alluvial-fan slope versus drainage basin area. Letters represent individual fan-basin relationships which are summarized in Table 12. Data points are for Davis County; heavy line designated "K" is the regression of the Davis County data.

Table 12. Selected data regarding relationships of alluvial-fan slope and drainage basin area.

Designation	Regression ^(a) Equation	Location	Köppen-Geiger ^(b) Climate Class	Reference
A	$Sf = 0.03 Ab^{-0.16}$	Fresno Co., CA, fine-grained source	Csb-Csa	Bull, 1964, p.95
B	$Sf = 0.03 Ab^{-0.32}$	Fresno Co. CA, coarse-grained source	Csb-Csa	Bull, 1964, p. 95
C	$Sf = 0.02 Ab^{-0.26}$	Death Valley, CA, Bat Mtn.	BWk	Denny, 1965, p. 53
D	$Sf = 0.03 Ab^{-0.27}$	Death Valley, CA, Shadow Mtn.	BWk	Denny, 1965, p. 53
E	$Sf = 0.08 Ab^{-0.10}$	Death Valley, CA, Johnson Canyon	BWk	Denny, 1965, p. 53
F	$Sf = 0.12 Ab^{-0.20}$	South eastern Spain	BSk	Harvey, 1984, p. 129
G	$Sf = 0.02 Ab^{-0.045}$	Ventura Co., CA, fine-grained source	Csb	Rockwell and others, 1985, p. 197
H	$Sf = 0.02 Ab^{-0.053}$	Ventura Co. CA, fine-grained source	Csb	Rockwell and others, 1985, p. 197
I	$Sf = 0.09 Ab^{-0.19}$	Ventura Co., CA, coarse-grained source	Csb	Rockwell and others, 1985, p. 197
J	$Sf = 0.11 Ab^{-0.21}$	Ventura Co., CA, coarse-grained source	Csb	Rockwell and others, 1985, p. 197
K	$Sf = 0.121 Ab^{-0.198}$ $r^2 = 0.315, n = 22$	Davis Co., UT	BSk	This study

(a) Sf is alluvial fan slope (dimensionless); Ab is drainage basin area in km².

(b) Köppen-Geiger climate classification from Strahler and Strahler (1984, p. 160)

the same size elsewhere, but the fan slopes decrease with increasing basin areas at about the same rate as elsewhere. Studies by Bull (1964; 1977) and Hooke (1972) suggested that fan slopes were a function of lithology of source area, particle size of the fan sediments, drainage basin area and discharge. Steeper fans generally are associated with coarser sediments and smaller drainage basins. These concepts were supported by observations in Ventura Co., CA (Rockwell and others, 1985, p. 200), and in Spain (Harvey, 1984, p. 131). Harvey (1984, p. 131) also suggests that relative abundance of deposition by debris flows contributes not only coarse sediment, but the debris-flow process inherently produces steeper deposition slopes than do fluvial processes. Such observations are supported by the findings of Hooke (1967) and Pierson and Costa (1987). Fine-grained source basins, reflected on Figure 22 by curves designated A, G, and H, have generally gentler regression curve slopes than coarse-grained source basins.

Harvey (1984, p. 130) found improved statistical correlation of alluvial-fan slope in a multiple regression with drainage basin area, Ab, basin relief, Rb, and basin slope

(relief ratio as defined above), R_r . Harvey's regression equation for fans in southeast Spain is

$$Sf = 0.00092 Ab^{-0.500} Rb^{0.748} Rr^{-0.107} \quad (54)$$

A similar regression computed for fans in Davis County yielded

$$Sf = 3.656 Ab^{-0.039} Rb^{-0.383} Rr^{0.712}, (r^2 = 0.396, n = 22) \quad (55)$$

The coefficient of determination for the multivariate regression (equation 55) indicates a modest 12 percent improvement in correlation from the bivariate regression listed as designation K in Table 12.

LEVEES AND BOULDER FRONTS

Levees are lateral ridges which have been observed on many debris-flow deposits. Early accounts described these features as "moraine" (Rickmers, 1913), but Sharp (1942) gave them the name "levees." Beaty (1963, p. 524) described levees in the White Mountains of California as steep-sided, paired, linear ridgelets of heterogeneous composition. Johnson (1970, p. 435) describes these features as lateral deposits and discusses the material properties required to preserve steep sides. Hooke (1967, p. 452) describes the threshold condition required for deposition of moving debris. Debris-flow material has a finite yield strength, τ_c , which must be exceeded by the applied shear stress, τ_o , for the debris to move. At such time as $\tau_o < \tau_c$, the debris stops. Sharp (1942, p. 225) noted that coarse material accumulating at the front of a debris flow is shoved aside by more rapidly moving debris, forming levees which confine the trailing portions of the flow. Hooke (1967, p. 452) noted that

$$\tau_o = \rho g h Sf \quad (56)$$

where ρ is density, g is acceleration of gravity, h is debris thickness, and Sf is the slope of the fan. As debris issues from the confinement of a canyon mouth and spreads on a gentler fan slope, the thickness, h , and the slope, Sf , decrease, resulting in a decrease in τ_o . The more fluid debris confined by the levees preserves a greater thickness, h , and, consequently, a greater τ_o , even though the slope, Sf , decreases in a down-fan direction.

Levees are characteristic features of Davis County alluvial fans, particularly at Ricks Creek where residential development has not yet obliterated the geomorphology. Levees of prehistoric debris flows are preserved on an abandoned part of the Ricks Creek fan, as shown on Figure 8. Additionally, levees associated with historic debris flows in 1923 and 1930 are preserved within the entrenched fanhead channel. Levees of prehistoric debris flows were observed on the Rudd Creek fan above the Wasatch fault trace, as shown on Figure 7. Levees were also created at Lightning Canyon during debris flows in 1984. Elsewhere in Utah, levees were created during debris flow events in 1983 (Lips and Wieczorek, 1987, written communication).

Accumulations of boulders in linear orientations approximately perpendicular to debris flow directions were observed by Lips and Wieczorek (1987, written communication) and named boulder fronts. Similar boulder fronts were observed on the Ricks Creek fan at locations indicated on Figure 8, suggesting that as many as 5 pulses or surges of debris occurred on the abandoned part of that fan. Boulder fronts were not observed elsewhere in Davis County, probably due, at least in part, to the degree of urbanization which obscures and obliterates geomorphic features.

PROGRESSIVE FAN DEVELOPMENT

Elements of progressive fan development were described by Denny (1967). He notes a complex history of shifting deposition, stream entrenchment, and fan enlargement to an ideal steady state condition in which the amount of sediment applied to the fan is equal to the amount eroded from the fan. Denny (1967, p. 84) discusses a hypothetical piedmont in an arid region in which initial deposits at the apex of a fan are incised near the mountain front so that the upper part is no longer receiving sediment. The incision in the Death Valley, California, region where Denny worked was related to steepening of the stream gradients across post-fan fault scarps. Many other reports of alluvial fans attribute their formation to fault scarps (Davis, 1925; Eckis, 1928; Sharp and Nobles, 1953; Blissenbach, 1954; Hunt and Mabey, 1966; Rahn, 1967; Beaty, 1970; Scott, 1971, 1973; Hooke, 1972; Wasson, 1974; Meckel, 1975; Tanner 1976; Bull, 1977; Heward, 1978; and Nilsen, 1982). Continued deposition with intermittent large-magnitude flood events results in shifting patterns of deposition accompanied by abandonment of some channels and creation of new ones elsewhere.

The relationships among the rate and magnitude of tectonic uplift, channel downcutting, and fan deposition were recognized and described by Bull (1977, p. 248 ff). He reasoned that as long as the amount of uplift equals or exceeds the sum of the amounts of channel downcutting in the mountains and deposition, accumulation of alluvial-fan deposits adjacent to the mountains would continue. Where channel downcutting exceeds the rate of mountain uplift, fanhead entrenchment will occur, shifting the zone of deposition in a downfan direction.

Heward (1978, p. 684 ff) developed hypothetical behavioral models of fans in response to a) prolonged fanhead entrenchment, b) scarp retreat and lowering of relief, c) tectonic uplift where the rate of uplift exceeds the rate of stream dissection, and d) tectonic uplift where stream dissection exceeds the uplift rate. Prolonged fanhead entrenchment naturally results in progressive downfan shifting of deposition. Decreasing sediment supply or lowering of the local base level can be responsible for such entrenchment. Scarp retreat and lowering of relief in the mountains tends to maintain deposition in the proximal fan area. Steep, proximal-fan deposition occurs in response to tectonic uplift exceeding the rate of stream dissection. If stream dissection exceeds tectonic uplift, then fanhead entrenchment occurs and deposition shifts to distal fan areas.

Alluvial-fan deposits in Davis County occur below the Bonneville Shoreline, and, in general, below the Wasatch fault trace, as shown in Appendix D. Long-term uplift rates on the Wasatch fault zone in Davis County have been estimated by Naeser and others (1983) on the basis of fission-track ages of apatite in gneiss and schist of the Precambrian Farmington Canyon Complex. They assumed a geothermal gradient of 30° C/km and considered that apatite annealing could occur at temperatures as low as about 150° if the minerals remained at that temperature for at least 1 Ma; thus, an effective annealing depth would be approximately 5 km. Naeser and others (1983, p. 35) found apparent ages of the Precambrian apatites ranging from 5 to 94 Ma; the older apparent ages were developed from samples near the crest of the Wasatch Range, while the younger ages were from the base of the range near the Wasatch fault zone. They concluded that uplift along the Wasatch fault zone for the past 5 to 10 Ma occurred at an average rate of about 0.8 to 0.4 m/ka, respectively.

The Wasatch fault zone was exposed in a trench excavation between Baer Canyon and Half Canyon (Swan and others, 1980). An average slip rate of about 1.3 m/ka was determined from faulted sediments that were found to be 8 ± 1-2 ka old (Schwartz and

Coppersmith, 1984, p. 5687). Precise releveing following the 1983 Borah Peak, Idaho, earthquake by Stein and Barrientos (1985) revealed that surface displacement along the Lost Hills fault was proportioned approximately 0.24 in an upward direction on the upthrown side of the fault and 0.76 in a downward direction on the downthrown side. A theoretical elastic dislocation model developed by Okada (1985) was applied to estimate tectonic deformation along the Wasatch fault zone by Keaton (1987). The results of the elastic model indicates that the amount of deformation is greatest at the fault zone, as would be expected, and attenuates to zero at distances of approximately 15 and 30 km on the upthrown and downthrown sides of normal faults, respectively. The shape of the deformation curve (Keaton, 1987, p. 22) indicates that about half of the maximum deformation on the upthrown side should be present at a distance of about 5 km away from the fault trace. The distance from the surface trace of the Wasatch fault zone to the crest of the Wasatch Range is about 5 km. The anticipated surface displacement accompanying a major Wasatch fault zone earthquake would be on the order of 1.6 m (Schwartz and Coppersmith, 1984, p. 5687), thus, uplift of 0.4 m at the fault trace could have occurred in response to each surface faulting earthquake. At the crest of the Wasatch Range, uplift of 0.2 m could have occurred during each earthquake. The average uplift across the west-facing drainage basins in the study area could have been 0.2 to 0.4 m per earthquake. Schwartz and others (1983) report three surface faulting events in central Davis County in the past 8 ka, two of which were within the past 1.58 ka. The average effective uplift rate of the Wasatch Range in the study area since mid- to late-Holocene time can be calculated as

$$UR_{MH} = (0.4 \text{ m/event}) \cdot (3 \text{ events} / 8 \text{ ka}) = 0.15 \text{ m/ka} \quad (57)$$

$$UR_{LH} = (0.4 \text{ m/event}) \cdot (2 \text{ events} / 1.58 \text{ ka}) = 0.5 \text{ m/ka} \quad (58)$$

where UR_{MH} is the mid-Holocene uplift rate and UR_{LH} is the late-Holocene uplift rate. This is considered effective uplift in the sense that it contributes to lowering the base level controlling erosion in the mountains. This range of average uplift rate compares well with the long-term uplift rate estimated from fission-track ages of apatite. However, a considerable amount of the long-term uplift must have been regional since the elevation of the crest of the Wasatch Range in the study area is approximately 2800 m; therefore, at an uplift rate of 0.4 m/ka, 4 km of uplift would have occurred in the past 10 Ma, and what is now at an elevation of 2800 m would have been 1200 m below sea level in late Miocene time. Rocks deposited in a coastal marine environment in latest Cretaceous to early Paleogene time (approximately 60 Ma old) are located in the northern Colorado Plateau and Wasatch Plateau Provinces in central Utah at elevations as high as 3600 m (Hintze, 1977; 1980), indicating a long-term (Cenozoic) average regional uplift on the order of 0.06 m/ka.

The steepness and relief of the Wasatch Range indicates that erosion has not equalled uplift. Rapid uplift of the Wasatch Range in the past 10 Ma indicated by the distribution of fission-track ages in rocks of the Farmington Canyon Complex is interpreted to have occurred chiefly by normal slip on the Wasatch fault zone. An average long-term erosion rate for the Wasatch Range in Davis County was estimated on the basis of the volume of missing rock between the existing ground surface and the upward projection of the plane of the Wasatch fault (Keaton, 1986a). The volume eroded from the mountain block was assumed to be defined by the plane of the fault projected upward at 60° to an elevation of 2835 m, about 13 m higher than Bountiful Peak on the crest of the range between Steed Canyon and Ricks Creek. Lateral limits of the drainage basins were taken as vertical projections of the divides. The area used to calculate the long-term erosion rate was approximately 63 km², from Rudd Creek on the north to Ward Canyon on the south. The volume as defined suggests that about 43 km³ were eroded from the upthrown side of the Wasatch fault zone, presumably during the past 10 Ma. The corresponding erosion rate, Er , is

$$Er = Ve / Ae / Te \quad (59)$$

$$= 43 \text{ km}^3 / 63 \text{ km}^2 / 10 \text{ Ma} \quad (60)$$

$$= 0.07 \pm 0.04 \text{ m / ka} \quad (61)$$

where Ve is the eroded volume, Ae is the area over which the erosion occurs, and Te is the time during which erosion occurs. A relatively large error (about 50 percent, or ± 0.04 m/ka) was estimated for the erosion rate because of the uncertainty inherent in the planimetering technique on which the erosion rate was based and on the arbitrary boundary surfaces of the eroded volume. This erosion rate suggests that long-term uplift is approximately 6 times greater than erosion.

Erosion rates evaluated for other locations have been used to predict sediment yield and denudation rates. The Pacific Southwest Inter-Agency Committee (PSIAC) of the U.S. Department of Agriculture created a Task Force to evaluate factors affecting sediment yield (PSIAC, 1968; Branson and others, 1981, p. 119 - 121). This group developed an empirical rating system based on nine factors to estimate annual sediment yield from moderate-sized drainage basins. The PSIAC method was applied to conditions in the study area using rating values for the nine factors shown in Table 13. The PSIAC method relates

Table 13. PSIAC sediment yield factors and ratings for Davis County conditions.

Factor	Characteristics	Rating Range	Davis County Conditions	Davis County Rating Value
Surface Geology	Rock type; Hardness; Weathering; Fracturing	0 - 10	Gneiss and Schist	0
Soils	Texture; Organic Matter; Shrink-swell; Salinity	0 - 10	High Content of Rock Fragments	0
Climate	Storm Frequency; Intensity; Duration	0 - 10	Infrequent Convective Storms	5
Runoff	Volume per area; Peak flow per area	0 - 10	Moderate Peak Flows	5
Topography	Steepness of Upland; Relief; Flood Plain	0 - 20	Steep to Moderate Upland Slopes	15
Ground Cover	Vegetation; Litter; Rocks; Understory	-10 - +10	Cover Between Complete and 40%	-5
Land Use	Cultivation; Roads; Grazing; Logging	-10 - +10	No Cultivation, Logging, Grazing; Few Roads	-10
Upland Erosion	Rills; Gullies; Landslides; Wind Deposits	0 - 25	About 5% of Area with Gullies and Slides	2.5
Channel Erosion and Sediment Transport	Bank and Bed Erosion; Headcuts; Flow Depths; Channel Vegetation	0 - 25	Moderate Flow Depths; Medium Durations; Rocky Channels	<u>5</u>

Summation of Davis County Ratings 17.5

sediment yield to the sum of the nine rating factors as

$$\log SY = -1.4104 + 0.0166 \sum RF \quad (62)$$

where SY is estimated sediment yield in m/ka, and $\sum RF$ is the sum of the nine rating factors in Table 13. The average sediment yield for the Davis County area predicted with the PSIAC method is 0.076 m/ka, which is nearly identical to the average long-term erosion rate described above.

Strand (1975) predicted sediment yield for eight U.S. Bureau of Reclamation reservoirs in New Mexico, Arizona, and California on drainage basins ranging in area from about 25 to 10,000 km². His regression equation, converted to the metric system, is

$$Er = 1.41 Ab^{-0.229} \quad (63)$$

where Er is erosion rate in m/ka, and Ab is drainage basin area in km². The negative exponent indicates that the erosion rate for larger basins is less than for smaller basins; however, the volume of sediment discharged from larger basins is greater than for smaller basins because of the larger area over which the erosion rate is applied. Erosion rates for Davis County drainage basins calculated with equation 63 are 1.040 ± 0.208 m/ka, 2.5 times greater than the long-term uplift rate. If such an erosion rate actually existed in Davis County, the Wasatch Range would not have the steep character that it does.

Megahan (1975) presented data for small (0.26 to 6.6 km²) undisturbed basins in granitic rock of the Idaho batholith in east central Idaho. Although the basins Megahan studied are relatively steep ($0.14 < Rr < 0.32$), they are in a relatively stable tectonic environment and Köppen-Geiger climate classification of H (Strahler and Strahler, 1984, p. 160), but nearby classification BSk or Csb probably describes the local climate. Data presented by Megahan (1975) were regressed with logarithmic transformations and yielded

$$Er = 0.006 Ab^{-0.473}, (r^2 = 0.36, n = 12) \quad (64)$$

$$Er = 0.019 Ab^{-0.462} Rr^{0.775}, (r^2 = 0.46, n = 12) \quad (65)$$

where Er is erosion rate in m/ka, Ab is drainage basin area in km², and Rr is dimensionless relief ratio (nominal basin slope). The multivariate analysis (equation 65) shows a 13-percent improvement in correlation over the bivariate analysis (equation 64). Erosion rates calculated with equation 64 for Davis County basins yield 0.003 ± 0.002 m/ka, while equation 65 yields 0.004 ± 0.002 m/ka. Such erosion rates are 100 times smaller than the long-term uplift rate. The tectonic stability in east central Idaho undoubtedly contributes to relatively small erosion rates.

An analysis of denudation rates in coastal southern California was conducted by Taylor (1983). He differentiated drainage basins on the basis of topographic expression into plains, hills, and mountains, and derived multivariate regression equations

$$Er = 0.094 L_t^{3.1} Ab^{-0.14} \quad (66)$$

where $L_t = \{L_{pl} = 1; L_h = 2.03; \text{ and } L_m = 2.74\}$ (67)

were calculated from graphic presentation (Taylor, 1983, p. 80).

Thus, $Er_{pl} = 0.094 Ab^{-0.14}$ (68)

$$Er_h = 0.84 Ab^{-0.14} \quad (69)$$

and $Er_m = 2.15 Ab^{-0.14}$ (70)

In these equations, Er is erosion rate in m/ka; L_t is ordinaly ranked land type with subscript pl designating plains, h designating hills, and m designating mountains; Ab is drainage basin area in km². Equations 68, 69, and 70 applied to Davis County drainage basins results in erosion rates of 0.08 ± 0.01 m/ka for plains, 0.70 ± 0.08 m/ka for hills, and 1.78 ± 0.21 m/ka for mountains. Clearly, the Davis County basins are mountainous;

however, the drainages in southern California studied by Taylor (1983) are in an area tectonically more active, climatically more vigorous, and lithologically more erodible than the conditions in Davis County. Thus, erosion rates developed from plains in southern California appears to be comparable to those developed from mountains in Davis County.

Griggs and Hein (1980) studied erosion rates from coastal and inland drainage basins in northern and central California. They found an average erosion rate of 0.43 m/ka for northern California coastal basins, 0.07 m/ka for central California coastal basins, and 0.014 m/ka for central California inland basins. Coastal climates are designated Köppen-Geiger classifications Csb while inland climates in central California are Csa. The California coast ranges are tectonically active (the northern coastal and central inland basins are on the east side of the San Andreas fault while the central coastal basins are on the west side), and characterized by varied lithologies ranging from fine-grained sedimentary rocks to crystalline rocks.

The volumes of the alluvial fans in Davis County were estimated by multiplying an average fan thickness by the fan area. Pertinent data used to estimate fan volumes are summarized in Table 14. Subsurface data for estimation of fan thickness were available for the Ricks Creek fan only; other fan thicknesses were estimated from fan-surface convexities as represented on topographic maps at scales of 1:24,000 and 1:2,400. Deposits of Lake Bonneville on which the post-lake alluvial fans accumulated were assumed to have a uniform configuration represented by the generally linear topographic contours between fans. Fan thickness estimates were based on the slope of the ground surface along the axis of maximum convexity, as shown on Figure 23, and the deviation of the topographic contour from the linear projection of the contour across the axis of maximum convexity. Thus, the mean fan thickness, T_{fm} , for each topographic contour on 1:24,000-scale maps was calculated as

$$T_{fm} = T_f / 2 \quad (71)$$

$$\text{where } T_f = L_p \cdot S_f \quad (72)$$

$$\text{and } S_f = CI / L_a \quad (73)$$

where T_f is the maximum fan thickness along the axis of maximum convexity, L_p is the length from the contour to the projection along the axis of maximum convexity, S_f is the slope of the fan along the axis of maximum convexity, CI is the contour interval, and L_a is the length between successive contours along the axis of maximum convexity. Equation 71 is based on an assumed triangular cross section along the projection of the topographic contour. On 1:2,400-scale maps, the contour interval was sufficiently small that the projection of a topographic contour intersected several higher contours. Thus,

$$T_{fm} = \sum A_i / \sum L_i \quad (74)$$

$$A_i = [(H_i + H_{i-1}) / 2] \cdot [L_i - L_{i-1}] \quad (75)$$

where A_i is the incremental area along the projection of the contour computed as a trapezoid, $\sum A_i$ is the total area, H_i and H_{i-1} are the differences in elevation from the projected contour to the i th and $i-1$ th contour, L_i and L_{i-1} are the lengths from the edge of the contour convexity to the i th and $i-1$ th contours along the projected contour. Both methods were used to calculate average thicknesses for those fans where both scales of maps were available; the results were nearly identical. The fan thickness values presented in Table 14 were considered to have errors on the order of 40 percent of the mean values due to the accuracies of the topographic maps and uncertainties in the estimation procedures. The ± 40 percent value was taken to represent the standard deviation of the thickness.

Table 14. Summary of alluvial-fan areas, thicknesses, and volumes.

Basin Name	Fan Area Af (km ²)	Fan Thickness Tf (m) (a)		Fan Volume Vf (10 ⁶ m ³) (b)	
		Mean	Standard Deviation	Mean	Standard Deviation
Corbett	0.130	2.2	0.9	0.286	0.117
Hobbs	0.069	4.1	1.6	0.283	0.110
Lightning	0.080	4.6	1.8	0.368	0.144
Kays (Middle)	0.146	4.3	1.7	0.628	0.248
Kays (South)	0.118	5.1	2.0	0.602	0.236
Snow	0.256	4.3	1.7	1.101	0.435
Adams	0.162	4.4	1.8	0.713	0.292
Webb	0.168	5.1	2.0	0.857	0.336
Baer	0.254	4.1	1.6	1.041	0.406
Half	0.029	4.4	1.8	0.128	0.052
Shepard	0.518	6.1	2.4	3.160	1.243
Farmington	1.356	8.2	4.5	11.119	6.102
Rudd	0.197	3.7	1.5	0.729	0.296
Steed	0.382	2.3	0.9	0.879	0.344
Davis	0.264	3.3	1.3	0.871	0.343
Halfway	0.056	2.3	0.9	0.129	0.050
Ricks	0.556	1.9	0.7	1.056	0.389
Barnard	0.406	2.2	0.9	0.893	0.365
Parrish	0.280	2.2	0.9	0.616	0.252
Centerville	0.852	2.9	1.2	2.471	1.022
Buckland	0.072	2.8	1.1	0.202	0.079
Ward	0.896	3.1	1.6	2.778	1.434
Mean	0.329	3.8	1.6	1.405	0.650
Standard Deviation	0.332	1.5	0.8	2.320	1.272

(a) Thickness values are based on convexity of alluvial fans represented on topographic maps; standard deviations are assumed to be 40 percent of the thickness values. See text for discussion.

(b) Volumes are calculated by multiplying fan area by fan thickness.

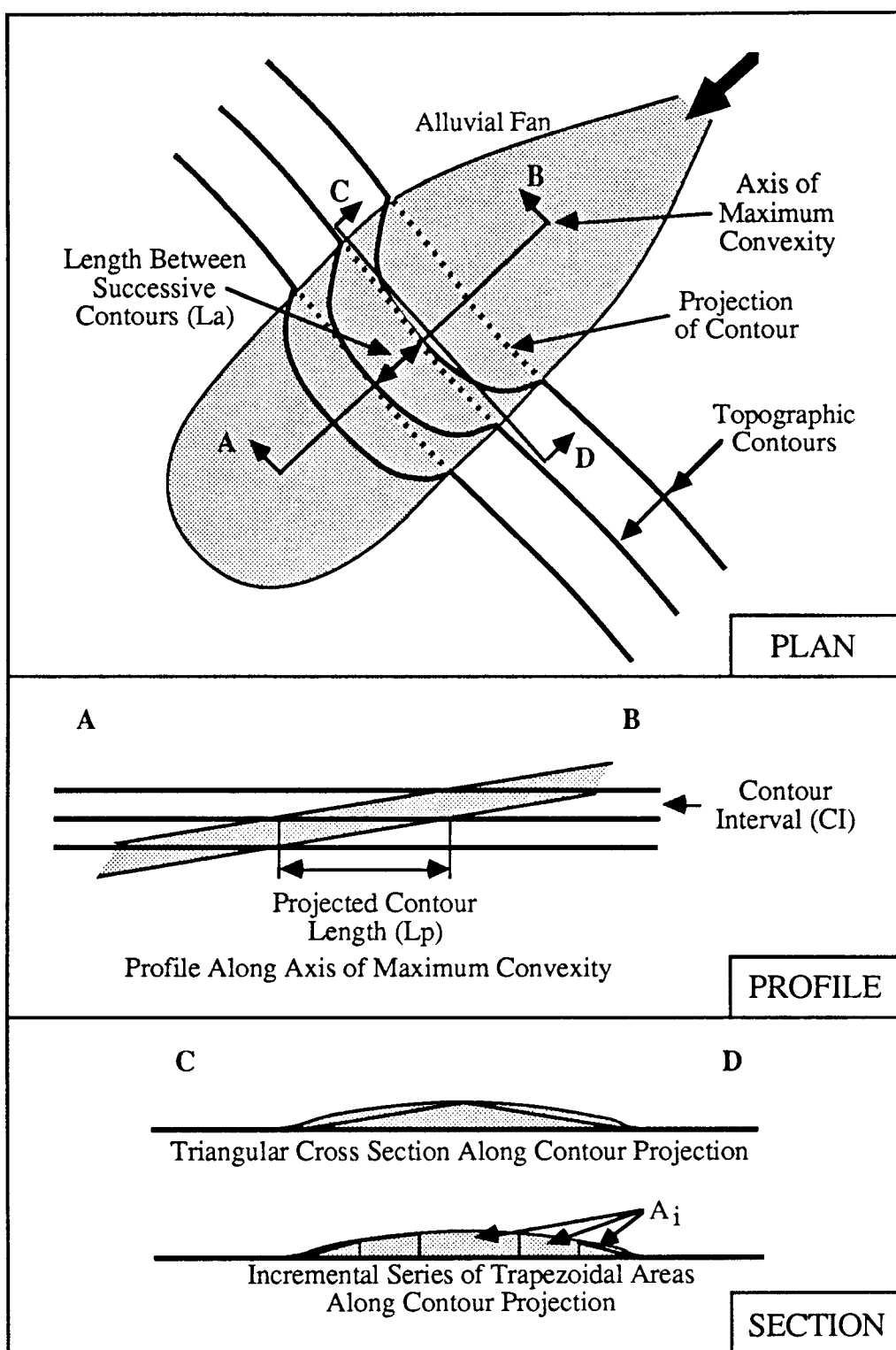


Figure 23. Schematic diagram showing components of alluvial-fan geometry used to compute fan volumes.

Rates of accumulation of alluvial-fan deposits were estimated on the basis of subaerial exposure beginning at the time Lake Bonneville receded past the apex and toe elevations of the fans. Pertinent data regarding ages of alluvial fans in Davis County are summarized in Table 15. Transgression of Lake Bonneville across the west-facing Davis County landscape was assumed to have been sufficiently vigorous to erode most preexisting alluvial-fan deposits. Assuming that storms affecting northern Utah in late Pleistocene time arrived from the west, as they do now, an effective 200-km long fetch length would have existed for the approximately 1 ka that Lake Bonneville occupied the Bonneville Shoreline. Thus all waves affecting the Davis County mountain front would have been duration-limited (Mathewson, 1981, p. 192). Sedimentation events in the Davis

Table 15. Pertinent age data regarding alluvial fans in Davis County.

Basin	Elevation (m) ^(a)		First Inundation (b) Of Toe Elevation (ka)	First Exposure (c) Of Apex Elevation (ka)	Complete Exposure (c) Of Toe Elevation (ka)
	Apex	Toe			
Corbett	1495	1400	22.1	15.0	13.1
Hobbs	1585	1500	19.0	15.0	15.0
Lightning	1585	1500	19.0	15.0	15.0
Kays (Middle)	1570	1485	19.5	15.0	15.0
Kays (South)	1565	1480	19.6	15.0	15.0
Snow	1525	1460	20.3	15.0	13.9
Adams	1525	1450	21.9	15.0	13.8
Webb	1520	1460	20.3	15.0	13.9
Baer	1475	1385	22.5	15.0	12.9
Half	1465	1420	21.5	14.0	13.4
Shepard	1465	1355	23.5	14.0	12.6
Farmington	1385	1300	25.1	12.9	11.8
Rudd	1365	1305	25.0	12.7	11.9
Steed	1385	1300	25.1	12.9	11.8
Davis	1350	1290	25.4	12.5	11.7
Halfway	1370	1320	24.5	12.8	12.1
Ricks	1370	1290	25.4	12.8	11.7
Barnard	1355	1295	25.3	12.6	11.8
Parrish	1370	1300	25.1	12.8	11.8
Centerville	1385	1305	25.0	12.9	11.9
Buckland	1450	1410	21.8	13.8	13.3
Ward	1435	1365	23.2	13.6	12.7
Mean	1454	1381	22.7	13.9	13.0
Standard Deviation	82	78	2.3	1.0	1.2

(a) Elevations based on 1:24,000-scale topographic maps.

(b) Transgression of Lake Bonneville based on time-altitude relationship by Currey and Oviatt (1985, p. 1091); $At = 64.42 - 0.03 (Et)$, where At is age in ka and Et is elevation of transgression in m.

(c) Recession of Lake Bonneville based on time-altitude relationship by Currey and Oviatt (1985, p. 1091); $Ar = 15$ ka for $Er > 1465$ m due to the Bonneville Flood; $Ar = -5.28 + 0.013 (Er)$ for $1465 \geq Er < 1275$, where Ar is age in ka and Er is elevation of recession in m.

County drainage basins during the high stand of Lake Bonneville were assumed to have been incorporated into and distributed by the littoral currents in the lake. A subaqueous debris-flow deposit was observed intercalated within sandy near-shore and silty deep water deposits at an elevation of about 1380 m in the Ricks Creek fan (location 12 on Figure 8). This deposit was overlain by fine sandy silt with ostracode fossils (*Candona* ?) interpreted to represent the white marl of Gilbert (1890) dating from the 16-ka old high stand of Lake Bonneville. The subaqueous debris flow underlying the ostracode-bearing layer represents a debris flow which occurred during the rise of Lake Bonneville to the Bonneville Shoreline. Other debris flows probably were derived from unstable shoreline sediments generated by the rapid drop of the lake level in response to the Bonneville Flood (Currey and others, 1984); however, evidence of such sedimentation events was not found during the examination of exposures in Davis County.

Rates of erosion in the drainage basins and deposition on the alluvial fans were computed from data summarized in Appendix D and Tables 8 and 15. The resulting rates presented in Table 16 were based on the time since first exposure of the apex of the fans and on the time since complete exposure of the toes of the fans. Erosion rates were calculated by normalizing the fan volumes to the respective drainage basin areas and then dividing by the time since Lake Bonneville receded past the apexes and toes. This calculation yields erosion rates in $\text{m}^3/\text{m}^2/\text{ka}$ or m/ka . The resulting average erosion rates, 0.017 ± 0.012 to 0.018 ± 0.013 m/ka , summarized in Table 16 are approximately 25 percent of the long-term erosion rate of 0.07 m/ka described above. Average deposition rates were calculated by normalizing the fan volumes to the respective fan areas and dividing by the time since Lake Bonneville receded past the fan apexes and toes. The resulting average deposition rates, 0.273 ± 0.114 to 0.291 ± 0.122 m/ka , summarized in Table 16 are not directly comparable to the long-term erosion rate because of differences in normalization (basin area versus fan area); however, the deposition rates as well as the erosion rates are based on estimated fan volumes and timing of Lake Bonneville recession, hence, they are equivalent values in different terms.

The estimated volumes of sediment produced in the drainage basins in the study area and delivered to the alluvial fans are summarized in Table 17. These volumes have been estimated by four different computations. A long-term average annual sediment volume was developed by multiplying the average long-term erosion rate by the drainage basin area. A Holocene average annual sediment volume was developed by dividing the fan volume by the time since Lake Bonneville retreated; 15 ka was used for the basins from Baer Creek to the north and 10 ka was used for the basins south of Baer Creek (these volumes collectively are called Holocene even though a pre-Holocene age of 15 ka is used for some of the basins). A late Holocene average annual sediment volume was developed by dividing the sum of historic sedimentation event volumes by 4 ka. A historic average annual sediment volume was developed by dividing the sum of the historic sedimentation event volumes by 140 yr. The large variability in the volumes estimated by the different methods is emphasized by the standard deviations reported in Table 17; for Holocene, late Holocene, and historic time periods, the standard deviations are larger than the mean values.

Historic Sedimentation Events

Settlement of Davis County began in 1847 and the first reported flood events were in 1878 (Woolley, 1946, Plate 22). A chronological listing of reported major cloudburst and snowmelt floods in Davis County is presented in Appendix A. Most of the reported flood events were accompanied by sedimentation on the alluvial fans at the mouths of the

Table 16. Summary of average erosion and deposition rates in Davis County. Erosion rates were computed by normalizing alluvial-fan volumes to drainage basin areas and dividing by time of recession of Lake Bonneville past fan apexes or fan toes. Deposition rates were computed by normalizing alluvial-fan volumes to alluvial-fan areas.

Basin	Erosion Rate (m/ka)		Deposition Rate (m/ka)	
	Apex Recession ^(a)	Toe Recession ^(b)	Apex Recession ^(a)	Toe Recession ^(b)
Corbett	0.006±0.002	0.007±0.003	0.147±0.060	0.168±0.069
Hobbs	0.006±0.002	0.006±0.002	0.273±0.107	0.273±0.107
Lightning	0.045±0.018	0.045±0.018	0.307±0.120	0.307±0.120
Kays (Middle)	0.010±0.004	0.010±0.004	0.287±0.113	0.287±0.113
Kays (South)	0.009±0.004	0.009±0.004	0.340±0.133	0.340±0.133
Snow	0.036±0.014	0.039±0.015	0.287±0.113	0.309±0.122
Adams	0.009±0.004	0.009±0.004	0.293±0.120	0.319±0.130
Webb	0.009±0.003	0.010±0.004	0.340±0.133	0.367±0.144
Baer	0.008±0.003	0.009±0.004	0.273±0.107	0.318±0.124
Half	0.008±0.003	0.009±0.004	0.314±0.129	0.328±0.134
Shepard	0.038±0.015	0.042±0.017	0.436±0.171	0.484±0.190
Farmington	0.032±0.017	0.035±0.019	0.636±0.349	0.695±0.381
Rudd	0.032±0.013	0.034±0.014	0.291±0.118	0.311±0.126
Steed	0.010±0.004	0.011±0.004	0.178±0.070	0.195±0.076
Davis	0.016±0.006	0.017±0.007	0.264±0.104	0.282±0.111
Halfway	0.006±0.002	0.007±0.003	0.180±0.070	0.190±0.074
Ricks	0.013±0.005	0.014±0.005	0.148±0.055	0.162±0.060
Barnard	0.019±0.008	0.020±0.008	0.175±0.071	0.186±0.076
Parrish	0.009±0.004	0.010±0.004	0.172±0.070	0.186±0.076
Centerville	0.024±0.010	0.025±0.011	0.225±0.093	0.244±0.101
Buckland	0.006±0.002	0.006±0.002	0.203±0.080	0.211±0.083
Ward	0.018±0.009	0.019±0.010	0.228±0.118	0.244±0.126
Mean	0.017±0.007	0.018±0.007	0.273±0.114	0.291±0.122
Standard Deviation	0.012±0.005	0.013±0.006	0.109±0.060	0.119±0.066

(a) Apex recession refers to recession of Lake Bonneville past the elevation of the apex of the alluvial fan; timing of recession with respect to elevation is presented in Table 15.

(b) Toe recession refers to recession of Lake Bonneville past the elevation of the toe of the alluvial fan; timing of recession with respect to elevation is presented in Table 15.

Table 17. Average annual sediment volumes for drainage basins and alluvial fans in Davis County.

Basin Name	Average Annual Sediment Volume, m ³			
	Long-Term ^(a)	Holocene ^(b)	Late Holocene ^(c)	Historic ^(d)
Corbett	236	19.1	0	0
Hobbs	227	18.9	0	0
Lightning	40	24.5	2.3	64.3
Kays (Middle)	309	41.9	0.4	10.7
Kays (South)	328	40.1	22.6	644.3
Snow	148	73.4	0	0
Adams	400	47.5	0	0
Webb	472	57.1	0.8	21.4
Baer	621	69.4	40.4	1154.3
Half	80	12.8	0	0
Shepard	435	31.6	3.8	107.1
Farmington	1982	1111.9	214.8	6137.1
Rudd	130	72.9	17.3	495.4
Steed	490	87.9	62.9	1796.4
Davis	313	87.1	44.1	1259.3
Halfway	119	12.9	0	0
Ricks	463	105.6	59.0	1685.7
Barnard	272	89.3	18.7	532.9
Parrish	398	61.6	109.1	3115.7
Centerville	595	247.1	0.5	14.3
Buckland	178	20.2	0	0
Ward	825	277.8	3.9	110.7
Mean	412	118.7	27.3	779.5
Standard Deviation	401	232.0	50.6	1446.9

(a) Basin area from Appendix D times the average long-term erosion rate of 0.073 m/ka (0.000073 m/yr).

(b) Fan volume from Table 14 divided by the age of the post-Lake Bonneville fan (15 ka from Baer Creek to the north, 10 ka south of Baer Creek).

(c) Volume of historic sedimentation events from Table 18 divided by 4 ka.

(d) Volume of historic sedimentation events from Table 18 divided by 140 yr.

canyons. The temporal distribution of flood events for each of the 22 drainage basins in Davis County which comprise the study area is shown on Figure 24. The cumulative number of reported flood events (77 events) in the study area since 1850 is presented on Figure 25. Woolley (1946, p. 121) notes the direct correlation of increasing population and increasing incidence of reported flood events. Some of the floods appear to have been clear water, judging from their descriptions which are summarized in Appendix A; therefore, not all flood events contributed significant amounts of sediment to the alluvial fans at the canyon mouths. Furthermore, reported flood events were considered only if specific reference was made to a canyon name or a community located in a position such that it could be flooded only by a specific canyon. Consequently, general references to wide-spread flooding (e.g., snowmelt flooding in 1922 and 1952) was not used in the analysis of flood events.

The largest number of reported flood events (14 events) was for Farmington Canyon, the largest of all the canyons in the study area; consequently, it was separated from the other canyons in the cumulative frequency plot shown on Figure 25. Curves are also presented on Figure 25 for the 10 canyons south of Farmington Canyon (38 events), and the 11 canyons north of Farmington Canyon (25 events). The 77 flood events reported in the 22-basin study area in the 140 years since settlement corresponds to an average report rate of 0.55 per year or an average recurrence of 1.8 years. The 14 events reported at Farmington Canyon corresponds to an average report rate of 0.10 per year or an average recurrence of 10 years. The 10-basin segment of the study area south of Farmington Canyon had a higher incidence of flood reporting than the 11-basin segment north of Farmington Canyon. Thirty-eight flood events were reported in the south area, corresponding to an average report rate of 0.27 per year or an average recurrence of 3.7 years. Twenty-five flood events were reported in the north area, corresponding to an average report rate of 0.18 per year or an average recurrence of 5.5 years.

The floods of 1930 prompted Governor Dern to appoint a commission to study the problem and make recommendations about protecting the communities, as discussed earlier. The response to the flooding included construction of sediment catch basins at the mouths of the canyons, acquiring the watersheds into public ownership (U.S. Forest Service), and creating contour trenches to promote infiltrating and inhibit runoff. The contour trenches were constructed beginning in 1934 in the upper parts of the watersheds from Farmington Canyon to Centerville Canyon. The effectiveness of these contour trenches is indicated on Figure 25 by the small number of reported flood events in the canyons south of Farmington Canyon between 1935 and 1982. The cumulative departure from mean precipitation at the Salt Lake City airport from 1875 to 1985 is presented on Figure 26. It can be seen that a deficit exceeding nearly 90 cm of precipitation existed from about 1935 to 1972. Thus, a paucity of precipitation could have contributed to the reduction in reported flooding. Nonetheless, 5-minute rainfall intensities measured at a gage in the upper part of Parrish Creek were 128.0 mm/hr on July 10, 1936, and 173.7 mm/hr on August 19, 1945 (Bailey and others, 1947, p. 16). The July 10, 1936 storm dropped 29.0 mm while 26.9 mm fell on August 19, 1945. Croft (1967, p. 6) reports a remarkable 5-minute rainfall intensity of 225.0 mm/hr in a storm with a total rainfall of 26.2 mm measured on August 10, 1947 at a gage at Rice Creek (one of the tributary drainages of Farmington Canyon).

Historic flood events are summarized in Table 18. The data in this table were compiled from a number of sources, and in most cases the volumes of sediment contributed to the fans is approximated on the basis of damage descriptions or proportioned to other canyons where flood events occurred in the same years. Data tabulated by Croft (1967, p. 16) provided information on total sediment delivery between 1923 and 1947, in most cases. In some cases, Croft (1967, p. 16) included volumes for specific years. The

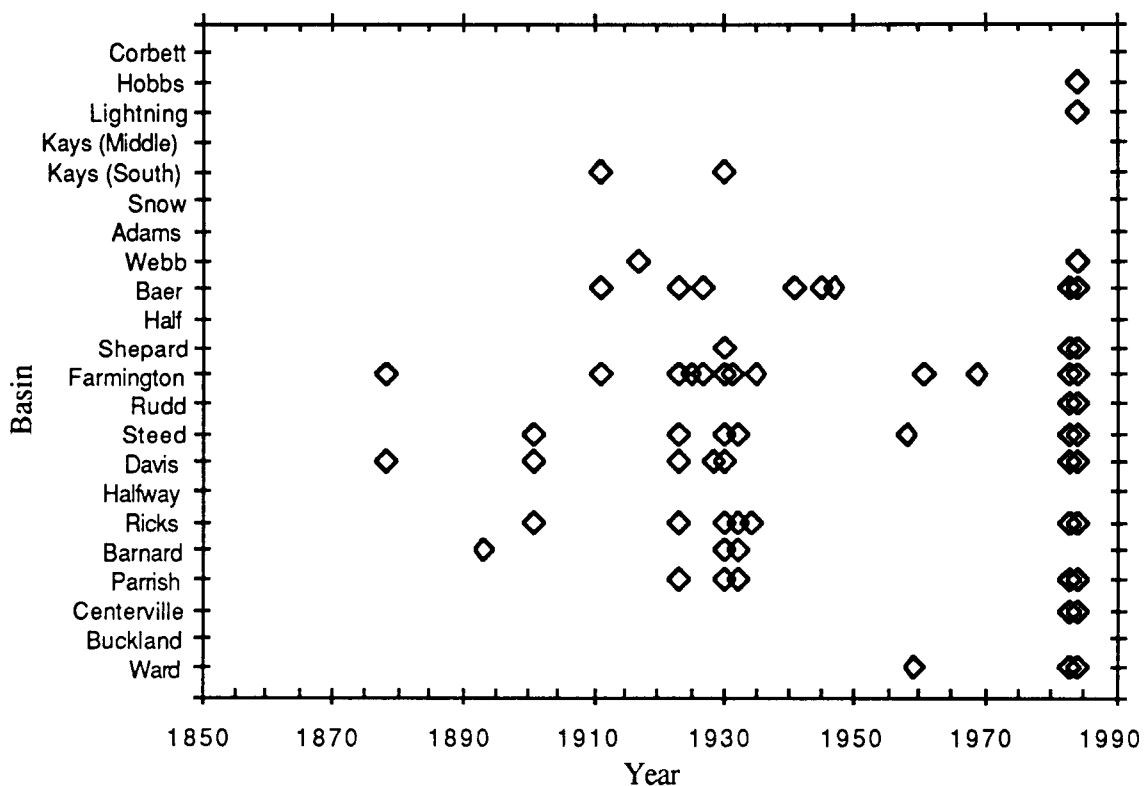


Figure 24. Temporal distribution of historic flood events in Davis County.

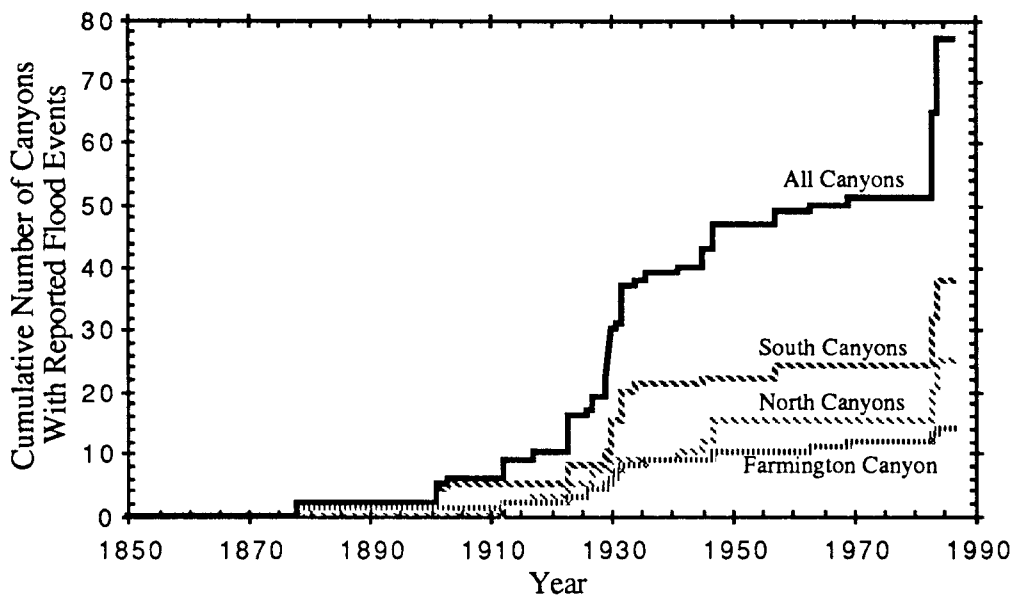


Figure 25. Cumulative number of historic flood events in Davis County. Curves are shown for all 22 canyons in the study area, the 10 canyons south of Farmington Canyon, the 11 canyons north of Farmington Canyon, and Farmington Canyon.

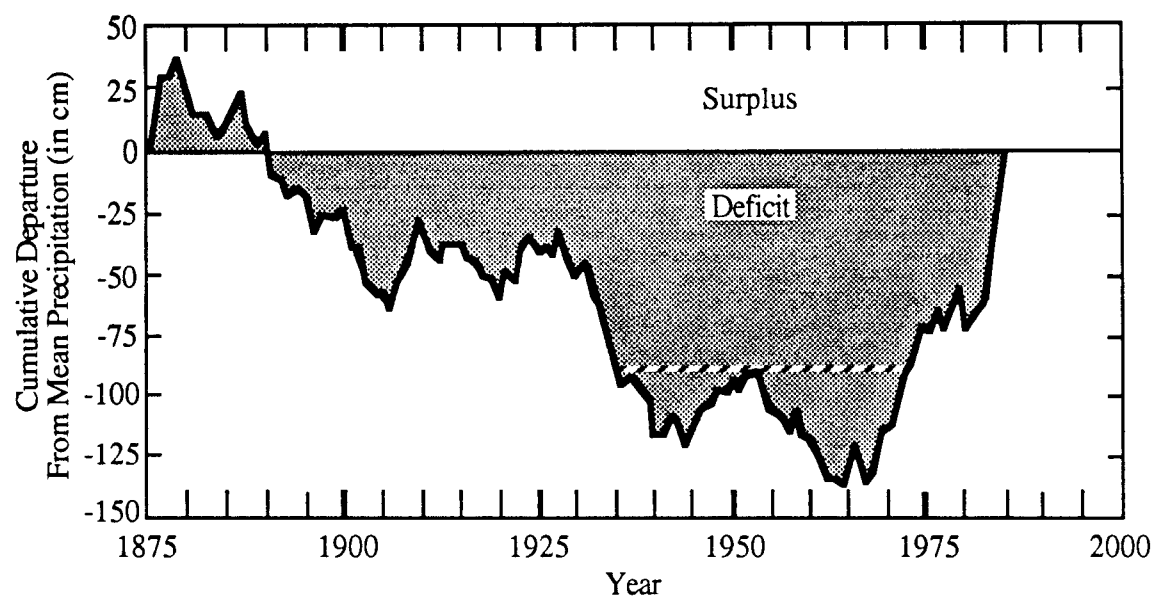


Figure 26. Cumulative departure from mean precipitation at Salt Lake City from 1875 to 1985. Dotted line from 1935 to 1972 marks 90 cm of precipitation deficit.

Table 18. Summary of historic flood events in Davis County from 1847 to 1987.

Basin	Year	Approximate Sediment Magnitude, M		References
		Volume, V (m ³)	(M = log V)	
Corbett	None Reported			
Hobbs	1984	---	---	Wieczorek and others, 1988
Lightning	1984	9,000	3.95	Olson, 1985; Mathewson and Santi, 1987
Kays (Middle)	1947	1,000	3.00	Wieczorek and others, 1983
	1983	500	2.70	Wieczorek and others, 1983
Kays (South)	1912	51,000	4.71	Croft, 1981
	1923	1,500	3.18	Wieczorek and others, 1983
	1927	1,200	3.08	Wieczorek and others, 1983
	1930	19,000	4.28	Croft, 1962, 1981
	1945	1,000	3.00	Croft, 1962; Wieczorek and others, 1983
	1947	16,000	4.20	Croft, 1962; Wieczorek and others, 1983
	1983	500	2.70	Wieczorek and others, 1983
Snow	None Reported			
Adams	None Reported			
Webb	1917	2,500	3.40	Woolley, 1946
	1983	500	2.70	Wieczorek and others, 1983
	1984	---	---	Wieczorek and others, 1988
Baer	1912	51,000	4.71	Croft, 1962, 1967, 1981
	1923	39,700	4.60	Croft, 1962, 1967, 1981
	1927	12,000	4.08	Croft, 1962, 1967, 1981
	1941	---	---	Butler and Marsell, 1972
	1945	24,000	4.38	Croft, 1962, 1967, 1981
	1947	32,500	4.51	Croft, 1962, 1967, 1981
	1983	2,400	3.38	Wieczorek and others, 1983
	1984	---	---	Wieczorek and others, 1988
Half	None Reported			
Shepard	1930	10,000	4.00	Woolley, 1946
	1983	5,000	3.70	Wieczorek and others, 1983
	1984	---	---	Wieczorek and others, 1988
Farmington	1878	100,000	5.00	Woolley, 1946
	1912	---	---	Woolley, 1946
	1923	528,000	5.72	Woolley, 1946; Croft, 1967
	1926	31,000	4.49	Woolley, 1946; Croft, 1967
	1929	40,000	4.60	Woolley, 1946; Croft, 1967
	1930	---	---	Woolley, 1946; Croft, 1967
	1931	61,700	4.79	Woolley, 1946; Croft, 1967
	1932	29,400	4.47	Woolley, 1946; Croft, 1967
	1936	23,100	4.36	Woolley, 1946; Croft, 1967
	1945	---	---	Bailey and others, 1947; Croft, 1967
	1947	10,000	4.00	Croft, 1967, 1981
	1963	---	---	Butler and Marsell, 1972
	1969	16,000	4.20	Butler and Marsell, 1972
	1983	20,000	4.30	Wieczorek and others, 1983
	1984	---	---	Wieczorek and others, 1988

Table 24. Continued.

Basin	Year	Approximate Sediment		Magnitude, M (M = log V)	References
		Volume, V (m ³)			
Rudd	1983	68,000	4.83	Vandre, 1983; Wieczorek and others, 1983	
	1984	1,350	3.13	Forbush, 1984, oral communication	
Steed	1901	—	—	Woolley, 1946	
	1923	156,200	5.19	Woolley, 1946; Croft, 1967	
	1930	53,000	4.72	Woolley, 1946; Croft, 1967	
	1932	26,300	4.42	Rigby, 1987, oral comm.; Woolley, 1946	
	1957	—	—	Butler and Marsell, 1972	
	1983	16,000	4.20	Wieczorek and others, 1983	
	1984	—	—	Wieczorek and others, 1988	
	Davis	1878	6,000	3.78	Woolley, 1946
1901		16,000	4.20	Woolley, 1946	
1903		—	—	Wieczorek and others, 1983	
1923		112,400	5.05	Woolley, 1946; Croft, 1967	
1929		12,000	4.08	Croft, 1967; Wieczorek and others, 1983	
1930		20,700	4.32	Woolley, 1946; Croft, 1967	
1932		8,700	3.94	Rigby, 1987, oral comm.; Woolley, 1946	
1983		500	2.70	Wieczorek and others, 1983	
1984		—	—	Wieczorek and others, 1988	
Halfway	None Reported				
Ricks	1901	—	—	Woolley, 1946	
	1923	72,000	4.86	Woolley, 1946; Croft, 1967	
	1929	—	—	Wieczorek and others, 1983; Rigby, 1987, oral	
	1930	100,000	5.00	Woolley, 1946; Croft, 1967	
	1932	34,000	4.53	Rigby, 1987, oral comm.; Woolley, 1946	
	1934	22,000	4.34	Bailey and others, 1947; Croft, 1967	
	1983	8,000	3.90	Wieczorek and others, 1983; Rigby, 1987, oral	
	1984	—	—	Wieczorek and others, 1988	
Barnard	1930	43,300	4.64	Woolley, 1946; Croft, 1967	
	1932	21,600	4.33	Rigby, 1987, oral comm.; Woolley, 1946	
	1983	9,700	3.99	Wieczorek and others, 1983	
Parrish	1930	402,000	5.60	Woolley, 1946; Croft, 1967	
	1932	33,000	4.52	Rigby, 1987, oral comm.; Wooley, 1946	
	1983	1,600	3.20	Wieczorek and others, 1983	
	1984	—	—	Wieczorek and others, 1988	
Centerville	1983	2,000	3.30	Wieczorek and others, 1983	
Buckland	None Reported				
Ward	1957	—	—	Butler and Marsell, 1972	
	1983	15,500	4.19	Wieczorek and others, 1983	
	1984	—	—	Wieczorek and others, 1988	
Total Flood Events		77			
Total Sediment Volume		2,401,350			

volume of sediment delivered to the fans was taken as a measure of the size of the flood event. The logarithm of sediment volume in cubic meters normalized to a unit volume is used as the magnitude of the flood event.

Prehistoric Sedimentation Events

The alluvial fans studied as part of this research were deposited on, and therefore are younger than, sediments of Lake Bonneville. Evidence of prehistoric sedimentation events is contained in the stratigraphic record which is poorly exposed and the geomorphic expression of the fans which is largely obscured by urbanization, mining of sand and gravel resources, and construction of debris basins. A uniquely preserved and exposed alluvial fan is located at the mouth of Ricks Creek. Erosion caused by the floods of 1930 exposed the stratigraphy of the fan in several locations below the Wasatch fault and much of the fan is currently undeveloped.

Erosion in 1983 exposed the stratigraphy of the fan at Rudd Creek above the Wasatch fault; however, most of this fan has been used for urban development and a substantial portion of it was altered during construction of a debris basin in 1983. Croft (1962) discussed the characteristics of prehistoric sedimentation events at Baer Creek, but this fan has been extensively developed also. Personius (1987, written communication) mapped post-Lake Bonneville deposits at the mouths of all of the canyons in the study area as part of the U.S. Geological Survey Earthquake Hazard Reduction Program. The fan at Ricks Creek is uniquely preserved, in the sense that it is not totally developed, and uniquely created, in the sense that diversion of Ricks Creek along the Wasatch fault near the apex of the fan caused subsequent sedimentation events to be deposited without obscuring the evidence of the earlier events. Consequently, the Ricks Creek fan proved to be an exceptional resource for this research and is discussed in detail below.

Substantial volumes of frost-shattered and solifluction rock debris undoubtedly were produced in the Wasatch Range by the alpine glacial climate which must have existed in late Pleistocene time when Lake Bonneville achieved its maximum extent (Madsen and Currey, 1979). Geomorphic evidence of small cirque glaciers exists on east-facing slopes in Farmington Canyon at Bountiful Peak (elevation 2820 m) and east of Webb Canyon (elevation 2860 m). Thus, substantial volumes of sediment extremely susceptible to sheet erosion probably existed in the drainage basins in the study area at the time Lake Bonneville was receding at its most rapid rate.

Reconstructions of the paleoclimate have been based on the effects of variations in the earth's orbit on irradiated solar energy (Bradley, 1985, p. 39). Systematic evaluation of changes in solar energy and its potential effects on paleoclimate were first assessed by Milutin Milankovitch beginning in 1912 (Imbrie and Imbrie, 1979, p. 97 ff). Deviations of solar irradiation from their 1950 values at 40° north latitude, one degree south of the study area, have been summarized by Benson (1986, p. 19). The summer deviation, shown on Figure 27, shows a small negative deviation approximately 23 ka ago and a large positive deviation approximately 11 ka ago. Studies of the physiology and biogeography of *Quercus gambelii* and *Quercus turbinella* in Utah, Arizona, New Mexico, and Colorado have indicated that "the northernmost populations of these species were established under a climate with greater summer precipitation than the current climate" (Neilson and Wullstein, 1985, p. 269). Neilson and Wullstein (1985, p. 269) further suggest that an expansion of the "Arizona Monsoon" during the early- to mid-Holocene Hypsithermal interval of Deevey and Flint (1957) could have provided the conditions needed for their establishment. Thus, a summer "monsoon" climate, with vigorous convective cloudburst storms, probably accompanied the Milankovitch-type summer insolation abnormality (Figure 27). The

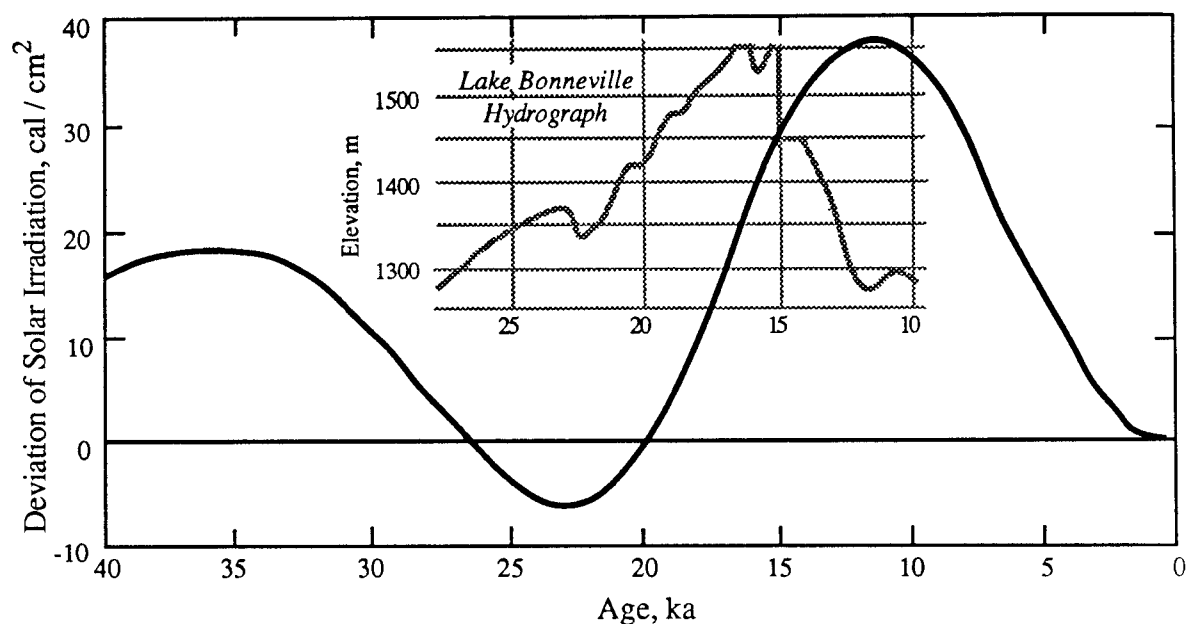


Figure 27. Deviation of summer solar irradiation from 1950 value at 40° North Latitude. Irradiation curve is modified from Benson (1986, p. 19). For comparison, the Lake Bonneville hydrograph, modified from Currey and Oviatt (1985, p. 1091), is also presented. The peak of Lake Bonneville at about elevation 1550 m is the Bonneville level; the bench at about elevation 1450 m is the Provo level; the minor peak at about 1280 m is the Gilbert level.

combination of easily eroded material and frequent, intense convective cloudburst storms would be expected to cause major accumulations of sediment on the alluvial fans in Davis County.

The rise of Lake Bonneville to the Gilbert Shoreline (elevation 1290 m) approximately 10.5 ka ago (Currey and Oviatt, 1985, p. 1091) probably was caused by the vigorous summer monsoon climate that accompanied the Milankovitch-type summer insolation abnormality (Figure 27). The details of the Holocene history of the ancestral Great Salt Lake are not clearly understood, but Currey and others (1984) postulate decline to near playa conditions in early- to mid-Holocene time. Thus, following a possibly brief period of intense sediment production in earliest Holocene time, during which most of the available sediment may have been stripped from the slopes in the drainage basins, the climate in Davis County may have moderated, resulting in conditions favorable for weathering of the bedrock and production of colluvial material on the slopes. Such a sequence of events would suggest major sediment production immediately following the decline of Lake Bonneville with only minimal mid- to late-Holocene sedimentation in Davis County.

Ricks Creek Fan

The Ricks Creek fan is situated on the downthrown side of the Wasatch fault zone, as shown on Figure 28. The geomorphology, stratigraphy, and modern history of this fan

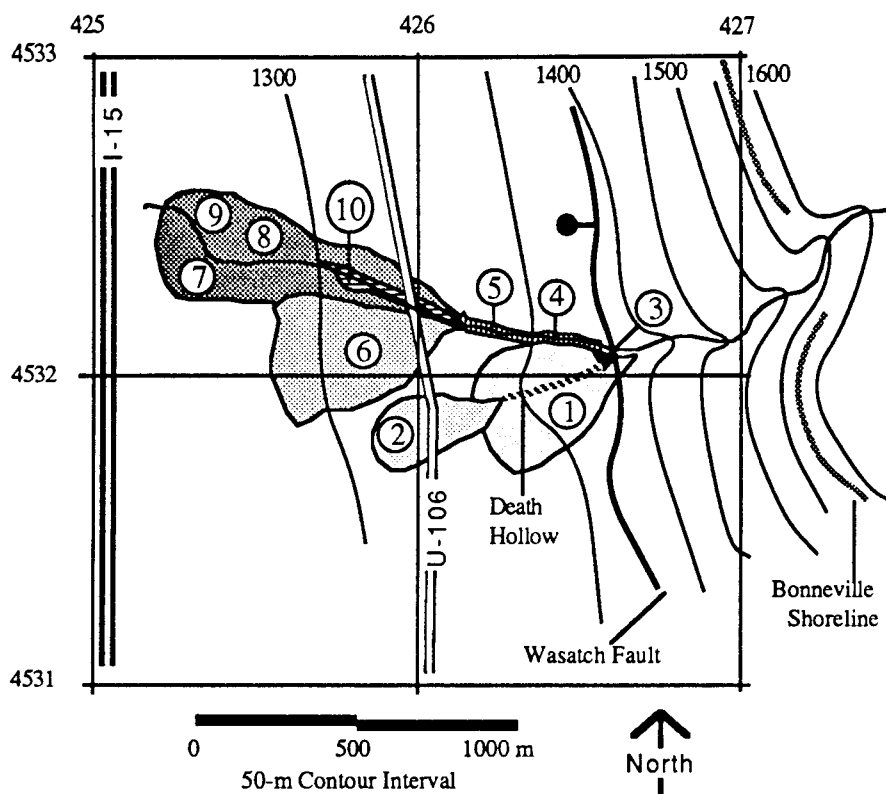


Figure 28. Geomorphic map of the Ricks Creek fan. Circled numbers represent sequential sedimentation events for five prehistoric post-Lake Bonneville events (1 - 5) and five historic events (6 - 10). The abandoned channel of Ricks Creek is identified as Death Hollow. A prehistoric sedimentation event intercalated within Lake Bonneville stratigraphy is not identified on this figure (see text for discussion). Grid numbers are Universal Transverse Mercator Zone 12 coordinates shown as km.

indicate that it was constructed by 10 major sedimentation events, five of which occurred during historic time. The historic events are listed in Table 18. Detailed mapping of the alluvial fan (Figure 8) revealed deposits of one subaqueous debris flow and probably five prehistoric post-Bonneville sedimentation events. The subaqueous debris-flow deposits are interbedded in deposits of Lake Bonneville. They are overlain by clean, stratified fine to coarse sand and a layer of ostracode-bearing fine sandy silt. The fine sandy silt is interpreted to represent the deep-water deposit of Lake Bonneville which Gilbert (1890) named the White Marl. Thus, the subaqueous debris-flow is interpreted to have occurred prior to the rapid 108-m drop in the level of Lake Bonneville from the Bonneville Level to the Provo Level approximately 15 ka ago (Currey and Oviatt, 1985, p. 1091). Exposure of lacustrine shore facies between the Bonneville and Provo levels of the lake would have contributed an abundance of sand to the littoral currents, explaining the stratified sand above the subaqueous debris-flow deposits and the ostracode-bearing layer.

Test pit excavations on the largest fan surface penetrated the debris-flow deposits and exposed lacustrine sand at an average depth of about 2 m (Appendix B). The test pit data confirmed an interpretation that the debris-flow deposits were thin based on exposures on the south side of the Ricks Creek channel approximately 200 m west of the Wasatch fault.

The oldest post-Lake Bonneville alluvial-fan sedimentation event appears to have been the largest. Sediment from this event apparently issued from the mouth of Ricks Creek canyon and covered a 0.166-km² area. If older subaerial deposits had existed at Ricks Creek, they were completely masked by this event. Four boulder fronts were observed at locations shown on Figure 8, indicating that this sedimentation event consisted of four or five surges or pulses. The volume of this part of the fan was estimated using the procedure outlined earlier in this chapter and found to be 315,000±129,000 m³.

The soil developed on the oldest fan segment consists of an A-C profile and is part of the Kilburn series (Erickson and others, 1968) and is described in Table 19. This soil series is classified in the 1938 system as a Zonal soil Order and the Brunizems great group (Erickson and others, 1968). The current soil taxonomy classification system, this soil is in the Mollisols order, Typic Haploxerolls subgroup, and the loamy-skeletal, mixed, mesic family (Erickson and others, 1968). The degree of soil development observed in the test pit exposures was uniform across the oldest post-Lake Bonneville fan and on fan deposits of clearly younger relative ages. The uniformity of the soil and the absence of soils formation on contacts separating deposits within the alluvial fan suggests that massive, rapid sedimentation was followed by an extensive period of landscape stability, during which the soil developed.

Table 19. Description of soil formed on the Ricks Creek fan surface.

Horizon	Depth (cm)	Description
A1	0 - 15	Very dark brown (10YR 2/2m) to very dark grayish brown (10YR 3/2m) silty coarse sand with gravel; very fine granular structure; friable; very slightly sticky; very slightly plastic; abundant fine roots; gradual smooth boundary.
A2	15 - 35	Very dark brown (10YR 2/2m) to very dark grayish brown (10YR 3/2m) gravelly silty coarse sand; weak, fine granular structure; friable; nonsticky; nonplastic; few fine roots; gradual smooth boundary.
C2	35 - 70	Dark yellowish brown (10YR 3/4 to 4/4m) gravelly silty coarse sand; massive; friable; nonsticky; nonplastic; few fine pores; gradual smooth boundary.
C3	70 - 100+	Dark yellowish brown (10YR 4/4m) to yellowish brown (10YR 5/6m) cobbly gravelly silty sand; friable; nonsticky; nonplastic; few fine pores.

Prominent levees containing the largest boulders present on the fan surface are preserved along the flanks of the abandoned prehistoric channel of Ricks Creek which local residents call Death Hollow (Mr. Rulon Ford, 1987, oral communication). The confining levees along Death Hollow resulted in a downfan shift in sedimentation for the second post-Lake Bonneville event. An intersection point was created in Death Hollow approximately 375 m west of the Wasatch fault zone, downslope from which a 0.062-km² fan was deposited. This fan probably was composed in part of reworked sediment eroded from the channel of Death Hollow, but erosion from Ricks Creek drainage basin undoubtedly also contributed to the volume of the fan which is estimated to be approximately 118,000±45,000 m³. The degree of soil development observed in a test pit excavated in this fan was the same as observed elsewhere and described in Table 19, suggesting that the deposits are approximately the same age.

The side slopes of the Death Hollow stream channel probably were relatively steep while Death Hollow was the active channel of Ricks Creek. Following the abandonment of Death Hollow, the side slopes gradually degraded to their present configurations. Scarp degradation rates have been evaluated extensively since 1977, with particular emphasis on fault scarps (Wallace, 1977; Bucknam and Anderson, 1979; Colman and Watson, 1983; Nash, 1980, 1984, 1986; Hanks and others, 1983; Hanks and Wallace, 1986; Pierce and Colman, 1986). Scarp degradation models are based on the concept that the rate of elevation change is proportional to the rate of accumulation of sediment. This can be expressed mathematically as

$$\partial y/\partial t = \partial(r)/\partial x + \partial(r)/\partial y + \partial(r)/\partial z = \nabla(r) \quad (76)$$

$\partial y/\partial t$ is the rate of change of elevation, and $\nabla(r)$ is the difference between the mass entrance rate and the mass exit rate, or the rate of accumulation. Assuming conservation of mass, this concept indicates that slope segments will decline in elevation if more mass leaves than enters, and conversely, slope segments will increase in elevation if more mass enters than leaves. Uniform segments of scarps can be found such that topographic curvature is restricted to profiles and mass movement is restricted to the x-y plane, or

$$\partial(r)/\partial y = \partial(r)/\partial z = 0 \quad (77)$$

Therefore, at specific locations along scarps, away from the influence of gullies or ridges,

$$\partial y/\partial t = \partial(r)/\partial x \quad (78)$$

Nash (1980, p. 354) notes that field and theoretical studies indicate that the rate of debris transfer on a hillslope is proportional to the sine of the slope angle, or

$$r = c \cdot \sin \theta \approx c \cdot \tan \theta \quad (79)$$

where c is a constant of proportionality and θ is the slope angle; for small values of θ , $\tan \theta \approx \sin \theta$. Furthermore,

$$\tan \theta = \partial y/\partial x \quad (80)$$

Therefore,

$$\partial y/\partial t = \partial(c \cdot \tan \theta)/\partial x = \partial(c \cdot \partial y/\partial x)/\partial x = c \cdot \partial^2 y/\partial x^2 \quad (81)$$

which is the diffusion equation where c is the rate coefficient. This equation states that the rate of change of elevation ($\partial y/\partial t$) at any point on a profile is proportional to the curvature ($\partial^2 y/\partial x^2$) of the profile at that point. Positive curvatures correspond to concave upward profile segments and elevations will increase. Similarly, negative curvatures correspond to convex upward profile segments and elevations will decrease.

Pierce and Colman (1986, p. 874) assumed a rectilinear profile at the angle of repose of the slope material and developed an analytical solution for equation 81 using previously developed relationships in Colman and Watson (1983)

$$c \cdot t = \{H_s/[4 \cdot \tan \alpha \cdot \text{erf}^{-1}(\tan \theta / \tan \alpha)]\}^2 \quad (82)$$

where c is the rate coefficient or diffusivity, t is time since diffusion processes began, H_s is the height of the scarp, α is the angle at which diffusion processes begin (assumed to be the angle of repose), θ is the maximum slope angle, and $\text{erf}^{-1}()$ is the inverse error function. The inverse error function is the argument which has an error function equal to the value in parentheses, where

$$\text{erf}(\beta) = (2/\sqrt{\pi}) \int_0^\beta e^{-\epsilon^2} d\epsilon \quad (83)$$

Thus,

$$\beta = \text{erf}^{-1} \{ (2/\sqrt{\pi}) \int_0^\beta e^{-\epsilon^2} d\epsilon \mid 0 \leq \epsilon \leq \beta \} \quad (84)$$

The error function is well behaved and $0 \leq (\tan \theta / \tan \alpha) \leq 1.0$. A polynomial regression with the error function as the independent variable was developed with StatView (by BrainPower, Inc.) on a Macintosh 512K personal computer and revealed

$$\beta = -0.00008 + 0.913 \text{erf} - 0.571 \text{erf}^2 + 4.649 \text{erf}^3 - 16.233 \text{erf}^4 \\ + 30.889 \text{erf}^5 - 29.168 \text{erf}^6 + 11.131 \text{erf}^7 \quad (r^2 = 1; n = 32) \quad (85)$$

The values of β predicted with equation 85 were found to be virtually identical to values developed with the iterative, converging algorithm used by Pierce and Colman (1986) for solving the inverse error function (Colman, 1988, written communication). Thus, equation 82 can be rewritten as

$$c \cdot t = \{H_s/[4 \cdot \tan \alpha \cdot \beta]\}^2 \quad (86)$$

Pierce and Colman (1986) evaluated the influence of height and orientation on the diffusivity, c , in the diffusion-equation model described above. They found that higher scarps degrade faster than lower scarps and that south-facing scarps degrade faster than north-facing slopes. Pierce and Colman (1986, p. 878) evaluated scarp height-maximum slope angle data for east- or west-facing Lake Bonneville shoreline scarps known to be about 15 ka old and developed an apparent diffusivity of

$$c^* = 0.303 + 0.135 H_s \quad (87)$$

where c^* is the diffusivity in m^2/ka corrected for the effect of height, H_s . This relationship was taken to represent the diffusivity for slopes with northwest aspects because it plots between the diffusivity relationships for north-facing scarps and due west-facing scarps shown by Pierce and Colman (1986, p. 880) for late-glacial terrace scarps in Idaho. Thus, equation 83 was used to develop values of c^*_{NW} . A relationship presented by Pierce and Colman (1986, p. 880) for diffusivities of south-facing slopes was compared to the relationship for northwest- to west-facing slopes. The ratio of diffusivities for south-facing slopes (assumed to be valid also for southeast-facing slopes) was found to be greater than the values for northwest- to west-facing slopes by a linear relationship with H_s

$$c^*_{\text{SE}}:c^*_{\text{NW}} = 1.420 + 0.057 H_s, \quad (r^2 = 0.788, n = 4) \quad (88)$$

Thus, the diffusivities for southeast-facing slopes can be expressed as the product of equation 87 and 88, or

$$c^*_{\text{SE}} = 0.430 + 0.209 H_s + 0.008 H_s^2 \quad (89)$$

The diffusion-equation model was applied to six profiles of the Death Hollow channel (Figure 29) measured in the field with a 1-m long rigid frame to which a circle level was attached (a Slope-A-Scope; Lips and Keaton, 1988). Three profiles were on northwest-facing slopes and three were on southeast-facing slopes. The relationships between maximum slope angle, θ , and slope height, H_s , are shown on Figure 30. A BASIC program called SCARP.DIF written to solve the diffusion-equation model for scarp

ages is presented in Appendix G. The results of the diffusion-equation model using the Death Hollow profile data are summarized in Table 20. The estimated age of the scarps forming the Death Hollow channel based on the diffusion-equation model is 10.5 ± 1.8 ka.

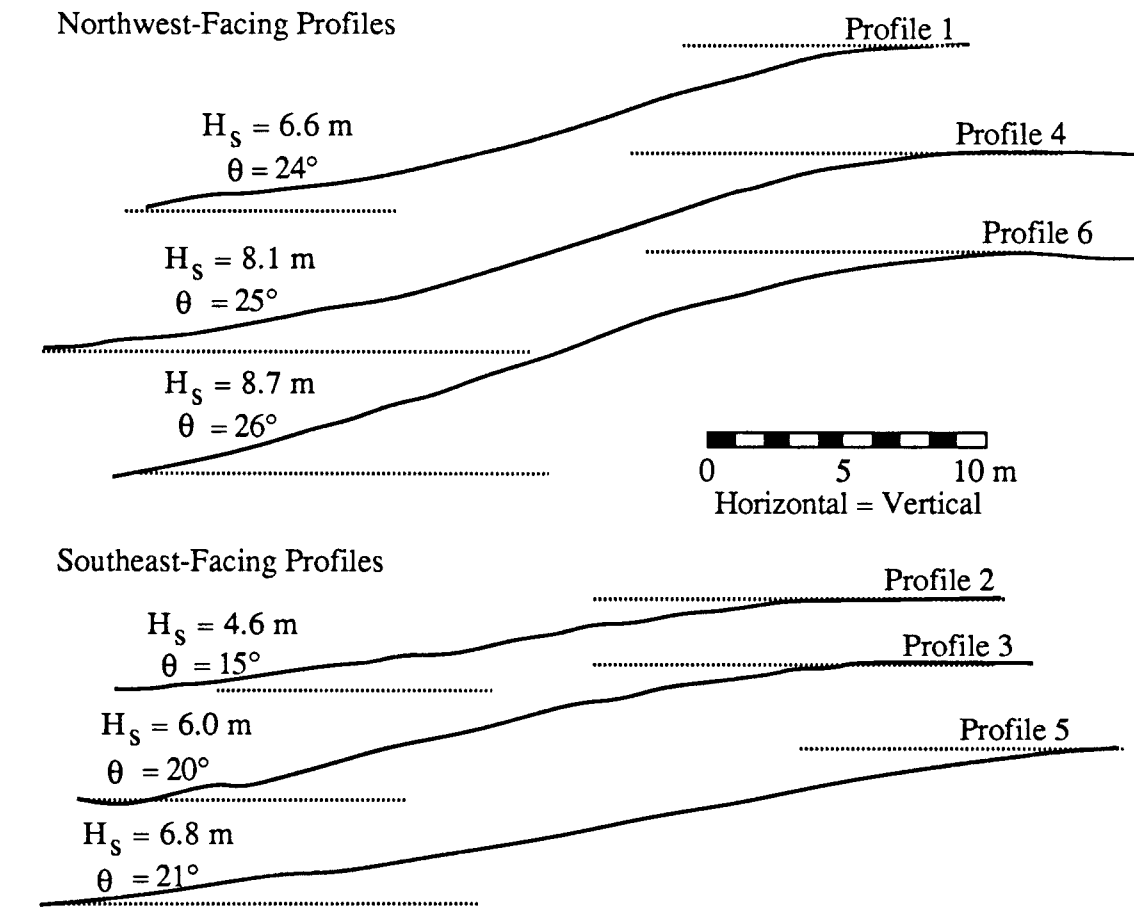


Figure 29. Profiles of Death Hollow channel slopes. Slope height, H_s , and maximum slope angle, θ , are indicated for each profile; profiles are grouped into two principal facing directions.

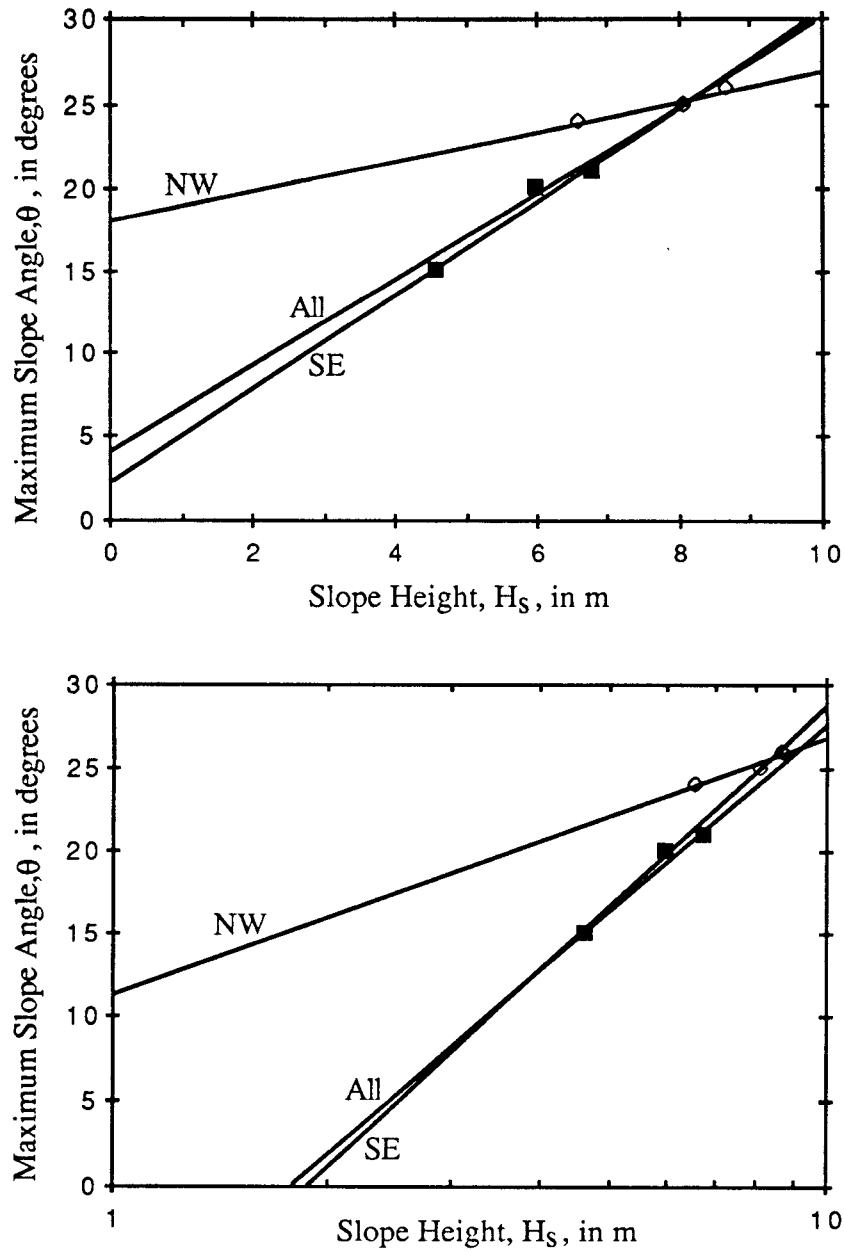


Figure 30. Relationships between maximum slope angle and slope height. Abbreviations NW signifies northwest slope aspect, SE signifies southeast aspect, All signifies both aspects combined. Upper diagram uses arithmetic expression of height while lower diagram uses a logarithmic transformation of height. Regression equations:

$$\begin{aligned} \theta_{All} &= 4.2 + 2.6 H_s \quad (r^2 = 0.88, n = 6); & \theta_{All} &= -10.6 + 39.4 \log H_s \quad (r^2 = 0.91, n = 6); \\ \theta_{NW} &= 18.0 + 0.9 H_s \quad (r^2 = 0.94, n = 3); & \theta_{SE} &= 2.3 + 2.8 H_s \quad (r^2 = 0.96, n = 3); \\ \theta_{NW} &= 11.2 + 15.5 \log H_s \quad (r^2 = 0.93, n = 3); & \theta_{SE} &= -9.1 + 36.6 \log H_s \quad (r^2 = 0.97, n = 3). \end{aligned}$$

Table 20. Geomorphic parameters of the Death Hollow channel used in the diffusion-equation model. The parameters of aspect, H_s , and θ were measured in the field; the parameters erf^{-1} , c^*t , c^*_{NW} , and c^*_{SE} were calculated using equations 85, 86, 87, and 89, respectively; the value of t was computed by dividing c^*t by c^*_{NW} or c^*_{SE} , depending on the aspect of the slope. A value of 31.5° was used as α , the starting angle for diffusion processes.

Profile	Aspect	Slope Height	Maximum Slope		c^*t	c^*_{NW}	c^*_{SE}	t
		H_s , m	Angle, θ°	$\text{erf}^{-1}(\tan \theta / \tan \alpha)$	m^2	m^2/ka	m^2/ka	ka
1	Northwest	6.6	24	0.77428	12.093	1.194	---	10.1
2	Southeast	4.6	15	0.40911	21.041	---	1.554	13.5
3	Southeast	6.0	20	0.58758	17.354	---	1.961	8.8
4	Northwest	8.1	25	0.83225	15.765	1.397	---	11.3
5	Southeast	6.8	21	0.62933	19.432	---	2.207	8.8
6	Northwest	8.7	26	0.89776	15.630	1.478	---	10.6
Mean		6.8	21.8	0.68839	16.886	1.356	1.907	10.5
Standard Deviation		1.47	4.07	0.18086	3.155	0.146	0.330	1.8

This age represents the approximate age since diffusion processes began and the actual age of abandonment of the channel is older by the time required for the scarps to degrade to the angle of repose. The angle of repose was taken to be 31.5° because this value was required to reproduce an example of scarp degradation presented by Pierce and Colman (1986, p. 869) using the SCARP.DIF program in Appendix G. An age of 10 ka was used in subsequent analyses. Therefore, the oldest and second oldest fans at Ricks Creek (Figure 28) apparently are slightly older than 10 ka and the younger prehistoric fans at Ricks Creek are slightly younger than 10 ka.

The third major sedimentation event (number 3 on Figure 28) apparently was a debris flow which came down Ricks Creek, crossed the Wasatch fault zone, and plugged the upper part of Death Hollow, preventing subsequent flows from flowing down Death Hollow. The diversion of Ricks Creek probably was caused by one of the three surface faulting earthquakes reported by Schwartz and others (1983) from the trench site in central Davis County, approximately 10 km north of Ricks Creek. The surface faulting event probably occurred some period of time before the third major sedimentation event to permit a substantial channel to form because the plug in Death Hollow does not appear to be sufficiently massive to have diverted the trailing portion of a major debris flow. Additionally, no additional deposits were observed in the vicinity of the plug in Death Hollow which would suggest that the plug was responsible for the diversion. Consequently, some relief must have existed in Ricks Creek along the trace of the Wasatch fault zone at the time of the sedimentation event to contain virtually all of the sediment except the small portion which was deposited as a plug in Death Hollow. An excavation (Test Pit 8 in Appendix B) in the plug near the precipitous slope on the southwest side of Ricks Creek exposed soils with approximately the same degree of development as other exposures elsewhere at Ricks Creek (Table 19). Therefore, on the basis of degree of soil development, all deposits on the upper surface of the Ricks Creek fan appear to be about the same age. This observation supports the conclusion based on paleoclimatic arguments that major sedimentation occurred shortly following the decline of Lake Bonneville in latest Pleistocene or earliest Holocene time, and the 10-ka age estimated from diffusion-equation

modeling of the Death Hollow scarps appears to be corroborated. The volume of the third prehistoric sedimentation event is estimated to be $183,000 \pm 64,000 \text{ m}^3$. This event is considered to have been relatively large by the character of the sediment in the plug and the presence of a megaclast which exceeded 2.5 m (Location 13 on Figure 8 and Appendix B). This event must have nearly filled the channel of Ricks Creek diverted along the Wasatch fault and spilled onto the plain beyond the fan. Subsequent prehistoric and historic sedimentation events eroded the deposits of the third event which were left in the channel and buried and reworked the deposits at lower elevations.

Exposures within the incised channel of the modern Ricks Creek approximately 200 m west of the Wasatch fault zone reveal deposits of two sedimentation events preceding the first historic sedimentation event in 1923 (see Appendix A). Location 7 exposes lacustrine sand unconformably overlain by matrix- to clast-supported transitional flow sandy gravel with cobbles which is unconformably (?) overlain by matrix- to clast-supported transitional flow sandy gravel (see Appendix B). The ground surface above Location 7 is a levee created in 1923. The two transitional flow deposits have distinctly different character, as demonstrated by the data presented in Appendix B and C; therefore, they are interpreted to represent different sedimentation events. The relationship between the 1923 levee and the sandy gravel at Location 7 is uncertain. The thickness of the sandy gravel is greater at Location 7 than the thickness of the 1923 deposits elsewhere at Ricks Creek; therefore, the sandy gravel is interpreted to represent the deposit of an independent sedimentation event. The fourth and fifth prehistoric sedimentation events at Ricks Creek were estimated to have volumes of $118,000 \pm 45,000$ and $80,000 \pm 20,000 \text{ m}^3$, respectively. Deposits of these sedimentation events have been eroded, buried, and/or reworked by subsequent historic events, and possibly by prehistoric events for which evidence was not discovered.

The 1923 sedimentation event at Ricks Creek was described by Pack (1923) and Paul and Baker (1925). Local resident Mr. Rulon Ford (1987, oral communication) recalled that the 1923 flood extended to the Bamberger railroad tracks, approximately 600 m west of the intersection point of the fan, with a width ranging from 20 to 40 m and a thickness of 1.5 to 3 m. These dimensions yield an estimated volume of 18,000 to 72,000 m^3 . Data presented by Croft (1967, p. 16) suggest that the larger value may be the more accurate. Approximately 2 m of erosion occurred in Ricks Creek above the intersection point in 1923, cutting a small canal used to divert water for irrigation. The canal was repaired by suspending a pipe across Ricks Creek, and Mr. Wesley Ford (1987, oral communication) recalled that the pipe could be reached by a person of average height (1.8 m) standing in the channel of Ricks Creek.

Mr. Rulon Ford described cattle and sheep herding on the slopes of the Wasatch Range in Davis County before the land was acquired into the public domain. He recalled that prior to 1923 the sheep herders cut brush and burned the watersheds to protect the sheep's wool. Burned and charred oak branches were found underlying the 1923 deposits within the incised channel of Ricks Creek at Location 11 (see Figure 8). Pickford (1932, p. 171) noted that promiscuous burning and heavy grazing in the Wasatch Range depleted about 85 percent of the perennial grasses and 80 percent of the sage brush cover.

Wieczorek and others (1983, Table 1) report that a debris flow occurred at Ricks Creek in 1929. This event is listed as a reported flood event in Table 18; however, it is not given a sediment volume because none of the local residents interviewed during this research mentioned such a sedimentation event in 1929. Woolley (1946) mentions sediment discharge from Davis Canyon in 1929 (see Appendix A) but makes no mention of Ricks Creek.

A series of four sedimentation events occurred at Ricks Creek in 1930. Mr. Wesley Ford described the events as being similar to the 1923 sedimentation event with the exception that the sediment was dominated by sand, and the last of the major floods was chiefly water. The sediment apparently spread over a greater area, but was generally thinner than the 1923 event. The dominant feature of the 1930 events was approximately 15 m of erosion in the incised part of Ricks Creek about 200 m west of the Wasatch fault. The channel of Ricks Creek cut into the easily eroded lacustrine sand deposit and contributed to the dominance of sand in the sedimentation event. The ability of the flow to erode probably was related to an assumed absence of available debris in the drainage basin due to the 1923 sedimentation event. The 1930 sedimentation deposits were removed or modified by human activities below the intersection point of the fan; above the intersection point, no 1930 deposits were preserved probably because of the sloughing of the steep slopes in the lacustrine sand as well as the fluid character of the flow. Data presented by Croft (1967, p. 16) suggests that the 1930 deposition probably amounted to about 100,000 m³.

Mr. Bill Rigby (1987, oral communication) commented that most of the drainage basins from Parrish Creek to Farmington Canyon experienced sediment discharge in 1932. Bailey and others (1947, p. 16) reported boulders up to 2.75 m long being carried onto the Ricks Creek fan in 1934. Croft (1967, p. 16) reported a total sediment delivery at the Ricks Creek fan of 228,000 m³ between 1923 and 1947. Based on this volume and the values for the 1923 and 1930 events, volumes of 34,000 and 22,000 m³ were estimated for the 1932 and 1934 events, respectively.

Sedimentation also occurred at Ricks Creek in 1983. Based on descriptions by Mr. Bill Rigby (1987, oral communication), this event was characterized by hyperconcentrated sediment flow and normal stream flow. Wicczorek and others (1983, Table 1) report that the largest single debris flow at Ricks Creek in 1983 had a volume of 1,040±200 m³. The total amount of sediment transported beyond the intersection point of the fan was estimated to be about 8,000 m³.

Rudd Creek Fan

The development of the Rudd Creek fan is interpreted from exposures on the upthrown side of the Wasatch fault trace, as shown on Figure 7. An access road to repair some of the 1983 debris-flow damage was excavated into the scarp of the fault, exposing lacustrine sand overlain by alluvial-fan deposits. These fan deposits were also exposed in a borrow pit excavation about 50 m north of the point where Rudd Creek crosses the fault. Tufa-cemented transgressive lacustrine gravel was exposed in the borrow pit (Location 2, Figure 7, and Appendix B) at about elevation 1370 m. Tufa-cemented lacustrine gravel at this elevation elsewhere in the Bonneville Basin has been dated at approximately 22 ka (Currey and others, 1983) and corresponds to the Stansbury Shoreline of Lake Bonneville. This gravel is overlain by several meters of deep-water lacustrine micaceous, clayey and fine sandy silt.

Alluvial-fan deposits are exposed in the borrow pit excavation, along the access road, and in the banks of the Rudd Creek channel scoured by the 1983 sedimentation event. Evidence for two modest-sized and one large sedimentation event were exposed at Location 3 (Figure 7 and Appendix B). The base of the exposure at Location 3 was transgressive lacustrine gravel and cobbles overlain by deep-water micaceous fine sandy silt. Scoured into the deep-water deposits were alluvial-fan deposits. The lowest fan

deposits are interpreted to represent Units 3 and 4 of the ideal sedimentation package described earlier. The lowest unit was clast-supported, silty, sandy gravel which was deposited as a hyperconcentrated sediment flow. The next unit was stratified, gravelly, silty sand which was deposited as normal fluvial streamflow. These two units were 1.1 m in combined thickness and appear to comprise the earliest post-Lake Bonneville sedimentation event at Rudd Creek.

Scoured into the units described in the previous paragraph were a second pair of Units 3 and 4 (Location 3 on Figures 7 and Appendix B). The lower of this pair of units was clast-supported, cobbly, sandy gravel which was deposited as a hyperconcentrated sediment flow. The upper of this pair of units was stratified micaceous, silty sand and coarse sand which was deposited as normal fluvial streamflow. These units have a combined thickness of 1.2 m and appear to comprise the second post-Lake Bonneville sedimentation event at Rudd Creek.

Unconformably overlying the two pairs of units described above was matrix-supported sandy gravel with cobbles which was deposited as a debris flow. This Unit 1 deposit at Location 3 was greater than 3 m thick and appears to comprise the third post-Lake Bonneville sedimentation event at Rudd Creek. The upper part of Location 3 had been disturbed by the borrow operation; consequently, evidence of additional sedimentation events, if any, had been destroyed.

Exposures at Locations 4 and 5 (Figure 7 and Appendix B) show evidence of four alluvial-fan sedimentation events overlying lacustrine sand. The lowest deposit at both locations was matrix- to clast-supported sandy gravel which was deposited as a transitional flow (Unit 2). This Unit 2 deposit was 0.4 m thick in both Locations 4 and 5, and could represent either the first or the second sedimentation event interpreted from Location 3.

At Location 4, the Unit 2 deposit was overlain by a 0.5- to 0.8-m thick layer of matrix-supported silty sandy gravel with boulders deposited as a debris flow (Unit 1), which was overlain by a layer of clast-supported sandy gravel, 0.8 to 1.1 m thick, deposited as hyperconcentrated sediment flow (Unit 3); At Location 5, the Unit 2 deposit was overlain by a 1.6-m thick layer of matrix-supported sandy and cobbly gravel which was deposited as a debris flow (Unit 1). A thin (0.1 m) layer of stratified sandy gravel (Unit 4) was present over the Unit 3 deposit at Location 4 and over the Unit 1 deposit at Location 5. At Location 4, an additional 1.1-m thick layer of clast-supported sandy gravel deposited as hyperconcentrated sediment (Unit 3) overlain by a 0.1-m thick layer of stratified fluvial sandy gravel (Unit 4) were present. These Unit 1 deposits at both Locations 4 and 5 appear to correlate with the Unit 1 deposit at Location 3, and probably represent the third sedimentation event at Rudd Creek. The Unit 3 and Unit 4 deposits at Location 4 probably are part of the waning stages of the third event, but the upper pair of Unit 3 and 4 deposits at Location 4 could represent a fourth independent sedimentation event.

Matrix-supported sandy gravel with boulders deposited as a debris flow (Unit 1) overlies the deposits described above at Locations 4 and 5. This Unit 1 deposit is 1.8 to 5.5 m thick and extends to the ground surface where a prominent debris-flow levee is evident. This Unit 1 deposit represents the fifth sedimentation event at Rudd Creek and appears to have been the largest and most massive.

Other locations at Rudd Creek where detailed observations of alluvial-fan stratigraphy were made provide additional evidence supporting the interpretation outlined above. Buried stratigraphy in the alluvial fan on the downthrown side of the Wasatch fault at Rudd Creek could contain evidence for additional sedimentation events; however, the

degree of urbanization on the fan and disturbance following the 1983 sedimentation event has obliterated or prevented access to such evidence. The absence of pedogenic features developed on the upper surfaces of any of the alluvial-fan deposits suggests that all post-Lake Bonneville sedimentation occurred over a relatively short period of time. Soils developed on the levees at Rudd Creek appeared to have approximately the same degree of development as those observed at Ricks Creek (Table 19), suggesting that the sedimentation at both fans was contemporaneous. The distribution of the five prehistoric sedimentation events at Rudd Creek is shown on Figure 31.

The volumes of the five prehistoric sedimentation events at Rudd Creek were estimated on the basis that they were proportional to the volume of the fan with the same ratios as at Ricks Creek. The five prehistoric sedimentation events at Ricks Creek constituted approximately 0.38, 0.22, 0.16, 0.14, and 0.10 times the fan volume after the cumulative volume of historic sedimentation events had been subtracted. The estimated volume of the Rudd Creek fan is 729,000 m³; the volume of historic sedimentation is approximately 69,400 m³, as discussed below. Thus, the volumes of the prehistoric sedimentation events at Rudd Creek are estimated to have been 250,000, 146,000, 105,000, 94,000, and 64,000 m³.

A sample of the debris flow collected at Location 4 about 0.5 m above the contact with the underlying lacustrine sand was submitted to Dr. Vaughn Bryant at Texas A&M University for palynologic evaluation. The sample was processed with standard procedures, using 25 ml of sediment and introducing two laboratory tablets of *Lycopodium* spp. spores. The sample was then dissolved, first in HCl, and then in HF, and remaining heavy minerals were separated with a solution of ZnBr₂. The remaining sample was examined at 400-power with a Nikon microscope in the palynology laboratory. One complete slide was counted until 100 spores of *Lycopodium* spp. had been observed. The sample was very clean, with only a few small flecks of charcoal and small amounts of organics; no fungal spore were observed (Bryant, 1987, written communication). The results of the palynologic evaluation suggest that the oxidizing environment of the alluvial fan completely destroyed all evidence of pollen, if it had been present in the sediment at the time of deposition.

Rapid snow melt in 1983 caused a slope failure in the Rudd Creek drainage at about elevation 2050 m which mobilized into a series of debris flows, scouring the channel of the creek and depositing approximately 55,050 to 68,050 m³ of sediment on the alluvial fan on the downthrown side of the Wasatch fault in the community of Farmington over a period of nearly 2 weeks (Vandre, 1983, p. 8). Wieczorek and others (1983, Table 1) report that the largest single debris flow had a volume of about 64,000 m³. The extent of the 1983 sedimentation event in Farmington is shown on Figure 32. A debris basin with a capacity of approximately 49,700 m³ was constructed in the October 1983 (Figure 33) in an attempt to protect the community from future sedimentation events. Approximately 1350 m³ of additional sediment was deposited in the debris basin in 1984, bringing the total sediment volume for the two years to 56,400 to 69,400 m³. The historic sedimentation events at Rudd Creek were of small enough magnitude that they did not approach the capacity of the channel on the upthrown side of the Wasatch fault; consequently, deposits from these events were present almost exclusively on the downthrown side of the fault. Evidence of the historic sedimentation events within the channel on the upthrown side of the fault was restricted to very minor levees marking the "high mud" level and scour, with associated oversteepening of the channel banks. Thus, prehistoric sedimentation events of similar or

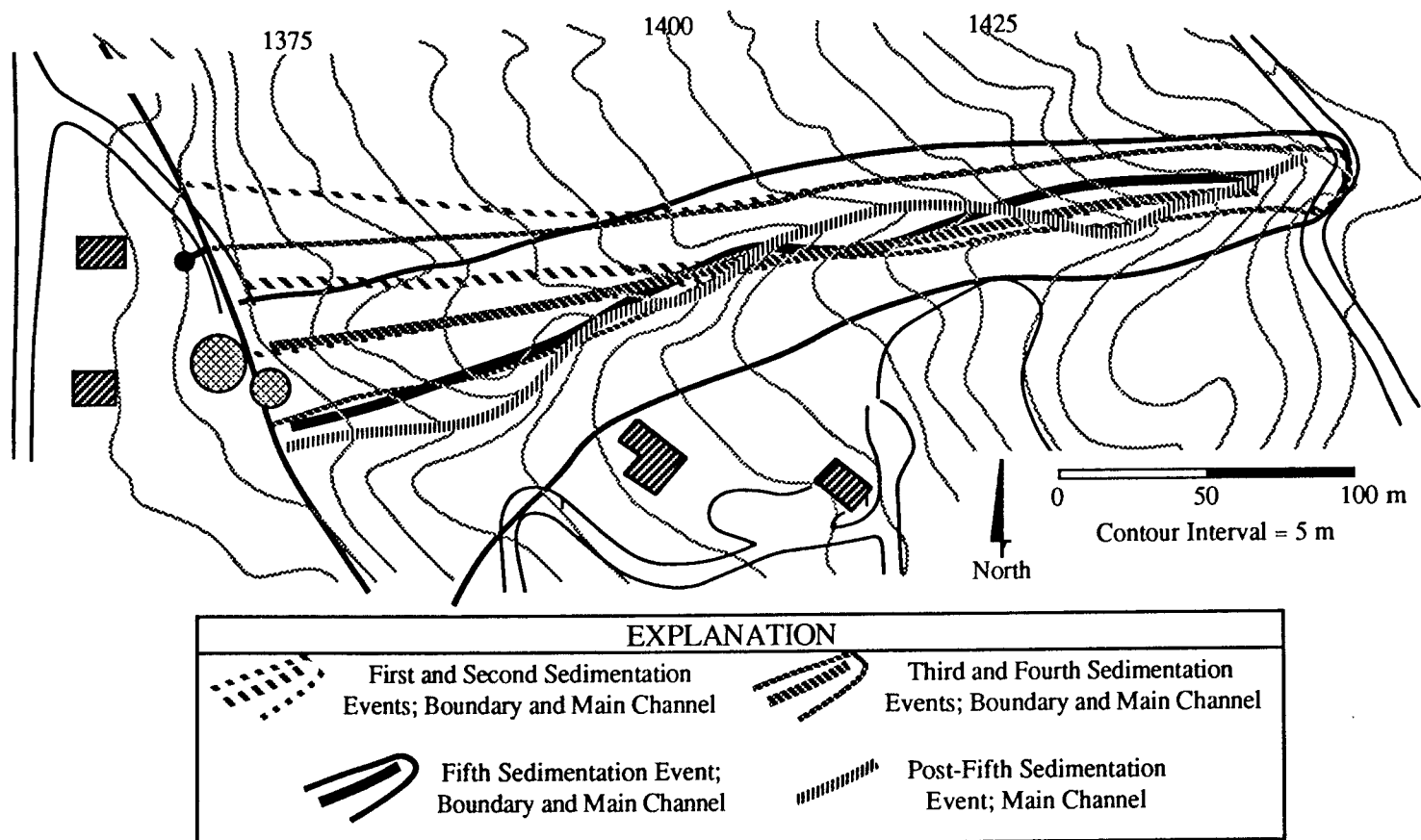


Figure 31. Distribution of prehistoric sedimentation events at the Rudd Creek fan. Base map was modified from Davis County orthotopographic map of Sec. 18, T. 3 N., R. 1 E. prepared in 1982. Hachured rectangles are structures; cross-hatched circles are water tanks. Solid heavy line is the approximate location of the Wasatch fault. Prehistoric event distribution is shown on the foot wall of the Wasatch fault only.

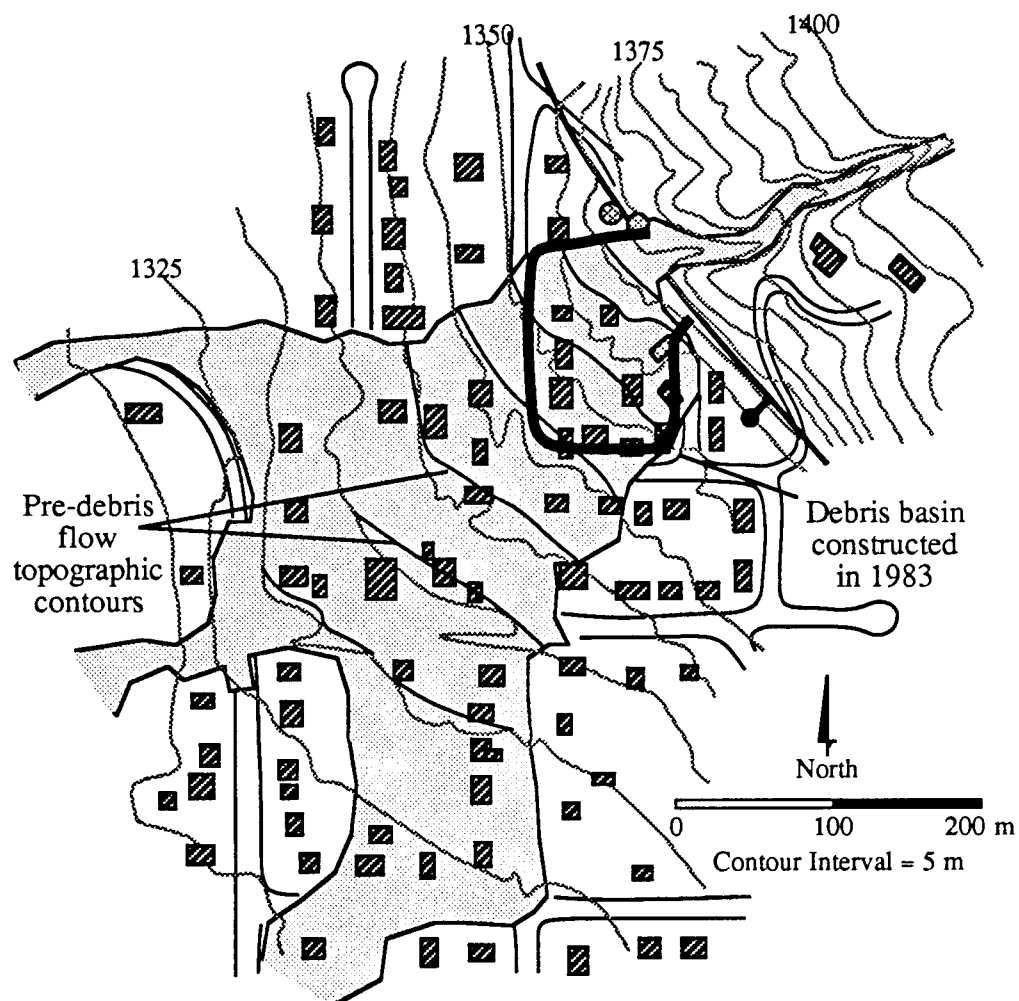


Figure 32. Area covered by the 1983 sedimentation event at the Rudd Creek fan. Topographic base map is from U.S. Department of Agriculture, Forest Service, Geomtronics - Intermountain Region at a scale of 1:2,400 prepared by photo-grammetric techniques from aerial photographs taken in 1983. Hachured rectangles are structures; cross-hatched circles are water tanks. Solid line with bar-and-ball is the approximate location of the Wasatch fault.

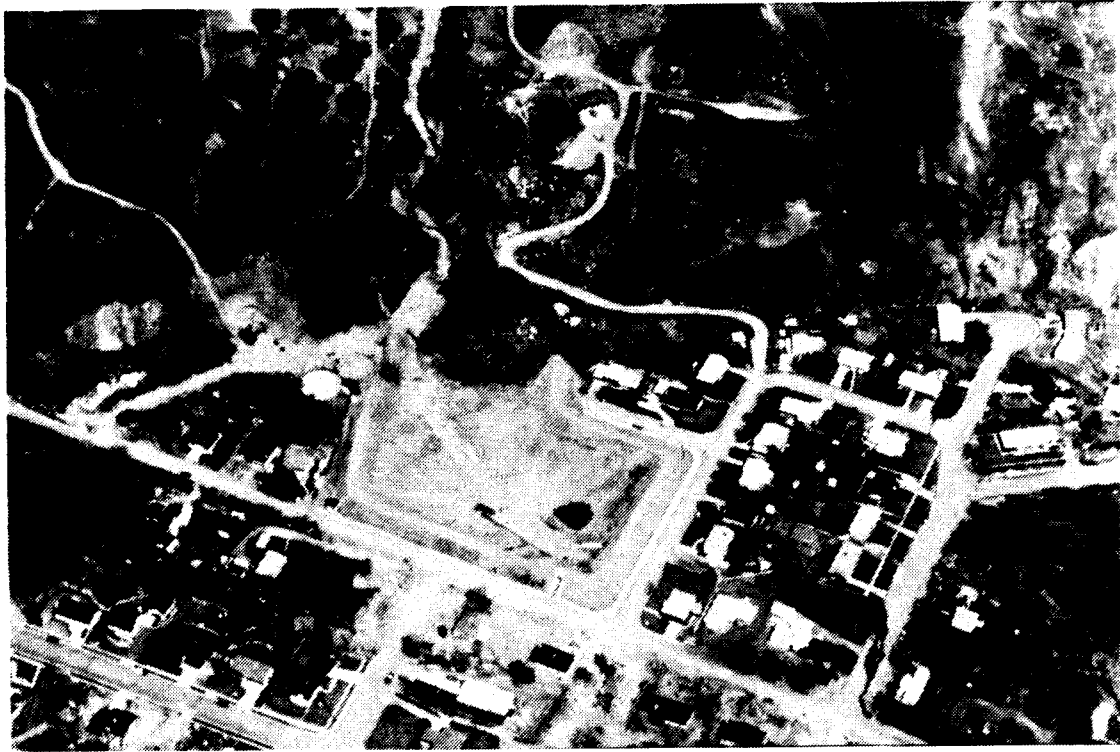


Figure 33. Photograph of debris basin constructed at Rudd Creek, Farmington, Utah, in 1983.

smaller magnitude could have occurred at Rudd Creek without being detected by the investigation described above.

Lightning Canyon Fan

Exposures at the Lightning Canyon fan are very poor. A sedimentation event and subsequent water flows in 1984 resulted in a channel being eroded into alluvial-fan deposits comprising the scarp of the Wasatch fault zone. Lacustrine sand overlain by approximately 2 m of prehistoric alluvial-fan deposits were exposed in the channel, indicating sedimentation events prior to 1984 had occurred at Lightning Canyon. Excavations for buildings approximately 200 m west of the Wasatch fault trace exposed matrix-supported debris-flow deposits to a depth greater than about 2.5 m. The total volume of the Lightning Canyon fan is estimated to be 368,000 m³. Using the same volumetric proportion for five prehistoric sedimentation events as discerned at Ricks Creek, and subtracting the 9,000-m³ sedimentation event in 1984, described below, the volumes of the prehistoric sedimentation events are estimated to have been 136,000, 79,000, 58,000, 50,000, and 36,000 m³.

The 1984 sedimentation event resulted in deposition which extended 256 m west of the Wasatch fault, had an average width of about 25 m, and an average depth of about 1.4 m, corresponding to a volume of approximately 8960 m³ (Olson, 1985, p. 18). The 1984 sedimentation event covered an area of about 6400 m², as shown on Figure 6. The temporal sequence of sedimentation in 1984 was described by Mathewson and Santi (1987, p. 256), and consisted of the four ideal stratigraphic unit processes described earlier in this report.

Samples of sediment were collected from the 1984 deposits at three locations (Figure 6) and used in the sedimentologic analysis (Appendix C). One of the samples was obtained from the wheel of a tractor which had been pushed aside by the debris flow. Part of this sample was submitted to Dr. Vaughn Bryant at Texas A&M University for palynologic evaluation. The sample was prepared in the same manner as described above for the sample from Rudd Creek. The pollen count summarized in Table 21 was based on examination of two slides (Bryant, 1987, written communication).

Other Fans

Historic sedimentation events for the canyons in the study area are listed in Table 18. The degree of urbanization and access restrictions on most fan surfaces obscured evidence of prehistoric progressive development. Therefore, because of the excellent preservation and apparently complete sequence of alluvial-fan deposits at Ricks Creek, and because of the general similarities among the drainage basins in the study area, the prehistoric record of five significant events so well expressed at Ricks Creek was considered to be representative of the other canyons. This assumption is supported by the stratigraphic evidence of five prehistoric sedimentation events at Rudd Creek, and knowledge that Ricks Creek is a "full" drainage basin which extends to the main divide of the Wasatch Range while Rudd Creek is a "half" basin which terminates approximately 68 percent of the distance to the main divide. The estimated volumes and magnitudes of prehistoric sedimentation events comprising the alluvial fans in the study area are listed in Table 22.

Table 21. Results of palynologic evaluation of the 1984 Lightning Canyon sedimentation event. Pollen analysis by Bryant (1987, written communication).

Identification	Count
<i>Lycopodium</i> spp. spores	85
Cheno/Am	30
<i>Quercus</i>	10
<i>Pinus</i>	41
<i>Artemisia</i>	8
Cyperaceae	2
<i>Ephedra</i> (<i>nevadensis</i> -type)	3
<i>Typha</i>	2
<i>Juniperus</i>	7
Liliaceae	6
<i>Salix</i>	5
<i>Myrica</i>	1
Fabaceae	2
Brassicaceae	4
cf. <i>Populus</i>	1
High-spine Asteraceae	1
Low-spine Asteraceae	20
Poaceae	19
<i>Celtis</i>	2
<i>Erodium</i>	1
Unknown	4
Indeterminant	35
Total grains	204

Notes: A moderate number of fungal spores were noted. Preservation ranged from excellent to "ghost images." Because of the great variety of grains encountered, and the variable preservation of grains of identical taxons, the sample is interpreted to consist of mixed sediments.

Table 22. Summary of estimated prehistoric sedimentation event data.

Fan	Estimated Volume 10^6 m^3	Magnitude
Corbett	0.109	5.04
	0.063	4.80
	0.046	4.66
	0.040	4.60
	0.027	4.46
Hobbs	0.107	5.03
	0.062	4.79
	0.045	4.66
	0.040	4.60
	0.028	4.45
Lightning	0.136	5.13
	0.079	4.90
	0.057	4.76
	0.050	4.70
	0.036	4.56
Kays (Middle)	0.238	5.38
	0.138	5.14
	0.100	5.00
	0.088	4.94
	0.063	4.80
Kays (South)	0.194	5.29
	0.113	5.05
	0.082	4.91
	0.072	4.86
	0.051	4.71
Snow	0.418	5.62
	0.242	5.38
	0.176	5.24
	0.154	5.19
	0.110	5.04
Adams	0.271	5.43
	0.157	5.20
	0.114	5.06
	0.100	5.00
	0.071	4.89
Webb	0.345	5.51
	0.188	5.27
	0.137	5.14
	0.120	5.08
	0.085	4.93
Baer	0.334	5.52
	0.193	5.29
	0.141	5.15
	0.123	5.09
	0.088	4.94

Table 28. Continued.

Fan	Estimated Volume 10^6 m^3	Magnitude
Half	0.049	4.69
	0.028	4.45
	0.020	4.31
	0.018	4.25
	0.013	4.11
Shepard	0.797	5.90
	0.461	5.66
	0.398	5.60
	0.335	5.52
	0.293	5.47
	0.231	5.36
	0.210	5.32
	0.168	5.22
	0.147	5.17
	0.105	5.02
Farmington	1.115	6.05
	0.929	5.97
	0.743	5.87
	0.646	5.81
	0.558	5.75
	0.538	5.73
	0.469	5.67
	0.430	5.63
	0.411	5.61
	0.391	5.59
	0.372	5.57
	0.342	5.53
	0.323	5.51
	0.313	5.50
	0.293	5.47
	0.274	5.44
	0.245	5.39
	0.235	5.37
	0.215	5.33
	0.205	5.31
	0.196	5.29
	0.186	5.27
	0.156	5.19
	0.147	5.17
	0.137	5.14
	0.108	5.03
	0.098	4.99
	0.078	4.89
	0.068	4.83
	0.049	4.69

Table 28. Continued.

Fan	Estimated Volume 10^6 m^3	Magnitude
Rudd	0.250	5.40
	0.146	5.16
	0.105	5.02
	0.094	4.97
	0.064	4.80
Steed	0.239	5.38
	0.138	5.14
	0.100	5.00
	0.088	4.94
	0.063	4.80
Davis	0.264	5.42
	0.153	5.18
	0.111	5.05
	0.097	4.99
	0.070	4.84
Halfway	0.049	4.69
	0.028	4.45
	0.021	4.32
	0.018	4.26
	0.013	4.11
Ricks	0.315	5.50
	0.183	5.26
	0.132	5.12
	0.118	5.07
	0.080	4.90
Barnard	0.311	5.49
	0.180	5.26
	0.131	5.12
	0.115	5.06
	0.082	4.91
Parrish	0.068	4.84
	0.040	4.60
	0.029	4.46
	0.025	4.40
	0.018	4.26

Table 28. Continued.

Fan	Estimated Volume 10^6 m^3	Magnitude
Centerville	0.939	5.97
	0.544	5.73
	0.395	5.60
	0.346	5.54
	0.247	5.39
Buckland	0.077	4.89
	0.044	4.65
	0.032	4.51
	0.028	4.45
	0.020	4.31
Ward	1.050	6.02
	0.608	5.78
	0.442	5.65
	0.387	5.59
	0.276	5.44

Five major prehistoric sedimentation events were deduced from a detailed examination of the stratigraphy and geomorphology at both Ricks Creek and Rudd Creek; therefore, five major prehistoric sedimentation events were assumed to account for the volumes of all other fans in the study area, except the fans at Shepard Creek and Farmington Canyon. Fans at these canyons were so large that volumetric proportion would have resulted in numerous sedimentation event volumes $> 10^6 \text{ m}^3$, which were considered excessively large. Therefore, the Shepard Creek fan was assumed to have been constructed by ten prehistoric sedimentation events, the volumes of which were estimated by first subdividing the fan volume into five volumes on the basis of the proportions of the five events deduced from stratigraphic and geomorphic evidence at Ricks Creek, and then subdividing each incremental volume into 1/3 and 2/3. This procedure is arbitrary but resulted in ten reasonable volumes ranging from 105,000 to 797,000 m^3 , as shown in Table 22.

The fan at Farmington Canyon was assumed to have been constructed by 30 prehistoric sedimentation events. The volumes of these events were estimated by first separating the prehistoric volume into five volumes on the basis of the proportions of the five events deduced from the evidence at Ricks Creek. Then, each of the five major volumes was subdivided into six smaller volumes with arbitrary proportions of 1/21, 2/21, 3/21, 4/21, 5/21, and 6/21. This procedure resulted in 30 sedimentation events with reasonable volumes ranging from about 49,000 to 1,115,000 m^3 , as shown in Table 22.

HAZARD EVALUATION

HAZARD VERSUS RISK

Hazards are naturally occurring or man-induced processes which have the potential to cause damage or injury. Risk is exposure of something of value to potential damage or individuals to potential injury as a result of the occurrence of hazardous processes. Rowe (1977) defines risk as "the potential (probability) for the realization of unwanted consequences from impending events." Petak and Atkisson (1982, p. 11) define risk analysis as including three related operational elements: Risk identification, risk estimation, and risk evaluation. The *risk identification* element focuses on the description of a candidate problem or impact. The *risk estimation* element focuses on quantitative descriptions of 1) the population at risk, 2) the impact-causing events, 3) the probability that such events will occur, 4) the consequences associated with the range of event magnitudes, and 5) the integration of these magnitude/event probabilities into a quantitative measure of risk. The *risk evaluation* element consists of a social, political, and/or engineering assessment of the results of the risk estimation element. It is in the risk evaluation element that a most difficult question is addressed: How safe is safe enough?

Bowles and others (1987) have developed a risk-based method for assessing possible improvements for dam safety. Their method consists of four elements: Risk identification, risk estimation, risk aversion, and risk acceptance. These elements, modified to reflect sedimentation hazards, are shown on Figure 34. The *risk identification* element involves listing the various factors which could contribute to potential losses and organizing these into logical event sequences which cover all expected events and responses. Such event sequences commonly are configured into event trees which serve as risk models for evaluating existing conditions and the effectiveness of proposed mitigation or aversion alternatives. The *risk estimation* element involves assigning probabilities to each branch of the event tree model and assessing the consequences of each event and response along separate pathways in the event tree. If the expected losses (damage and/or injury) are unacceptable under existing conditions, then some form of *risk aversion* may be desirable to reduce the probability associated with an initiating event, a system response, or an outcome, or to reduce the exposure to the hazard. Alternative responses for dealing with hazards are described in a subsequent section of this report. The *risk acceptance* element deals with deciding what degree of safety is appropriate or what residual risk will be accepted.

The primary purpose of this report is to elucidate the variety of hazards associated with sedimentation processes on alluvial fans and develop a method for assessing them in Davis County. Therefore, in the context of risk assessment, sedimentation processes on alluvial fans have been identified as the candidate problem for study in the risk estimation element. Quantitative descriptions of the initiating events, responses within the drainage basins, and exposure of the population at risk is beyond the scope of this research; however, quantitative descriptions of the impact-causing events (hazardous processes) or outcomes and the probability that such events will occur are the primary focus of this report. The consequences associated with the range of event magnitudes and the integration of these magnitude/event probabilities into a quantitative measure of risk are addressed only in an abstract way as *potential* consequences because an inventory of the population at risk has not been developed. The results of the research presented in this report should have value in a future risk evaluation element regarding alluvial-fan sedimentation hazards specifically in Davis County and possibly elsewhere.

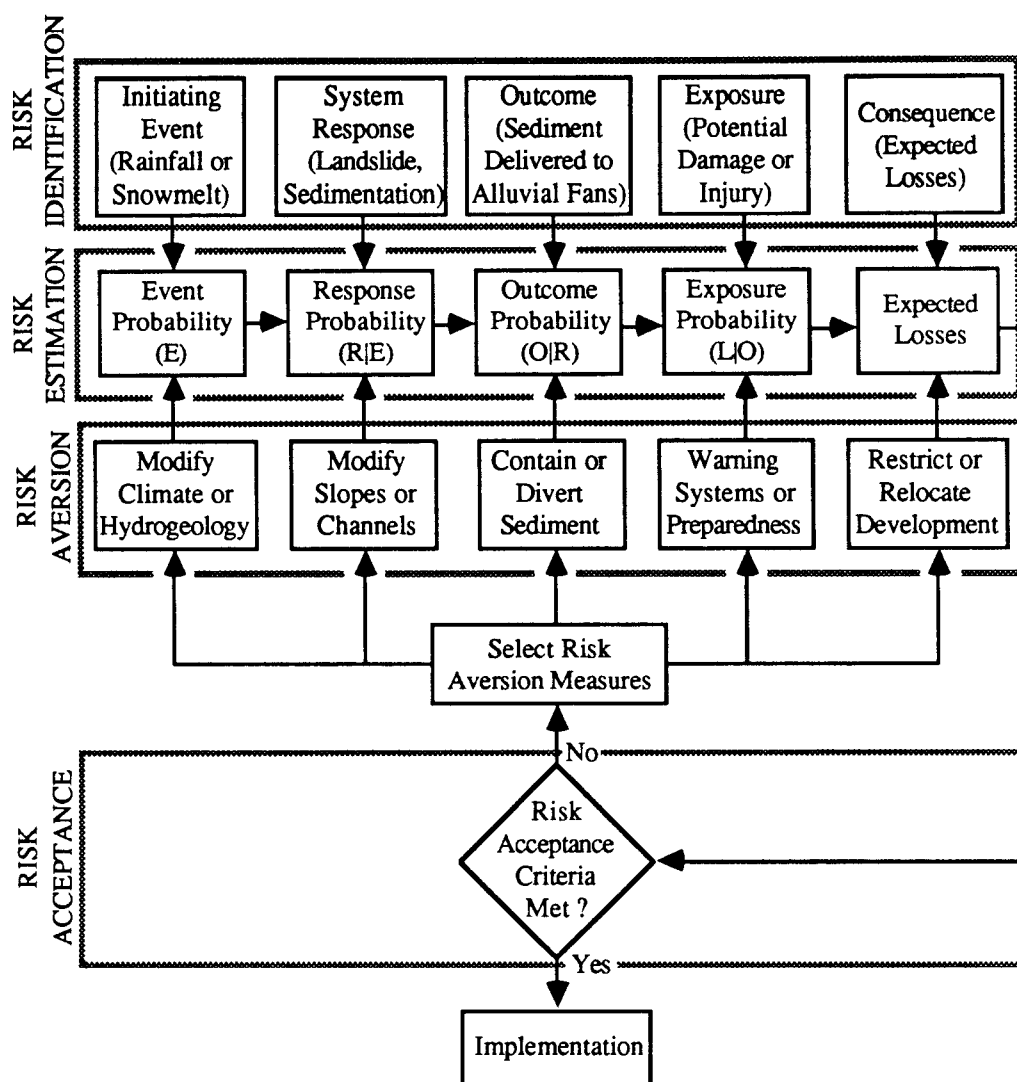


Figure 34. Risk-based method for assessing hazards and responses. Modified from Bowles and others (1987, p. 213).

HAZARD VARIABILITY

A complete hazard evaluation of potentially damaging processes consists of 1) identifying their locations, 2) estimating their frequencies, 3) estimating their magnitudes, 4) estimating the rates at which they occur, 5) estimating their durations, 6) estimating the certainty with which they can be forecasted, and 7) estimating their possible effects. Damage commonly is directly associated with hazards, even though hazardous processes can occur in remote areas where no facilities exist to be damaged. Sedimentation events have caused extensive damage, as described earlier, and the damage issue will be discussed in the context of the hazard evaluation prior to systematic treatment of the factors listed above.

Damage

Damage caused by sedimentation events on alluvial fans in Davis County in 1983 included collapse of structures, translation of structures off of foundations, flood-like inundation of structures, battering and lateral impact by boulders and debris with parked vehicles, clogging of surface drainage devices with resultant diversion of surface water, scour, and normal water flooding. In general, the heaviest damage occurred in the proximal fan areas and at some normally short distance away, no damage occurred. Such a distribution of damage is consistent with general concepts of attenuation with distance which is a well established characteristic feature of other hazards, such as earthquakes.

Degrees of damage have been subdivided into intensity classifications ranging from none to extreme. A six-level intensity scale for alluvial-fan sedimentation event damage is presented in Table 23.

Temporal Variations

The most recent damaging sedimentation events in Davis County were caused by rapidly melting snow in May and June 1983 (Anderson and others, 1984). At Rudd Creek in Farmington, for example, the initial damaging pulse of sediment occurred on May 30, and subsequent pulses of smaller magnitude occurred daily for the following two weeks. Pierson (1985b, p. 137 ff) observed and sampled a sedimentation event at Rudd Creek on June 5, 1983. He noted four surges occurring within 15 minutes of each other. The surges were distinguished on the basis of stage and velocity; sediment concentration peaked

Table 23. Intensity scale for alluvial-fan sedimentation event damage.

Intensity	Damage	Description
0	None	No sediment deposition; no damage.
1	Negligible	Sediment < 0.1 m thick; damage to landscape and access; no damage to structures; possibly minor scour and erosion.
2	Slight	Sediment generally < 0.5 m thick deposited against buildings without structural damage; sediment flooded around parked vehicles.
3	Moderate	Sediment generally ≥ 0.5 m thick deposited against buildings with easily repairable structural damage; basements partially filled with sediment; parked vehicles shoved by sediment with repairable damage.
4	Severe	Sediment ≥ 1 m thick deposited against buildings with repairable structural damage; basements completely filled with sediment; wood structures detached from foundations; parked vehicles shoved by sediment with nonrepairable damage (e.g., distorted frames).
5	Extreme	Sediment ≥ 1.5 m thick deposited against buildings with nonrepairable damage; structures collapsed by force (drag or impact) of flow; wood structures shoved from foundations; parked vehicles so badly damaged that they have small salvage value.

with the initial surge and decreased progressively. Prior to the arrival of the initial surge, Pierson (1985b, p. 137) estimated the discharge in Rudd Creek to be $0.1 \text{ m}^3/\text{s}$; however, peak discharge during the sedimentation event was computed to be $24 \text{ m}^3/\text{s}$. Although discharge quickly returned to pre-event levels, dilution to the pre-event sediment concentration required several hours. Sediment concentration in the debris flow range (Figure 11) persisted for about 8 minutes (Pierson, 1985b, p. 138), while sediment concentration in the transitional flow range lasted about 10 to 12 minutes and concentration in the hyperconcentrated sediment flow range apparently lasted less than 5 minutes. A sample collected 45 minutes after the sedimentation event began was found to have a C_w value of 0.18 and had the appearance of turbulent, muddy water (Pierson, 1985b, p. 143).

The ideal alluvial-fan stratigraphic sequence described above (Figure 19) was based on observed temporal sequence which begins with an initial plastic debris flow, which is followed by a viscous transitional flow, which is followed by a liquid hyperconcentrated sediment flow, and is completed by fluid normal streamflow. Thus, in the proximal fan area during an ideal sedimentation event, initial damage of Intensity 5 is likely to be experienced. Since many sedimentation events appear to have pulses or surges with progressively decreasing sediment concentrations, subsequent damage of Intensity <5 may be likely. In proximal fan areas, however, this may be a moot point if the initial pulse destroys all features at risk, since damage cannot exceed 100 percent.

Medial and distal fan areas can be exposed to somewhat different temporal variations in possible damage. Generally, the intensity of damage caused by sedimentation events decreases in a down-fan direction; therefore, in medial fan areas, initial damage of Intensity 3 or 4 may represent the maximum intensity, with subsequent damage of Intensity 1 or 2. This is a valid point in medial and distal fan areas because damage during the initial sediment pulse is not likely to reach 100 percent.

Long-term temporal variations in potential damage depend on changes in fan geomorphology. Heward (1978) discussed behavioral models of fans in response to tectonic uplift and fanhead entrenchment. Fan development in Davis County appears to result in a progressive downfan shift in deposition. Thus, at proximal fan locations, the intensity of potential sedimentation event damage might change from extreme to none as a fanhead trench becomes established and the intersection point on the fan shifts to medial or distal fan locations. Similarly, at medial or distal fan locations, the intensity of potential sedimentation event damage might change from negligible or moderate to severe or extreme as the intersection point progressively shifts closer.

Spatial Variations

The discussion of temporal variations presented above also indicates marked spatial variations in sedimentation event damage. Extremes in potential damage can be demonstrated by comparing proximal fan areas to locations between adjacent fans, where essentially no sedimentation hazard exists. The presence of a fanhead trench could result in a very low hazard level adjacent to the trench in the proximal fan area but a high hazard level in the medial fan area below the intersection point. This condition existed at Rudd Creek in Farmington in 1983. The intersection point coincided with the scarp of the Wasatch fault; above the fault, Rudd Creek was entrenched approximately 10 m (Pierson, 1985, p. 135) and no damage occurred at a residence located less than 15 m from the channel. Alternatively, Intensity 5 damage was experienced as much as 150 m from the intersection point, which effectively is the apex of the active fan.

The attenuation of damage from the apex of the active fan is shown on Figure 34 for the 1983 M 4.8 sedimentation event at Rudd Creek in Farmington and the 1984 M 3.9 sedimentation event at Lightning Canyon in Layton. An apparent linear decline in intensity with the logarithm of distance from the active fan apex can be seen in Figure 35. The equations describing the attenuation at Farmington and Layton, respectively, are

$$I_{M=4.8} = 14.161 - 4.558 \log D_a, (r^2 = 0.918, n = 5) \quad (90)$$

$$I_{M=3.9} = 19.256 - 7.477 \log D_a, (r^2 = 1, n = 3) \quad (91)$$

where I is intensity of sedimentation event damage and D_a is the distance, in m, from the apex of the active fan. Insufficient data are available to permit development of a family of attenuation curves; however, the intensity scale appears to have potential merit in describing the effects of sedimentation events. The values of intensity for the Farmington event shown on Figure 35 appear to describe a curvilinear relationship with the logarithm of distance and may reflect nonlinearity in the intensity scale or a nonlinear relationship between intensity and distance.

Debris basins have been constructed at the mouths of a number of canyons in Davis County. These debris basins probably affect the spatial variability of sedimentation event damage for events which do not exceed the volume of the basins. Early designs of debris basins apparently were flawed, as described by Croft (1981, p. 12), "Mud-rock floods went straight through the basins and breached the end dikes, leaving the elaborate spillways dry, or nearly so." Therefore, debris basins appear to provide protection from small- to moderate-magnitude sedimentation events, but probably do not protect above a threshold magnitude which is equal to some proportion of the basin volume. The constant of proportionality would be a function of the shape of the basin as it affects the probability that a sedimentation event would overtop or breach the basin.

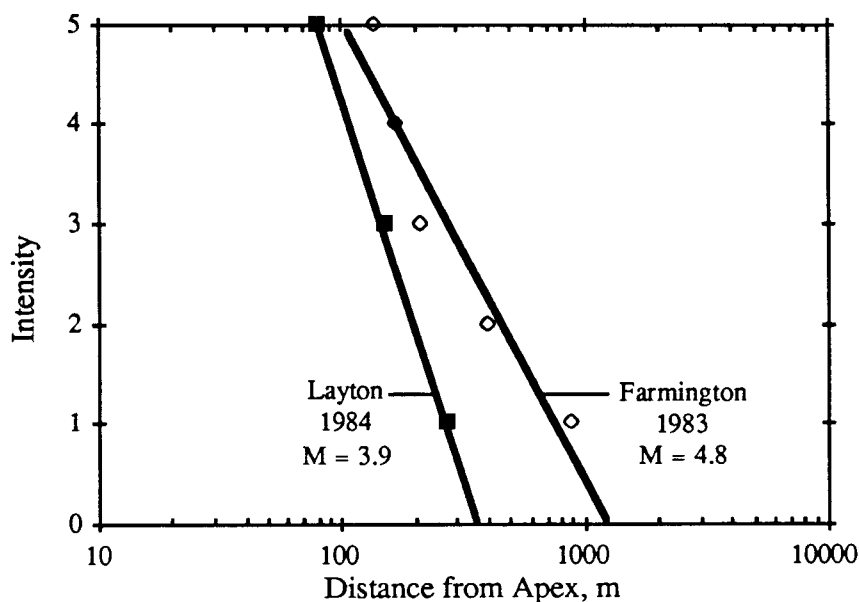


Figure 35. Attenuation of damage with distance. Intensity scale from Table 29. Farmington 1983 refers to the Rudd Creek sedimentation event; Layton 1984 refers to the Lightning Canyon sedimentation event.

Locations

A procedure for estimating flood frequency on alluvial fans was developed by Dawdy (1979) to provide an alternative to conventional methods which could not be used because the flow paths on alluvial fans are subject to lateral migration and sudden relocation during a single flood event. Dawdy (1979, p. 1407) notes that flows rarely spread evenly over the surface on an alluvial fan and "the probability with which a flood occurs at the apex of the fan does not alone determine the probability of flooding ... at any point on the fan below the apex." He concluded that this unpredictable behavior subjects all portions of the fan to potential flood hazard, and that "a site distant from an identifiable channel has approximately the same potential for flooding as a site at the same elevation near an identifiable flowpath" (Dawdy, 1979, p. 1408).

The factors affecting spatial variability discussed above certainly need to be included in a hazard model. Dawdy's (1979) method was developed to provide a means for computing flood parameters (depth and velocity) for events with 100-year average return periods, or annual probabilities of 0.01, so that damage estimates and insurance premiums could be established for the National Flood Insurance Program (NFIP). This program currently covers floodlike damage caused by sedimentation events (Committee on Methodologies for Predicting Mudflow Area, 1982), but it does not cover landslide-like damage. As shown on Figures 2 and 11, a continuous gradation in sediment concentration exists from normal streamflow to solid or semisolid deformation; consequently, no clear distinction currently exists for identifying the limits of coverage of the NFIP. Thus, Dawdy's (1979) method can be considered an interim approach to alluvial fan flood hazards because it permits computation of parameters needed for establishing insurance premiums with existing procedures. Dawdy's (1979) method considers clear water flooding without appreciable sediment. Such floods undoubtedly occur on alluvial fans with much greater frequency than floods with higher concentrations of sediment.

Frequencies

Blackwelder (1928, p. 468) observed the damage caused by the 1923 sedimentation events at Farmington and at Willard (approximately 50 km north of Farmington in Box Elder County). He considered the sedimentation at Willard to be "a normal but rare occurrence" and thought that the conditions in the mountains suggested that "two such events may be separated by centuries of time, during which the soil covering, talus slopes, and vegetation are regenerated" (Blackwelder, 1928, p. 469).

Bailey and others (1934) shared Blackwelder's (1928) views but did not reference his work in their paper. They noted that the post-Bonneville deposits were very small and concluded that if increments of sediment equal to the volumes deposited in 1930 had been added to the alluvial fans in Davis County one or more times per century since Lake Bonneville receded, the fans certainly would be impressive landforms extending westward into the Great Salt Lake (Bailey and others, 1934, p. 8). They concluded that anthropogenic degradation of the watersheds permitted accelerated erosion during historic time.

A theoretical model of alluvial-fan deposition was developed by Price (1976). He employed a random-walk simulation and used stochastic representations of mountain-block uplift and storm-event frequency. Although many aspects of this digital, three dimensional model are interesting, one of the input parameters Price used bears directly on the issue of frequency. Price (1976, p. 58) recognized that the character of deposition on an alluvial fan is directly related to the volume of weathered material immediately available for erosion

from the source basin. Price considered the areal extent of material to be constant, but its thickness increased with time according to the relation

$$y_s = m_s (1 - e^{-\eta t}) \quad (92)$$

where y_s is the thickness of the weathered layer, m_s is a maximum thickness of the weathered layer, η is a constant related to the rate of weathering, and t is a time period. Price (1976, p. 58) established threshold values of weathered layer thickness which corresponded to eroding water flow if the thickness of weathered material was small, water flow if the thickness was moderate, and debris flow if the thickness was large (Figure 36). The source basins essentially were "cleaned out" after each storm of a certain magnitude; thus, frequent large storms inhibited debris flows on the fan while infrequent storms promoted debris flows. This concept was demonstrated in Davis County in 1983 by the largest volume of sediment being produced at a canyon which had not produced sediment in historic time (Rudd Creek). Those canyons with histories of sediment production (Kays (South), Baer, Farmington, Steed, Davis, Ricks, and Parrish Canyons) produced only modest volumes in 1983 (Table 18). A significant observation at Rudd Creek in 1983 and Lightning Canyon in 1984 in support of this concept is that the bulk of sediment deposited on the fans at these canyons was scoured from the channel bed and banks. A significant amount of time should be required for a mantle of sediment to accumulate in the channels between scour events.

A significant difference exists between snowmelt and cloudbursts in the erosion of sediment from drainage basins. The damaging sedimentation events of 1983 were caused by sustained rapid melting of heavy snowpack. Snowmelt flooding without sedimentation events also occurred in 1922 and 1952, and the influence of the snowmelt on ground water levels and slope stability and subsequent sediment production has been addressed by Anderson and others (1984), Mathewson and Santi (1987), and Mathewson and Keaton

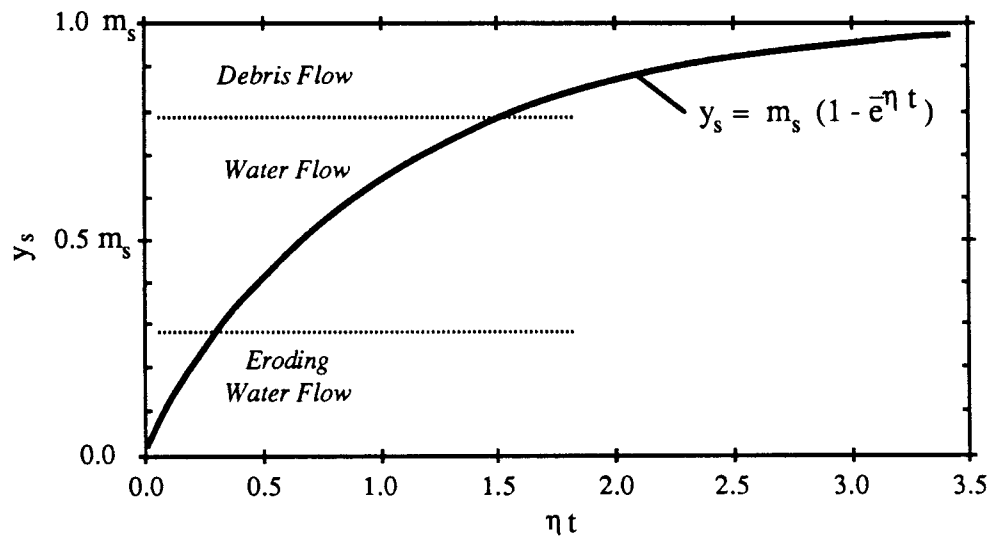


Figure 36. Alluvial fan flow events as a function of the thickness of the weathered layer in the mountains. Modified from Price (1976). y_s is the thickness of the weathered layer; m_s is the maximum thickness of the weathered layer; ηt is the rate of development of the weathered layer.

(1986). The damaging sedimentation events of the 1920's and 30's were caused by cloudburst rainstorms which apparently occur with greater frequency than rapid melting of heavy, late spring snowpack.

Magnitude

A relationship appears to exist between frequency and magnitude. Large magnitude sedimentation events appear to occur less frequently than small magnitude events. A possible explanation for such a relationship was described above in the context of the time required for development of a threshold thickness of weathered material available for erosion. Thus, if major cloudburst storms or rapid snowmelt events occur sufficiently infrequently that significant amounts of sediment are available for scour in stream channels, then large magnitude sedimentation events probably result. However, if the channels have been recently scoured at the time of a major cloudburst or snowmelt event, then the volume of sediment delivered to the fan would be more directly related to the volume eroded from slopes or generated by landslides. Thus, frequent sedimentation events should be relatively small while rare events could be of large volume.

Rates

The rate at which a hazardous process reaches its peak is a fundamental aspect of the hazard, and certainly an aspect which can affect hazard response. Alluvial fan sedimentation events have many characteristics similar to flash flood events. Thus, the sedimentation events progress quickly from nondamaging to damaging intensities. Pierson (1985b, p. 137-139) recorded discharge associated with a sedimentation event at Rudd Creek on June 5, 1983, and found that it increased from 0.1 to 24 m³/s in a period of about 1 minute. During this minute, therefore, the discharge increased at an average rate of about 0.4 m³/s/s. The sediment concentration (by weight) during this period increased from about 0.1 to over 0.9 at an average rate of 0.013/s. Such rapid rates preclude virtually all hazard responses once the process is detected by direct observation on the fan.

Hydraulic engineering modeling of the debris flow at Rudd Creek has been attempted by the Omaha District of the U.S. Army Corps of Engineers (Anciaux, 1987). The input "mudflow hydrograph" was compressed from a more typical "clear water hydrograph" to model observed behavior on the fan. The discharge on the input hydrograph increased from zero to nearly 200 m³/s in the first 10 s, a rate of nearly 20 m³/s/s (Anciaux, 1987). The discharge increased at a decreasing rate for the next approximately 280 s, to a peak discharge of about 260 m³/s (Anciaux, 1987). The discharge terminated instantaneously at the end of the sedimentation event.

Durations

A substantial difference in duration exists between cloudburst-generated sedimentation events and snowmelt-generated events. Blackwelder (1928, p. 469) noted that the 1923 sedimentation event at Willard "burst" out of its canyon with sufficient force that it descended halfway down the fan and was "followed by a typical water flood, which lasted with diminishing power for several hours." The residents of Centerville interviewed during the present research indicated that the damaging intensities of the sedimentation

events of 1923 and 1930 lasted for periods of 30 minutes or less at Ricks Creek and Parrish Creek.

During 1930, four damaging sedimentation events occurred at several canyons in Davis County; other damaging cloudburst events apparently occurred no more frequently than once in any given year. The snowmelt sedimentation events on 1983 consisted of a series of individual pulses which occurred over a two-week period. Individual pulses during the two-week period probably were similar to the cloudburst events; however, the sustained source of water from melting snow resulted in single or multiple sedimentation events on a daily basis.

Morton and others (1979) documented a 40-day period in May and June, 1969, at Wrightwood, California, when melting heavy snowpack generated daily sedimentation events. They classified the 40-day period into three stages: waxing, climactic, and waning. The durations and volumes of individual sedimentation events increased during the waxing stage, was maximum during the climactic stage, and decreased during the waning stage. The daily sedimentation events tended to be controlled by diurnal variations in temperature and the diminishing snowpack.

The Omaha District U.S. Army Corps of Engineers modeling of the debris flow at Rudd Creek was based on a hydrograph with a duration of only 300 s (5 minutes) to deliver nearly 69,000 m³ of sediment (Anciaux, 1987).

Forecastabilities

An important aspect of hazard evaluation pertains to the ability to forecast them. Keefer and others (1987) describe a real-time warning system developed in the San Francisco area, California, and tested in February, 1986. Their system is based on antecedent rainfall amount, rainfall intensity, rainfall duration, and susceptibility of slope systems (topography, geology, pore water pressure). They conclude that improvements to their system are needed but that it could serve as a prototype for systems in other landslide-prone areas.

Insufficient understanding presently exists in Davis County on which to base a reliable warning system. Pack (1985) used multivariate statistical techniques to study the landslide susceptibilities of slopes in Davis County. Jadkowski (1987) used multispectral remote sensing data for a landslide susceptibility evaluation of Davis County. Brooks (1986) summarized the results of real-time monitoring of pore water pressure in a partly-detached landslide mass in Steed Canyon. Keaton (1986b) prepared an inventory of landslide deposits in the southern part of Davis County. Additional understanding is needed regarding the relationship of infiltration of rainfall and snowmelt on slope instability and sediment yield before these valuable components can be integrated into a warning system. Thus, sedimentation events in Davis County are forecastable only in the broadest general terms in the context of the hydrometeorologic parameters (i.e., the presence of heavy spring snowpack or development of concentrated storm cells) required to cause sedimentation events. The length of time since the last sedimentation event which cleaned the canyon also is important in forecasting sediment delivery; if virtually all available sediment in the channel was recently removed, then the likelihood of a major sediment discharge is greatly diminished. Alternatively, the likelihood of clear water flooding certainly is not diminished and may be enhanced by the absence of major amounts of sediment in the channels.

Effects

The effects of sedimentation events can be divided into two issues: life safety and property damage. Injuries and fatalities were caused by sedimentation events in Davis County in 1923, but none of the other reported events had references to injuries. Nonetheless, the sedimentation events in Centerville in 1930, Farmington in 1983, and Layton in 1984 certainly had the potential for loss of life.

The risk estimation element of the method developed by Bowles and others (1987) is expressed in terms of the probabilities of events, responses, and outcomes. Their risk model is in the form of an event tree with a number of pathways, each of which represents an outcome associated with a response to an event. For an event tree with n possible pathways, Bowles and others (1987, p. 216) report that the pathway probability for the i th pathway is

$$P(P_i) = P(E) \cdot P(R|E) \cdot P(O|R) \quad (93)$$

where $P(P_i)$ is the pathway probability for the i th pathway, $P(E)$ is the probability that event E will occur, $P(R|E)$ is the conditional probability that response R will occur given that event E occurs, and $P(O|R)$ is the conditional probability that outcome O will occur given that response R occurs. The partial risk cost for the i th pathway is

$$C(P_i) = P(P_i) \cdot L_e \quad (94)$$

where $C(P_i)$ is the partial risk cost for the i th pathway, $P(P_i)$ is the pathway probability for the i th pathway, and L_e is the possible economic loss. The total risk cost is obtained by summing the partial risk costs over all n mutually exclusive pathways in the event tree, or

$$C = \sum_{i=1}^n C(P_i) \quad (95)$$

where C is the total risk cost and $C(P_i)$ is the partial risk cost for each of n pathways. For a population at risk, the magnitude of life loss due to events along the i th pathway is given by

$$L_l = P(L|O) \cdot PAR \quad (96)$$

where L_l is the magnitude of life loss, $P(L|O)$ is the conditional probability of life loss L given that outcome O occurs, and PAR is the population at risk.

The property damage aspect of sedimentation events was addressed above in the description of damage. The only significant issue to add in this section regarding effects is that of business interruption and property value reduction. Access and egress clearly can be disrupted by deposition and/or scour during a sedimentation event. Croft (1981, p. 18-19) summarized some of the results of a damage survey he conducted following the floods of 1930. In addition to damage to real property, Croft found that 1) farmers had crops destroyed and fields rendered less productive for a period of years, 2) bankers could not collect interest or principal on loans made on property in the "flood zone," 3) bankers refused to loan money on "flood property," 4) home and farm buyers moved out after deciding that they were too near the potential "flood zone," and 5) the Farmington-Centerville area was in a state of economic stagnation, even five years after the last large floods of 1930.

HAZARD MODEL

The principal goal of any hazard model should be quantification of the hazard in meaningful terms which can be used for actuarial purposes, investment decisions, and engineering design. Alluvial-fan sedimentation hazards must be quantified in terms which are compatible with other quantitative hazard models to permit systematic assessments of multiple hazards. Other hazards which have been modeled quantitatively are flooding (Benson, 1968) and earthquakes (Schwartz and Coppersmith, 1986). The most commonly used methods for flood frequency analysis are the log normal, log Pearson Type III, and extreme-value methods, described by McCuen and Snyder (1986). These methods require discharge values for each year, and numerous years of zero or near zero discharge result in strongly skewed distributions. The most commonly used model for earthquake hazard evaluation is the Poisson-exponential model (Schwartz and Coppersmith, 1986, p. 227). This model is based on two fundamental assumptions: 1) earthquakes occur randomly in time as well as space, and 2) the distribution of earthquake magnitudes is exponential.

Sedimentation events on alluvial fans in Davis County probably are not random in time, and certainly are not random in space. Arguments have been presented earlier supporting the concept that most of the volumes of the post-Lake Bonneville alluvial fans in Davis County were deposited during a brief period of intense sedimentation approximately 10 ka ago. Arguments have also been presented supporting the concept that the historic sedimentation events represent not only the historic period (140 yr) but also late Holocene time (4 ka). Therefore, temporal non-randomness can be addressed by a family of relationships representing frequencies for each of the principal time periods: Holocene, late Holocene, and historic. Some element of randomness must be accepted until considerable additional knowledge is available regarding factors which contribute to erosion within drainage basins (rates of weathering, rates of colluvium formation, climate variation, effects of fire, and effects of anthropogenic activities). Spatial non-randomness can be addressed simply by resisting the temptation to develop a single "universal" hazard relationship for Davis County. The alternative clearly is to develop separate hazard relationships for each alluvial fan.

An exponential distribution of sedimentation event magnitudes probably does exist. Such a distribution indicates that a small number of large events and a large number of small events occur on any individual fan. Evidence for the larger events certainly exists at Ricks Creek, and the uniform trend in fan size with drainage basin size in Davis County suggests that the processes at Ricks Creek probably are representative of the other fans. Local residents of Centerville, Farmington, and Layton (Bill Rigby, Cammon Arrington, and Jeff Warburton, respectively, 1987, oral communication) indicate that, during "normal" years, virtually no sediment is added to the alluvial fans. This undiscernable volume of sediment was represented as 0.001 m^3 , corresponding to a sedimentation event of $M -3$. This is an arbitrary volume, but one which was considered to be realistic and to approach zero. Such a small volume could be deposited in an imperceptible fashion on any alluvial fan. Thus, most fans in Davis County can be characterized by sedimentation events ranging from $M -3$ to $M 6$.

The elements of the complete hazard evaluation which are being addressed during this research consist of the locations, frequencies, and magnitudes, and to a lesser extent rates and durations. Forecastabilities require separate treatment as research which can build upon the results included in this dissertation. Effects are included in this model only in an abstract way, in as much as the character of the effect is reflected in the magnitude of the sedimentation event.

The factors described above and in earlier chapters were synthesized into the model shown in the flow diagram on Figure 37. The initial component of the model pertains to the historic record, which can contain the most specific information about flood events at individual canyons. From the historic record, the number of historic sedimentation events is determined or estimated. If specific historic records of sufficient detail are available, the volumes of the historic sedimentation events can be estimated directly. If specific historic records are not available, then in the Davis County area, the volumes of the sedimentation events were proportioned to the historic events at Ricks Creek because they are relatively well known and appear to be representative of Davis County alluvial-fan flood events.

The total volume of the post-Lake Bonneville alluvial fan is then estimated using the procedure described earlier. The total volume of prehistoric sedimentation events at each fan is determined by subtracting the total volume of historic sedimentation events from the total fan volume. If the fan is well preserved and accessible, the number of prehistoric sedimentation events can be estimated directly from the stratigraphic record and geomorphic expression of the fan. Such preservation exists in Davis County only on the Ricks Creek fan and to a lesser extent at the Rudd Creek fan. Therefore, the volumes of the prehistoric sedimentation events (Table 22) were estimated by volumetric proportion.

Magnitude-frequency relationships were required to quantify the sedimentation events in terms which could be incorporated with the results of evaluations of other hazards, such as earthquake hazards. The procedure used to develop magnitude-frequency relationships for sedimentation events on fans in Davis County is described in the next section of this chapter. The magnitude-frequency relationships were then transformed into exceedance probabilities in a manner commonly used for earthquake or flood risk assessment. Exceedance probabilities were developed for normal (binomial and Poisson) and extreme-value distributions. The assumptions and procedures used to develop the exceedance probabilities are described below.

Fan hazard classifications are based on presence or absence of three features on the alluvial fans: fanhead trenches, intersection points below mid-fan locations, and debris basins. Fan hazard classifications are also based on the time since the last sediment discharge event and the general condition of the main channel with respect to the possibility of large volumes of sediment being entrained into a sedimentation event by scour or liquefaction. Hazard classifications are developed separately for proximal, medial, and distal fan areas, and the historic sedimentation record and combined for an average fan hazard classification. The average fan hazard classification is a simple average of ordinal ranking of the separate classifications using 0 for very low hazard, 1 for low, 2 for moderate, and 3 for high hazard.

Variations on a Specific Fan

Dawdy (1979) developed a method of evaluating flood frequencies on alluvial fans. His method is based on three fundamental assumptions: 1) the distribution of flood magnitudes can be described adequately with the log Pearson III method of flood frequency analysis (Benson, 1968), 2) each flood event forms a single channel and flow remains in that channel throughout the event, and 3) flood channels are distributed uniformly across any contour. Consideration was given to expanding Dawdy's (1979) method to account for high sediment concentrations, but the log Pearson III method requires a value of flood flow for each year. Since many, if not most, of the fans in Davis County have experienced essentially zero flood flow for most of the years, the log Pearson III distribution probably

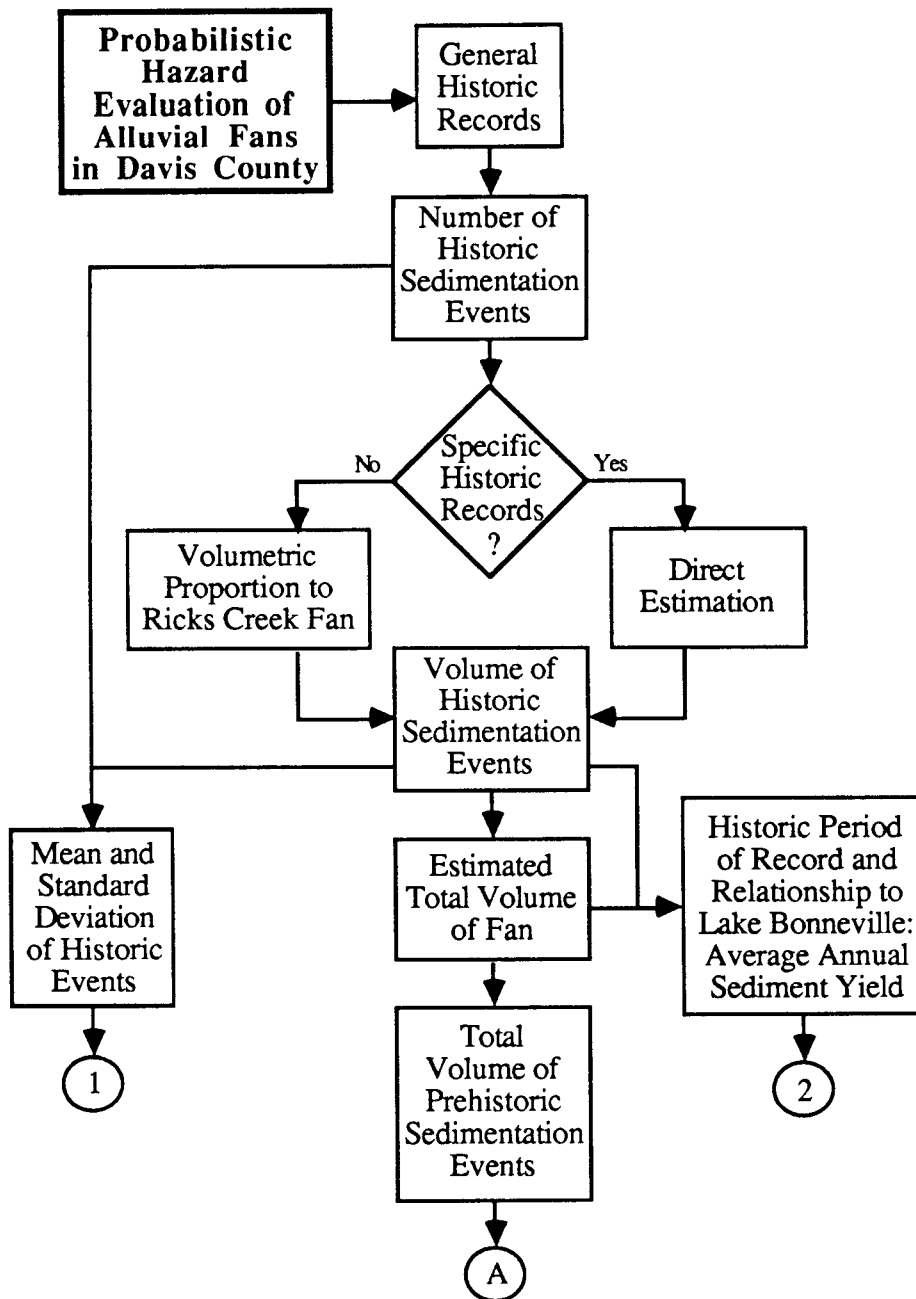


Figure 37. A model for hazards related to sedimentation processes on alluvial fans in Davis County, Utah.

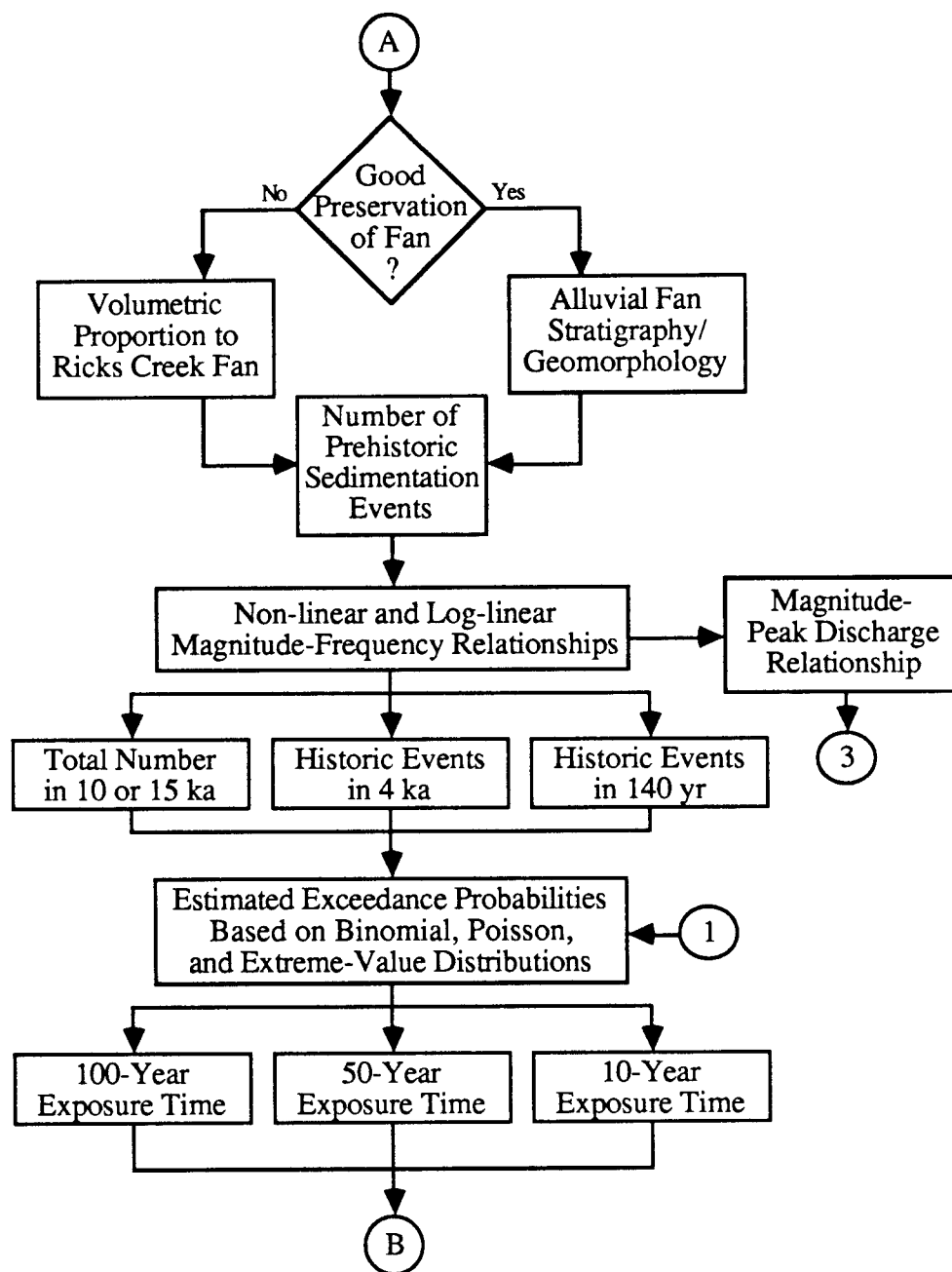


Figure 37. Continued.

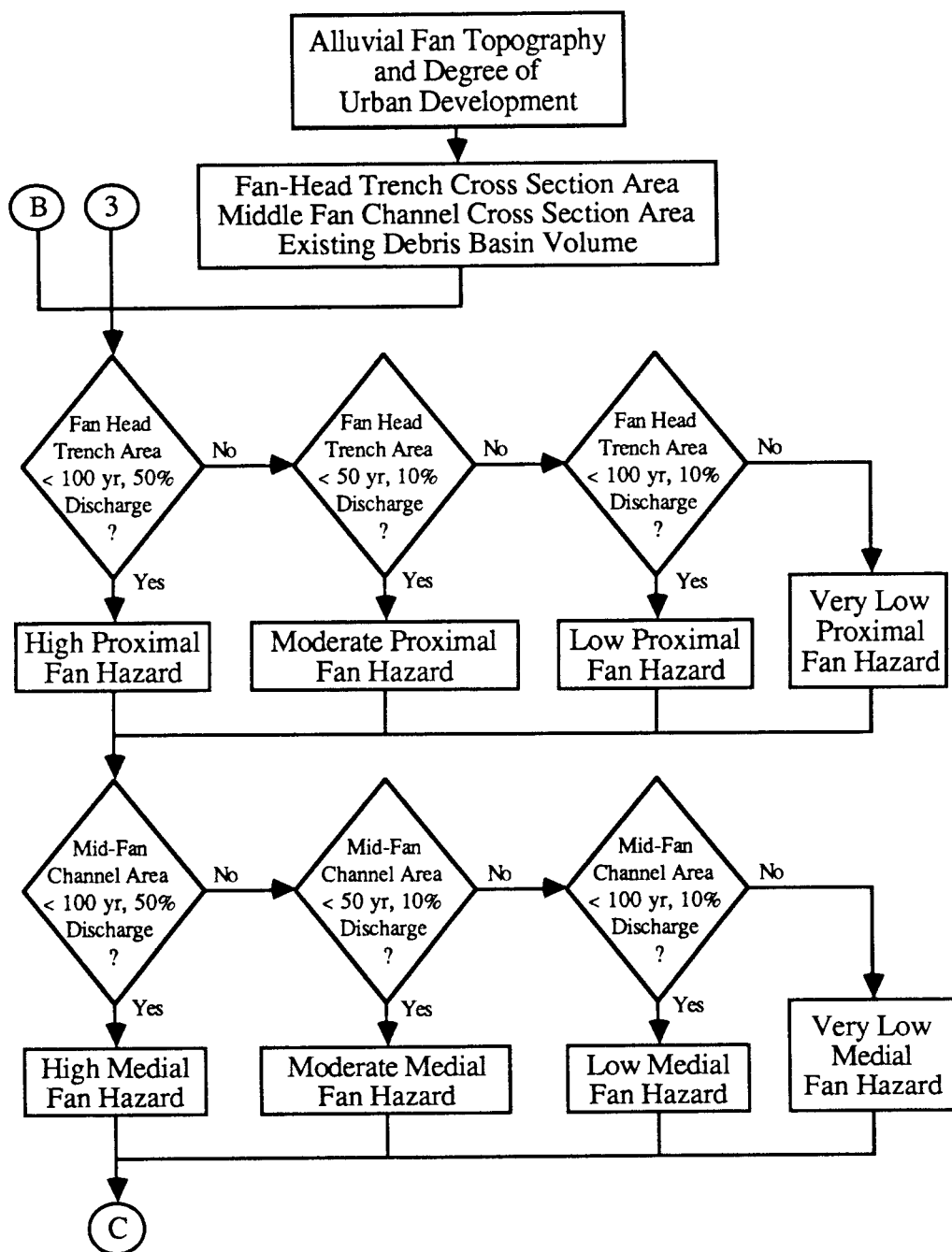


Figure 37. Continued.

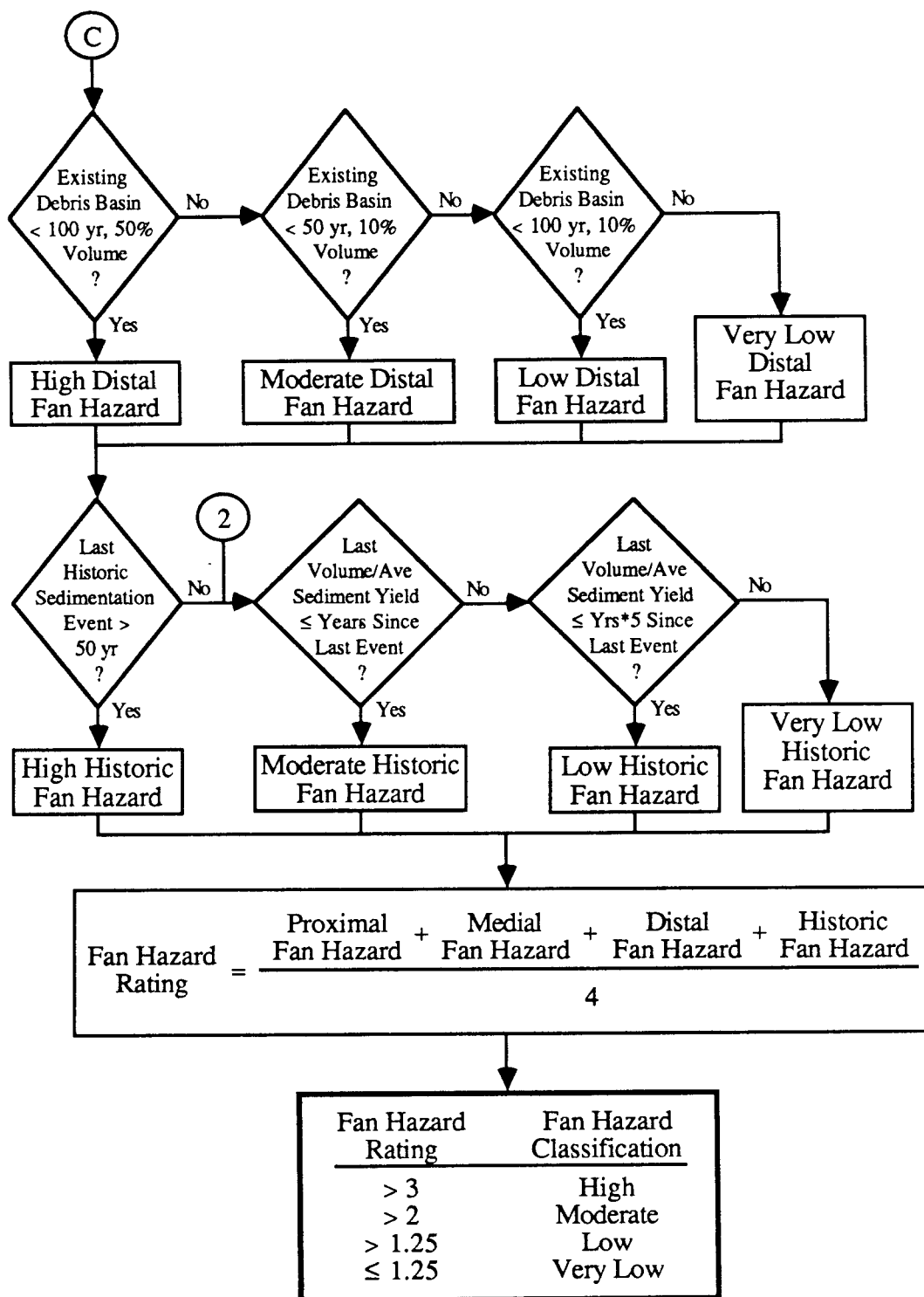


Figure 37. Continued.

would be excessively skewed and yield results with little relation to the physical conditions on a fan.

Additionally, the sedimentation events at sediment concentrations in the transitional flow and debris flow range, by their very nature, are self-diverting and avulsions should be expected to occur. Dawdy (1979, p. 1412) notes that avulsions can be problems and has an "avulsion coefficient" to modify the result to be more reasonable. He also notes that valid assumptions regarding distribution of channels that differ from the uniform distribution assumption used in his model would result in different probabilities. Thus, variations on a specific fan are treated in Dawdy's (1979) model rather simplistically as statistical uncertainty.

Schamber (1987) developed a finite element model with a moving front for transient simulation of debris flows. This model was used by Ancaix (1987) to compute debris flow thicknesses on alluvial fans in Davis County for input hydrographs representing events with 100-year average recurrence intervals. Apparently, the 100-year events were proportioned on the basis that the volume of the principal sedimentation event at Rudd Creek was, in fact, the 100-year event. The hydrographs were generated by compressing the leading and trailing tails to generate, for example, 64,000 m³ in 5 minutes with a peak discharge of about 260 m³/s at Rudd Creek. Neither the details of the method nor the results have been published, but it seems like a straightforward engineering approach to quantifying the problem although variability on a specific fan appears to be neglected by the method.

The model developed as part of the present research deals with variability on specific fans by recognizing the importance of fanhead trenches, intersection points, and debris basins. Although specific "sediment routing" is beyond the scope of this research, general aspects of geomorphology have been incorporated into the model. The self-diverting character of alluvial-fan sedimentation events is a fundamental aspect of the hazard; after all, that is why alluvial fans are fan-shaped landforms. Consequently, immediately following the next sedimentation event on any fan, the locations of hazards probably will shift. In some respects, Dawdy's (1979, p. 1412) "avulsion coefficient" approaches the problem of diversion during an event. Dawdy's (1979) model, however, appears to be incapable of accommodating sediment concentrations in the higher range of hyperconcentrated sediment flow, not to mention debris flow.

Variations Between Fans

Variations between fans certainly exists; however, uniformity between fans is suggested by trends discussed earlier in the section regarding morphometric correlations. Specifically, Figures 21 and 22 suggest that larger fans are associated with larger drainage basins and gentler fan slopes are associated with larger drainage basins. These figures also show that, in general, the Davis County fans are smaller and steeper than fans associated with drainage basins of similar size elsewhere.

Nonetheless, marked variation between fans is considered to be a fundamental aspect of the hazard model shown in Figure 37. Therefore, rather than apply the model once to develop a single result for all fans in Davis County, each fan is treated independently, and separate results are developed. Unavoidable dependence among fans results from the proportioning of sedimentation event volumes for individual fans where specific data are lacking to the volumes at the Ricks Creek fan.

MAGNITUDE-FREQUENCY RELATIONSHIPS

The magnitude of sedimentation events is defined as the logarithm of the volume of sediment deposited in cubic meters normalized to a unit volume to result in a dimensionless number:

$$M = \log (V / V_o) \quad (97)$$

where M is sedimentation event magnitude, V is the volume of sediment deposited in m³, and V_o is 1 m³.

The number of sedimentation events which created the post-Lake Bonneville alluvial fans in Davis County was determined from historic records and deduced from geomorphic expression of the fans. The frequencies of sedimentation events were computed with procedures described in Appendix E. Two fundamentally different assumptions were used to develop magnitude-frequency relationships for each of the alluvial fans, as shown in the figures in Appendix E. One assumption was that the entire range of sedimentation event magnitudes from very small to very large contributed to the development of the alluvial fans; this assumption was modeled with a log-linear distribution of event magnitudes, in the form of

$$\log N = a + b M \quad (98)$$

where N is the annualized frequency of occurrence of events equal to or larger than magnitude M, and a and b are coefficients of regression. The frequency is annualized with the Weibull plotting position formula

$$N_{PR} = Re / (PR + 1) \quad (99)$$

where N_{PR} is the annual frequency for a period of record PR in years and Re is the event rank (modified from McCuen and Snyder, 1986, p. 113). The largest event in the period of record is given a rank of 1 and the smallest event is given a rank of PR/(PR+1). The smallest event was taken to be 0.001 m³, or M -3, as discussed in Appendix E.

The second assumption used to develop magnitude-frequency relationships was that the largest events were few in number and discernable in the stratigraphy and geomorphology of the alluvial fans and that all other years had sedimentation events of negligible volume (0.001 m³). This assumption was modeled with a non-linear distribution of event magnitudes for each of the alluvial fans, as shown in the figures in Appendix E.

The historic record appears to be reasonably accurate and indicates that a log-linear distribution of event magnitudes on the alluvial fans is not representative of the historic period (the past 140 years). Alternatively, progressive changes on the alluvial fan surfaces and the paucity of exposures of the stratigraphy suggest that events of small to intermediate magnitude could have occurred on the alluvial fans during Holocene time without being readily distinguishable. Thus, it appears that actual distribution of event magnitudes probably lies between log-linear and non-linear.

PROBABILISTIC HAZARD EVALUATION

Earthquake and flood hazards commonly are evaluated on the basis of the probability that a certain size of event will be equalled or exceeded in a specified period of time, known as exceedance probability. The specified period of time represents an exposure time and commonly is called a "design life" or an "economic life" for the facility or feature under consideration. Earthquake engineering commonly employs two levels of

"design" earthquake events: a lower-level event (LLE) and an upper-level event (ULE). The LLE is an event which has a relatively high probability of occurring during the design life, while the ULE has a relatively low probability; consequently, the LLE has a smaller magnitude (hence, lower level) than the ULE (hence, upper level). Typical design lives range from as little as 10 years to as much as 100 years or more, depending on the critical or noncritical nature of the facility. Commonly accepted probabilities for design range from 50 to 10 percent. For example, the LLE usually is taken as the earthquake acceleration which has a 50 percent probability of being equalled or exceeded during a 50-year period, while the ULE has a 10 percent probability in the same 50 years. An exposure time of 100 years was used by Anderson and others (1982) in their evaluation of earthquake-induced liquefaction hazards in Davis County, and by Keaton and others (1987) in their evaluation of earthquake-induced landslide hazards in Davis County. Studies of bedrock accelerations by Algermissen and others (1982) and ground surface accelerations by Youngs and others (1987), both of which included Davis County, were based on exposure times of 250, 50 and 10 years. Urban flood hazards commonly are evaluated in the context of the "100-year" flood plain.

The probabilistic evaluation of sedimentation hazards in Davis County is based on exposure times of 100, 50, and 10 years to permit the results of this research to be incorporated with quantitative representations of other hazards. The method used in this research and the results of the probabilistic analyses of sedimentation events are presented in Appendix F. Probabilistic analyses were conducted using normal (binomial and Poisson) and extreme-value distributions, as described in Appendix F. The results of the binomial and Poisson distributions were nearly identical. Flood hazard analyses commonly are based on binomial distributions, while earthquake hazard analyses commonly are based on Poisson distributions. Sedimentation events are associated with flood-like damage and the binomial distribution, rather than the Poisson distribution, was used in the hazard evaluation in this research. The extreme-value distribution was used for the historic period of record only because the distributions were excessively skewed toward M -3 for the longer Holocene period of record.

The actual distribution of event magnitudes probably lies between log-linear and non-linear, as discussed earlier. Therefore, the probabilistic evaluation of sedimentation hazards on alluvial fans in Davis County in this research was developed by averaging the binomial distribution over the Holocene period and the extreme-value distribution over the historic period. These results were calculated with MAGPRO.4 (Appendix G) and are presented on Figures 38 to 59; the individual results are presented in Appendix F.

The magnitude values for exceedance probabilities of 0.5 and 0.1 for exposure times of 100, 50, and 10 years are summarized in Table 24. These values were needed for the hazard model shown in Figure 37 and described below.

HAZARD CLASSIFICATIONS

Sedimentation event hazards at each of the alluvial fans in the study area were classified with the procedure outlined above and presented diagrammatically on Figure 37. Hazard ratings for each fan were computed with an interactive program called "HAZ.MOD" (Appendix G) written in BASIC and executed on a Macintosh SE personal computer. A flow diagram for this program is presented on Figure 60. Input parameters to this model consist of 1) the fan-head trench (channel) area, 2) the middle fan channel area, 3) the existing debris basin storage volume, 4) the number of years since the last historic sedimentation event, 5) the volume of the last historic sedimentation event, 6) the average annual sediment yield volume, 7) the magnitude of the 100-year, 50 percent probability

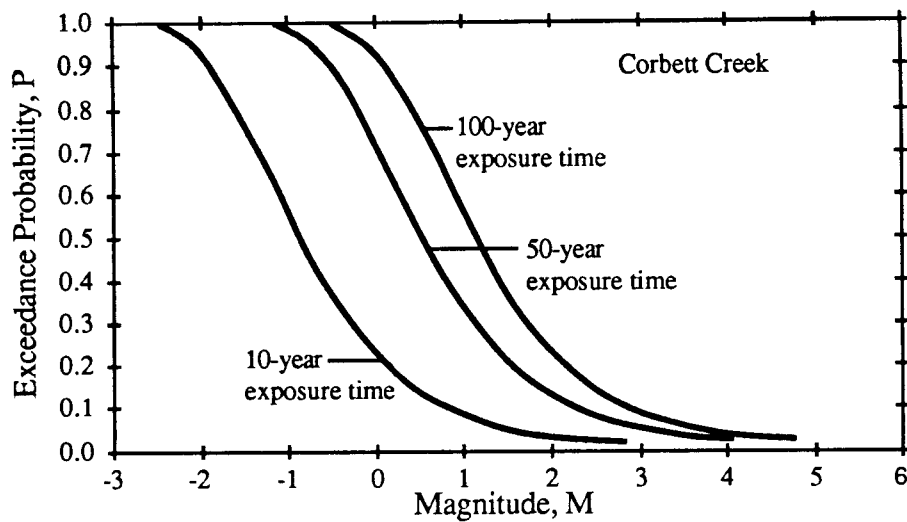


Figure 38. Representative exceedance probability curves for sedimentation events on the Corbett Creek fan.

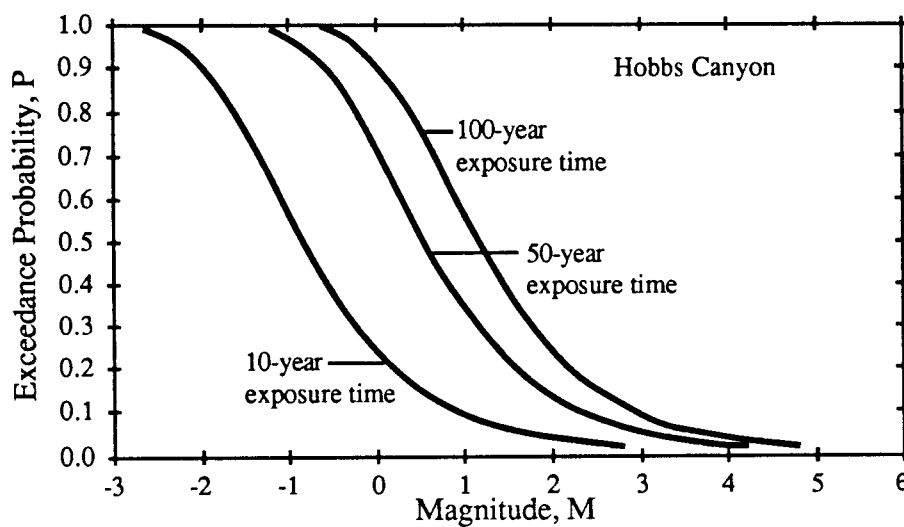


Figure 39. Representative exceedance probability curves for sedimentation events on the Hobbs Canyon fan.

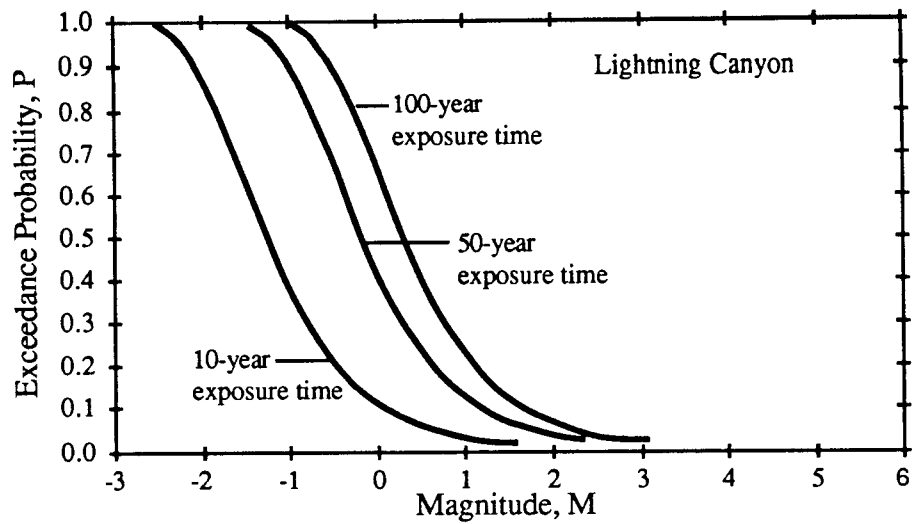


Figure 40. Representative exceedance probability curves for sedimentation events on the Lightning Canyon fan.

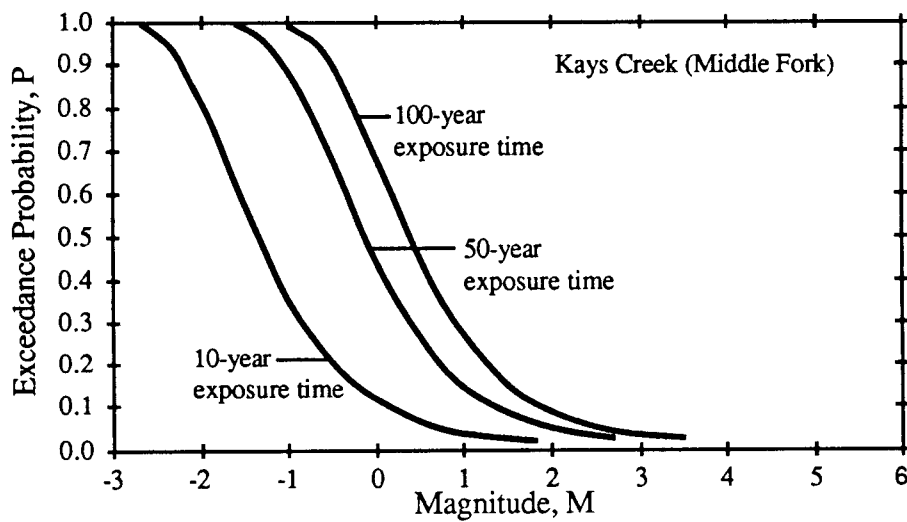


Figure 41. Representative exceedance probability curves for sedimentation events on the Kays Creek (Middle Fork) fan.

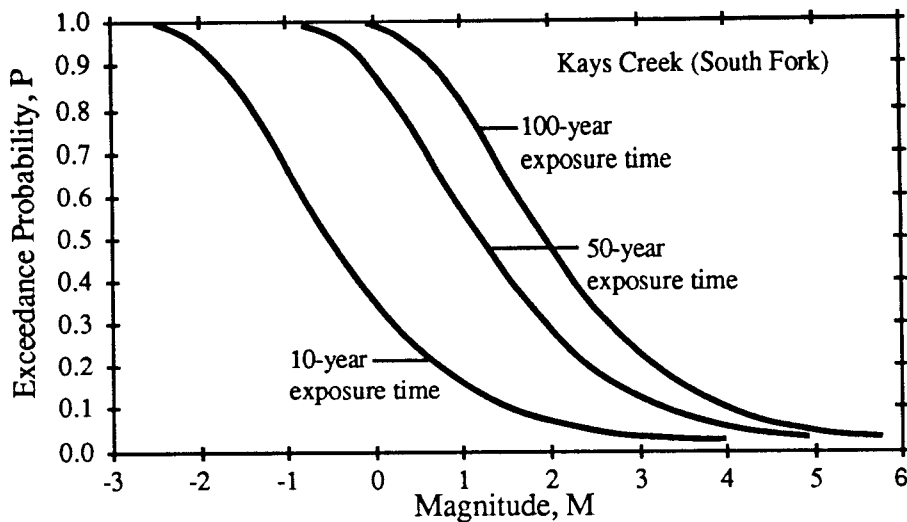


Figure 42. Representative exceedance probability curves for sedimentation events on the Kays Creek (South Fork) fan.

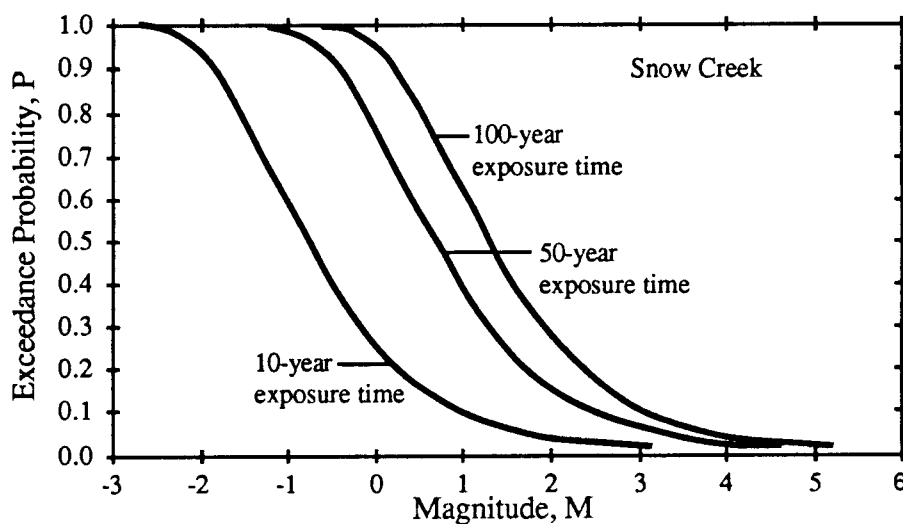


Figure 43. Representative exceedance probability curves for sedimentation events on the Snow Creek fan.

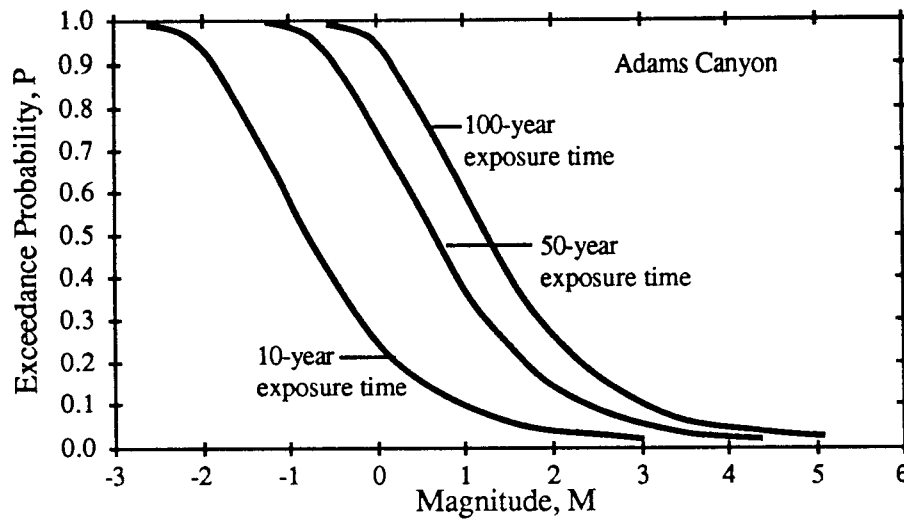


Figure 44. Representative exceedance probability curves for sedimentation events on the Adams Canyon fan.

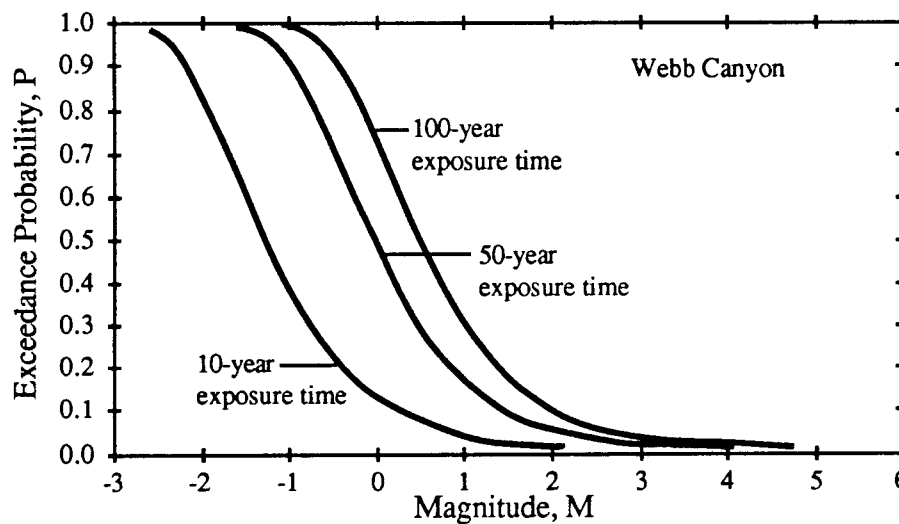


Figure 45. Representative exceedance probability curves for sedimentation events on the Webb Canyon fan.

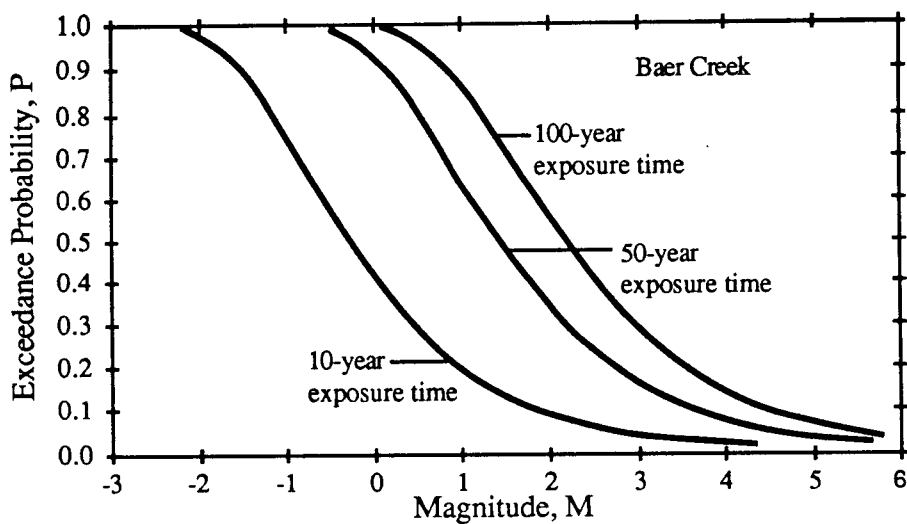


Figure 46. Representative exceedance probability curves for sedimentation events on the Baer Creek fan.

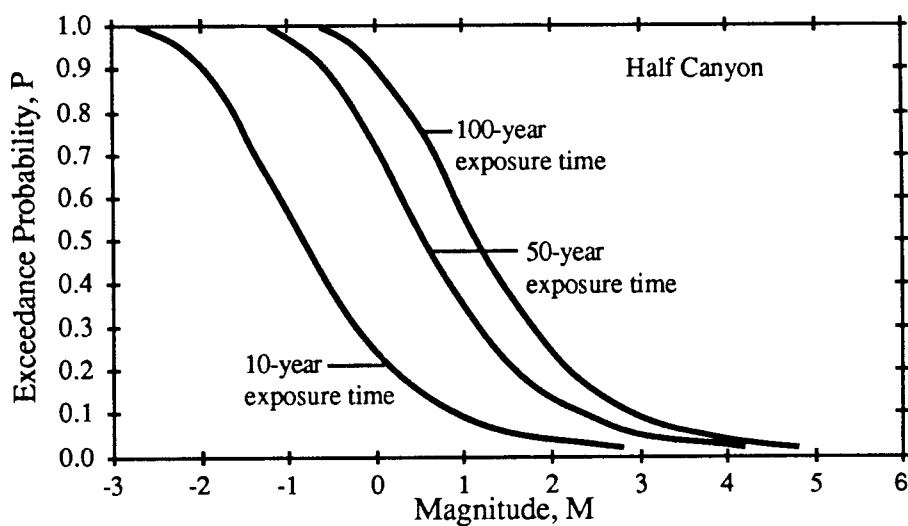


Figure 47. Representative exceedance probability curves for sedimentation events on the Half Canyon fan.

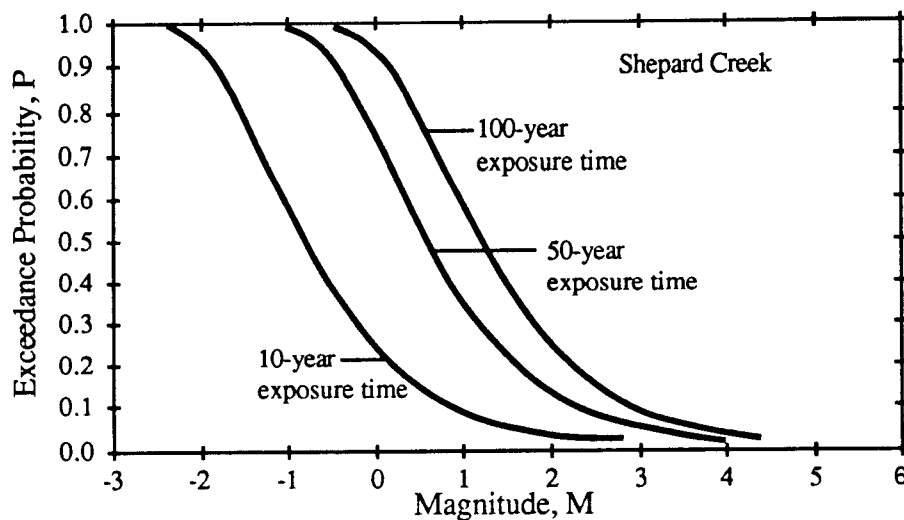


Figure 48. Representative exceedance probability curves for sedimentation events on the Shepard Creek fan.

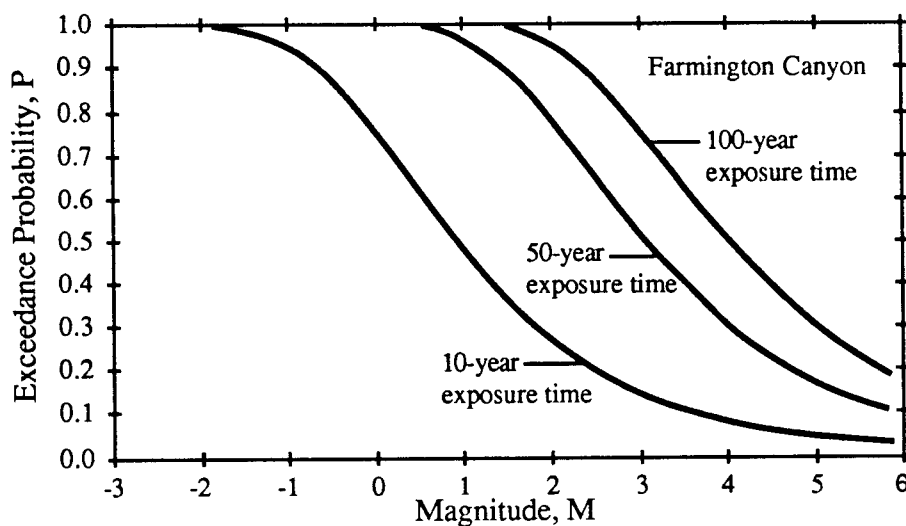


Figure 49. Representative exceedance probability curves for sedimentation events on the Farmington Canyon fan.

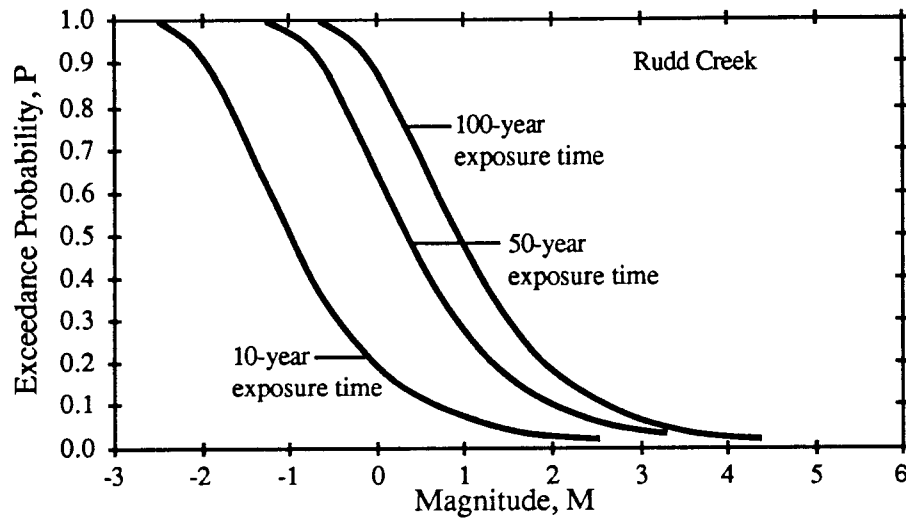


Figure 50. Representative exceedance probability curves for sedimentation events on the Rudd Creek fan.

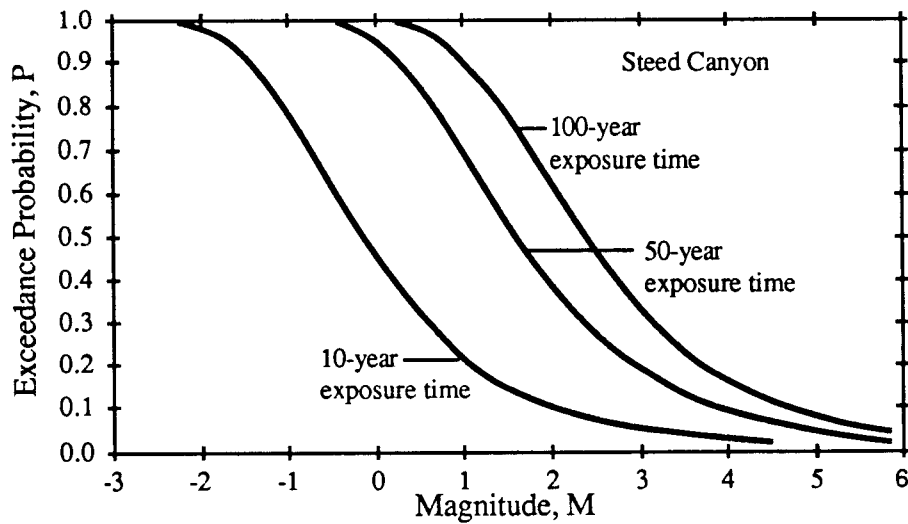


Figure 51. Representative exceedance probability curves for sedimentation events on the Steed Canyon fan.

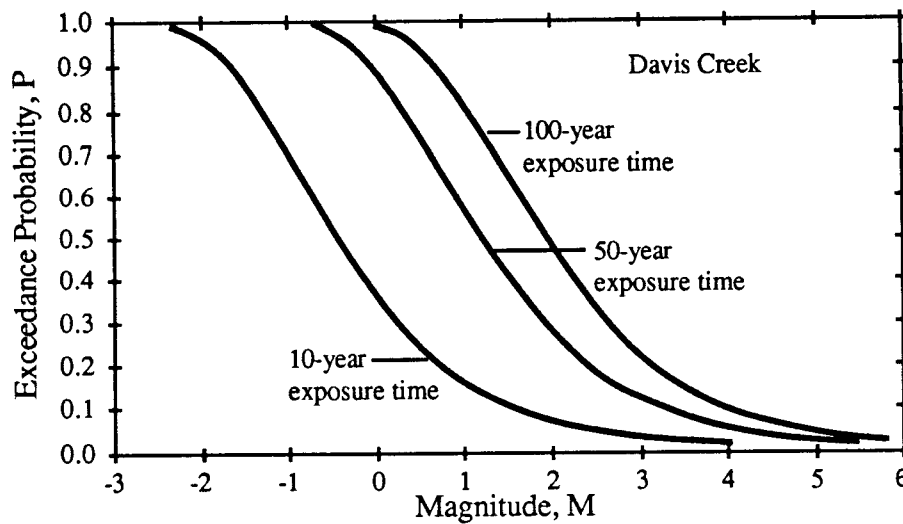


Figure 52. Representative exceedance probability curves for sedimentation events on the Davis Creek fan.

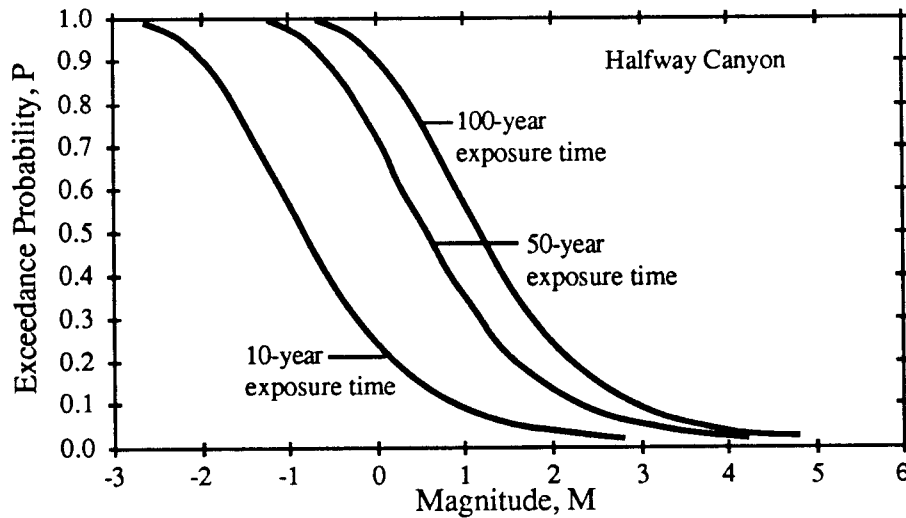


Figure 53. Representative exceedance probability curves for sedimentation events on the Halfway Canyon fan.

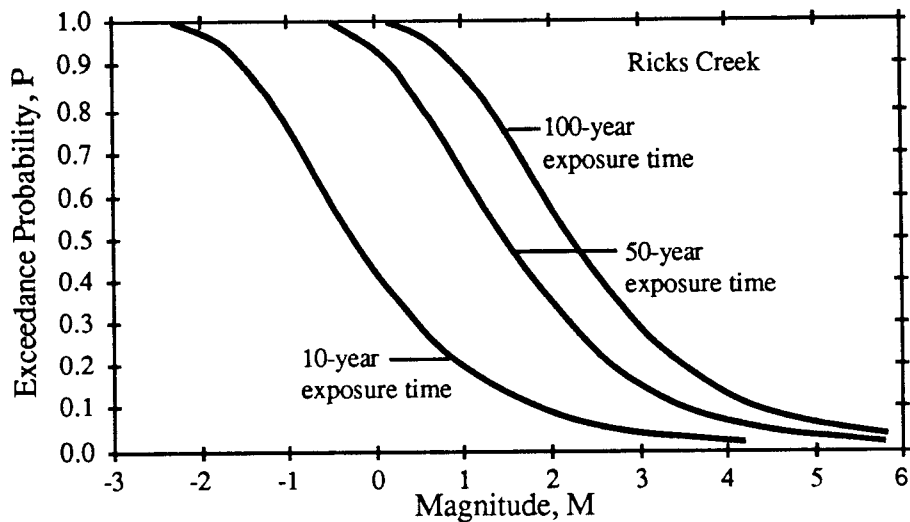


Figure 54. Representative exceedance probability curves for sedimentation events on the Ricks Creek fan.

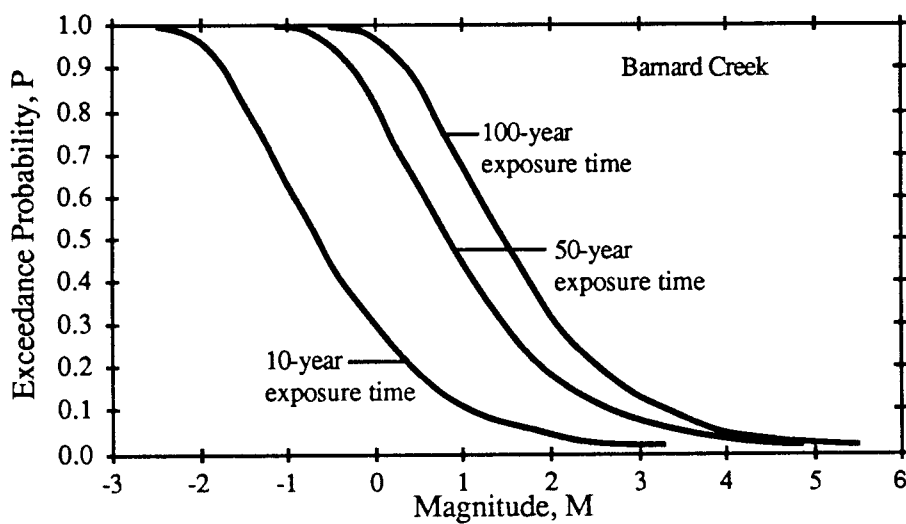


Figure 55. Representative exceedance probability curves for sedimentation events on the Barnard Creek fan.

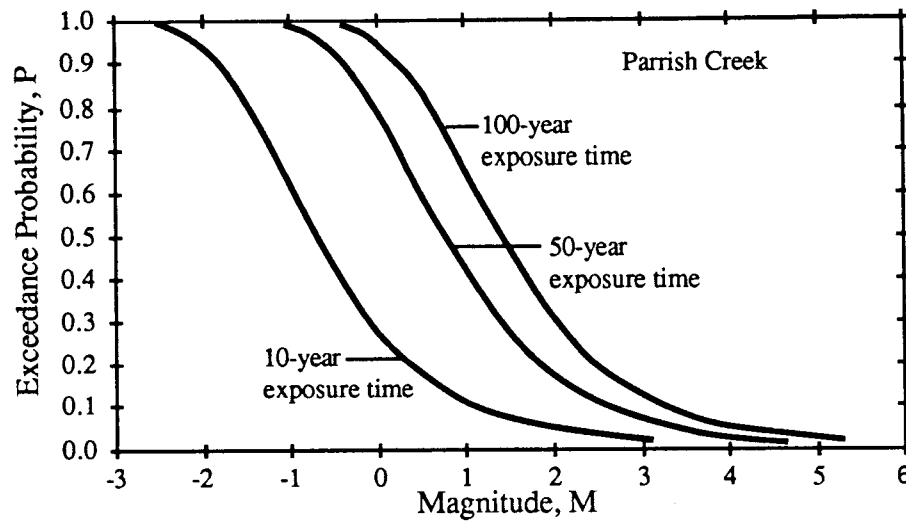


Figure 56. Representative exceedance probability curves for sedimentation events on the Parrish Creek fan.

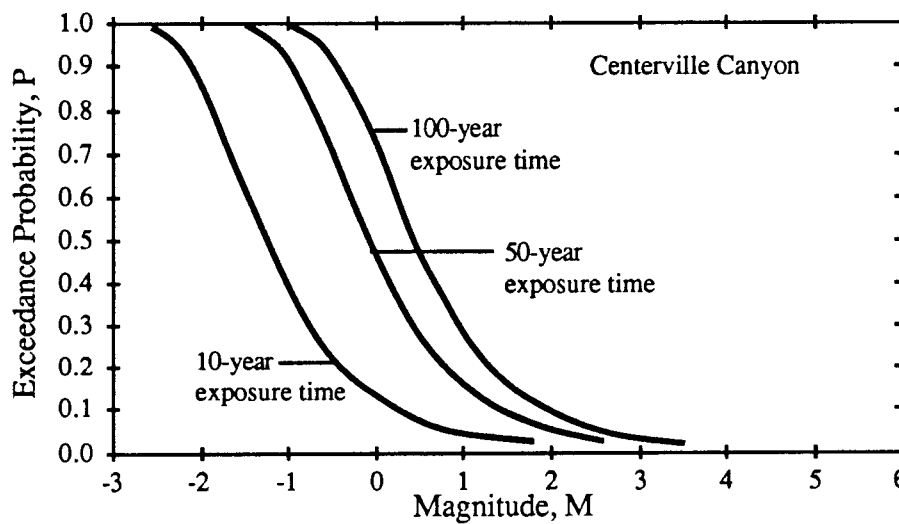


Figure 57. Representative exceedance probability curves for sedimentation events on the Centerville Canyon fan.

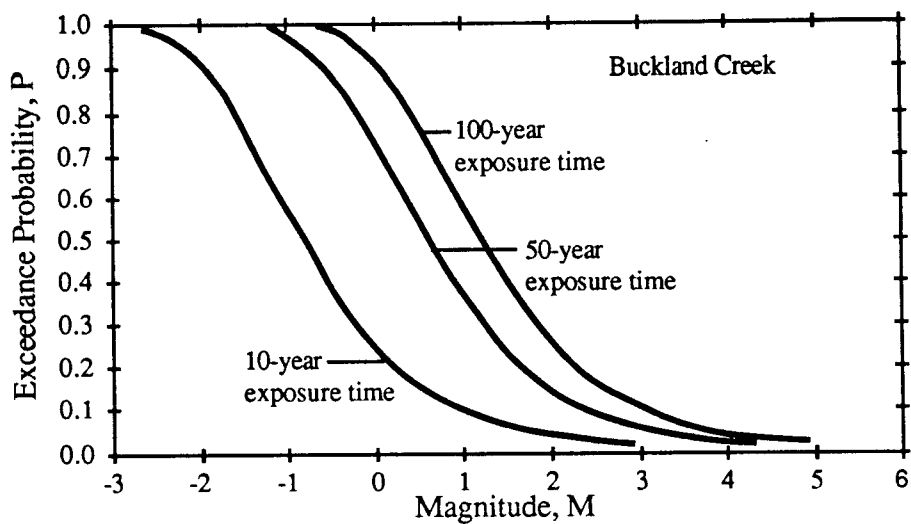


Figure 58. Representative exceedance probability curves for sedimentation events on the Buckland Creek fan.

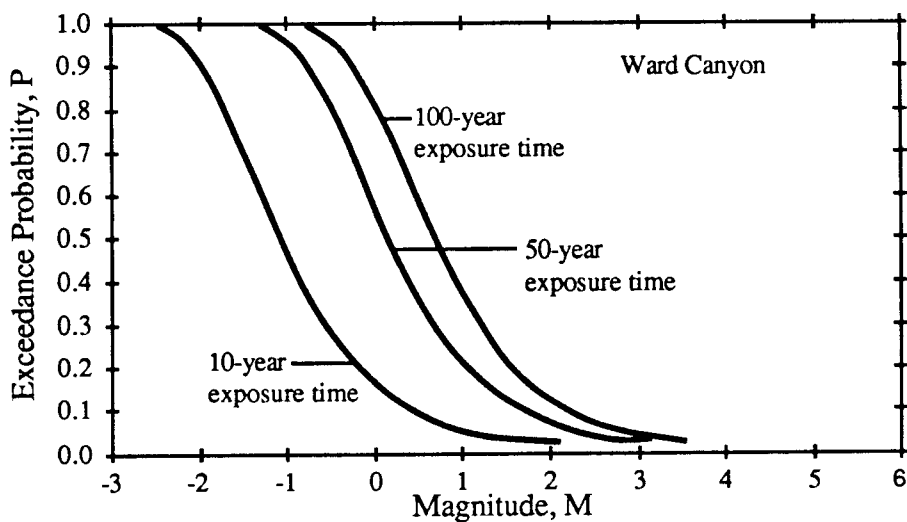


Figure 59. Representative exceedance probability curves for sedimentation events on the Ward Canyon fan.

Table 24. Summary of probabilistic evaluation of sedimentation hazards on alluvial fans in Davis County. Magnitudes of sedimentation events were calculated with a BASIC program "MAGPRO.3" (Appendix G). Values are average of binomial and extreme-value types of probability analyses associated with Holocene and historic periods of record; see text.

Fan	Calculated Magnitude of Sedimentation Event					
	100-Year Exposure Time		50-Year Exposure Time		10-year Exposure Time	
	P=0.5	P=0.1	P=0.5	P=0.1	P=0.5	P=0.1
Corbett	1.16	2.82	0.55	2.21	-0.86	0.79
Hobbs	1.16	2.82	0.55	2.21	-0.86	0.79
Lightning	0.33	1.63	-0.15	1.15	-1.24	0.04
Kays (Middle)	0.42	1.85	-0.11	1.32	-1.33	0.10
Kays (South)	1.96	3.98	1.21	3.23	-0.50	1.51
Snow	1.32	3.05	0.69	2.41	-0.77	0.94
Adams	1.27	2.97	0.67	2.35	-0.80	0.89
Webb	0.51	1.98	-0.03	1.44	-1.27	0.19
Baer	2.22	4.27	1.47	3.51	-0.27	1.77
Half	1.16	2.82	0.55	2.21	-0.86	0.79
Shepard	1.21	2.86	0.60	2.25	-0.80	0.84
Farmington	4.07	6.67	3.12	5.71	0.92	3.50
Rudd	0.95	2.53	0.37	1.95	-0.97	0.60
Steed	2.41	4.52	1.64	3.74	-0.14	1.95
Davis	1.95	3.90	1.21	3.18	-0.45	1.50
Halfway	1.16	2.82	0.55	2.21	-0.86	0.79
Ricks	2.22	4.24	1.47	3.50	-0.25	1.77
Barnard	1.48	3.23	0.84	2.59	-0.64	1.10
Parrish	1.40	3.14	0.76	2.50	-0.71	1.02
Centerville	0.47	1.88	-0.05	1.36	-1.23	0.16
Buckland	1.22	2.90	0.60	2.28	-0.83	0.85
Ward	0.70	2.16	0.17	1.62	-1.06	0.38

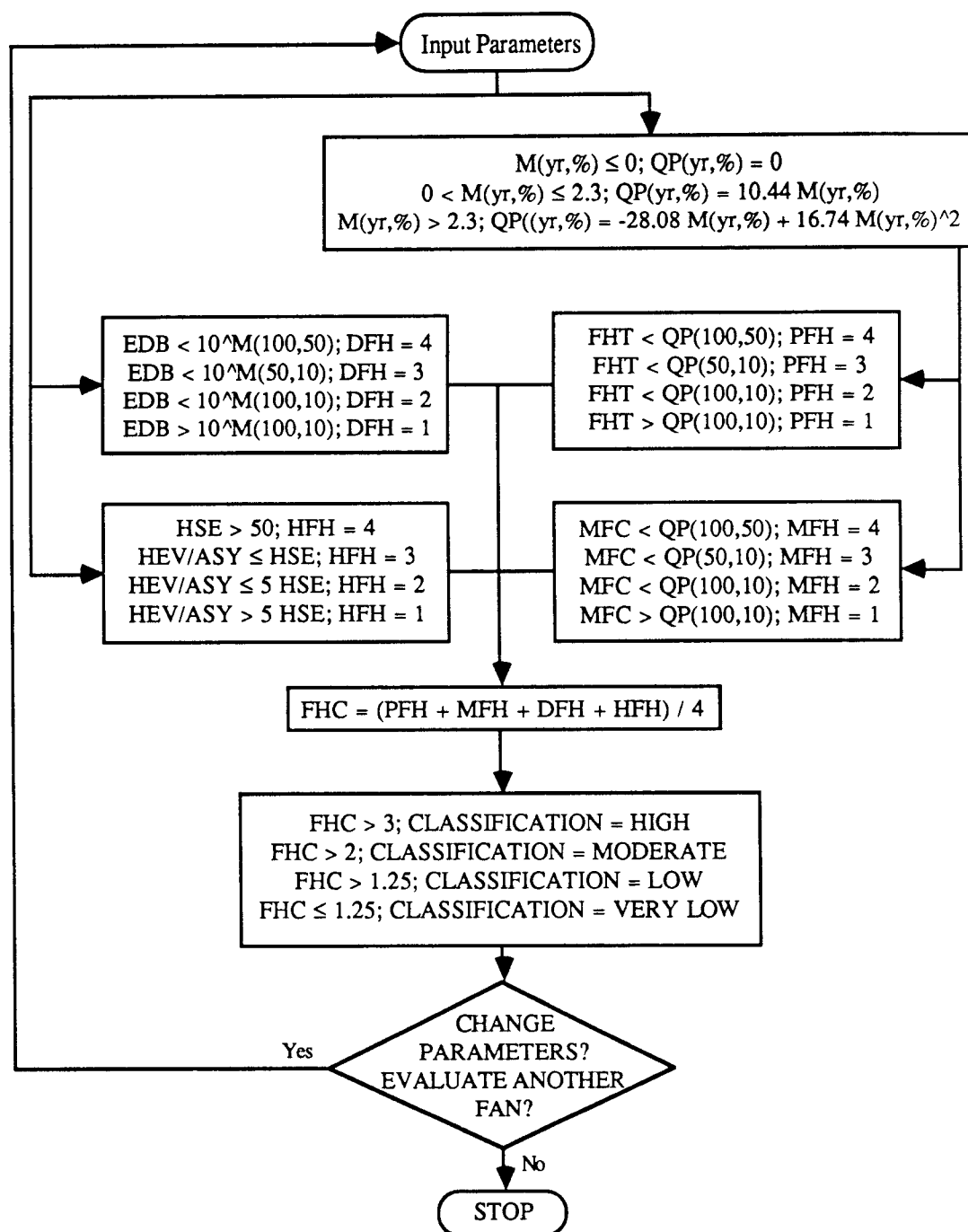


Figure 60. Flow diagram for program HAZ.MOD. $M(yr, \%)$ denotes the sedimentation event magnitude associated with a specific exposure time, yr, and exceedance probability, %; $QP(yr, \%)$ denotes probabilistic peak discharge. FHT denotes fan head trench area; MFC denotes middle fan channel area; EDB denotes existing debris basin volume; HSE denotes the time since the last historic sedimentation event; HEV denotes historic event volume; ASY denotes average sediment yield. PFH denotes proximal fan hazard; MFH denotes medial fan hazard; DFH denotes distal fan hazard; HFH denotes historic flow hazard; FHC denotes fan hazard classification.

sedimentation event, 8) the magnitude of the 50-year, 10 percent probability sedimentation event, and 9) the magnitude of the 100-year, 10 percent probability sedimentation event.

Values of fan-head trench and middle fan channel areas were estimated from the 1:2,400-scale orthotopographic maps of Davis County. These areas were estimated at positions where damage to existing structures could occur if the channels were overtopped. The volumes of existing debris basins were estimated from the orthotopographic maps or from geotechnical reports (Dames & Moore, 1984a, b, c, d, and e) for construction or repair of the debris basins which were planned in response to the 1983 damage. The fan-head trench areas, middle fan channel areas, and debris basin volumes are summarized in Table 25. The number of years since the last historic sedimentation event and the event volume are summarized in Table 18. Average annual sediment yield volumes are summarized in Table 17. Sedimentation event magnitudes for the exposure times and exceedance probabilities used in the model are summarized in Table 24.

Table 25. Summary of fan-head trench and middle fan channel areas, and debris basin volumes.

Fan	Fan-Head Trench Area (m ²)(a)	Middle Fan Channel Area (m ²)(a)	Existing Debris Basin Volume (m ³)
Corbett	80	8	0
Hobbs	185	5	300
Lightning	45	5	0
Kays (Middle)	140	10	1,400
Kays (South)	410	25	0
Snow	75	90	0
Adams	185	40	3,000
Webb	35	25	0
Baer	475	25	2,150
Half	10	0	0
Shepard	60	35	0
Farmington	115	15	57,350
Rudd	85	0	49,700
Steed	300	0	20,400
Davis	105	205	0
Halfway	115	0	0
Ricks	240	10	30,600
Barnard	20	0	4,600
Parrish	110	25	4,600
Centerville	55	10	7,600
Buckland	540	15	0
Ward	2,000	30	100,000

(a) The areas of the fan-head trench and middle fan channels were estimated from 1:2,400 scale orthotopographic maps using assumed simple triangular cross section shape unless trapezoidal shape appeared more appropriate. The channel areas were located where, if overtopped, damage to existing structures would occur.

Proximal and medial fan hazard ratings were derived by comparing the cross section areas of the fan head trench and the principal middle fan channel to the anticipated peak discharge associated with sedimentation event magnitudes which have exceedance probabilities of 50 percent in 100 years, 10 percent in 50 years, and 10 percent in 100 years. The annual frequencies for these three threshold events are 0.0069, 0.0021, and 0.0011, respectively; the average recurrence intervals for these events are 145, 475, and 950 years, respectively. Peak discharge values were estimated on a very limited basis consisting of Pierson's (1985b) observations of a small ($M = 2.3$) sedimentation event at Rudd Creek and Anciaux's (1987) proposed design inflow hydrograph of the major ($M = 4.83$) sedimentation event which caused damage at Farmington in 1983. Pierson (1985b) observed a peak discharge of $24 \text{ m}^3/\text{s}$ while Anciaux (1987) proposed a peak discharge of $255 \text{ m}^3/\text{s}$.

A non-linear relationship should exist between peak discharge and sedimentation event magnitude. Very small sedimentation events ($M \leq 0$) probably are associated with peak discharges which are so small that they may be taken to be zero. For use in this model, peak discharges were assumed to be linear from $M = 0$ to $M = 2.3$, and quadratic for $M > 2.3$. This relationship is shown graphically on Figure 61; the equations describing this relationship are

$$Q_p = 0 \quad \{M \leq 0\} \quad (99)$$

$$Q_p = 10.44 \cdot M \quad \{0 < M \leq 2.3\} \quad (100)$$

$$Q_p = -28.08 \cdot M + 16.74 \cdot M^2 \quad \{M > 2.3\} \quad (101)$$

where Q_p is the peak discharge in m^3/s and M is the sedimentation event magnitude. Since probabilistic values of magnitude were used to compute peak discharge, the corresponding peak discharge values were considered to be associated with the same exposure times and exceedance probabilities as the magnitudes. The hazard ratings were assigned by

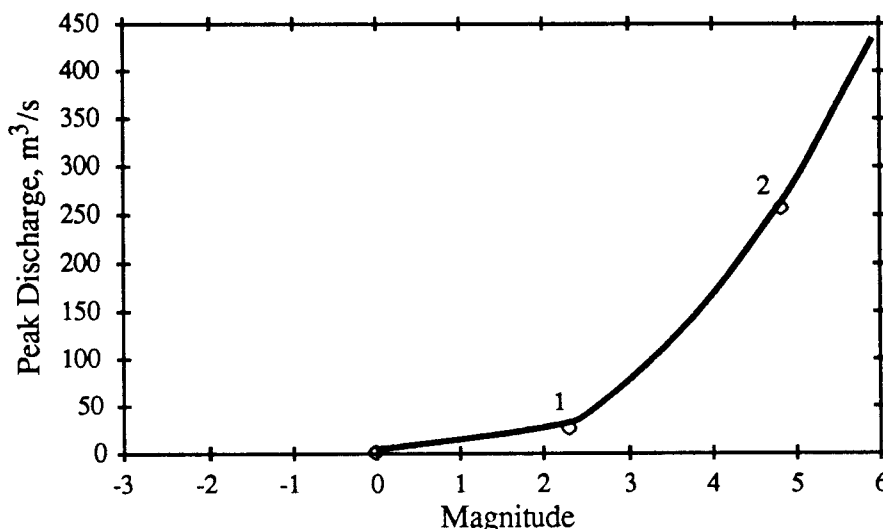


Figure 61. Peak discharge as a function of sedimentation event magnitude. Point 1 represents a peak discharge of $24 \text{ m}^3/\text{s}$ at an event magnitude of 2.3 (derived from Pierson, 1985b); point 2 represents a peak discharge of $255 \text{ m}^3/\text{s}$ at a magnitude of 4.83 (derived from Anciaux, 1987).

comparing the fan head trench and middle fan channel areas to the probabilistic peak discharge values. The channel areas were assumed to be constant for distances of 1 m to convert the cross section areas to equivalent volumes and the peak discharges were assumed to act for periods of 1 s to convert the discharges to equivalent volumes. If the channel areas were smaller than the 100-year, 50 percent peak discharge, hazard ratings of high were assigned. High hazard ratings were given ordinal rank of 4 in the HAZ.MOD program (Figure 60). Similarly, channel areas between the 100-year, 50 percent and the 50-year, 10 percent discharge values were assigned hazard ratings of moderate (rank 3); channel areas between the 50-year, 10 percent and the 100-year, 10 percent discharge values were assigned hazard ratings of low (rank 2); and channels larger than the 100-year, 10 percent discharge value were assigned hazard ratings of very low (rank 1).

The volumes of existing debris basins were compared to the volumes of the probabilistic sedimentation event magnitudes ($V = 10^M$). Basins with volumes smaller than the volume of the 100-year, 50 percent sedimentation event were assigned hazard ratings of high (rank 4); basin volumes between the 100-year, 50 percent and 50-year, 10 percent event volumes were assigned hazard ratings of moderate (rank 3); basin volumes between the 50-year, 10 percent and the 100-year, 10 percent event volumes were assigned hazard ratings of low (rank 2); basin volumes larger than the 100-year, 10 percent event volume were assigned hazard ratings of very low (rank 1).

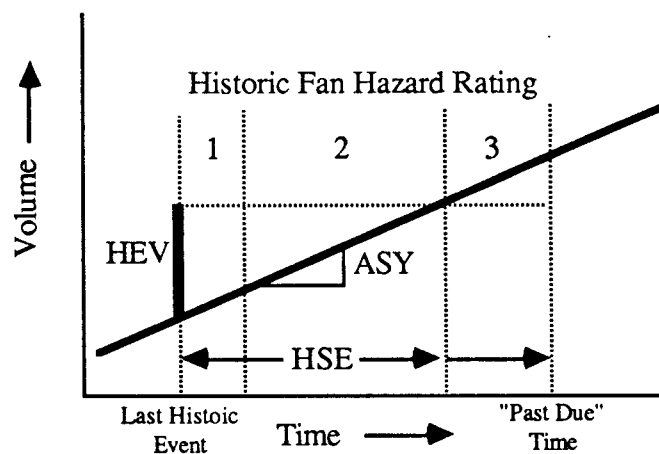
The number of years since the last historic sedimentation event at each fan was used two ways in the HAZ.MOD program: first, a hazard rating of high (rank 4) was assigned if the last historic sedimentation event occurred more than 50 years ago; second, the number of years was compared to the volume of the last sedimentation event and the average annual sediment yield for the basin (Figure 62). Fans with the ratio of the last sedimentation event volume (HEV) to the average sediment yield (ASY) less than or equal to the number of years since the last sedimentation event (HSE) were assigned hazard ratings of moderate (rank 3). This expression is

$$\text{HEV} / \text{ASY} \leq \text{HSE} \quad (102)$$

Fans with the ratio of HEV to ASY between HSE and five times HSE were assigned hazard ratings of low (rank 2) and fans with HEV/ASY greater than five times HSE were assigned hazard ratings of very low (rank 1). The overall hazard classification for each fan was taken as the simple arithmetic average of the individual hazard ratings. Overall fan hazard classifications were assigned according to the subdivisions listed in Table 26.

Wieczorek and others (1983, Plate 1) prepared a map showing relative potential for debris flows and debris floods to reach canyon mouths for drainage basins between Salt Lake City and Willard. The results of their study are summarized in Table 27 for the canyons in Davis County and compared to the results of this research. The basis for Wieczorek and others (1983) evaluation consisted of two lines of reasoning: First, the presence and size of partly-detached landslide masses within drainage basins; and second, geomorphic or historic evidence of past debris flows or debris floods reaching canyon mouths. Thus, their study was deterministic while the present research is probabilistic.

The classifications which Wieczorek and others (1983) used to describe the relative potential for debris flow consisted of very high, high, moderate, and low; the criteria they used to differentiate these classes are described in the footnote to Table 27. The classifications they used to describe the relative potential for debris flood consisted of very high, high, and low; the criteria they used to differentiate these classes also are described in the footnote to Table 27. Overall fan hazard classifications based on Holocene sediment yield values from Table 17 are also presented on Table 27. Wieczorek and others (1983) classified 9 canyons as having high or very high debris flow potential and 19 canyons as



Historic Sedimentation Event Characteristic	Historic Fan Hazard Rating
No historic events	4 - High
$HEV/ASY \leq HSE$	3 - Moderate
$HEV/ASY \leq 5 \cdot HSE$	2 - Low
	1 - Very Low

Figure 62. Relationships among the time since the last sedimentation event, the volume of the last event, and the average annual sediment yield. HSE is the time in years since the last historic sedimentation event; HEV is the volume of the last historic event; ASY is the average annual sediment yield.

having high or very high debris flood potential. The results of the present research (Table 27) indicate that only 4 fans have overall fan hazard classifications of high, while 9 are classified as low and 1 as very low.

The geologic arguments described earlier in this report suggest that the most realistic classifications of hazards due to sedimentation events on the alluvial fans in Davis County are based on an average between the binomial distribution of event magnitudes during Holocene time and the extreme-value distribution of event magnitudes during the historic period. The most appropriate sediment yield values for the hazard model are based on sedimentation during Holocene (post-Lake Bonneville) time.

Table 26. Overall fan hazard classifications for average hazard rating values. FHC, as used in the program HAZ.MOD, is the arithmetic average of PFH, MFH, DFH, and HFH (where high hazard was given a rank of 4; moderate, a rank of 3; low, a rank of 2; and very low, a rank of 1).

Average Hazard Rating Value	Overall Fan Hazard Classification
FHC > 3	High Hazard
$3 \geq \text{FHC} > 2$	Moderate Hazard
$2 \geq \text{FHC} > 1.25$	Low Hazard
$\text{FHC} \leq 1.25$	Very Low Hazard

Table 27. Comparison of fan hazard classifications from this study with potential for debris flow and debris flood (Wieczorek and others, 1983, Plate 1). Overall fan hazard classification (from Table 26) is based on Holocene sediment yield value (Table 17). It is important to note that the analysis by Wieczorek and others (1983) was based on 1983 conditions and described the relative potential for debris flows or debris floods to reach canyon mouths based on deterministic parameters. The overall fan hazard classification developed during the present research is based on 1987 conditions and probabilistic parameters.

Fan	<u>Wieczorek and others, 1983, Plate 1</u>		<u>Overall Fan Hazard Classification</u> Based on Holocene Sediment Yield Value And Average of Holocene Binomial and <u>Historic Extreme-value Distributions</u>	
	Potential For Debris Flow (a)	Potential For Debris Flood (b)	Classification	Numerical Value
Corbett	—	High	High	3.25
Hobbs	Low	Low	Moderate	2.5
Lightning	—	—	Moderate	2.25
Kays (Middle)	Moderate	High	Low	1.75
Kays (South)	High	High	Moderate	2.5
Snow	Low	High	Moderate	2.5
Adams	Low	Low	Moderate	2.0
Webb	Moderate	High	Moderate	2.0
Baer	Very High	Very High	Moderate	2.5
Half	Moderate	High	High	4.0
Shepard	Low	Very High	Low	2.0
Farmington	Very High	Very High	High	3.25
Rudd	Very High	Very High	Low	1.75
Steed	Very High	Very High	Low	2.0
Davis	High	High	Moderate	2.25
Halfway	Moderate	High	High	3.25
Ricks	High	Very High	Low	1.75
Barnard	Moderate	Very High	Moderate	2.25
Parrish	Very High	Very High	Low	1.5
Centerville	Low	High	Low	1.75
Buckland	—	High	Moderate	3.0
Ward	High	Very High	Very Low	1.0

(a) Very High: Canyons with existing partly-detached landslide of volume sufficient for debris flow to reach canyon mouth.

High: Evidence of more than one past debris flow reaching canyon mouth, indicating a recurrent long-term potential for debris flow.

Moderate: Evidence of only one past debris flow reaching canyon mouth, or historic debris-flow scar or path suggesting volume sufficient for debris flow to reach canyon mouth.

Low: No evidence for past debris flows reaching canyon mouth.

(b) Very High: Canyons with existing partly-detached landslides that could become mobilized as debris flow and subsequently diluted into debris floods.

High: At least one historic debris-flow or debris flood scar or path regardless of volume, or evidence of past debris-flow or debris flood at canyon mouth (fans mapped by Miller, 1980). This suggests recurrent long-term potential for debris flood.

Low: No old debris-flow scars or evidence of past debris floods.

HAZARD RESPONSE ALTERNATIVES

INTRODUCTION

Many alternative actions are available for responding to or reducing potential hazards. Kockelman (1986) notes that public acquisition of hazardous areas is one of the actions well known to the planning profession, construction of control structures is commonly used by the engineering profession, and highway departments typically place warning signs at areas subject to flash flood and rock fall hazards. The techniques identified by Kockelman (1986, p. 65) for reduction of hazards are summarized in Table 28.

Possible responses to hazards or potentially hazardous processes summarized by Varnes (1984, p. 28) include some the alternatives identified in Table 28. Varnes (1984) reports that fact-finding, or delineation of areas of hazard and degrees of risk, probably is the most common first action for natural hazard assessment. Dissemination of information to governing bodies and the public, along with education and warnings, is a common second action. Once the hazards are identified, actions can include enacting land-use regulation and building ordinances, acquisition of land, and evacuation in the event the hazard occurs. Discouraging development of hazardous areas can be accomplished by tax-assessment practices and financing policies. Hazards can be removed and facilities at risk can be protected with control works.

Table 28. Some techniques for reducing natural hazards. From Kockelman, 1986.

- **Discouraging new development in hazardous areas**
 - Disclosing the hazard to real-estate buyers
 - Informing and educating the public
 - Adopting utility and public-facility service-area policies
 - Posting warnings of potential hazards
 - Making a public record of hazards
- **Removing or converting existing development**
 - Acquiring or exchanging hazardous property
 - Reconstructing damaged areas after natural hazards occur
 - Clearing and redeveloping blighted areas before natural hazards occur
 - Discontinuing nonconforming uses
 - Removing unsafe structures
- **Providing financial incentives or disincentives**
 - Providing tax credits or lower assessments
 - Adopting lending policies that reflect risk of loss
 - Clarifying the legal liability of property owners
 - Requiring insurance related to level of hazard
 - Placing conditions on federal and state financial assistance
- **Regulating new development in hazardous areas**
 - Enacting grading ordinances
 - Amending land-use zoning districts and regulations
 - Creating special hazard-reduction zones and regulations
 - Placing moratoriums on rebuilding
 - Adopting hillside-development regulations
 - Enacting sanitary ordinances
 - Enacting subdivision ordinances
- **Protecting existing development**
 - Controlling landslides and slumps
 - Controlling rockfalls
 - Establishing monitoring, warning, and evacuating systems
 - Controlling mudflows and debris flows
 - Creating improvement districts

A model for hazard and risk management was developed as part of the research for this dissertation and is presented on Figure 63. Responsible management of hazards and risks begins with recognition of the hazards affecting an area. Failure to recognize hazards in the contemporary legal atmosphere in the United States may constitute negligence and probably invites liability for damage in the event a hazard occurs with damaging intensity. Similarly, ignoring hazards after they have been recognized probably also constitutes negligence. Motivations for ignoring hazards do exist, however, and are described below.

The first major step in hazard and risk management following recognition of hazards is evaluation of both hazards and risks (Figure 63). Evaluation of hazards was described earlier and includes quantifying the probabilities that hazards will occur with intensities which exceed a damage threshold (exceedance probabilities) within a specific exposure time (design life). Evaluation of risk includes inventorying population, property, and business function which might be injured, damaged, or interrupted by the occurrence of a hazard. After hazards and risks have been evaluated, decisions must be made regarding the level of exposure, or risk, which is acceptable (Figure 63). Commonly, establishment of acceptable levels of risk is a public policy issue. However, for private facilities, autonomous decisions can be made within the constraints of governmental regulations and ordinances which specify certain minimum levels of risk (e.g., code requirements for structural design).

Following evaluation of hazards and risks, and establishment of acceptable risks, hazard response alternatives may be assessed systematically, as shown on Figure 64. Each of the alternatives should be assessed sequentially, beginning with the "do nothing" alternative. Assessment of the alternatives consists of two steps: First, comparing the acceptable levels of risk with the risk associated with the alternative, and second, estimating costs associated with the alternative. If the risk associated with the alternative is acceptable, the cost associated with the alternative is estimated and stored for subsequent benefit-cost optimization. On the other hand, if the risk associated with the alternative is deemed unacceptable, estimating the cost is not meaningful and need not be done. The alternative responses are described systematically below.

Risk management consists of a continuous triple loop (Figure 63). One of the loops provides for periodic reevaluation of the hazard, another loop provides for reevaluation of the risk, and another loop provides for reevaluation of the perception of acceptable risk. New information or technology may become available which indicates the hazardous processes are more or less dangerous than originally thought. For example, the probability of a damaging flood event may be diminished if a flood control dam is constructed upstream from a community. Similarly, community growth may change the inventory of population and property at risk and perception of risk may change due to economic factors. For example, the loss of a large number of jobs by the closing of a factory may outweigh the perception of health risks associated with inferior air quality caused by factory emissions. The model of hazard and risk management described on Figures 63 and 64 provides a systematic framework for dealing with hazards in a responsible manner.

ALTERNATIVES

In addition to the irresponsible alternative of ignoring hazards, response alternatives can be subdivided into five basic categories as outlined on Figure 64: 1) continue current practices, 2) modify the hazard, 3) modify what is at risk, 4) modify procedural and/or operational aspects, and 5) avoid the hazard. Any of these five possible alternatives could be applied to hazards related to sedimentation processes on alluvial fans.

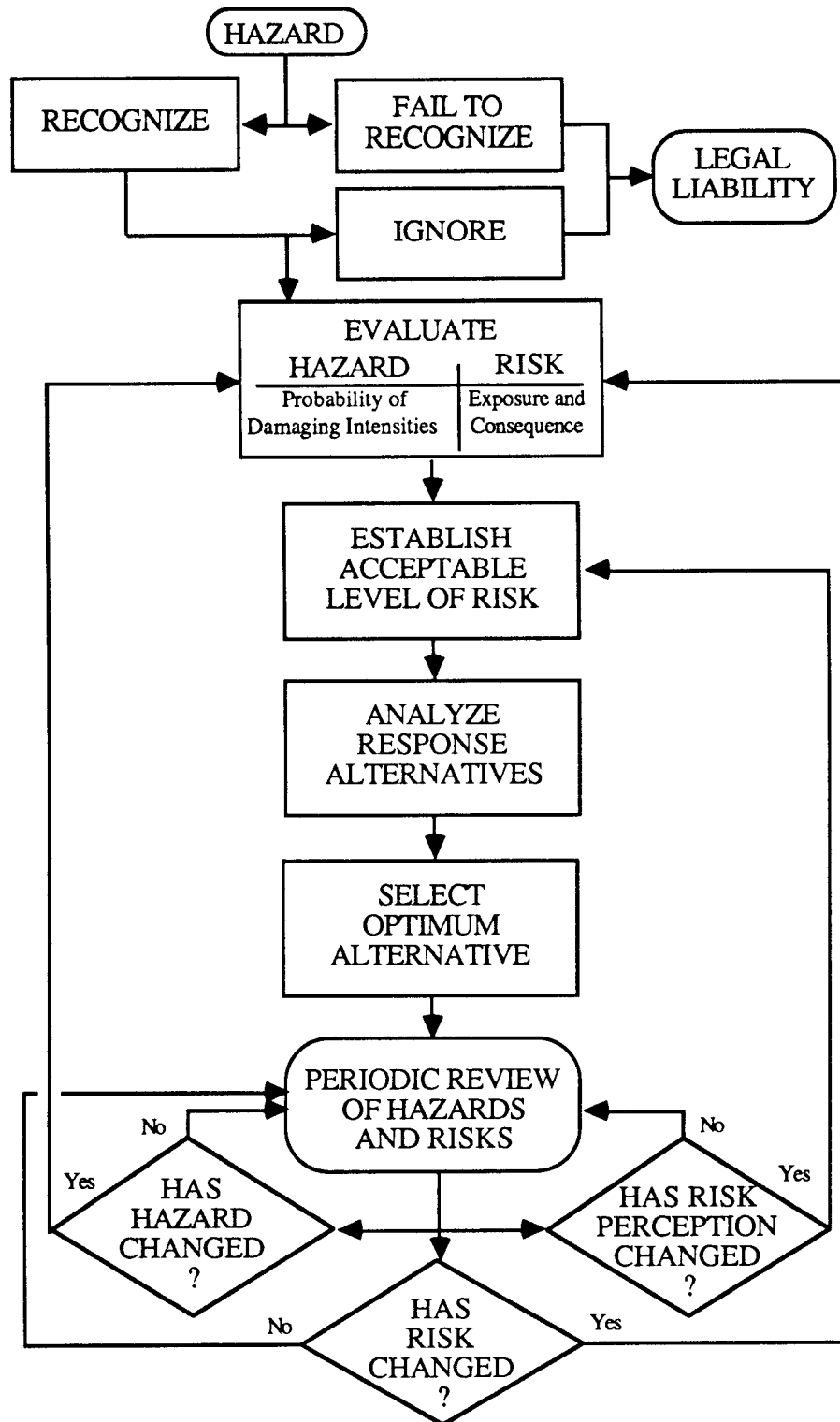


Figure 63. A model for hazard and risk management. The element entitled "Analyze Response Alternatives" is described on Figure 64.

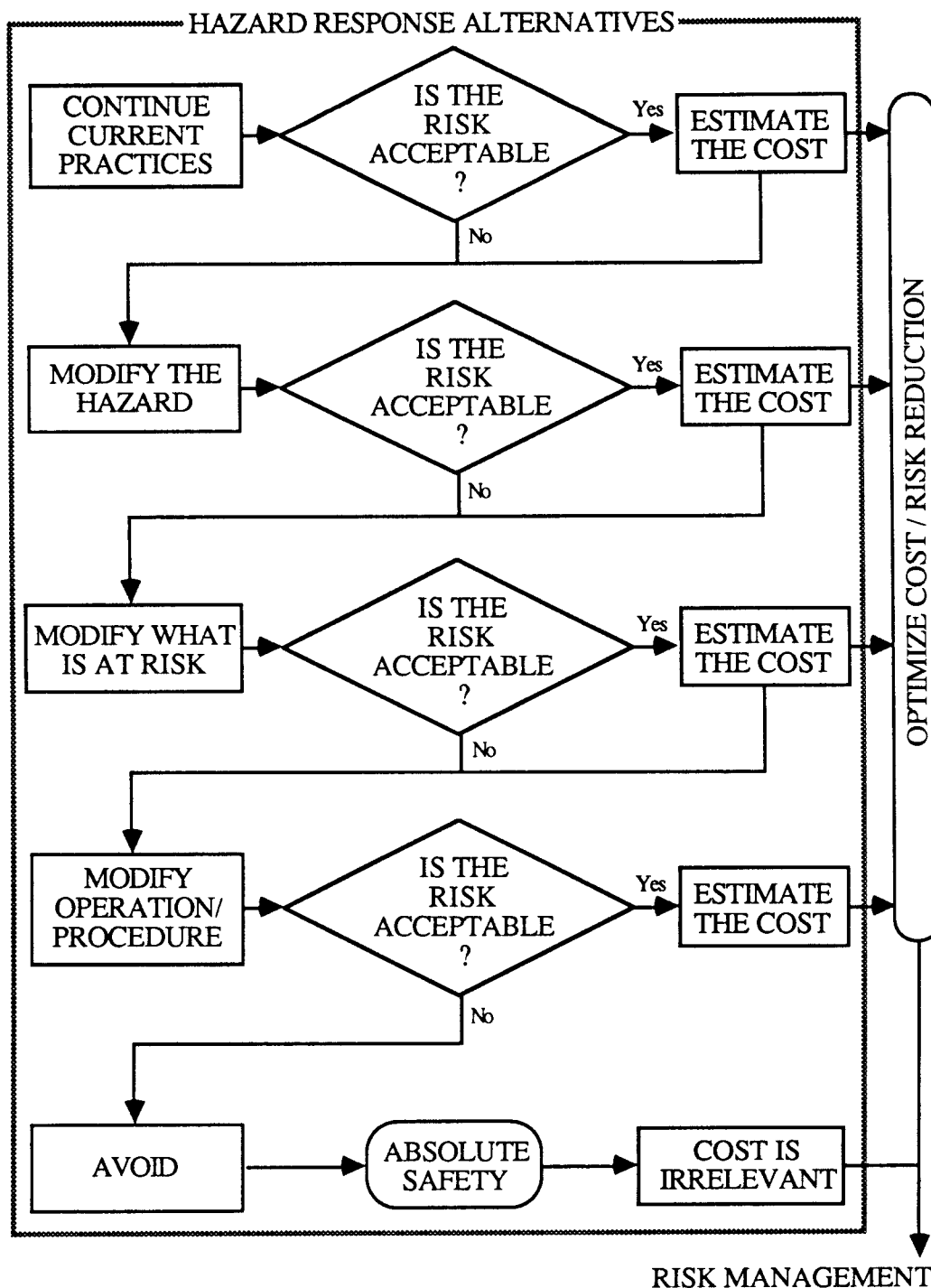


Figure 64. A model for hazard response alternatives. The details on this figure represent the element entitled "Analyze Response Alternatives" on Figure 63.

Ignore the Hazard

The simplest and probably most commonly adopted hazard response is to ignore the existence of the hazard and do nothing. Justifications for this alternative could be 1) investigating hazard distributions costs money, 2) identifying hazards could result in restricting development, 3) facilities probably already exist in hazard areas, and 4) if hazards are not known to exist then nothing will have to be done about them. A substantial part of the direct financial losses caused by natural hazards in the United States have been shifted to the federal government in the form of disaster relief (Petak and Atkisson, 1982, p. 238). This effectively distributes the losses to taxpayers in areas not exposed to loss-producing hazards and actually may encourage irresponsible actions with respect to hazards. Ignoring hazards is equivalent to de facto acceptance of the risk of damage, even though neither the level of risk nor the extent of potential damage are known.

Continue Current Practices

This essentially is a "do nothing" alternative which is different from ignoring the hazards because the hazards have been quantified and the risks judged to be acceptable. The continuous loops for reevaluation of the hazards, risks, and risk perception (Figure 63) provides periodic review of changes which may modify the understanding of the hazard, the perception of the risk, or actually the character of the hazardous process. Even if continuing current practices satisfies the acceptable risk criteria, the other alternatives must be evaluated to provide a basis for optimizing of benefits and costs. Realistically, however, if doing nothing satisfies the acceptable risk criteria, the other alternatives probably would not be thoroughly evaluated.

Modify the Hazard

Once hazards have been identified, a viable alternative may be to modify them (Figure 64). In some cases, modification of the hazard is not technically possible, and in many cases, modification is not economically feasible. Modification of a volcano, for example, to prevent it from erupting exceeds technological capabilities. Modification of flood hazards, on the other hand, by building dikes to contain large flood discharges is a proven technique; however, as demonstrated by Costa and Baker (1981, p. 386), flood control dikes encourage development in flood zones and expose that development to hazards associated with floods which exceed the design capacity of the dikes. Constructing dikes large enough to contain the largest conceivable flood probably would cost far more than the value of the development which would benefit from the protection, making the dikes economically unfeasible or requiring the cost burden to be distributed over a large population which extends well beyond the area protected by the dikes. Such is the case with sediment catch basins as well.

Sedimentation hazards have been modified to provide protection to communities located on alluvial fans. Among the more common approaches to sedimentation hazard modification are sediment catch basins and channel improvements (Wieczorek and others, 1983, p. 14 ff). Sediment source modifications also have been used to modify sedimentation hazards; these measures commonly include construction of contour terraces, to retard rapid runoff of heavy precipitation, and protection from fire and overgrazing, to promote erosion-resistant vegetation (Bailey and Croft, 1937).

Sediment Catch Basins

One of the approaches which seems to directly modify sedimentation hazards is construction of sediment catch basins. This approach is similar to construction of dikes to contain flood discharges in that some design capacity is selected as providing an acceptable level of safety. In the case of floods, the dikes are designed to contain a discharge which waxes, peaks, and wanes, leaving the dikes unchanged and ready for the next flood discharge. Sediment catch basins, however, are designed to contain a volume of sediment which otherwise would be discharged into a community where damage could occur. The sediment contained in the basin must be removed to preserve the capacity of the basin for the next event. Among the geologic factors considered in the design of the sediment catch basins following the damaging sedimentation events in 1983 were earlier historic sedimentation events and volumes of partly detached landslide masses in the drainage basins (Wieczorek and others, 1983). Non-geologic factors included cost of land acquisition and cost of construction.

Channel Improvements

Channel improvements consist of increased capacity for transport of sediment and dissipation of energy with features such as drop-structures. An increased channel capacity is intended to provide a means for sediment to be transported through certain areas and deposited in areas where little or no damage will result. This approach generally is based on hydraulic considerations and probably is more successful for hyperconcentrated sediment flows and normal streamflows than for debris flows because of the tendency for debris flows to be self-diverting. Wieczorek and others (1983, p. 20) note that deposition and erosion commonly occur unpredictably not only from storm to storm, but also within a single storm. Dawdy (1979, p. 1407) also notes the propensity for sudden relocation of flood flows on alluvial fans during a single runoff event.

Other channel improvements include straightening curves and protecting curves from erosion and undercutting. Where existing development encroaches on watercourses, Wieczorek and others (1983, p. 21) recommended block walls at rear and side yards to provide some containment within streets and some protection for structures. Hollingsworth and Kovacs (1981) suggest diversion walls ("A" walls) and debris fences to protect structures directly in the paths of debris flows. The "A"-shaped wall is intended to divert flowing sediment between structures, normally residences in a relatively high density neighborhood. The debris fence is intended to retard the rate of the flow, catch a portion of the flow, and generally disrupt the flow to reduce its damage potential.

Check dams have also been used as a means of creating local base levels and dissipating energy with drop structures (Ferrell, 1959). Check dams have been used in series in mountain channels above communities in Los Angeles County. The design gradient of the stream is projected upward from the crest of the lowest check dam to provide a means for selecting the location of the next dam. By reducing the gradient between check dams, deposition of sediment is promoted; by having a free-fall from the crest of a check dam onto an erosion-resistant apron, flow energy is dissipated which is intended to reduce damage potential. These check dams can be viewed as a series of small sediment catch basins and are commonly constructed in canyons with sediment catch basins at the canyon mouths. Thus, sediment which is trapped behind check dams within canyons does not contribute to the volume of sediment which must be removed from the sediment catch basins to preserve their effectiveness. Therefore, economic evaluations are needed to compare the cost of constructing the check dams with the cost of maintaining the sediment catch basins. In areas such as Los Angeles County where large quantities of sediment are

discharged from canyons at relatively frequent intervals, check dams may represent economical alternatives. However, in Davis County, the relative infrequency of sedimentation events combined with the inaccessability of the canyons may make check dams so expensive that periodic maintenance of sediment catch basins may be the preferred alternative.

Far-reaching environmental and economic ramifications should not be overlooked in evaluating local mitigation measures. For example, arresting sediment in catch basins at canyon mouths could promote down-stream erosion of stream channels or coastlines, possibly threatening existing developments and requiring expensive erosion protection to be constructed where otherwise it would not have been needed.

Sediment Source Modifications

The damaging sedimentation events in Davis County in 1930 resulted in construction of sediment catch basins at a number of canyons. Mr. Bill Rigby's father, when asked for his opinion regarding the basin at Ricks Creek, replied that he didn't doctor his big toe when he had a headache (Mr. Bill Rigby, 1987, oral communication). A prominent state official translated Mr. Rigby's intent into a more graphic statement, "To attempt to control floods by putting debris basins at the mouth of the canyon is like putting a diaper on a baby to control diarrhea" (Croft, 1981, p. 12).

With the realization that the sediment catch basins provide limited, but immediate, protection, the U.S. Forest Service began to implement modifications at higher elevations within the drainage basins which contributed damaging sediment in 1930. Bailey and others (1934, p. 14 ff) noted that sources of the damaging floods in 1930 constituted very small areas where plant cover had been denuded by overgrazing and other anthropogenic degradation (e.g., promiscuous burning, Pickford, 1932). The denuded areas permitted rapid, concentrated runoff from cloudburst storms, eroding rills which quickly converged into gullies. The sediment concentration achieved debris-flow level well before the discharge reached the communities at the mouths of the canyons. With recognition that small areas probably were responsible for most of the damage, a technique of contour trenching was formulated and implemented after the land was acquired into the public domain (Bailey and Croft, 1937). The contour trenches were intended to contain intense rainfall, promote infiltration, inhibit runoff, and promote growth of erosion-resisting vegetation. The frequency of sedimentation events declined dramatically following the construction of the contour trenches (Bailey and others, 1947, p. 16). Thus, the contour trenches, protection from overgrazing, and protection from promiscuous burning appear to have successfully controlled sediment production during cloudburst rainstorms; however, the increased infiltration of snowmelt may have contributed to ground water pressures in fractured bedrock which could have promoted shallow landsliding which mobilized into debris flows in 1983.

Modify What is at Risk

A logical alternative to modifying a hazard is to modify the structure or population at risk. Examples of modifying what is at risk can be obtained from experiences with flood hazards. A hypothetical site within a zone where flooding is expected to occur need not adopt a policy to ignore the flood hazard. This site is located within a flood hazard zone; therefore, avoiding the hazard is not possible unless the site is to be left undeveloped. For some critical landuses (e.g., hospitals, fire stations), sites within flood hazard zones may be unacceptable because the critical facilities will be depended upon for relief and service

during and immediately following disasters. However, most noncritical facilities can be modified to reduce the risk of damage to an acceptable level. Mathewson (1981, p. 186) uses an office building in a flood zone as an example to illustrate the influence of insurance costs on average annual costs for four alternatives of flood "proofing." One of his alternatives is establishing parking on the ground level with the office space above. The anticipated flood would inundate the parking level with potential damage to parked vehicles and the elevator of the building, but other elements of the building would be undamaged.

Two kinds of risk exist and must be treated separately: potential loss of life and potential economic loss. These risks must be separated because of the generally great differences in the level of risk deemed to be acceptable for each. Protection of life safety by modifying what is at risk commonly involves methods of early warning of impending life-threatening processes (e.g., smoke detectors for fire) and formulation of contingency plans for rapid evacuation. Such methods and plans represent procedural and/or operational aspects which are discussed in a subsequent section of this chapter. Protection of life safety also is provided by structural integrity of buildings. Therefore, the design of new buildings and improvement of existing buildings to resist forces of hazardous processes constitutes modification of what is at risk.

Once the life safety issue is addressed and an acceptable level of risk is established, an assessment of potential economic losses can be made. Economic loss can be direct (e.g., damage to structures and contents) and indirect (e.g., damaged access to a business and reduced land value). Structures can be designed to withstand impact and drag forces; existing structures could be upgraded, if economically feasible. Deflection walls, described above as features which can be used to modify the hazard (i.e., the path of the sedimentation event), can also be used to modify what is at risk by absorbing or deflecting impact and drag forces.

Damage to contents of buildings can be minimized with the techniques described below for protection of life safety.

Modify Procedural and/or Operational Aspects

Understanding hazards and evaluating risks and possible mitigation alternatives permits comparison of procedural and/or operational modifications for risk management. Understanding hazards and evaluating risks comprise the risk estimation and risk evaluation elements of Petak and Atkisson (1982, p. 11). As described earlier, risk estimation focuses on quantitative descriptions of the population at risk, the hazardous events, the probabilities that the hazardous events will occur, the consequences associated with the occurrence of the hazardous events, and integration of the magnitude/event probabilities into a quantitative measure of risk. Risk evaluation consists of a social, political, and/or engineering assessment of the result of the risk estimation; in essence, how safe is safe enough? Within the context of this alternative response, life safety issues and economic issues must be separated because of the great differences in acceptable levels of risk.

Life Safety Issues

Seven persons were killed in Farmington in the sedimentation event in 1923 (Woolley, 1946). No records indicate that any other lives have been lost in sedimentation events in Davis County. Effective, although unintentional, warnings of the impending sedimentation damage were given at Rudd Creek in 1983 and at Lightning Creek in 1984

by the sounds of bumping boulders and snapping tree branches as debris flow material moved down the channels (Mr. Cammon Arrington and Mr. Jeff Warburton, 1987, oral communication). McCarter and Kaliser (1985) installed extensometers and inclinometers on partly detached landslide masses with radio frequency telemetry to local law enforcement agencies. The good success with which these instruments were able to detect landslide movements and mobilized debris in the channel at Rudd Creek is summarized by McCarter and Kaliser (1985, p. 45). Criteria and instructions for evacuation could be developed to minimize loss of life in areas exposed to sedimentation hazards.

Potentially life threatening damage to residential structures included collapse due to impact of rapidly moving debris and inundation of basements and ground level rooms by transitional flows and hyperconcentrated sediment flows entering through windows and doors. A systematic assessment of the structural quality of the collapsed residences apparently was not conducted; consequently, it is not known whether the collapsed structures were old unreinforced masonry or modern wood frame construction. A relatively modern wood frame structure at Rudd Creek was shoved intact from its foundation without collapsing (Figure 3). Nonetheless, more modern construction is designed to withstand some lateral force due to earthquake and, in general, should perform better than older construction under lateral force due to sediment impact and drag. Local ordinances prohibiting basement and ground-level windows on upstream sides of residences in high hazard areas would serve to minimize life loss potential by removing the dominant locus of sediment entrance into structures, such as occurred in Davis County in 1983 and 1984. Another alternative operational action would be local ordinances prohibiting bedrooms in basements to eliminate the possibility of individuals being overcome by sediment while they were sleeping.

A systematic assessment of seasonal aspects of cloudburst floods along the Wasatch Front was prepared by Butler and Marsell (1972, p. 33). They included the data presented by Woolley (1946) and found that 99.8 percent of the cloudburst floods from 1850 to 1969 occurred in the spring and summer months (April to September). Furthermore, 90.1 percent of the flood events occurred in the summer months (June to September). The snowmelt floods in 1922, 1952, 1983, and 1984 occurred chiefly in the months of May and June. Therefore, restrictions on usage of basement bedrooms could be implemented only during high risk months to maximize utility of the facilities while minimizing potential loss of life.

Economic Loss Issues

Typically, potential economic losses are viewed with more objectivity than potential loss of life. Therefore, numerical probabilities of loss developed with methods presented earlier can be very useful for actuarial purposes, engineering design, and investment decisions. If the probability of a damaging sedimentation event is sufficiently low that the risk of damage is deemed acceptable, then for practical purposes, continuing current practices (essentially "doing nothing") may be the appropriate hazard response. Choosing to do nothing to reduce potential consequences of hazards after the risks associated with them have been evaluated is considerably different than the *de facto* acceptance of risk associated with ignoring hazards with no specific knowledge of them.

If the probability of a damaging sedimentation event is low, but the risk of damage is deemed marginal, then an economic evaluation can be implemented to provide a means for comparing the cost of reducing the risks below what they are to the cost of repairing the damage in the event the hazardous process actually occurs. The method described by Bowles and others (1987) provides a means for combining probabilities and potential

losses. The methods of reducing risk can involve modifying the hazardous process, modifying the facility at risk, or both. In many cases, the risk is in a range where no risk reduction seems to be warranted, but some protection from potential losses is desirable. In these cases, compensation of potential losses may be provided with some level of insurance coverage. Such a situation could exist at a site outside, but near, the 100-year flood plain. The probability of a flood event in any year large enough to cause damage at such a site is less than 0.01. However, since most insurance rates are set on the basis of the 100-yr flood, the cost of insurance at the hypothetical site probably would be very low, yet compensation for losses in the unlikely event of a rare flood would be available.

Avoid the Hazard

Once a hazard has been identified and all of the alternative responses have been evaluated, if none of the alternatives provide a means for reducing risks to within acceptable limits, then the only remaining alternative is avoidance. This approach for surface fault rupture hazards has been codified in the Alquist-Priolo Special Studies Zones Act in California (Hart, 1980, p. 19), which provides "policies and criteria to assist cities, counties, and state agencies in the exercise of their responsibility to prohibit the location of developments and structures for human occupancy across the trace of active faults..." Such a policy, although well meaning, essentially discriminates against fault rupture hazards as being worse than other earthquake-related hazards and worse than non-earthquake hazards. In many cases, avoiding hazards may be prudent; however, if life safety can be protected, building across a fault which may move with an average recurrence interval of 1500 yr probably is no worse than building within the 1500-yr flood plain. The potential consequences of a 1500-yr flood probably are no more severe, and actually may be worse, than the potential consequences associated with fault rupture hazards (not including the hazards of strong ground shaking, liquefaction, etc.) on the "1500-yr" fault. Existing facilities exposed to hazards do not have the option of avoiding them unless the facilities are abandoned.

Alluvial-fan sedimentation hazards can be avoided by facilities located off of fans. In some cases, fanhead trenches provide protection for proximal fan areas for all but exceptionally large events. Such appears to be the case on the abandoned segment of the fan at Ricks Creek. Hence, facilities on the abandoned fan segment at Ricks Creek could be considered to be located in positions where the sedimentation hazards have been avoided.

SUMMARY AND CONCLUSIONS

The research described in this report was focused on the problem of quantifying hazards related to sedimentation processes on alluvial fans. Davis County, Utah, was selected as a study area because 1) damaging debris flow and debris flood events occurred repeatedly during historic time, 2) controversy exists regarding the influence of watershed degradation on sediment production in the 1920's and 30's, 3) the most recent damaging events were caused by rapid snowmelt rather than intense cloudburst rainstorms, 4) community response consisted of constructing new debris basins and refurbishing old ones, and 5) stratigraphy of Lake Bonneville provided a well-known base from which to study the development of post-Lake Bonneville alluvial fans. The alluvial fans in Davis County follow the world-wide trends of fan area and fan slope to drainage basin area; however, the fan in Davis County are smaller and steeper than fans developed in other regions for drainage basins of the same size.

The objectives of the research were to 1) assess hazards related to sedimentation processes on alluvial fans, 2) develop an intensity scale of alluvial-fan sedimentation event damage, 3) quantify alluvial-fan sedimentation events in the context of size and frequency of occurrence, and 4) estimate in probabilistic terms the risk of sedimentation event magnitudes for specific exposure times.

A complete evaluation of sedimentation hazards should include the location, frequency, magnitude, rate, duration, forecastability, and effects of the various sedimentation processes. The hazards are restricted to the alluvial fans at canyon mouths; however, the hazard locations can be affected significantly by stream channels on the fans themselves.

The frequency of occurrence of sedimentation processes appears to be directly related to climatic patterns (intensity of cloudburst or snowmelt) and the availability of sediment in the drainage basin. The sedimentation events of 1983 and 1984 demonstrated that most (90 percent) of the sediment delivered to the fans came from mobilization of sediment in the stream channels rather than from slope failures, *per se*. Additionally, post-Lake Bonneville sedimentation in Davis County consists of debris-flow, transitional flow, hyperconcentrated flow, and normal streamflow deposits without intercalated soils or other evidence of subaerial weathering. Thus, the alluvial-fan sediments appear to have accumulated very quickly. The soils developed on the modern surface of the alluvial fans have features which suggest that they have been developing since early Holocene time. Consequently, post-Lake Bonneville sedimentation events in Davis County appear to be rare. The frequency of sedimentation events was quantified in a manner similar to that used to quantify other types of flood events. The sedimentation events for each year in three periods of record were ranked and the rank values were divided by the number of years in the period of record plus 1 to give an estimated annualized frequency.

The magnitudes of post-Lake Bonneville sedimentation events in Davis County appear to be either large or very small with few being medium in size. The large events have left distinctive geomorphic expressions; the very small events constitute typical years of clear water discharge observed by local residents who report virtually no sediment deposition. These observations are supported by the stratigraphy of the alluvial-fan deposits which apparently do not contain intercalated soils. The magnitudes of sedimentation events were defined as the logarithm of the volume in cubic meters of deposited sediment. The volumes of historic sedimentation event deposits were estimated from published or eyewitness accounts of the events. The volumes of prehistoric

sedimentation events were estimated from geomorphic expression or volumetric proportion based on the excellent expression at the Ricks Creek fan. Event magnitude-frequency relationships were developed for both log-linear and non-linear distributions of events; however, because geomorphic evidence of moderate size events appears to be absent, and average of the log-linear and non-linear distribution appears to be most appropriate for describing sedimentation events on alluvial fans in Davis County.

The rates and durations of sedimentation events have been described by eyewitnesses. The rate at which events of high sediment concentration reach peak discharge is extremely rapid, almost instantaneous. Events of low sediment concentration behave according to conventional hydraulic engineering laws; in the semi-arid climate of Davis County, normal streamflows commonly are flash-flood discharges from intense rainstorms or minor discharges from spring snowmelt. Sedimentation events generated by cloudburst rainstorms (e.g., the events of the 1920's and 1930's) have been described as having durations of 30 to 45 minutes. Sedimentation events generated by rapid snowmelt (e.g., the events of 1983 and 1984) have been described as having durations of days to weeks with diurnal fluctuations and individual pulses of 30- to 45- minute duration.

Sedimentation events are forecastable to the extent that development of antecedent conditions in the source areas leading to sedimentation events on alluvial fans can be recognized. The present state of knowledge of hillslope hydrogeology is insufficient to permit specific forecasting of slope failures leading to sedimentation events on alluvial fans. Furthermore, the present state of knowledge of the kinematics and dynamics of flowing sediment-water mixtures at higher sediment concentrations is insufficient to permit specific forecasting of avulsions and distribution of sediment deposition on alluvial fans. Sedimentation events were forecasted quantitatively by computing exceedance probabilities for specific exposure times of 10, 50, and 100 years. Exceedance probabilities were computed on the basis of binomial and extreme-value distributions of event magnitudes for post-Lake Bonneville and historic periods of record. The results of calculations using Poisson distributions were not significantly different from those based on binomial distributions.

The effects of sedimentation processes can be damaging to man-made facilities constructed on alluvial fans. The damage experienced in Davis County in 1983 included collapse of structures, translation of structures off of foundations, flood-like inundation of structures, battering and lateral impact of parked vehicles by boulders and debris, clogging of surface drainage devices with resultant diversion of surface water, scour, and normal water flooding. In general, the heaviest damage occurred in the proximal fan areas and diminished in a downfan direction. Additionally, short distances laterally away from areas of major sediment deposition, no damage occurred.

Hazards are naturally occurring or man-induced processes which have the potential to cause damage or injury. Risk is exposure of something of value or individuals to potential damage or injury as a result of the occurrence of hazardous processes. This research has focused on the quantitative description of hazardous processes and the probability that such events will occur. Quantitative description of the initiating events and population at risk are beyond the scope of this research and assessment of consequences associated with the range of event magnitudes and the integration of magnitude/event probabilities into a quantitative measure of risk have been addressed only in an abstract way because of the at-risk inventory has not been developed. A hazard evaluation was prepared by Wieczorek and others (1983) in response to the damaging sedimentation events in May and June, 1983. Their evaluation was based chiefly on features within the drainage basins (partly-detached landslide masses) with only cursory consideration of the alluvial fans at the canyon mouths. This research focused on the stratigraphy and geomorphology of the

alluvial fans to elucidate the variety of hazards associated with sedimentation processes. Sedimentation event hazards at each of the alluvial fans in the study area were classified by systematically comparing selected features of the fans to the sizes of selected probabilistic sedimentation events. The cross-sectional area of the channel in the apex of the fan (the fan-head trench), the area of the channel in the middle fan, the volume of any existing debris basin, the number of years since the last historic sedimentation event, the volume of the last historic sedimentation event, and the average annual sediment yield volume were compared to the magnitudes of sedimentation events with probabilities of 10 and 50 percent in 100 years and 10 percent in 50 years. In general, the evaluation by Wieczorek and others (1983) suggests high to very high potential for sediment to reach canyon mouths in Davis County. The results presented in this report suggest high hazard for only a 4 fans and low hazard for approximately half of the 22 fans studied. The assessment of sedimentation hazard was based on an average of binomial analyses of log-linear magnitude distribution based on the post-Lake Bonneville period of record and extreme-value analyses of non-linear magnitude distribution based on the historic period of record. The results of the present research are not directly comparable to the results presented by Wieczorek and others (1983), but they can be compared for a general impression of the degree of risk to which existing facilities on the alluvial fans may be exposed.

Alternative hazard response actions consist of continuing current practices, modifying the hazard, modifying what is at risk, modifying operations and/or procedures to reduce risk, or avoiding the hazard by not building or abandoning facilities exposed to hazardous processes. The response of the Davis County communities to the damaging sedimentation events of the 1930's and again in 1983 was to construct sediment catch basins (debris basins). These basins were intended to limit the amount of sediment which could enter the communities; thus, the basins were an attempt to modify the nature of the hazard. In the 1930's, contour terraces were constructed in the mountains where sediment was being eroded; these terraces also were an attempt to modify the nature of the hazard. The debris basins will provide effective protection against damage caused by sedimentation events small enough to be contained in the basins; however, they will provide only limited protection against damage caused by events which exceed the volume of the basins. Current studies by the U.S. Army Corps of Engineers appear to be based on the concept that the largest sedimentation event which occurred in 1983 may represent the 100-year event. The results of the present research suggests that the largest event in 1983 may represent the 500- to 3,700-year event.

Alternative hazard responses could include accepting the risk associated with sedimentation event damage (continuing current practices). The probabilities summarized in this dissertation suggest that the likelihood of sedimentation events is relatively low; possibly low enough to represent an acceptable level of risk. The facilities on the alluvial fans could be modified to reduce the risk of damage (modifying what is at risk). Appropriate modifications could include an ordinance prohibiting basement windows on the up-fan sides of homes or prohibiting bedrooms in basements where floodlike inundation by sediment is anticipated. An additional response to sedimentation event hazards could include an ordinance prohibiting sleeping in bedrooms in basements during times of spring snowmelt or cloudburst rainstorms (modifying operations and/or procedures). The final alternative to sedimentation event hazards would be to abandon all existing facilities and prohibit new construction of the alluvial fans (avoiding the hazard). Intuitively, avoiding the hazards is not a reasonable alternative, especially since the probability of damaging sedimentation events appears to be relatively low.

The debris basins constructed in response to the 1983 sedimentation events have two benefits. First, by their construction, the local residents who had been damaged or threatened by the events could see that something was being done to protect them; thus, the

debris basins provided an immediate psychological benefit to the community. Second, the debris basins have a capacity to contain a certain volume of sediment which otherwise would be discharged into the community. In most cases, however, the capacities of the debris basins are relatively small and would provide complete protection only from small sedimentation events. Additionally, the debris basins must be maintained periodically to preserve their effectiveness.

Other hazards are present on the alluvial fans in Davis County. Clear water floods are hazardous even if they do not carry significant amounts of sediment. The Wasatch fault cuts alluvial-fan deposits at the base of the Wasatch Range in Davis County. Earthquake hazards certainly exist but have not been addressed in this research. It appears that fluctuations of the local base level (the Great Salt Lake) have contributed to the entrenchment of streams on the fans in Davis County. Consequently, the primary locus of sediment deposition has shifted in a downfan direction. Accompanying this downfan shift in deposition is deepening of the channels on the fan. At the Ricks Creek fan during the first historic sedimentation event (1923), the bouldery sediment passed through the channel in the apex of the fan, left levees along the channel, and was deposited below the intersection point of the active fan. In 1930, because the channel in the mountain had been cleaned of sediment in 1923, the discharge on the fan had the capacity to erode. Consequently, the channel in the apex of the fan was cut into easily erodible lacustrine sand below the bouldery alluvial-fan deposits and the bulk of the sediment discharged beyond the intersection point of the active fan was sand. The potential for this type of sedimentation event exists at other fans, particularly those fans where sedimentation events have cleaned the channels in the mountains. The hazards associated with these types of sedimentation events have not been addressed during the present research because the stratigraphy of the alluvial-fan deposits, which was the basis of the research, does not include such sandy deposits. Additional research is needed to quantify the hazards associated with erosion of sediment from the alluvial fans and/or lacustrine deposits underlying the alluvial fans.

Additional research should be directed at predicting the locations, magnitudes, and frequencies of slope failures in the drainage basins. Some research has been directed at this difficult topic by graduate students at Utah State University (Pack, 1985; Brooks, 1986; Jackowski, 1987; and Monteith, 1988) and Texas A&M University (Ala, in progress; and Colman, in progress). The parameters in the risk estimation element of the risk assessment model developed by Bowles and others (1987) should be systematically quantified.

The hazard model described in this dissertation should be applied to other locations where sedimentation processes represent hazards. Notable locations for additional research are elsewhere along the Wasatch Front, the Reno-Carson City area, the Los Angeles area, and areas in Arizona, Colorado, and New Mexico. Additional research also should be directed toward improving the ability to use drill hole data to aid in differentiating alluvial-fan stratigraphy on the basis of predicted clast support mechanism.

REFERENCES

- Algermissen, S. T., Perkins, D. M., Thenhaus, P. C., Hanson, S. L., and Bender, B. L., 1982, Probabilistic estimates of maximum acceleration and velocity in rock in the contiguous United States: U.S. Geological Survey Open-file Report 82-1033, 99 p.
- American Society for Testing and Materials, 1984, Standard test method for classification of soils for engineering purposes, and Standard practice for description and identification of soils (visual-manual procedure): ASTM Standards D 2487 83 and D 2488-84, p. 395-423.
- Anciaux, A., 1987, Mud and debris flow case studies in Davis County, Utah, *in* Mud and Debris Flow Workshop, Civil Engineering Department, University of Utah, and Federal Emergency Management Agency, Park City, Utah, September 10-11, unpaginated.
- Anderson, L. R., Keaton, J. R., Saarinen, T. F., and Wells, W. G., II, 1984, The Utah landslides, debris flows, and floods of May and June 1983: Washington, D.C., National Academy Press, 96 p.
- Anderson, L. R., Keaton, J. R., Aubry, K., and Ellis, S. J., 1982, Liquefaction potential map for Davis County, Utah: Utah State University final report to U.S. Geological Survey for contract no. 14-08-0001-19127, 46 p.
- Bailey, R. W., and Croft, A. R., 1937, Contour-trenches control floods and erosion on range lands: U. S. Department of Agriculture, Forestry Publication No. 4, 22 p.
- Bailey, R. W., Forsling, C. L., and Becraft, R. J., 1934, Floods and accelerated erosion in northern Utah: U.S. Department of Agriculture Miscellaneous Publication No. 196, 21 p.
- Bailey, R. W., Craddock, G. W., and Croft, A. R., 1947, Watershed management for summer flood control in Utah: U.S. Department of Agriculture, Forest Service, Miscellaneous Publication No. 639, 24 p.
- Beaty, C. B., 1963, Origins of alluvial fans, White Mountains, California and Nevada: *Annals of the Association of American Geographers*, v. 53, p. 516-535.
- Benson, M. A., 1968, Uniform flood-frequency estimating methods for Federal agencies: *Water Resources Research*, v. 4, p. 891-908.
- Benson, L., 1986, The sensitivity of evaporation rate to climate change -- results of an energy-balance approach: U.S. Geological Survey Water-Resources Investigations Report 86-4148, 40 p.
- Berg, R. R., 1986, *Reservoir Sandstones*: Englewood Cliffs, New Jersey, Prentice-Hall, 481 p.
- Beverage, J. P., and Culbertson, J. K., 1964, Hyperconcentrations of suspended sediment: *American Society of Civil Engineers Journal of the Hydraulics Division*, v. 90, no. HY6, p. 117-126.
- Birkeland, P. W., 1984, *Soils and geomorphology*: New York, Oxford University Press, 372 p.
- Blackwelder, E., 1928, Mudflow as a geologic agent in semi-arid mountains: *Geological Society of America Bulletin*, v. 39, p. 465-480.
- Blissenbach, E., 1954, Geology of alluvial fans in semi-arid regions: *Geological Society of America Bulletin*, v. 65, p. 175-190.
- Bluck, B. J., 1964, Sedimentation of an alluvial fan in southern Nevada: *Journal of Sedimentary Petrology*, v. 34, p. 395-400.
- , 1967, Deposition of some Upper Old Red Sandstone conglomerates in the Clyde area -- a study in the significance of bedding: *Scottish Journal of Geology*, v. 3, p. 139-167.

- Bowles, D. S., Anderson, L. R., and Glover, T. F., 1987, Design level risk assessment for dams, *in* Roesset, J. M., ed., *Dynamics of structures*: New York, American Society of Civil Engineers, p. 210-225.
- Bradley, R. S., 1985, *Quaternary paleoclimatology*: Boston, Allen & Unwin, 472 p.
- Branson, F. A., Gifford, G. F., Renard, K. G., and Hadley, R. F., 1981, *Rangeland hydrology*: Dubuque, Iowa, Kendall/Hunt Publishing Company, Second Edition, 340 p.
- Brooks, R. K., 1986, Instrumentation of the Steed Canyon landslide [M.S. thesis]: Logan, Utah, Utah State University, 183 p.
- Bryant, B., 1984, Reconnaissance geologic map of the Precambrian Farmington Canyon Complex and surrounding rocks in the Wasatch Mountains between Ogden and Bountiful, Utah: U.S. Geological Survey Map I-1447.
- Bucknam, R. C., and Anderson, R. E., 1979, Estimation of fault-scarp ages from a scarp-height-slope-angle relationship: *Geology*, v. 7, p. 11-14.
- Bull, W. B., 1962, Relation of textural (CM) patterns to depositional environment of alluvial-fan deposits: *Journal of Sedimentary Petrology*, v. 32, p. 211-216.
- , 1964, Alluvial fans and near-surface subsidence in western Fresno County, California: U. S. Geological Survey Professional Paper 437-A, 71 p.
- , 1972, Recognition of alluvial-fan deposits in the stratigraphic record, *in* Rigby, K. J., and Hamblin, W. K., eds., *Recognition of Ancient Sedimentary Environments*, Society of Economic Paleontologists and Mineralogists Special Publication 16, p. 68-83.
- , 1977, The alluvial fan environment: *Progress in Physical Geography*, v. 1, p. 222-270.
- Bull, W. B., and McFadden, L. D., 1977, Tectonic geomorphology north and south of the Garlock fault, California, *in* Doehring, D. O., ed., *Geomorphology in arid regions*: London, Allen & Unwin, p. 118-138.
- Burke, R. M., and Birkeland, P. W., 1979, Re-evaluation of multiparameter relative dating techniques and their application to the glacial sequence along the eastern escarpment of the Sierra Nevada, California: *Quaternary Research*, v. 11, p. 21-51.
- Butler, E., and Marsell, R. E., 1972, Developing a state water plan: Cloudburst floods in Utah, 1939-69: Utah Division of Water Resources Cooperative-Investigations Report No. 11, 103 p.
- Caine, N., 1980, The rainfall intensity-duration control of shallow landslides and debris flows: *Geografiska Annaler*, v. 62A, p. 23-27.
- Campbell, R. H., 1975, Soil slips, debris flows, and rainstorms in the Santa Monica Mountains and vicinity, southern California: U.S. Geological Survey Professional Paper 851, 51 p.
- Cannon, S. Q., and others, 1931, Torrential floods in northern Utah, 1930: Logan, Utah, Utah State University, Agricultural Experiment Station, Circular 92, 51 p.
- Chorley, R. J., Malm, D. E. G., and Pogorzelski, H. A., 1957, A new standard for estimating basin shape: *American Journal of Science*, v. 255, p. 138-141.
- Chorley, R. J., Schumm, S. A., and Sugden, D. E., 1984, *Geomorphology*: London, Methuen & Co., 605 p.
- Colman, S. M., and Watson, K., 1983, Ages estimated from a diffusion equation model for scarp degradation: *Science*, v. 221, p. 263-265.
- Committee on Methodologies for Predicting Mudflow Areas, 1982, *Selecting a methodology for delineating mudslide hazard areas for the National Flood Insurance Program*: Washington, D.C., National Academy Press, 35 p.
- Costa, J. E., 1984, Physical geomorphology of debris flows, *in* Costa, J. E., and Fleisher, P. J., eds., *Developments and applications of geomorphology*: Berlin, Springer-Verlag, p. 268-317.
- Costa, J. E., and Baker, V. R., 1981, *Surficial geology -- building with the earth*: New York, Wiley & Sons, 498 p.

- Costa, J. E., and Jarrett, R. D., 1981, Debris flows in small mountain stream channels of Colorado and their hydrologic implications: Association of Engineering Geologists Bulletin, v. 18, p. 309-322.
- Crawford, A. L., and Thackwell, F. E., 1931, Some aspects of the mudflows north of Salt Lake City, Utah: Proceedings, Utah Academy of Sciences, v. 8, p. 97-105.
- Croft, A. R., 1962, Some sedimentation phenomena along the Wasatch Mountain Front: Journal of Geophysical Research, v. 67, p. 1511-1524.
- , 1967, Rainstorm debris floods -- A problem in public welfare: Agricultural Experiment Station, Tucson, Arizona, University of Arizona, 36 p.
- , 1981, History of development of the Davis County Experimental Watershed: Ogden, Utah, U.S. Department of Agriculture, Forest Service, special publication, 42 p.
- Crozier, M. S., 1986, Landslides -- causes, consequences & environment: London, Dover, 252 p.
- Currey, D. R., Oviatt, C. G., and Plyler, G. B., 1983, Lake Bonneville stratigraphy, geomorphology, and isostatic deformation in west-central Utah, *in* Gurgel, K. D., ed., Geologic excursions in neotectonics and engineering geology in Utah, Guidebook - Part IV: Utah Geological and Mineral Survey Special Studies 62, p. 63-82.
- Currey, D. R., Atwood, G., and Mabey, D. R., 1984, Major levels of Great Salt Lake and Lake Bonneville: Utah Geological and Mineral Survey Map 73, 1 sheet.
- Currey, D. R., and Oviatt, C. G., 1985, Durations, average rates, and probable causes of Lake Bonneville expansions, stillstands, and contractions during the last deep-lake cycle 32,000 to 10,000 years ago: Geographical Journal of Korea, v. 10, p. 1085-1099.
- Dames & Moore, 1984a, Report, geotechnical consultation services, proposed Rudd Creek debris basin, Farmington, Utah, for Davis County Flood Control: Salt Lake City, unpublished consultant's report, 22 p.
- , 1984b, Report, geotechnical consultation services, proposed Ricks Creek debris basin, Centerville, Utah, for Davis County Flood Control: Salt Lake City, unpublished consultant's report, 20 p.
- , 1984c, Report, geotechnical consultation services, proposed Barnard Creek debris basin, Centerville, Utah, for Davis County Flood Control: Salt Lake City, unpublished consultant's report, 15 p.
- , 1984d, Report, geotechnical consultation services, proposed Parrish Creek debris basin, Centerville, Utah, for Davis County Flood Control: Salt Lake City, unpublished consultant's report, 24 p.
- , 1984e, Report, geotechnical consultation services, proposed Deuel Creek [Centerville Canyon] debris basin, Centerville, Utah, for Davis County Flood Control: Salt Lake City, unpublished consultant's report, 20 p.
- Davis, W., M., 1925, The Basin Range problem: Proceedings of the National Academy of Sciences, v. 11, p. 387-392.
- Dawdy, D. R., 1979, Flood frequency estimates on alluvial fans: American Society of Civil Engineers Journal of the Hydraulics Division, v. 105, p. 1407-1413.
- Deevey, E. S., and Flint, R. F., 1957, Postglacial hypsithermal interval: Science, v. 125, p. 182-184.
- Denny, C. S., 1965, Alluvial fans in the Death Valley region, California and Nevada: U. S. Geological Survey Professional Paper 466, 62 p.
- , 1967, Fans and pediments: American Journal of Science, v. 265, p. 81-105.
- Dohrenwend, J. C., 1987, Basin and Range, *in* Graf, W. L., ed., Geomorphic systems of North America: Geological Society of America, Centennial Special Volume 2, p. 303-342.
- Eckis, R., 1928, Alluvial fans of the Cucamonga district, southern California: Journal of Geology, v. 36, p. 224-247.

- Erickson, A. J., and others, 1968, Soil survey, Davis-Weber area, Utah: U. S. Department of Agriculture, Soil Conservation Service, 149 p.
- Ferrell, W. R., 1959, Report on debris reduction studies for mountain watersheds: Los Angeles County Flood Control District, unpublished, 164 p.
- Folk, R. L., 1980, Petrology of sedimentary rocks: Austin, Texas, Hemphill Publishing Company, 185 p.
- Gilbert, G. K., 1890, Lake Bonneville: U. S. Geological Survey Monograph 1, 438 p.
- Glancy, P. A., 1985, The Ophir Creed debris flood of May 30, 1983 -- a real test of geohydrologic hazard mapping, *in* Bowles, D. S., ed., Delineation of landslide, flash flood, and debris flow hazards in Utah: Utah Water Research Laboratory publication G-85/03, Logan, Utah, Utah State University, p. 195.
- Gloppen, T. G., and Steel, R. J., 1981, The deposits, internal structure and geometry in six alluvial fan-fan delta bodies (Devonian, Norway) -- a study in the significance of bedding sequences in conglomerates, *in* Ethridge, F. G., and Flores, R. M., eds., Recent and Ancient Non-Marine Depositional Environments: Models for Exploration, Society of Economic Paleontologists and Mineralogists, Special Publication 31, p. 49-69.
- Goudie, A., ed., 1981, Geomorphological techniques: London, Allen & Unwin, 395 p.
- Griggs, G. B., and Hein, J. R., 1980, Sources, dispersal, and clay mineral composition off central and northern California: *Journal of Geology*, v. 88, p. 541-566.
- Gumbel, E. J., 1958, Statistics of extremes: New York, Columbia University Press, 375 p.
- Haggett, P., 1965, Locational analysis in human geography: New York, St. Martin's Press, 339 p.
- Hampton, M.A., 1979, Bouyancy in debris flows: *Journal of Sedimentary Petrology*, v. 49, p. 753-758.
- Hanks, T. C., Bucknam, R. C., Lajoie, K. R., and Wallace, R. E., 1984, Modification of wave-cut and faulting-controlled landforms: *Journal of Geophysical Research*, v. 89, p. 5771-5790.
- Hanks, T. C., and Wallace, R. E., 1985, Morphological analysis of the Lake Lahontan shoreline and beachfront fault scarps, Pershing County, Nevada: *Seismological Society of America Bulletin*, v. 75, p. 835-846.
- Hansen, A., 1984, Landslide hazard analysis, *in* Brunsden, D., and Prior, D. B., eds., Slope instability: Chichester, England, Wiley and Sons, p. 523-602.
- Hart, E. W., 1980, Fault-rupture hazard zones in California -- Alquist-Priolo special studies zones act of 1972 with index to special studies zones maps: California Division of Mines and Geology Special Publication 42, 25 p.
- Harvey, A. M., 1984, Debris flow and fluvial deposits in Spanish Quaternary alluvial fans: implications for fan morphology, *in* Koster, E.H., and Steel, R.J., eds., Sedimentology of Gravels and Conglomerates, Canadian Society of Petroleum Geologists, Memoir 10, p. 123-132.
- Heward, A. P., 1978, Alluvial fan sequence and megasequence models: With examples from Westphalian D -- Stephanian B coalfields, N. Spain, *in* Miall, A. D., ed., Fluvial Sedimentology: Canadian Society of Petroleum Geologists, Memoir 5, p. 669-702.
- Hintze, L. F., 1977, Geologic history of Utah: Provo, Utah, Brigham Young University Geology Studies, v. 20, pt. 3, 181 p.
- _____, 1980, Geologic map of Utah: Utah Geological and Mineral Survey, 2 sheets.
- Hollingsworth, R. A., and Kovacs, G. S., 1981, Soil slumps and debris flows -- prediction and protection: *Association of Engineering Geologists Bulletin*, v. 18, p. 17-28.
- Hooke, R. L. B., 1967, Processes on arid-region alluvial fans: *Journal of Geology*, v. 75, p. 438-460.

- _____, 1968, Steady-state relationships on arid-region alluvial fans in closed basins: *American Journal of Science*, v. 266, p. 609-629.
- _____, 1972, Geomorphic evidence for late-Wisconsin and Holocene tectonic deformation, Death Valley, California: *Geological Society of America Bulletin*, v. 83, p. 2073-2098.
- Horton, R. E., 1932, Drainage basin characteristics: *American Geophysical Union Transactions*, v. 14, p. 350-361.
- Huggett, R. J., 1985, *Earth surface systems*: Berlin, Springer-Verlag, 270 p.
- Hunt, C. B., and Mabey, D. R., 1966, Stratigraphy and structure, Death Valley, California: U. S. Geological Survey Professional Paper 494-A, 162 p.
- Imbrie, J., and Imbrie, K. P., 1979, Ice ages -- solving the mystery: *Short Hills*, New Jersey, Enslow, 224 p.
- Innes, J. L., 1983, Debris flows: *Progress in Physical Geography*, v. 7, p. 469-501.
- Jadkowski, M. A., 1987, Multispectral remote sensing of landslide susceptible areas [Ph.D. thesis]: Logan, Utah, Utah State University, 260 p.
- Jahns, R. H., 1949, Desert floods; *Engineering and Science Monthly*, California Institute of Technology, May, p. 1-14.
- Johnson, A. M., 1965, A model for debris flow [Ph.D. thesis]: University Park, Pennsylvania, Pennsylvania State University, 232 p.
- _____, 1970, *Physical processes in geology*: San Francisco, Freeman, Cooper & Company, 576 p.
- Johnson, A. M., and Rodine, J. R., 1984, Debris flow, *in* Brunsden, D., and Prior, D. B., eds., *Slope instability*: Chichester, England, Wiley and Sons, p. 257-361.
- Keaton, J. R., 1986a, Debris flow recurrence estimated from long-term erosion: *Geological Society of America Abstracts with Program*, v. 18, no. 6, p. 652.
- _____, 1986b, Landslide inventory and preliminary hazard assessment, southeast Davis County, Utah: San Francisco, Association of Engineering Geologists 29th Annual Meeting, Abstracts and Program, p. 59.
- _____, 1987, Potential consequences of earthquake-induced regional tectonic deformation along the Wasatch Front, north-central Utah, *in* McCalpin, J., ed., *Proceedings of the 23rd Symposium on Engineering Geology and Soils Engineering*, Logan, Utah, Utah State University, p. 19-34.
- Keaton, J. R., and Mathewson, C. C., 1987, Proposed ideal alluvial fan stratigraphy for risk assessment: *Geological Society of America Abstracts with Program*, v. 19, no. 7, p. 723.
- Keaton, J. R., Mathewson, C. C., and Anderson, L. R., 1987a, Hazards and risks associated with alluvial fan processes in Davis County, Utah: *Association of Engineering Geologists Abstracts with Program*, Atlanta, GA, 30th annual meeting, p. 42.
- Keaton, J. R., Topham, D. E., Anderson, L. R., and Rathbun, D. J., 1987b, Earthquake-induced landslide potential in and development of a seismic slope stability map of the urban corridor of Davis and Salt Lake Counties, Utah, *in* McCalpin, J., ed., *Proceedings of the 23rd Symposium on Engineering Geology and Soils Engineering*, Logan, Utah, Utah State University, p. 57-80.
- Keaton, J. R., Anderson, L. R., and Mathewson, C. C., 1988, Assessing debris flow hazards on alluvial fans in Davis County, Utah, *in* Fragaszy, R. J., ed., *Proceedings, 24th Symposium on Engineering Geology and Soils Engineering*, Coeur d'Alene, Idaho, Washington State University, p. 89-108.
- Keefer, D. K., and others, 1987, Real-time landslide warning during heavy rainfall: *Science*, v. 238, p. 921-925.
- Kellerhals, R., and Bray, D. I., 1971, Sampling procedures for coarse fluvial sediments: *American Society of Civil Engineers, Proceedings*, v. 45, no. HY8, p. 1165-1180.
- Knighton, D. 1984, *Fluvial forms and processes*: Baltimore, Arnold, 218 p.

- Kochel, R. C., and Johnson, R. A., 1984, Geomorphology and sedimentology of humid-temperate alluvial fans, central Virginia, *in* Koster, E. H., and Steel, R. J., eds., *Sedimentology of Gravels and Conglomerates: Canadian Society of Petroleum Geologists, Memoir 10*, p. 109-122.
- Kockelman, W. J., 1986, Community planning to reduce mudflow and mudflood hazards, *in* *Proceedings of a Western State High Risk Flood Areas Symposium, Improving the effectiveness of floodplain management in arid and semi-arid regions: Las Vegas*, Association of State Floodplain Managers, p. 65-71.
- Koster, E. H., and Steel, R. J., eds., 1984, *Sedimentology of gravels and conglomerates: Canadian Society of Petroleum Geologists, Memoir 10*, 441 p.
- Krumbein, W. C., 1934, Size frequency distributions of sediments: *Journal of Sedimentary Petrology*, v. 4, p. 65-77.
- Lambe, T. W., 1951, *Soil testing for engineers*: New York, John Wiley & Sons, 165 p.
- Langbein, W. B., and Leopold, L. B., 1964, Quasi-equilibrium states in channel morphology: *American Journal of Science*, v. 262, p. 782-794.
- Larsen, V., and Steel, R. J., 1978, The sedimentary history of a debris-flow dominated, Devonian alluvial fan -- A study of textural inversion: *Sedimentology*, v. 25, p. 37-59.
- Lawson, D. E., 1982, Mobilization, movement and deposition of active subaerial sediment flows, Matanuska Glacier, Alaska: *Journal of Geology*, v. 90, p. 279-300.
- Leopold, L. B., and Maddock, T., Jr., 1953, The hydraulic geometry of stream channels and some physiographic implications: *U. S. Geological Survey Professional Paper 252*, 57 p.
- Lindskov, K. L., 1984, Floods of May to June 1983 along the northern Wasatch Front, Salt Lake City to North Ogden, Utah: *Utah Geological and Mineral Survey, Water Resources Bulletin 24*, 11 p.
- Lips, E. W., and Keaton, J. R., 1988, Slope-A-Scope -- a convenient tool for rapid topographic profiling: *Kansas City, Association of Engineering Geologists 31st Annual Meeting, Abstracts and Program*, p. 51.
- Lowe, D. R., 1979, Sediment gravity flows -- Their classification and some problems of application to natural flows and deposits, *in* Doyle, L. J., and Pilkey, O. H., eds., *Geology of continental slopes: Society of Economic Paleontologists and Mineralogists Special Publication No. 27*, p. 75-82.
- , 1982, Sediment gravity flows II -- Depositional models with special reference to the deposits of high-density turbidity currents: *Journal of Sedimentary Petrology*, v. 52, p. 279-297.
- Lustig, L. K., 1965, *Clastic sedimentation in Deep Springs Valley, California*: U.S. Geological Survey Professional Paper 352-F, 131 p.
- Machette, M. N., Personius, S. F., and Nelson, A. R., 1987, Quaternary geology along the Wasatch fault zone -- segmentation, recent investigations, and preliminary conclusions: *U. S. Geological Survey, Open-file Report 87-585*, p. A1-A72.
- Madole, R. F., and others, 1987, Rocky Mountains, *in* Graf, W. L., ed., *Geomorphic systems of North America: Geological Society of America, Centennial Special Volume 2*, p. 211-257.
- Madsen, D. B., and Currey, D. R., 1979, Late Quaternary glacial and vegetation changes, Little Cottonwood Canyon area, Wasatch Mountains, Utah: *Quaternary Research*, v. 12, p. 254-270.
- Mandelbrot, B. B., 1967, How long is the coast of Britain? -- Statistical self-similarity and the fractional dimension: *Science*, v. 156, p. 636-638.
- Marsell, R. E., 1972, Cloudburst and snowmelt floods, *in* *Environmental Geology of the Wasatch Front, 1971: Utah Geological Association Publication 1*, p. N1-N18.
- Mathewson, C. C., 1981, *Engineering Geology*: Columbus, Merrill, 410 p.
- , 1987, The disaster cycle, a combination of geologic and human processes: *Geological Society of America Abstracts with Program*, v. 19, no. 3, p. 173.

- Mathewson, C. C., and Keaton, J. R., 1986, The role of bedrock groundwater in the initiation of debris flows: San Francisco, Association of Engineering Geologists 29th Annual Meeting, Abstracts and Program, p. 56.
- Mathewson, C. C., and Santi, P. M., 1987, Bedrock ground-water -- source of sustained post-debris flow stream discharge, *in* McCalpin, J., ed., Proceedings of the 23rd Symposium on Engineering Geology and Soils Engineering, Logan, Utah, Utah State University, p. 25 -265.
- McCarter, M. K., and Kaliser, B. N., 1985, Prototype instrumentation and monitoring programs for measuring surface deformation associated with landslide processes, *in* Bowles, D. S., ed., Delineation of landslide, flash flood, and debris flow hazards in Utah: Utah Water Research Laboratory publication G-85/03, Logan, Utah, Utah State University, p. 30-49.
- McCuen, R. H., and Snyder, W. M., 1986, Hydrologic modeling -- statistical methods and applications: Englewood Cliffs, New Jersey, Prentice-Hall, 568 p.
- McGee, W.J., 1897, Sheetflood erosion: Geological Society of America Bulletin, v. 8, p. 87-112.
- McManus, D. A., 1963, A criticism of certain usage of the phi notation: Journal of Sedimentary Petrology, v. 33, p. 670-674.
- Mears, A. I., 1977, Debris-flow hazard analysis and mitigation -- an example from Glenwood Springs, Colorado: Colorado Geological Survey Information Series 8, 45 p.
- Meckel, L. D., 1975, Holocene sand bodies in the Colorado Delta area, northern Gulf of California, *in* Broussard, M. L., ed., Delta Models for Exploration: Houston Geological Society, p. 239-265.
- Megahan, W. F., 1975, Sedimentation in relation to logging activities in the mountains of central Idaho, *in* Present and prospective technology for predicting sediment yields and sources: U. S. Department of Agriculture, Agriculture Research Service, ARS-S-40, p. 74-82.
- Melton, M. A., 1965, The geomorphic and paleoclimatic significance of alluvial deposits in southern Arizona: Journal of Geology, v. 73, p. 1-38.
- Mills, H. H., 1982, Piedmont-cove deposits of the Dellwood Quadrangle, Great Smokey Mountains, North Carolina, U.S.A -- morphometry: Zeitschrift für Geomorphologie, Neue Folge, Band 26, p. 163-178.
- Monteith, S., 1988, Stability analysis of the Steed Canyon landslide [M.S. thesis]: Logan, Utah, Utah State University, 105 p.
- Morris, R. N., 1986, Geotechnical classification of debris flows and debris floods in the southern Rocky Mountains [M.S. thesis]: Ft. Collins, Colorado, Colorado State University, 187 p.
- Morton, D. M., and Campbell, R. H., 1974, Spring mudflows at Wrightwood, Southern California: Quarterly Journal of Engineering Geology, v. 7, p. 377-384.
- Morton, D. M., Campbell, R. H., Barrows, A. G., Jr., Kahle, J. E., and Yerkes, R. F., 1979, Wright Mountain mudflow -- Spring 1969: California Division of Mines and Geology Special Report 136, Part II, p. 7-21.
- Naeser, C. W., Bryant, B., Crittenden, M. D., and Sorensen, M. L., 1983, Fission-track ages of apatite in the Wasatch Mountains, Utah -- an uplift study: Geological Society of America Memoir 157, p. 29-36.
- Nardin, T. R., Hein, F. J., Gorsline, D. S., and Edwards, B. D., 1979, A review of mass movement processes, sediment and acoustic characteristics, and contrasts in slope and base-of-slope systems versus canyon-fan-basin floor systems: Society of Economic Paleontologists and Mineralogists Special Publication No. 27, p. 61-73.
- Nash, D. B., 1980, Morphologic dating of degraded normal fault scarps: Journal of Geology, v. 88, p. 353-360.

- _____, 1984, Morphologic dating of fluvial terrace scarps and fault scarps near West Yellowstone, Montana: *Geological Society of America Bulletin*, v. 95, p. 1413-1424.
- _____, 1986, Morphologic dating and modeling degradation of fault scarps, *in* *Active Tectonics*: Washington, D.C., National Academy Press, p. 181-194.
- Neilson, R. P., and Wullstein, L. H., 1985, Comparative drought physiology and biogeography of *Quercus gambelii* and *Quercus turbinella*: *The American Midland Naturalist*, v. 114, p. 259-271.
- Nemec, W., and Steel, R. J., 1984, Alluvial and coastal conglomerates -- Their significant features and some comments on gravelly mass-flow deposits, *in* Koster, E. H., and Steel, R. J., eds., *Sedimentology of gravels and conglomerates*: Canadian Society of Petroleum Geologists, Memoir 10, p. 1-31.
- Nilsen, T. H., 1982, Alluvial fan deposits, *in* Scholle, P. A., and Spearing, D., eds., *Sandstone depositional environments*: Tulsa, Oklahoma, American Association of Petroleum Geologists, p. 49-86.
- _____, ed., 1985, *Modern and ancient alluvial fan deposits*: New York, New York, Van Nostrand Reinhold Company, 372 p.
- O'Brien J., S., and Julien, P. Y., 1985, Physical properties and mechanics of hyperconcentrated sediment flows, *in* Bowles, D. S., ed., *Delineation of landslide, flash flood, and debris flow hazards in Utah*: Utah Water Research Laboratory publication G-85/03, Logan, Utah, Utah State University, p. 260-279.
- Okada, Y., 1985, Surface deformation due to shear and tensile faults in a half-space: *Seismological Society of America Bulletin*, v. 75, p. 1135-1154.
- Olson, E. P., 1985, East Layton debris flow: U.S. Department of Agriculture, Forest Service, Intermountain Region Report G-R-4-85-2, 24 p.
- Ott, L., 1984, *An introduction to statistical methods and data analysis*: Boston, Duxbury Press, 775 p.
- Pack, F.J., 1923, Torrential potential of desert waters: *Pan American Geologist*, v. 40, p. 349-356.
- Pack, R. T., 1985, Multivariate analysis of relative landslide susceptibility in Davis County, Utah [Ph.D. thesis]: Logan, Utah, Utah State University, 233 p.
- Paul, J. H., and Baker, F. S., 1925, The floods of 1923 in northern Utah: *University of Utah Bulletin*, v. 15, 20 p.
- PSIAC (Pacific Southwest Inter-Agency Committee), 1968, Factors affecting sediment yield and measures for the reduction of erosion and sediment yield: Portland, Oregon, U. S. Department of Agriculture, Soil Conservation Service, unpublished report, 10 p.
- Pe, G. G., and Piper, D. J. W., 1975, Textural recognition of mudflow deposits: *Sedimentology*, v. 13, p. 303-306.
- Petak, W. J., and Atkisson, A. A., 1982, Natural hazard risk assessment and public policy -- anticipating the unexpected: New York, Springer-Verlag, 489 p.
- Pierce, K. L., and Colman, S. M., 1986, Effect of height and orientation (microclimate) on geomorphic degradation rates and processes, late-glacial terrace scarps in central Idaho: *Geological Society of America Bulletin*, v. 97, p. 869-885.
- Pierson, T. C., 1980, Erosion and deposition by debris flows at Mount Thomas, North Canterbury, New Zealand: *Earth Surface Process*, v. 5, p. 227-247.
- _____, 1985a, Initiation and flow behavior of the 1980 Pine Creek and Muddy River lahars, Mount St. Helens, Washington: *Geological Society of America Bulletin*, v. 96, p. 1056-1069.
- _____, 1985b, Effects of slurry composition on debris flow dynamics, Rudd Canyon, Utah, *in* Bowles, D. S., ed., *Delineation of landslide, flash flood, and debris flow hazards in Utah*: Utah Water Research Laboratory publication G-85/03, Logan, Utah, Utah State University, p. 132-152.

- Pierson, T. C., and Costa, J. E., 1987, A rheologic classification of subaerial sediment-water flows, *in* Costa, J. E., and Wieczorek, G. F., eds., Debris flows/avalanches -- process, recognition, and mitigation: Geological Society of America Reviews in Engineering Geology, v. 7, p. 1-12.
- Pierson, T. C., and Scott, K. M., 1985, Downstream dilution of a lahar -- transition from debris flow to hyperconcentrated streamflow: *Water Resources Research*, v. 21, p. 1511-1524.
- Pickford, G. D., 1932, The influence of continued heavy grazing and on promiscuous burning on spring-fall ranges in Utah: *Ecology*, v. 13, p. 159-171.
- Price, W. E., 1976, A random-walk simulation model of alluvial-fan deposition, *in* Merriam, D. R., ed., *Random processes in geology*: New York, Springer-Verlag, p. 55-62.
- Rachocki, A., 1981, *Alluvial fans*: New York, New York, Wiley & Sons, 161 p.
- Rahn, P., 1967, Inselbergs and nickpoints in southwest Arizona: *Zeitschrift für Geomorphologie*, Band 10, p. 217-225.
- Rickmers, W. R., 1913, *The Duab of Turkestan*: Cambridge, Cambridge University Press, 278 p.
- Rockwell, T. K., Keller, E. A., and Johnson, D. L., 1985, Tectonic geomorphology of alluvial fans and mountains fronts near Ventura, California, *in* Morisawa, M., and Hack, J. T., eds., *Tectonic geomorphology*: Boston, Allen & Unwin, p. 183-207.
- Rodine, J. D., and Johnson, A. M., 1976, The ability of debris, heavily freighted with coarse clastic materials, to flow on gentle slopes: *Sedimentology*, v. 23, p. 213-234.
- Rowe, W. D., 1977, *An anatomy of risk*: New York, Wiley, 233 p.
- Ryder, J. M., 1971, Some aspects of the morphometry of paraglacial alluvial fans in south-central British Columbia: *Canadian Journal of Earth Sciences*, v. 8, p. 1252-1264.
- Santi, P. M., 1988, The kinematics of debris flow transport down a canyon [M.S. thesis]: College Station, Texas, Texas A&M University, 85 p.
- Santi, P. M., and Mathewson, C. C., 1988, What happens between the scar and the fan? -- The behavior of a debris flow in motion, *in* Frigaszy, R. J., ed., *Proceedings, 24th Symposium on Engineering Geology and Soils Engineering*, Coeur d'Alene, Idaho, Washington State University, p. 73-88.
- Schamber, D. R., 1987, One and two dimensional, transient simulations of mudflows: *in* Mud and Debris Flow Workshop, Civil Engineering Department, University of Utah, and Federal Emergency Management Agency, Park City, Utah, September 10-11, unpaginated.
- Scheidegger, A. E., 1961, *Theoretical geomorphology*: Berlin, Springer-Verlag, 333 p.
- Schumm, S. A., 1956, The evolution of drainage systems and slopes in badlands at Perth Amboy, New Jersey: *Geological Society of America Bulletin*, v. 67, p. 597-646.
- _____, 1977, *The fluvial system*: New York, John Wiley & Sons, 338 p.
- Schumm, S. A., Mosley, M. P., and Weaver, W. E., 1987, *Experimental fluvial geomorphology*: New York, John Wiley & Sons, 413 p.
- Schuster, R. L., and Fleming, R. W., 1986, Economic losses and fatalities due to landslides: *Association of Engineering Geologists Bulletin*, v. 23, p. 11-28.
- Schwartz, D. P., and Coppersmith, K. D., 1984, Fault behavior and characteristic earthquakes -- examples from the Wasatch and San Andreas faults: *Journal of Geophysical Research*, v. 89, p. 5681-5698.
- _____, 1986, Seismic hazards -- new trends in analysis using geologic data, *in* *Active Tectonics*: Washington, D.C., National Academy Press, p. 215-230.
- Schwartz, D. P., Hanson, K. L., and Swan, F. H., III, 1983, Paleoseismic investigations along the Wasatch fault -- an update, *in* Gurgel, K. D., ed., *Geologic excursions in neotectonics and engineering geology in Utah*, Guidebook - Part IV: Utah Geological and Mineral Survey Special Studies 62, p. 45-48.

- Scott, K. M., 1971, Origin and sedimentology of 1969 debris flows near Glendora, California: U. S. Geological Survey Professional Paper 750-C, p. C242-C247.
- , 1973, Scour and fill in Tujunga Wash -- fanhead valley in urban southern California -- 1969: U. S. Geological Survey Professional Paper 732-B, 29 p.
- , 1985, Lahars and lahar-runout flows in the Toutle-Cowlitz River system, Mount St. Helens, Washington -- origins, behavior, and sedimentology: U.S. Geological Survey Open-file Report 85-500, 202 p.
- Sharp, R. P., 1942, Mudflow levees: *Journal of Geomorphology*, v. 5, p. 222-227.
- Sharp, R. P., and Nobles, L. H., 1953, Mudflow of 1941 at Wrightwood, southern California: *Geological Society of America Bulletin*, v. 64, p. 547-560.
- Shreve, R. L., 1975, The probabilistic-topologic approach to drainage-basin geomorphology: *Geology*, v. 3, p. 527-529.
- Smith, G. A., 1986, Coarse-grained nonmarine volcanoclastic sediment -- terminology and depositional process: *Geological Society of America Bulletin*, v. 97, p. 1-10.
- Spangler, M. G., and Handy, R. L., 1982, *Soil Engineering*: New York, Harper & Row, 819 p.
- Spearing, D.R., 1974, Alluvial fan deposits: Geological Society of America Summary sheets of sedimentary deposits, Sheet 1.
- Strahler, A. N., 1952, Hypsometric (area-altitude) analysis of erosional topography: *Geological Society of America Bulletin*, v. 63, p. 1117-1142.
- Strahler, A. N., and Strahler, A. H., 1984, *Elements of physical geography*: New York, John Wiley & Sons, 538 p.
- Strand, R. I., 1975, Bureau of Reclamation procedures for predicting sediment yield, *in* Present and prospective technology for predicting sediment yields and sources: U. S. Department of Agriculture, Agriculture Research Service, ARS-S-40, p. 10-15.
- Stein, R. S., and Barrientos, S. E., 1985, Planar high-angle faulting in the Basin and Range -- geodetic analysis of the 1983 Borah Peak, Idaho earthquake: *Journal of Geophysical Research*, v. 90, p. 11,355-11,366.
- Swan, F. H., III, Schwartz, D. P., and Cluff, L. S., 1980, Recurrence of moderate to large magnitude earthquakes produced by surface faulting on the Wasatch fault, Utah: *Seismological Society of America Bulletin*, v. 70, p. 1431-1462.
- Takahashi, T., 1981, Debris flows: *Annual Reviews in Fluid Mechanics*, v. 13, p. 57-77.
- Tanner, W. F., 1976, Tectonically significant pebble types -- sheared, pocked, and second-cycle examples: *Sedimentary Geology*, v. 16, p. 69-83.
- Taylor, B. D., 1983, Sediment yields in coastal southern California: American Society of Civil Engineers, *Journal of the Hydraulics Division*, v. HY109, p. 71-85.
- Tinkler, K. J., 1971, Statistical analysis of tectonic patterns in areal volcanism -- the Bunyaruguru volcanic field in west Uganda: *Mathematical Geology*, v. 3, p. 335-355.
- VanDine, D. F., 1985, Debris flows and debris torrents in the southern Canadian Cordillera: *Canadian Geotechnical Journal*, v. 22, p. 44-68.
- Vandre, B. C., 1983, Geotechnical evaluation, Rudd Creek above Farmington: Ogden, Utah, U. S. Department of Agriculture, Forest Service, Intermountain Region, unpublished report, 11 p.
- Varnes, D. J., 1984, Landslide hazard zonation -- a review of principles and practice: Paris, France, UNESCO, Natural Hazards Series, No. 3, 63 p.
- Wallace, R. E., 1977, Profiles and ages of young fault scarps, north central Nevada: *Geological Society of America Bulletin*, v. 88, p. 1267-1281.
- Wasson, R. J., 1974, Intersection point deposition on alluvial fans -- an Australian example: *Geografiska Annaler*, v. 56, p. 83-92.
- Wieczorek, G. F., 1986, Debris flows and hyperconcentrated streamflows: American Society of Civil Engineers, *Proceedings, Water Forum '86: World Water Issues in Evolution*, p. 219-226.

- Wieczorek, G. F., Ellen, S., Lips, E. W., Cannon, S. H., and Short, D. N., 1983, Potential for debris flow and debris flood along the Wasatch Front between Salt Lake City and Willard, Utah, and measures for their mitigation: U.S. Geological Survey Open-file Report 83-635, 45 p.
- Wieczorek, G. F., Lips, E. W., and Ellen, S. D., 1988, Debris flows and hyperconcentrated floods along the Wasatch Front, Utah, 1983 and 1984: Association of Engineering Geologists Bulletin, in press.
- Williams, G. P., and Guy, H. P. 1973, Erosional and depositional aspects of Hurricane Camille in Virginia, 1969: U.S. Geological Survey Professional Paper 804, 84 p.
- Woolley, R.R., 1946, Cloudburst floods in Utah 1850-1928: U.S. Geological Survey Water Supply Paper 994, 128 p.
- Youngs, R. R., Swan, F. H., Power, M. S., Schwartz, D. P., and Green, R. K., 1987, Probabilistic analysis of earthquake ground shaking hazard along the Wasatch Front, Utah, *in* Gori, P. L., and Hays, W. W., eds., Assessment of regional earthquake hazards and risk along the Wasatch Front, Utah: U.S. Geological Survey Open-file Report 87-585, p. M1-110.

APPENDIX A
REPORTED MAJOR CLOUDBURST AND SNOWMELT FLOODS
IN DAVIS COUNTY, UTAH, SINCE 1848

<u>DATE</u>	<u>COMMUNITY</u>	<u>CANYON</u>	<u>COMMENTS</u>
July 23, 1878	Farmington	Farmington and Davis	Cloudburst over Wasatch Mountains. Farmington and Davis Creeks discharged an immense volume of water and debris. Farms and roads were covered with mud and boulders. A team and wagon swept away and the morning after "one of the mules was discovered embedded in the sand with only his head and neck visible above it. The other was found lodged against a rock a short distance below where it was caught. Both animals were badly bruised." Estimated damage to farms \$3,700. Rocks 20 to 30 tons in weight were carried 300 yards from canyon mouth over comparatively level ground. (Woolley, 1946).
June 15, 1892	Kaysville	Weber	Cloudburst in canyon threaten town. Bridges and tracks badly damaged. Fruit crops in Morgan and Weber Counties suffered appreciably, in some cases being literally swept away. (Woolley, 1946).
August 6, 1901	Farmington; Centerville	Steed, Davis, and Ford	Cloudburst in mountains caused floods in Davis Creek and high water in Steed and Ford Canyons. No damage was done below Steed or Ford Canyons, but the wash from Davis Creek was of great force, depositing on the farming lands below great quantities of mud, with tons of rocks and boulders, covering orchards and damaging croplands and other property. (Woolley, 1946).
1903	Centerville	Davis	Debris flood (Wieczorek and others, 1983).
July 31, 1912	Farmington	Farmington(?)	Cloudburst flooded powerhouse substation and damaged several portions of construction job. (Woolley, 1946).

APPENDIX A (Continued)

<u>DATE</u>	<u>COMMUNITY</u>	<u>CANYON</u>	<u>COMMENTS</u>
August 2, 1912	Northern Utah		Washouts on railroads halted all train service into Ogden. Wagon roads and bridges washed out. (Woolley, 1946).
August 2(?), 1912	Kaysville	Baer (Bairs) and Kays	The first rush of water down the mountain-side and through the canyon was laden with millions of tons of dirt and boulders. Near the nountain where the decent is rapid, the old creek bed has been cut down to massive boulders which have been buried for ages. Lower down where there is less fall the great deposits of mud reminds one of the lava flows from a volcano. This deposit of earth and mud is perhaps 10 feet where the creek crosses the road and 300 feet wide. The creek now flows on the crest of this dike. (Croft, 1962, p. 1515).
Summer of 1912	Northern Davis County	All canyons north of Farmington	"During the summer of 1912, all canyons between Farmington and Weber Canyon, exclusive of these two, produced mud-rock floods of varying size and intensity." (Croft, 1981, p. 5)
July 28, 1917	Kaysville	Webb	Cloudburst covered water-system intake with boulders and mud and swept debris onto farms near the mouth of the canyon. (Woolley, 1946).
Spring 1922	Northern Utah		Widespread snowmelt flooding (Marsell, 1972).
August 18, 1922	Bountiful		State highway and Interurban Railroad blocked by storm. (Woolley, 1946).
August 13, 1923	Farmington and Centerville	Farmington, Steed, Davis, and Ford	Seven persons drowned or died as a result of flood, the most disastrous in Utah history. Farming section largely destroyed, with houses, barns; orchards and the highway were covered with several feet of mud. One barn burned by lightning. Lagoon resort was flooded and patrons were rescued from trees, etc., where they sought refuge from the rapidly rising waters. Farmington Canyon

APPENDIX A (Continued)

<u>DATE</u>	<u>COMMUNITY</u>	<u>CANYON</u>	<u>COMMENTS</u>
			road, just completed at a cost of \$10,000, was completely destroyed. Bamberger Interurban Railway was washed out, and electric-power supply was cut off. Sixty miners were isolated in the canyon without a food supply. Considerable livestock destroyed. Observers in canyon reported crest to be 75 to 100 feet high in canyon, with width of 200 feet. Crest height at Baldwin mine reported to be 30 feet. (Woolley, 1946; Paul and Baker, 1925; Pack, 1923; Croft, 1962, p. 1511; Marsell, 1972; Croft, 1981, p. 9).
1923		Baer (Bairs)	Reference to 1923 in "well-known flood history." (Croft, 1962, p. 1513).
July 5, 1926	Farmington	Farmington	Flood filled forebay of power-plant intake with boulders and debris. Out of service eight days. (Woolley, 1946).
September 29, 1926	Farmington	Farmington	Flood filled power-plant intake with sand and gravel. Out of service two days. Woolley, 1946).
1927		Baer (Bairs)	Reference to 1927 in "well-known flood history." (Croft, 1962, p. 1513).
1927	Kaysville	Kays Creek	Debris flood in South Fork of Kays (Wieczorek and others, 1983).
August 4, 1929	Farmington	Davis	Heavy storms brought down deluge of boulders, tree trunks, rubbish, and water. Three autos crossing highway were buried. Property was damaged. (Woolley, 1946).
1929	Centerville	Ford (Ricks)	Debris flow according to Wieczorek and others (1983); not like other years according to Rigby (1987, oral communication).
July 10, 1930	Farmington and Centerville		Farms swept by water carrying tons of rock, sand, etc. One house and several farm buildings destroyed. Livestock loss negligible. Road blocked between Farmington and Centerville in three

APPENDIX A (Continued)

<u>DATE</u>	<u>COMMUNITY</u>	<u>CANYON</u>	<u>COMMENTS</u>
			places for eight days. Farm losses estimated at \$50,000. Relief fund of \$30,000 instituted. (Woolley, 1946; Cannon and others, 1931; Bailey and others, 1934).
August, 1930	Kaysville	Kays	Debris flow (Croft, 1967).
August 11, 1930	Farmington	Davis	Cloudburst in hills. No rain in Farmington. Rocks and debris over 8 feet deep on State Highway at Davis Creek. (Woolley, 1946; Cannon and others, 1931; Bailey and others, 1934).
August 13, 1930	Farmington (Kaysville)	Ford and Shepard	Slide 10 to 20 feet deep at Ford Canyon destroyed one home "as though it were paper." Bamberger Railway undermined at Shepard Canyon. (Woolley, 1946; Crawford and Thackwell, 1931; Bailey and others, 1934).
September 4, 1930	Centerville	Parrish	A new flood hit Davis County as a fierce rain struck in the hills. At Centerville at least one block of the State highway was under 15 feet of mud. Since property was already stricken, not a great amount of additional damage was done. (Woolley, 1946; Bailey and others, 1934).
September 4, 1930	Farmington (Centerville)	Steed, Davis, and Ford	Highway was buried. Bamberger Railway tracks were covered for a quarter of a mile with 2 to 4 feet of debris. Highway again covered by mudslide. A few autos were stalled. (Woolley, 1946; Cannon and others, 1931)
August 13, 1931	Farmington		Road blocked by rocks and silt. (Woolley, 1946).
August 27, 1932	Davis County	Parrish, Ford, Barnard, Steed, and Farmington	Salt Lake-Ogden road blocked at Beck's Hot Springs and between Centerville and Farmington by mudslides. (Woolley, 1946; Rigby, 1987, oral communication).

APPENDIX A (Continued)

<u>DATE</u>	<u>COMMUNITY</u>	<u>CANYON</u>	<u>COMMENTS</u>
July 4, 1934	Centerville	Ford	A mud flow carried boulders 9 feet long out of the canyon. (Bailey and others, 1947, p. 16).
July 10, 1936	Farmington	Farmington	Stream-gaging station at Miller Creek in Farmington Canyon was washed out. 1.14 inches of rain measured at the Parrish Creek gage in the Davis County Experimental Watershed with a maximum rate of 5.04 inches per hour for a 5-minute period. (Bailey and others, 1947, p. 16).
July 29, 1936	Farmington		Cloudburst brought debris down canyons (Woolley, 1946).
June 30, 1938	Bountiful		Cloudburst hit Davis County "in its annual devastating fashion." Two feet of water swiched across the highway at Perry Station. (Woolley, 1946).
August 10, 1941	Kaysville	Baer	Storms in Weber, Davis, Box Elder and Salt Lake Counties did little serious damage. Heaviest damage was at Fruit Heights east of Kaysville on Mountain Road near Jost Orchard. All runoff was held in established gullies. (Butler and Marsell, 1972).
1945		Baer (Bairs)	Reference to 1945 in "well-known flood history." (Croft, 1962, p. 1513).
August 19, 1945	Farmington	Farmington	Sub-basins in Farmington Canyon flooded. 1.06 inches of rain fell at the Parrish Creek gage in the Davis County Experimental Watershed with a maximum rate of 6.84 inches per hour for a 5-minute period. (Bailey and others, 1947, p. 16).
1945	Kaysville	Kays	Debris flood (Wieczorek and others, 1983).

APPENDIX A (Continued)

<u>DATE</u>	<u>COMMUNITY</u>	<u>CANYON</u>	<u>COMMENTS</u>
August 10, 1947		Baer (Bairs)	Large boulders were deposited at the canyon mouth where the flood burst from the confining canyon walls; concrete-like deposits extended more than 300 feet below the canyon mouth. (Croft, 1962, p. 1515).
1947	Farmington Kaysville	Farmington, S. Fork Kays M. Fork Kays	Debris flood or flow (Wieczorek and others, 1983; Croft, 1981).
August 5, 1948	Bountiful		A flash flood in business and residential districts between 8:30 and 9:00 p.m. caused several thousand dollars damage. (Butler and Marsell, 1972).
July 27, 1951	Bountiful		"Worst lightning storm in history of valley." Property damage in Salt Lake and southern Davis Counties estimated to be nearly \$500,000. (Butler and Marsell, 1972).
April 21 to May 7, 1952	Northern Utah		Widespread snowmelt flooding. (Marsell, 1972).
July 21, 1954	Bountiful		An electrical storm centered in Salt Lake and Davis Counties disrupted power, started a fire, and flooded basements. (Butler and Marsell, 1972).
August 4, 1954	Bountiful		Cloudburst caused gutters to overflow within a few minutes. The rain came with such force and quantity that many roofs, even some new ones, could not keep all the moisture out. Some basements were flooded. Residents "could not remember any in history as heavy as this storm." (Butler and Marsell, 1972).
July 24, 1955	Bountiful		Cloudburst poured water through the streets. Some basements flooded. (Butler and Marsell, 1972).

APPENDIX A (Continued)

<u>DATE</u>	<u>COMMUNITY</u>	<u>CANYON</u>	<u>COMMENTS</u>
May 27, 1956	Davis County		Severe crop damage reported in Davis County, but flood damage occurred in Salt Lake City, Ogden, and nearby farmland. (Butler and Marsell, 1972).
July 30, 1956	Syracuse		Water flooded practically all streets and soaked lawns and basements with over 8 inches of water. (Butler and Marsell, 1972).
May 20, 1957	Bountiful and Farmington	Ward and Steed	Many homes in Bountiful below Ward Canyon (Stone Creek) flooded. Steed Creek in Farmington flooded State highway. (Butler and Marsell, 1972).
April 28, 1960	Roy		Rain and hail hit the area shortly before noon. Water in streets and gutters was ankle deep and the Roy-Hooper road was partly under water. (Butler and Marsell, 1972).
August 25, 1961	Bountiful		Heavy flooding reported in Davis, Salt Lake, and Juab Counties. Water and debris blocked U.S. 91 for some time at various points near Levan and Salt Lake and Davis Counties. Basements were flooded in Bountiful. (Butler and Marsell, 1972).
June 1, 1963	Farmington		A cloudburst lasted about an hour; streets became rivers and the water poured into basements. (Butler and Marsell, 1972).
August 23, 1968	Bountiful		One of the heaviest rains in several years pelted the area. Gutters overflowed and caused damage to roads, garages, and basements. (Butler and Marsell, 1972).
June 24, 1969	Bountiful and Farmington	Farmington	Near Bountiful, heavy rains did serious damage to cherries and flood water 2-1/2 feet deep in one business establishment damaged company records and ruined telephone equipment. A layer of mud 1 foot deep covered the north lane in the 1600 block of Farmington's main street. (Butler and Marsell, 1972).

APPENDIX A (Continued)

<u>DATE</u>	<u>COMMUNITY</u>	<u>CANYON</u>	<u>COMMENTS</u>
July 29, 1969	Bountiful		A cloudburst completely inundated Fifth South Street with up to a foot of water. (Butler and Marsell, 1972).
May-June, 1983	Northern	All canyons	Widespread snowmelt flooding and debris flows (Wieczorek and others, 1983; Lindskov, 1984; Anderson and others, 1984).
May 14, 1984	Layton	Lightning	Five houses were destroyed or damaged by a debris flow generated by snowmelt (Olson, 1985; Mathewson and Santi, 1987).
May, June 1984	Farmington	Rudd	Small debris flows (Forbush, 1987, oral communication).

APPENDIX B

STRATIGRAPHIC SECTIONS

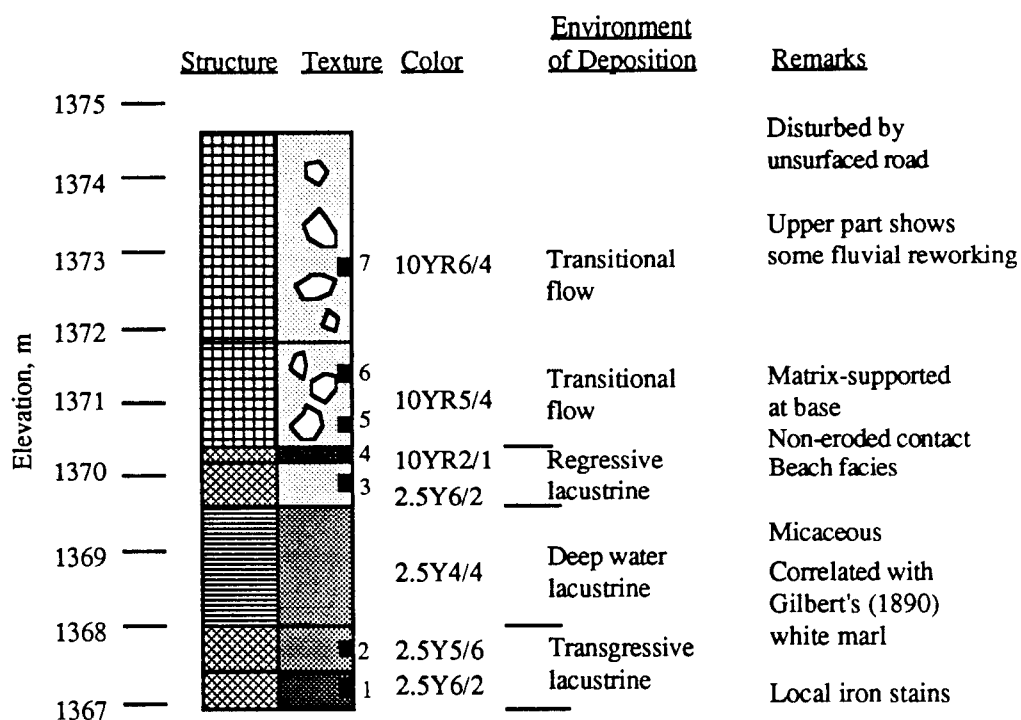
Introduction

Samples were collected from three alluvial fan areas in Davis County for subsequent laboratory testing. These fan areas are associated with Lightning Canyon, Rudd Creek, and Ricks Creek (Figure 1). Surface samples only were collected from the Lightning Canyon fan. These samples are identified as Lightning 1, Lightning 2, and Lightning 3; laboratory test results for these samples are presented in Appendix C, Summary of Experimental Data. The Lightning Canyon samples were obtained from sediment deposited by an alluvial-fan flooding event in May 1984 at locations shown on Figure 6.

Samples collected at Rudd Creek were obtained from stream-bank exposures, man-made cut slopes, and hand-dug pits at locations shown on Figure 7. These samples are identified as Rudd 1 through Rudd 29. Multiple samples were collected at several Rudd Creek sample locations; these multiple samples are identified with hyphenated numbers and letters (e.g., Rudd 4-3 and Rudd 4-4a). Laboratory test results for the Rudd Creek samples are presented in Appendix C. Stratigraphic sections of the Rudd Creek sample locations are illustrated on Figures B-1a through B-1n.

Samples collected at Ricks Creek were obtained from stream-bank exposures, man-made cut slopes, hand-dug pits, and test pits excavated by a hydraulic backhoe at locations shown on Figure 8. These samples are identified as Ricks 1 through Ricks 15 and Ricks TP-1 through Ricks TP-8. Multiple samples were collected at several Ricks Creek sample locations; these multiple samples are identified with hyphenated numbers. Laboratory test results for the Ricks Creek samples are presented in Appendix C. Stratigraphic sections of the Ricks Creek sample locations are illustrated on Figures B-2a through B-2j.

Rudd Creek, Location 1. UTM: N 37954.7; E 25731.9



EXPLANATION




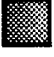









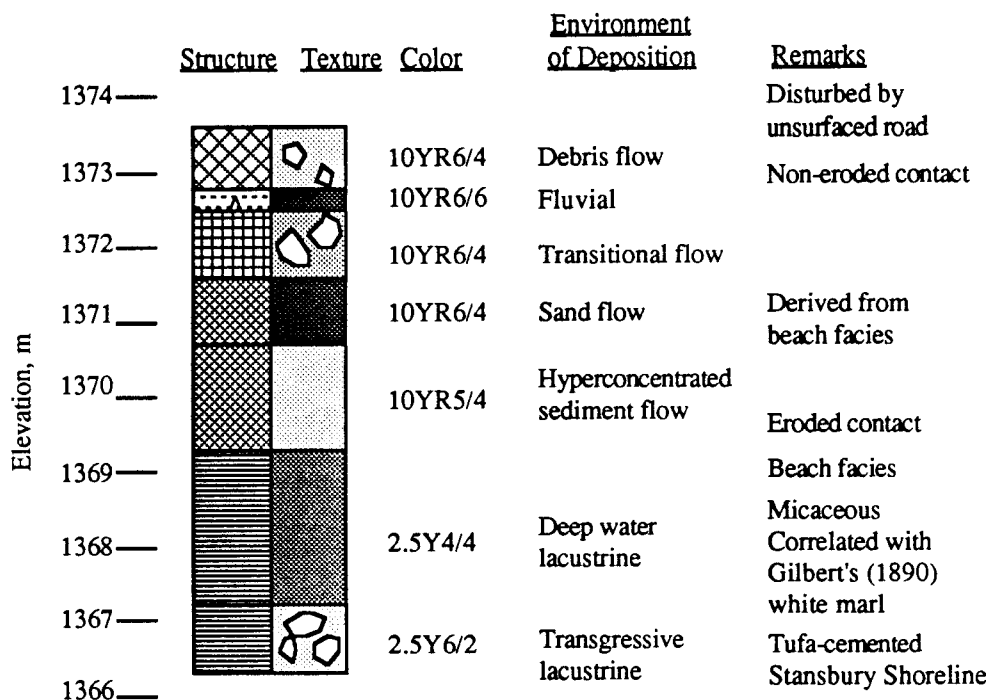
STRUCTURE	TEXTURE
 Horizontal to subhorizontal laminations.	 Silt to sandy silt.
 Clast-supported, graded bedding. Arrow points in direction of fining.	 Fine sand to silty sand.
 Clast-supported or massive.	 Coarse sand.
 Clast- to matrix-supported.	 Gravelly sand
 Matrix-supported	 Sandy gravel.
 Weak pedogenic development	 Boulders and megaclasts.
	 Sample location.

Figure B-1a. Stratigraphic section for Location 1 on the Rudd Creek Fan. UTM (Universal Transverse Mercator) coordinates, in m, truncated from Zone 12.

Rudd Creek, Location 2. UTM: N 37963.8; E 25722.1



Rudd Creek, Location 3. UTM: N 37943.4; E 25729.0

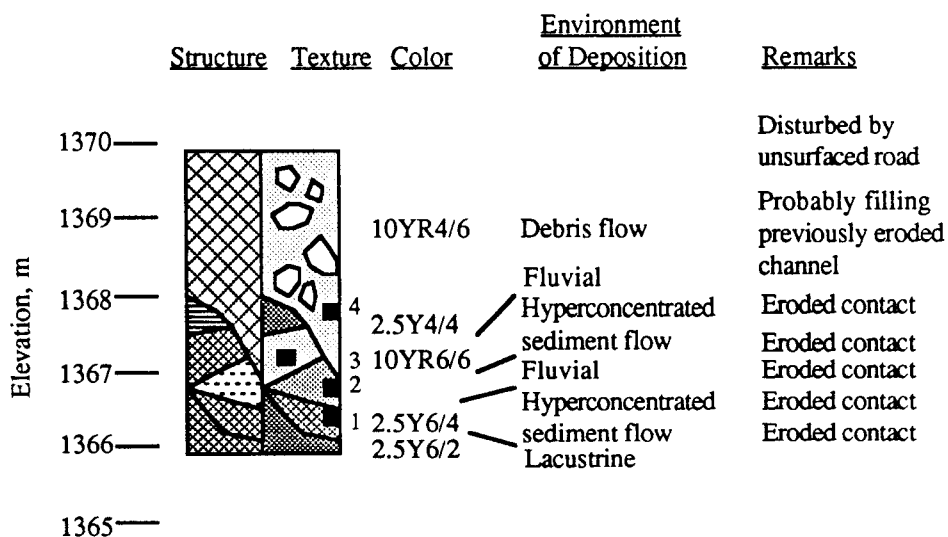
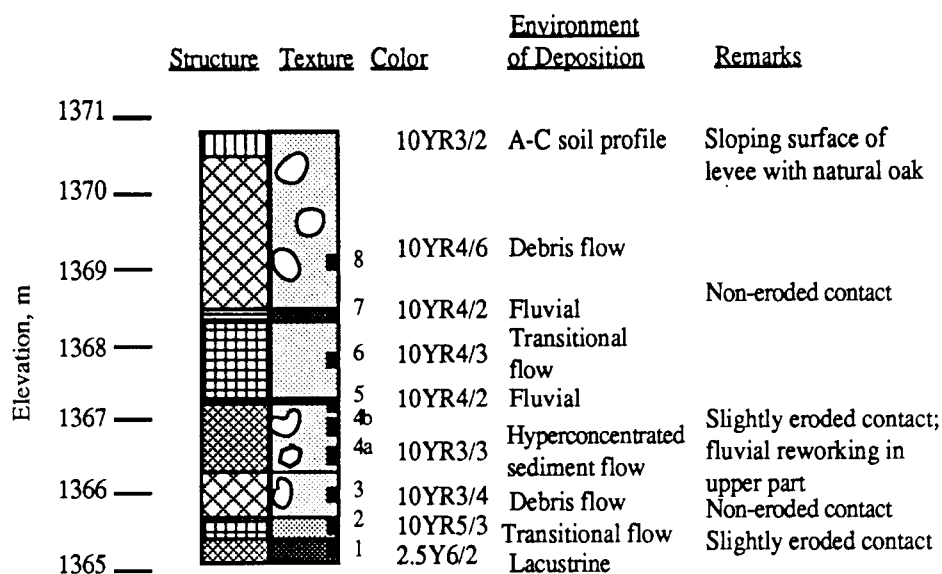


Figure B-1b. Stratigraphic sections for Locations 2 and 3 on the Rudd Creek Fan. See Figure B-1a for explanation of symbols.

Rudd Creek, Location 4. UTM: N 37922.8; E 25712.0



Rudd Creek, Location 5. UTM: N 37915.6; E 25717.5

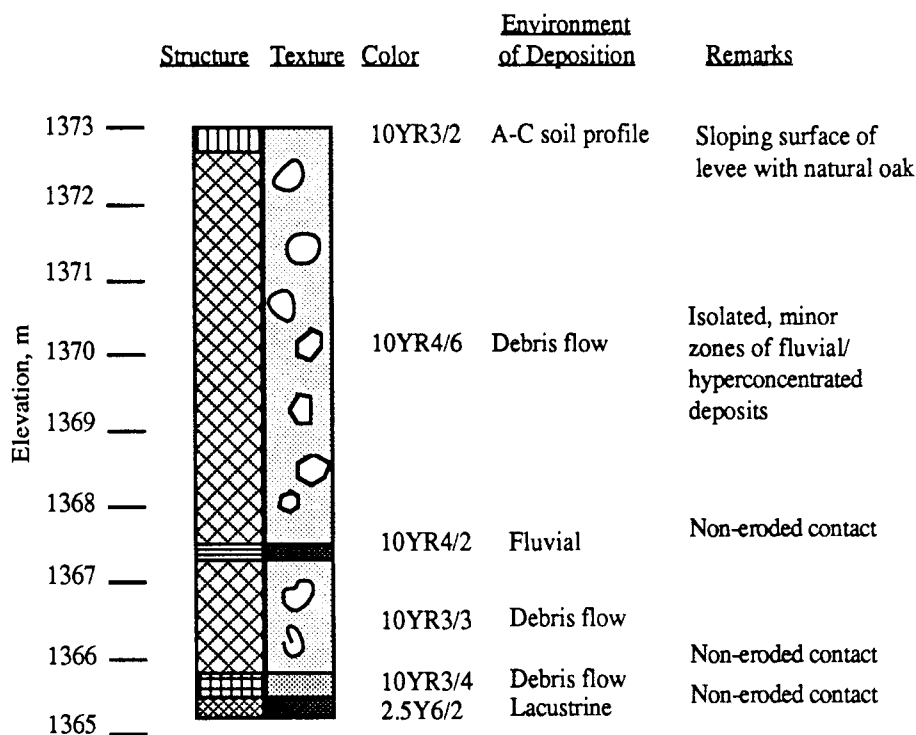
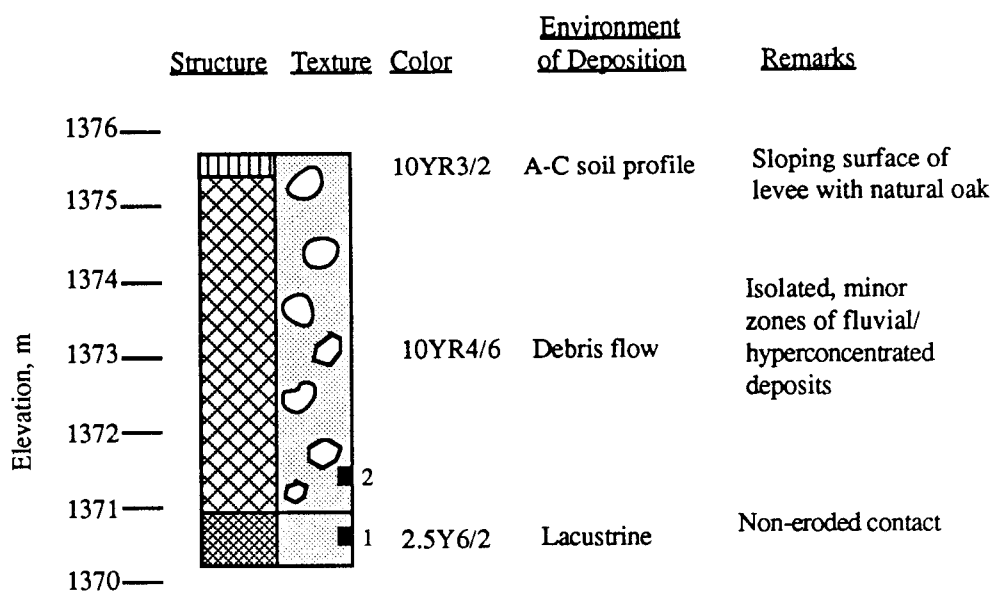


Figure B-1c. Stratigraphic sections for Locations 4 and 5 on the Rudd Creek Fan. See Figure B-1a for explanation of symbols.

Rudd Creek, Location 6. UTM: N 37880.8; E 25760.0



Rudd Creek, Location 7. UTM: N 37882.5; E 25769.7

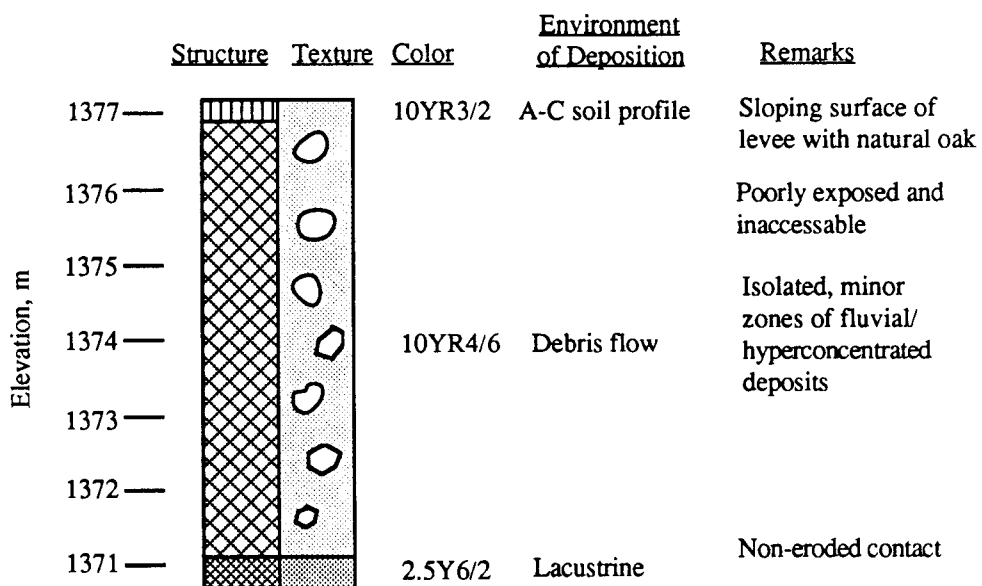
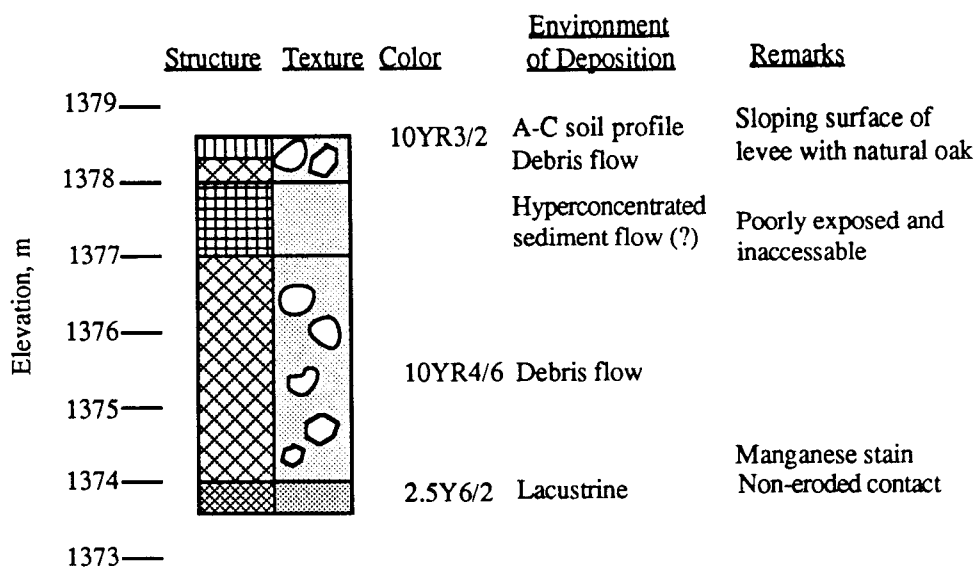


Figure B-1d. Stratigraphic sections for Locations 6 and 7 on the Rudd Creek Fan. See Figure B-1a for explanation of symbols.

Rudd Creek, Location 8. UTM: N 37883.0; E 25781.0



Rudd Creek, Location 9. UTM: N 37886.5; E 25783.8

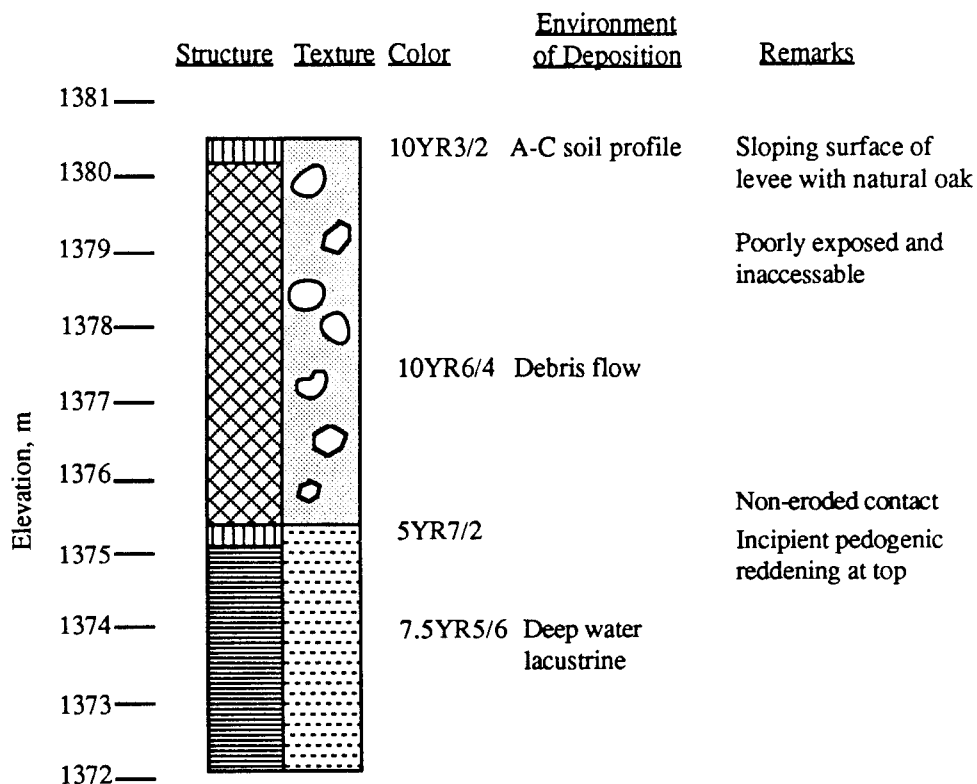
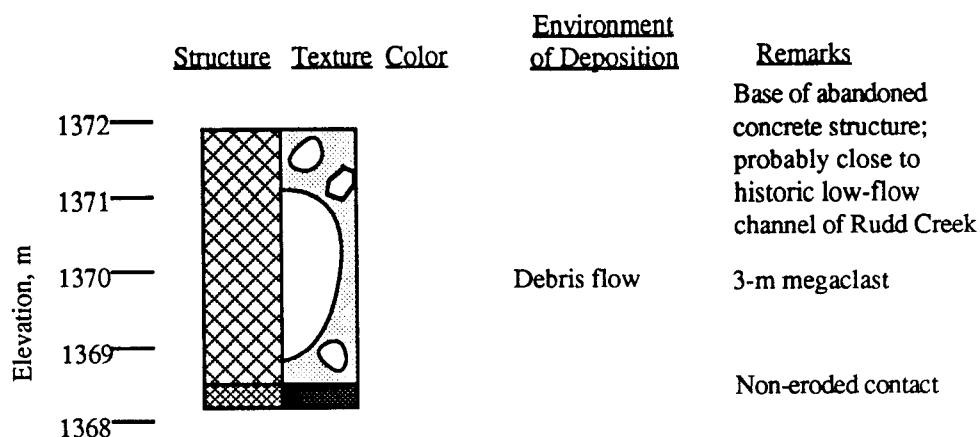
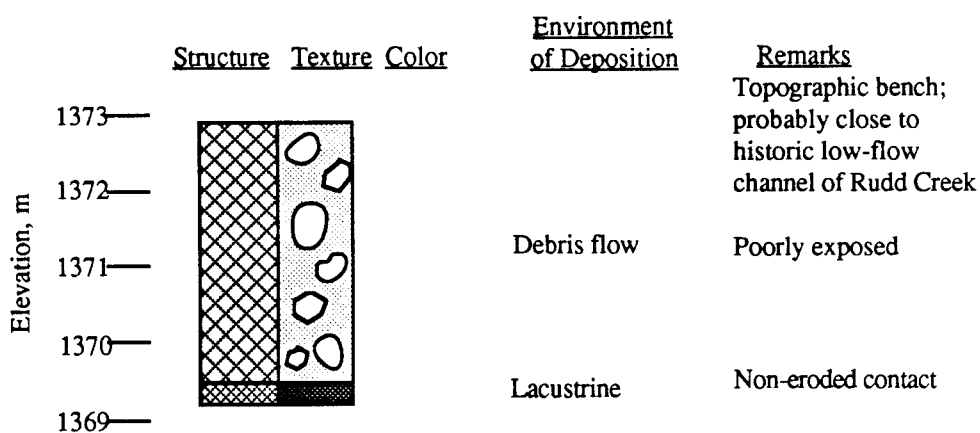


Figure B-1e. Stratigraphic sections for Locations 8 and 9 on the Rudd Creek Fan. See Figure B-1a for explanation of symbols.

Rudd Creek, Location 10. UTM: N 37892.6; E 25777.0



Rudd Creek, Location 11. UTM: N 37894.5; E 25783.8



Rudd Creek, Location 12. UTM: N 37898.8; E 25788.0

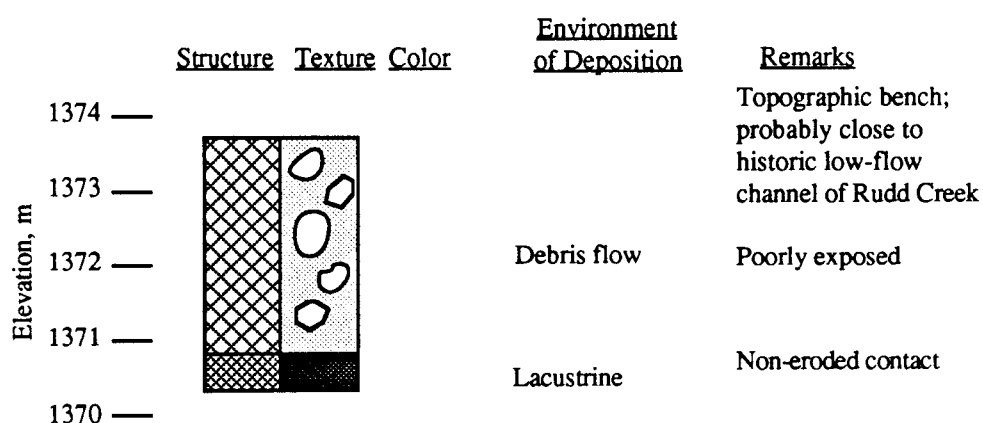
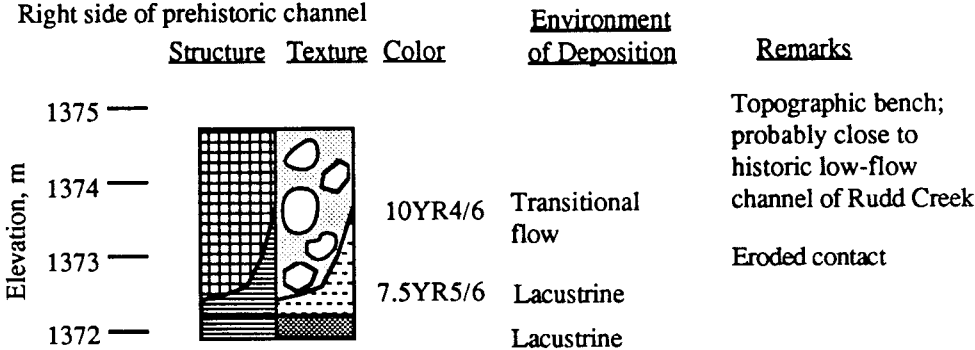


Figure B-1f. Stratigraphic sections for Locations 10, 11, and 12 on the Rudd Creek Fan. See Figure B-1a for explanation of symbols.

Rudd Creek, Location 13. UTM: N 37905.8; E 25790.4

Right side of prehistoric channel



Rudd Creek, Location 14. UTM: N 37908.2; E 25785.6

Left side of prehistoric channel

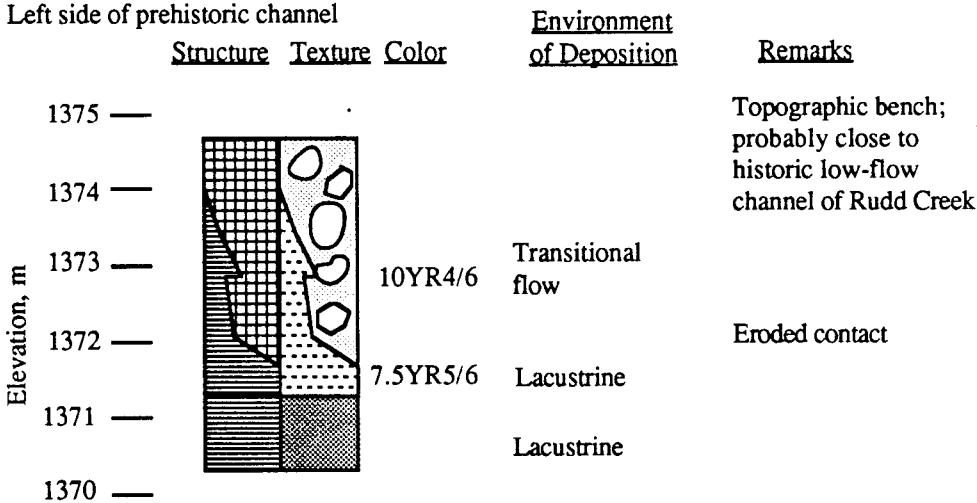
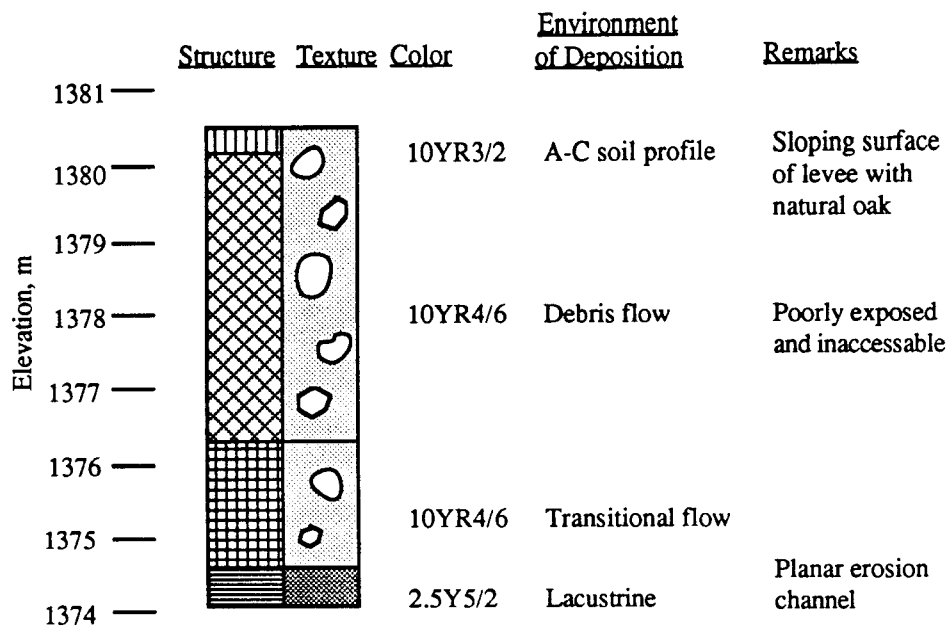


Figure B-1g. Stratigraphic sections for Locations 13 and 14 on the Rudd Creek Fan. See Figure B-1a for explanation of symbols.

Rudd Creek, Location 15. UTM: N 37916.3; E 25790.1



Rudd Creek, Location 16. UTM: N 37920.7; E 25790.4

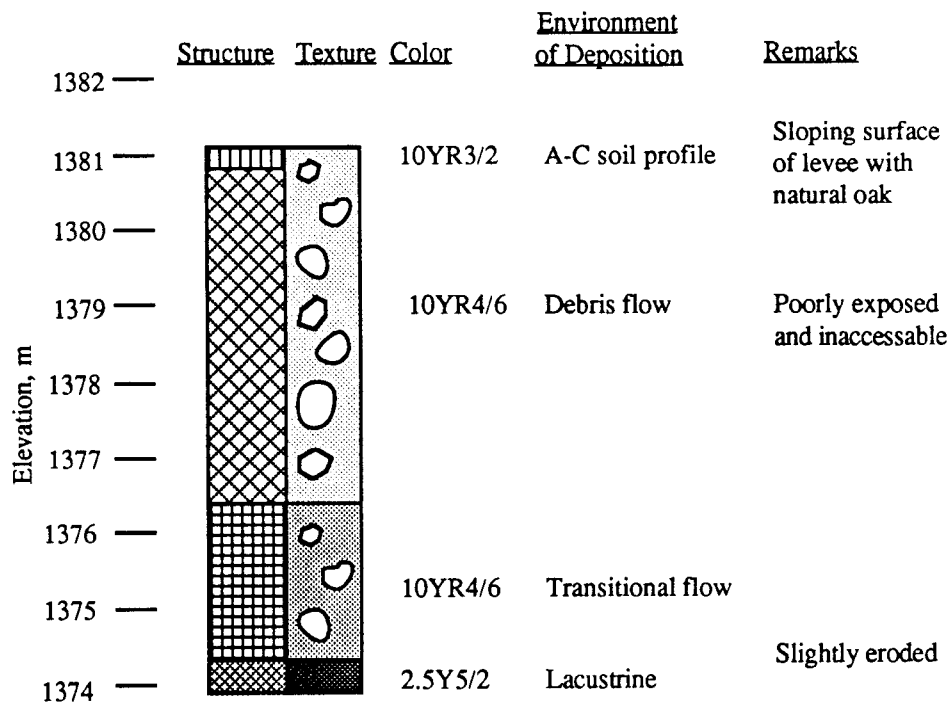
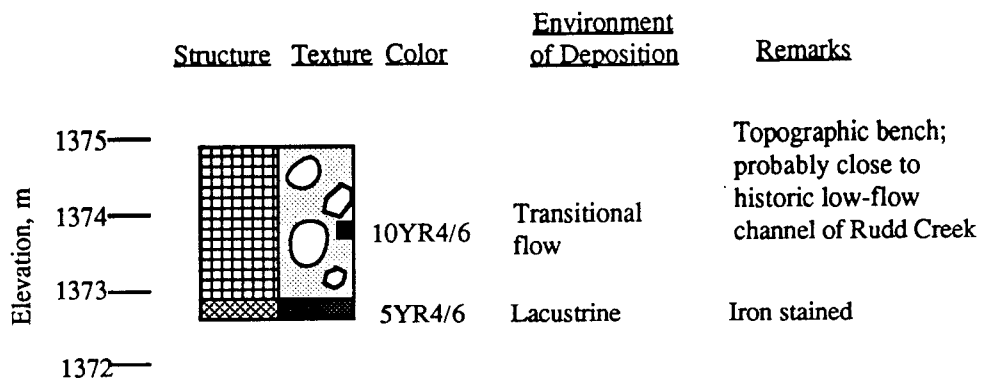


Figure B-1h. Stratigraphic sections for Locations 15 and 16 on the Rudd Creek Fan. See Figure B-1a for explanation of symbols.

Rudd Creek, Location 17. UTM: N 37912.7; E 25796.8



Rudd Creek, Location 18. UTM: N 37926.4; E 25795.6

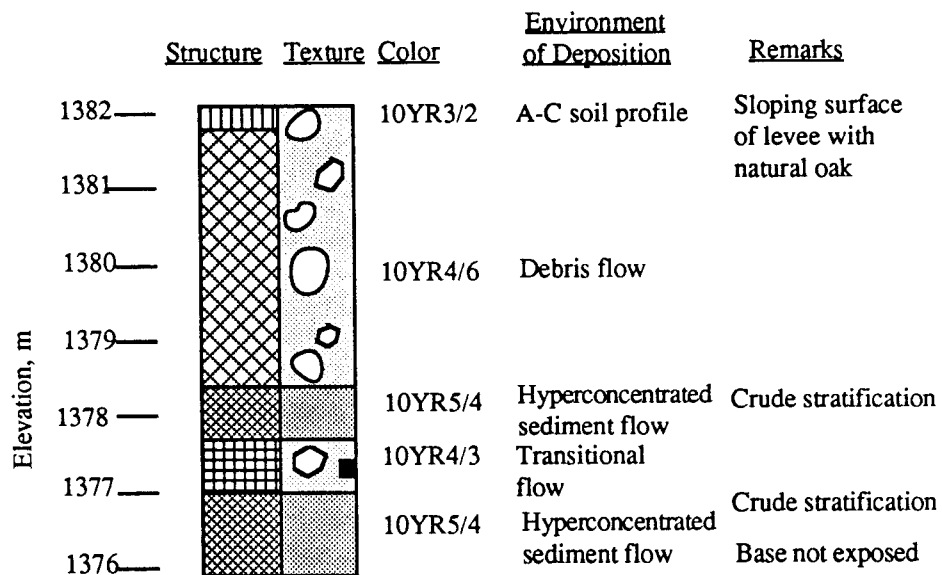
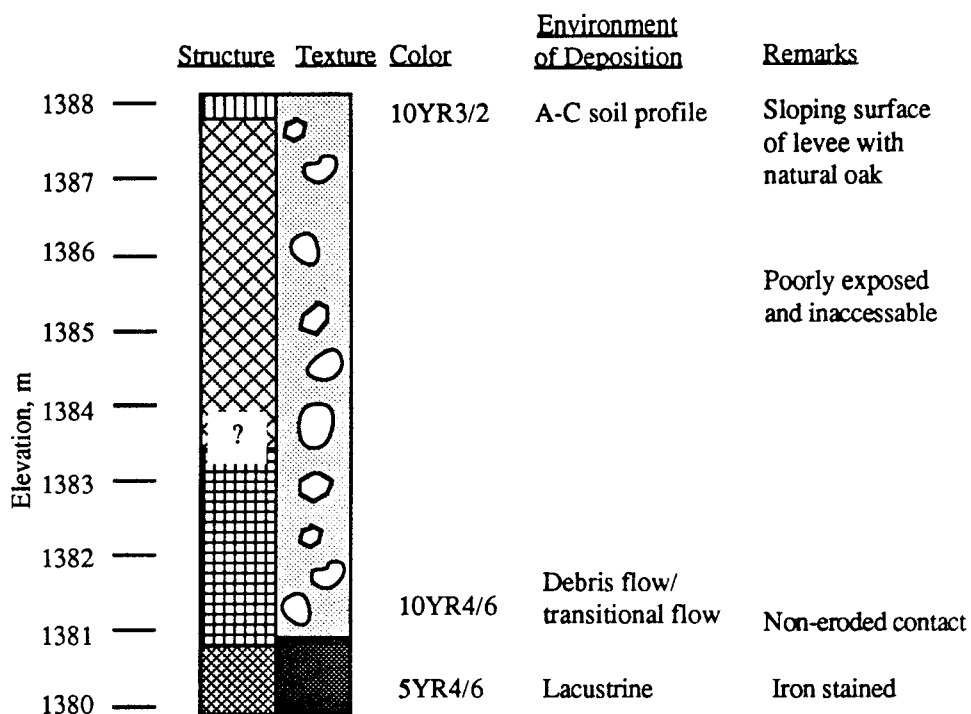


Figure B-1i. Stratigraphic sections for Locations 17 and 18 on the Rudd Creek Fan. See Figure B-1a for explanation of symbols.

Rudd Creek, Location 19. UTM: N 37929.7; E 25827.6



Rudd Creek, Location 20. UTM: N 37923.1; E 25837.2

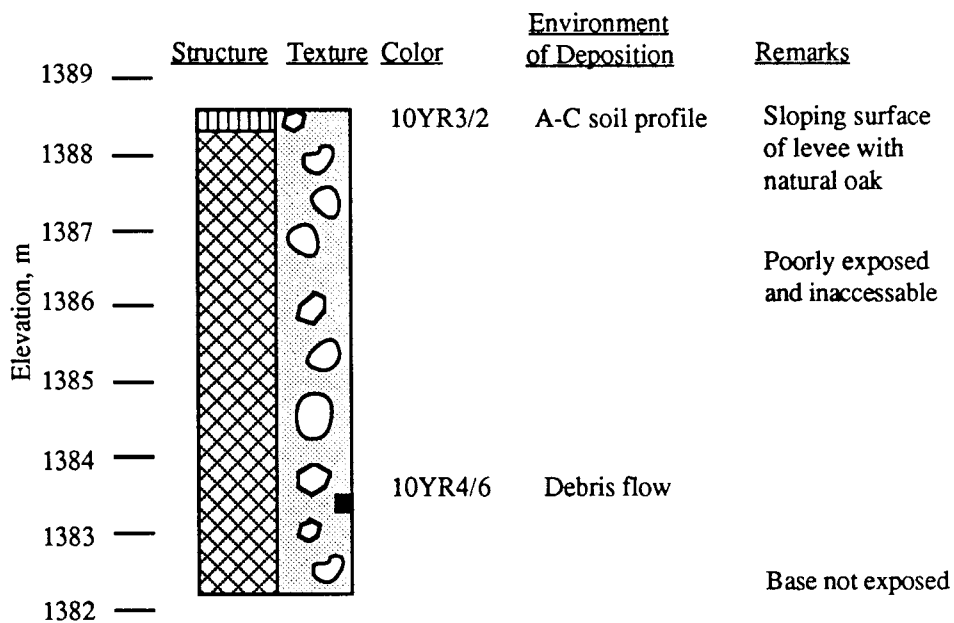
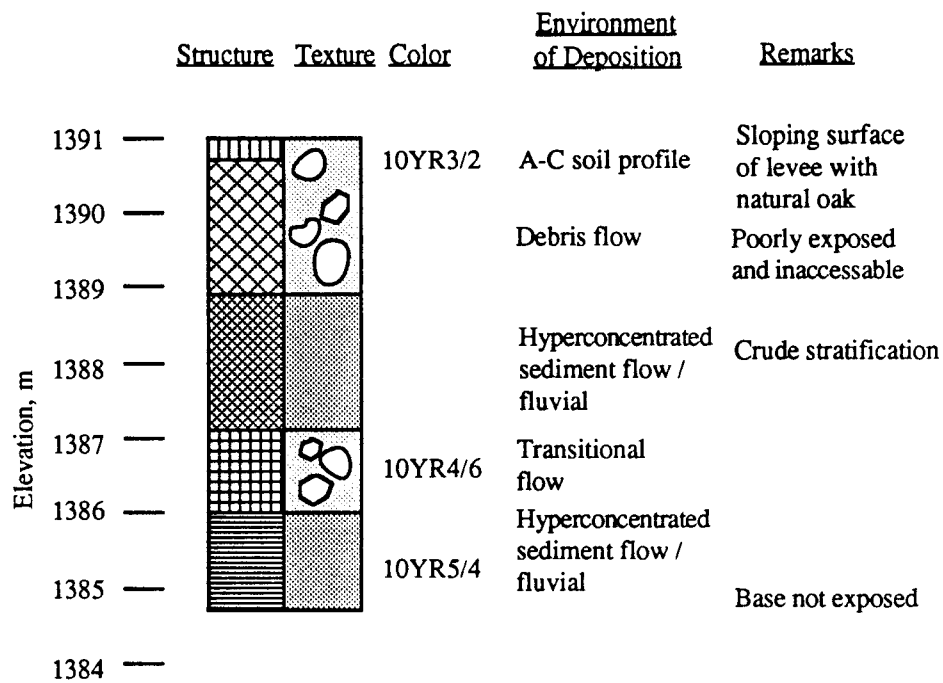


Figure B-1j. Stratigraphic sections for Locations 19 and 20 on the Rudd Creek Fan. See Figure B-1a for explanation of symbols.

Rudd Creek, Location 21. UTM: N 37945.3; E 25852.3



Rudd Creek, Location 22. UTM: N 37952.9; E 25857.4

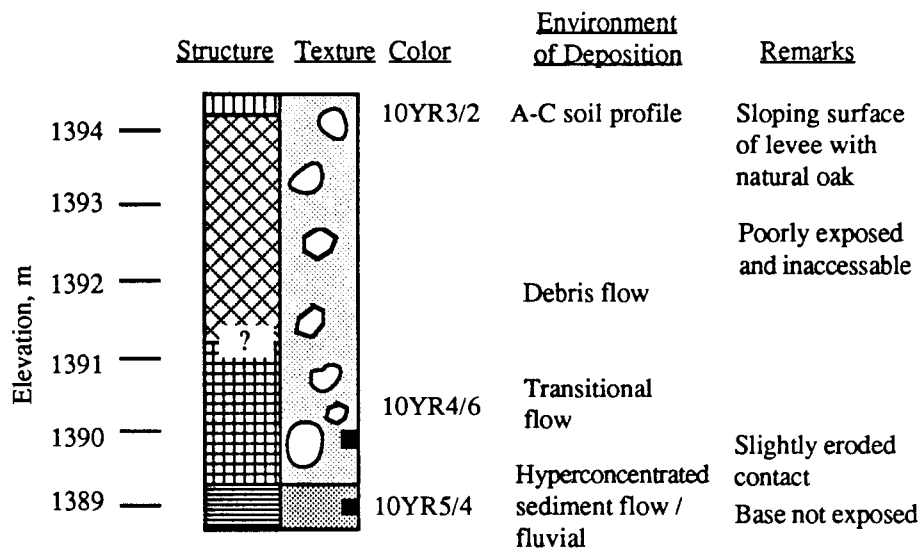
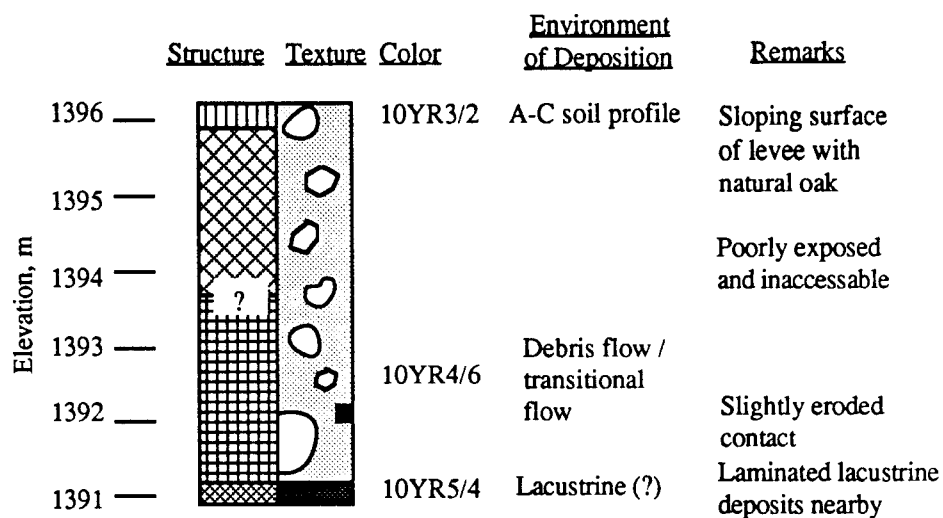


Figure B-1k. Stratigraphic sections for Locations 21 and 22 on the Rudd Creek Fan. See Figure B-1a for explanation of symbols.

Rudd Creek, Location 23. UTM: N 37951.1; E 25861.3



Rudd Creek, Location 24. UTM: N 37953.4; E 25867.8

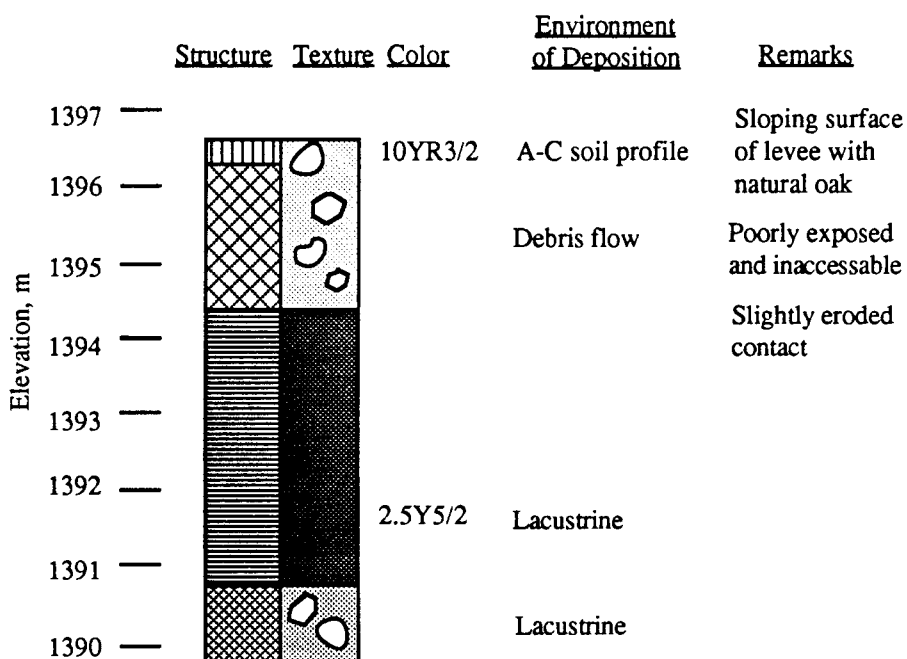
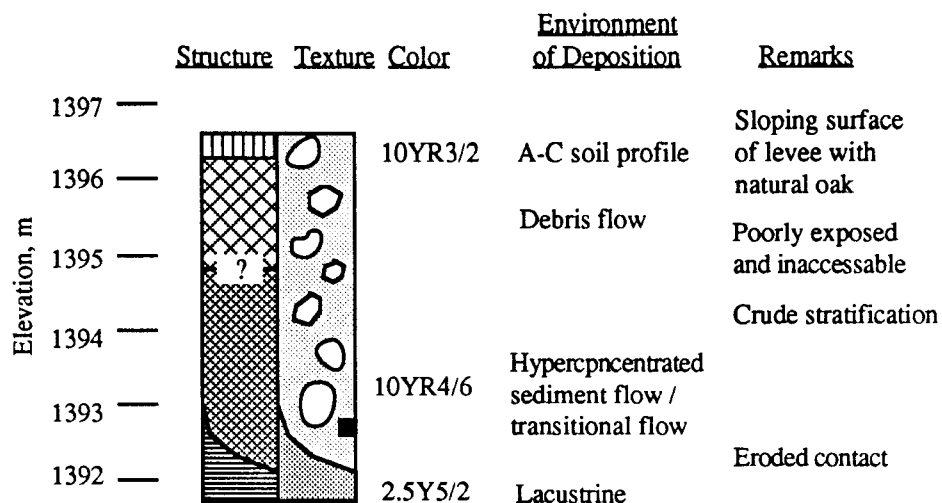


Figure B-11. Stratigraphic sections for Locations 23 and 24 on the Rudd Creek Fan. See Figure B-1a for explanation of symbols.

Rudd Creek, Location 25. UTM: N 37947.9; E 25878.8



Rudd Creek, Location 26. UTM: N 37951.5; E 25890.1

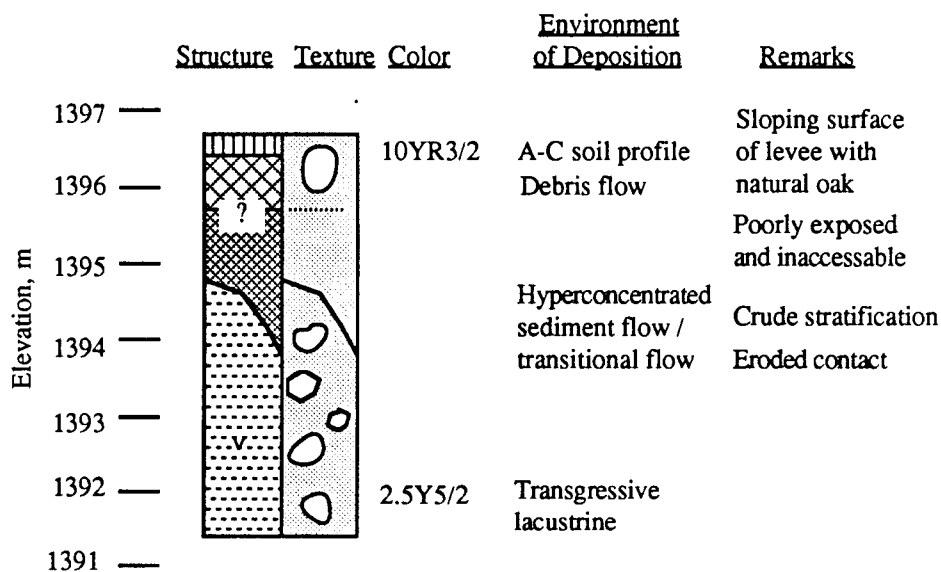
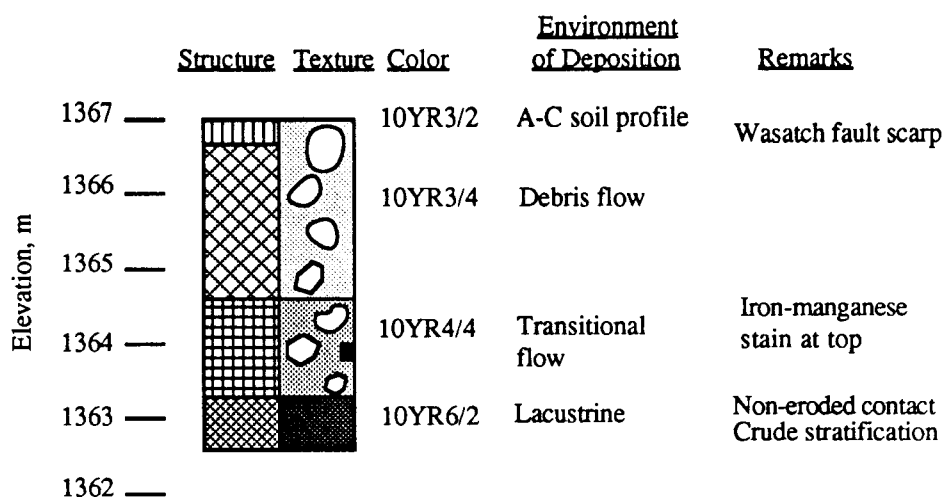
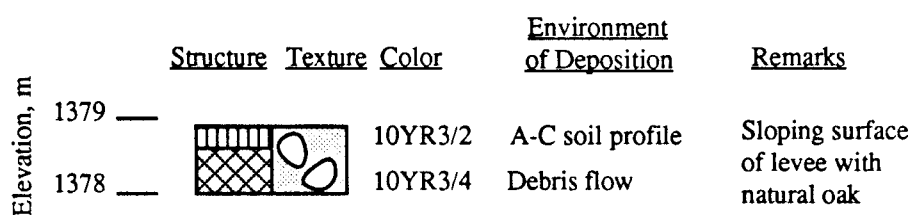


Figure B-1m. Stratigraphic sections for Locations 25 and 26 on the Rudd Creek Fan. See Figure B-1a for explanation of symbols.

Rudd Creek, Location 27. UTM: N 37877.2; E 25717.1



Rudd Creek, Test Pit 1. UTM: N 37879.3; E 25781.7



Rudd Creek, Test Pit 2. UTM: N 37922.9; E 25774.1

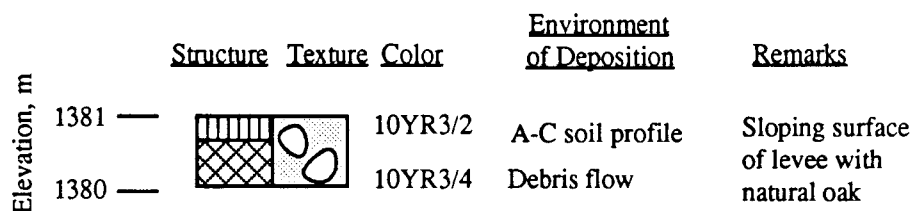
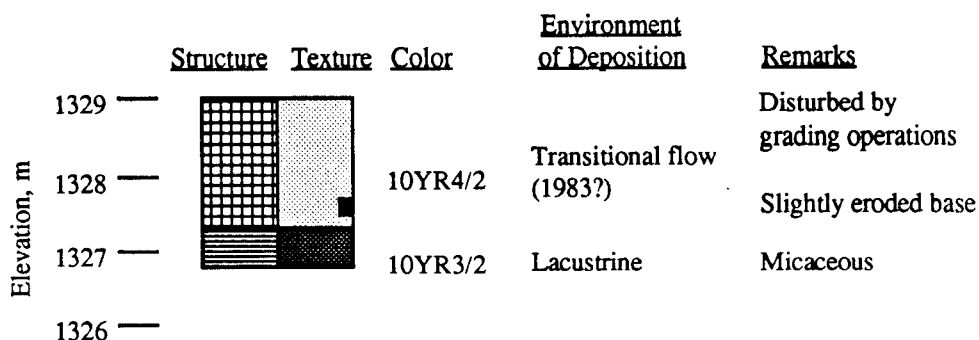
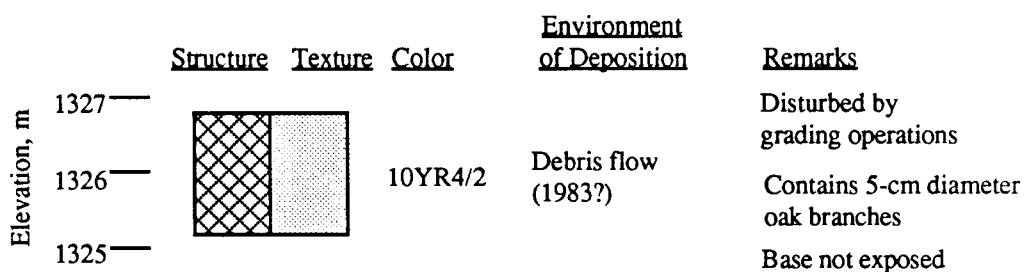


Figure B-1n. Stratigraphic sections for Location 27 and Test Pits 1 and 2 on the Rudd Creek Fan. See Figure B-1a for explanation of symbols.

Ricks Creek, Location 1. UTM: N 32176.1; E 26321.6



Ricks Creek, Location 2. UTM: N 32166.8; E 26329.5

EXPLANATION














STRUCTURE		TEXTURE	
	Horizontal to subhorizontal laminations.		Silt to sandy silt.
	Clast-supported, graded bedding. Arrow points in direction of fining.		Fine sand to silty sand.
	Clast-supported or massive.		Coarse sand.
	Clast- to matrix-supported.		Gravelly sand
	Matrix-supported		Sandy gravel.
	Weak pedogenic development		Boulders and megaclasts.
			Sample location.

Figure B-2a. Stratigraphic sections for Locations 1 and 2 on the Ricks Creek Fan. UTM (Universal Transverse Mercator) coordinated, in m, truncated from Zone 12.

Ricks Creek, Location 3. UTM: N 32153.5; E 26414.1

	<u>Structure</u>	<u>Texture</u>	<u>Color</u>	<u>Environment of Deposition</u>	<u>Remarks</u>
Elevation, m					
1341 —			10YR5/4	Hyperconcentrated sediment flow (1983?)	Grassy surface.
1340 —					Could be disturbed by grading operations
1339 —					Base not exposed

Ricks Creek, Location 4. UTM: N 32153.3; E 26410.6

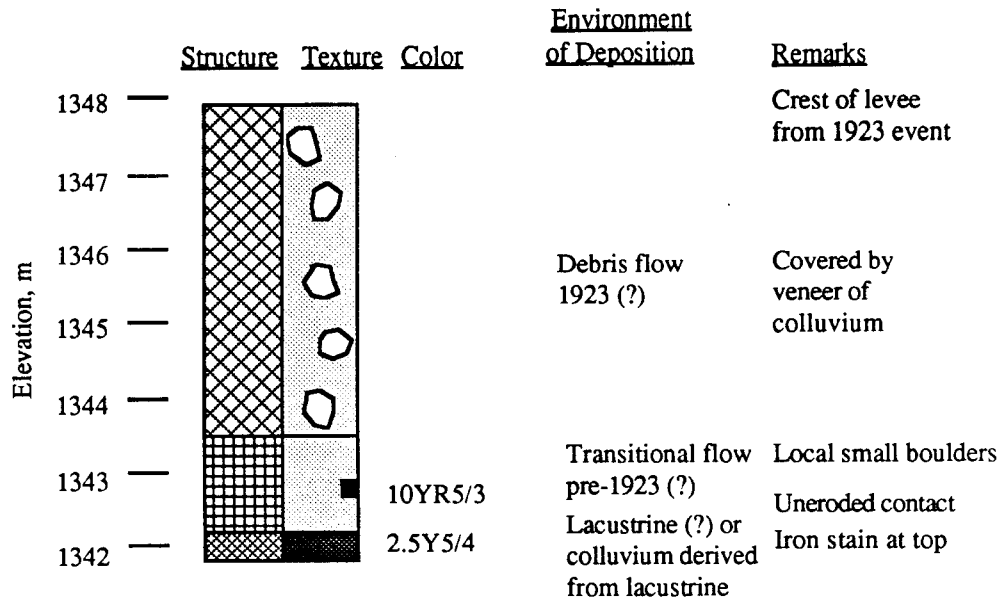
	<u>Structure</u>	<u>Texture</u>	<u>Color</u>	<u>Environment of Deposition</u>	<u>Remarks</u>
Elevation, m					
1342 —			10YR5/4	Hyperconcentrated sediment flow (1923?)	Below grading stake labeled "cut 9.91"
1341 —					
1340 —					Base not exposed

Ricks Creek, Location 5. UTM: N 32151.1; E 26435.4

	<u>Structure</u>	<u>Texture</u>	<u>Color</u>	<u>Environment of Deposition</u>	<u>Remarks</u>
Elevation, m					
1348 —			10YR5/4 7.5YR5/4 10R3/4- 2.5YR3/4 10YR5/2	Transitional flow (1923?)	Sloping vegetated surface
1347 —					
1346 —				Deep water lacustrine	Eroded contact
1345 —					
1344 —				Transgressive lacustrine	

Figure B-2b. Stratigraphic sections for Locations 3, 4, and 5 on the Ricks Creek Fan. See Figure B-2a for explanation of symbols.

Ricks Creek, Location 6. UTM: N 32153.5; E 26437.6



Ricks Creek, Location 7. UTM: N 32152.5; E 26458.1

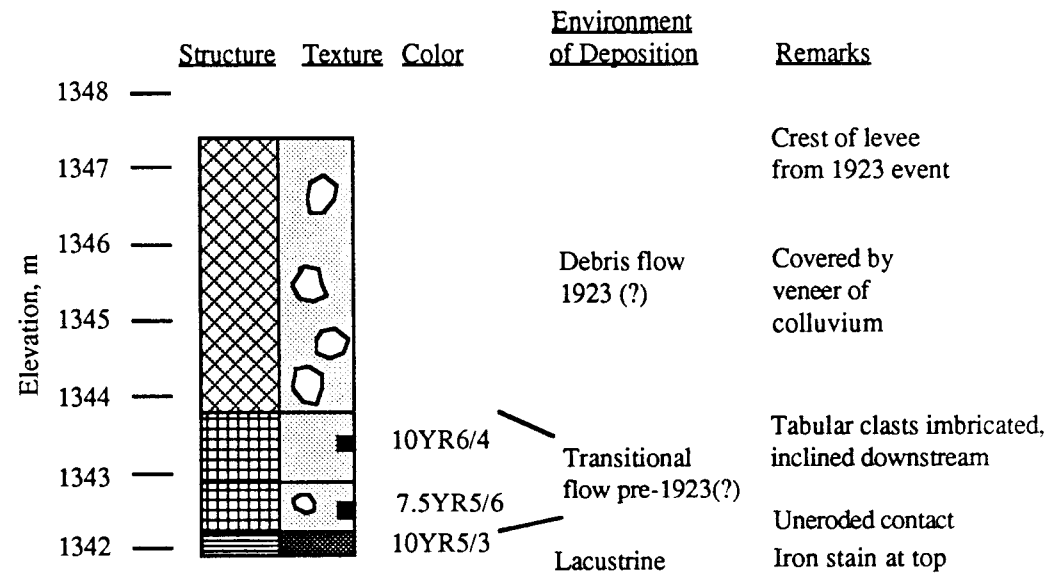
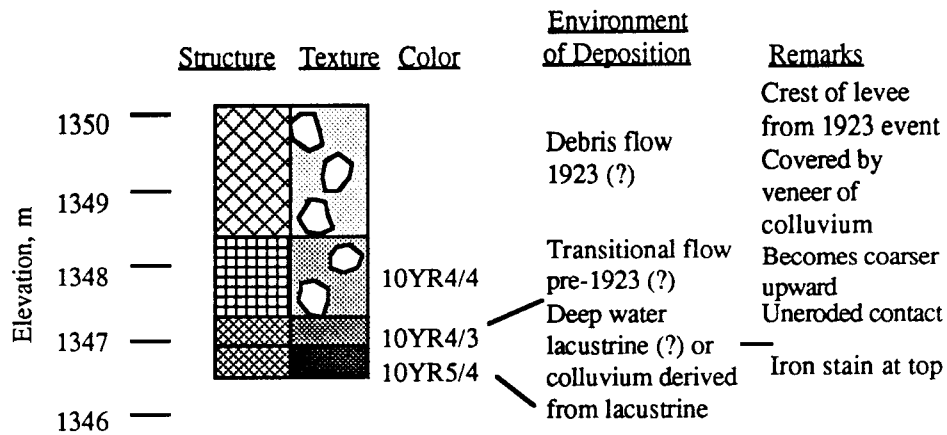


Figure B-2c. Stratigraphic sections for Locations 6 and 7 on the Ricks Creek Fan. See Figure B-2a for explanation of symbols.

Ricks Creek, Location 8. UTM: N 32148.2; E 26485.2



Ricks Creek, Location 9. UTM: N 32147.3; E 26503.6

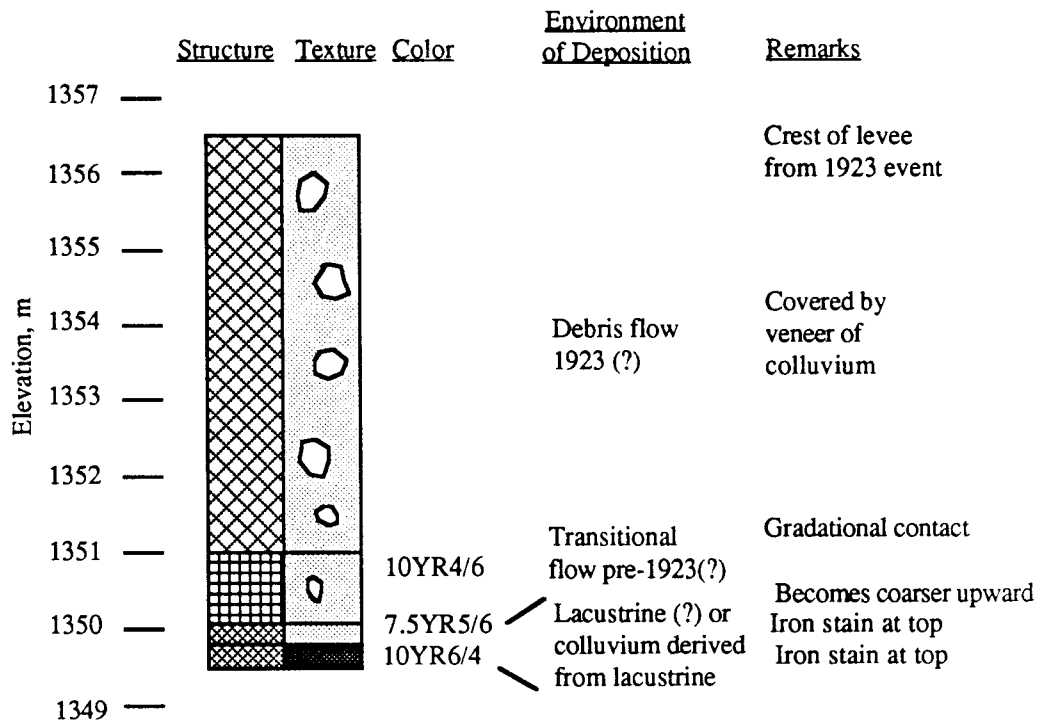
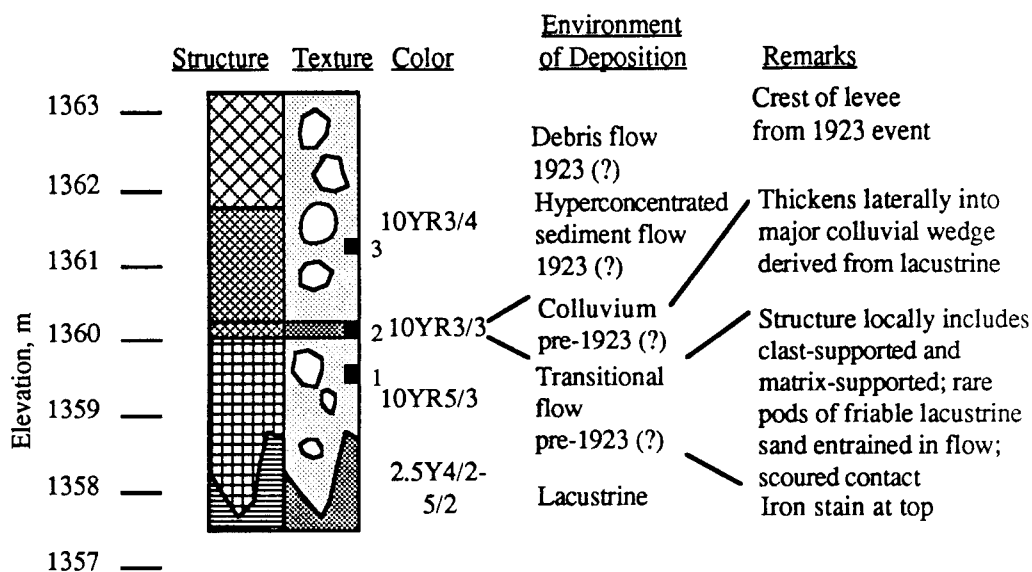


Figure B-2d. Stratigraphic sections for Locations 8 and 9 on the Ricks Creek Fan. See Figure B-2a for explanation of symbols.

Ricks Creek Location 10. UTM: N 32134.6, E. 26571.5.



Ricks Creek Location 11. UTM: N 32144.1, E. 26616.7.

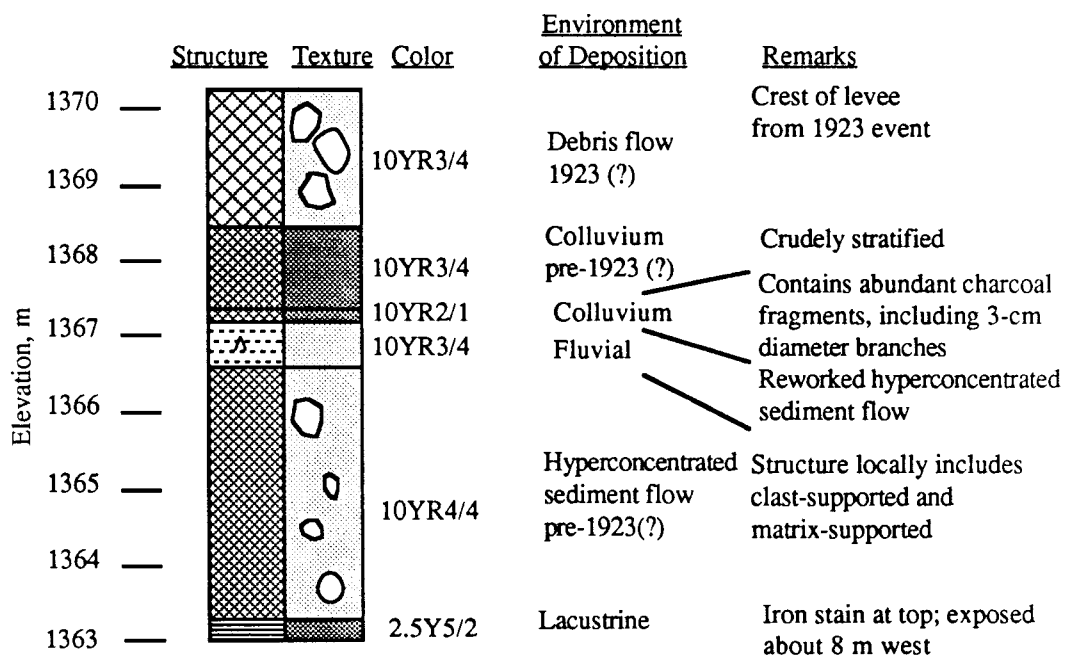
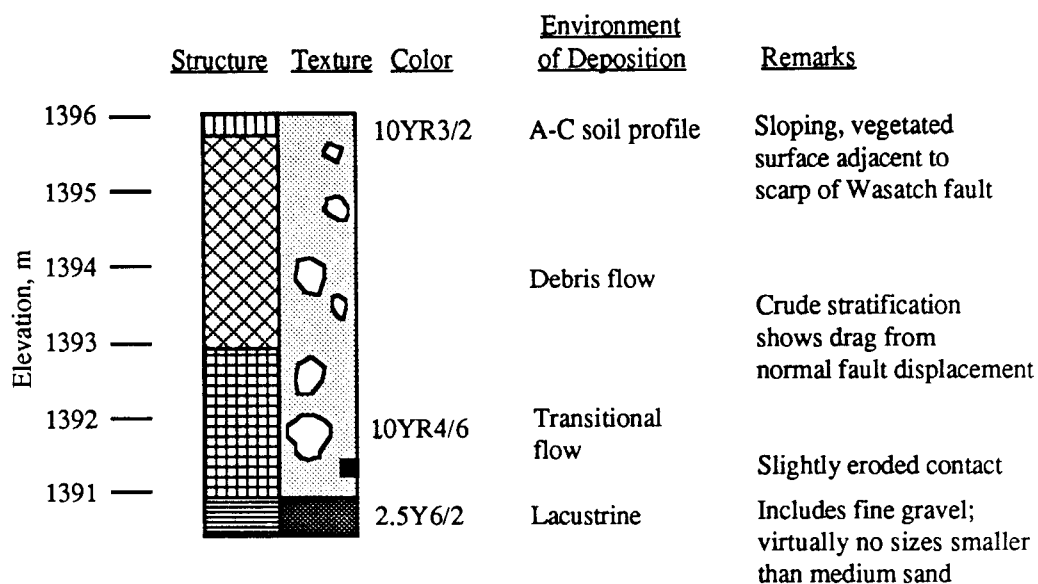


Figure B-2e. Stratigraphic sections for Locations 10 and 11 on the Ricks Creek Fan. See Figure B-2a for explanation of symbols.

Ricks Creek Location 14. UTM: N 32075.6, E. 26713.4.



Ricks Creek Location 15. UTM: N 31847.6, E. 26374.9. Retaining wall excavation at 103 Peach Tree Drive, Centerville.

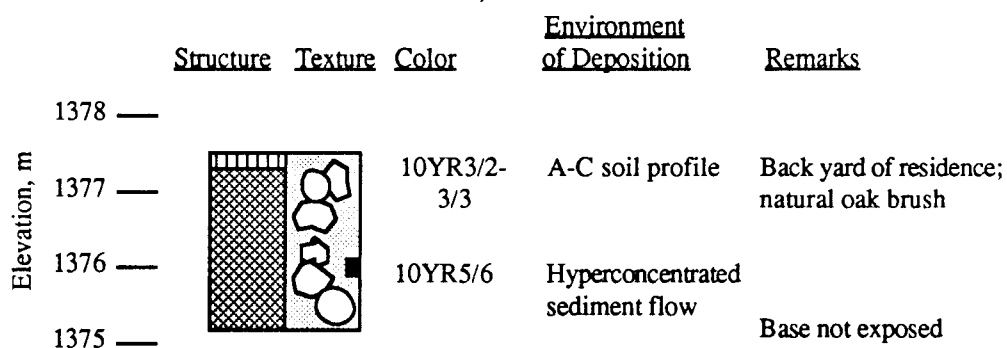


Figure B-2g. Stratigraphic sections for Locations 14 and 15 on the Ricks Creek Fan. See Figure B-2a for explanation of symbols.

Ricks Creek Location 12. UTM: N 32111.8, E. 26606.6.

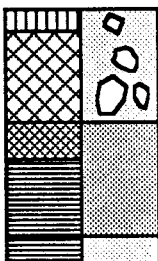

	<u>Structure</u>	<u>Texture</u>	<u>Color</u>	<u>Environment of Deposition</u>	<u>Remarks</u>
1377 —			2.5Y6/2	Lacustrine	Gilbert's (1890) white marl; correlates with candona-bearing deposit across Ricks Creek channel
1376 —			7.5YR5/4	Deep water lacustrine	
1375 —			2.5Y6/2	Lacustrine	
1374 —			10YR5/3	Subaqueous debris flow	
1373 —			2.5Y6/2	Lacustrine	

Ricks Creek Location 13. UTM: N 32081.7, E. 26685.2.

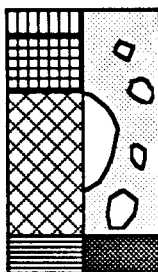

	<u>Structure</u>	<u>Texture</u>	<u>Color</u>	<u>Environment of Deposition</u>	<u>Remarks</u>
1389 —			10YR2/2-3/2	A-C soil profile	Plug filling Death Hollow channel
1388 —			10YR4/6	Debris flow	Minor fluvial-appearing lenses near top of unit
1387 —				Debris flow	
1386 —			10YR4/6	Transitional flow	
1385 —			2.5Y6/2	Lacustrine	

Figure B-2f. Stratigraphic sections for Locations 12 and 13 on the Ricks Creek Fan. See Figure B-2a for explanation of symbols.

Ricks Creek Test Pit 1. UTM: N 31875.7, E. 26286.6.

	<u>Structure</u>	<u>Texture</u>	<u>Color</u>	<u>Environment of Deposition</u>	<u>Remarks</u>		
1329 —			10YR2/2- 3/2	A-C soil profile	Gently sloping, grassy surface		
1328 —			10YR3/6- 3/4	Debris flow	Non-eroded contact		
1327 —			7.5YR3/4	Lacustrine			
1326 —			10YR4/6	Lacustrine			
				Lacustrine	Manganese layer		

Ricks Creek Test Pit 2. UTM: N 31893.3, E. 26406.9.

	<u>Structure</u>	<u>Texture</u>	<u>Color</u>	<u>Environment of Deposition</u>	<u>Remarks</u>
1345 —			10YR2/2- 3/2	A-C soil profile	Gently sloping, grassy surface
1344 —			7.5YR5/4- 4/4	Transitional flow	
1343 —			10YR5/4	Debris flow	Non-eroded contact
1342 —					
1341 —			10YR4/6	Lacustrine	Iron stain at top

Ricks Creek Test Pit 3. UTM: N 31955.5, E. 26615.4.

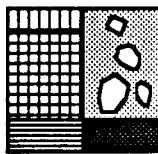

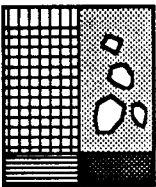

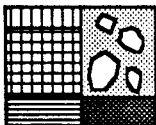

	<u>Structure</u>	<u>Texture</u>	<u>Color</u>	<u>Environment of Deposition</u>	<u>Remarks</u>
1373 —			7.5YR3/2	A-C soil profile	Gently sloping, grassy surface
1372 —			7.5YR4/6	Transitional flow	
1371 —			10YR5/6		Slightly eroded contact
1370 —			2.5YR5/6	Lacustrine	

Figure B-2h. Stratigraphic sections for Test Pits 1, 2, and 3 on the Ricks Creek Fan. See Figure B-2a for explanation of symbols.

Ricks Creek Test Pit 4. UTM: N 31972.9, E. 26381.0.

	<u>Structure</u>	<u>Texture</u>	<u>Color</u>	<u>Environment of Deposition</u>	<u>Remarks</u>
1345 —			10YR2/2-3/2	A-C soil profile	Gently sloping, grassy surface
1344 —			10YR3/4-4/4	Transitional flow	
1343 —			10YR4/6-5/6	Lacustrine	Slightly eroded contact
1342 —			2.5YR5/6		

Ricks Creek Test Pit 5. UTM: N 32043.9, E. 26425.2.

	<u>Structure</u>	<u>Texture</u>	<u>Color</u>	<u>Environment of Deposition</u>	<u>Remarks</u>
1350 —			10YR2/2-3/2	A-C soil profile	Gently sloping, grassy surface
1349 —			10YR3/6-4/6	Transitional flow	
1348 —			10YR3/4-4/4	Lacustrine	Slightly eroded contact
			2.5YR5/6		

Ricks Creek Test Pit 6. UTM: N 32082.9, E. 26602.0.

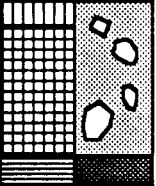

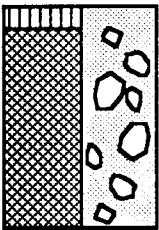
	<u>Structure</u>	<u>Texture</u>	<u>Color</u>	<u>Environment of Deposition</u>	<u>Remarks</u>
1376 —			10YR2/2-3/2	A-C soil profile	Gently sloping, grassy surface
1375 —			10YR3/6-4/6	Transitional flow	
1374 —			10YR4/4-4/6	Lacustrine	Locally matrix- supported Slightly eroded contact
1373 —			2.5YR5/6		

Figure B-2i. Stratigraphic sections for Test Pits 4, 5, and 6 on the Ricks Creek Fan. See Figure B-2a for explanation of symbols.

Ricks Creek Test Pit 7. UTM: N 31994.5, E. 26537.7.

	<u>Structure</u>	<u>Texture</u>	<u>Color</u>	<u>Environment of Deposition</u>	<u>Remarks</u>
1364 —					
1363 —				A-C soil profile	Gently sloping, grassy surface
1362 —					
1361 —				Diamicton; pockets of fluvial with abundant boulders	Severe caving of test pit walls
1360 —					Base not exposed

Ricks Creek Test Pit 8. UTM: N 32061.0, E. 26691.3.

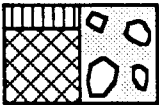
	<u>Structure</u>	<u>Texture</u>	<u>Color</u>	<u>Environment of Deposition</u>	<u>Remarks</u>
1382 —					
1381 —			10YR2/2- 3/2	A-C soil profile	Plug in Death Hollow channel
1380 —			10YR3/4- 4/4	Debris flow	Base not exposed

Figure B-2j. Stratigraphic sections for Test Pits 7 and 8 on the Ricks Creek Fan. See Figure B-2a for explanation of symbols.

APPENDIX C

SUMMARY OF EXPERIMENTAL DATA

Measured Parameters

Experiments performed in the laboratory consist of sieve analyses, hydrometer analyses, Atterberg Limits analyses, specific gravity determinations, and sediment-water slurry unit weight determinations.

Sieve Analyses

Samples collected in the field were subjected to sieve analyses using a stack of sieves as described in Table C-1. Sedimentologic parameters in this research are described in terms of phi (ϕ) units. The relationship between ϕ units and size in mm is shown in Figure C-1. Non-standard dry sieve procedures were used to develop grain size distributions because of the coarse nature of the sediments. Most samples required mechanical disaggregation of small clods; this was achieved by grinding the clods in a mortar with a pestal until only individual grains could be observed on the sieves. The samples were representative of that part of the deposit < 50 mm in nominal diameter. The deposits contained clasts > 50 mm which were incorporated into the grain size distribution using a modification of the procedure described by Williams and Guy (1973). The nominal areas of clasts > 50 mm were measured in a representative area of a stratigraphic unit. The ratio of the clast area to the representative area for clasts of different nominal size provided a means for estimating size distribution of the clasts > 50 mm. Frequency distributions of the sieve data and the field data were combined on the basis of a two-dimensional representation of the concept of Kellerhals and Bray (1971) that the area percentage of surface grains is proportional to the weight percentage of grains in a randomly distributed three-dimensional sample if all grains have the same specific gravity.

A map showing the locations of samples collected at the Rudd Creek fan is presented on Figure 7. Grain size distributions for samples collected at Rudd Creek are presented on Figures C-2a to C-2o. A map showing the locations of samples collected at the Ricks Creek fan is presented on Figure 8. Grain size distributions for samples collected at Ricks Creek are presented on Figures C-3a to C-3f. A map showing the locations of samples collected at the Lightning Canyon fan is presented on Figure 6. Grain size distributions for samples collected at Lightning Canyon are presented on Figures C-4a to C-4b.

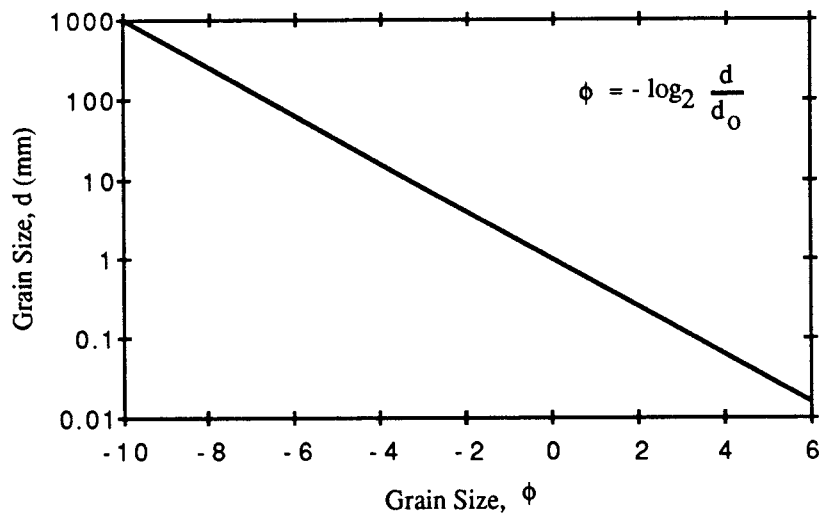
The results of sieve analyses were used to compute parameters for subsequent use in statistical analyses; these parameters are described below. In addition to these computed parameters, values of the fractions of the deposits smaller than the #200 sieve (fines) and the #40 sieve (matrix) were used and are listed in Tables C-2a to C-2c.

Hydrometer Analyses

Hydrometer analyses were performed on samples having 5 percent or more sediment passing the # 200 sieve (< 0.075 mm) using the procedure described by Lambe (1951, p. 29ff) and American Society for Testing and Materials (ASTM) Test D1140. Only the three samples from Lightning Canyon were found to have 5 percent or more

Table C-1. Summary of sieve opening sizes.

Standard U.S. Sieve Number	Sieve Opening Size	
	(mm)	(ϕ)
3 "	75	-6.229
2-1/2 "	63	-5.977
2 "	50	-5.644
1-1/2 "	37.5	-5.229
3/4 "	19	-4.248
1/2 "	12.5	-3.644
3/8 "	9.5	-3.248
#4	4.75	-2.248
#10	2.00	-1.000
#20	0.850	0.234
#40	0.425	1.234
#60	0.250	2.000
#120	0.125	3.000
#200	0.075	3.737



Wentworth Nomenclature					
-8	-6	-2	-1	4 ϕ	
b	c	p	g	s	m
b	c	g	s		m+c
300	75	4.75	0.075 mm		
American Society for Testing and Materials Nomenclature					

Figure C-1. Relationship between grain size in ϕ units and in mm. $d_0 = 1$ mm to make the ϕ value dimensionless. Wentworth grain size nomenclature: b, boulders; c, cobbles; p, pebbles; g, granules; s, sand; m, silt; (clay sizes begin at $\phi = 9$) (Folk, 1980, p. 23). American Society for Testing and Materials (ASTM) grain size nomenclature: b, boulders; c, cobbles; g, gravel; s, sand; m+c, silt and clay (ASTM, 1983, p. 396).

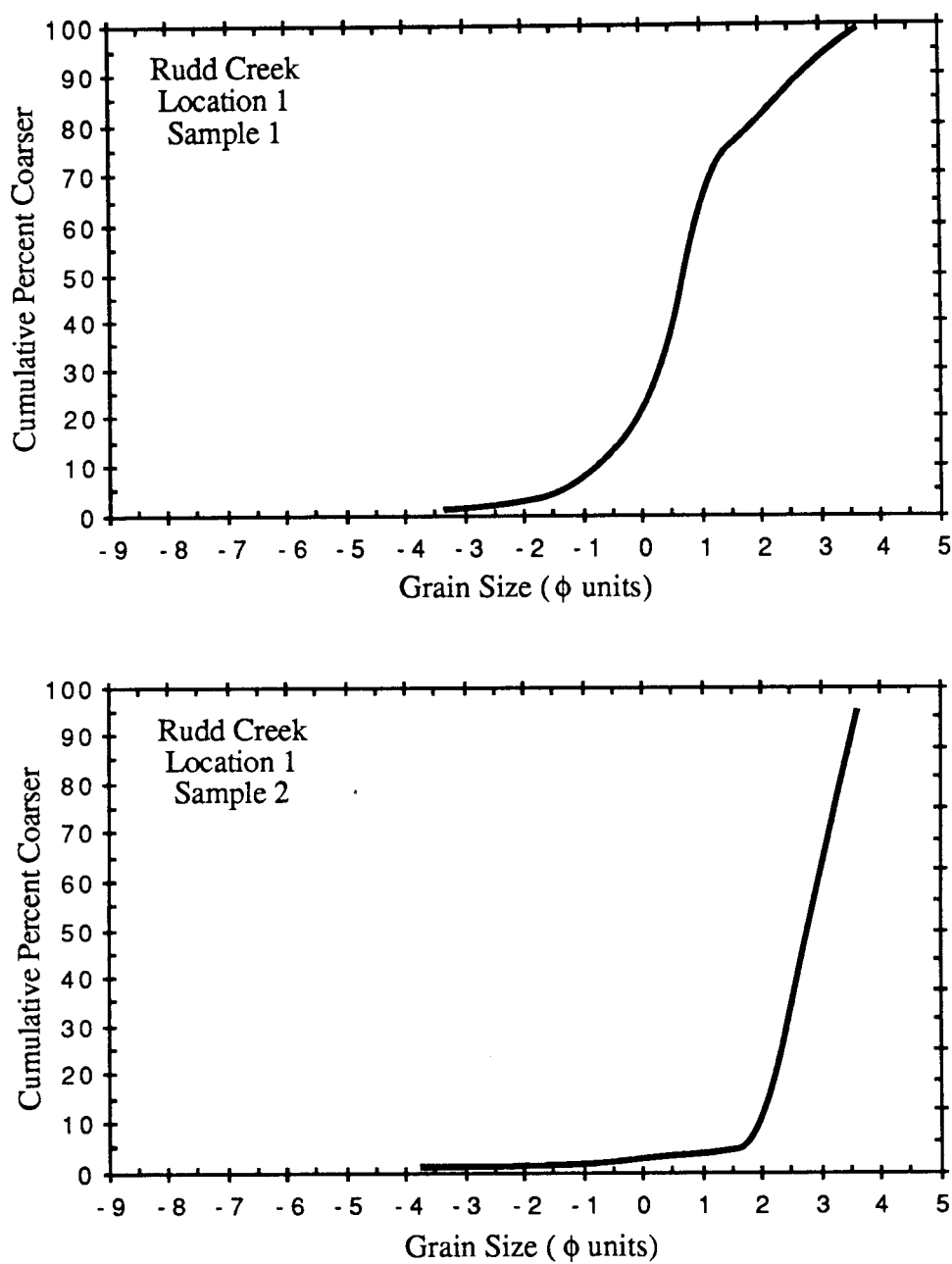


Figure C-2a. Grain size distributions for samples 1-1 and 1-2 from the Rudd Creek fan.

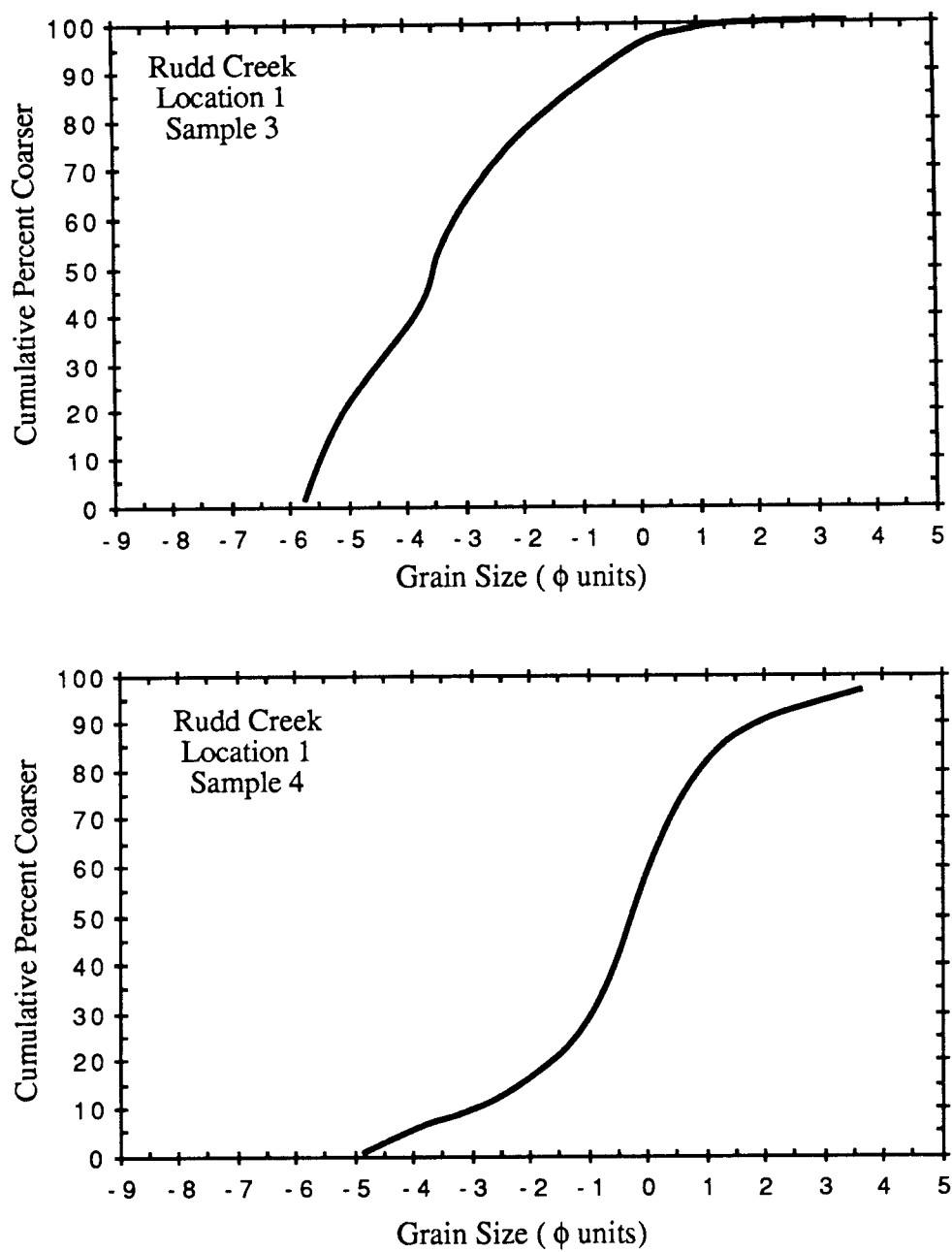


Figure C-2b. Grain size distributions for samples 1-3 and 1-4 from the Rudd Creek fan.

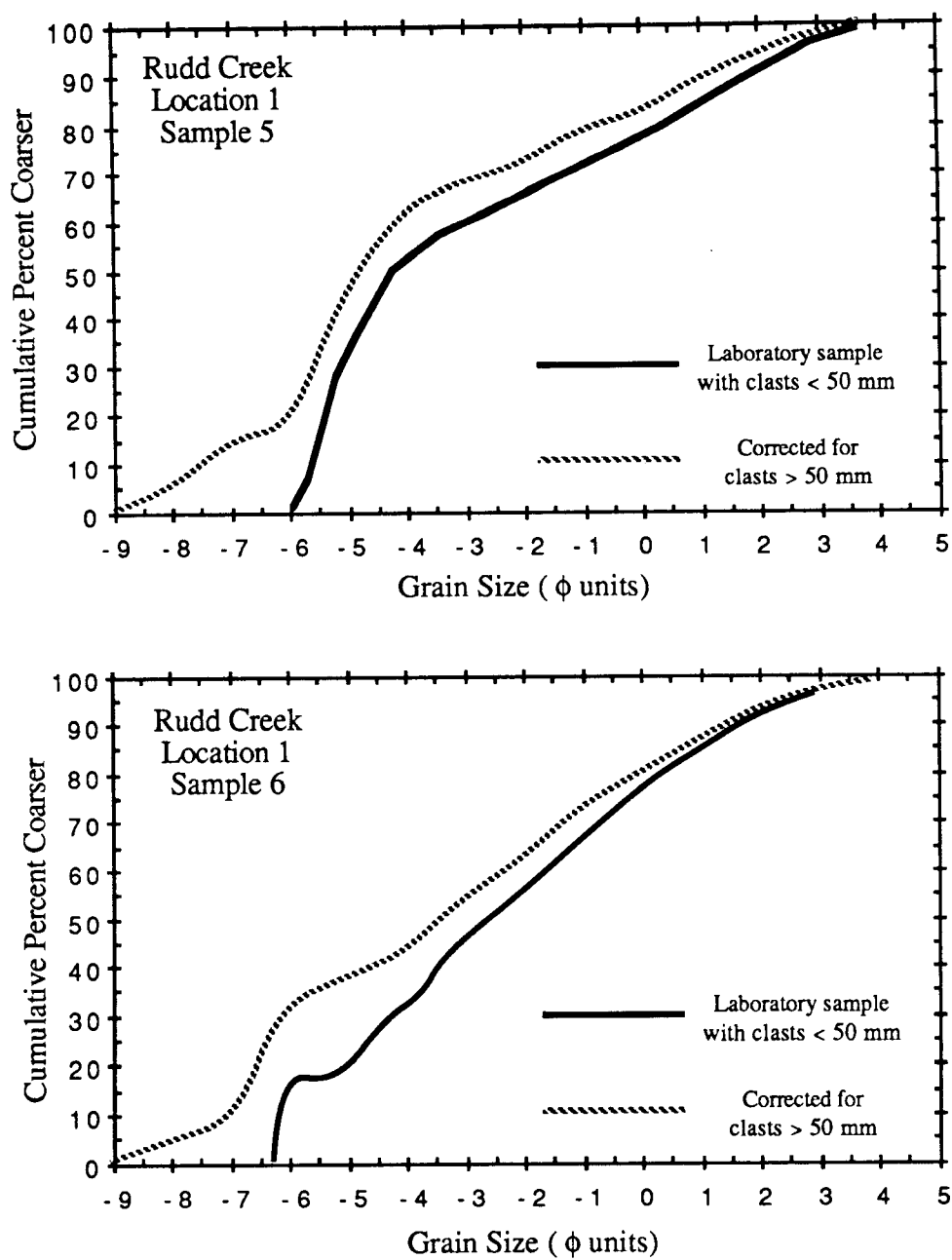


Figure C-2c. Grain size distributions for samples 1-5 and 1-6 from the Rudd Creek fan.

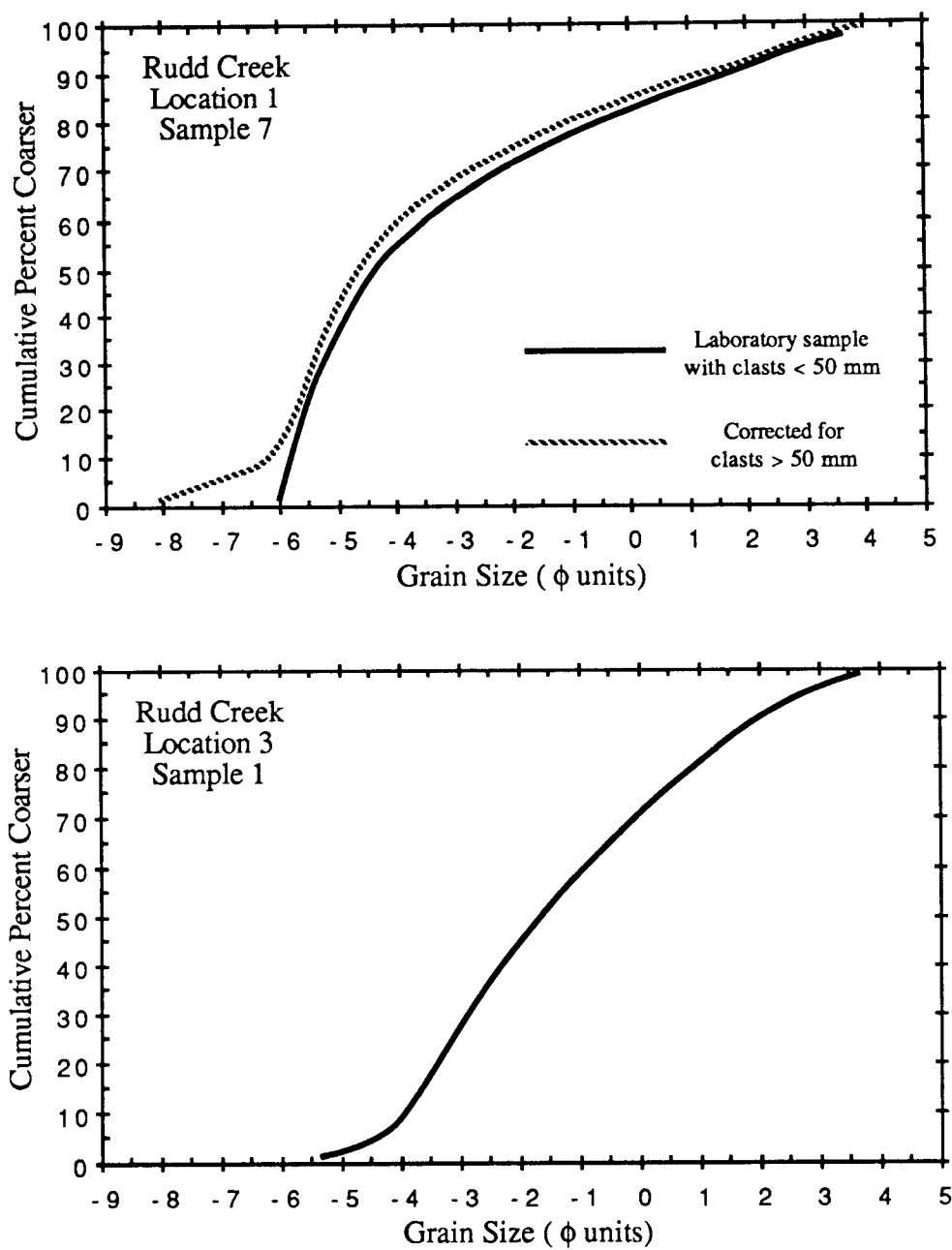


Figure C-2d. Grain size distributions for samples 1-7 and 3-1 from the Rudd Creek fan.

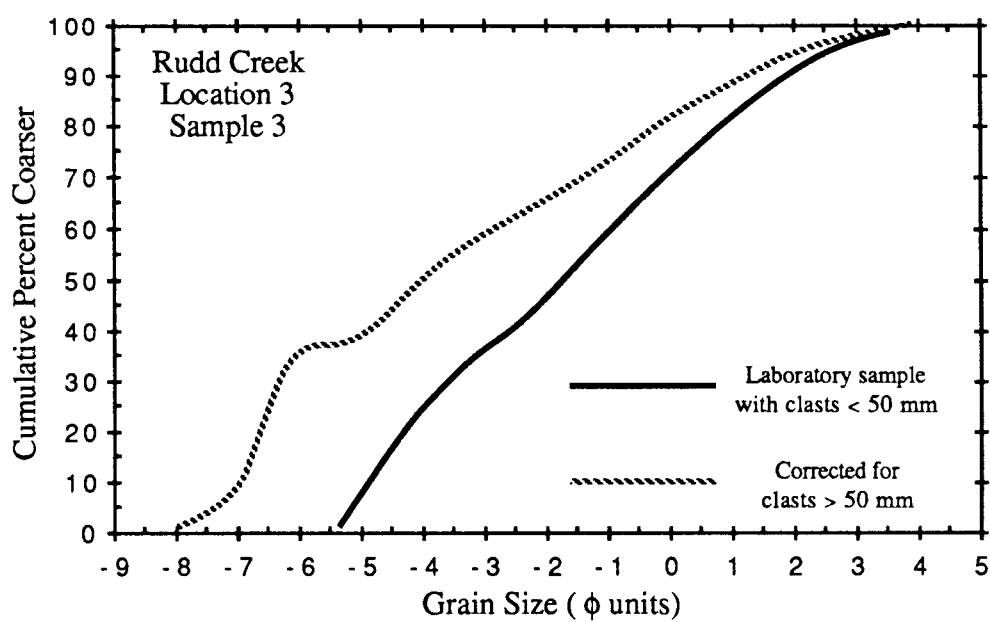
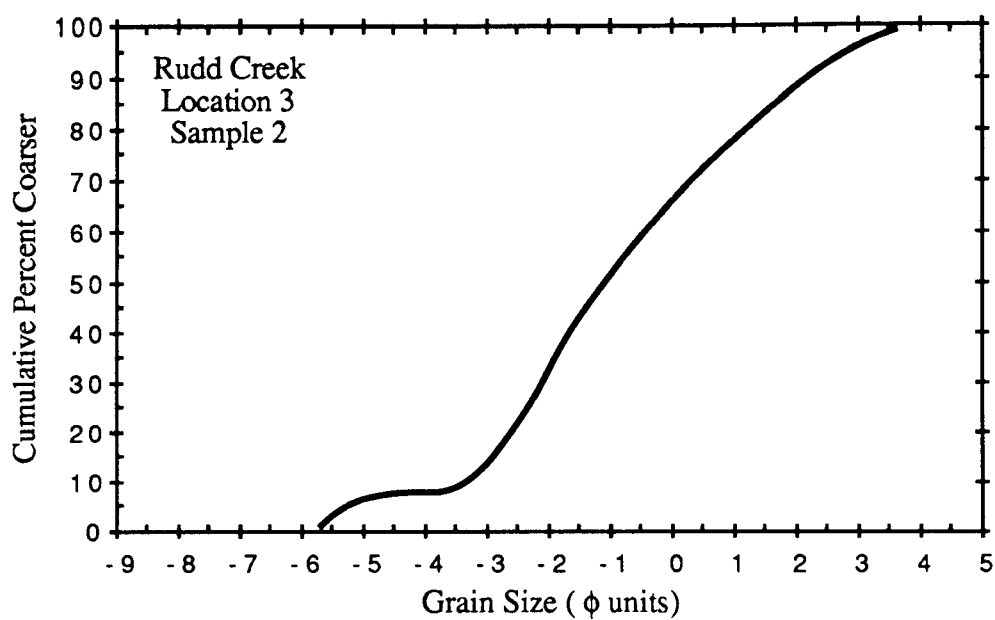


Figure C-2e. Grain size distributions for samples 3-2 and 3-3 from the Rudd Creek fan.

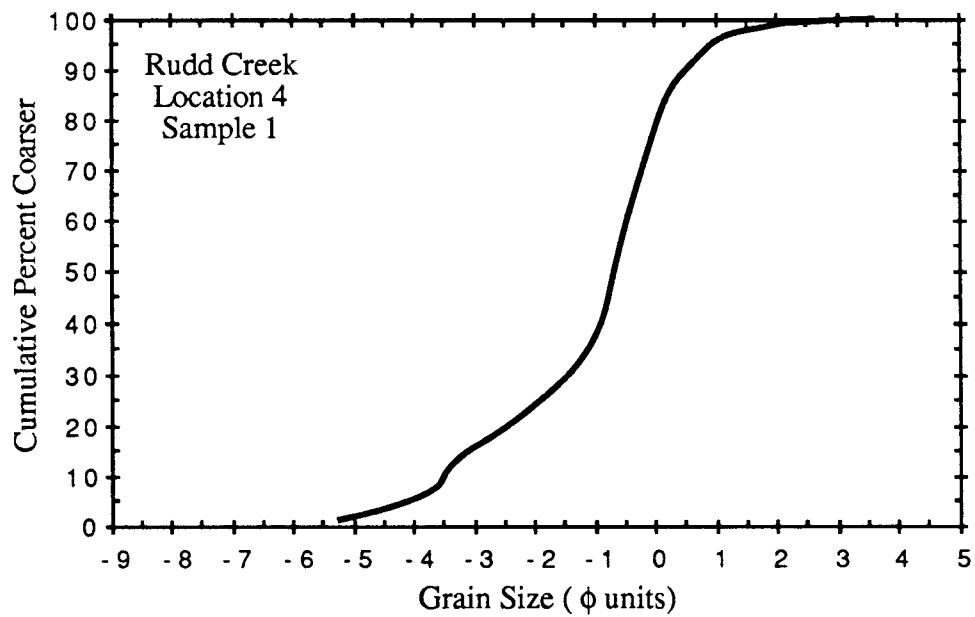
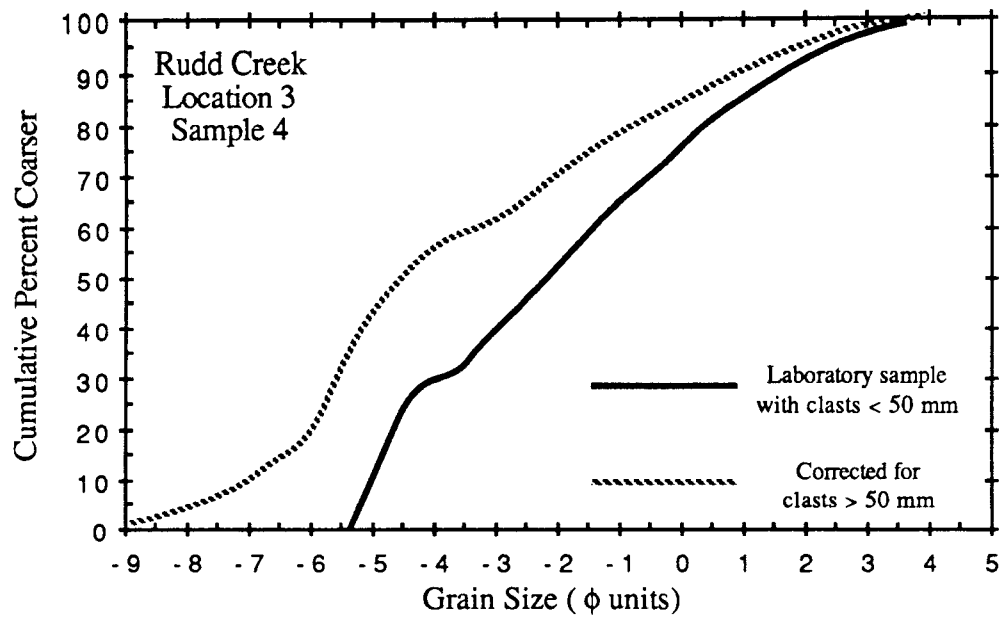


Figure C-2f. Grain size distributions for samples 3-4 and 4-1 from the Rudd Creek fan.

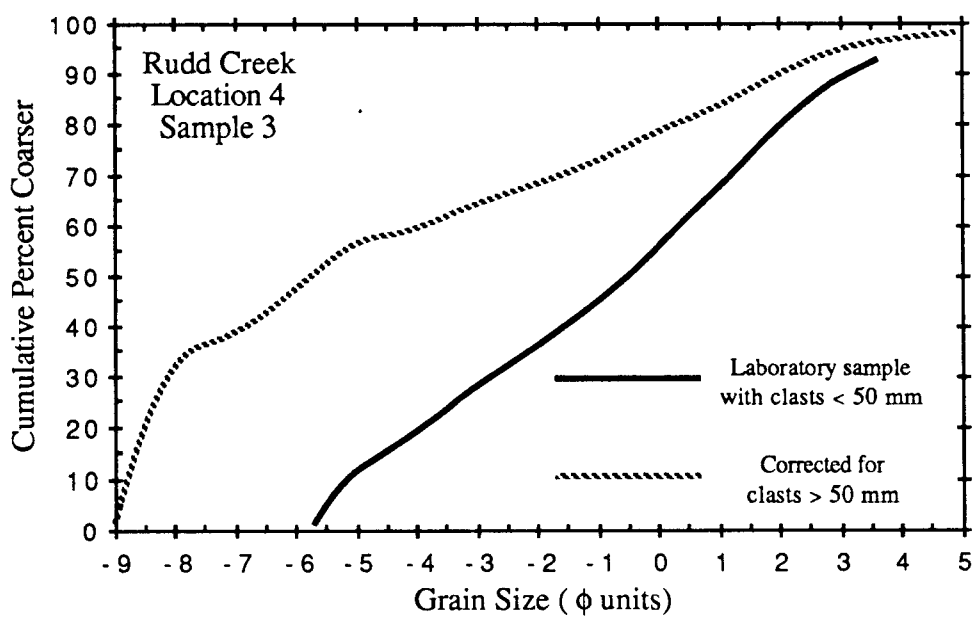
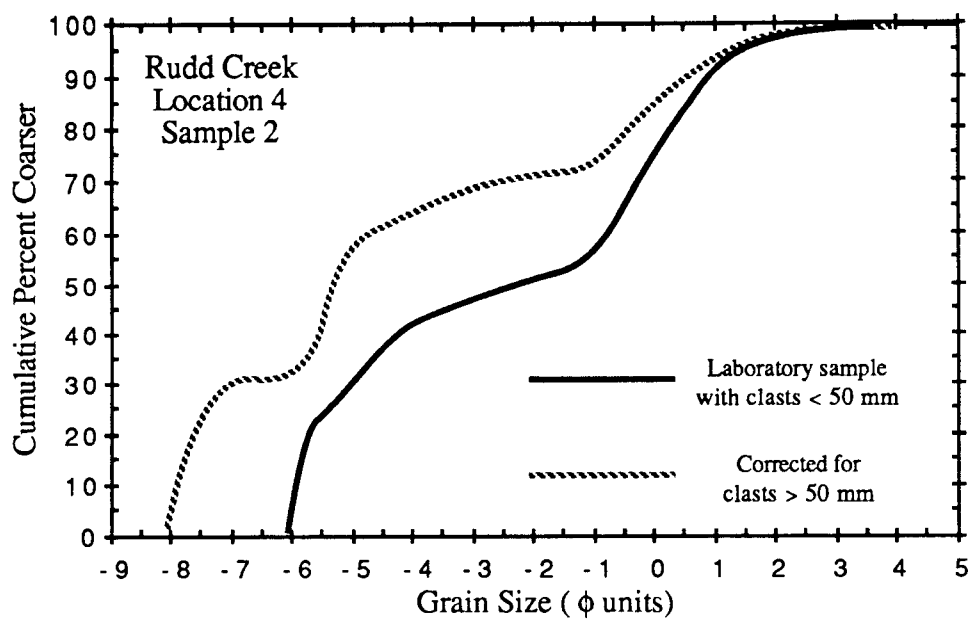


Figure C-2g. Grain size distributions for samples 4-2 and 4-3 from the Rudd Creek fan.

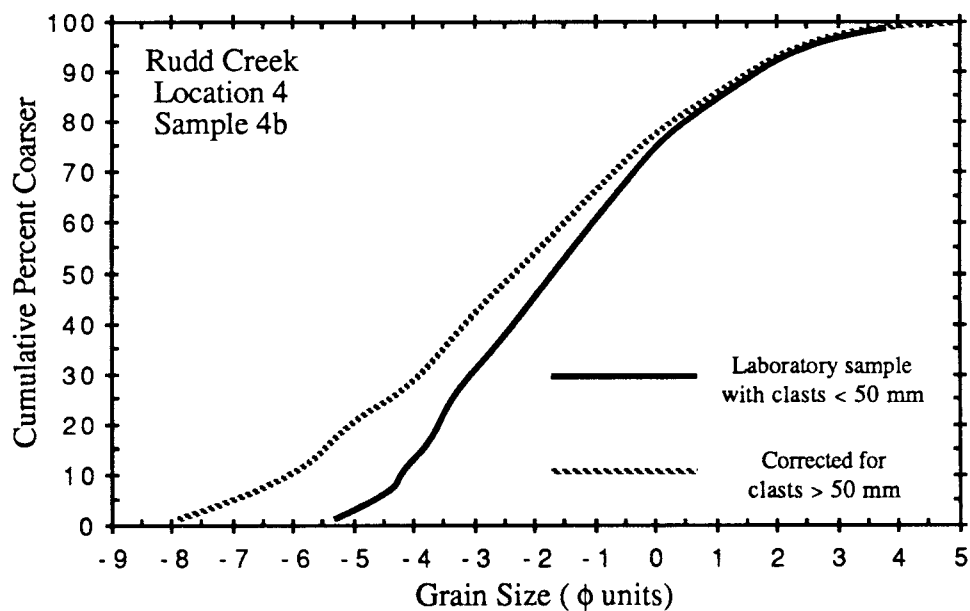
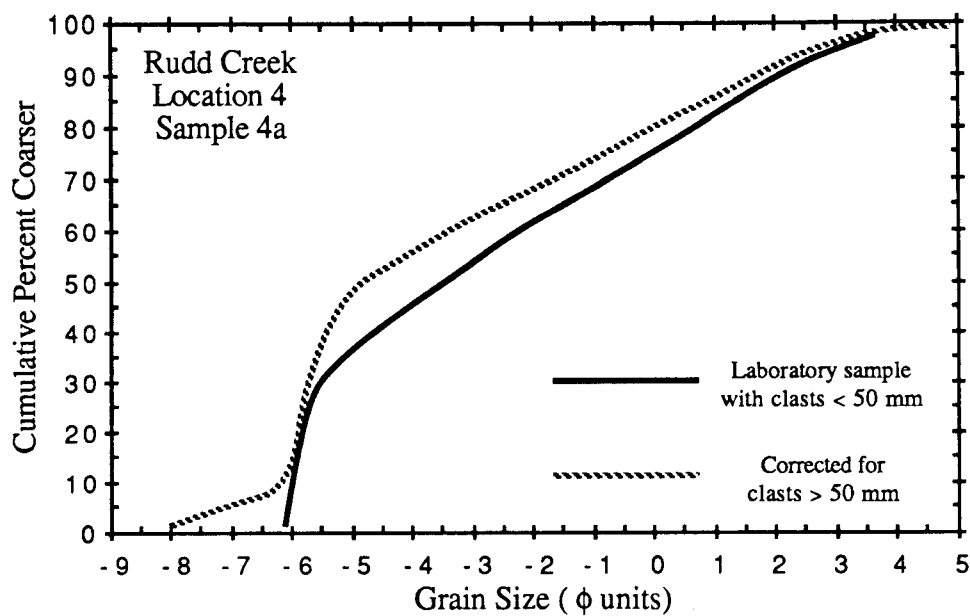


Figure C-2h. Grain size distributions for samples 4-4a and 4-4b from the Rudd Creek fan.

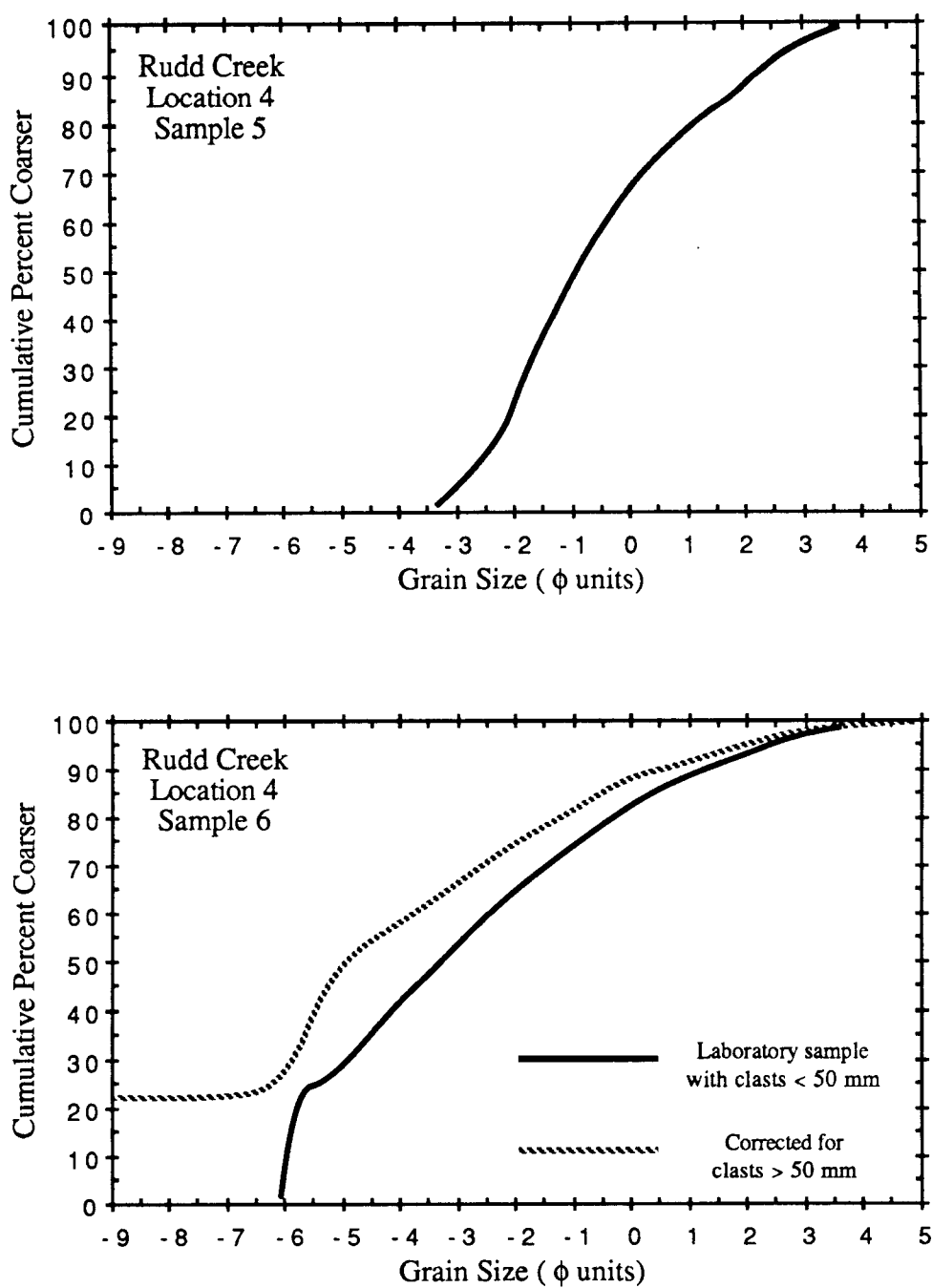


Figure C-2i. Grain size distributions for samples 4-5 and 4-6 from the Rudd Creek fan.

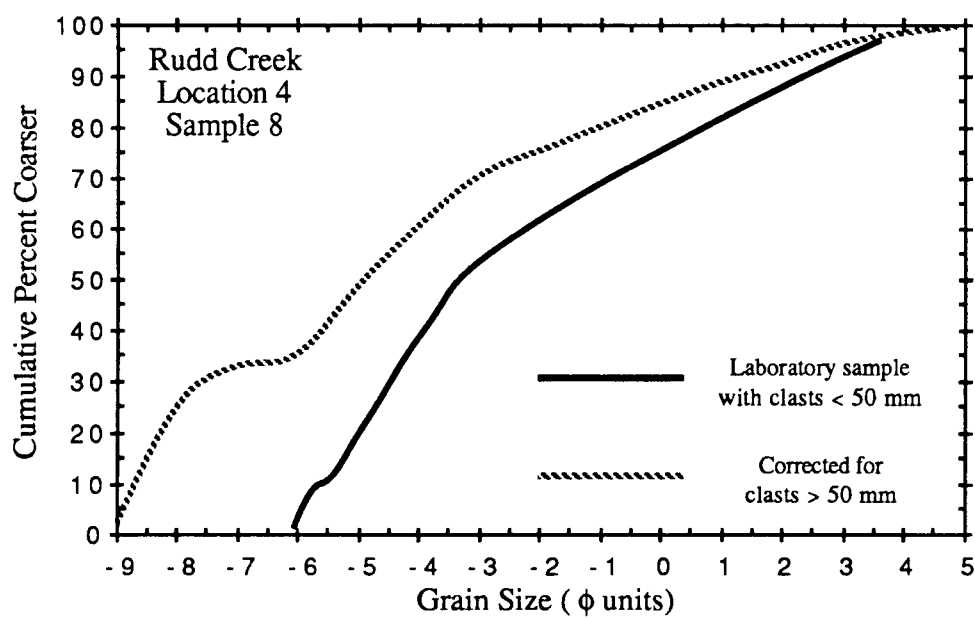
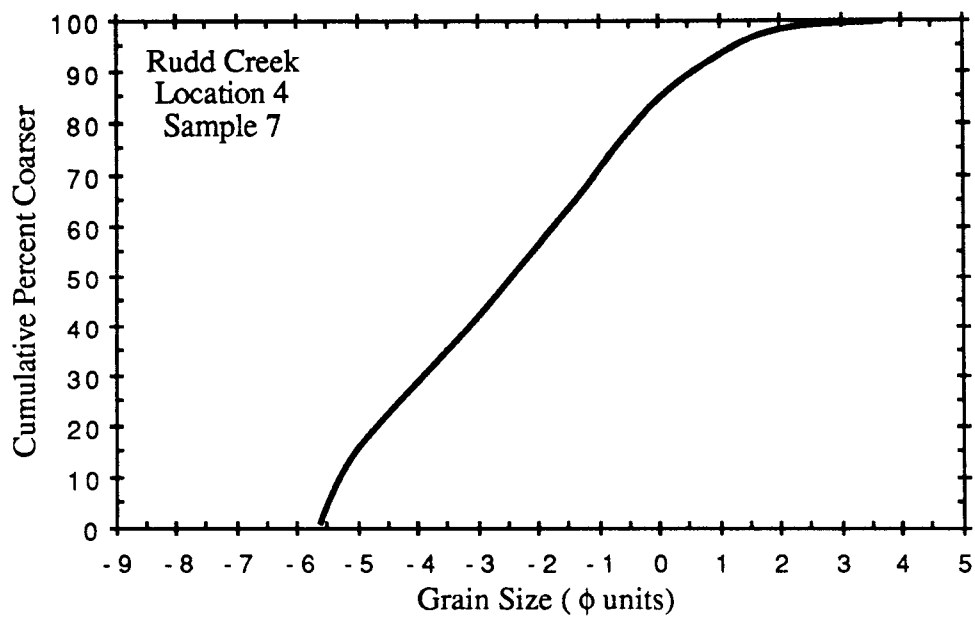


Figure C-2j. Grain size distributions for samples 4-7 and 4-8 from the Rudd Creek fan.

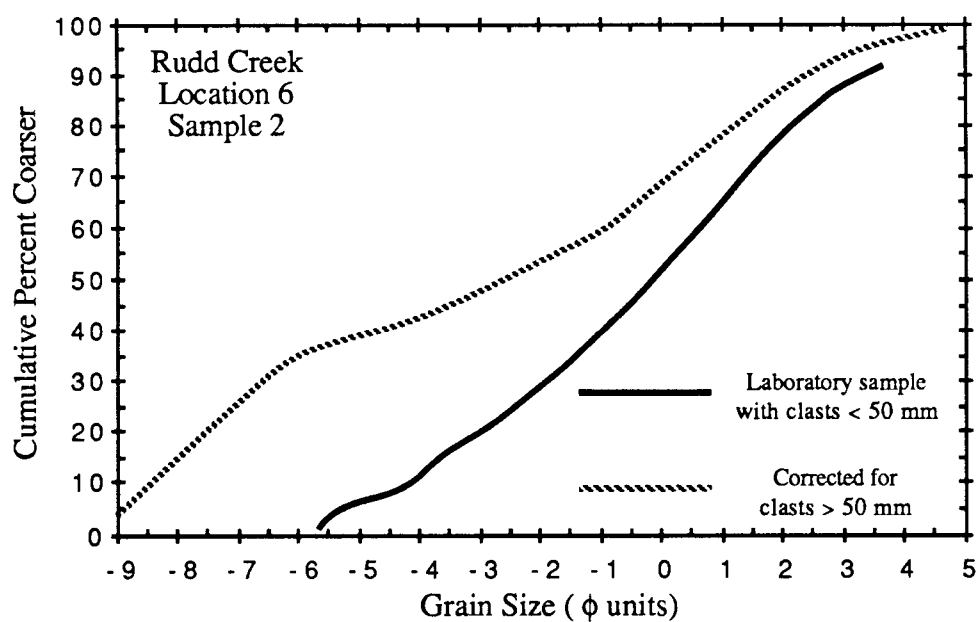
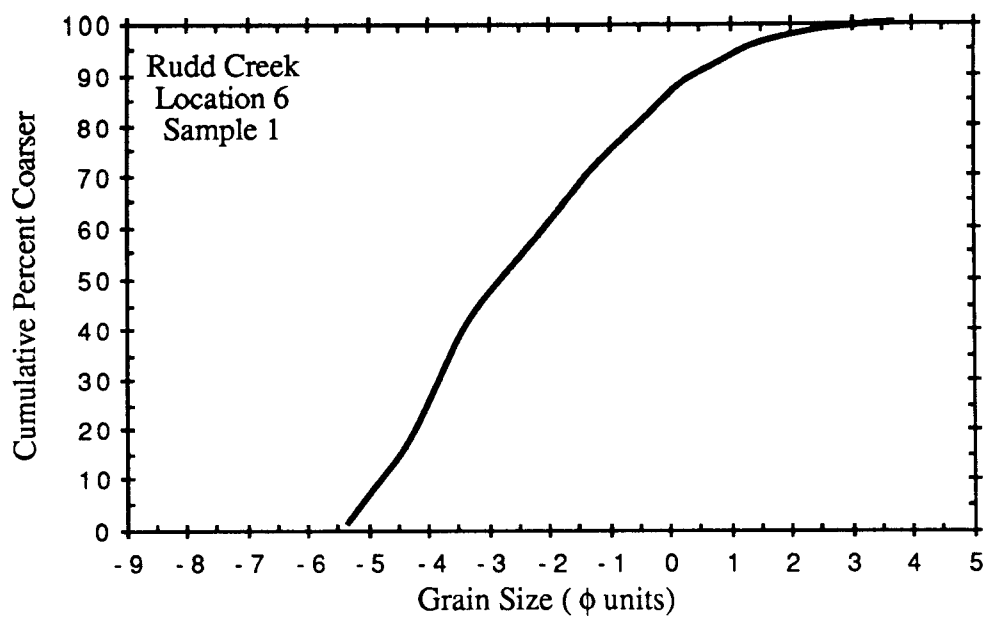


Figure C-2k. Grain size distributions for samples 6-1 and 6-2 from the Rudd Creek fan.

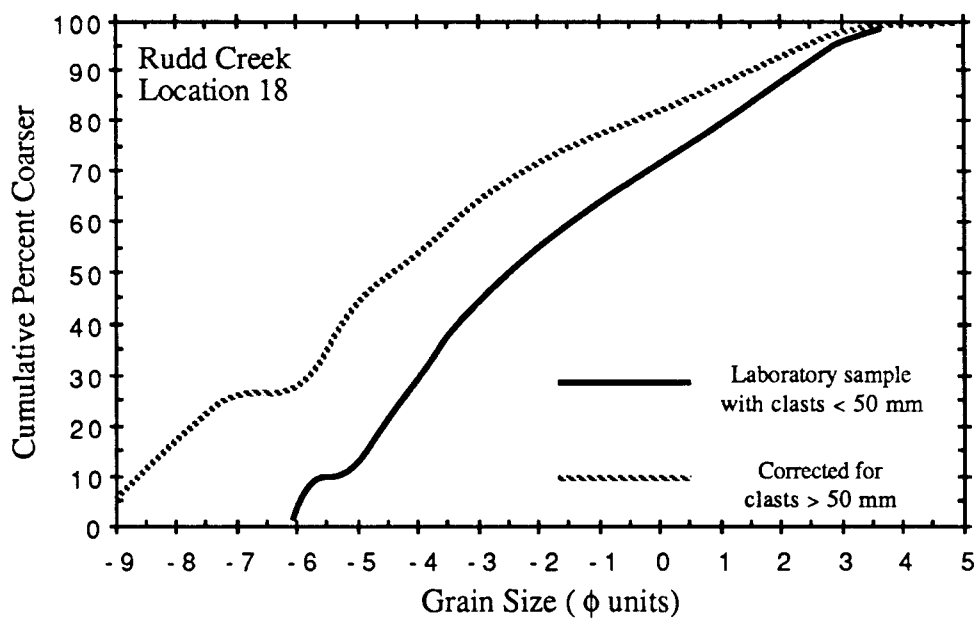
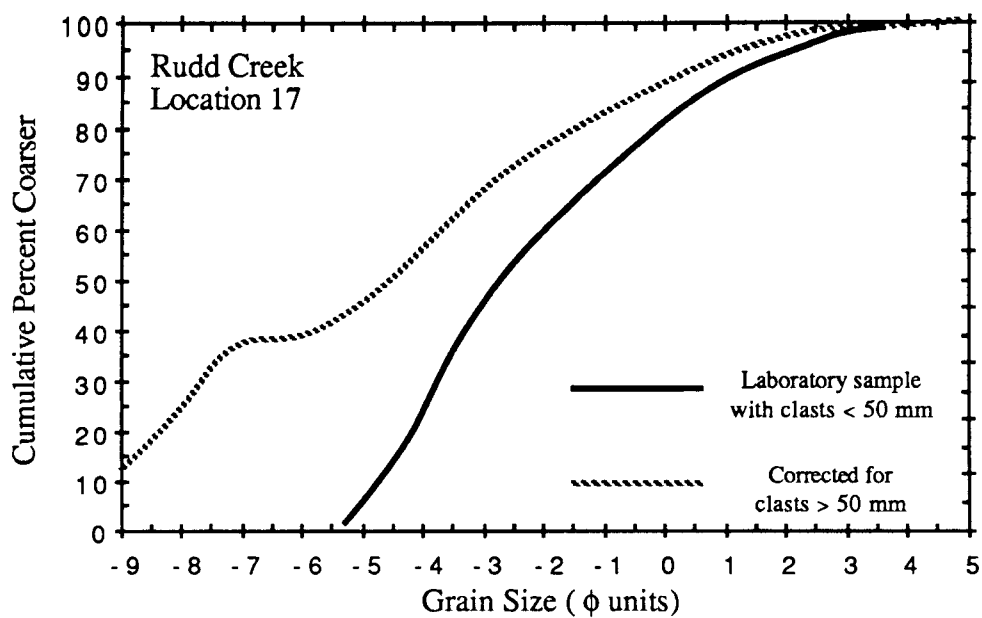


Figure C-21. Grain size distributions for samples 17 and 18 from the Rudd Creek fan.

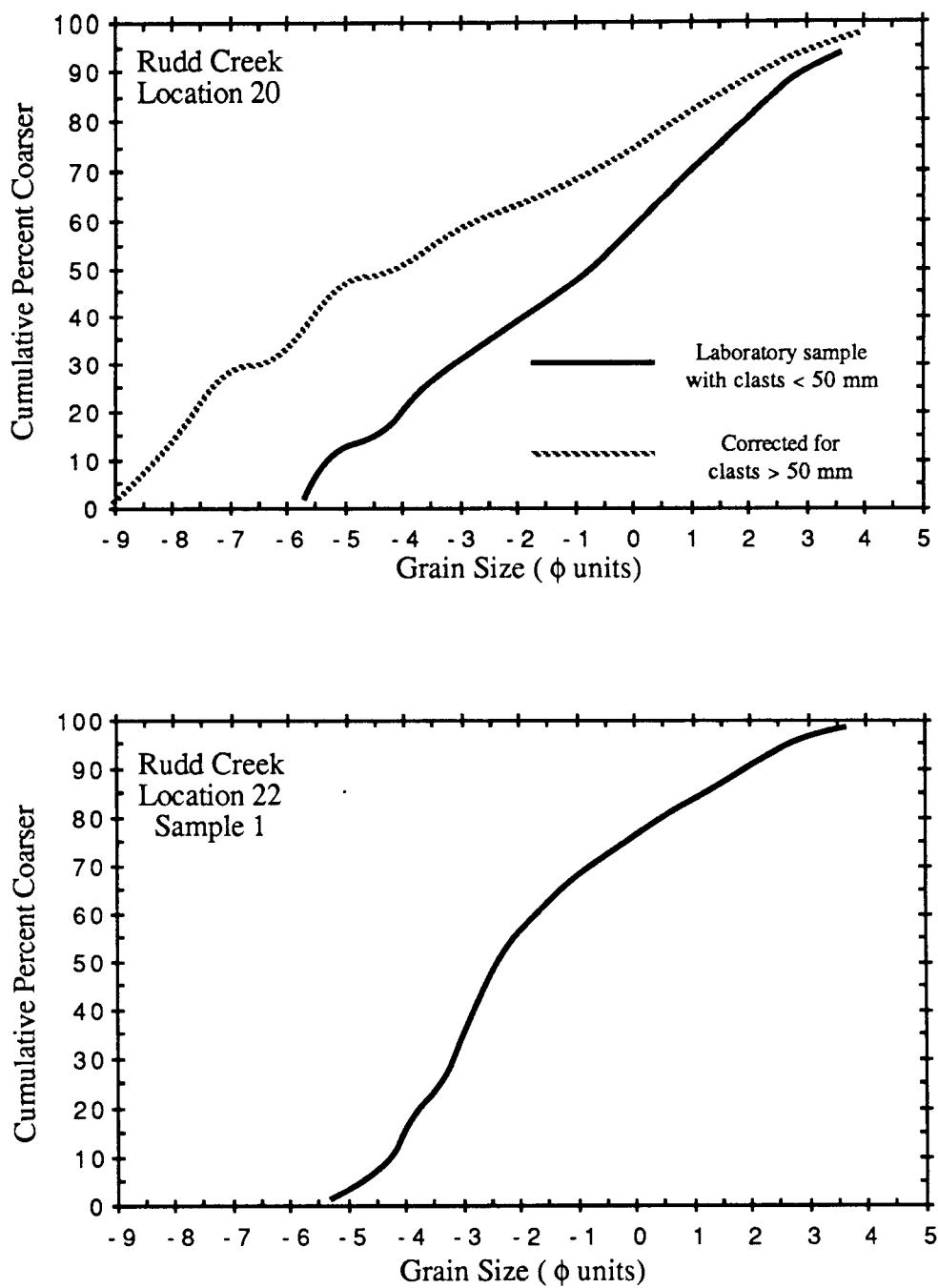


Figure C-2m. Grain size distributions for samples 20 and 22-1 from the Rudd Creek fan.

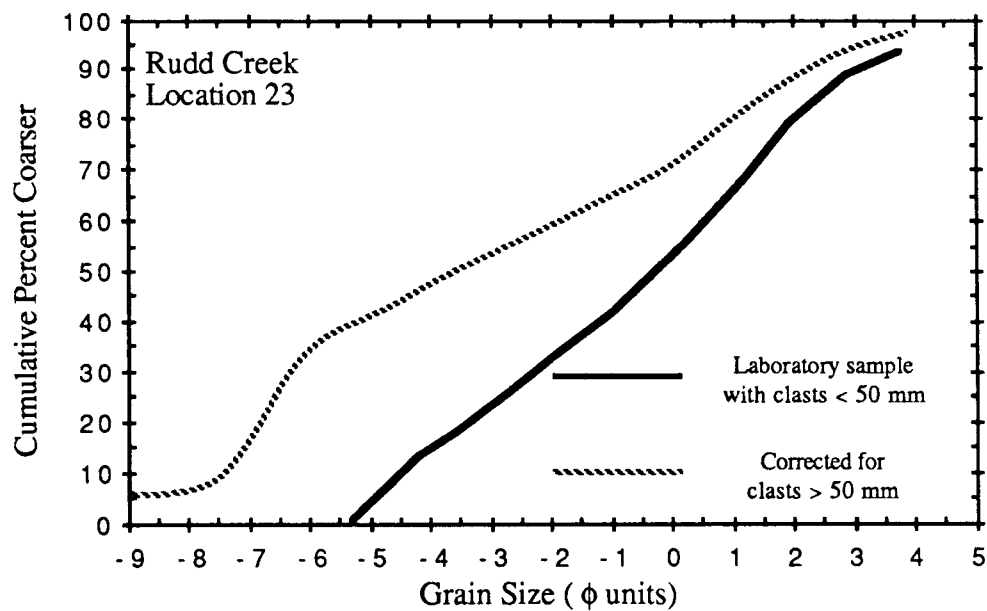
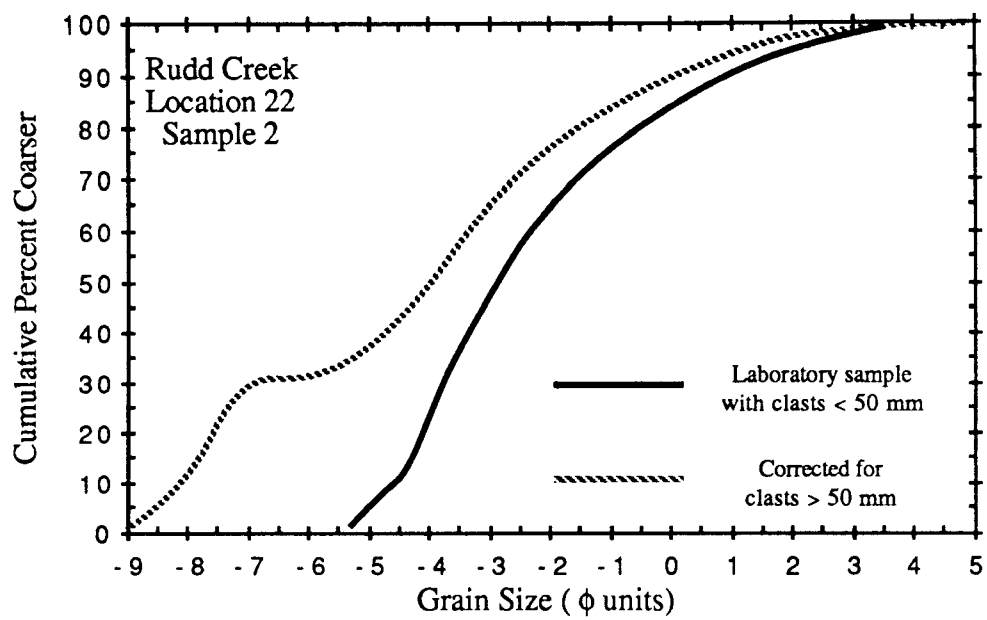


Figure C-2n. Grain size distributions for samples 22-2 and 23 from the Rudd Creek fan.

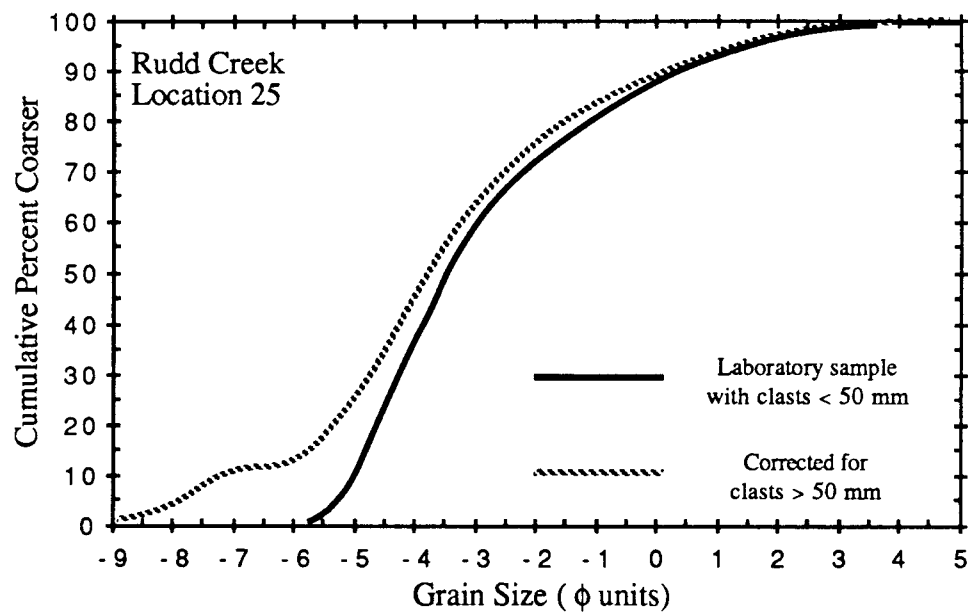


Figure C-2o. Grain size distribution for sample 25 from the Rudd Creek fan.

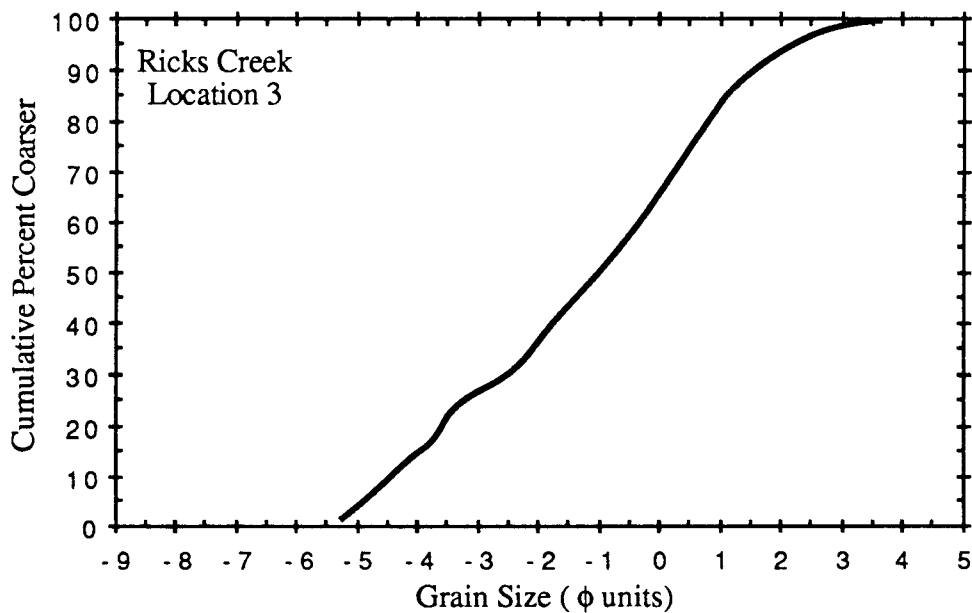
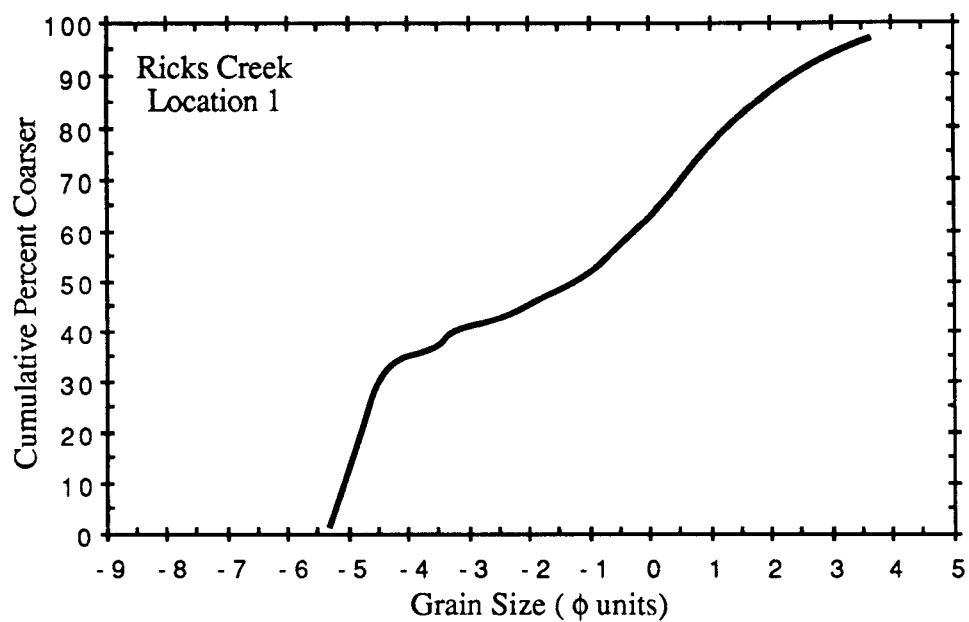


Figure C-3a. Grain size distributions for samples 1 and 3 from the Ricks Creek fan.

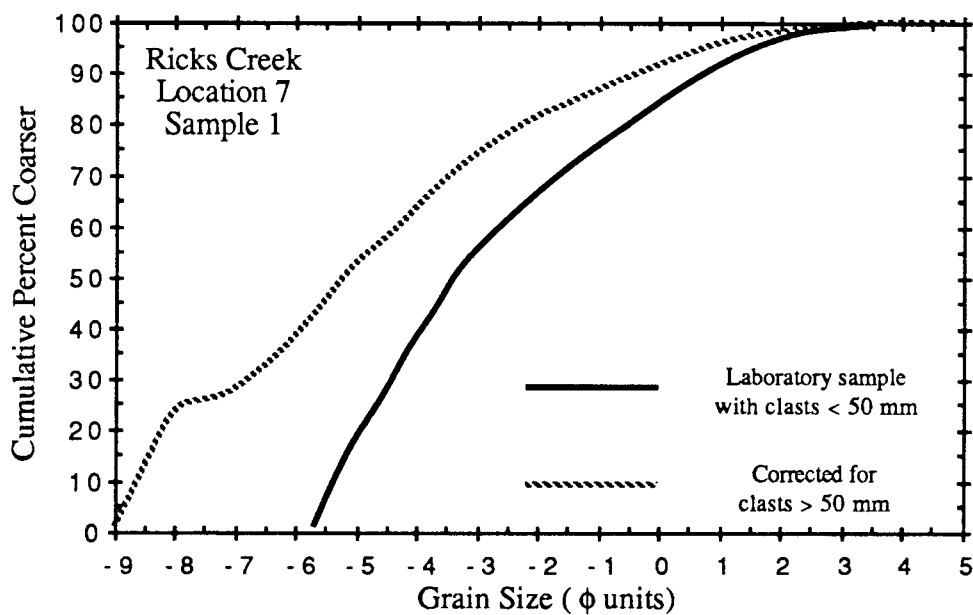
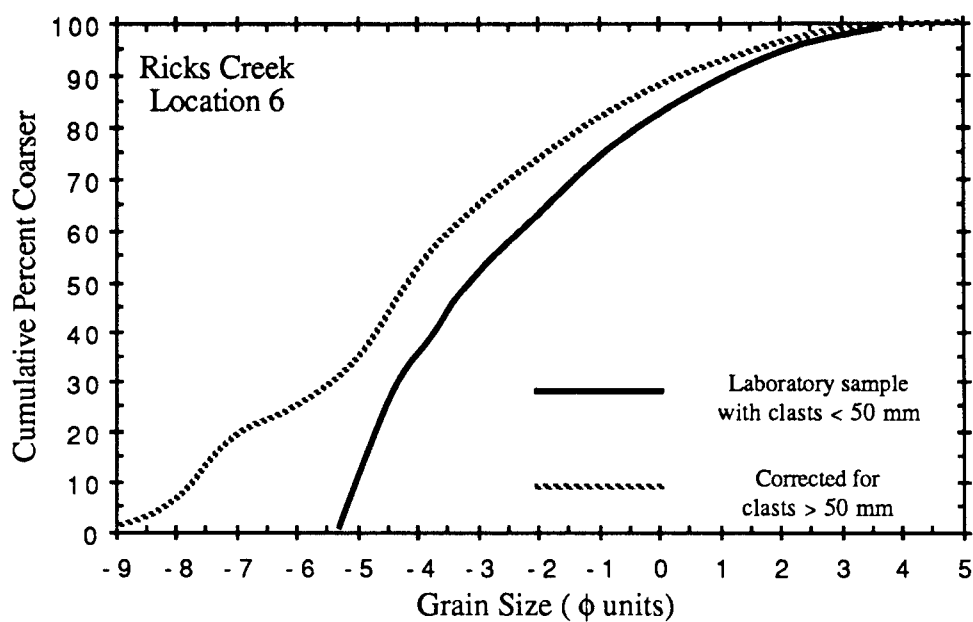


Figure C-3b. Grain size distributions for samples 6 and 7-1 from the Ricks Creek fan.

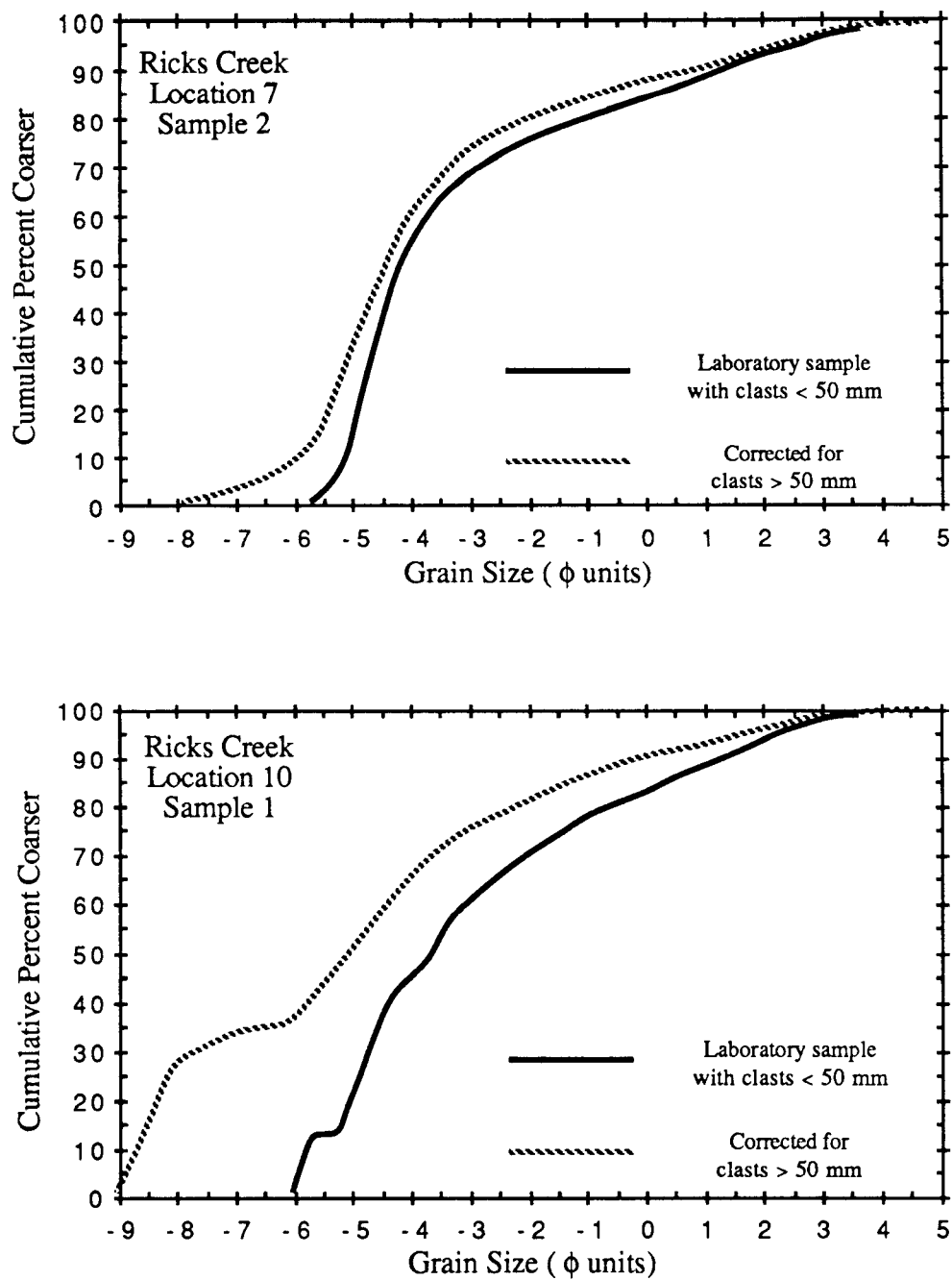


Figure C-3c. Grain size distributions for samples 7-2 and 10-1 from the Ricks Creek fan.

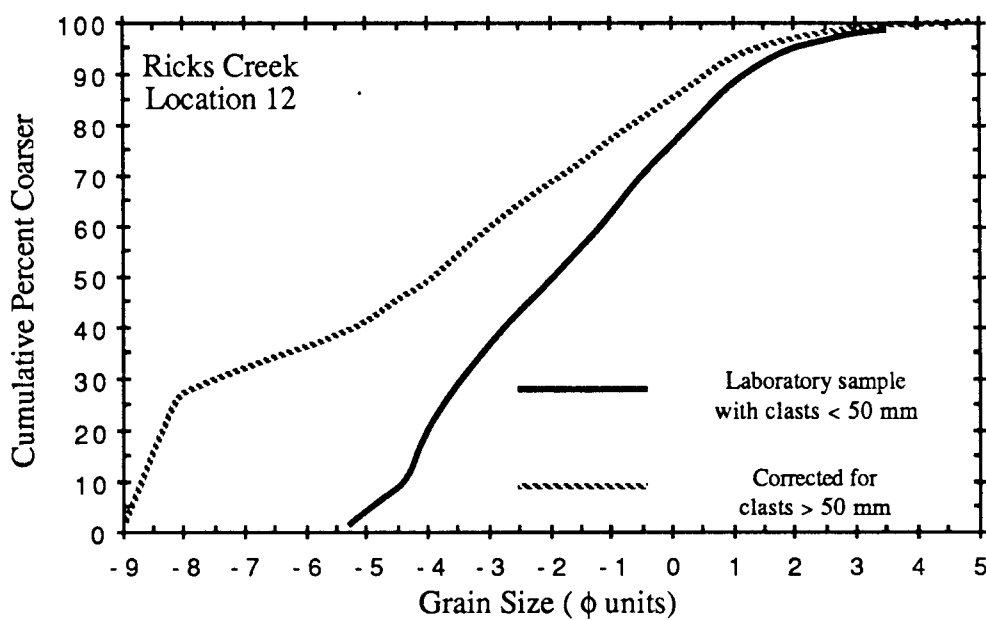
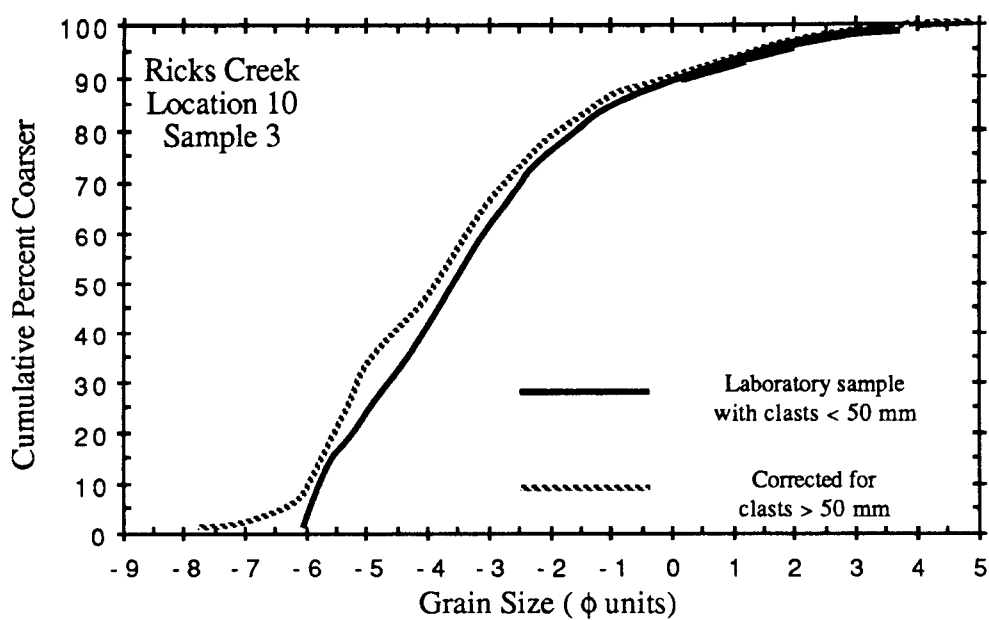


Figure C-3d. Grain size distributions for samples 10-3 and 12 from the Ricks Creek fan.

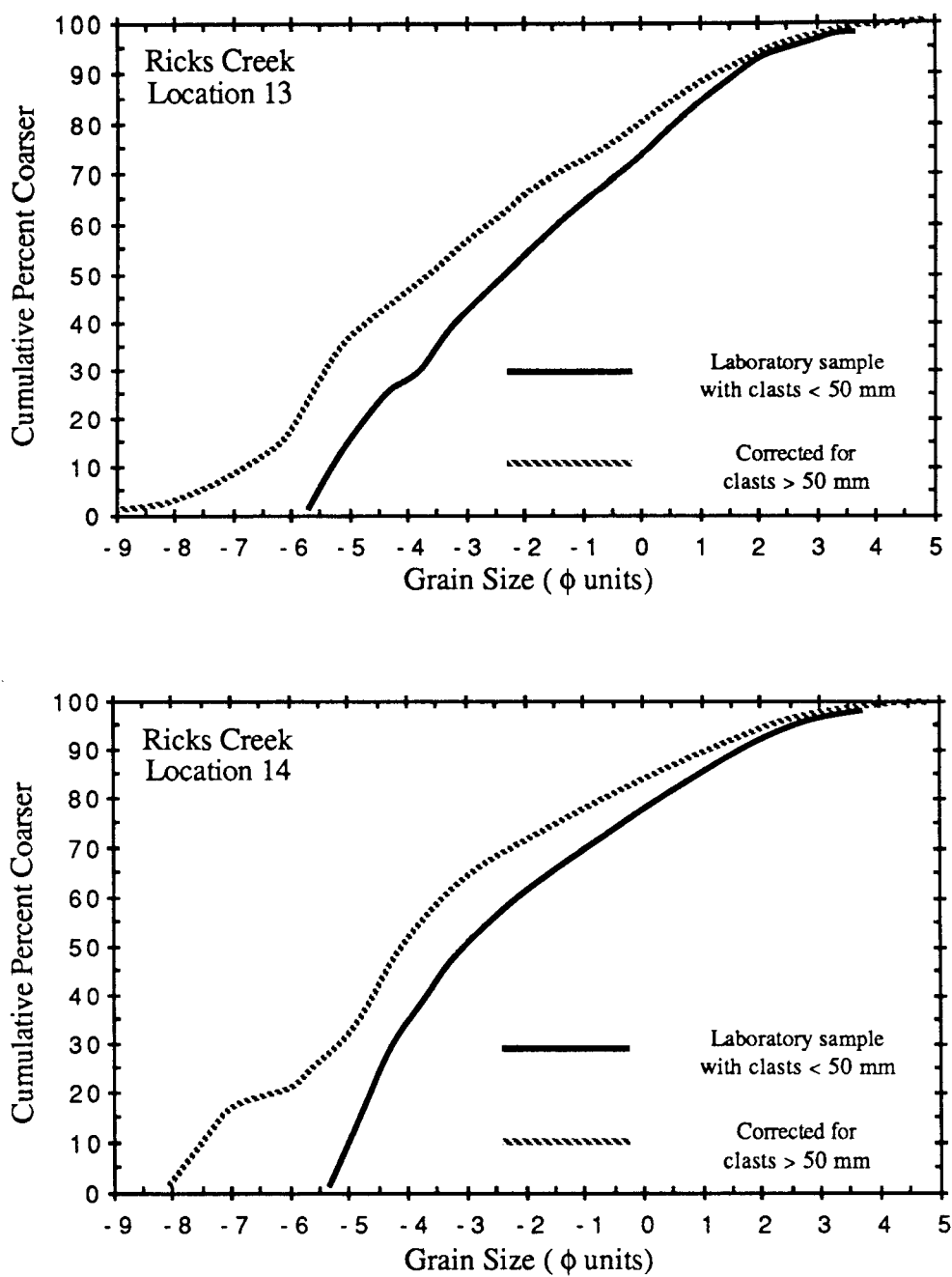


Figure C-3e. Grain size distributions for samples 13 and 14 from the Ricks Creek fan.

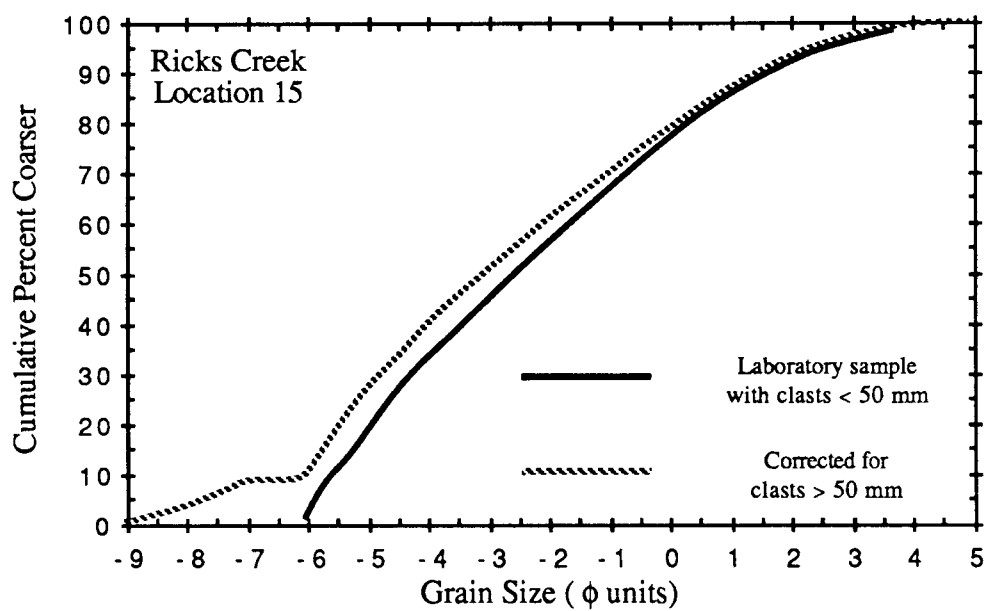


Figure C-3f. Grain size distribution for sample 15 from the Ricks Creek fan.

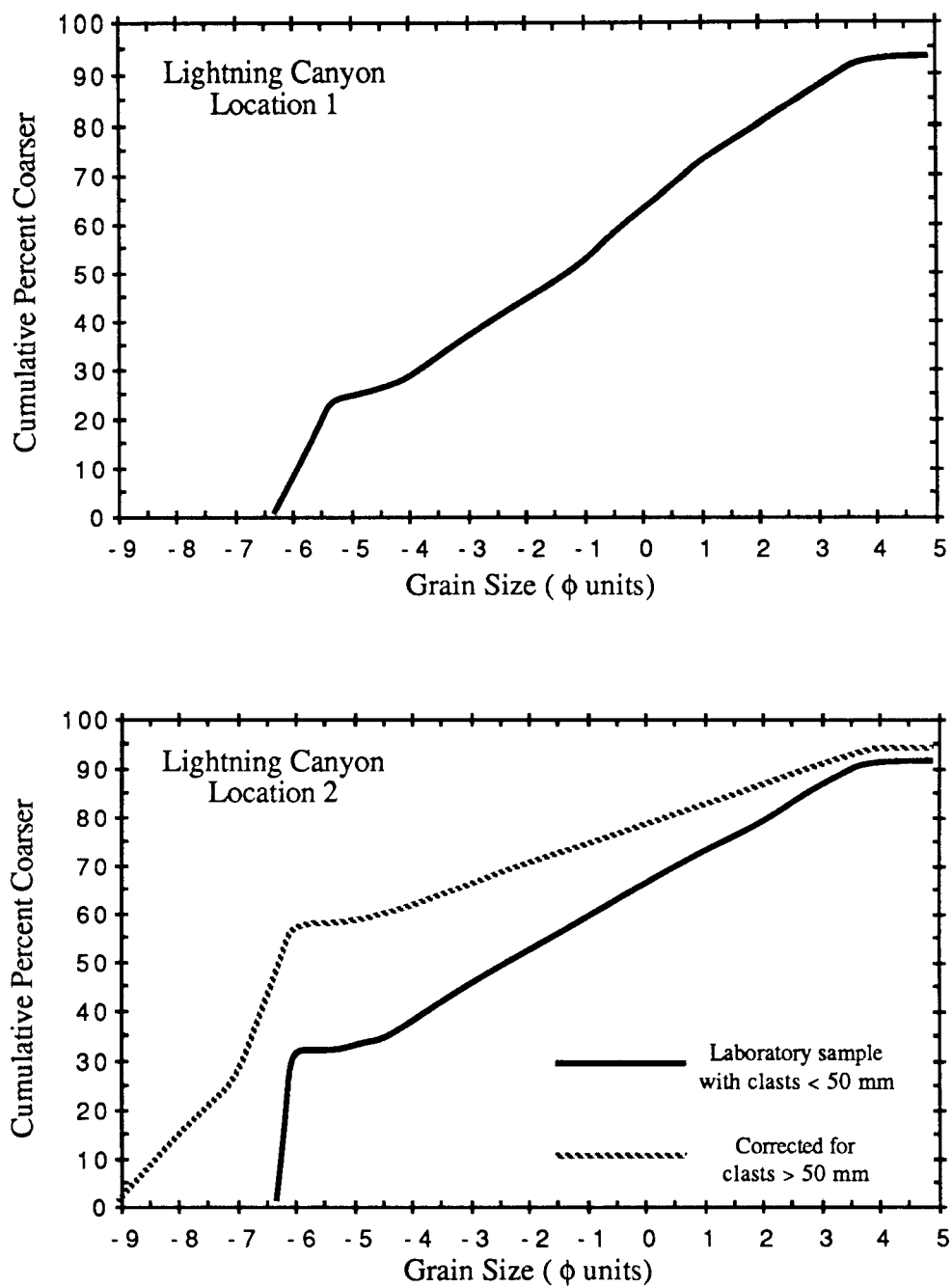


Figure C-4a. Grain size distributions for samples 1 and 2 from the Lightning Canyon fan.

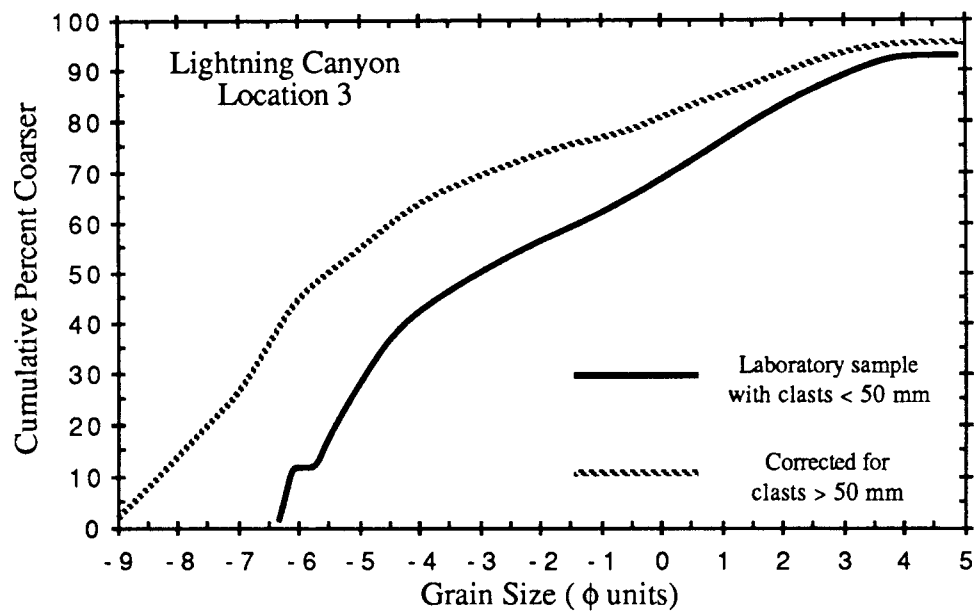


Figure C-4b. Grain size distribution for sample 3 from the Lightning Canyon fan.

Table C-2a. Fraction finer than the #200 and #40 sieves from samples from the Rudd Creek fan.

Sample	Fines Fraction (< #200 Sieve)	Matrix Fraction (< #40 Sieve)
1-5	0.012	0.133
1-6	0.022	0.126
1-7	0.032	0.117
3-1	0.021	0.182
3-2	0.021	0.214
3-3	0.012	0.115
3-4	0.003	0.089
4-2	0.010	0.061
4-3	0.042	0.161
4-4a	0.031	0.142
4-4b	0.026	0.139
4-6	0.018	0.085
4-8	0.031	0.113
6-1	0.003	0.062
6-2	0.047	0.215
17	0.001	0.056
18	0.015	0.126
20	0.040	0.179
22-1	0.017	0.163
22-2	0.012	0.065
23	0.039	0.190
25	0.010	0.060

Table C-2b. Fraction finer than the #200 and #40 sieves from samples from the Ricks Creek fan.

Sample	Fines Fraction (< #200 Sieve)	Matrix Fraction (< #40 Sieve)
6	0.014	0.077
7-1	0.007	0.041
7-2	0.021	0.097
10-1	0.007	0.071
10-2	0.013	0.065
13	0.019	0.113
14	0.023	0.106
15	0.017	0.117

Table C-2c. Fraction finer than the #200 and #40 sieves from samples from the Lightning Canyon fan.

Sample	Fines Fraction (< #200 Sieve)	Matrix Fraction (< #40 Sieve)
1	0.087	0.267
2	0.076	0.176
3	0.057	0.148

passing the # 200 sieve. The hydrometer data are summarized in Table C-3a to C-3c. A SoilTest, Inc. hydrometer with a range of specific gravity from 0.995 to 1.040 was used in a 1 L graduated cylinder. Sodium hexametaphosphate powder (Calgon) was used as a deflocculating agent.

Atterberg Limits

Atterberg Limits tests were performed on most samples following the procedures outlined in Lambe (1951, p. 22ff) and ASTM Tests D423 (liquid limit) and D424 (plastic limit). The Atterberg Limits consist of the threshold water contents separating solid, semi-solid, plastic, and liquid behaviors of sediment-water mixtures. The results of the Atterberg Limits tests are listed in Table C-4a to C-4c.

In geotechnical engineering, the liquid limit typically is not determined for non-plastic sediments (soils in the engineering sense). However, the liquid limit was determined even for non-plastic sediment because the transition from a plastic state to a liquid state was considered important and the standardized liquid limit test is based on flowage of a sediment-water mixture. The liquid limit is defined as the water content at which a standard groove in a pat of sediment-water mixture will close over a distance of about 12.7 mm in response to being tapped 25 times in a standard apparatus. The flow index is defined as the slope of the relationship between water content, w , and the logarithm of the number of taps required to close the groove, $\log B$; hence, $w = a - b \log B$. The plastic limit is defined as the minimum water content at which a small amount of sediment-water mixture may be rolled into a 3.2-mm diameter thread without crumbling. The plastic index is defined as the arithmetic difference between the liquid limit and the plastic limit. The toughness index is defined as the ratio of the plastic index to the flow index.

Specific Gravity

Specific gravity tests conducted on gravel-size clasts from five samples are summarized in Table C-5. These determinations were performed by first measuring the individual masses of oven-dried clasts and then measuring the displacement of a volumetric liquid in a graduated cylinder.

Slurry Experiments

Slurry experiments were conducted to evaluate the density of sediment-water mixtures at the threshold of mobility. Densities were evaluated using the procedure developed by Johnson and Rodine (1984, p. 292) which treats the mixtures as fine (< 19 mm) and coarse (> 19 mm) fractions. The fine fraction was placed in a shallow pan and mixed with the smallest amount of tap water which would permit the mixture to flow across the pan when it was tipped. In some cases, free water drained rapidly from the mixture as it was tipped. At the threshold of mobility, the mixture was poured into a graduated beaker, the volume was recorded, and the weight was measured. Slurry densities were computed by dividing the weight by the volume; the slurry densities were converted to debris densities by adding the slurry density to the bouyant density of the coarse fraction following the procedure described by Johnson and Rodine (1984, p. 292). The data used to compute densities of laboratory slurries are summarized in Tables C-6a to C-6c. Ordinal rank values and debris densities are summarized in Table C-7a to C-7c.

Table C-3a. Hydrometer data for the sample from Location 1 at Lightning Canyon. Analysis is based on the -#200 fraction and an assumed specific gravity of solids of 2.65 (25.98 kN/m³).

Elapsed Time (min)	Reading	Corrected Reading	Temperature (° C)	Specific Gravity of Water	Viscosity of Water (10 ⁻⁴ Pa-s)	Grain Size (mm)	Percent of -#200 Finer	Percent of Sample Coarser
2	1.0211	1.0216	23.2	0.9976	9.336	0.0309	94.36	91.84
5	1.0178	1.0183	23.2	0.9976	9.336	0.0203	81.11	92.98
15	1.0137	1.0142	23.2	0.9976	9.336	0.0123	64.65	94.41
30	1.0114	1.0119	23.0	0.9976	9.380	0.0089	55.41	95.21
60	1.0095	1.0100	23.0	0.9976	9.380	0.0064	47.78	95.87
130	1.0079	1.0084	23.4	0.9975	9.292	0.0044	41.36	96.42
460	1.0060	1.0065	23.4	0.9975	9.292	0.0024	34.13	97.05
1425	1.0045	1.0050	23.4	0.9975	9.292	0.0014	27.70	97.60

Table C-3b. Hydrometer data for the sample from Location 2 at Lightning Canyon. Analysis is based on the -#200 fraction and an assumed specific gravity of solids of 2.65 (25.98 kN/m³).

Elapsed Time (min)	Reading	Corrected Reading	Temperature (° C)	Specific Gravity of Water	Viscosity of Water (10 ⁻⁴ Pa-s)	Grain Size (mm)	Percent of -#200 Finer	Percent of Sample Coarser
2	1.0200	1.0205	23.6	0.9974	9.248	0.0312	94.73	90.94
5	1.0160	1.0165	23.6	0.9974	9.248	0.0206	77.96	92.55
15	1.0118	1.0123	23.6	0.9974	9.248	0.0124	60.36	94.23
30	1.0098	1.0103	23.6	0.9974	9.248	0.0090	51.97	95.03
60	1.0080	1.0085	23.6	0.9974	9.248	0.0064	44.43	95.75
130	1.0061	1.0066	23.4	0.9975	9.292	0.0045	36.05	96.55
660	1.0038	1.0043	23.4	0.9975	9.292	0.0020	26.41	97.47
1440	1.0031	1.0036	23.6	0.9974	9.248	0.0014	23.89	97.72

Table C-3c. Hydrometer data for the sample from Location 3 at Lightning Canyon. Analysis is based on the -#200 fraction and an assumed specific gravity of solids of 2.65 (25.98 kN/m³).

Elapsed Time (min)	Reading	Corrected Reading	Temperature (° C)	Specific Gravity of Water	Viscosity of Water (10 ⁻⁴ Pa-s)	Grain Size (mm)	Percent of -#200 Finer	Percent of Sample Coarser
2	1.0205	1.0210	23.6	0.9974	9.248	0.0310	92.75	92.15
5	1.0172	1.0177	23.6	0.9974	9.248	0.0204	79.50	93.27
15	1.0128	1.0133	23.6	0.9974	9.248	0.0123	61.83	94.77
30	1.0110	1.0115	23.6	0.9974	9.248	0.0089	54.61	95.38
60	1.0090	1.0095	23.4	0.9975	9.292	0.0064	46.18	96.09
130	1.0072	1.0077	23.2	0.9976	9.336	0.0044	38.55	96.74
600	1.0056	1.0061	23.4	0.9975	9.292	0.0021	32.52	97.25
1442	1.0042	1.0047	23.4	0.9975	9.292	0.0014	26.90	97.72

Table B-4a. Results of Atterberg Limits tests on samples from Rudd Creek.

Location and Sample No.	Flow Index Regression (a)				Liquid Limit	Plastic (b) Limit	Plastic (c) Index	Toughness (d) Index
	a	b	r ²	n				
1-2	0.367	0.074	0.99	4	0.263	0.260	0.003	0.041
1-5	0.185	0.001	0.89	4	0.184	N.P.	---	---
1-6	0.238	0.046	0.98	4	0.174	0.159	0.015	0.326
1-7	0.274	0.070	0.95	4	0.176	N.P.	---	---
3-1	0.215	0.019	0.92	4	0.189	N.P.	---	---
3-2	0.248	0.041	0.98	4	0.191	N.P.	---	---
3-3	0.259	0.041	0.89	4	0.201	N.P.	---	---
3-4	0.240	0.055	0.99	4	0.163	N.P.	---	---
4-2	0.182	0.035	0.89	3	0.133	N.P.	---	---
4-3	0.282	0.053	0.99	4	0.208	0.177	0.031	0.585
4-4a	0.288	0.070	0.99	4	0.190	0.160	0.030	0.429
4-4b	0.236	0.043	1.00	4	0.176	N.P.	---	---
4-6	0.235	0.045	0.93	4	0.172	0.159	0.013	0.289
4-8	0.258	0.048	0.92	4	0.190	0.184	0.006	0.125
6-1	0.297	0.074	0.88	3	0.193	N.P.	---	---
6-2	0.297	0.066	0.92	4	0.205	0.197	0.008	0.121
17	0.254	0.055	0.90	4	0.176	N.P.	---	---
18	0.245	0.038	0.94	4	0.192	N.P.	---	---
20	0.292	0.048	1.00	4	0.225	0.213	0.012	0.250
22-1	0.280	0.062	0.99	4	0.193	N.P.	---	---
22-2	0.235	0.052	0.70	4	0.163	N.P.	---	---
23	0.248	0.033	0.76	4	0.203	0.194	0.009	0.273
25	0.262	0.064	0.94	4	0.173	0.166	0.007	0.109

(a) Flow index regression values: $w = a - b \cdot \log B$, where w is water content, a is intercept, b is slope, B is number of taps required to close groove, r^2 is coefficient of determination, n is number of determinations; the flow index is b .

(b) N.P. designates that the sediment was non-plastic, that is, it would not roll into a thread at any water content.

(c) The plastic index is defined as the arithmetic difference between the liquid limit and the plastic limit.

(d) The toughness index is defined as the ratio of the plastic index to the flow index.

Table C-4b. Results of Atterberg Limits tests on samples from Ricks Creek.

Location and Sample No.	Flow Index Regression (a)				Liquid Limit	Plastic (b) Limit	Plastic (c) Index	Toughness (d) Index
	a	b	r ²	n				
6	0.255	0.051	0.91	4	0.184	0.172	0.012	0.235
7-1	0.281	0.056	0.98	3	0.202	N.P.	---	---
7-2	0.274	0.058	0.99	4	0.194	N.P.	---	---
10-1	0.295	0.057	0.95	4	0.216	N.P.	---	---
10-3	0.264	0.049	0.97	4	0.196	N.P.	---	---
13	0.232	0.045	0.84	4	0.169	N.P.	---	---
14	0.234	0.052	0.76	3	0.162	N.P.	---	---
15	0.290	0.073	0.98	4	0.188	N.P.	---	---

(a) Flow index regression values: $w = a - b \cdot \log B$, where w is water content, a is intercept, b is slope, B is number of taps required to close groove, r^2 is coefficient of determination, n is number of determinations; the flow index is b .

(b) N.P. designates that the sediment was non-plastic, that is, it would not roll into a thread at any water content.

(c) The plastic index is defined as the arithmetic difference between the liquid limit and the plastic limit.

(d) The toughness index is defined as the ratio of the plastic index to the flow index.

Table C-4c. Results of Atterberg Limits tests on samples from Lightning Canyon.

Location and Sample No.	Flow Index Regression (a)				Liquid Limit	Plastic (b) Limit	Plastic (c) Index	Toughness (d) Index
	a	b	r ²	n				
1	0.278	0.047	0.94	4	0.213	0.182	0.031	0.660
2	0.320	0.054	0.81	4	0.245	0.214	0.031	0.574
3	0.279	0.042	0.99	6	0.221	0.193	0.028	0.667

(a) Flow index regression values: $w = a - b \cdot \log B$, where w is water content, a is intercept, b is slope, B is number of taps required to close groove, r^2 is coefficient of determination, n is number of determinations; the flow index is b .

(b) N.P. designates that the sediment was non-plastic, that is, it would not roll into a thread at any water content.

(c) The plastic index is defined as the arithmetic difference between the liquid limit and the plastic limit.

(d) The toughness index is defined as the ratio of the plastic index to the flow index.

Table C-5. Results of specific gravity tests.

Sample	Rock Type	Mass (g)	Volume (cm ³)	Specific Gravity
Rudd 4-3	Gneiss	140.79	55.0	2.560
	Gneiss	29.86	11.0	2.715
	Pegmatite & Schist	16.54	6.5	2.545
	Pegmatite	18.85	7.0	2.693
	Gneiss	22.66	9.5	2.385
	Gneiss	44.91	<u>18.0</u>	<u>2.495</u>
Mean \pm Standard Deviation =				2.566 \pm 0.124
Rudd 4-4a	Pegmatite & Schist	272.66	100.0	2.727
	Gneiss	128.08	50.0	2.562
	Amphibolite	109.58	40.0	2.740
	Gneiss	35.16	15.0	2.344
	Gneiss	16.59	7.0	2.370
	Gneiss	25.87	9.5	2.723
	Gneiss	22.45	7.0	3.207
	Gneiss	21.05	8.5	2.476
	Pegmatite & Gneiss	16.00	6.0	2.667
	Gneiss	13.42	4.5	2.982
	Gneiss	13.30	5.5	2.418
	Quartz & Pegmatite	13.47	5.5	2.449
	Pegmatite	11.98	5.5	2.178
	Gneiss	10.24	4.5	2.276
	Gneiss	8.75	3.0	2.917
	Garnite Gneiss	359.8	<u>135.0</u>	<u>2.665</u>
Mean \pm Standard Deviation =				2.606 \pm 0.277
Rudd 4-8	Gneiss	59.67	22.0	2.712
	Gneiss	18.70	5.8	3.224
	Pegmatite	21.21	10.2	2.079
	Pegmatite	20.76	8.0	2.595
	Gneiss	19.99	7.0	2.856
	Gneiss	12.14	5.0	2.428
	Gneiss	17.94	6.5	2.760
	Gneiss	14.85	<u>5.5</u>	<u>2.700</u>
Mean \pm Standard Deviation =				2.669 \pm 0.331
Rudd 23	Schist	10.15	4.0	2.538
	Pegmatite	12.71	6.0	2.118
	Schist & Gneiss	22.14	7.0	3.163
	Pegmatite	27.41	11.0	2.492
	Gneiss	22.30	8.0	2.788
	Gneiss	18.24	7.0	2.606
	Gneiss	46.69	<u>16.0</u>	<u>2.918</u>
Mean \pm Standard Deviation =				2.660 \pm 0.336
Ricks 14	Gneiss	97.17	32.5	2.990
	Gneiss	81.37	30.5	2.668
	Pegmatite	61.71	22.0	2.805
	Pegmatite	23.19	9.0	2.577
	Gneiss	29.10	10.0	2.910
	Gneiss	22.30	9.0	2.478
	Schist	20.26	9.5	2.133
	Schist	9.46	2.5	3.784
	Schist	11.89	<u>4.0</u>	<u>2.973</u>
Mean \pm Standard Deviation =				2.813 \pm 0.456

Calculated Parameters

Calculated parameters were derived from gradation data and Atterberg Limits analyses. Seven parameters were calculated directly from the gradation data (sieve and hydrometer results) and eight parameters were calculated from a combination of the gradation data and Atterberg Limits data.

The equations describing the seven parameters calculated with gradation data are listed in Table C-8. The parameters were calculated with a BASIC program called "SED.STAT" (Appendix G) executed on a Macintosh 512K or SE personal Computer. The values of these parameters are summarized in Tables C-9a to C-9c. The mean grain size and standard deviation parameters are in phi units; all other parameters are dimensionless. The equations describing the eight parameters calculated on the basis on combined gradation and Atterberg Limits data are listed in Table C-10. These parameters are based on the amount of the sample finer than the #200 sieve or the #40 sieve, the liquid limit water content, and the flow index of the liquid limit determination. These parameters are summarized in Tables C-11a to C-11c; they are dimensionless and four are normalized because their ranges are unlimited. These parameters were also calculated with the program called "SED.STAT" (Appendix G).

Table C-6a. Results of laboratory slurry density determinations for samples from the Rudd Creek fan.

Sample	Slurry Mass (g)	Slurry Volume (cm ³)	Slurry Density (g/cm ³)	Water Content (Ww/Ws)	<u>Sediment Concentration</u> by Weight by Volume		Saturated Void Ratio
1-5	1452.0	700	2.074	0.151	0.869	0.714	0.400
1-6	1576.6	750	2.102	0.125	0.889	0.751	0.331
1-7	1226.9	550	2.231	0.123	0.890	0.754	0.326
3-1	1503.2	680	2.211	0.134	0.882	0.738	0.355
3-2	1744.8	820	2.128	0.119	0.894	0.760	0.315
3-3	1715.2	805	2.131	0.156	0.865	0.708	0.413
3-4	1566.0	715	2.190	0.145	0.873	0.722	0.384
4-2	1552.8	770	2.017	0.179	0.848	0.678	0.474
4-3	1545.5	745	2.074	0.171	0.854	0.688	0.453
4-4a	1578.3	730	2.162	0.136	0.880	0.735	0.360
4-4b	1459.8	695	2.100	0.148	0.871	0.718	0.392
4-6	1747.5	805	2.171	0.132	0.883	0.741	0.350
4-8	1826.4	875	2.087	0.134	0.882	0.738	0.355
6-1	1358.1	620	2.190	0.145	0.873	0.722	0.384
6-2	1802.7	830	2.172	0.153	0.867	0.712	0.405
17	1639.8	780	2.102	0.158	0.864	0.705	0.419
18	1788.9	810	2.209	0.114	0.898	0.768	0.302
20	1488.7	695	2.142	0.084	0.923	0.818	0.223
22-1	1602.1	740	2.165	0.146	0.873	0.721	0.387
22-2	1600.4	740	2.163	0.119	0.894	0.760	0.315
23	1201.5	550	2.185	0.143	0.875	0.725	0.379
25	1725.3	800	2.157	0.091	0.917	0.806	0.241
Mean 2.144				0.137	0.880	0.736	0.362
Standard Deviation 0.053				0.023	0.018	0.034	0.061

Table C-6b. Results of laboratory slurry density determinations for samples from the Ricks Creek fan.

Sample	Slurry Mass (g)	Slurry Volume (cm ³)	Slurry Density (g/cm ³)	Water Content (Ww/Ws)	<u>Sediment Concentration</u> by Weight by Volume		Saturated Void Ratio
6	813.3	355	2.291	0.104	0.906	0.784	0.276
7-1	1507.9	700	2.154	0.134	0.882	0.738	0.355
7-2	999.0	450	2.220	0.117	0.895	0.763	0.310
10-1	910.4	425	2.142	0.113	0.898	0.770	0.299
10-3	1081.8	505	2.142	0.152	0.868	0.713	0.403
13	1085.9	500	2.172	0.115	0.897	0.766	0.305
14	877.7	395	2.222	0.132	0.883	0.741	0.350
15	1730.4	825	2.097	0.138	0.879	0.732	0.366
Mean 2.180				0.126	0.889	0.751	0.333
Standard Deviation 0.057				0.015	0.012	0.022	0.039

Table C-6c. Results of laboratory slurry density determinations of samples from the Lightning Canyon fan.

Sample	Slurry Mass (g)	Slurry Volume (cm ³)	Slurry Density (g/cm ³)	Water Content (Ww/Ws)	<u>Sediment Concentration</u> by Weight by Volume		Saturated Void Ratio
1	1816.6	855	2.125	0.175	0.851	0.683	0.464
2	1105.4	540	2.047	0.177	0.850	0.681	0.469
3	1748.6	800	2.186	0.147	0.872	0.720	0.390
Mean				2.119	0.166	0.858	0.695
Standard Deviation				0.057	0.014	0.010	0.018
							0.441
							0.036

Table C-7a. Ordinal rank values and debris density determinations for samples from the Rudd Creek fan.

Sample	Ordinal Rank	Slurry Solid Content by Volume	Slurry Water Content by Volume	Slurry Air Content by Volume	Slurry Density (g/cm ³)	Coarse Fraction (> 50 mm)	Debris Density (g/cm ³)
1-5	40	0.680	0.272	0.048	2.074	0.57	2.402
1-6	30	0.705	0.234	0.061	2.102	0.42	2.332
1-7	30	0.750	0.244	0.006	2.231	0.54	2.457
3-1	20	0.736	0.261	0.003	2.211	0.05	2.233
3-2	10	0.718	0.226	0.056	2.128	0.07	2.164
3-3	20	0.696	0.288	0.017	2.131	0.46	2.370
3-4	40	0.722	0.277	0.001	2.190	0.53	2.434
4-2	30	0.645	0.306	0.048	2.017	0.60	2.397
4-3	40	0.669	0.303	0.029	2.074	0.57	2.403
4-4a	20	0.718	0.259	0.023	2.162	0.52	2.416
4-4b	20	0.690	0.271	0.039	2.100	0.45	2.348
4-6	30	0.724	0.253	0.023	2.171	0.55	2.434
4-8	40	0.695	0.247	0.059	2.087	0.56	2.402
6-1	0	0.722	0.277	0.001	2.190	0.16	2.264
6-2	40	0.711	0.288	0.001	2.172	0.40	2.363
17	30	0.685	0.287	0.028	2.102	0.56	2.409
18	30	0.748	0.226	0.026	2.209	0.50	2.429
20	40	0.746	0.166	0.088	2.142	0.49	2.391
22-1	10	0.713	0.276	0.011	2.165	0.08	2.204
22-2	30	0.729	0.230	0.041	2.163	0.44	2.377
23	40	0.721	0.273	0.005	2.185	0.45	2.394
25	20	0.746	0.180	0.074	2.157	0.40	2.354
Mean		0.712	0.257	0.031	2.144	0.426	2.363
Standard Deviation		0.027	0.036	0.026	0.053	0.173	0.078

Table C-7b. Ordinal rank values and debris density determinations for samples from the Ricks Creek fan.

Sample	Ordinal Rank	Slurry Solid Content by Volume	Slurry Water Content by Volume	Slurry Air Content by Volume	Slurry Density (g/cm ³)	Coarse Fraction (> 50 mm)	Debris Density (g/cm ³)
6	30	0.783	0.216	0.001	2.291	0.47	2.460
7-1	30	0.717	0.255	0.029	2.154	0.60	2.452
7-2	30	0.750	0.233	0.017	2.220	0.52	2.444
10-1	30	0.726	0.217	0.056	2.142	0.61	2.452
10-3	20	0.702	0.283	0.016	2.142	0.42	2.355
13	30	0.735	0.224	0.041	2.172	0.42	2.373
14	30	0.741	0.259	0.000	2.222	0.44	2.410
15	20	0.696	0.254	0.050	2.097	0.38	2.307
Mean		0.731	0.243	0.026	2.180	0.483	2.407
Standard Deviation		0.026	0.022	0.020	0.057	0.080	0.052

Table C-7c. Ordinal rank values and debris density determinations from samples from the Lightning Canyon fan.

Sample	Ordinal Rank	Slurry Solid Content by Volume	Slurry Water Content by Volume	Slurry Air Content by Volume	Slurry Density (g/cm ³)	Coarse Fraction (> 50 mm)	Debris Density (g/cm ³)
1	40	0.682	0.316	0.001	2.125	0.26	2.261
2	40	0.656	0.308	0.036	2.047	0.59	2.403
3	40	0.719	0.280	0.001	2.186	0.60	2.464
Mean		0.686	0.301	0.013	2.119	0.483	2.376
Standard Deviation		0.026	0.015	0.016	0.057	0.158	0.085

Table C-8. Parameters based on gradation data. Parameters involving ϕ are from Folk (1980); parameters involving d are from American Society for Testing and Materials (1984).

Parameter	Equation
Mean Grain Size	$M_z = (\phi_{16} + \phi_{50} + \phi_{84}) / 3$
Graphic Standard Deviation	$\sigma_G = (\phi_{84} - \phi_{16}) / 2$
Inclusive Graphic Standard Deviation	$\sigma_I = [(\phi_{84} - \phi_{16}) / 4] + [(\phi_{95} - \phi_5) / 6.6]$
Inclusive Graphic Skewness	$SK_I = [(\phi_{84} + \phi_{16} - 2 \phi_{50}) / 2 (\phi_{84} - \phi_{16})] + [(\phi_{95} + \phi_5 - 2 \phi_{50}) / 2 (\phi_{95} - \phi_5)]$
Graphic Kurtosis	$K_G = (\phi_{95} - \phi_5) / 2.44 (\phi_{75} - \phi_{25})$
Normalized Graphic Kurtosis	$K_G' = K_G / (1 + K_G)$
Coefficient of Uniformity	$C_U = d_{60} / d_{10}$
Coefficient of Curvature	$C_C = (d_{30})^2 / [(d_{10})(d_{60})]$

Table C-9a. Summary of parameters calculated based on gradation data for samples from the Rudd Creek fan. These parameters were calculated with SED.STAT (Appendix G).

Sample	Mean Grain Size (ϕ)	Graphic Standard Deviation (ϕ)	Inclusive Graphic Standard (ϕ)	Inclusive Graphic Skewness	Graphic Kurtosis	Normalized Graphic Kurtosis	Coefficient of Uniformity	Coefficient of Curvature
1-1	1.000	1.400	1.382	0.196	1.272	0.560	4.925	2.000
1-3	-3.250	1.925	1.811	0.183	0.883	0.469	9.514	1.464
1-4	-0.317	1.575	1.901	0.023	1.585	0.613	6.277	1.464
1-5	-3.503	3.720	3.427	0.422	0.988	0.497	111.430	2.362
1-6	-3.107	3.685	3.447	0.124	0.763	0.433	73.009	0.712
1-7	-3.337	3.020	2.983	0.532	1.027	0.507	106.891	3.160
3-1	-1.157	2.475	2.318	0.216	0.819	0.450	20.393	0.901
3-2	-0.693	2.290	2.363	0.094	1.053	0.513	14.723	1.000
3-3	-3.360	3.610	3.276	0.275	0.698	0.411	79.341	0.555
3-4	-3.597	3.080	3.037	0.381	0.922	0.480	68.593	0.859
4-1	-1.100	1.575	1.545	-0.384	1.171	0.539	3.031	1.231
4-2	-4.217	3.760	3.286	0.422	0.591	0.371	80.449	0.398
4-3	-4.303	4.870	4.290	0.447	0.644	0.392	515.561	0.285
4-4a	-3.790	2.440	2.708	0.533	0.803	0.445	144.007	0.785
4-4b	-2.197	3.145	3.030	0.018	0.945	0.486	27.474	0.895
4-5	-0.500	1.925	1.864	0.275	0.920	0.479	12.996	1.414
4-6	-4.850	4.390	4.016	0.081	1.148	0.535	72.004	1.257
4-7	-2.350	2.450	2.278	0.054	0.760	0.432	12.996	0.707
4-8	-4.350	4.210	3.870	0.240	0.807	0.446	146.018	3.972
6-1	-2.333	2.100	2.065	0.237	0.886	0.470	16.564	0.901
6-2	-2.753	4.780	4.275	-0.077	0.660	0.397	137.187	0.192
17	-5.063	4.070	3.726	0.049	0.745	0.427	165.421	0.540
18	-3.950	4.175	3.845	0.149	0.841	0.457	137.187	1.414
20	-3.403	4.625	4.135	0.217	0.666	0.400	232.325	0.272
22-1	-1.767	2.550	2.404	0.371	0.985	0.496	25.992	1.414
22-2	-4.120	3.425	3.258	-0.015	0.809	0.447	31.125	1.580
23	-2.927	4.245	3.845	0.194	0.668	0.400	172.446	0.171
25	-3.387	2.405	2.615	0.163	1.322	0.569	22.162	1.905

Table C-9b. Summary of parameters calculated based on gradation data for samples from the Ricks Creek fan. These parameters were calculated with SED.STAT (Appendix G).

Sample	Mean Grain Size (ϕ)	Graphic Standard Deviation (ϕ)	Inclusive Graphic Standard (ϕ)	Inclusive Graphic Skewness	Graphic Kurtosis	Normalized Graphic Kurtosis	Coefficient of Uniformity	Coefficient of Curvature
6	-3.963	3.365	3.193	0.135	0.968	0.492	41.070	1.558
7-1	-4.927	3.510	3.225	0.169	0.813	0.448	50.914	1.636
7-2	-3.560	2.470	2.633	0.469	1.461	0.594	57.680	7.516
10-1	-4.897	3.545	3.380	0.143	0.835	0.455	58.081	2.713
10-3	-3.517	2.210	2.320	0.272	1.043	0.511	23.588	1.395
12	-4.087	4.165	3.667	-0.028	0.616	0.381	50.914	0.511
13	-2.967	3.275	3.145	0.237	0.819	0.450	63.558	0.637
14	-3.560	3.640	3.364	0.216	0.978	0.494	57.680	2.042
15	-2.663	3.145	3.095	0.140	0.882	0.469	45.255	0.697

Table C-9c. Summary of parameters calculated based on gradation data for samples from the Lightning Canyon fan. These parameters were calculated with SED.STAT (Appendix G).

Sample	Mean Grain Size (ϕ)	Graphic Standard Deviation (ϕ)	Inclusive Graphic Standard (ϕ)	Inclusive Graphic Skewness	Graphic Kurtosis	Normalized Graphic Kurtosis	Coefficient of Uniformity	Coefficient of Curvature
1	-1.400	4.050	3.960	0.053	0.880	0.468	64.000	0.660
2	-4.127	4.710	4.585	0.664	0.947	0.486	754.826	1.266
3	-4.077	4.385	4.158	0.477	0.920	0.479	382.681	2.428

Table C-10. Parameters based on a combination of gradation and Atterberg Limits data. LL is liquid limit; F is fraction of sample < #200 sieve; M is fraction of sample < #40 sieve; FI is the flow index from the liquid limit test.

Parameter	Equation
Fines Activity	$FA = LL / F$
Normalized Fines Activity	$FA' = FA / (1 + FA)$
Matrix Activity	$MA = LL / M$
Normalized Matrix Activity	$MA' = MA / (1 + MA)$
Fines Flow Index	$FF = F / FI$
Normalized Fines Flow Index	$FF' = FF / (1 + FF)$
Matrix Flow Index	$MF = M / FI$
Normalized Matrix Flow Index	$MF' = MF / (1 + MF)$

Table C-11a. Summary of parameters calculated based on gradation and Atterberg Limits data for samples from the Rudd Creek fan. These parameters were calculated with SED.STAT (Appendix G).

Sample	Fines Activity	Normalized Fines Activity	Matrix Activity	Normalized Matrix Activity	Fines Flow Index	Normalized Fines Flow Index	Matrix Flow Index	Normalized Matrix Flow Index
1-5	15.333	0.939	1.383	0.580	12.000	0.923	133.000	0.993
1-6	7.909	0.888	1.381	0.580	0.478	0.324	2.739	0.733
1-7	5.500	0.846	1.504	0.601	0.457	0.314	1.671	0.626
3-1	9.000	0.900	1.038	0.509	1.105	0.525	9.579	0.905
3-2	9.095	0.901	0.893	0.472	0.512	0.339	5.220	0.839
3-3	16.750	0.944	1.748	0.636	0.293	0.226	2.805	0.737
3-4	54.333	0.982	1.831	0.647	0.055	0.052	1.618	0.618
4-2	13.300	0.930	2.180	0.686	0.286	0.222	1.743	0.635
4-3	4.952	0.832	1.292	0.564	0.792	0.442	3.038	0.752
4-4a	6.129	0.860	1.338	0.572	0.443	0.307	2.029	0.670
4-4b	6.769	0.871	1.266	0.559	0.605	0.377	3.233	0.764
4-6	9.556	0.905	2.024	0.669	0.400	0.286	1.889	0.654
4-8	6.129	0.860	1.681	0.627	0.646	0.392	2.354	0.702
6-1	64.333	0.985	3.113	0.757	0.041	0.039	0.838	0.456
6-2	4.362	0.813	0.953	0.488	0.712	0.416	3.258	0.765
17	176.000	0.994	3.143	0.759	0.018	0.018	1.018	0.505
18	12.800	0.928	1.524	0.604	0.395	0.283	3.316	0.768
20	5.675	0.850	1.268	0.559	0.833	0.455	3.729	0.789
22-1	11.353	0.919	1.184	0.542	0.274	0.215	2.629	0.724
22-2	13.583	0.931	2.508	0.715	0.231	0.188	1.250	0.556
23	5.205	0.839	1.068	0.517	1.182	0.542	5.758	0.852
25	17.300	0.945	2.883	0.742	0.156	0.135	0.937	0.484

Table C-11b. Summary of parameters calculated based on gradation and Atterberg Limits data for samples from the Ricks Creek fan. These parameters were calculated with SED.STAT (Appendix G).

Sample	Fines Activity	Normalized Fines Activity	Matrix Activity	Normalized Matrix Activity	Fines Flow Index	Normalized Fines Flow Index	Matrix Flow Index	Normalized Matrix Flow Index
6	13.143	0.929	2.390	0.705	0.275	0.215	1.510	0.602
7-1	28.857	0.967	4.927	0.831	0.125	0.111	0.732	0.423
7-2	9.238	0.902	2.000	0.667	0.362	0.266	1.672	0.626
10-1	30.857	0.969	3.042	0.753	0.123	0.109	1.246	0.555
10-3	15.077	0.938	3.015	0.751	0.265	0.210	1.327	0.570
13	8.895	0.899	1.496	0.599	0.422	0.297	2.511	0.715
14	7.043	0.876	1.528	0.604	0.442	0.307	2.038	0.671
15	11.059	0.917	1.607	0.616	0.233	0.189	1.603	0.616

Table C-11c. Summary of parameters calculated based on gradation and Atterberg Limits data for samples from the Lightning Canyon fan. These parameters were calculated with SED.STAT (Appendix G).

Sample	Fines Activity	Normalized Fines Activity	Matrix Activity	Normalized Matrix Activity	Fines Flow Index	Normalized Fines Flow Index	Matrix Flow Index	Normalized Matrix Flow Index
1	2.448	0.710	0.798	0.444	1.851	0.649	5.681	0.850
2	3.224	0.763	1.392	0.582	1.407	0.585	3.259	0.765
3	3.877	0.795	1.493	0.599	1.357	0.576	3.524	0.779

Sample Classification

The samples tested and described above have been classified according to geologic and engineering nomenclature (Folk, 1980; American Society for Testing and Materials, 1984). The results of these classifications are presented below in Tables C-12a to C-12c.

Table C-12a. Classification of samples from the Rudd Creek fan.

Sample	Description	Unified Soil Classification Symbol
1-1	Coarse sand, poorly sorted, fine-skewed, leptokurtic	SP
1-2	Fine to very fine sand	SM
1-3	Sandy, fine to medium gravel, poorly sorted, fine-skewed, platykurtic	GW
1-4	Gravelly, coarse to very coarse sand, poorly sorted, near symmetrical very leptokurtic	SW
1-5	Sandy gravel, very poorly sorted, strongly fine-skewed, mesokurtic	GW
1-6	Sandy gravel, very poorly sorted, fine-skewed, platykurtic	GP
1-7	Sandy gravel, very poorly sorted, strongly fine-skewed, mesokurtic	GP
3-1	Sandy gravel, very poorly sorted, fine-skewed, platykurtic	GP
3-2	Gravelly sand, very poorly sorted, near symmetrical, mesokurtic	SW
3-3	Sandy gravel, very poorly sorted, fine-skewed, platykurtic	GP
3-4	Sandy gravel, very poorly sorted, strongly fine-skewed, mesokurtic	GP
4-1	Gravelly sand, poorly sorted, strongly coarse-skewed, leptokurtic	SP
4-2	Sandy gravel, very poorly sorted, strongly fine-skewed, very platykurtic	GP
4-3	Sandy gravel, extremely poorly sorted, strongly fine-skewed, platykurtic	GP
4-4a	Sandy gravel, very poorly sorted, strongly fine-skewed, platykurtic	GP
4-4b	Sandy gravel, very poorly sorted, near symmetrical, mesokurtic	GP
4-5	Gravelly sand, poorly sorted, fine-skewed, mesokurtic	SW
4-6	Sandy gravel, extremely poorly sorted, near symmetrical, leptokurtic	GW
4-7	Sandy gravel, very poorly sorted, near symmetrical, platykurtic	GP
6-1	Sandy gravel, very poorly sorted, fine-skewed, platykurtic	GP
6-2	Sandy gravel with boulders and cobbles, extremely poorly sorted, near symmetrical, platykurtic	GP
17	Boulders and cobbles with pebbles and sand, very poorly sorted, near symmetrical, platykurtic	GP
18	Bouldery sandy gravel with cobbles, very poorly sorted, fine-skewed, platykurtic	GW
20	Cobbly sandy gravel, extremely poorly sorted, fine-skewed, very platykurtic	GP
22-1	Sandy gravel, very poorly sorted, strongly fine-skewed, mesokurtic	GW
22-2	Sandy gravel with cobbles, very poorly sorted, near symmetrical, platykurtic	GW
23	Sandy gravel, very poorly sorted, fine-skewed, very platykurtic	GP
25	Sandy gravel, very poorly sorted, fine-skewed, leptokurtic	GW

Table C-12b. Classification of samples from the Ricks Creek fan.

Sample	Description	Unified Soil Classification Symbol
6	Sandy and cobbly gravel, very poorly sorted, fine-skewed, mesokurtic	GW
7-1	Sandy gravel with cobbles, very poorly sorted, fine-skewed, platykurtic	GW
7-2	Sandy gravel, very poorly sorted, strongly fine-skewed, leptokurtic	GP
10-1	Sandy gravel with cobbles, very poorly sorted, fine-skewed, platykurtic	GW
10-3	Sandy gravel, very poorly sorted, fine-skewed, mesokurtic	GW
12	Sandy and cobbly gravel, very poorly sorted, near symmetrical, very platykurtic	GP
13	Sandy gravel, very poorly sorted, fine-skewed, platykurtic	GP
14	Sandy gravel, very poorly sorted, fine-skewed, mesokurtic	GW
15	Sandy gravel, very poorly sorted, fine-skewed, platykurtic	GP

Table C-12c. Classification of samples from the Lightning Canyon fan.

Sample	Description	Unified Soil Classification Symbol
1	Gravelly sand, very poorly sorted, near symmetrical, platykurtic	SP-SM
2	Sandy gravel with cobbles, extremely poorly sorted, strongly fine-skewed, mesokurtic	GW-GM
3	Sandy gravel with cobbles, extremely poorly sorted, strongly fine-skewed, mesokurtic	GW-GM

APPENDIX D

SUMMARY OF SELECTED GEOMORPHIC PARAMETERS

The study area comprises 22 drainage basins, as shown on Figure 1; selected morphometric data and parameters regarding these basins are presented in Table D-1. These traditional geomorphic parameters were developed for the drainage basins in the study area to provide a means for comparing the study area to other areas where aspects of sedimentation have been published. The drainage basins range in order from 2 to 5, as shown on Figures D-1 to D-22. The stream order system developed by Strahler (1952) was used to classify the basins in Davis County. Basin area, A_b , was determined by planimetry of basin outlines on conventional U.S. Geological Survey topographic quadrangles at a scale of 1:24,000; measurements were made using a Numonics Corp. Model 1224 Electronics Graphic Calculator.

Basin length, L_b , was measured on topographic quadrangles as the horizontal distance from the basin mouth to the most distant point on the basin divide; in most cases, the most distant point was also the highest point. The basin length ratio, L_r , is a dimensionless parameter defined as

$$L_r = L_b / L_d \quad (D-1)$$

where L_b is the basin length and L_d is the length from the basin mouth to the principal divide of the Wasatch Range measured in the same direction as basin length. Those basins which do not extend to the principal divide were called "half canyons" by Wieczorek and others (1983, p. 10). Wieczorek and others (1983, Plate 1) applied the informal names of "Half" and "Halfway" for the basins between Baer and Shepard and between Davis and Ricks, respectively, which were unnamed on the topographic quadrangles. These names have been used in this dissertation; however, it should be noted that Halfway Canyon is also the name of one of the tributaries in Farmington Canyon (Croft, 1981) and is shown on the Peterson Quadrangle, Utah (7.5-minute series).

Basin relief, R_b , is the difference in elevation from the highest point in the basin to the mouth. The elevations were determined from 1:24,000-scale topographic quadrangles and converted from feet to meters. Basin relief for the research area was found to correlate moderately well in a power function with basin area as

$$R_b = 950.6 A_b^{0.184}, (r^2 = 0.617, n = 22) \quad (D-2)$$

The relief ratio, R_r , is a dimensionless parameter equivalent to the nominal basin slope and is defined as

$$R_r = R_b / L_b \quad (D-3)$$

where R_b is the basin relief in m and L_b is the basin length in m.

The basin ruggedness factor, R_u , is a dimensionless parameter developed by Melton (1965, p. 23) and defined as

$$R_u = R_b / (A_b)^{0.5} \quad (D-4)$$

Table D-1. Morphometric data and parameters of drainage basins in Davis County.

Basin	Order ^(a)		Area Ab (km ²)	Length Lb (m)	Length ^(b)		Relief Rb (m)	Relief ^(c)		Ruggedness ^(d)		Form ^(e)		Elongation ^(f)		Lemniscate ^(g) Factor K
	O	R			Ratio Lr	Ratio Rr		Ratio Rr	Factor Ru	Factor Fo	Factor Eb					
Corbett	3		3.233	4115	1.00	0.309	1270	0.309	0.706	0.191	0.493	0.191	0.493			4.113
Hobbs	3		3.115	3764	0.91	0.296	1113	0.296	0.630	0.220	0.529	0.220	0.529			3.573
Lightning	2		0.547	1920	0.44	0.359	689	0.359	0.931	0.148	0.435	0.148	0.435			5.294
Kays (Middle)	4		4.238	4450	1.00	0.300	1337	0.300	0.649	0.214	0.522	0.214	0.522			3.670
Kays (South)	4		4.491	4450	1.00	0.313	1392	0.313	0.657	0.227	0.537	0.227	0.537			3.463
Snow	3		2.022	3719	0.85	0.334	1244	0.334	0.875	0.146	0.431	0.146	0.431			5.371
Adams	4		5.485	4907	1.00	0.292	1435	0.292	0.613	0.228	0.539	0.228	0.539			3.448
Webb	5		6.465	4877	1.00	0.282	1375	0.282	0.541	0.272	0.588	0.272	0.588			2.889
Baer	4		8.502	5304	1.00	0.271	1435	0.271	0.492	0.302	0.620	0.302	0.620			2.598
Half	2		1.090	2438	0.51	0.368	896	0.368	0.858	0.183	0.483	0.183	0.483			4.284
Shepard	3		5.958	4892	1.00	0.280	1370	0.280	0.561	0.249	0.563	0.249	0.563			3.155
Farmington	5		27.145	10119	1.00	0.142	1438	0.142	0.276	0.265	0.581	0.265	0.581			2.963
Rudd	3		1.781	3307	0.68	0.347	1146	0.347	0.859	0.163	0.455	0.163	0.455			4.823
Steed	4		6.706	5029	1.00	0.285	1435	0.285	0.554	0.265	0.581	0.265	0.581			2.962
Davis	4		4.283	4968	0.92	0.285	1414	0.285	0.683	0.174	0.470	0.174	0.470			4.526
Halfway	3		1.627	3658	0.69	0.295	1079	0.295	0.846	0.122	0.394	0.122	0.394			6.458
Ricks	4		6.341	5395	1.00	0.269	1451	0.269	0.576	0.218	0.527	0.218	0.527			3.605
Barnard	4		3.730	5334	0.92	0.247	1318	0.247	0.683	0.131	0.409	0.131	0.409			5.991
Parrish	4		5.452	5883	1.00	0.228	1342	0.228	0.575	0.158	0.448	0.158	0.448			4.985
Centerville	4		8.148	6401	1.00	0.202	1291	0.202	0.452	0.199	0.503	0.199	0.503			3.949
Buckland	3		2.436	4511	0.70	0.187	843	0.187	0.540	0.120	0.390	0.120	0.390			6.561
Ward	5		11.302	6126	1.00	0.199	1221	0.199	0.363	0.301	0.619	0.301	0.619			2.608
Mean	3.6		5.641	4799	0.89	0.277	1252	0.277	0.633	0.204	0.505	0.204	0.505			4.150
Standard Deviation	0.8		5.492	1622	0.17	0.057	212	0.057	0.168	0.056	0.071	0.056	0.071			1.209

(a) Stream order is by Strahler's (1952) method.

(b) Length ratio is basin length divided by length from basin mouth to principal Wasatch Range divide.

(c) Relief ratio is basin relief divided by basin length ($Rr = Rb/Lb$); it is nominal basin slope.(d) Ruggedness factor is basin relief divided by the square root of basin area ($Ru = Rb/Ab^{0.5}$) (Melton, 1965).(e) Form factor is basin area divided by basin length squared ($Fo = Ab/Lb^2$) (Horton, 1932).(f) Elongation factor is 2 divided by basin length times the square root of basin area divided by pi ($Eo = 2[Ab/\pi]^{0.5}/Lb$) (Schumm, 1956).(g) Lemniscate factor is π times basin length squared divided by 4 times basin area ($K = \pi Lb^2/4Ab$) (modified from Chorley and others, 1957).

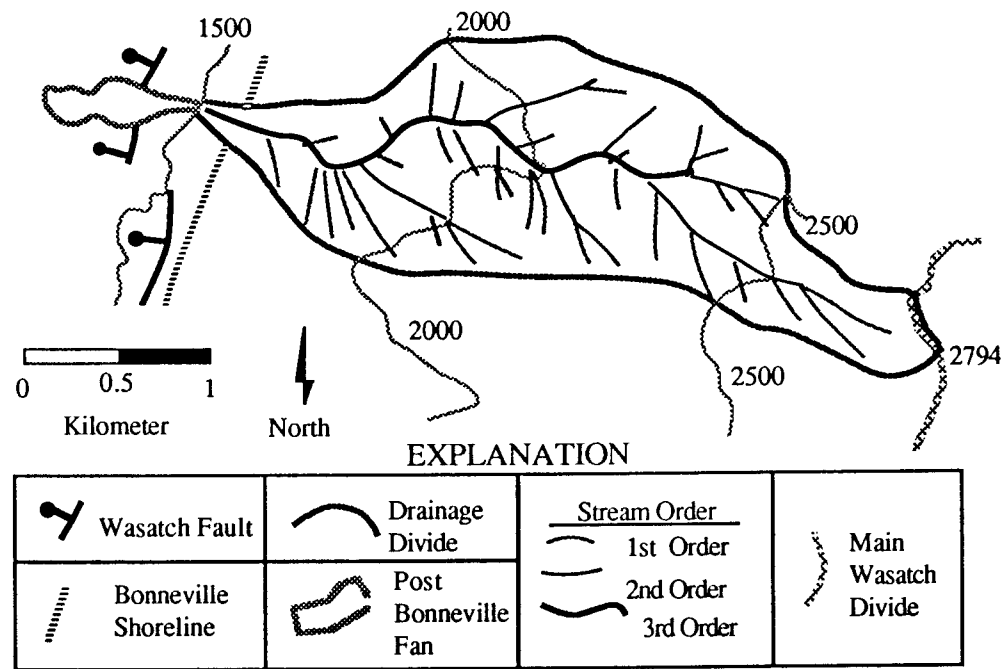


Figure D-1. Corbett Creek drainage basin and fan showing selected geomorphic features. 500-m contour interval.

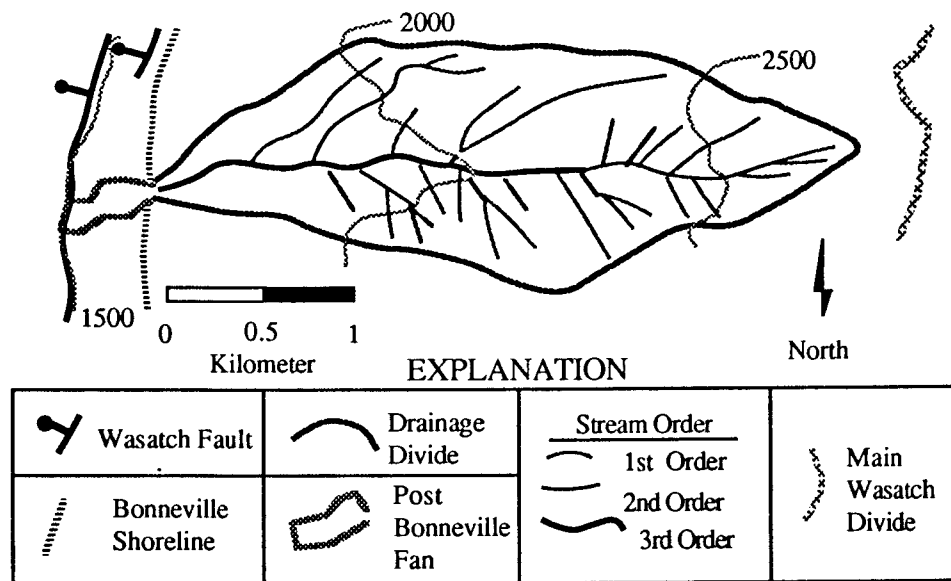
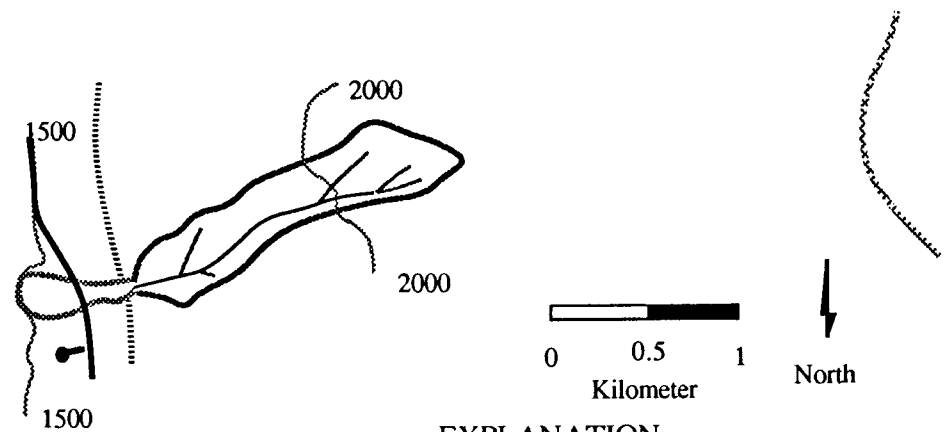


Figure D-2. Hobbs Canyon drainage basin and fan showing selected geomorphic features. 500-m contour interval.









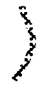
EXPLANATION			
	Wasatch Fault		Drainage Divide
	Bonneville Shoreline		Post Bonneville Fan
		<u>Stream Order</u>  1st Order  2nd Order	 Main Wasatch Divide

Figure D-3. Lightning Canyon drainage basin and fan showing selected geomorphic features. 500-m contour interval.

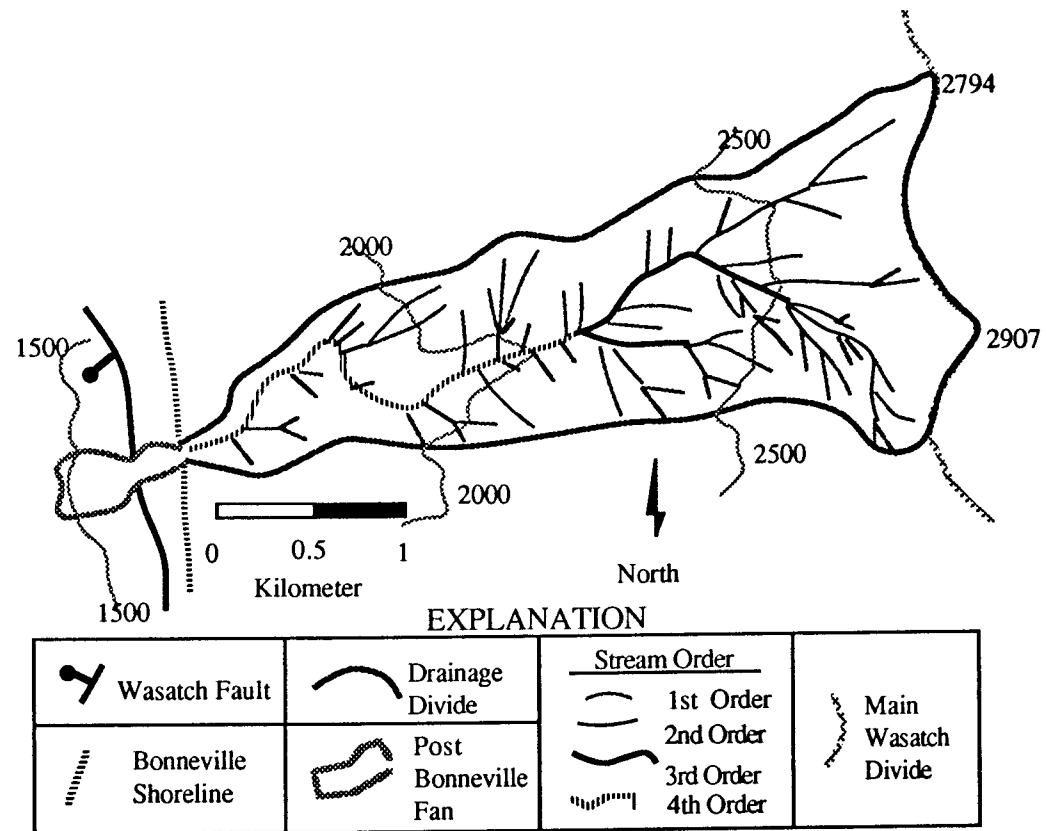


Figure D-4. Kays Creek (Middle Fork) drainage basin and fan showing selected geomorphic features. 500-m contour interval.

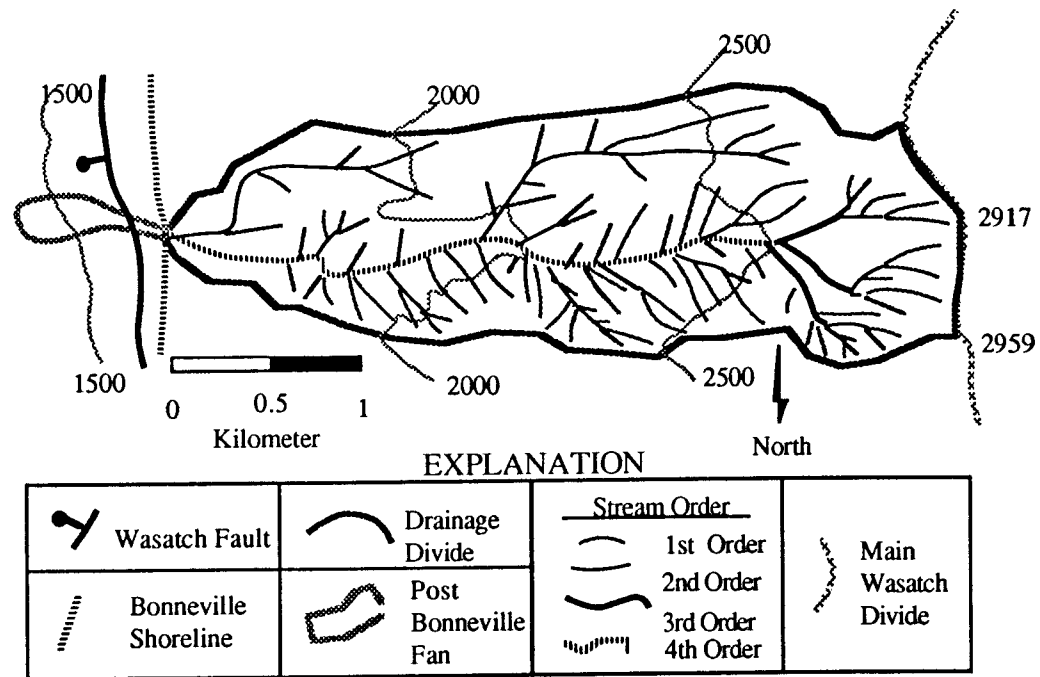
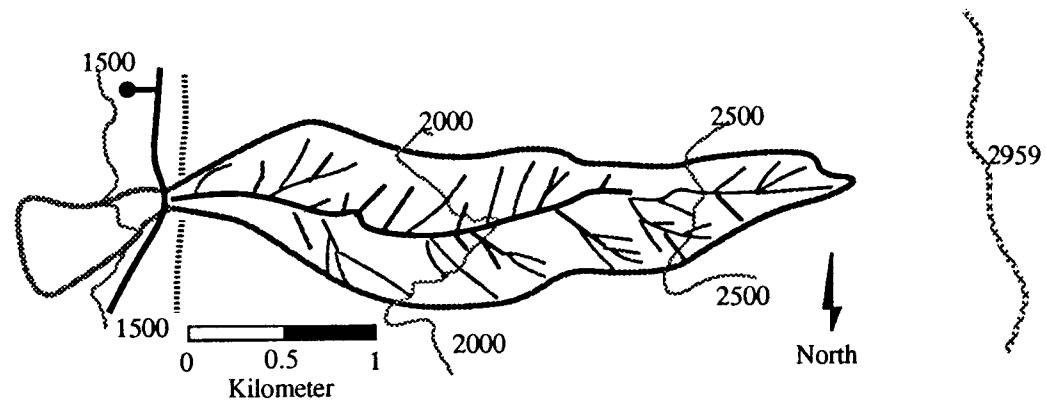


Figure D-5. Kays Creek (South Fork) drainage basin and fan showing selected geomorphic features. 500-m contour interval.



EXPLANATION









	Wasatch Fault		Drainage Divide	<u>Stream Order</u>	
	Bonneville Shoreline		Post Bonneville Fan		1st Order
					2nd Order
					3rd Order
					Main Wasatch Divide

Figure D-6. Snow Creek drainage basin and fan showing selected geomorphic features. 500-m contour interval.

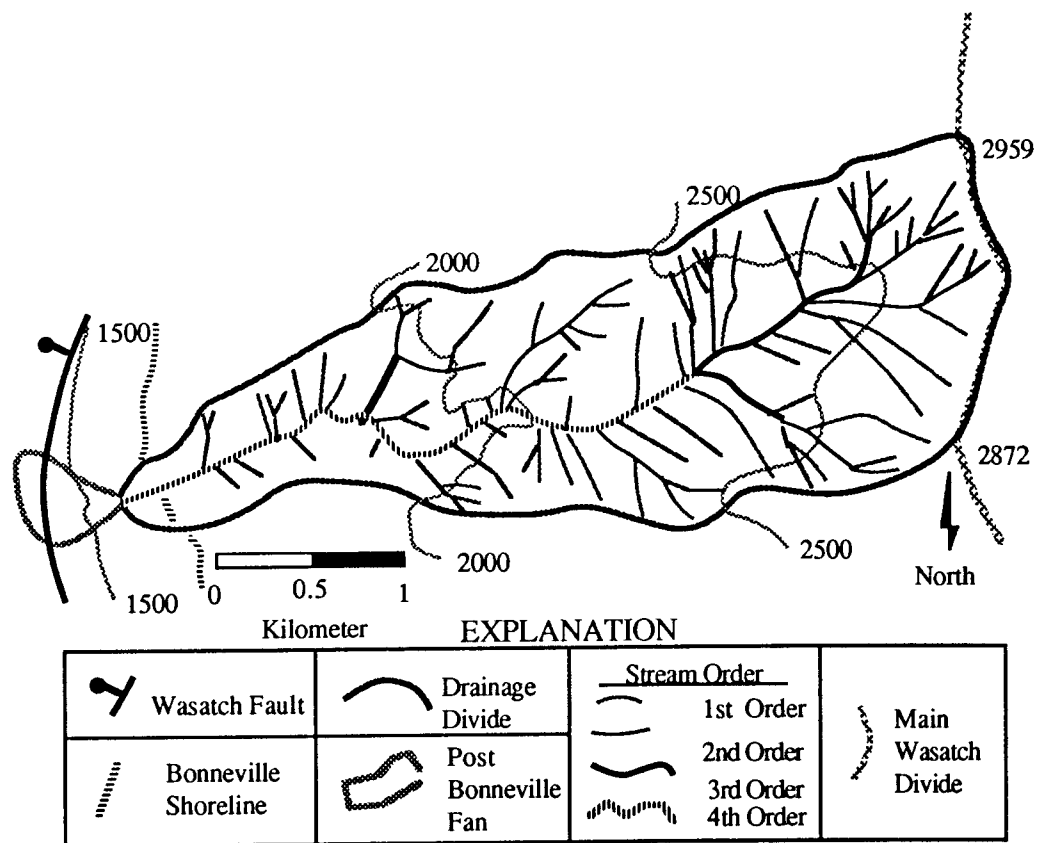


Figure D-7. Adams Canyon drainage basin and fan showing selected geomorphic features. 500-m contour interval.

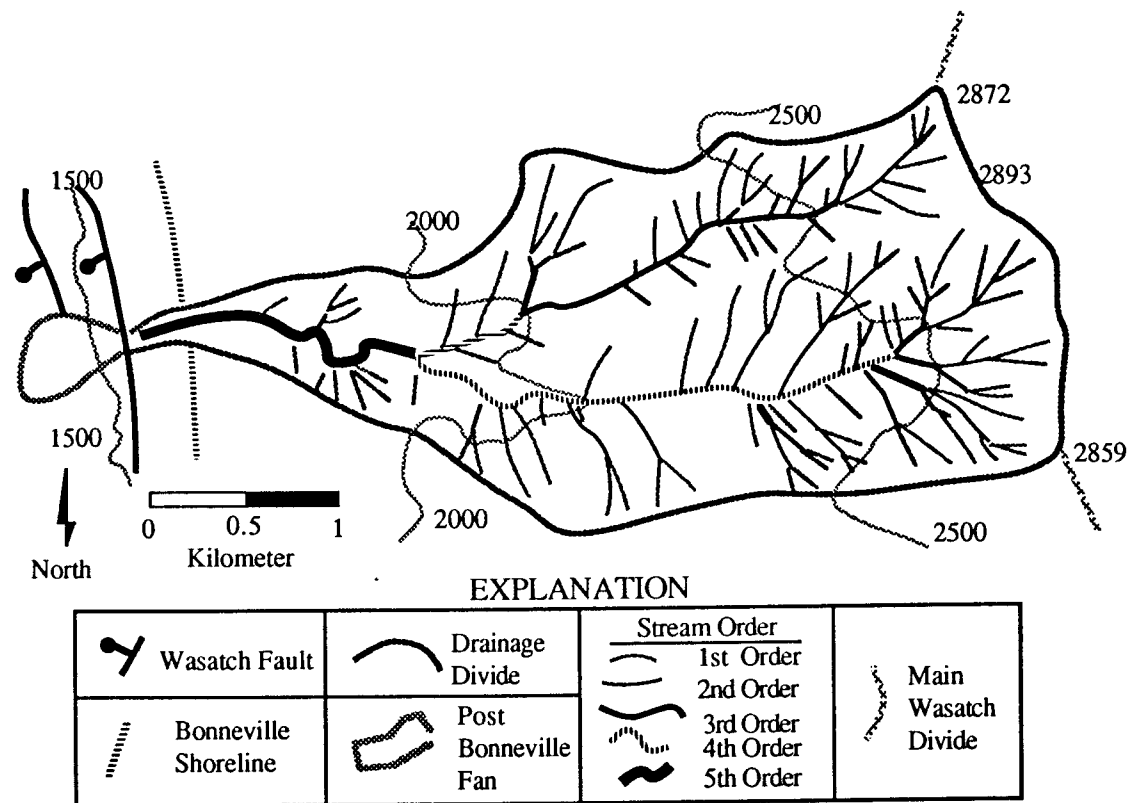


Figure D-8. Webb Canyon drainage basin and fan showing selected geomorphic features. 500-m contour interval.

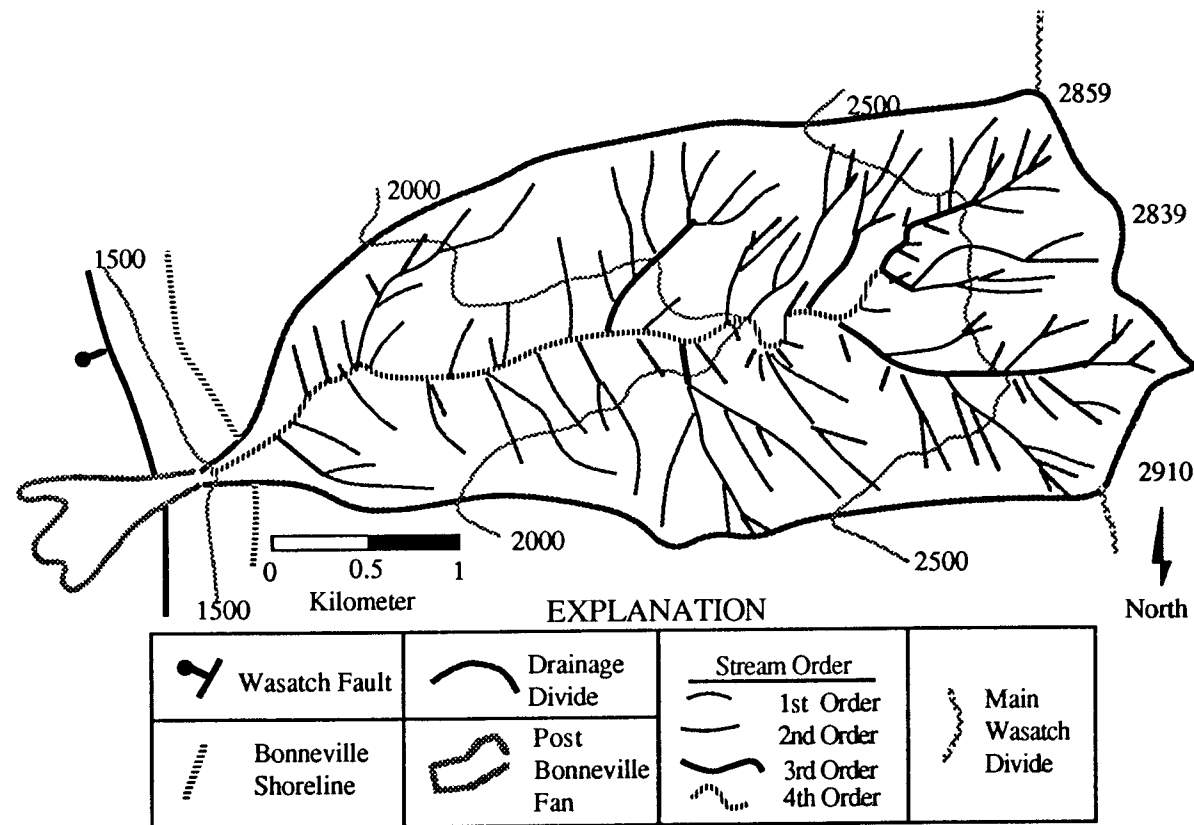


Figure D-9. Baer Creek drainage basin and fan showing selected geomorphic features. 500-m contour interval.

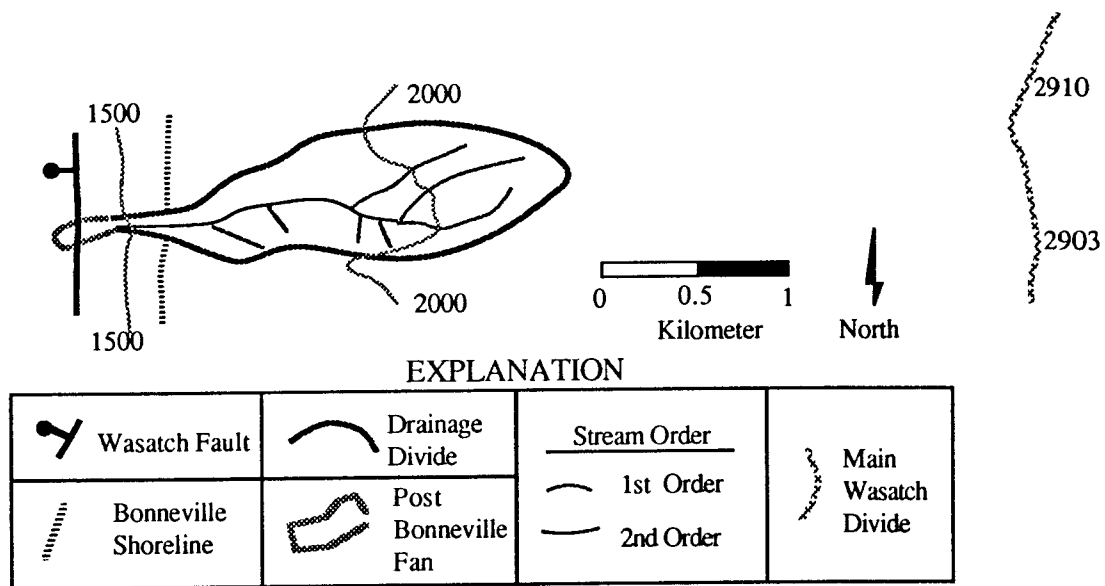


Figure D-10. Half Canyon drainage basin and fan showing selected geomorphic features. 500-m contour interval.

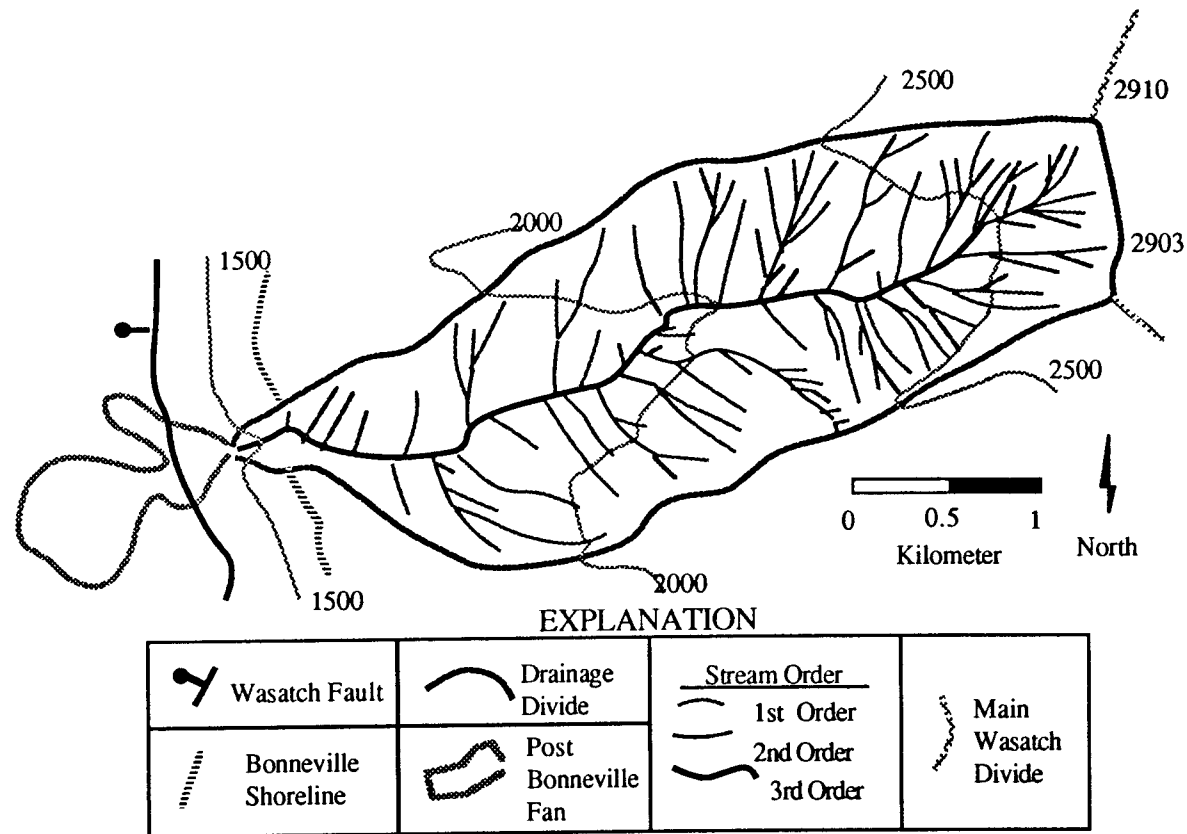


Figure D-11. Shepard Creek drainage basin and fan showing selected geomorphic features. 500-m contour interval.

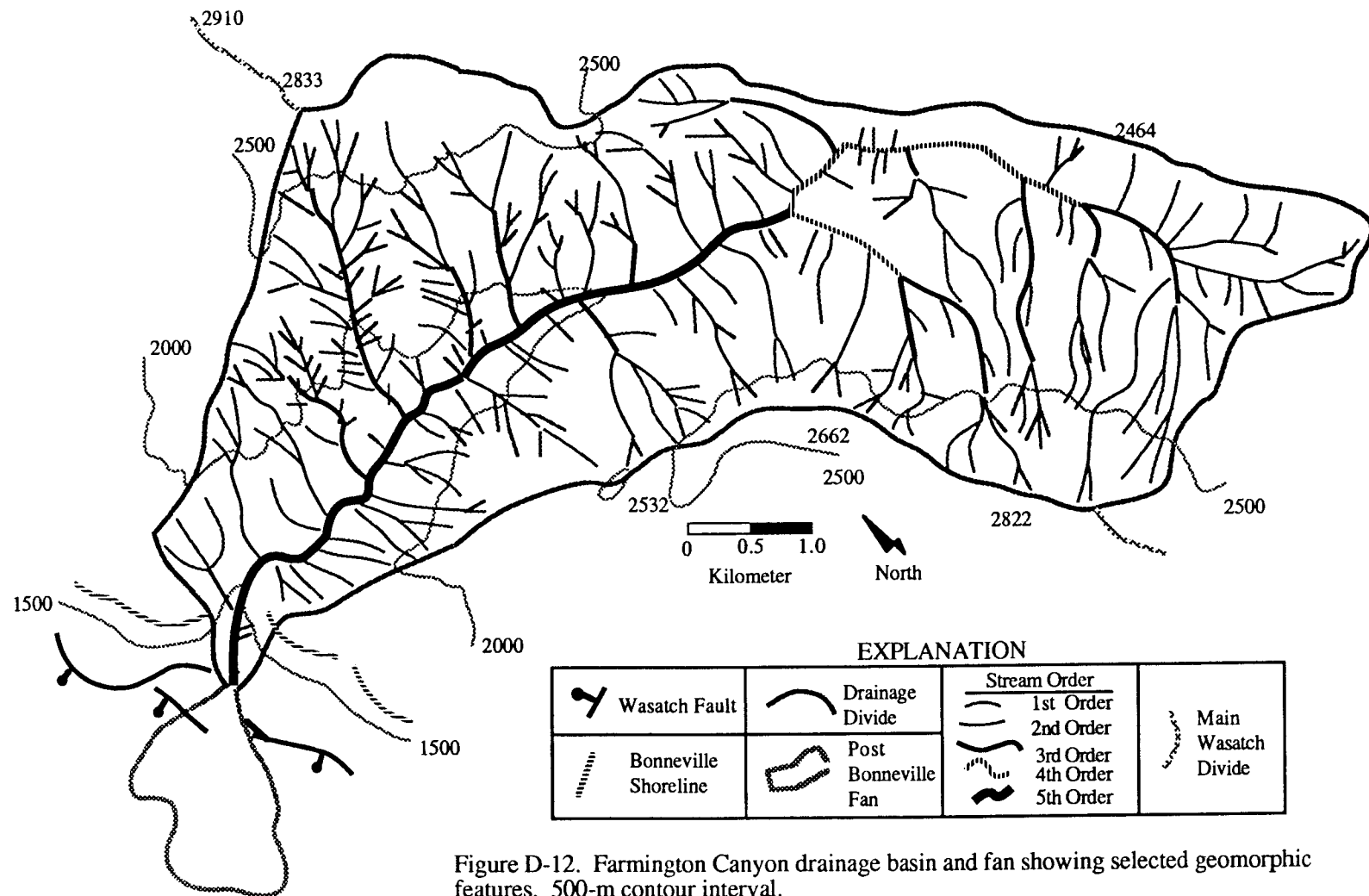


Figure D-12. Farmington Canyon drainage basin and fan showing selected geomorphic features. 500-m contour interval.

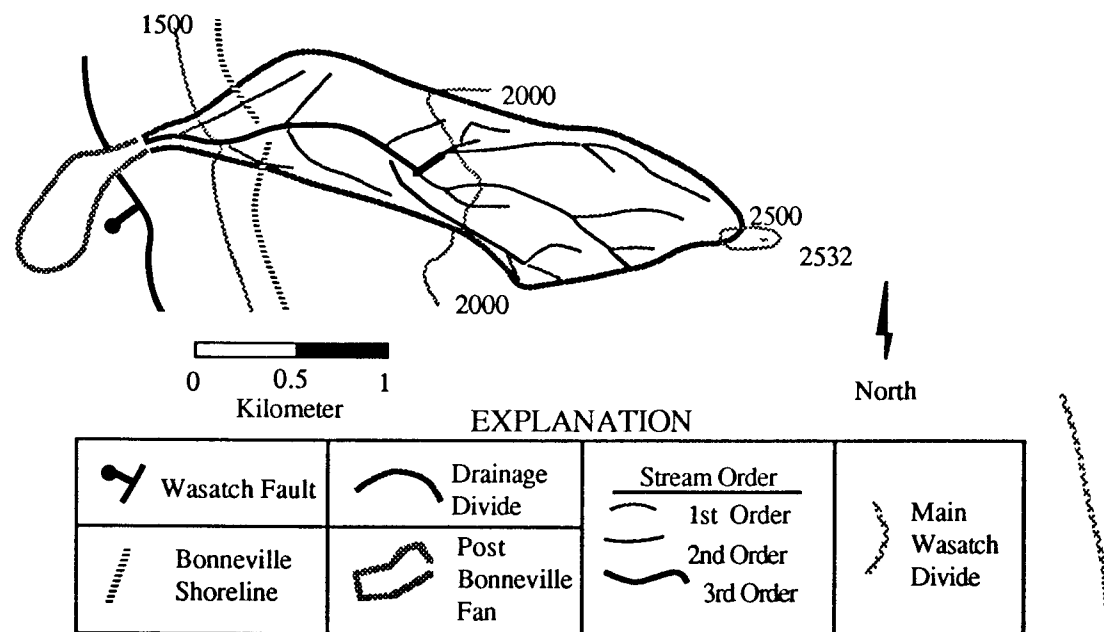


Figure D-13. Rudd Creek drainage basin and fan showing selected geomorphic features. 500-m contour interval.

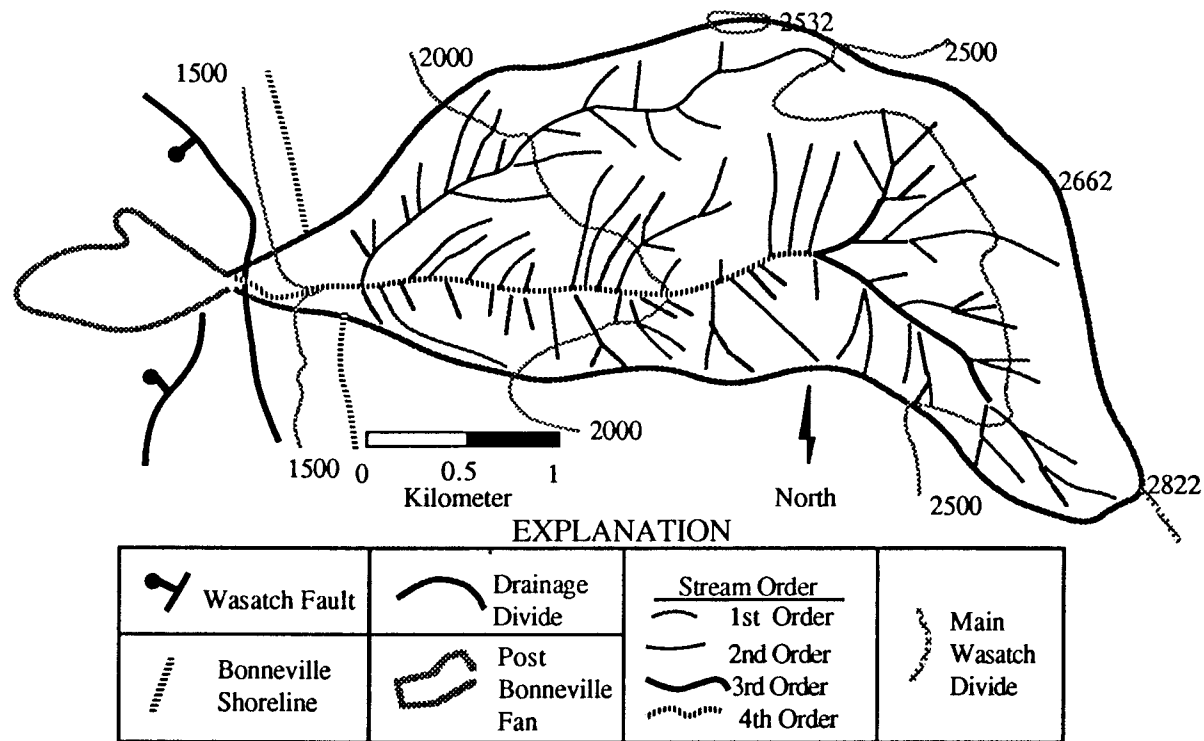


Figure D-14. Steed Canyon drainage basin and fan showing selected geomorphic features. 500-m contour interval.

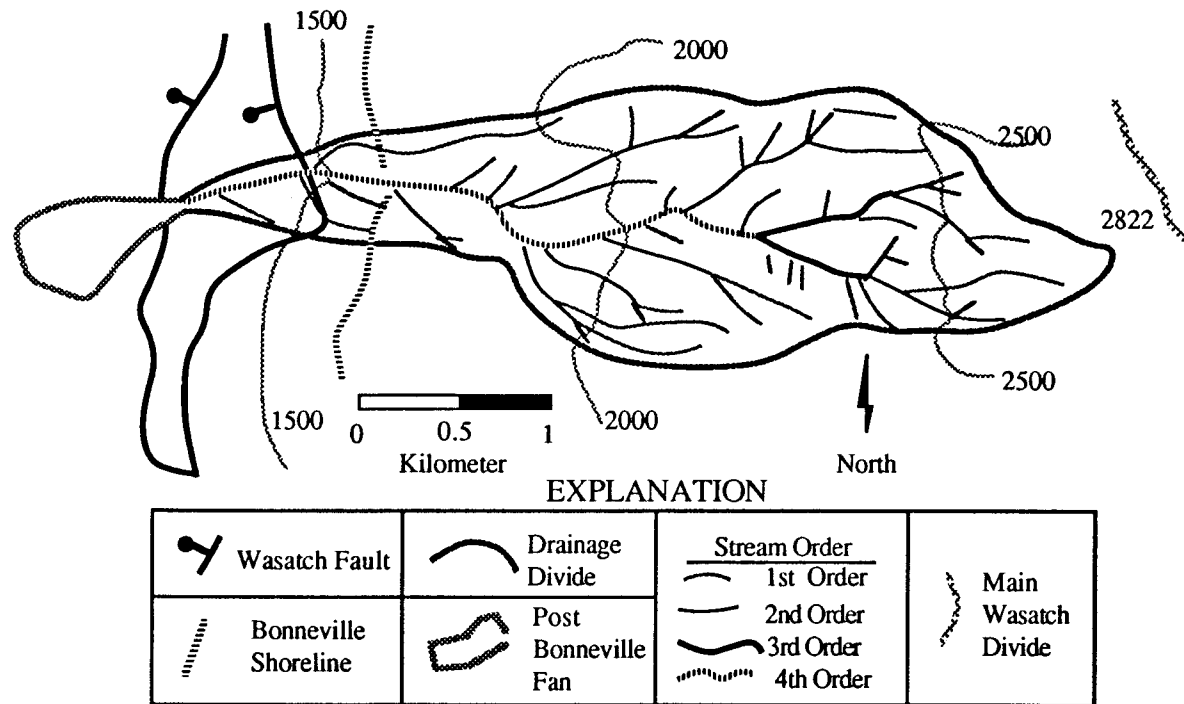


Figure D-15. Davis Creek drainage basin and fan showing selected geomorphic features. 500-m contour interval.

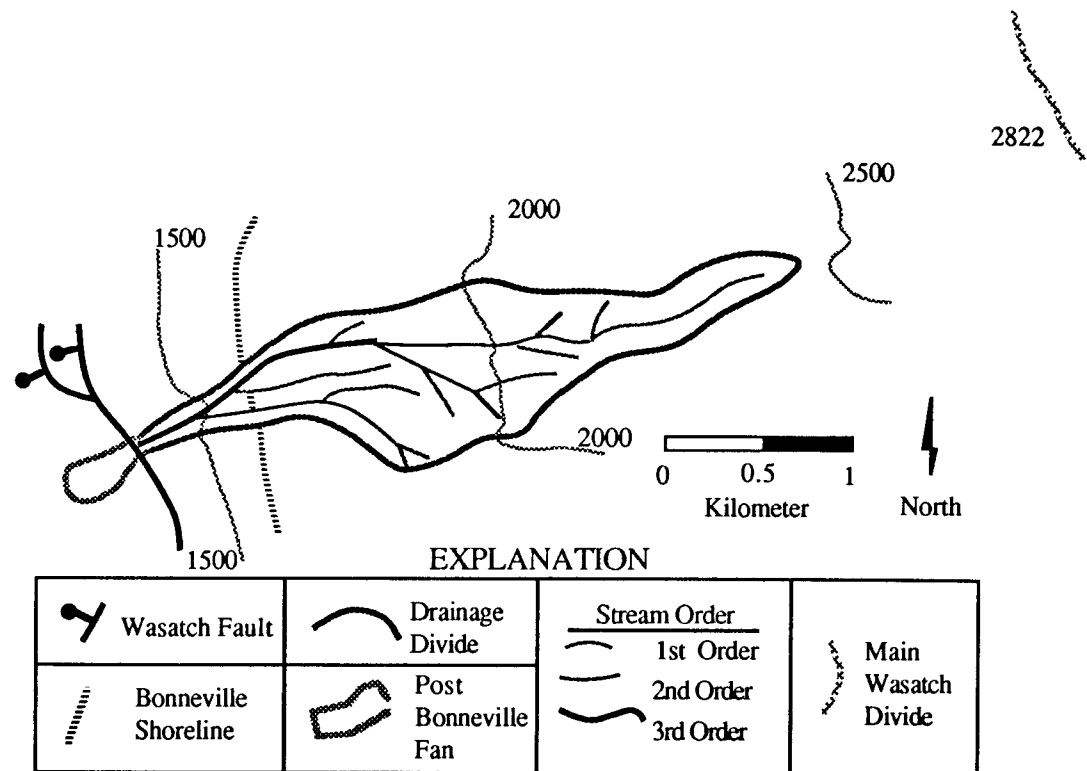


Figure D-16. Halfway Canyon drainage basin and fan showing selected geomorphic features. 500-m contour interval.

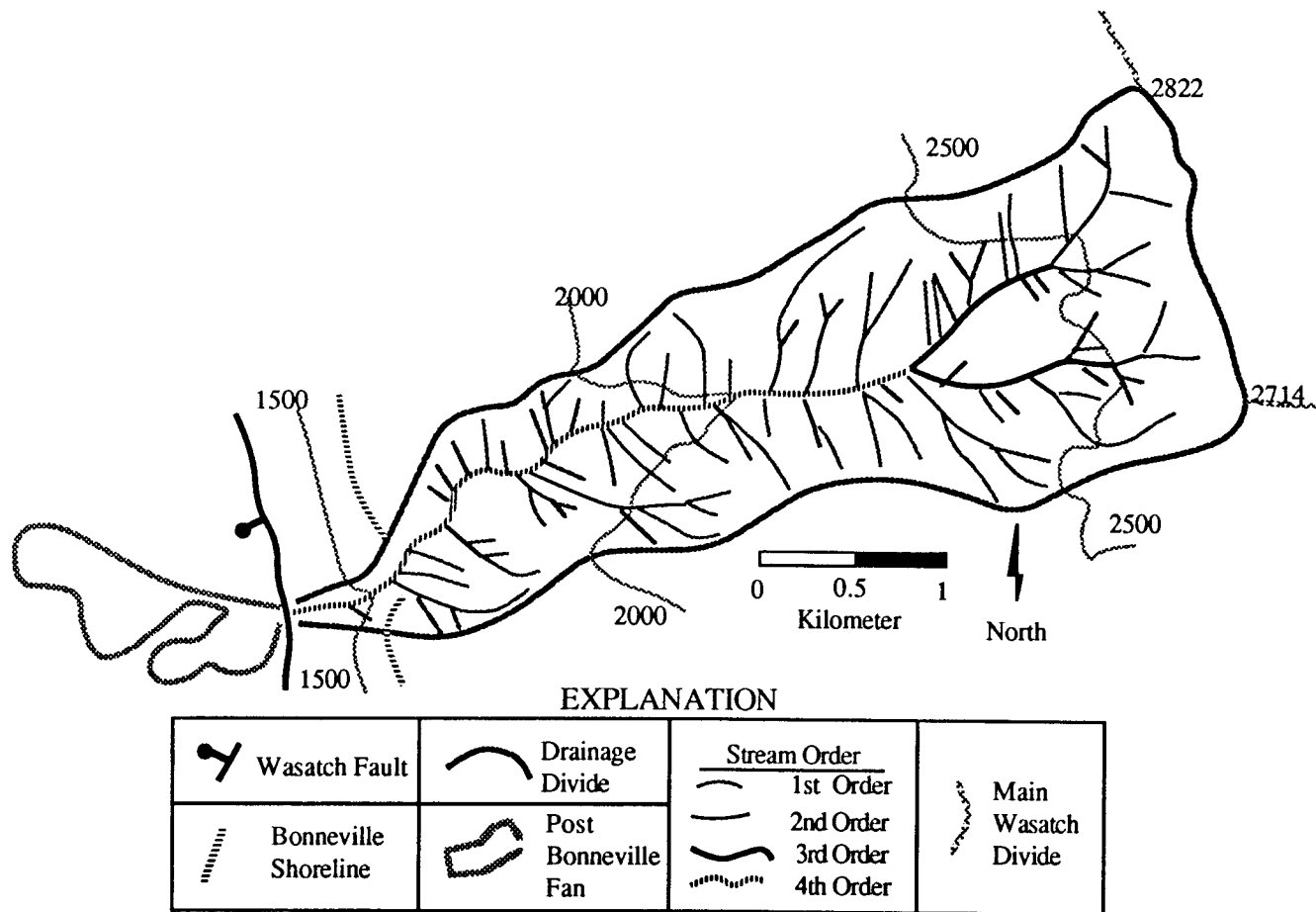


Figure D-17. Ricks Creek drainage basin and fan showing selected geomorphic features. 500-m contour interval.

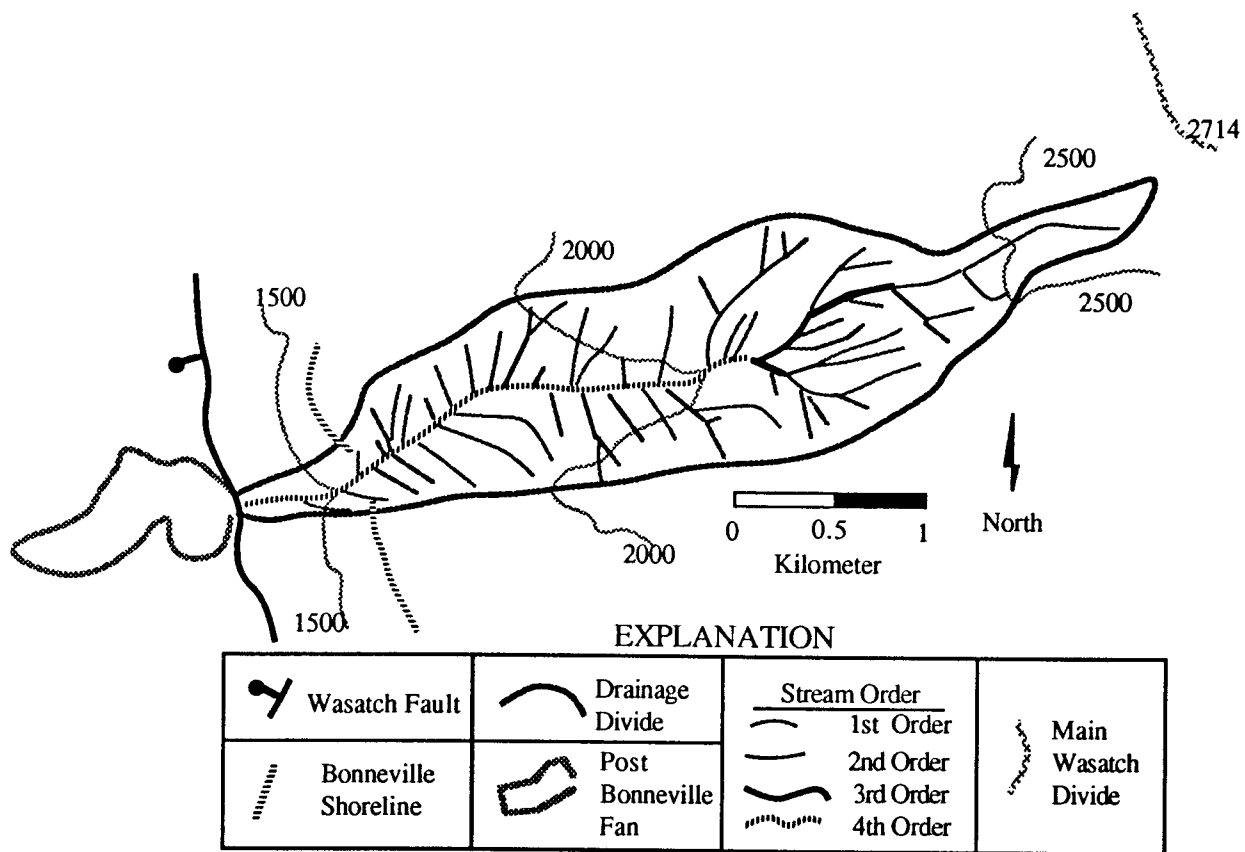


Figure D-18. Barnard Creek drainage basin and fan showing selected geomorphic features. 500-m contour interval.

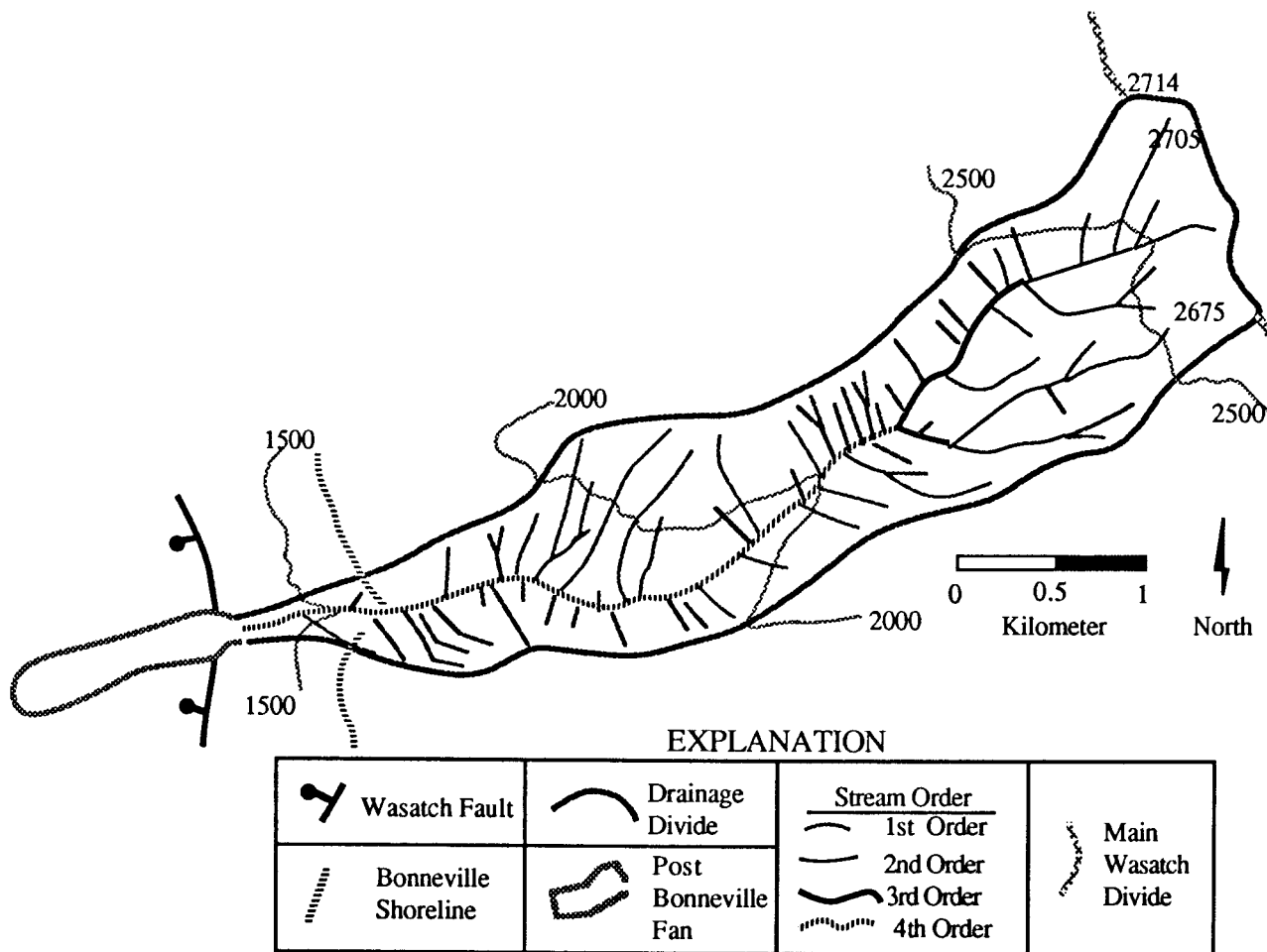


Figure D-19. Parrish Creek drainage basin and fan showing selected geomorphic features. 500-m contour interval.

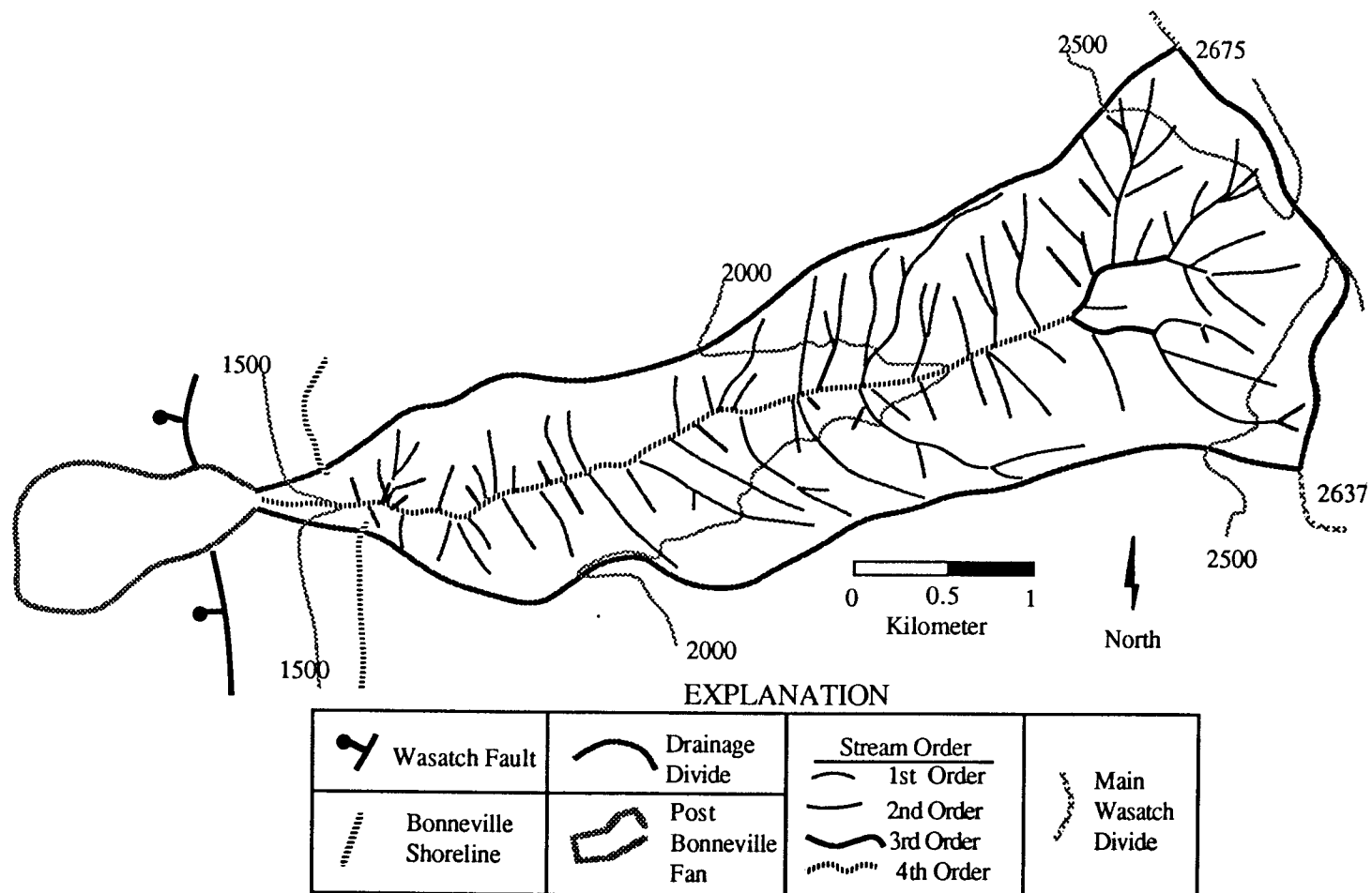


Figure D-20. Centerville Canyon drainage basin and fan showing selected geomorphic features. 500-m contour interval.

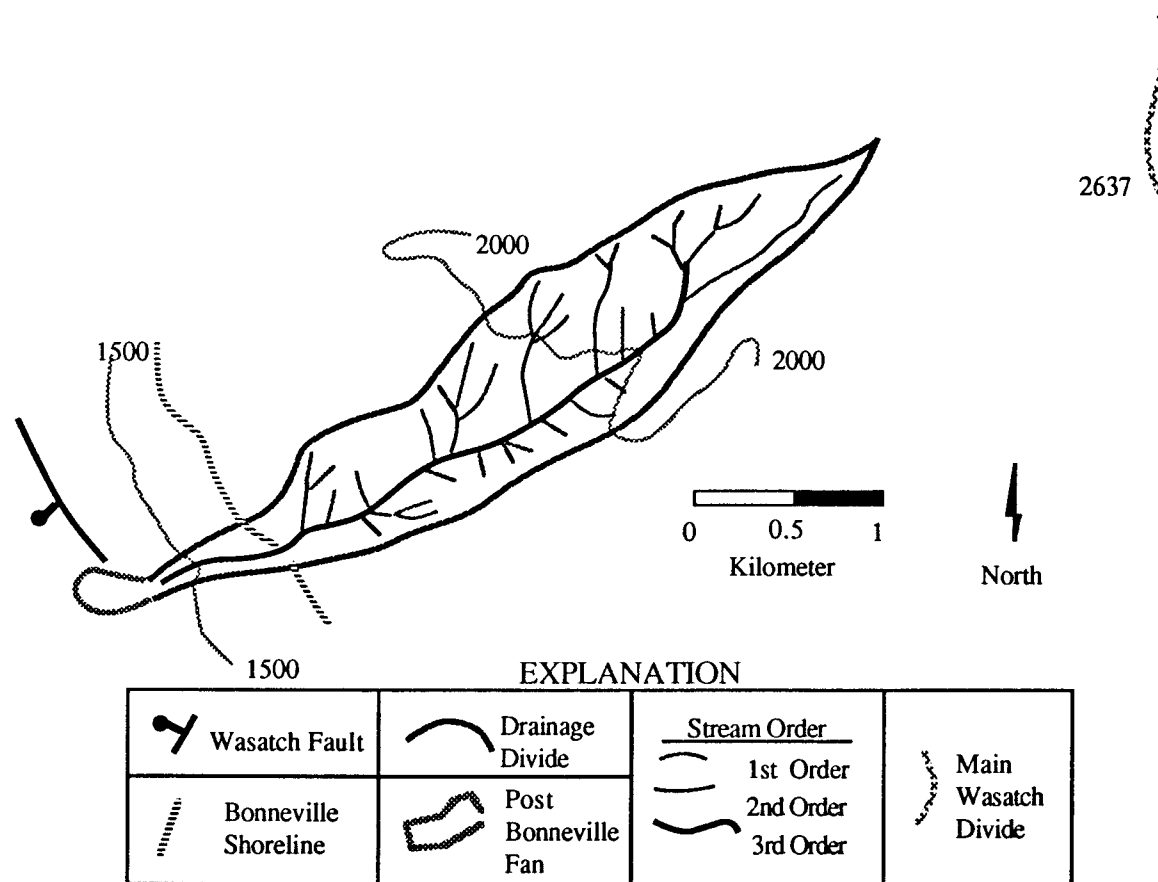


Figure D-21. Buckland Creek drainage basin and fan showing selected geomorphic features. 500-m contour interval.

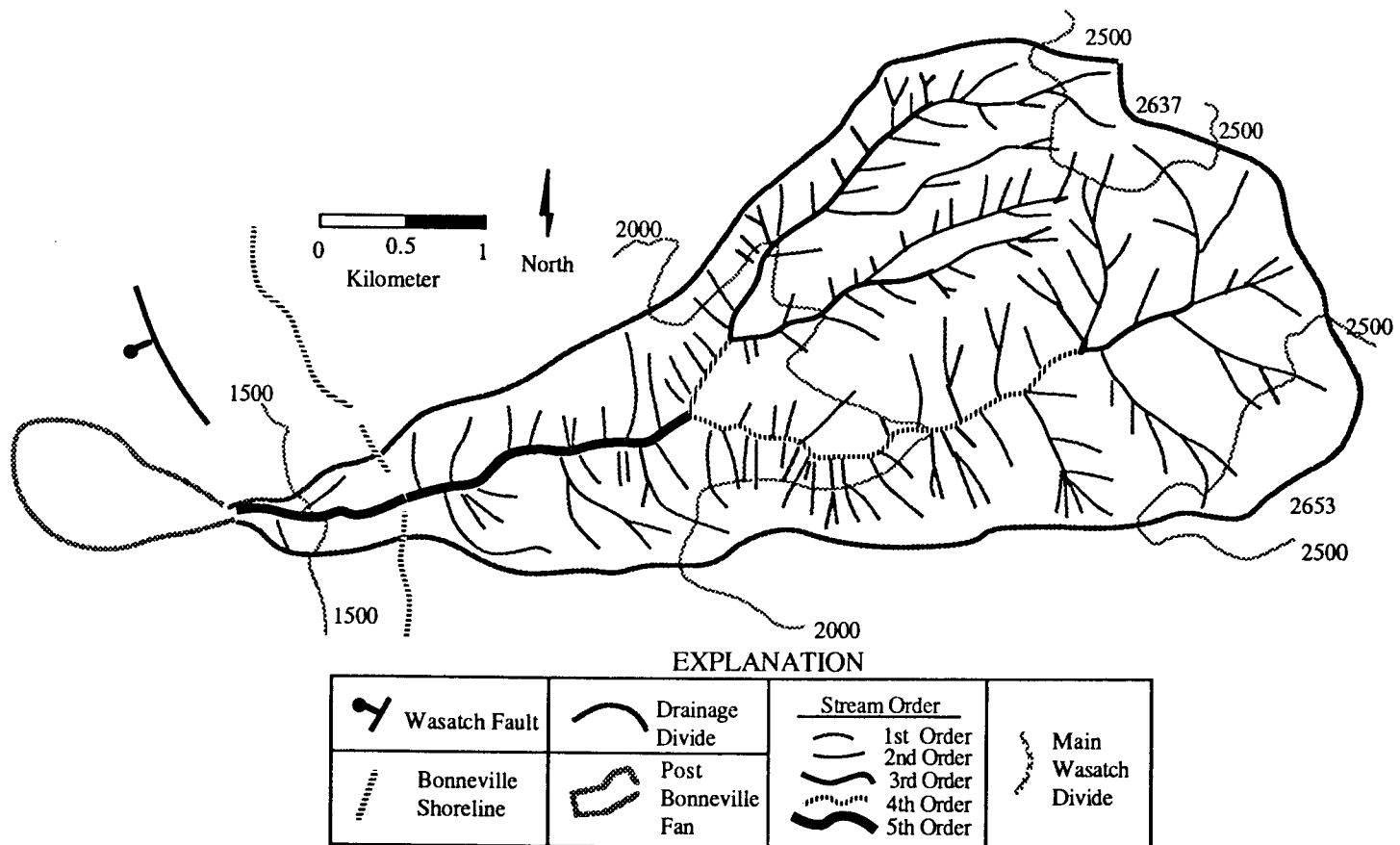


Figure D-22. Ward Canyon drainage basin and fan showing selected geomorphic features. 500-m contour interval.

where R_b is the basin relief in m and A_b is the basin area in m^2 . An R_u factor of 1.0 indicates that the basin relief and the nominal basin dimension are equal. The nominal basin dimension, D_b , is

$$D_b = (A_b)^{0.5} \quad (D-5)$$

$$= (L_b + W_b) / 2 \quad (D-6)$$

and $W_b = A_b / L_b \quad (D-7)$

where A_b is basin area in m^2 , L_b is basin length and W_b is nominal basin width, in m.

The basin form factor, F_o , was developed by Horton (1932) and defined as

$$F_o = A_b / (L_b)^2 \quad (D-8)$$

where A_b is basin area in m^2 and L_b is basin length in m. An F_o factor of 1.0 would correspond to a square basin while an F_o factor of $\pi/4$ ($= 0.785$) would indicate a circular basin. Elliptical basins would have F_o factors of $e_b \pi/4$ where the eccentricity, e_b , is defined as

$$e_b = W_b / L_b \quad (D-9)$$

where W_b is the basin width in m and L_b is the basin length in m.

The basin elongation factor, E_b , was developed by Schumm (1956) and is a comparison of the basin length to the diameter of a circle with the same area as the basin. The factor E_b is defined as

$$E_b = 2 (A_b/\pi)^{0.5} / L_b \quad (D-10)$$

where A_b is the basin area in m and L_b is the basin length in m. A basin elongation factor of 1.0 indicates a circular basin.

The lemniscate factor, K , developed by Chorley and others (1957) and defined as

$$K = L_b^2 / 4 A_b \quad (D-11)$$

where L_b is the basin length in m and A_b is the basin area in m^2 . The lemniscate factor reported in Table 13 is a modification of the factor developed by Chorley and others (1957). The equation of a lemniscate in polar coordinates is

$$r = L \cos (kt) \quad (D-12)$$

where L is the length of the long axis and k is a measure of the elongation (Scheidegger, 1961, p. 275). The area of a lemniscate is

$$A = \pi L^2 / 4 k \quad (D-13)$$

Therefore, the elongation of a lemniscate of length L_b required to approximate the area of a drainage basin, A_b , can be expressed as

$$K = \pi L_b^2 / 4 A_b \quad (D-14)$$

Thus, the lemniscate factor, K , reported in Table D-1 is π times the factor developed by Chorley and others (1957). Circular basins have lemniscate factors of 1.0; long, thin basins have lemniscate elongation factors > 1 while short, wide basins have factors < 1 . Goudie (1981, p. 44) notes that the lemniscate elongation (equation D-14) corresponds to the ellipticity index of Tinker (1971) and the reciprocal of Horton's (1932) form factor (equation D-8) as modified by Haggett (1965) and the squared reciprocal of Schumm's (1956) elongation factor (equation D-10).

APPENDIX E

SUMMARY OF MAGNITUDE - FREQUENCY RELATIONSHIPS

Magnitude-Frequency Relationships

The number of sedimentation events responsible for the post-Lake Bonneville alluvial fans in Davis County has been obscured by urbanization, mining of sand and gravel resources, and construction of debris basins. The unique preservation of the fan at Ricks Creek made it the best to use as a basis for this model. Incremental volumes of the ten historic and prehistoric sedimentation events at the Ricks Creek fan summarized in the text were used to develop annual frequency relationships using the Weibull plotting position formula

$$N_{PR} = Re / (PR+1) \quad (E-1)$$

where N_{PR} is the annual frequency for a period of record, PR, in years and Re is the event rank (modified from McCuen and Snyder, 1986, p. 113). Thus, the largest event is assigned a rank, Re, of 1, the second largest event is assigned a rank of 2, and the smallest event is assigned a rank of PR. The period of record, PR, was taken to be 10 ka for Holocene relationships, 4 ka for late Holocene relationships, and 140 yr for historic relationships. The smallest event was taken to be 0.001 m^3 , corresponding to M -3, as discussed above. The annual frequencies for this event were 0.9999 for a PR of 10 ka, 0.9998 for a PR of 4 ka, and 0.9929 for a PR of 140 yr.

A log linear relationship between sedimentation event magnitude and annual frequency is given by

$$\log N_{PR} = a + b M \quad (E-2)$$

where N_{PR} and M are as previously defined, a is the intercept coefficient, and b is the slope coefficient. Because $M = \log V$,

$$N_{PR} = 10^a \cdot V^b \quad (E-3)$$

is also true, where V is the volume of the sedimentation event. Prediction limits were also computed using standard statistical procedures (Ott, 1984, p. 298).

Evidence for intermediate sediment discharges appears to be lacking on alluvial fans in the study area; therefore, a non-linear relationship between sedimentation event magnitude and annual frequency is suggested. The discussion presented in the text suggests that sedimentation events in Davis County are relatively rare and virtually no sediment is discharged during a "normal" year. Therefore, a non-linear relationship is suggested in which the large events are known or estimated from geomorphic expression and historic records and all other events are taken to be 0.001 m^3 (M -3). Thus, at Ricks Creek during the 140-year historic period, 5 years had documented sediment discharges and 135 years are assumed to have virtually no sediment discharge.

Estimated volumes of historic and prehistoric sedimentation events in Davis County listed in Tables 18 and 22 were combined and ranked to compute magnitude-frequency relationships considered to be representative of the past 10 or 15 ka (Holocene time). Only historic sedimentation events (Table 18) were used in computing magnitude-frequency

relationships considered to be representative of the past 4 ka (late Holocene time) and 140 yr (historic time). As stated above, the smallest sedimentation event was taken to be M -3. The annual frequencies computed from the data in Tables 18 and 22 represent the cumulative number of sedimentation events normalized to the periods of record. Linear regression of these data was accomplished with a commercially available program called StatView (BrainPower, Inc., 1984) executed on a Macintosh 512K or Macintosh SE personal computer to yield mathematical expressions in the form of equation (E-2). Magnitude was taken as the independent variable and logarithmic transformations were applied to the frequency values. The regression coefficients for the magnitude-frequency relationships for the 22 alluvial fans in the study area are summarized in Table E-1.

Also included in Table E-1 are regression coefficients for 90 and 10 percent prediction limits using the relationship

$$N_{PR} \pm t_{\alpha/2} s_e \{1 + (1/n) + [(M - \bar{M})^2 / S_{MM}]\}^{0.5} \quad (E-4)$$

where $t_{\alpha/2}$ is Student's t parameter for 100(1- α) percent prediction, s_e is the standard error of regression, n is the number of observations in the sample, M is event magnitude, \bar{M} is the mean value of magnitude, and S_{MM} is the sum of squares about the mean value of M ;

$$S_{MM} = (\sum M^2 - [\sum M]^2 / n) \quad (E-5)$$

These regression coefficients were developed by computing 90 and 10 percent prediction values of N_{PR} at $M = -3$ and $M = 6$ with the aid of a program called "90PL.MN" written in BASIC and executed on a Macintosh 512K or Macintosh SE personal computer. The source code for program "90PL.MN" is presented in Appendix G. Values of Student's t statistic for $\alpha/2 = 0.05$ and $(n - 2)$ degrees of freedom were obtained from Ott (1984, p. 697). Linear regression of the values of $N_{PR,M=-3}$ and $N_{PR,M=6}$ were accomplished with keystroke statistical functions on a Hewlett-Packard 15C pocket calculator using magnitude as the independent variable and applying logarithmic transformations of frequency. The magnitude-frequency relationships for the 90 and 10 percent prediction limits are presented graphically on Figures E-1 to E-22. The ordinates of Figures E-1 to E-22 are represented as annual frequency on the left sides and as average recurrence interval on the right sides. The average recurrence interval is the reciprocal of annual frequency, expressed as

$$RI_{PR,M} = 1/N_{PR,M} \quad (E-6)$$

where $RI_{PR,M}$ is the average recurrence interval of events of magnitude M in a period of record of PR years and $N_{PR,M}$ is the annualized cumulative number of events of magnitude M or greater in that period.

For the historic period of record, 140 years, means and standard deviations of sedimentation event magnitudes were calculated on the basis of the volumes of historic sedimentation events (Table 18) assuming all other years had sediment delivery volumes of 0.001 m^3 ($M = -3$); the calculations were performed with statistical functions in a commercially available spreadsheet program (Excel by Microsoft) executed on a Macintosh SE personal computer. The mean and standard deviation values are listed in Table E-2. Fans with no historic sedimentation events clearly have mean event magnitudes of -3, but rather than report standard deviations of zero for these fans, the mean values of the standard deviations for those fans with historic sedimentation events are reported. The

magnitude-frequency relationships for these extreme-value distributions are shown on Figures E-1 to E-22, but no mathematical expressions were developed to describe them.

Table E-1. Summary of regression coefficients describing magnitude-frequency relationships. Regression coefficients are in the form $\log N_{PR} = a + b M$ and are valid for $-3 \leq M \leq 6$. The periods of record are Holocene, late Holocene, and historic; Holocene is taken to be 10 ka for fans with apex elevations < 1450 m and 15 ka for fans with apex elevations ≥ 1450 m; late Holocene is taken to be 4 ka; historic is taken to be 140 yr. Fans with no historic sedimentation events have relationships computed for Holocene periods of record only. Mean relationships computed from data in Tables 18 and 22. Prediction limits based on standard statistical procedures and computed with BASIC program "90PL.MN" (Appendix G). Coefficient of determination, r^2 , pertains to mean relationship; number of data values, n , includes $M - 3$ for all fans; Student's t parameter from Ott (1984, p. 697) for $\alpha/2 = 0.05$ and $(n-2)$ degrees of freedom. Student's t parameter and prediction limits are not reported for those fans with only one late Holocene or historic sedimentation event because they would have zero degrees of freedom.

Fan	Period of Record	90 Percent Prediction Limit		Mean Relationship		10 Percent Prediction Limit		r^2	n	Student's t
		a	b	a	b	a	b			
Corbett	Holocene	-0.992	-0.500	-1.452	-0.490	-1.912	-0.479	0.989	6	2.132
Hobbs	Holocene	-0.991	-0.501	-1.453	-0.490	-1.915	-0.478	0.989	6	2.132
Lightning	Holocene	-1.043	-0.494	-1.440	-0.484	-1.838	-0.474	0.989	7	2.015
	Late Holocene	—	—	-1.555	-0.518	—	—	1	2	—
	Historic	—	—	-0.929	-0.309	—	—	1	2	—
Kays (Middle)	Holocene	-0.744	-0.473	-1.601	-0.454	-2.459	-0.435	0.943	8	1.943
	Late Holocene	-0.954	-0.581	-1.769	-0.591	-2.584	-0.601	0.999	3	6.314
	Historic	0.271	-0.327	-1.025	-0.342	-2.321	-0.357	0.993	3	6.314
Kays (South)	Holocene	-1.038	-0.464	-1.553	-0.452	-2.068	-0.440	0.954	13	1.796
	Late Holocene	-1.114	-0.462	-1.424	-0.457	-1.733	-0.451	0.990	8	1.943
	Historic	-0.386	-0.261	-0.711	-0.255	-1.036	-0.249	0.966	8	1.943
Snow	Holocene	-0.870	-0.468	-1.349	-0.456	-1.828	-0.444	0.990	6	2.132
Adams	Holocene	-0.907	-0.478	-1.381	-0.466	-1.855	-0.454	0.991	6	2.132
Webb	Holocene	-0.738	-0.467	-1.563	-0.448	-2.387	-0.429	0.946	8	1.943
	Late Holocene	-1.081	-0.563	-1.713	-0.569	-2.345	-0.575	0.999	3	6.314
	Historic	-0.542	-0.327	-0.991	-0.331	-1.440	-0.335	0.999	3	6.314
Baer	Holocene	-0.996	-0.464	-1.356	-0.453	-1.717	-0.443	0.980	12	1.812
	Late Holocene	-0.823	-0.441	-1.285	-0.431	-1.748	-0.421	0.983	7	2.015
	Historic	-0.118	-0.248	-0.671	-0.236	-1.224	-0.224	0.923	7	2.015
Half	Holocene	-0.971	-0.500	-1.450	-0.490	-1.930	-0.480	0.990	6	2.132
Shepard	Historic	-0.715	-0.414	-1.213	-0.399	-1.711	-0.384	0.953	13	1.796
	Late Holocene	-0.568	-0.506	-1.511	-0.505	-2.455	-0.504	0.999	3	6.314
	Historic	0.469	-0.293	-0.875	-0.292	-2.219	-0.291	0.992	3	6.314

Table E-1. Continued.

Fan	Period of Record	90 Percent Prediction Limit		Mean Relationship		10 Percent Prediction Limit		r^2	Student's	
		a	b	a	b	a	b		n	t
Farmington	Holocene	-0.309	-0.396	-0.826	-0.380	-1.343	-0.364	0.827	40	1.687
	Late Holocene	-0.807	-0.407	-1.136	-0.398	-1.465	-0.389	0.983	10	1.860
	Historic	-0.019	-0.228	-0.545	-0.214	-1.072	-0.200	0.868	10	1.860
Rudd	Holocene	-0.756	-0.453	-1.381	-0.437	-2.006	-0.421	0.967	8	1.943
	Late Holocene	1.778	-0.489	-1.506	-0.481	-4.790	-0.473	0.983	3	6.314
	Historic	0.259	-0.284	-0.868	-0.281	-1.996	-0.278	0.994	3	6.314
Steed	Holocene	-0.832	-0.448	-1.264	-0.436	-1.696	-0.424	0.977	10	1.860
	Late Holocene	-1.030	-0.434	-1.274	-0.429	-1.518	-0.424	0.998	5	2.353
	Historic	-0.199	-0.250	-0.697	-0.240	-1.195	-0.230	0.973	5	2.353
Davis	Holocene	-0.920	-0.440	-1.355	-0.429	-1.790	-0.418	0.964	13	1.796
	Late Holocene	-0.950	-0.442	-1.329	-0.434	-1.708	-0.426	0.985	8	1.943
	Historic	-0.230	-0.249	-0.666	-0.240	-1.101	-0.231	0.983	8	1.943
Halfway	Holocene	-0.965	-0.500	-1.450	-0.490	-1.934	-0.480	0.989	6	2.132
Ricks	Holocene	-0.842	-0.444	-1.255	-0.432	-1.668	-0.420	0.975	11	1.833
	Late Holocene	-0.909	-0.434	-1.262	-0.426	-1.614	-0.418	0.993	6	2.132
	Historic	-0.150	-0.248	-0.674	-0.236	-1.198	-0.225	0.951	6	2.132
Barnard	Holocene	-0.936	-0.450	-1.295	-0.440	-1.654	-0.430	0.987	9	1.895
	Late Holocene	-0.977	-0.463	-1.366	-0.458	-1.754	-0.453	0.998	4	2.920
	Historic	-0.138	-0.268	-0.770	-0.260	-1.401	-0.252	0.982	4	2.920
Parrish	Holocene	-1.017	-0.463	-1.384	-0.454	-1.750	-0.445	0.986	9	1.895
	Late Holocene	-0.223	-0.450	-1.390	-0.433	-2.557	-0.417	0.979	4	2.920
	Historic	-0.448	-0.254	-0.773	-0.250	-1.097	-0.245	0.995	4	2.920
Centerville	Holocene	-0.564	-0.430	-1.351	-0.410	-2.137	-0.390	0.959	7	2.015
	Late Holocene	—	—	-1.715	-0.572	—	—	1	2	—
	Historic	—	—	-1.025	-0.341	—	—	1	2	—
Buckland	Holocene	-0.927	-0.488	-1.412	-0.477	-1.898	-0.466	0.989	6	2.132
Ward	Holocene	-0.744	-0.429	-1.263	-0.415	-1.782	-0.401	0.982	7	2.015
	Late Holocene	—	—	-1.503	-0.501	—	—	1	2	—
	Historic	—	—	-0.899	-0.298	—	—	1	2	—

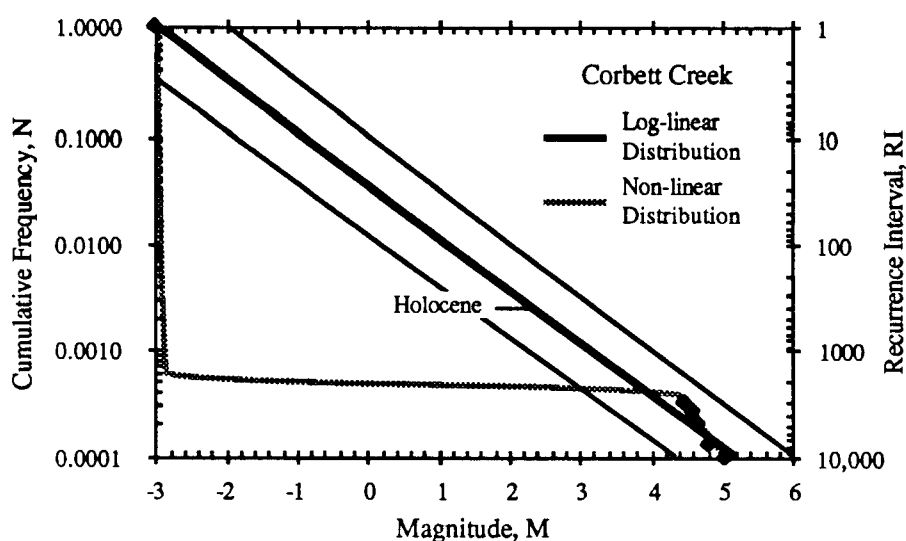


Figure E-1. Magnitude-frequency relationship for sedimentation events on the Corbett Creek fan. Cumulative frequency, N , is the average number of events of magnitude M per year; recurrence interval, RI , is the average number of years between re-occurrences of magnitude M events. Heavy solid line represents an assumed exponential distribution of event magnitudes; thin solid lines represent ± 90 percent prediction limits. Shaded line represents apparent "actual" distribution of event magnitudes. Holocene refers to post-Lake Bonneville period of sediment accumulation, taken to be 10 ka.

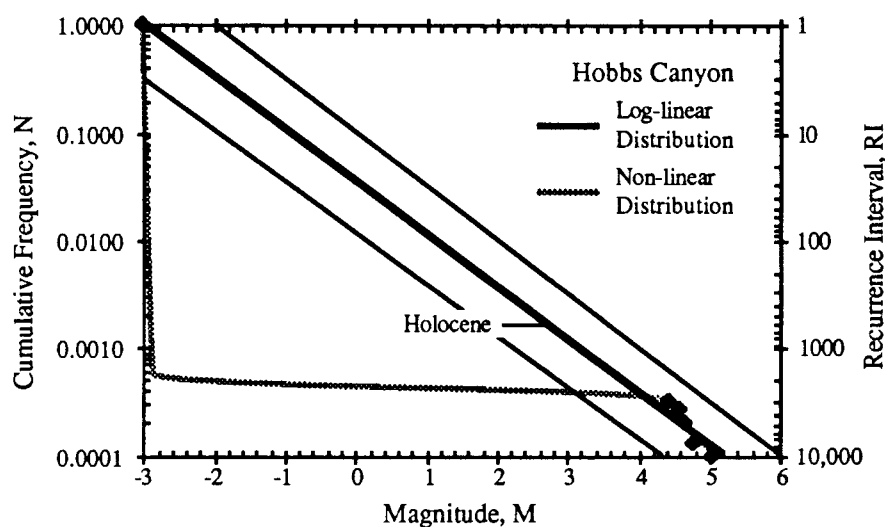


Figure E-2. Magnitude-frequency relationship for sedimentation events on the Hobbs Canyon fan. Cumulative frequency, N , is the average number of events of magnitude M per year; recurrence interval, RI , is the average number of years between re-occurrences of magnitude M events. Heavy solid line represents an assumed exponential distribution of event magnitudes; thin solid lines represent ± 90 percent prediction limits. Shaded line represents apparent "actual" distribution of event magnitudes. Holocene refers to post-Lake Bonneville period of sediment accumulation, taken to be 10 ka.

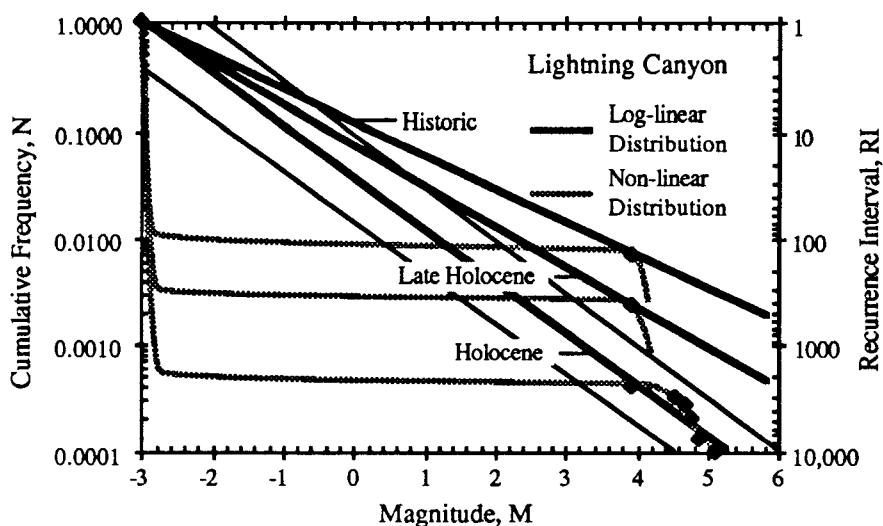


Figure E-3. Magnitude-frequency relationship for sedimentation events on the Lightning Canyon fan. Cumulative frequency, N , is the average number of events of magnitude M per year; recurrence interval, RI , is the average number of years between re-occurrences of magnitude M events. Heavy solid line represents an assumed exponential distribution of event magnitudes; thin solid lines represent ± 90 percent prediction limits. Shaded line represents apparent "actual" distribution of event magnitudes. Holocene refers to post-Lake Bonneville period of sediment accumulation, taken to be 10 ka; Late-Holocene is taken to be the last 4 ka; Historic is 140 years.

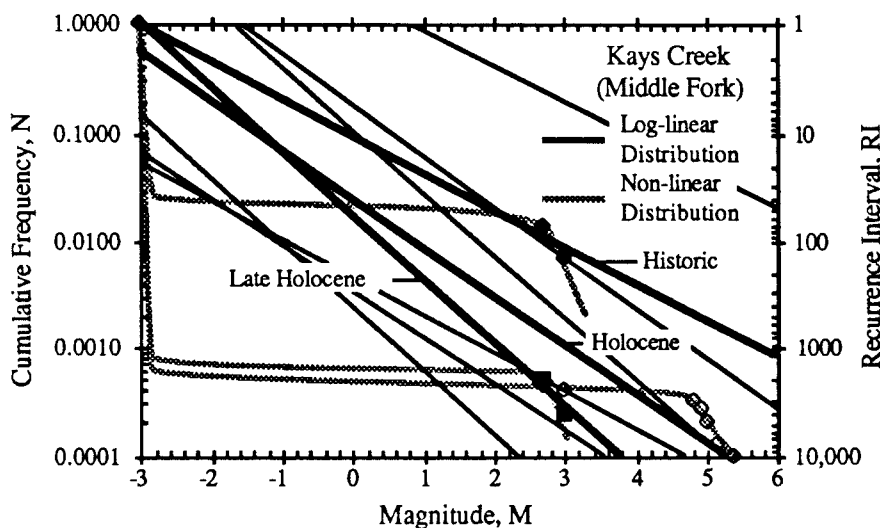


Figure E-4. Magnitude-frequency relationship for sedimentation events on the Kays Creek (Middle Fork) fan. Cumulative frequency, N , is the average number of events of magnitude M per year; recurrence interval, RI , is the average number of years between re-occurrences of magnitude M events. Heavy solid lines represent an assumed exponential distribution of event magnitudes; thin solid lines represent ± 90 percent prediction limits. Shaded lines represent apparent "actual" distribution of event magnitudes. Holocene refers to post-Lake Bonneville period of sediment accumulation, taken to be 10 ka; Late-Holocene is taken to be the last 4 ka; Historic is 140 years.

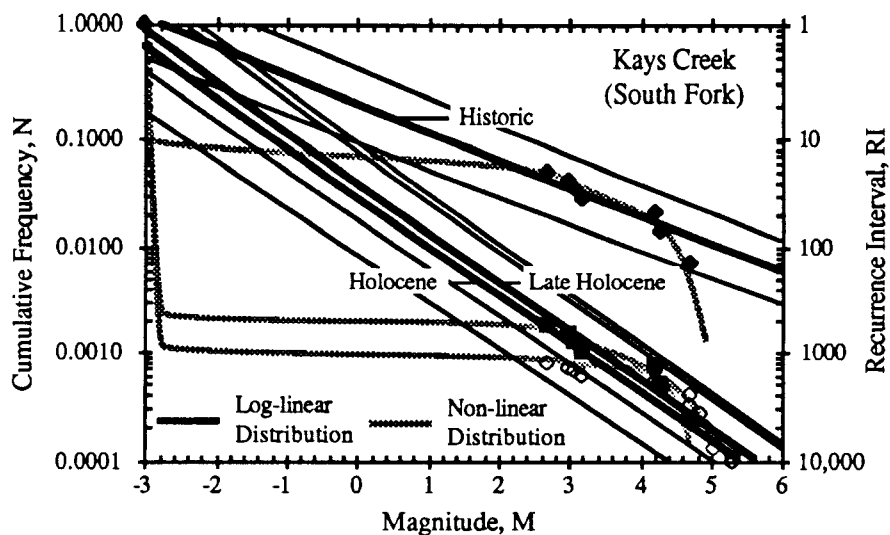


Figure E-5. Magnitude-frequency relationship for sedimentation events on the Kays Creek (South Fork) fan. Cumulative frequency, N , is the average number of events of magnitude M per year; recurrence interval, RI , is the average number of years between re-occurrences of magnitude M events. Heavy solid lines represent an assumed exponential distribution of event magnitudes; thin solid lines represent ± 90 percent prediction limits. Shaded lines represent apparent "actual" distribution of event magnitudes. Holocene refers to post-Lake Bonneville period of sediment accumulation, taken to be 10 ka; Late-Holocene is taken to be the last 4 ka; Historic is 140 years.

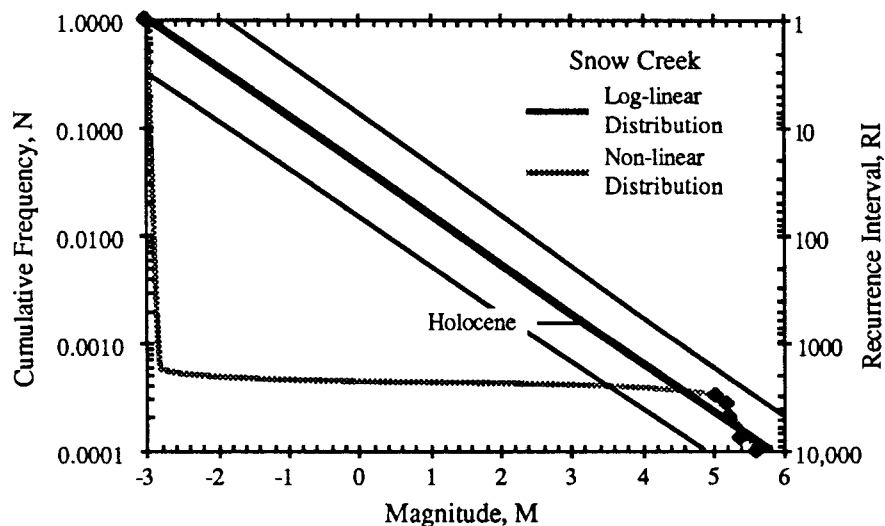


Figure E-6. Magnitude-frequency relationship for sedimentation events on the Snow Creek fan. Cumulative frequency, N , is the average number of events of magnitude M per year; recurrence interval, RI , is the average number of years between re-occurrences of magnitude M events. Heavy solid line represents an assumed exponential distribution of event magnitudes; thin solid lines represent ± 90 percent prediction limits. Shaded line represents apparent "actual" distribution of event magnitudes. Holocene refers to post-Lake Bonneville period of sediment accumulation, taken to be 10 ka.

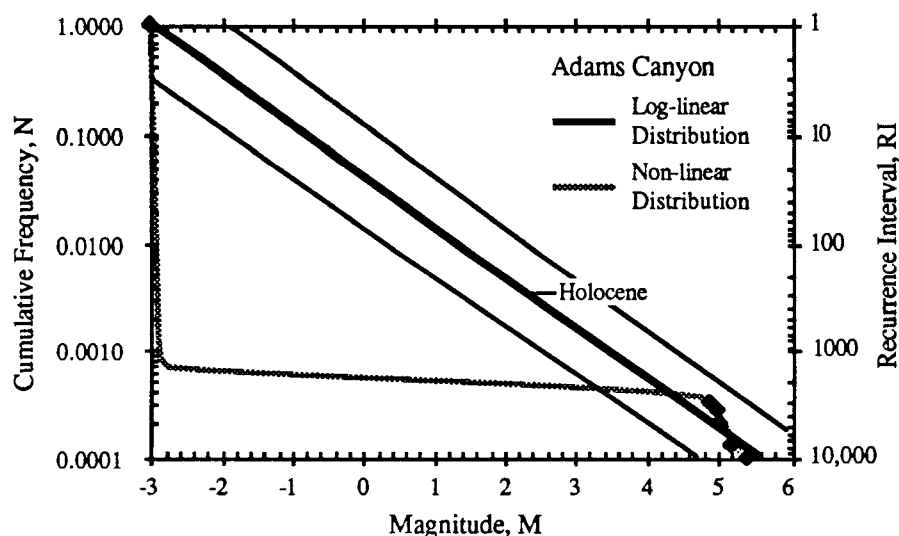


Figure E-7. Magnitude-frequency relationship for sedimentation events on the Adams Canyon fan. Cumulative frequency, N , is the average number of events of magnitude M per year; recurrence interval, RI , is the average number of years between re-occurrences of magnitude M events. Heavy solid line represents an assumed exponential distribution of event magnitudes; thin solid lines represent ± 90 percent prediction limits. Shaded line represents apparent "actual" distribution of event magnitudes. Holocene refers to post-Lake Bonneville period of sediment accumulation, taken to be 10 ka.

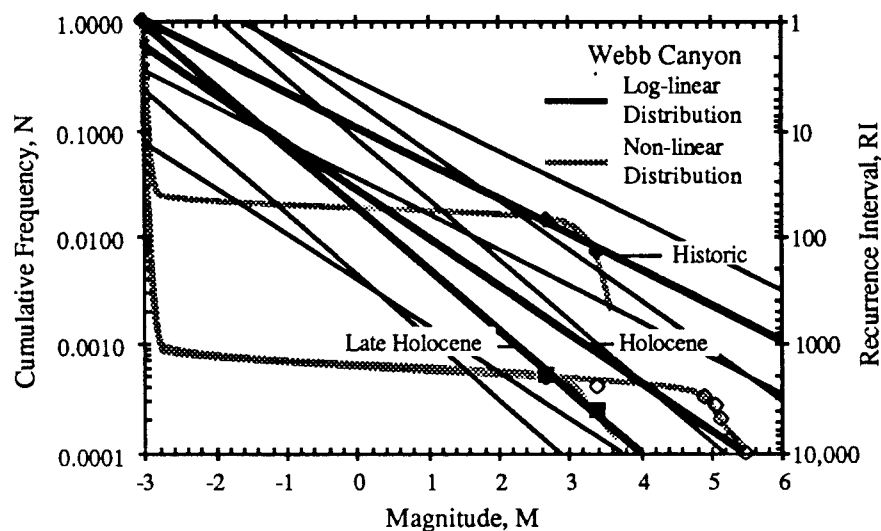


Figure E-8. Magnitude-frequency relationship for sedimentation events on the Webb Canyon fan. Cumulative frequency, N , is the average number of events of magnitude M per year; recurrence interval, RI , is the average number of years between re-occurrences of magnitude M events. Heavy solid lines represent an assumed exponential distribution of event magnitudes; thin solid lines represent ± 90 percent prediction limits. Shaded lines represent apparent "actual" distribution of event magnitudes. Holocene refers to post-Lake Bonneville period of sediment accumulation, taken to be 10 ka; Late-Holocene is taken to be the last 4 ka; Historic is 140 years.

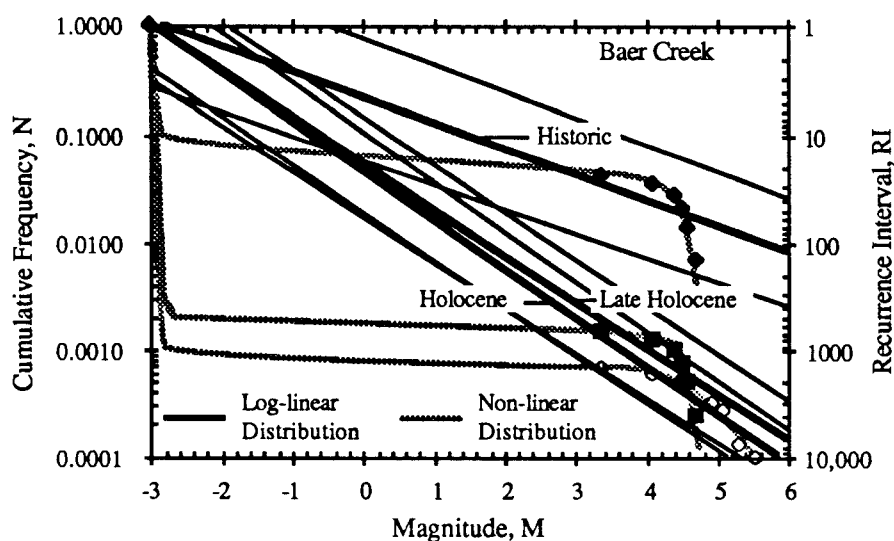


Figure E-9. Magnitude-frequency relationship for sedimentation events on the Baer Creek fan. Cumulative frequency, N , is the average number of events of magnitude M per year; recurrence interval, RI , is the average number of years between re-occurrences of magnitude M events. Heavy solid lines represent an assumed exponential distribution of event magnitudes; thin solid lines represent ± 90 percent prediction limits. Shaded lines represent apparent "actual" distribution of event magnitudes. Holocene refers to post-Lake Bonneville period of sediment accumulation, taken to be 10 ka; Late-Holocene is taken to be the last 4 ka; Historic is 140 years.

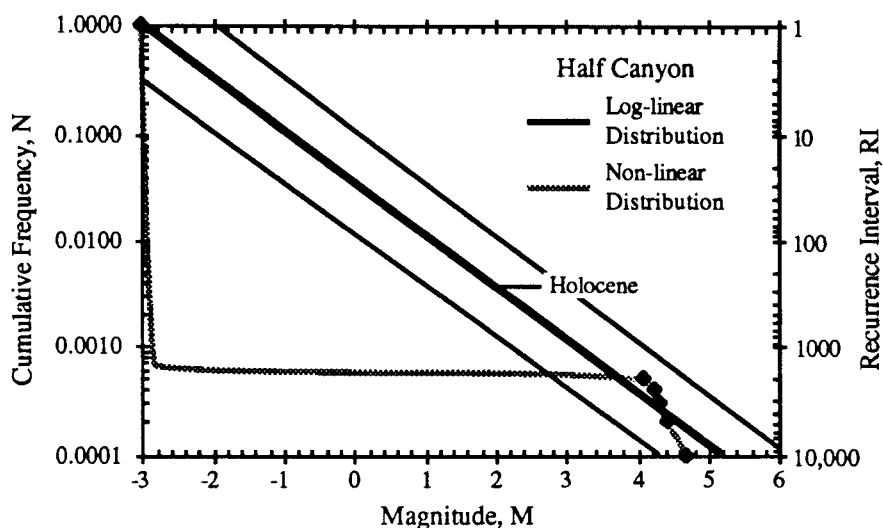


Figure E-10. Magnitude-frequency relationship for sedimentation events on the Half Canyon fan. Cumulative frequency, N , is the average number of events of magnitude M per year; recurrence interval, RI , is the average number of years between re-occurrences of magnitude M events. Heavy solid line represents an assumed exponential distribution of event magnitudes; thin solid lines represent ± 90 percent prediction limits. Shaded line represents apparent "actual" distribution of event magnitudes. Holocene refers to post-Lake Bonneville period of sediment accumulation, taken to be 10 ka.

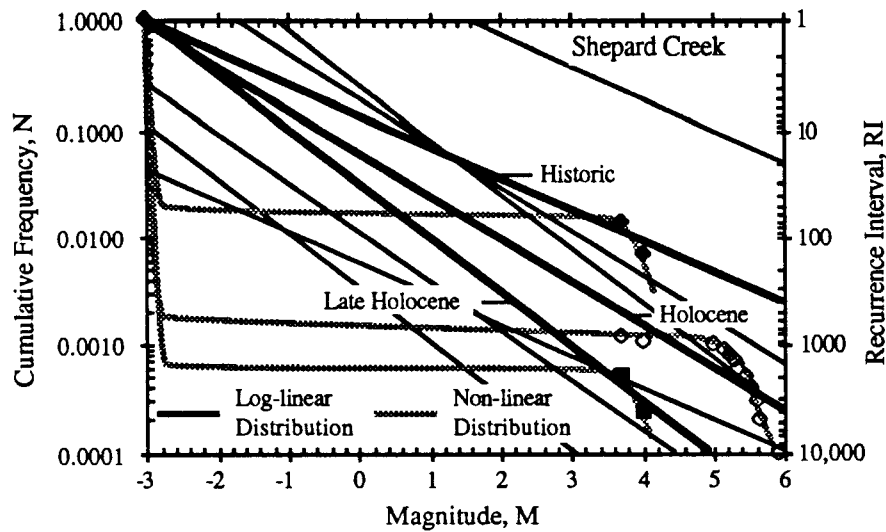


Figure E-11. Magnitude-frequency relationship for sedimentation events on the Shepard Creek fan. Cumulative frequency, N , is the average number of events of magnitude M per year; recurrence interval, RI , is the average number of years between re-occurrences of magnitude M events. Heavy solid lines represent an assumed exponential distribution of event magnitudes; thin solid lines represent ± 90 percent prediction limits. Shaded lines represent apparent "actual" distribution of event magnitudes. Holocene refers to post-Lake Bonneville period of sediment accumulation, taken to be 10 ka; Late-Holocene is taken to be the last 4 ka; Historic is 140 years.

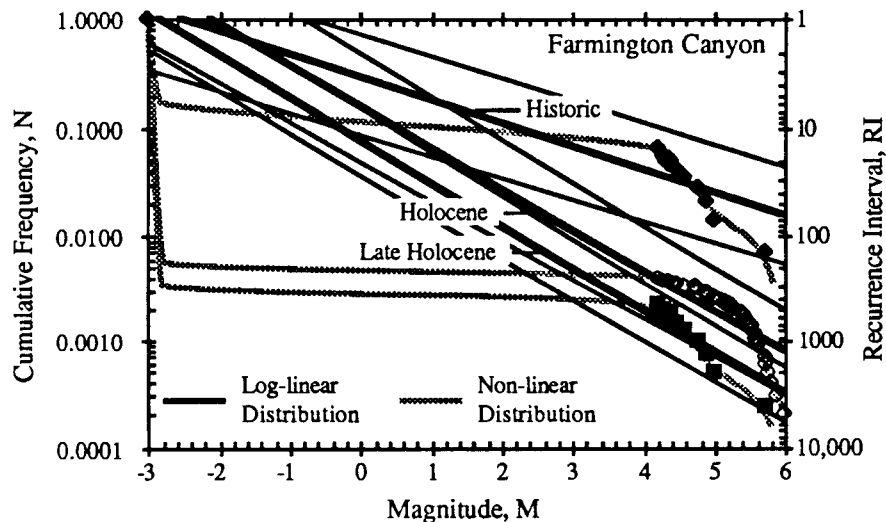


Figure E-12. Magnitude-frequency relationship for sedimentation events on the Farmington Canyon fan. Cumulative frequency, N , is the average number of events of magnitude M per year; recurrence interval, RI , is the average number of years between re-occurrences of magnitude M events. Heavy solid lines represent an assumed exponential distribution of event magnitudes; thin solid lines represent ± 90 percent prediction limits. Shaded lines represent apparent "actual" distribution of event magnitudes. Holocene refers to post-Lake Bonneville period of sediment accumulation, taken to be 10 ka; Late-Holocene is taken to be the last 4 ka; Historic is 140 years.

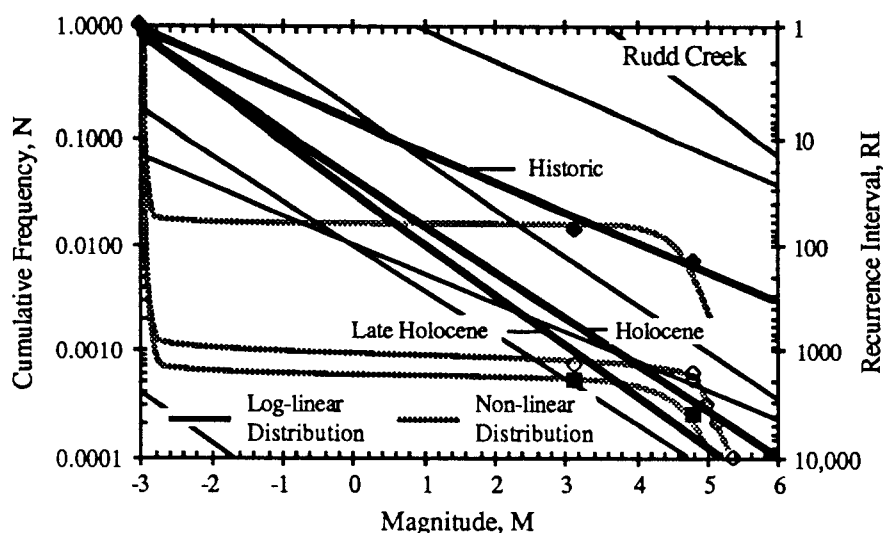


Figure E-13. Magnitude-frequency relationship for sedimentation events on the Rudd Creek fan. Cumulative frequency, N , is the average number of events of magnitude M per year; recurrence interval, RI , is the average number of years between re-occurrences of magnitude M events. Heavy solid lines represent an assumed exponential distribution of event magnitudes; thin solid lines represent ± 90 percent prediction limits. Shaded lines represent apparent "actual" distribution of event magnitudes. Holocene refers to post-Lake Bonneville period of sediment accumulation, taken to be 10 ka; Late-Holocene is taken to be the last 4 ka; Historic is 140 years.

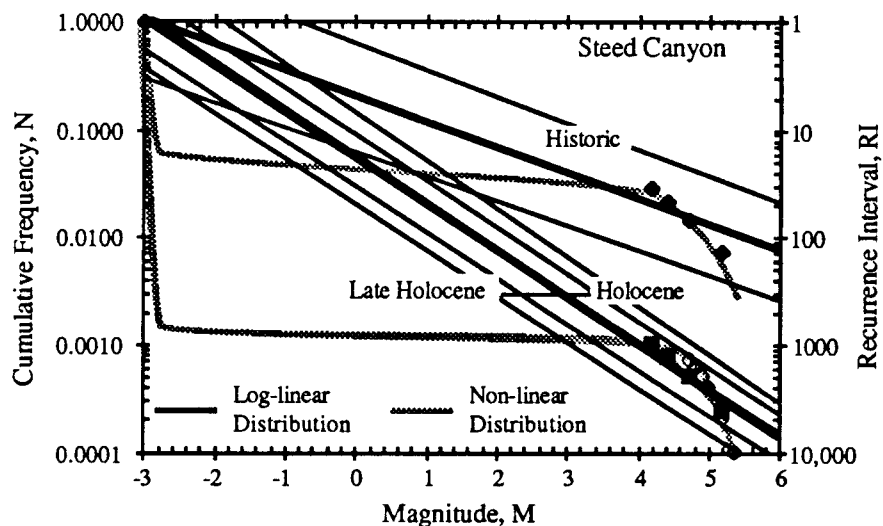


Figure E-14. Magnitude-frequency relationship for sedimentation events on the Steed Canyon fan. Cumulative frequency, N , is the average number of events of magnitude M per year; recurrence interval, RI , is the average number of years between re-occurrences of magnitude M events. Heavy solid lines represent an assumed exponential distribution of event magnitudes; thin solid lines represent ± 90 percent prediction limits. Shaded lines represent apparent "actual" distribution of event magnitudes. Holocene refers to post-Lake Bonneville period of sediment accumulation, taken to be 10 ka; Late-Holocene is taken to be the last 4 ka; Historic is 140 years.

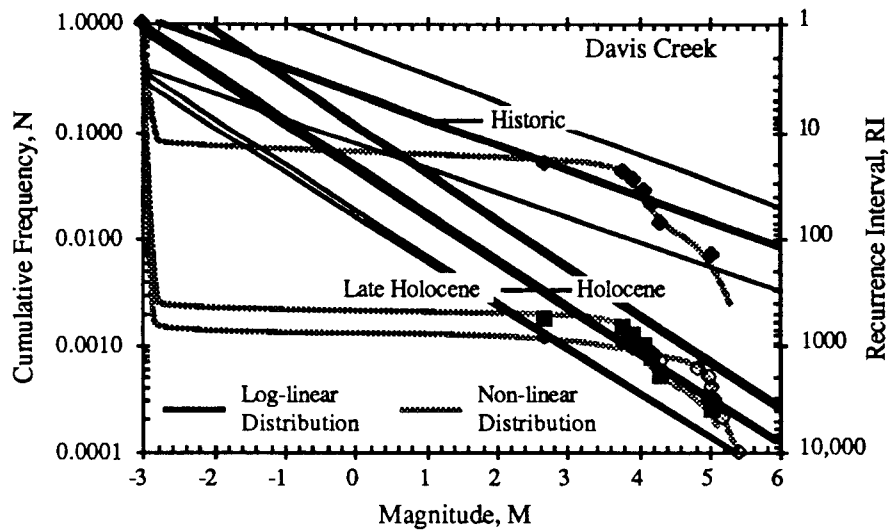


Figure E-15. Magnitude-frequency relationship for sedimentation events on the Davis Creek fan. Cumulative frequency, N , is the average number of events of magnitude M per year; recurrence interval, RI , is the average number of years between re-occurrences of magnitude M events. Heavy solid lines represent an assumed exponential distribution of event magnitudes; thin solid lines represent ± 90 percent prediction limits. Shaded lines represent apparent "actual" distribution of event magnitudes. Holocene refers to post-Lake Bonneville period of sediment accumulation, taken to be 10 ka; Late-Holocene is taken to be the last 4 ka; Historic is 140 years.

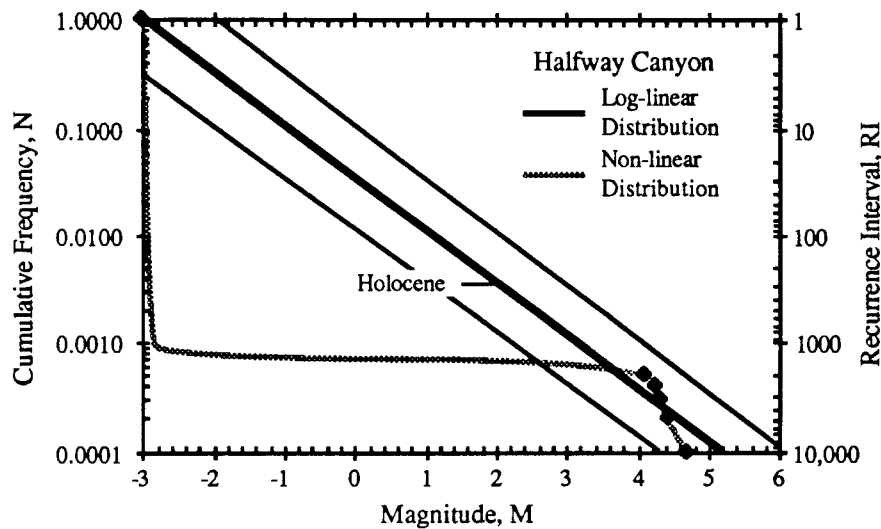


Figure E-16. Magnitude-frequency relationship for sedimentation events on the Halfway Canyon fan. Cumulative frequency, N , is the average number of events of magnitude M per year; recurrence interval, RI , is the average number of years between re-occurrences of magnitude M events. Heavy solid line represents an assumed exponential distribution of event magnitudes; thin solid lines represent ± 90 percent prediction limits. Shaded line represents apparent "actual" distribution of event magnitudes. Holocene refers to post-Lake Bonneville period of sediment accumulation, taken to be 10 ka.

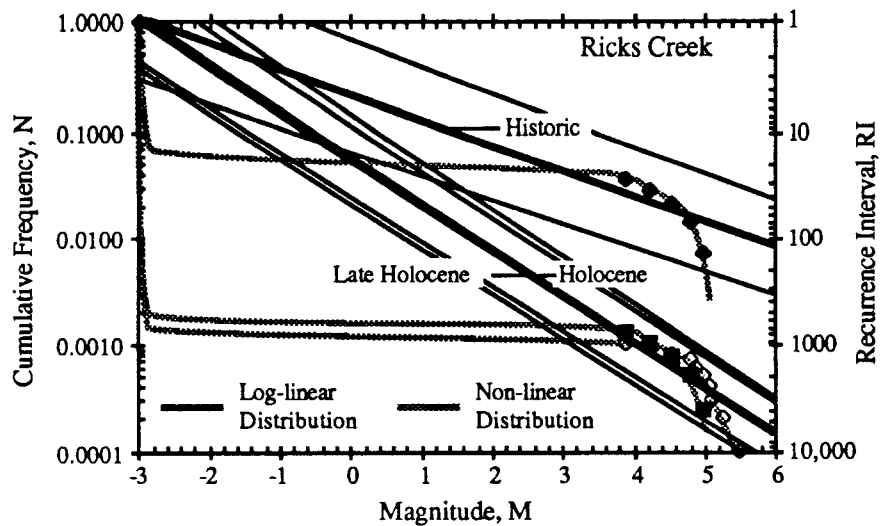


Figure E-17. Magnitude-frequency relationship for sedimentation events on the Ricks Creek fan. Cumulative frequency, N , is the average number of events of magnitude M per year; recurrence interval, RI , is the average number of years between re-occurrences of magnitude M events. Heavy solid lines represent an assumed exponential distribution of event magnitudes; thin solid lines represent ± 90 percent prediction limits. Shaded lines represent apparent "actual" distribution of event magnitudes. Holocene refers to post-Lake Bonneville period of sediment accumulation, taken to be 10 ka; Late-Holocene is taken to be the last 4 ka; Historic is 140 years.

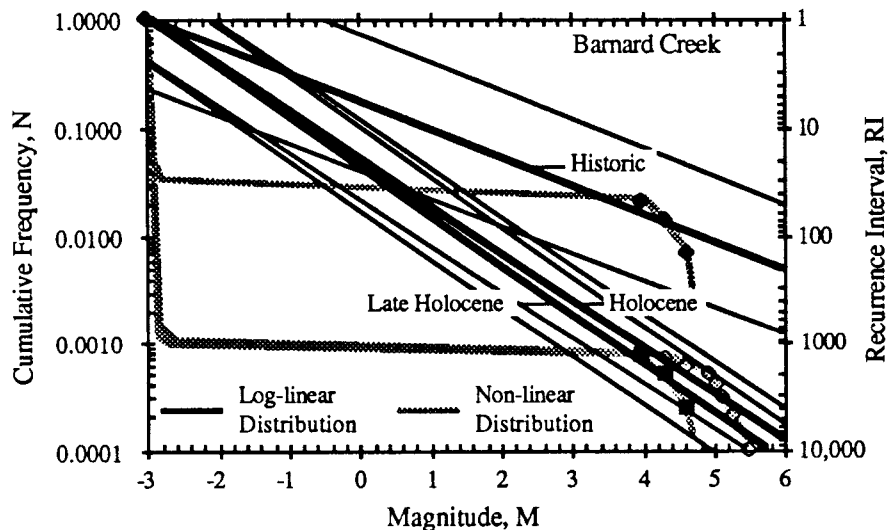


Figure E-18. Magnitude-frequency relationship for sedimentation events on the Barnard Creek fan. Cumulative frequency, N , is the average number of events of magnitude M per year; recurrence interval, RI , is the average number of years between re-occurrences of magnitude M events. Heavy solid lines represent an assumed exponential distribution of event magnitudes; thin solid lines represent ± 90 percent prediction limits. Shaded lines represent apparent "actual" distribution of event magnitudes. Holocene refers to post-Lake Bonneville period of sediment accumulation, taken to be 10 ka; Late-Holocene is taken to be the last 4 ka; Historic is 140 years.

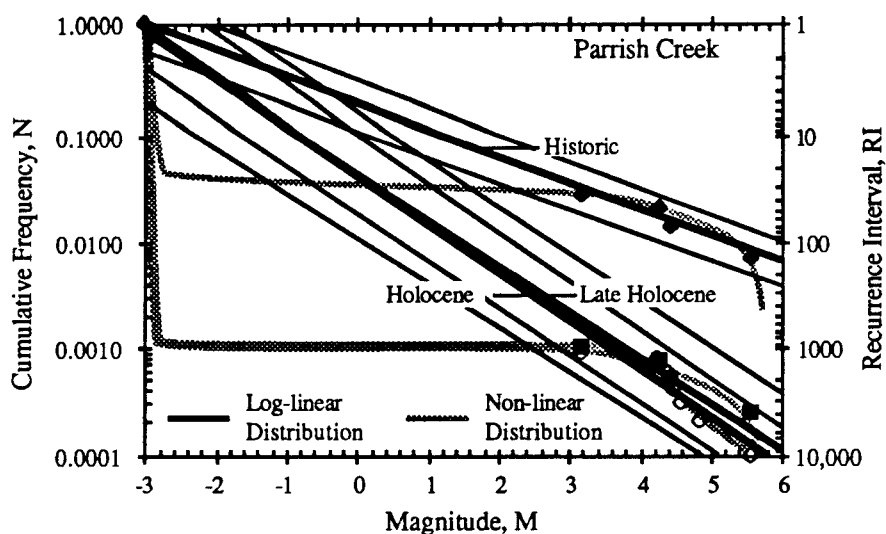


Figure E-19. Magnitude-frequency relationship for sedimentation events on the Parrish Creek fan. Cumulative frequency, N , is the average number of events of magnitude M per year; recurrence interval, RI , is the average number of years between re-occurrences of magnitude M events. Heavy solid lines represent an assumed exponential distribution of event magnitudes; thin solid lines represent ± 90 percent prediction limits. Shaded lines represent apparent "actual" distribution of event magnitudes. Holocene refers to post-Lake Bonneville period of sediment accumulation, taken to be 10 ka; Late-Holocene is taken to be the last 4 ka; Historic is 140 years.

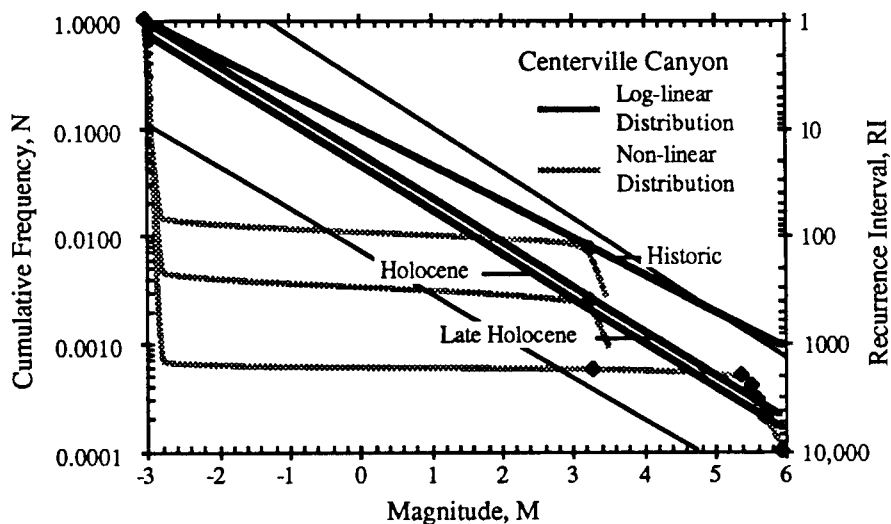


Figure E-20. Magnitude-frequency relationship for sedimentation events on the Centerville Canyon fan. Cumulative frequency, N , is the average number of events of magnitude M per year; recurrence interval, RI , is the average number of years between re-occurrences of magnitude M events. Heavy solid line represents an assumed exponential distribution of event magnitudes; thin solid lines represent ± 90 percent prediction limits. Shaded line represents apparent "actual" distribution of event magnitudes. Holocene refers to post-Lake Bonneville period of sediment accumulation, taken to be 10 ka; Late-Holocene is taken to be the last 4 ka; Historic is 140 years.

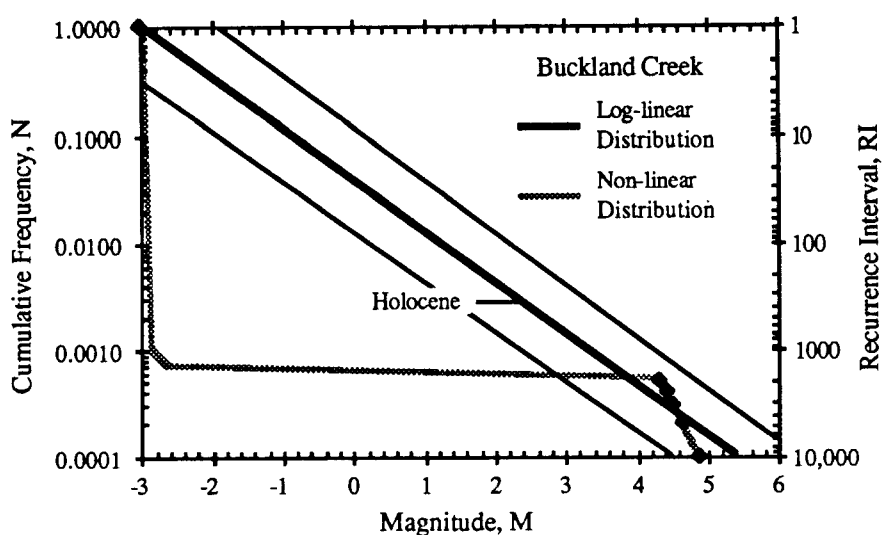


Figure E-21. Magnitude-frequency relationship for sedimentation events on the Buckland Creek fan. Cumulative frequency, N , is the average number of events of magnitude M per year; recurrence interval, RI , is the average number of years between re-occurrences of magnitude M events. Heavy solid line represents an assumed exponential distribution of event magnitudes; thin solid lines represent ± 90 percent prediction limits. Shaded line represents apparent "actual" distribution of event magnitudes. Holocene refers to post-Lake Bonneville period of sediment accumulation, taken to be 10 ka.

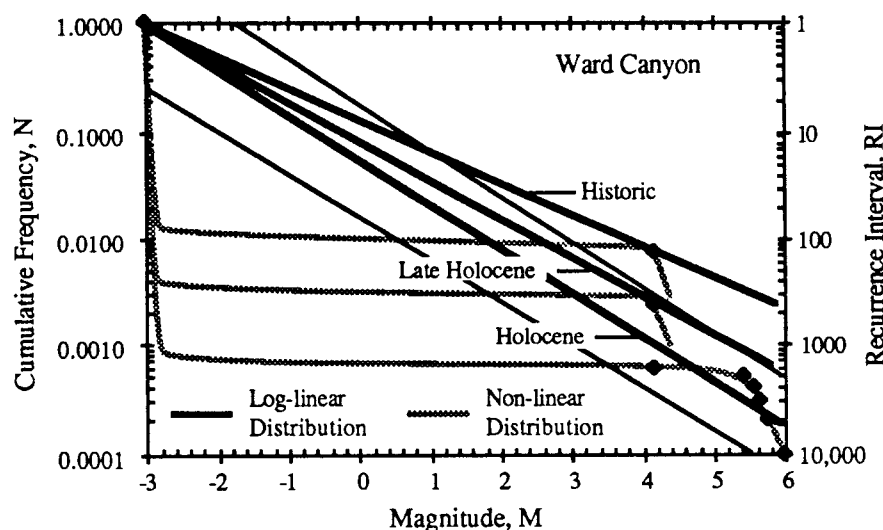


Figure E-22. Magnitude-frequency relationship for sedimentation events on the Ward Canyon fan. Cumulative frequency, N , is the average number of events of magnitude M per year; recurrence interval, RI , is the average number of years between re-occurrences of magnitude M events. Heavy solid line represents an assumed exponential distribution of event magnitudes; thin solid lines represent ± 90 percent prediction limits. Shaded line represents apparent "actual" distribution of event magnitudes. Holocene refers to post-Lake Bonneville period of sediment accumulation, taken to be 10 ka; Late-Holocene is taken to be the last 4 ka; Historic is 140 years.

Table E-2. Summary of mean sediment magnitudes and standard deviations for 140-year historic period. This summary is based on the assumption that all years without records of documented sediment delivery actually experienced 0.001 m^3 of sediment (M -3). For those years without documented sediment delivery, mean sedimentation magnitudes were taken to be -3 and standard deviations were taken to be the mean of the standard deviations for all years with sedimentation records (1.072). Extreme value mean and standard deviation are from Gumbel (1958, p. 228) for $n = 140$.

Fan	Mean Magnitude	Standard Deviation
Corbett	-3	1.072
Hobbs	-3	1.072
Lightning	-2.950	0.587
Kays (Middle)	-2.916	0.697
Kays (South)	-2.670	1.451
Snow	-3	1.072
Adams	-3	1.072
Webb	-2.914	0.722
Baer	-2.688	1.482
Half	-3	1.072
Shepard	-2.902	0.816
Farmington	-2.458	1.966
Rudd	-2.900	0.837
Steed	-2.682	1.511
Davis	-2.749	1.315
Halfway	-3	1.072
Ricks	-2.731	1.404
Barnard	-2.843	1.065
Parrish	-2.841	1.091
Centerville	-2.955	0.532
Buckland	-3	1.072
Ward	-2.949	0.608
Reduced Extreme Value	0.564	1.222

APPENDIX F

SUMMARY OF EXCEEDANCE PROBABILITY CALCULATIONS

Probabilistic Hazard Evaluation

Three types of probabilistic analyses were used in this hazard evaluation, each with a distribution of possible sedimentation event magnitudes: binomial, Poisson, and extreme-value distributions. The binomial distribution applies to experiments of a certain number of independent trials with only two possible outcomes each of which has a constant probability from one trial to the next (McCuen and Snyder, 1986, p. 33). The independent trials for the sedimentation processes in Davis County would be some exposure time, measured in years, during which the risk of damage is to be assessed. The two possible outcomes to each trial consist of sediment discharge larger than magnitude M or smaller than magnitude M. Arguments have been presented earlier about possible lack of independence due to cleaning of channels by major debris flows and the influence this may have on constancy of trial outcomes. Nonetheless, binomial analyses are commonly used in flood hazard evaluations, which represent one end of the continuum of sediment-water discharges. The binomial distribution probability is given by

$$P(i,t) = \{t! / [i! (t-i)!]\} \cdot p^i \cdot (1 - p)^{t-i} \quad (F-1)$$

where $P(i,t)$ is the probability of exactly i outcomes in t trials if each outcome has a probability of p . The binomial distribution can be applied to the sedimentation processes by computing the probability associated with exactly zero outcomes of sediment discharge equal to or larger than some volume or magnitude. This probability would be a non-exceedance probability given by

$$P(0,t) = \{t! / 0! (t-0)!\} \cdot p^0 \cdot (1 - p)^{t-0} \quad (F-2)$$

$$\text{or,} \quad P(0,t) = (1 - p)^t \quad (F-3)$$

because $0! = 1$ and $p^0 = 1$. Thus, this binomial probability can be expressed as a non-exceedance probability by

$$P(i < I, t) = (1 - p)^t \quad (F-4)$$

where $P(i < I, t)$ is the probability of an event, i , not exceeding a threshold value, I . The exceedance probability is 1 minus the non-exceedance probability, or

$$P(i \geq I, t) = 1 - (1 - p)^t \quad (F-5)$$

where $P(i \geq I, t)$ is the probability of an event, i , greater than or equal to a threshold value, I . Substituting appropriate terms for the sedimentation processes in Davis County yields

$$P(e \geq M, t) = 1 - [1 - (1/R_{IPR,M})]^t \quad (F-6)$$

where $P(e \geq M, t)$ is the probability of occurrence of an event, e , greater than or equal to a specified magnitude, M , within an exposure time, t years, and $R_{IPR,M}$ is the average recurrence interval of events of magnitude M based on a period of record of PR years, and

$1/RI_{PR,M}$ is the cumulative average number of events of magnitude M or larger in any one year. Substituting $RI_{PR,M}$ from equation (E-6) into equation (F-6) yields

$$P(e \geq M, t) = 1 - [1 - N_{PR,M}]^t \quad (F-7)$$

where the terms are as previously defined.

The Poisson distribution is commonly used in earthquake hazard modeling (Schwartz and Coppersmith, 1986, p. 227), as described earlier in this chapter. The Poisson equation is given by

$$P(i, t) = [(vt)^i \exp(-vt)] / i! \quad (F-8)$$

where $P(i, t)$ is the probability of occurrence of i number of events during time t , v is the average number of events per unit time, and $\exp(-vt)$ is the base of Naperian logarithms raised to the $-vt$ power. Setting $i = 0$ for non-exceedance probability as described above,

$$P(0, t) = \exp(-vt) \quad (F-9)$$

The average number of events per unit time can be given by $N_{PR,M}$. Converting this to exceedance probability and substituting $N_{PR,M}$ for v yields

$$P(e \geq M, t) = 1 - \exp(-N_{PR,M} \cdot t) \quad (F-10)$$

The extreme-value distribution is used most frequently in estimating the probability of flood events (McCuen and Snyder, 1986, p. 122). Flood histories usually are described by the discharge of the largest flood which occurred during each year of record. Consequently, such flood histories are composed of extreme events. The extreme-value distribution was initially described by Gumbel (1958) in terms of a double exponential equation using the mean and standard deviation of a sample and the mean and standard deviation of normally distributed extreme values called reduced extremes (Gumbel, 1958, p. 228). The extreme-value distribution is given by

$$P(i, t) = \exp\{-t \cdot \exp[-A(I - U)]\} \quad (F-11)$$

$$A = \sigma_G / \sigma_I \quad (F-12)$$

$$U = \mu_I - (\mu_G / A) \quad (F-13)$$

where $P(i, t)$ is previously defined, μ_G and σ_G are the mean and standard deviation of Gumbel's reduced extreme, μ_I and σ_I are the mean and standard deviation of the events to which I is being compared. For reasons described above, this may be converted to exceedance probability in terms of the sedimentation processes in Davis County by

$$P(e \geq M, t) = 1 - \exp\{-t \cdot \exp[-A(M - U)]\} \quad (F-14)$$

where μ_M and σ_M are the mean and standard deviation of the annual sedimentation events, and μ_G and σ_G are from Gumbel (1958, p. 228). This extreme-value analysis appears to be valid only for the historic period of record because most of the fans in the study area have

less than 10 years of the 140-year historic period with documented sediment delivery. Such a history strongly skews the event distribution toward extremely small sediment event magnitudes. Values of $\mu_G = 0.56369$ and $\sigma_G = 1.22157$ represent a sample size of $n = 140$ (Gumbel, 1958, p. 228). Gumbel's table does not extend past $n = 1000$; therefore, extreme-value distributions were not analyzed for late Holocene (4 ka) or Holocene (10 or 15 ka) periods of record.

A statistical analysis was performed on the regression coefficients for mean magnitude-frequency relationships (Table E-1) to test the hypothesis that the coefficients for the different periods of record were statistically different. The results of this statistical analysis are presented in Table F-1. This analysis shows that both the intercept value (a in Table E-1) and the slope value (b in Table E-1) cannot be distinguished for the Holocene and late Holocene periods of record; however, the analysis also shows that the values for the historic period do appear to be different from both of the other periods at a significance of $\alpha = 0.05$. Therefore, probabilistic analyses were performed for Holocene and historic periods of record, but not for late Holocene periods.

The exceedance probability relationships described in equations F-6, F-10, and F-14 were solved for exposure times of 100, 50, and 10 years. The binomial and Poisson distribution expressions (equations F-6 and F-10) were evaluated on the basis of values of $N_{PR,M}$ developed from the regression coefficients for the mean relationships (Table E-1). An interactive BASIC program called "EXPRAN" (Appendix G) was written to solve equations F-6, F-10, and F-14 for each exposure time at each fan for magnitudes ranging from -3 to 6 in increments of 0.1; the program was executed on a Macintosh SE personal computer.

In a chapter on deductive stochastic models, Huggett (1985, p. 56) notes that, in some cases, the probability generated by the binomial distribution is closely approximated by the Poisson distribution. To test this hypothesis for the Davis County fans, EXPRAN was run for the Corbett Creek fan for an exposure time of 10 years. The 91 values of probability estimated by the binomial and Poisson relationships for $-3 \leq M \leq 6$ at a magnitude interval of 0.1 were evaluated statistically. For each of the 91 magnitude values, the probability generated by the Poisson distribution was subtracted from the probability generated by the binomial distribution. The results of the statistical analysis are summarized in Table F-2 and indicate that the differences between the probabilities estimated with these two distributions are not actually zero; however, the probabilities are within 0.005 of each other. This difference is so small that the two probabilities are virtually the same; therefore, exceedance probabilities were evaluated systematically for binomial and extreme-value distributions only. The exceedance probability relationships are presented graphically on Figures F-1 to F-22.

Sedimentation event magnitudes for exceedance probabilities of 50 and 10 percent for each of the three exposure times and periods of record for each fan were calculated with the aid of a BASIC program called "MAGPRO.2" (see Appendix G) which is based on

$$M_{P,t} = (\log N_{P,t} - a)/b \quad (F-15)$$

for binomial distributions, where $M_{P,t}$ is the magnitude associated with a specific probability, P , in a specific exposure time, t , $N_{P,t}$ is the annual frequency of events with the specific probability and exposure time, and a and b are the regression coefficients from Table E-1. For extreme-value distributions, the mean and standard deviations of magnitude

Table F-1. Summary of statistical analysis of regression coefficients for mean magnitude-frequency relationships listed in Table E-1. Subscript Ho signifies Holocene and indicates a period of record of 15 ka or 10 ka; subscript LH signifies late Holocene and indicates a period of record of 4 ka; subscript Hi signifies historic and indicates a period of record of 140 yr. Values of the F and t distributions are from Ott (1984, p. 700 and 697, respectively). Regression coefficients for the late Holocene and historic periods for Lightning, Centerville, and Ward fans were not used in the statistical analysis because in each case only one sedimentation event was known for either period of record.

Parameter	Mean Value	Standard Deviation	Number of Samples	Test Statistic (F)	Rejection Region (95% Confidence)	Equal Variance Hypothesis
a_{Ho}	-1.366	0.158	22	1.386 (Ho-LH)	$F > 2.23$	Accept
a_{LH}	-1.414	0.186	12	1.221 (Ho-Hi)	$F > 2.23$	Accept
a_{Hi}	-0.772	0.143	12	1.692 (LH-Hi)	$F > 2.69$	Accept
b_{Ho}	-0.449	0.031	22	3.746 (Ho-LH)	$F > 2.23$	Reject
b_{LH}	-0.468	0.060	12	1.583 (Ho-Hi)	$F > 2.23$	Accept
b_{Hi}	-0.265	0.039	12	2.367 (LH-Hi)	$F > 2.69$	Accept

Comparison	Test Statistic (t)	Degrees of Freedom	Rejection Region (90% Confidence)	Null Hypothesis	Conclusion
$a_{Ho}-a_{LH}$	0.796	32	$ t > 1.694$	$a_{Ho} = a_{LH}$	Accept
$a_{Ho}-a_{Hi}$	-10.814	32	$ t > 1.694$	$a_{Ho} = a_{Hi}$	Reject
$a_{LH}-a_{Hi}$	-9.479	22	$ t > 1.717$	$a_{LH} = a_{Hi}$	Reject
$b_{Ho}-b_{LH}$	1.025	14	$ t > 1.761$	$b_{Ho} = b_{LH}$	Accept
$b_{Ho}-b_{Hi}$	-15.096	32	$ t > 1.694$	$b_{Ho} = b_{Hi}$	Reject
$b_{LH}-b_{Hi}$	-9.827	22	$ t > 1.717$	$b_{LH} = b_{Hi}$	Reject

Table F-2. Summary of statistical analysis of exceedance probabilities generated by binomial and Poisson distributions of sedimentation event magnitudes at the Corbett Creek fan. The Holocene period of record and an exposure time of 10 years were used. P_B denoted probability generated by the binomial distribution while P_P denotes the probability for the Poisson distribution. The value of t for $\alpha/2 = 0.005$ is from Ott (1984, p. 697) interpolated between 60 and 120 degrees of freedom.

$P_B - P_P$			Null Hypothesis (H_0)	Test Statistic (t)	Rejection Region (99% confidence)	Conclusion
Mean	Standard Deviation	n				
0.00479	0.00840	91	$P_B - P_P = 0$	5.439	$ t = 2.639$	Reject H_0
			$P_B - P_P = 0.005$	-0.240	$ t = 2.639$	Accept H_0

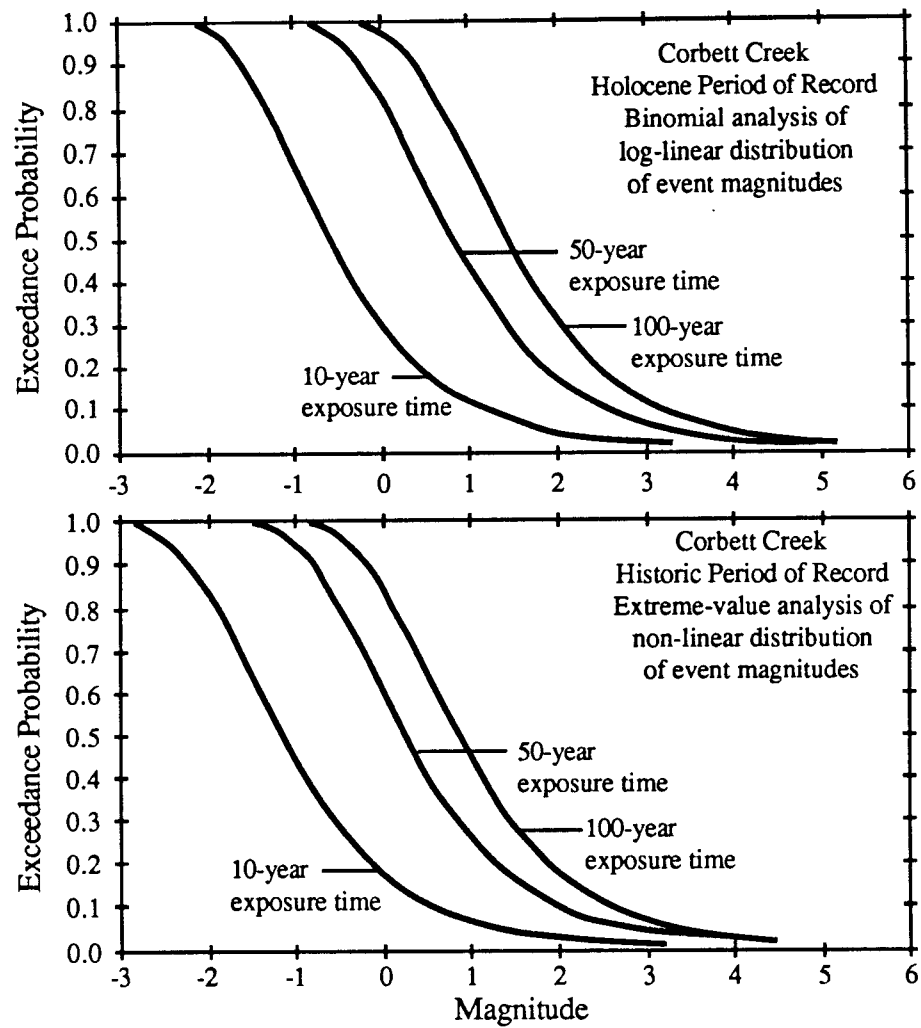


Figure F-1. Exceedance probability curves for sedimentation events on the Corbett Creek fan.

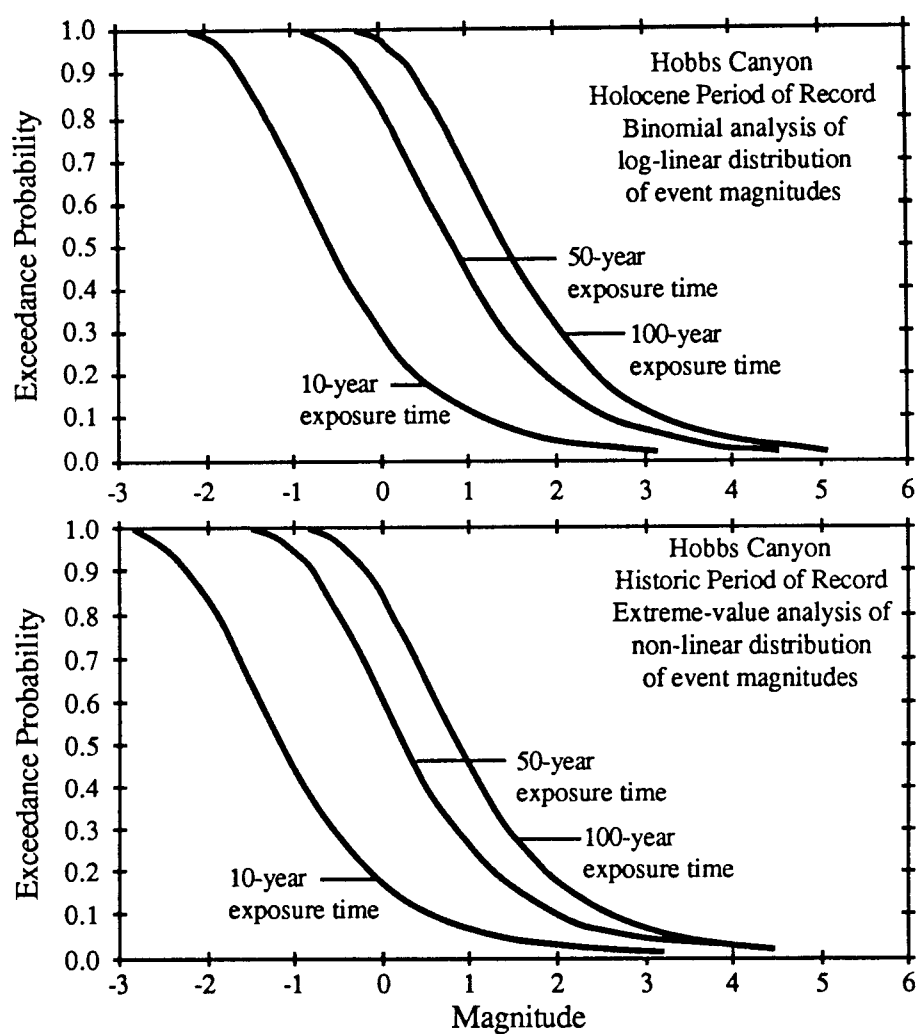


Figure F-2. Exceedance probability curves for sedimentation events on the Hobbs Canyon fan.

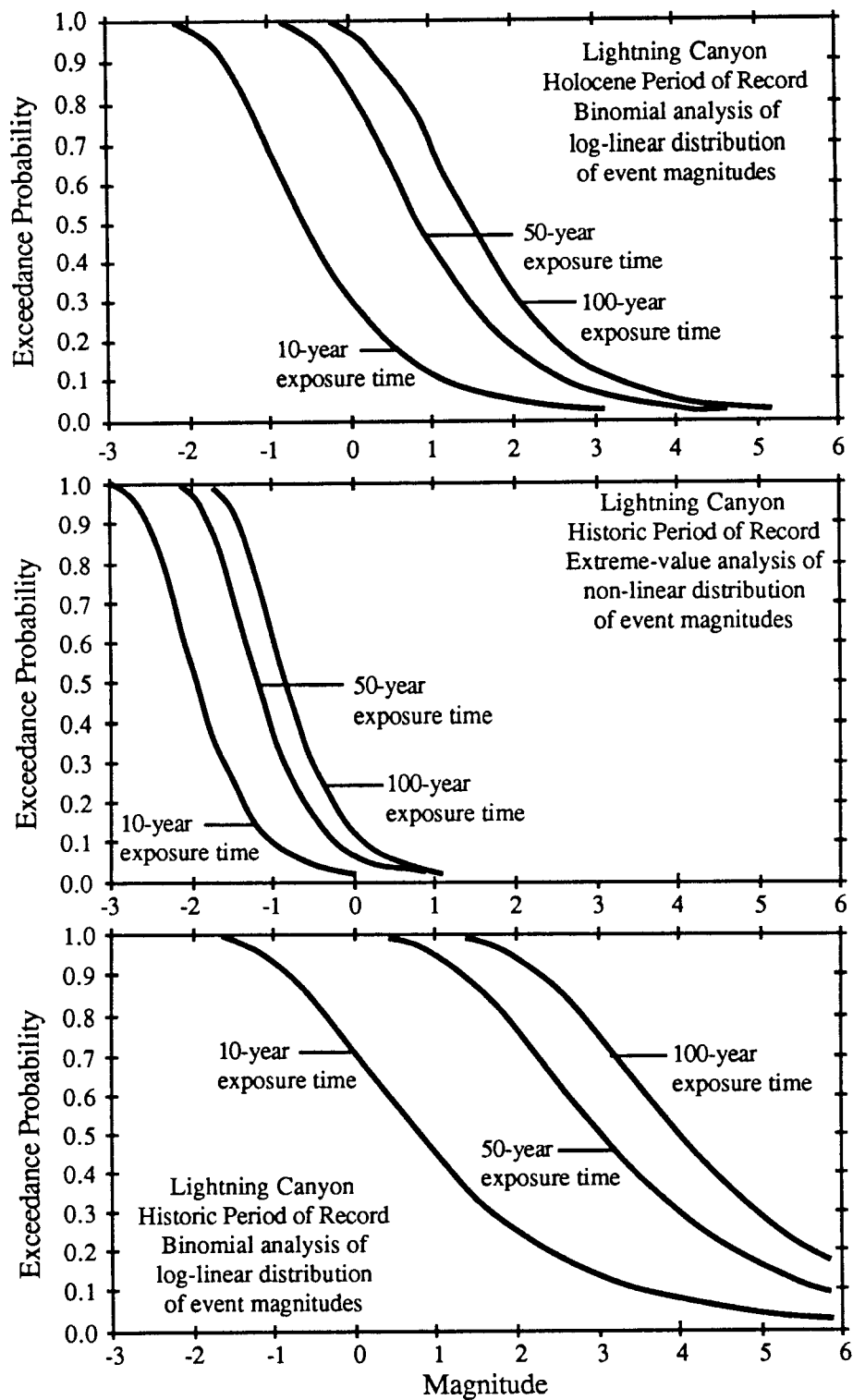


Figure F-3. Exceedance probability curves for sedimentation events on the Lightning Canyon fan.

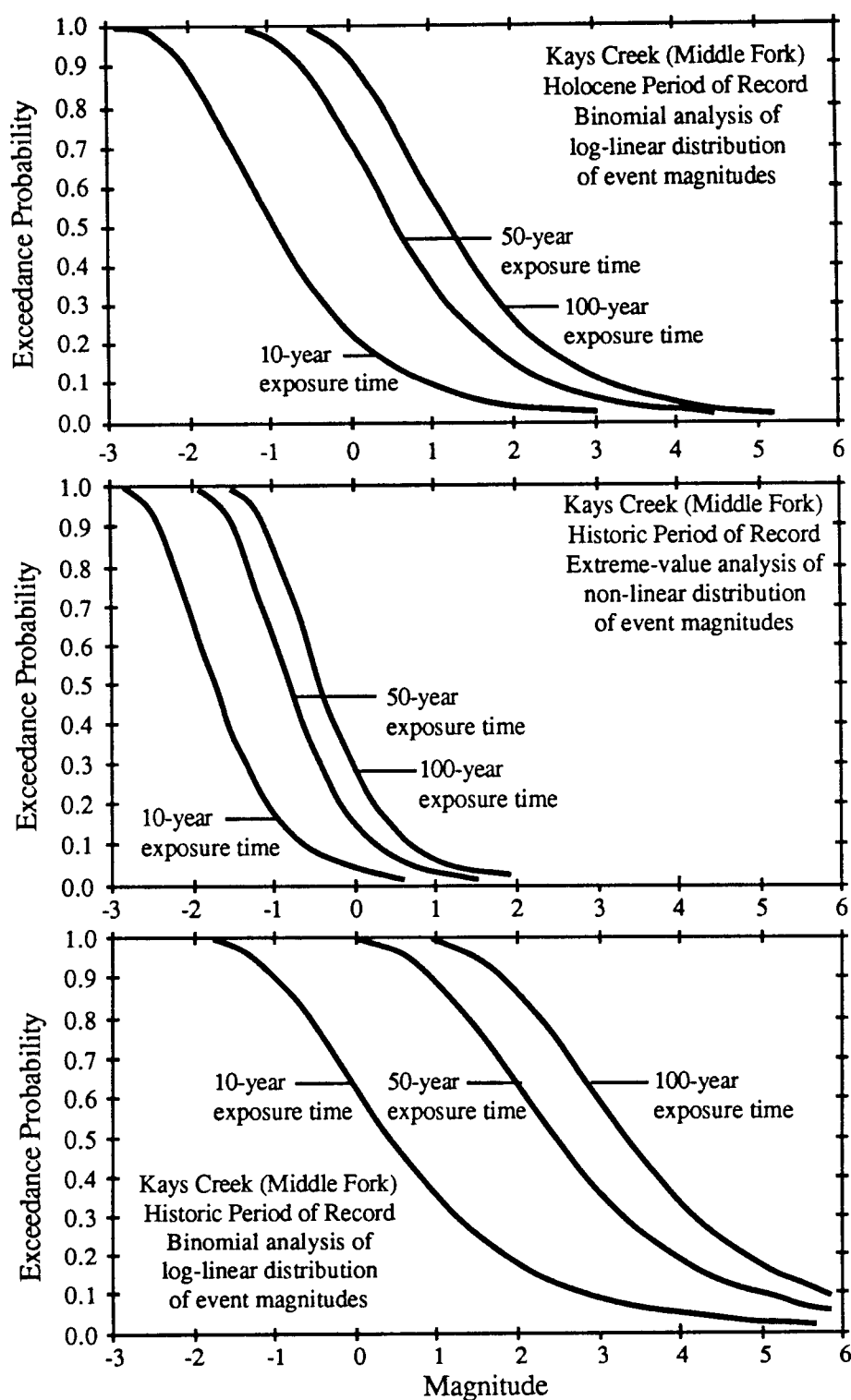


Figure F-4. Exceedance probability curves for sedimentation events on the Kays Creek (Middle Fork) fan.

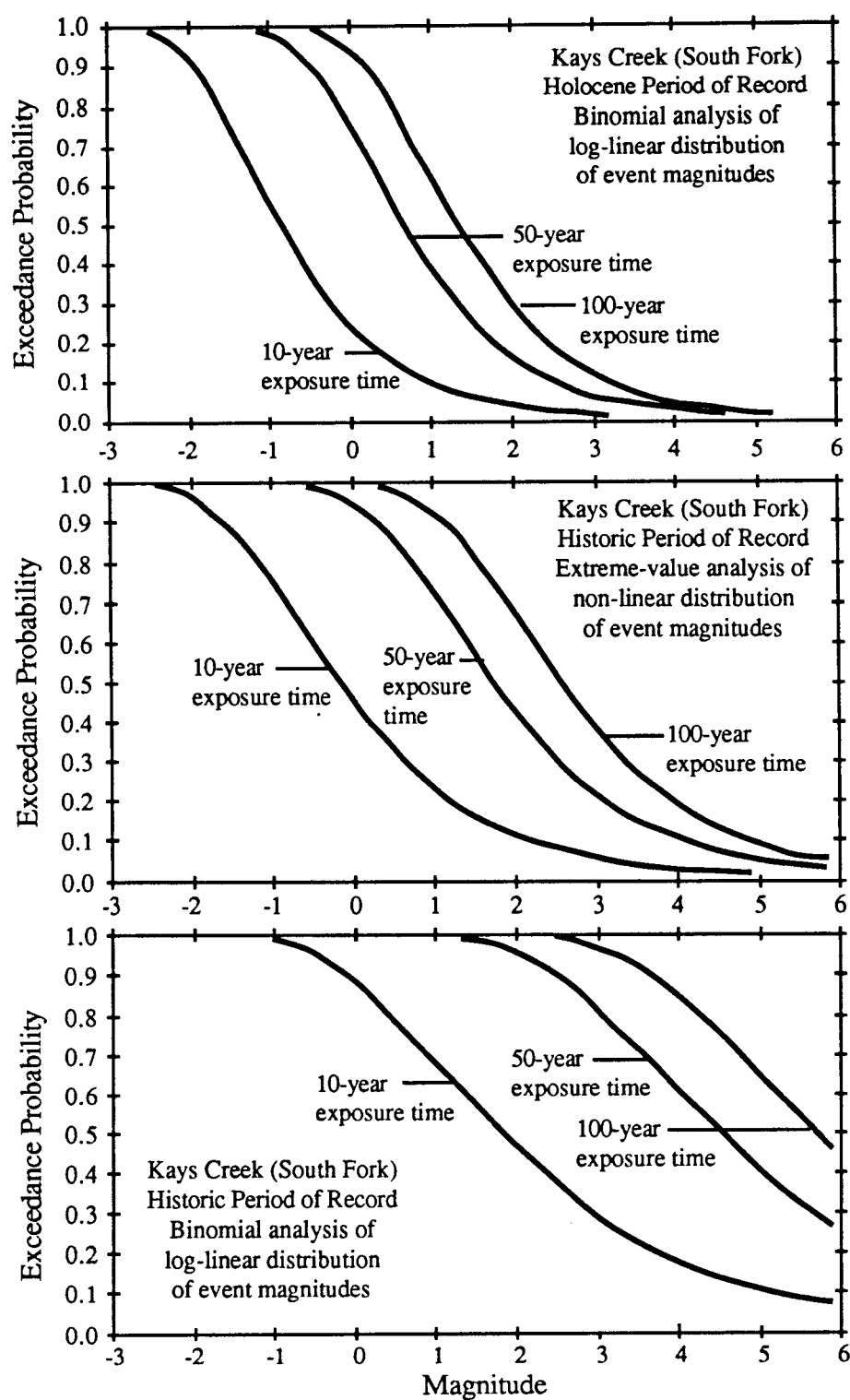


Figure F-5. Exceedance probability curves for sedimentation events on the Kays Creek (South Fork) fan.

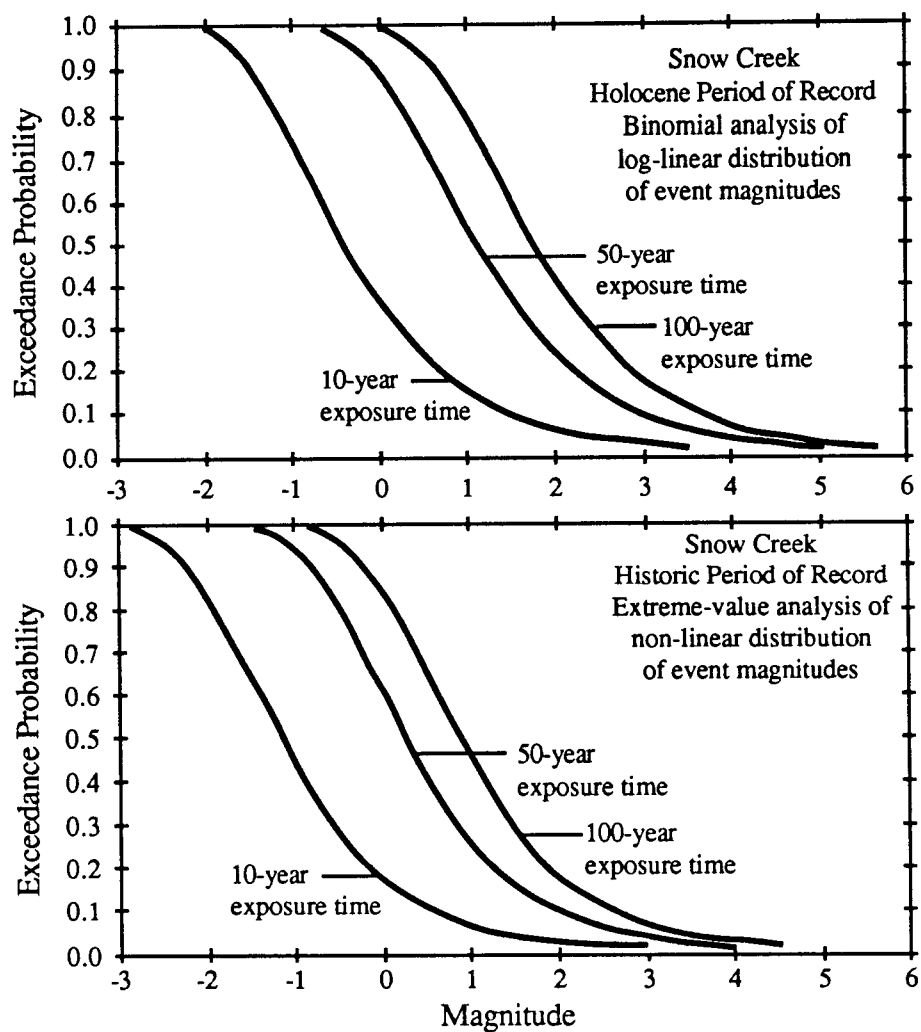


Figure F-6. Exceedance probability curves for sedimentation events on the Snow Creek fan.

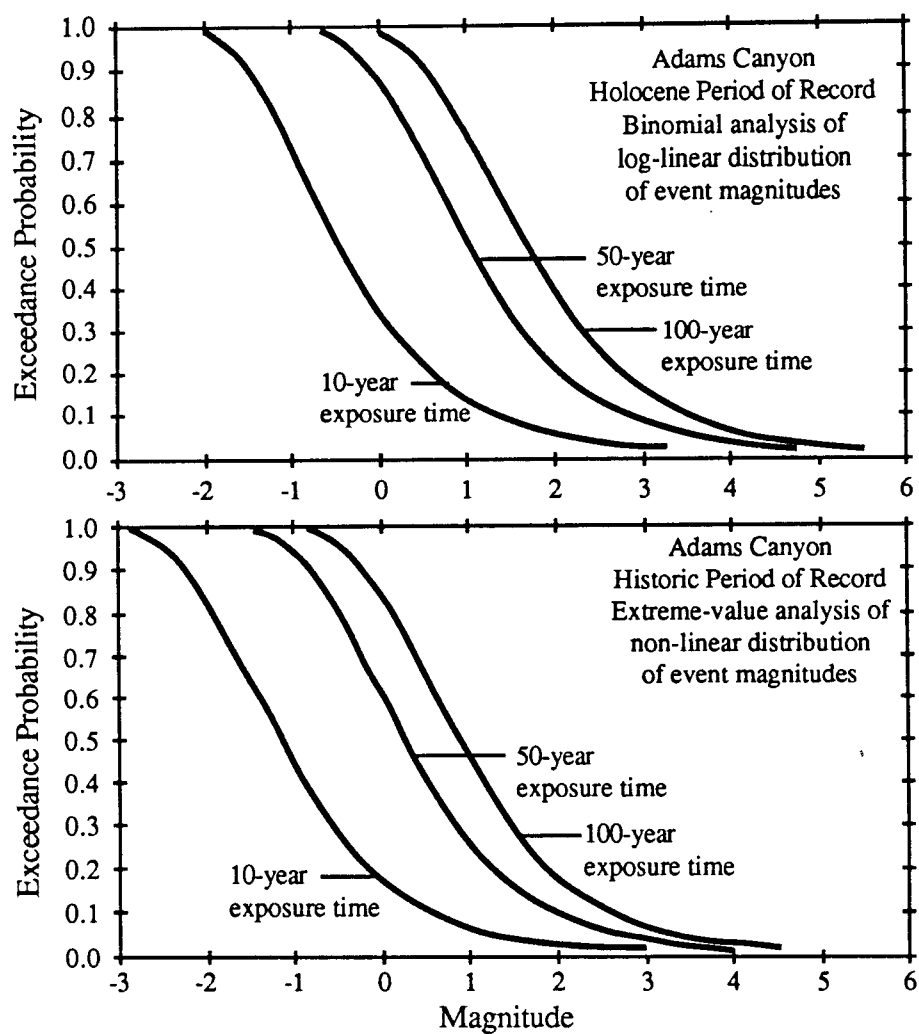


Figure F-7. Exceedance probability curves for sedimentation events on the Adams Canyon fan.

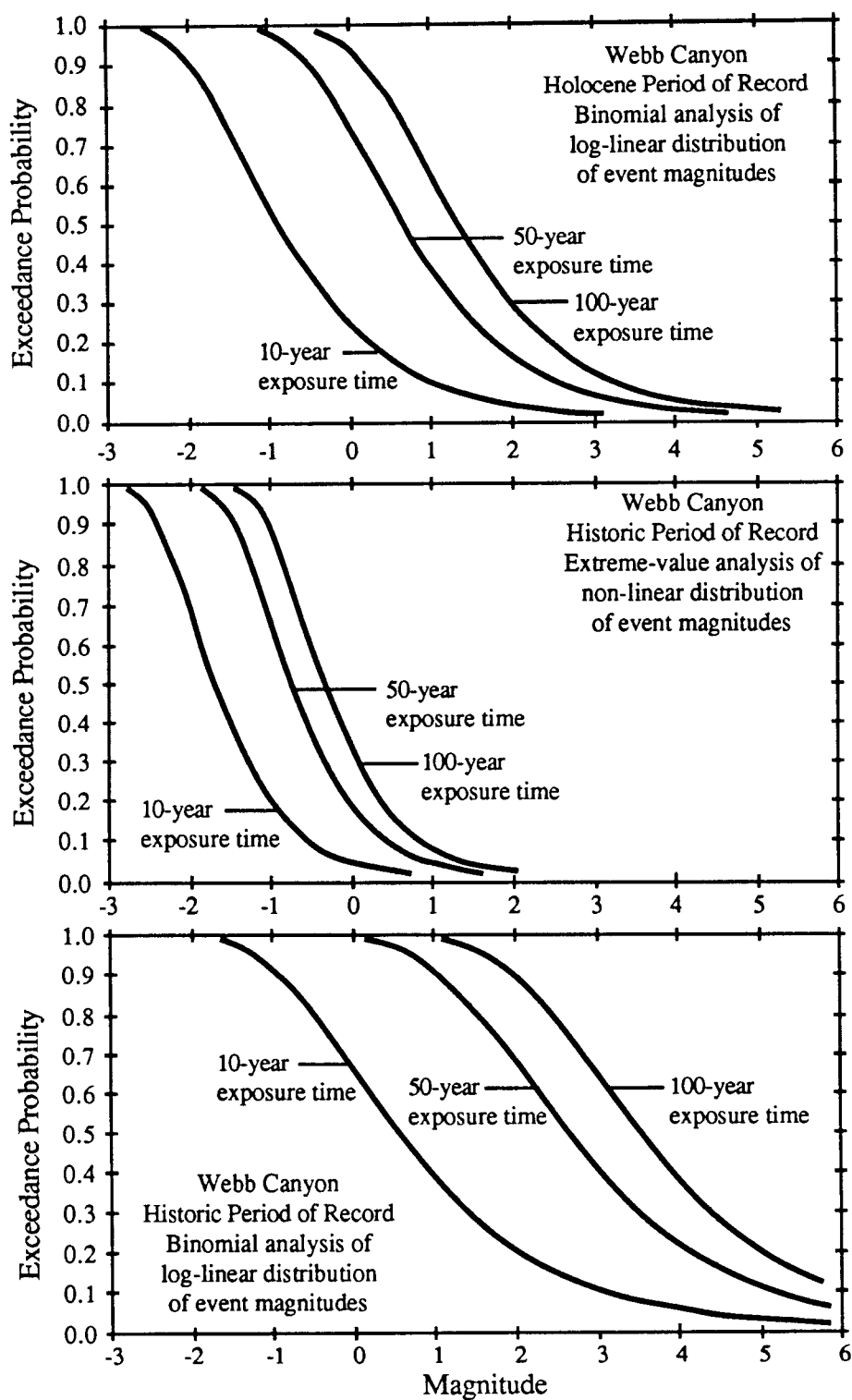


Figure F-8. Exceedance probability curves for sedimentation events on the Webb Canyon fan.

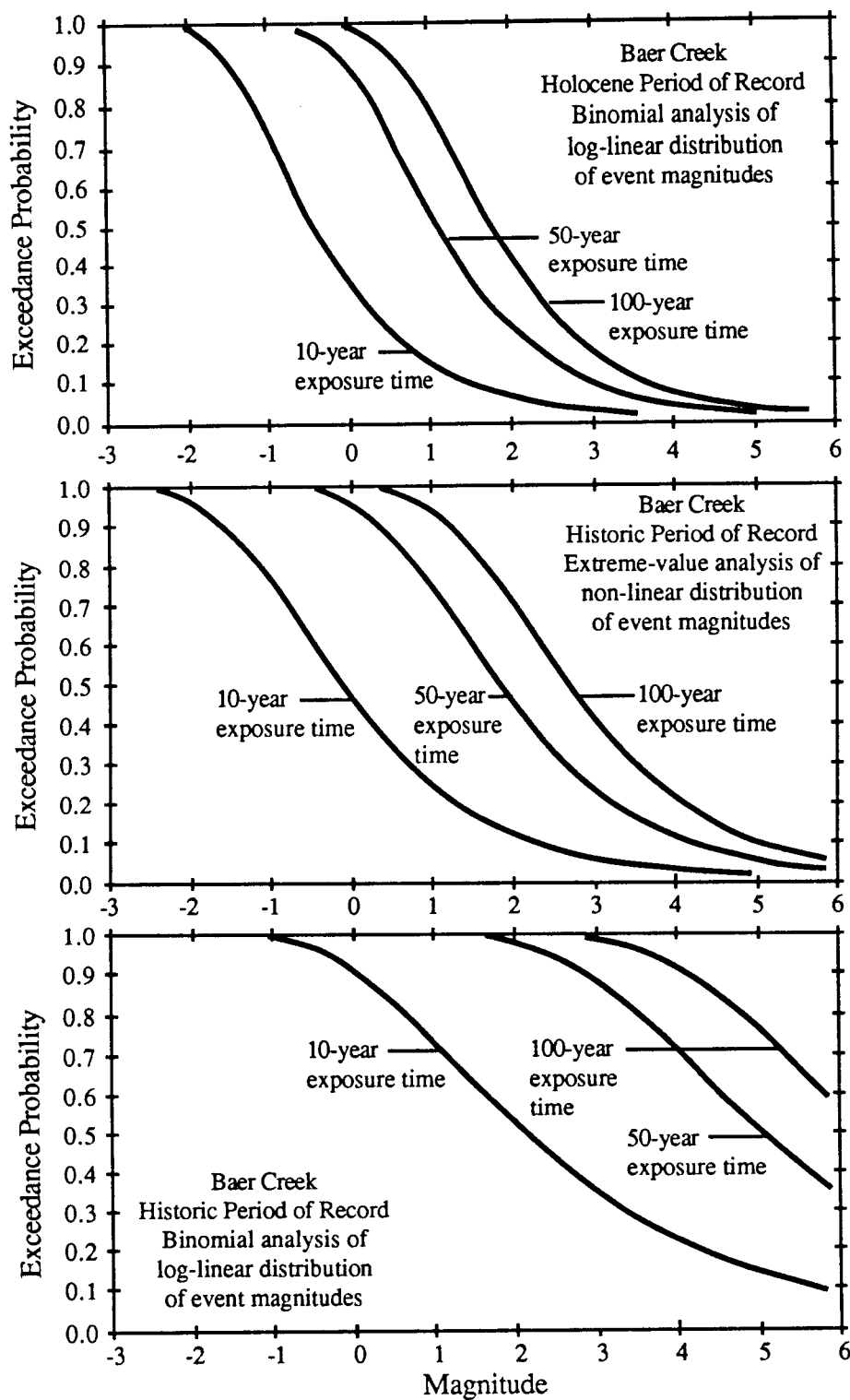


Figure F-9. Exceedance probability curves for sedimentation events on the Baer Creek fan.

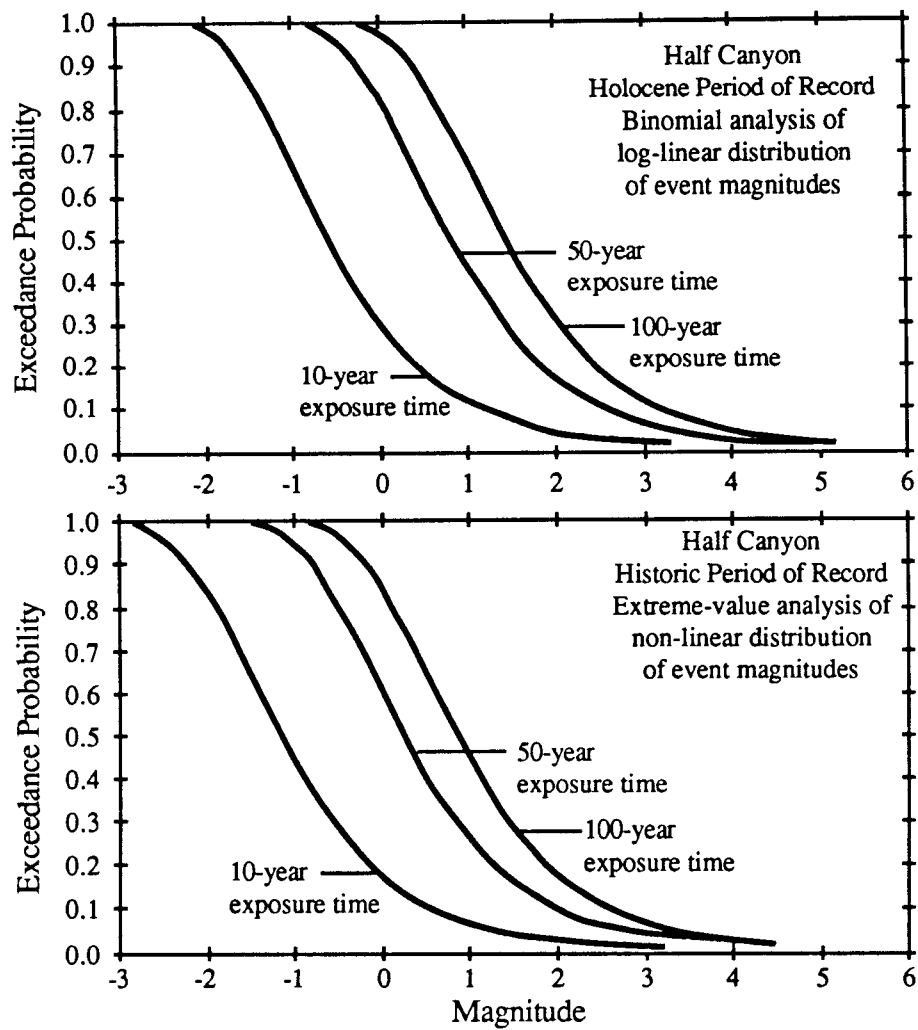


Figure F-10. Exceedance probability curves for sedimentation events on the Half Canyon fan.

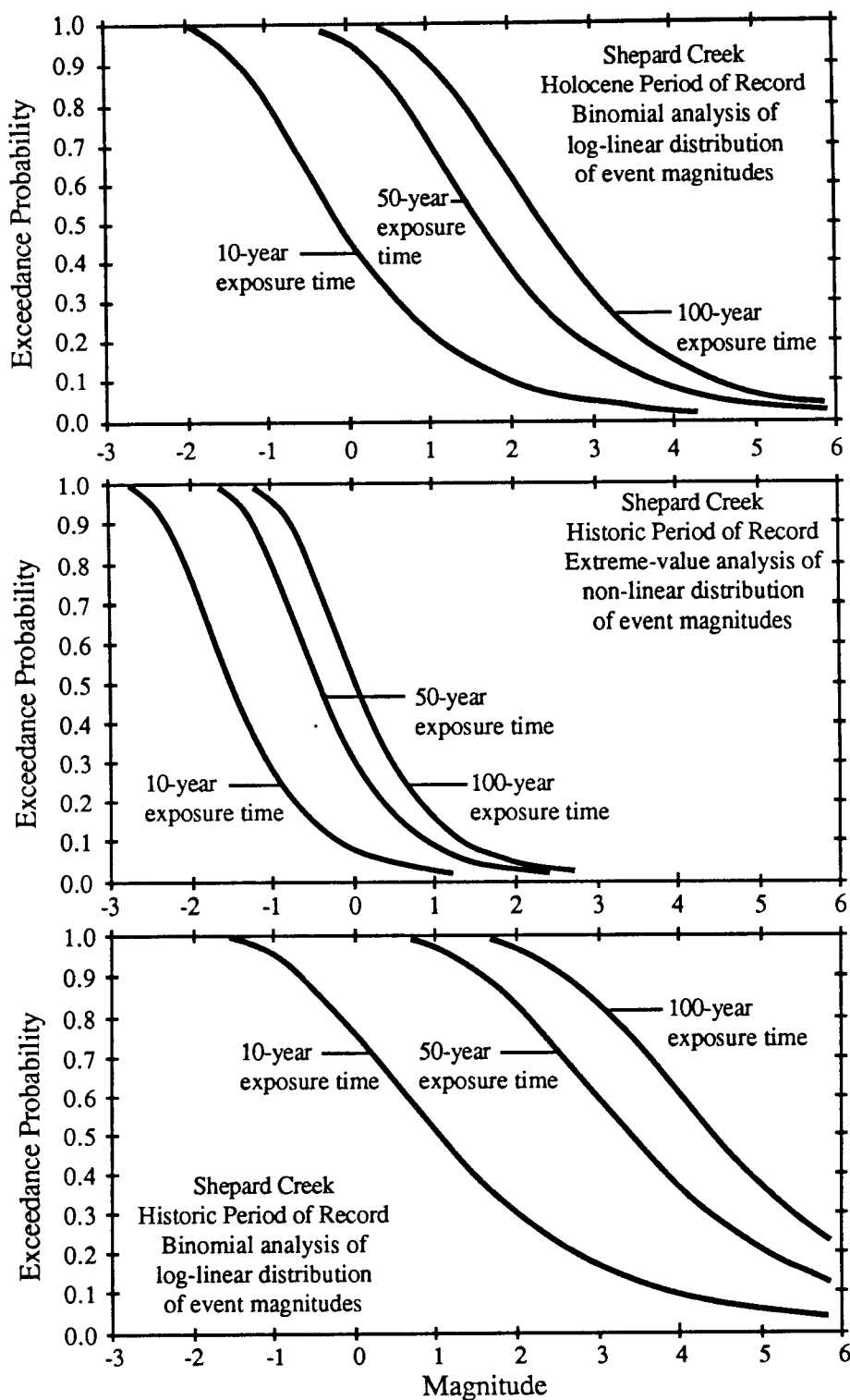


Figure F-11. Exceedance probability curves for sedimentation events on the Shepard Creek fan.

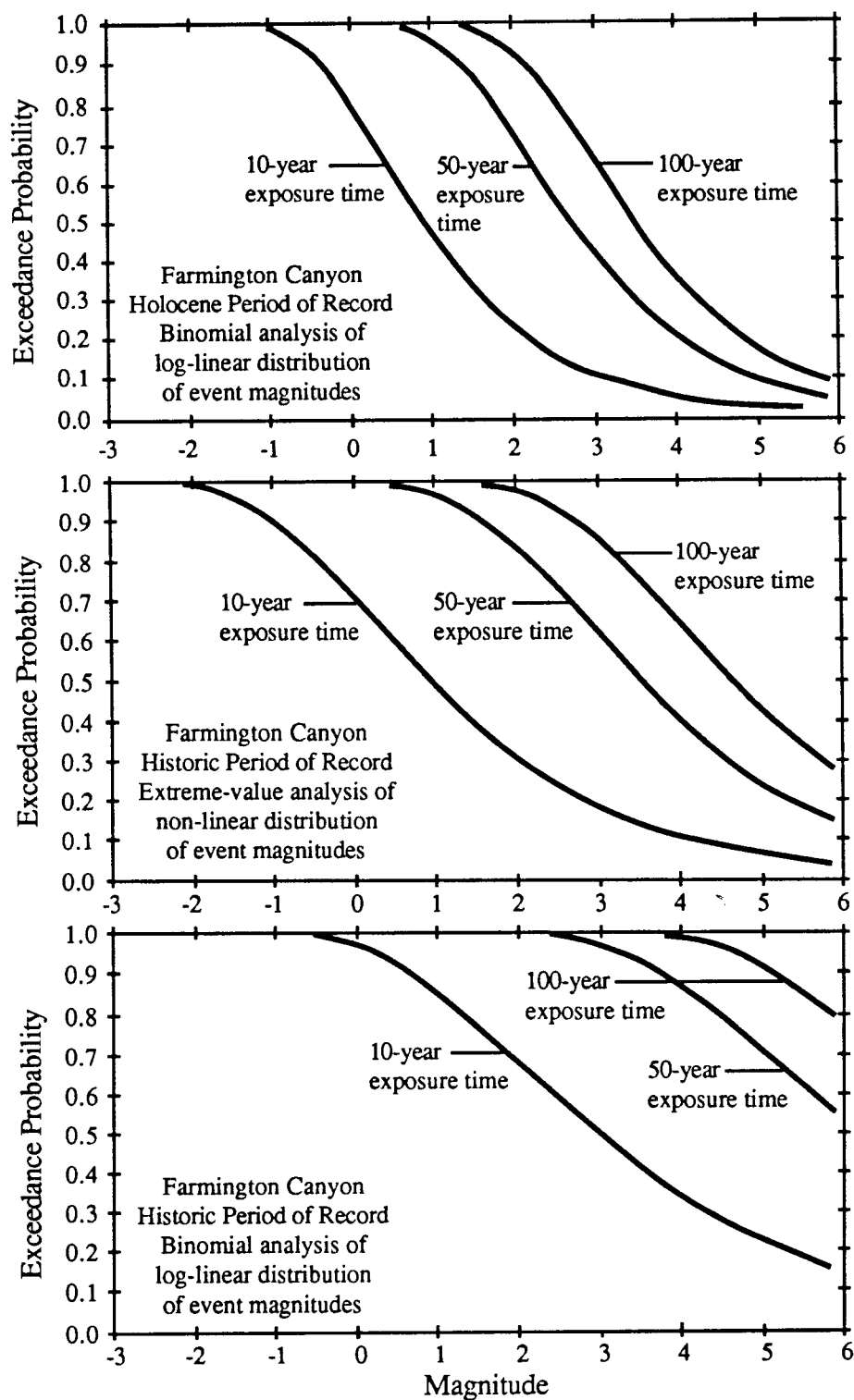


Figure F-12. Exceedance probability curves for sedimentation events on the Farmington Canyon fan.

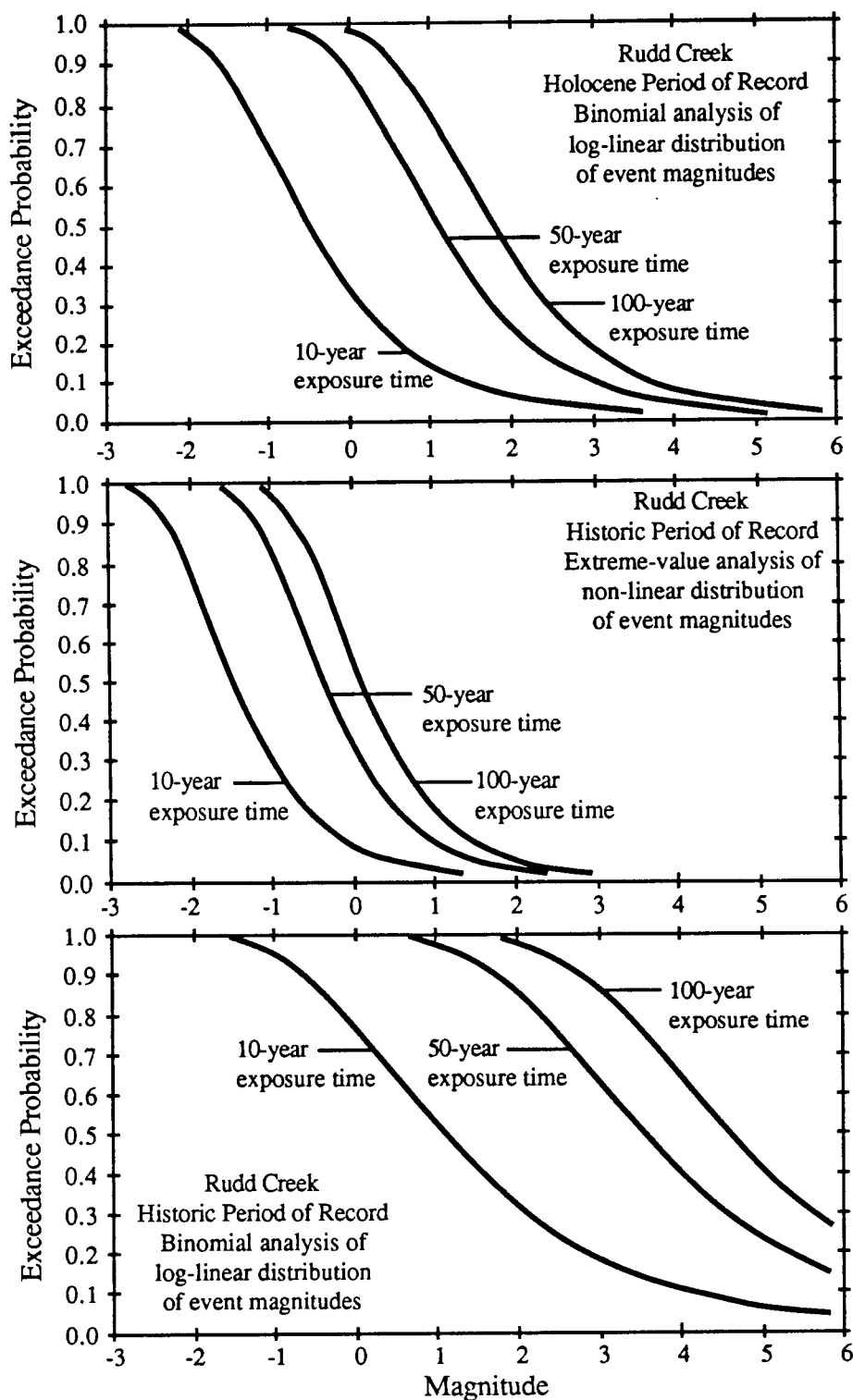


Figure F-13. Exceedance probability curves for sedimentation events on the Rudd Creek fan.

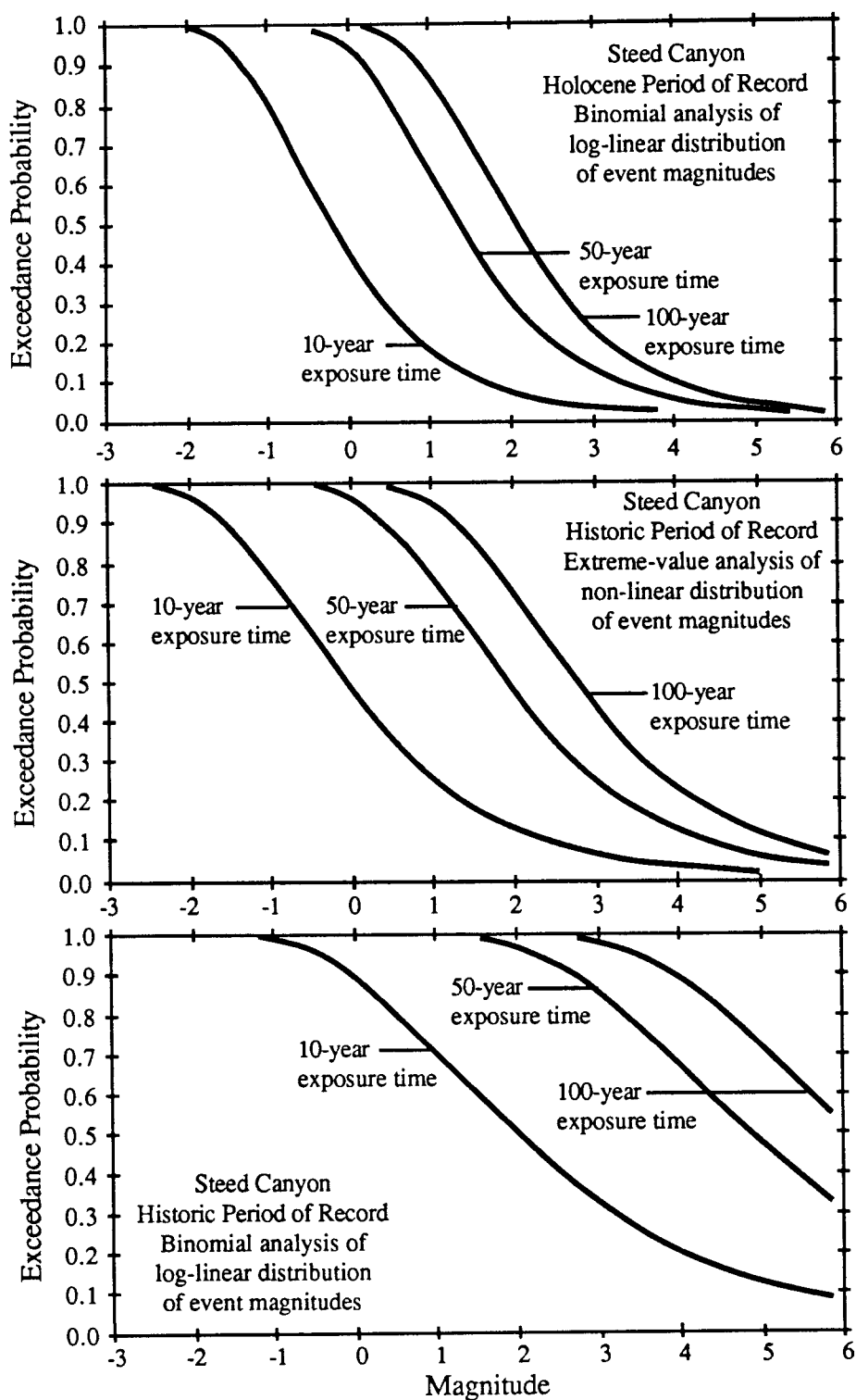


Figure F-14. Exceedance probability curves for sedimentation events on the Steed Canyon fan.

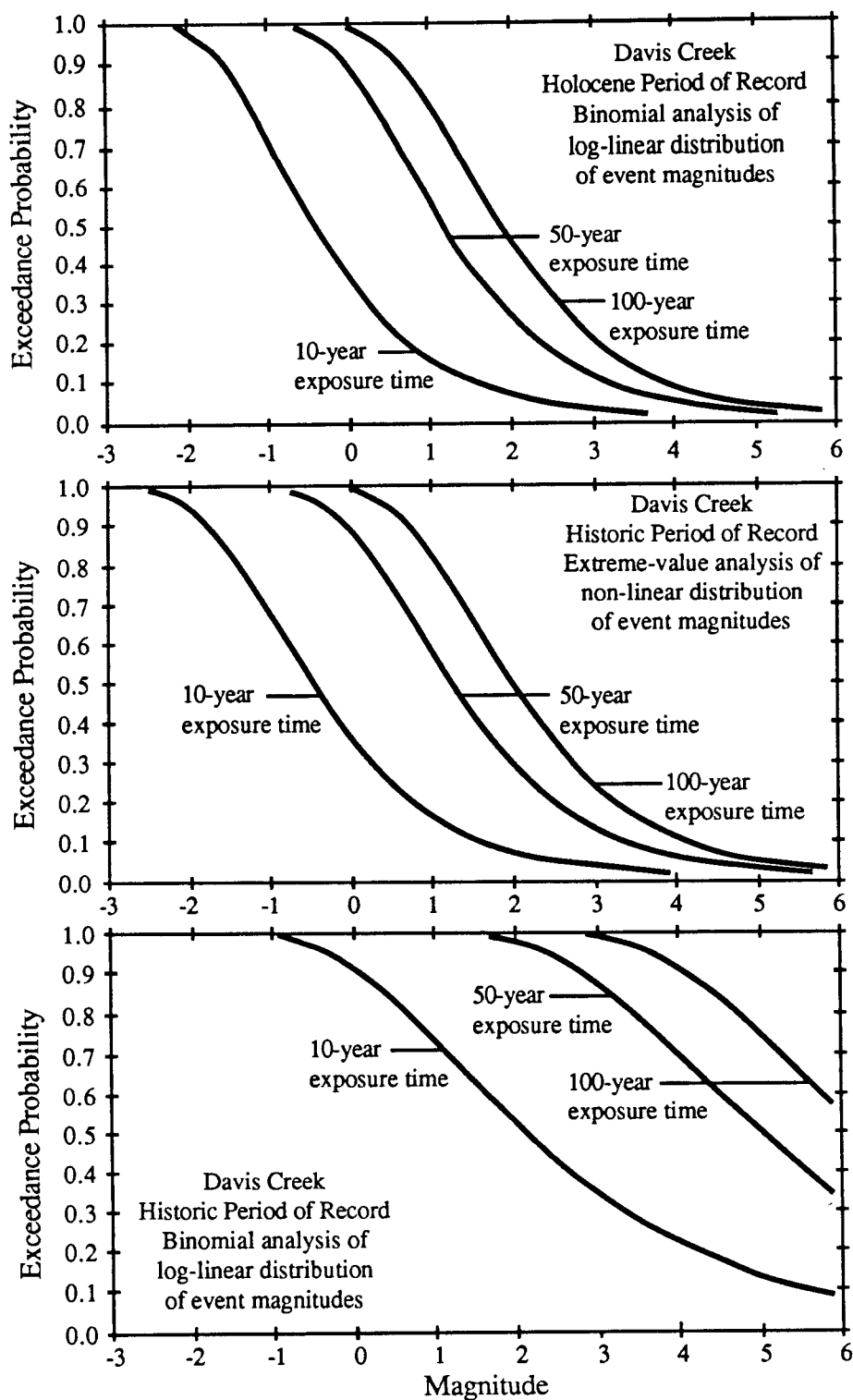


Figure F-15. Exceedance probability curves for sedimentation events on the Davis Creek fan.

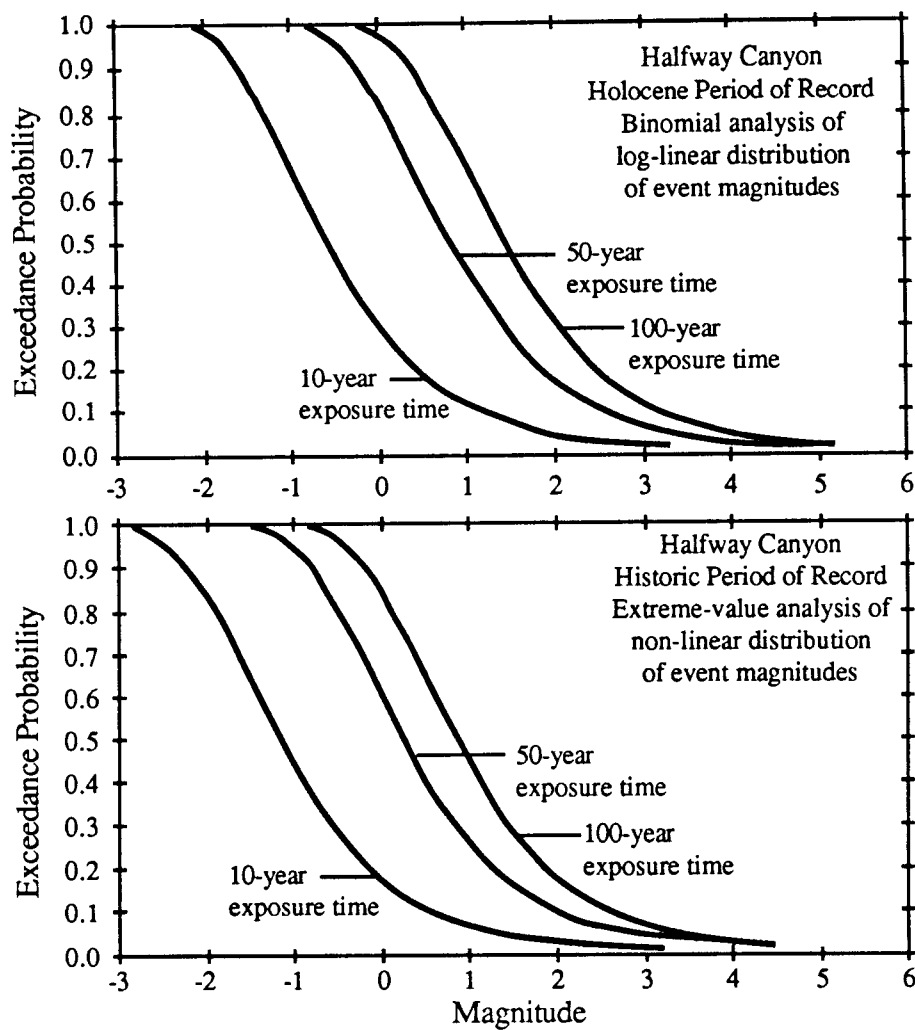


Figure F-16. Exceedance probability curves for sedimentation events on the Halfway Canyon fan.

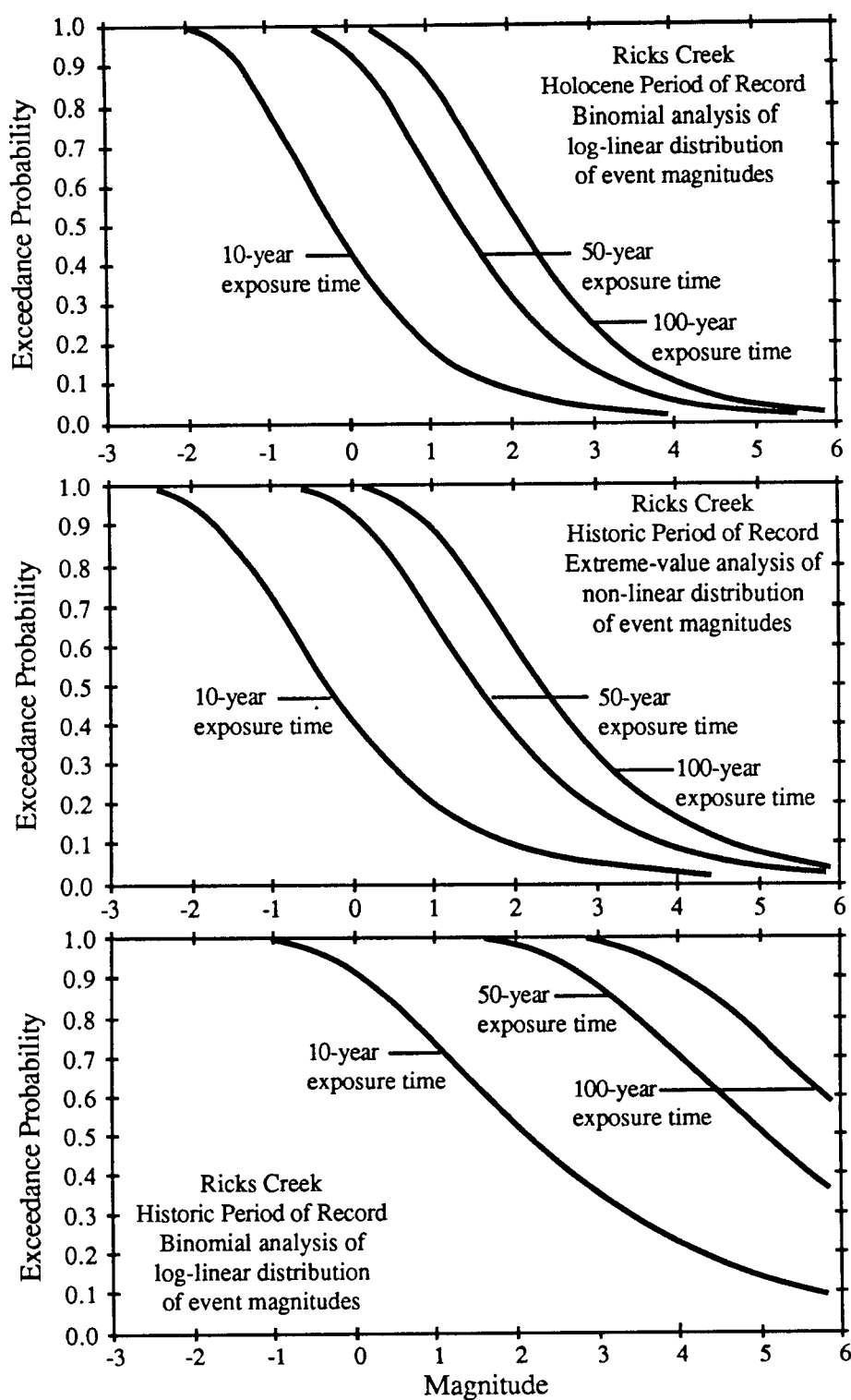


Figure F-17. Exceedance probability curves for sedimentation events on the Ricks Creek fan.

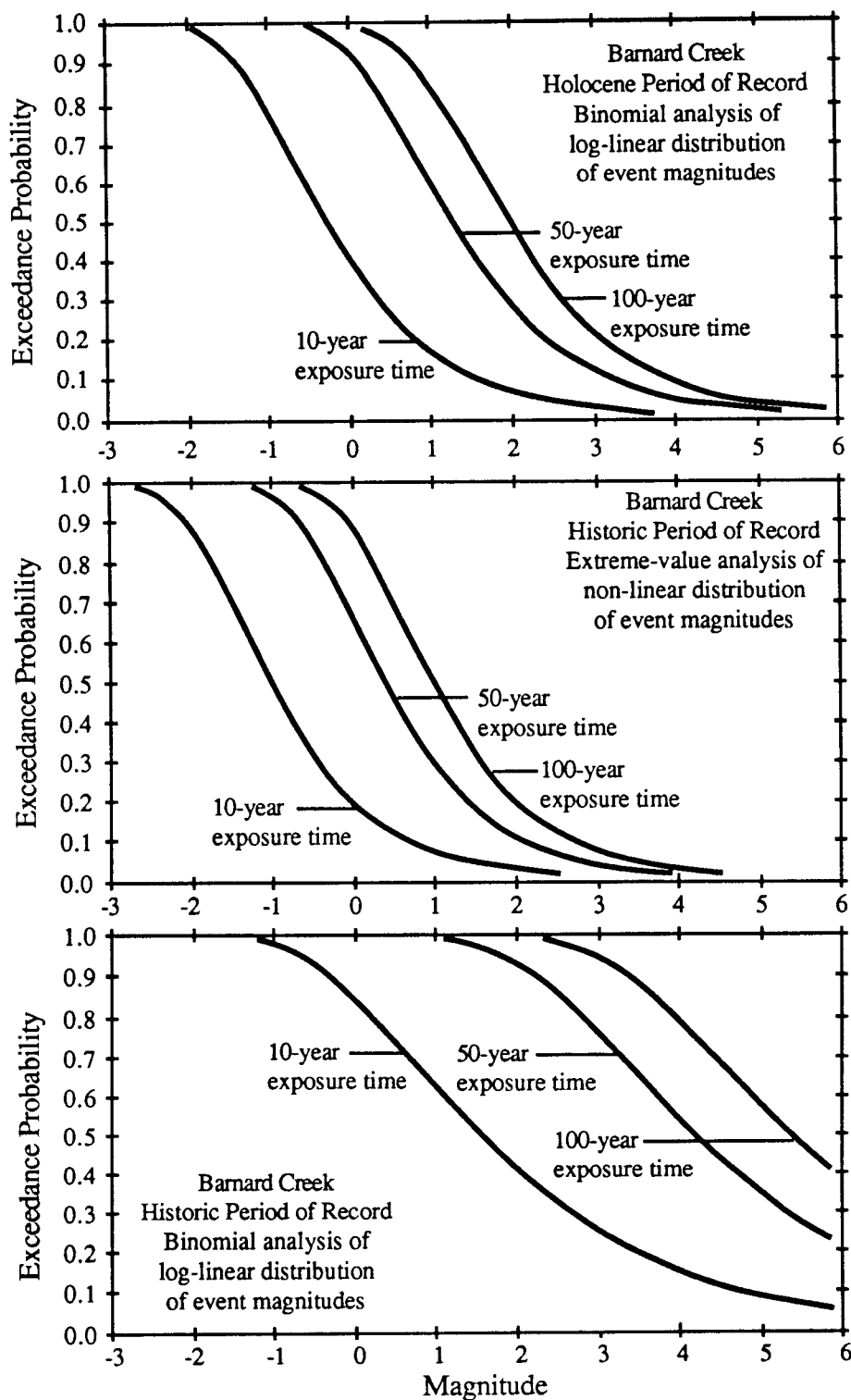


Figure F-18. Exceedance probability curves for sedimentation events on the Barnard Creek fan.

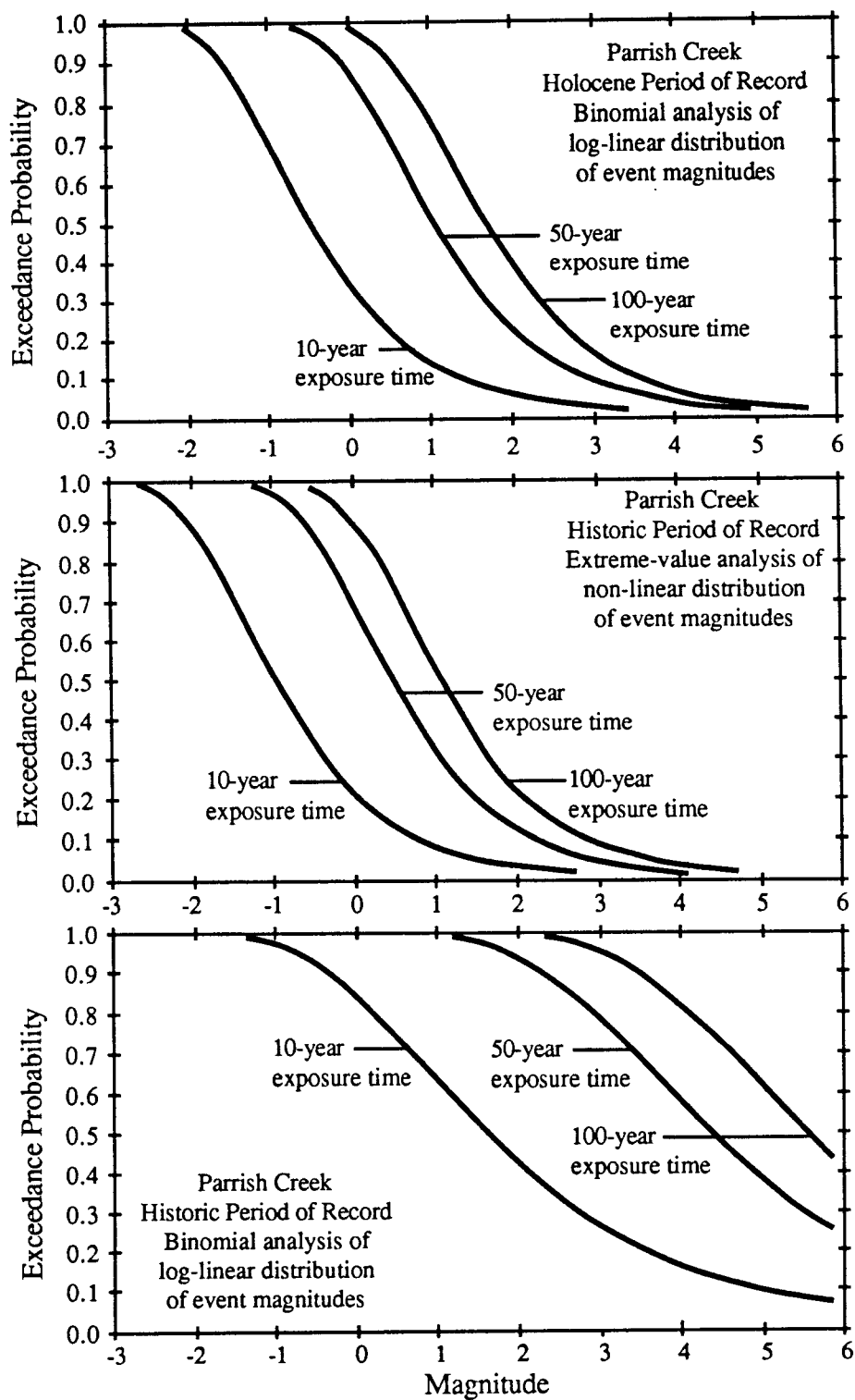


Figure F-19. Exceedance probability curves for sedimentation events on the Parrish Creek fan.

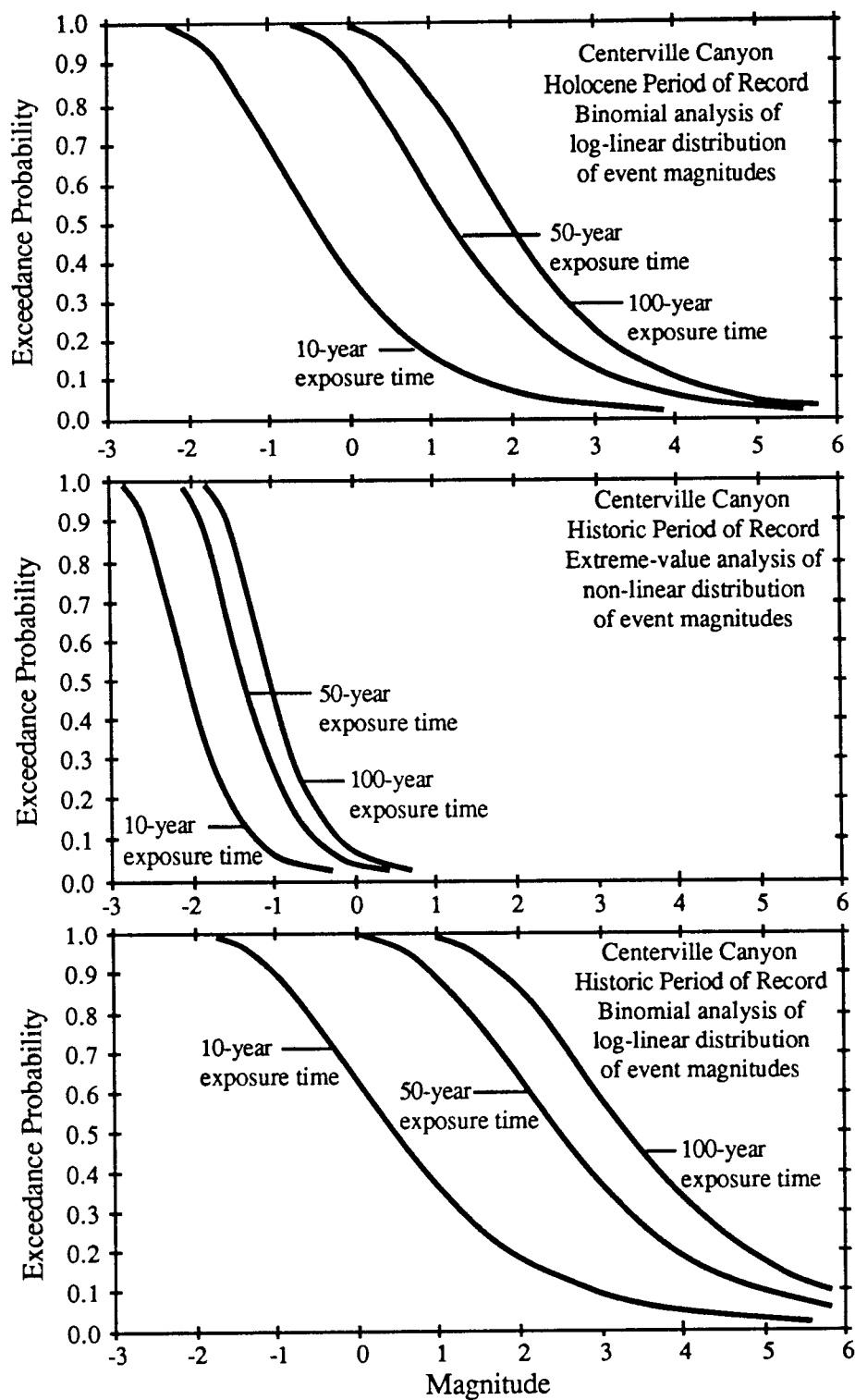


Figure F-20. Exceedance probability curves for sedimentation events on the Centerville Canyon fan.

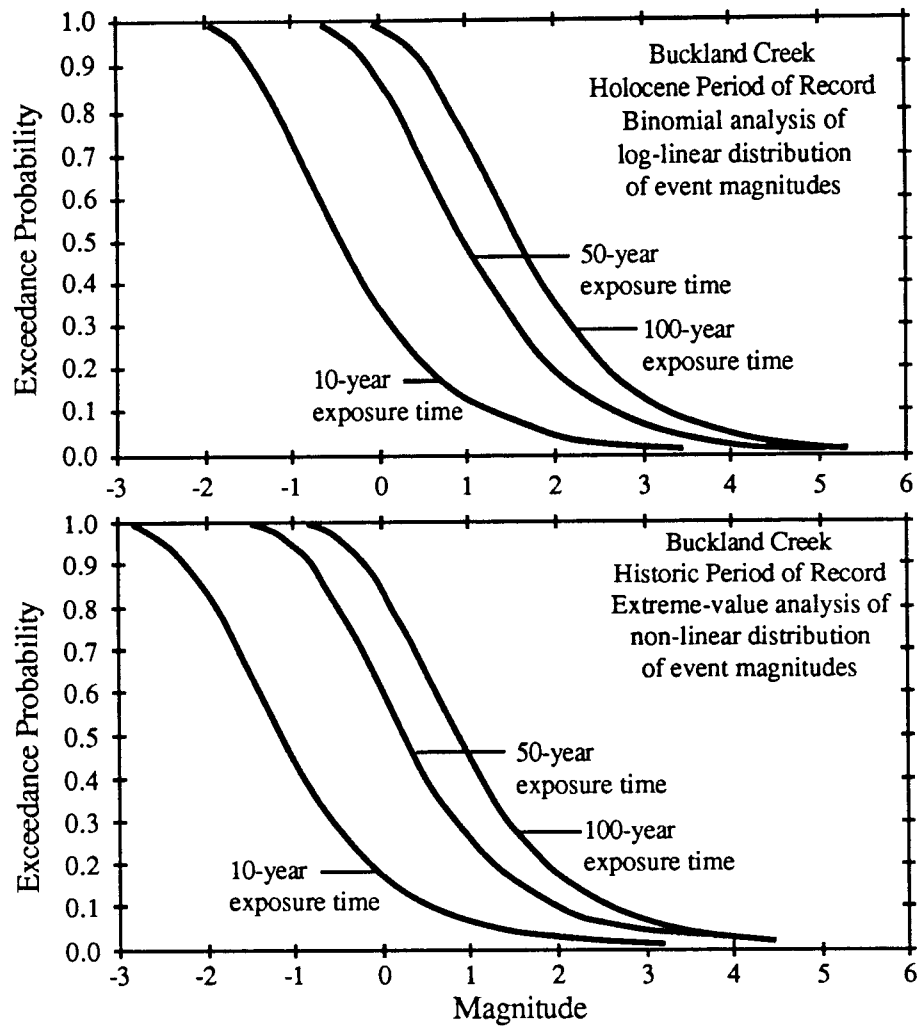


Figure F-21. Exceedance probability curves for sedimentation events on the Buckland Creek fan.

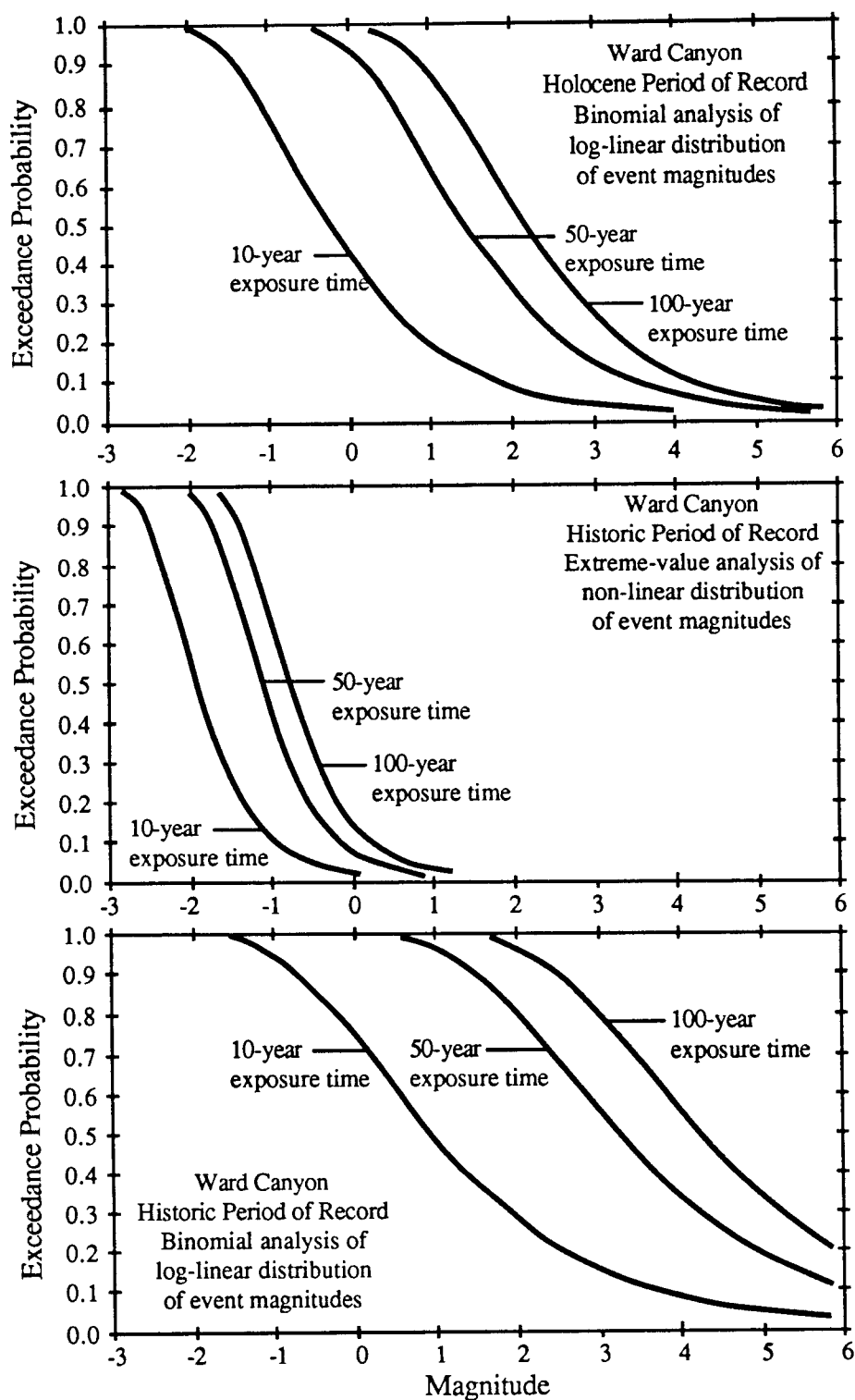


Figure F-22. Exceedance probability curves for sedimentation events on the Ward Canyon fan.

were computed for the historic period of record, as summarized in Table E-2. For binomial distributions, equation (F-6) may be rewritten as

$$N_{P,t} = 1 - [1 - P(e \geq M, t)]^{1/t} \quad (F-16)$$

and substituting in equation (F-15),

$$M_{P,t} = \{\log [1 - [1 - P(e \geq M, t)]^{1/t}] - a\} / b \quad (F-17)$$

For Poisson distributions, equation (F-10) may be rewritten as

$$N_{P,t} = \{\ln [1 - P(e \geq M, t)]\} / -t \quad (F-18)$$

and substituting in equation (F-15),

$$M_{P,t} = \{\log (\ln [1 - P(e \geq M, t)]) / -t\} - a\} / b \quad (F-19)$$

For extreme-value distributions, equation (F-11) may be rewritten as

$$M_{P,t} = \{\ln [\ln (1 - P(e \geq M, t)) / -t] / -A\} + U \quad (F-20)$$

where A and U are defined in equations (F-12) and (F-13).

The magnitude values for exceedance probabilities of 0.5 and 0.1 for exposure times of 100, 50, and 10 years are summarized in Table F-3. Probabilistic sedimentation event magnitudes calculated on the basis of binomial distributions for the historic period of record commonly exceed 6, suggesting that either 1) the magnitude-frequency relationship is nonlinear, or 2) the historic period of record is unrepresentative of the sedimentation history of the fans. The extreme-value distribution of probabilistic event magnitudes for the historic period of record is less than the binomial distribution for the historic period in all cases. However, the extreme-value distribution magnitudes for the historic period are greater than the binomial distribution for the Holocene period for fans with significant historic sedimentation events (Kays Creek (South Fork), Baer Creek, Farmington Canyon, and Steed Canyon). In most cases, the extreme-value distributions magnitudes for the historic period are less than the binomial distribution magnitudes for the Holocene period.

Table F-3. Summary of probabilistic evaluation of sedimentation hazards on alluvial fans in Davis County. Magnitudes of sedimentation events with exceedance probabilities of 0.5 and 0.1 in exposure times of 100, 50, and 10 years were calculated with a BASIC program "MAGPRO.2" (Appendix G). Holocene period of record refers to post-Lake Bonneville time; historic period of record is taken to be 140 years. Binomial and extreme-value types of probability analyses are described in the text.

Fan	Period of Record	Type of Probability Analysis	Calculated Magnitude of Sedimentation Event					
			100-Year Exposure Time		50-Year Exposure Time		10-year Exposure Time	
			P=0.5	P=0.1	P=0.5	P=0.1	P=0.5	P=0.1
Corbett	Holocene	Binomial	1.45	3.11	0.84	2.50	-0.57	1.08
	Historic	Extreme-value	0.87	2.52	0.26	1.19	-1.15	0.50
Hobbs	Holocene	Binomial	1.44	3.11	0.83	2.50	-0.57	1.08
	Historic	Extreme-value	0.87	2.52	0.26	1.19	-1.15	0.50
Lightning	Holocene	Binomial	1.49	3.18	0.87	2.56	-0.55	1.11
	Historic	Extreme-value	-0.83	0.08	-1.16	-0.26	-1.94	-1.03
	Historic	Binomial	3.99	6.63	3.02	5.66	0.79	3.40
Kays (Middle)	Holocene	Binomial	1.23	3.03	0.57	2.37	-0.94	0.83
	Historic	Extreme-value	-0.40	0.67	-0.80	0.28	-1.72	-0.64
	Historic	Binomial	3.32	5.71	2.44	4.83	0.44	2.79
Kays (South)	Holocene	Binomial	1.34	3.15	0.68	2.49	-0.84	0.94
	Historic	Extreme-value	2.57	4.80	1.74	3.98	-0.17	2.07
	Historic	Binomial	5.69	8.89	4.51	7.71	1.82	4.97
Snow	Holocene	Binomial	1.78	3.57	1.12	2.91	-0.38	1.38
	Historic	Extreme-value	0.87	2.52	0.26	1.19	-1.15	0.50
Adams	Holocene	Binomial	1.67	3.43	1.03	2.78	-0.44	1.29
	Historic	Extreme-value	0.87	2.52	0.26	1.19	-1.15	0.50
Webb	Holocene	Binomial	1.33	3.16	0.67	2.49	-0.87	0.93
	Historic	Extreme-value	-0.31	0.80	-0.72	0.39	-1.67	-0.56
	Historic	Binomial	3.53	6.00	2.63	5.09	0.55	2.99
Baer	Holocene	Binomial	1.78	3.58	1.12	2.92	-0.40	1.38
	Historic	Extreme-value	2.66	4.95	1.82	4.10	-0.13	2.15
	Historic	Binomial	6.31	9.77	5.04	8.50	2.13	5.54
Half	Holocene	Binomial	1.45	3.12	0.84	2.50	-0.56	1.08
	Historic	Extreme-value	0.87	2.52	0.26	1.19	-1.15	0.50
Shepard	Holocene	Binomial	2.38	4.42	1.62	3.67	-0.10	1.92
	Historic	Extreme-value	0.04	1.30	-0.42	0.84	-1.50	-0.24
	Historic	Binomial	4.40	7.20	3.38	6.17	1.02	3.78

Table F-3. Continued.

Fan	Period of Record	Type of Probability Analysis	<u>Calculated Magnitude of Sedimentation Event</u>					
			<u>100-Year Exposure Time</u>		<u>50-Year Exposure Time</u>		<u>10-year Exposure Time</u>	
			P=0.5	P=0.1	P=0.5	P=0.1	P=0.5	P=0.1
Farmington	Holocene	Binomial	3.51	5.66	2.72	4.87	0.92	3.04
	Historic	Extreme-value	4.64	7.67	3.52	6.55	0.93	3.96
	Historic	Binomial	7.55	11.37	6.15	9.96	2.94	6.70
Rudd	Holocene	Binomial	1.78	3.65	1.10	2.97	-0.47	1.37
	Historic	Extreme-value	0.12	1.41	-0.35	0.94	-1.46	-0.17
	Historic	Binomial	4.60	7.51	3.53	6.44	1.09	3.96
Steed	Holocene	Binomial	2.06	3.93	1.37	3.24	-0.21	1.64
	Historic	Extreme-value	2.77	5.10	1.91	4.24	-0.08	2.25
	Historic	Binomial	6.10	9.50	4.85	8.25	1.99	5.34
Davis	Holocene	Binomial	1.88	3.78	1.18	3.08	-0.42	1.46
	Historic	Extreme-value	2.00	4.02	1.25	3.28	-0.48	1.54
	Historic	Binomial	6.23	9.63	4.98	8.38	2.12	5.47
Halfway	Holocene	Binomial	1.45	3.12	0.84	2.50	-0.56	1.08
	Historic	Extreme-value	0.87	2.52	0.26	1.19	-1.15	0.50
Ricks	Holocene	Binomial	2.10	3.99	1.40	3.29	-0.19	1.68
	Historic	Extreme-value	2.33	4.50	1.54	3.70	-0.31	1.85
	Historic	Binomial	6.30	9.76	5.03	8.49	2.12	5.53
Barnard	Holocene	Binomial	1.97	3.82	1.29	3.14	-0.27	1.56
	Historic	Extreme-value	1.00	2.64	0.39	2.04	-1.01	0.63
	Historic	Binomial	5.35	8.49	4.20	7.33	1.55	4.65
Parrish	Holocene	Binomial	1.71	3.51	1.05	2.85	-0.46	1.31
	Historic	Extreme-value	1.10	2.78	0.48	2.16	-0.96	0.72
	Historic	Binomial	5.55	8.82	4.35	7.61	1.60	4.83
Centerville	Holocene	Binomial	1.97	3.97	1.24	3.23	-0.43	1.53
	Historic	Extreme-value	-1.03	-0.21	-1.34	-0.51	-2.04	-1.22
	Historic	Binomial	3.33	5.73	2.45	4.84	0.44	2.80
Buckland	Holocene	Binomial	1.57	3.28	0.94	2.65	-0.50	1.19
	Historic	Extreme-value	0.87	2.52	0.26	1.19	-1.15	0.50
Ward	Holocene	Binomial	2.16	4.13	1.44	3.41	-0.21	1.73
	Historic	Extreme-value	-0.76	0.18	-1.10	-0.16	-1.90	-0.96
	Historic	Binomial	4.23	6.98	3.23	5.97	0.92	3.63

APPENDIX G

COMPUTER PROGRAMS

Program SED.STAT

This program computes the sedimentologic parameters used in the multivariate analysis of clast support mechanism.

```

REM    PROGRAM "SED.STAT"; 10 JUNE 87; MODIFIED 4 JULY; J.R. KEATON
REM    INPUT FROM EXTERNAL FILE: FILE NAME; TITLE; PHI VALUES FOR
REM    5, 16, 25, 40, 50, 70, 75, 84, 90, 95 PERCENT COARSER;
REM    FINES (% PASSING # 200); MATRIX (% PASSING # 40); LIQUID LIMIT;
REM    FLOW INDEX; AND PLASTICITY INDEX.
REM    CALCULATES MEAN, STANDARD DEVIATION, SKEWNESS, KURTOSIS
REM    (AFTER FOLK,1980); COEFFICIENT OF UNIFORMITY AND
REM    COEFFICIENT OF CURVATURE FROM UNIFIED SOIL CLASSIFICATION
REM    SYSTEM DEFINITIONS; FINES ACTIVITY, MATRIX ACTIVITY, FINES
REM    FLOW INDEX, AND MATRIX FLOW INDEX

150    SELECT$ = FILE$(0,"DATA FROM WHICH FILE?")
IF SELECT$="" THEN END
OPEN SELECT$ FOR INPUT AS #1

INPUT #1, FILENAME$, TITLE$, PH5, PH16, PH25, PH40, PH50, PH70, PH75
INPUT #1, PH84, PH90, PH95, F, M, LL, FI, PI
CLOSE #1

REM    MEAN GRAIN SIZE, MZ
MZ = (PH16 + PH50 + PH84)/3

REM    GRAPHIC STANDARD DEVIATION, SIGG, AND INCLUSIVE, SIGI
SIGG = (PH84 - PH16)/2
SIGI = ((PH84 - PH16)/4) + ((PH95 - PH5)/6.6)

REM    INCLUSIVE GRAPHIC SKEWNESS, SKI, NORMALIZED, SKI1
SK1 = (PH16 + PH84 - (2*PH50))/(2*(PH84 - PH16))
SK2 = (PH5 + PH95 - (2*PH50))/(2*(PH95 - PH5))
SKI = SK1 + SK2
SKI1 = SKI/(1 + SKI)

REM    GRAPHIC KURTOSIS, KG, NORMALIZED, KG1
KG = (PH95 - PH5)/(2.44*(PH75 - PH25))
KG1 = KG / (1 + KG)

REM    CONVERT PHI TO MM FOR ENGINEERING VALUES
D60 = 2^(-PH40)
D10 = 2^(-PH90)
D30 = 2^(-PH70)

REM    COEFFICIENT OF UNIFORMITY, CU, AND CURVATURE, CZ
CU = D60 / D10
CZ = (D30^2) / (D10*D60)

REM    FINES ACTIVITY, FA, AND NORMALIZED, FA1
FA = LL/F
FA1 = FA/(1+ FA)

```

```

REM    MATRIX ACTIVITY, MA, AND NORMALIZED, MA1
MA  = LL/M
MA1 = MA/(1+ MA)

IF FI = 0 GOTO 100

REM    FINES FLOW INDEX, FF, AND NORMALIZED, FF1
FF  = F / FI
FF1 = FF / (1 + FF)

REM    MATRIX FLOW INDEX, MF, AND NORMALIZED, MF1
MF  = M / FI
MF1 = MF / (1 + MF)

100    LPRINT TAB(10);
        LPRINT TITLE$;
        LPRINT TAB(50);
        LPRINT "MEAN GRAIN SIZE      = ";
        LPRINT USING "#####.###"; MZ;
        LPRINT "  PHI"
        LPRINT TAB(10);
        LPRINT "GRAPHIC ST. DEV.      = ";
        LPRINT USING "#####.###"; SIGG;
        LPRINT "  PHI";
        LPRINT TAB(50);
        LPRINT "INCLUSIVE ST. DEV. = ";
        LPRINT USING "#####.###"; SIGI;
        LPRINT "  PHI"
        LPRINT TAB(10);
        LPRINT "INCLUSIVE SKEWNESS = ";
        LPRINT USING "#####.###"; SKI;
        LPRINT TAB(50);
        LPRINT "NORMAL INCLUS SKEW = ";
        LPRINT USING "#####.###"; SKI1
        LPRINT TAB(10);
        LPRINT "GRAPHIC KURTOSIS      = ";
        LPRINT USING "#####.###"; KG;
        LPRINT TAB(50);
        LPRINT "NORMALIZED KURTOSIS = ";
        LPRINT USING "#####.###"; KG1
        LPRINT TAB(10);
        LPRINT "UNIFORMITY COEF.      = ";
        LPRINT USING "#####.###"; CU;
        LPRINT TAB(50);
        LPRINT "CURVATURE COEF.      = ";
        LPRINT USING "#####.###"; CZ
        LPRINT TAB(10);
        LPRINT "LIQUID LIMIT          = ";
        IF LL = 0 GOTO 10
        LPRINT USING "#####.###"; 100*LL;
        LPRINT " %";
        GOTO 20
10    LPRINT " ----";
20    LPRINT TAB(50);
        LPRINT "PLASTICITY INDEX      = ";
        IF LL = 0 GOTO 25
        IF PI = 0 GOTO 30

```

```

        LPRINT USING "####.###"; 100*PI; LPRINT " %"
        GOTO 40
25      LPRINT " ----"
        GOTO 40
30      LPRINT " NONPLASTIC"
40      LPRINT TAB(10);
        LPRINT "FLOW INDEX          = ";
        IF LL = 0 GOTO 50
        LPRINT USING "####.###"; FI;
        GOTO 60
50      LPRINT " ----";
60      LPRINT TAB(50);
        LPRINT "MINUS #200 FRACTION = ";
        LPRINT USING "####.###"; 100*F;
        LPRINT " %"
        IF LL = 0 GOTO 70
        LPRINT TAB(10);
        LPRINT "FINES ACTIVITY          = ";
        LPRINT USING "####.###"; FA;
        LPRINT TAB(50);
        LPRINT "NORMAL FINES ACT          = ";
        LPRINT USING "####.###"; FA1
        LPRINT TAB(10);
        LPRINT "MATRIX ACTIVITY          = ";
        LPRINT USING "####.###"; MA;
        LPRINT TAB(50);
        LPRINT "NORMAL MATRIX ACT          = ";
        LPRINT USING "####.###"; MA1
        LPRINT TAB(10);
        LPRINT "FINES FLOW INDEX          = ";
        LPRINT USING "####.###"; FF;
        LPRINT TAB(50);
        LPRINT "NORMAL FINES FLOW          = ";
        LPRINT USING "####.###"; FF1
        LPRINT TAB(10);
        LPRINT "MATRIX FLOW INDEX          = ";
        LPRINT USING "####.###"; MF;
        LPRINT TAB(50);
        LPRINT "NORMAL MATRIX FLOW          = ";
        LPRINT USING "####.###"; MF1
        GOTO 80
70      LPRINT TAB(10);
        LPRINT "FINES ACTIVITY          = ";
        LPRINT " ----";
        LPRINT TAB(50);
        LPRINT "NORMAL FINES ACT          = ";
        LPRINT " ----"
        LPRINT TAB(10);
        LPRINT "MATRIX ACTIVITY          = ";
        LPRINT " ----";
        LPRINT TAB(50);
        LPRINT "NORMAL MATRIX ACT          = ";
        LPRINT " ----"
        LPRINT TAB(10);
        LPRINT "FINES FLOW INDEX          = ";
        LPRINT " ----";
        LPRINT TAB(50);
        LPRINT "NORMAL FINES FLOW          = ";

```

```

      LPRINT " ----"
      LPRINT TAB(10);
      LPRINT "MATRIX FLOW INDEX    = ";
      LPRINT " ----";
      LPRINT TAB(50);
      LPRINT "NORMAL MATRIX FLOW    = ";
      LPRINT " ----"
80    LPRINT
      LPRINT

INPUT "ANOTHER ANALYSIS FOLLOWS?", STATEMENT$
IF LEFT$(STATEMENT$,1) = "Y" THEN GOTO 150

STOP

```

Program SCARP.DIF

This program computes the age since diffusion processes became dominant on a scarp.

```

REM    THIS IS PROGRAM "SCARP.DIF", WRITTEN 20 JAN 88 BY J.R. KEATON
REM    MODIFIED 22 JAN 88 FOLLOWING DISCUSSION WITH STEVE COLMAN.
REM    MODIFIED 30 JAN 88 TO INCORPORATE ASPECT INTO CSTAR VALUE.
REM    USER-INPUT PARAMETERS ARE USED TO COMPUTE THE AGE (IN KA)
REM    OF SCARPS USING DIFFUSIVITIES OF THE BONNEVILLE SHORELINE
REM    FROM PIERCE AND COLMAN (1986) UNLESS USER-INPUT VALUE IS
REM    PROVIDED. ALL PARAMETERS ARE SELF-EXPLANATORY. B IS POLY-
REM    NOMIAL REGRESSION OF ERROR FUNCTION WITH ARGUMENT AS
REM    DEPENDENT AND ERROR FUNCTION AS INDEPENDENT VARIABLE;
REM    R-SQUARED = 1; STANDARD ERROR = 0.0000836.

INPUT "LOCATION OF PROFILE IS ...", LOCAT$
INPUT "PROFILE NO. IS ...", PROF$
INPUT "SLOPE ASPECT IS ...", ASP$
INPUT "SCARP HEIGHT IS ...", H
INPUT "MAXIMUM SLOPE ANGLE IS ...", THETA
INPUT "ANGLE AT WHICH DIFFUSION PROCESS BEGINS IS ...", ALFA

R = 3.14159/180
THETR = THETA*R
ALFR = ALFA*R
ERF = TAN(THETR)/TAN(ALFR)

B1 = -.00007747#+.913#*(ERF)-(.571#*(ERF)^2)+(4.649#*(ERF)^3)
B2 = -(16.233#*(ERF)^4)+(30.889#*(ERF)^5)-(29.168#*(ERF)^6)
B3 = (11.131#*(ERF)^7)
B = B1 + B2 + B3

CT = (H/(4*TAN(ALFR)*B))^2

INPUT "USE BONNEVILLE SHORELINE C*"; AN$
IF LEFT$(AN$,1)="Y" GOTO 10

INPUT "C* VALUE IS ...", CSTAR
GOTO 20

10    CSTAR = .303 + (.135*H)

```

```

INPUT "COMPENSATE FOR NON-NORTH ASPECT"; RE$
IF LEFT$(RE$,1)="N" GOTO 20

INPUT "FOR S:N, INPUT 30; FOR W:N, INPUT 40; FOR S:W, INPUT 50", X
IF X = 30 GOTO 30 ELSE IF X = 40 GOTO 40 ELSE IF X = 50 GOTO 50

30  CSTAR = CSTAR*(1.715 + (.289*H))
    GOTO 20
40  CSTAR = CSTAR*(1.265 + (.098*H))
    GOTO 20
50  CSTAR = CSTAR*(1.42 + (.057*H))
20  T = CT/CSTAR

CLS  'CLEAR SCREEN

PRINT LOCAT$
PRINT PROF$
PRINT ASP$
PRINT "SCARP HEIGHT IN M IS "; H
PRINT "MAXIMUM SLOPE ANGLE IN DEGREES IS "; THETA
PRINT "ANGLE AT WHICH DIFFUSION PROCESSES BEGIN IS "; ALFA
PRINT "VALUE OF C*T IN SQUARE M IS "; CT
PRINT "VALUE OF C* IN SQUARE M / KA IS "; CSTAR
PRINT "ESTIMATED AGE OF SCARP IN KA IS "; T

STOP

```

Program 90PL.MN

This program computes the 90 percent and 10 percent prediction limits of the magnitude-frequency relationship of sedimentation events on alluvial fans in Davis County, Utah.

```

REM  THIS PROGRAM IS "90PL.MN" WRITTEN 16 JAN 88 BY J.R. KEATON
REM  IT COMPUTES 90% PREDICTION LIMITS FOR MAGNITUDE-FREQUENCY
REM  RELATIONSHIPS FOR ALLUVIAL FAN SEDIMENTATION IN DAVIS CO.
REM  IT IS INTERACTIVE WITH USER-INPUT OF VALUES IN LOGICAL FASHION.

10  INPUT "NUMBER OF DATA POINTS= ", NO
    INPUT "T-VALUE (A=0.05, DF = N-2) =", T
    INPUT "STANDARD ERROR FROM REGRESSION = ", SE
    INPUT "SUM OF X^2 = ", SX2
    INPUT "SUM OF X = ", SX
    INPUT "MEAN X = ", XBAR
    INPUT "REGRESSION COEFFICIENT A = ", A
    INPUT "REGRESSION COEFFICIENT B = ", B
    SXX = SX2 - ((SX)^2)/NO

20  INPUT "MAGNITUDE VALUE =", X
    LGN = A + (B*X)
    P90 = T*SE*SQR(1+(1/NO)+((X-XBAR)^2)/SXX)
    N1 = 10^(LGN + P90)      '90% PROBABILITY THAT ALL DATA ARE LESS
    N2 = 10^(LGN)           'MEAN VALUE: 50% PROBABILITY DATA ARE <
    N3 = 10^(LGN - P90)     '10% PROBABILITY THAT ALL DATA ARE LESS
    PRINT X, N1, N2, N3

```

```

INPUT "CHANGE MAGNITUDE VALUE"; AN$
IF LEFT$(AN$,1) = "Y" GOTO 20

INPUT "CALCULATE ANOTHER SERIES OF 90% PREDICTION LIMITS"; RE$
IF LEFT$(RE$,1) = "Y" GOTO 10

STOP

```

Program EXPRAN

This program computes exceedance probabilities based on input parameters and selection of binomial, Poisson, or extreme value distributions.

```

REM    PROGRAM "EXPRAN" J.R. KEATON  28 JUNE 1988
REM    THIS PROGRAM CAN COMPUTE EXCEEDANCE PROBABILITY
REM    AS A FUNCTION OF MAGNITUDE.  USER SELECTS TYPE OF
REM    ANALYSIS: 1 = BINOMIAL; 2 = POISSON; 3 = EXTREME
REM    FOR EXTREME-VALUE ANALYSIS, SAMPLE SIZE IS TAKEN AS
REM    140 FOR THE HISTORIC PERIOD OF RECORD IN DAVIS COUNTY.
REM    PROGRAM CAN ALSO COMPUTE DIFFERENCES IN PROBABILITIES
REM    COMPUTED FROM THE THREE TYPES OF ANALYSIS

CALL TEXTFONT (4)          'MONACO FONT
CALL TEXTSIZE (9)          '9 POINT LETTERS

INPUT "FAN OR BASIN TO BE ANALYZED IS "; ID$
INPUT "PERIOD OF RECORD IS "; PR$
INPUT "EXPOSURE TIME, T = ", T

OPEN "CLIP:" FOR OUTPUT AS #1

INPUT "EVALUATE DIFFERENCES BETWEEN TYPES OF ANALYSES"; RE$
IF LEFT$(RE$,1)="N" GOTO 10

PRINT "SPECIFY TYPES OF ANALYSES TO BE COMPARED"
PRINT "BINOMIAL-POISSON, COM = 1; BINOMIAL-EXTREME, COM = 2;"
PRINT "POISSON-EXTREME, COM = 3."

INPUT "DESIRED COMPARISON, COM = ", COM
IF COM = 1 GOTO 50
IF COM = 2 GOTO 60
IF COM = 3 GOTO 70

10    PRINT "SPECIFY TYPE OF EXCEEDANCE PROBABILITY ANALYSIS"
PRINT "BINOMIAL, TYP = 1;  POISSON, TYP = 2;  EXTREME, TYP = 3."
INPUT "TYP = ", TYP

IF TYP = 2 GOTO 20
IF TYP = 3 GOTO 30

REM    BINOMIAL EXCEEDANCE PROBABILITY

INPUT "REGRESSION INTERCEPT, A = ", A
INPUT "REGRESSION SLOPE, B = ", B
FOR M = -3# TO 6# STEP .1#
N = 10^(A + B*M)
PBI = 1 - (1 - N)^T

```

```

IF PBI > .99# GOTO 5
IF PBI < .01# GOTO 5
WRITE #1, M,PBI
PRINT M,PBI
5    NEXT M

```

```

GOTO 40

```

```

20    REM    POISSON EXCEEDANCE PROBABILITY

```

```

INPUT "REGRESSION INTERCEPT, A = ", A
INPUT "REGRESSION SLOPE, B = ", B

```

```

    FOR M = -3 TO 6 STEP .1
    N = 10^(A + B*M)
    PPO = 1 - EXP(-N*T)
    IF PPO > .99# GOTO 6
    IF PPO < .01# GOTO 6
    PRINT M,PPO
    WRITE #1, M,PPO
6    NEXT M

```

```

GOTO 40

```

```

30    REM    EXTREME-VALUE EXCEEDANCE PROBABILITY

```

```

INPUT "MEAN MAGNITUDE, MM = ", MM
INPUT "STANDARD DEVIATION OF MAGNITUDE, SM = ", SM
A = 1.22157/SM
U = MM - (.56369/A)
FOR M = -3# TO 6# STEP .1#
PEX = 1 - EXP(-T * EXP(-A * (M - U)))
IF PEX > .99# GOTO 7
IF PEX < .01# GOTO 7
WRITE #1, M,PEX
PRINT M,PEX
7    NEXT M

```

```

GOTO 40

```

```

50    REM    DIFFERENCE BETWEEN BINOMIAL AND POISSON PROBABILITIES

```

```

INPUT "REGRESSION INTERCEPT, A = ", A
INPUT "REGRESSION SLOPE, B = ", B

```

```

    FOR M = -3# TO 6# STEP .1#
    N = 10^(A + B*M)
    PBI = 1 - (1 - N)^T
    PPO = 1 - EXP(-N*T)
    DBP = PBI - PPO
    PRINT M,DBP
    WRITE #1, M,DBP
    NEXT M

```

```

GOTO 40

```

```

60    REM    DIFFERENCE BETWEEN BINOMIAL AND EXTREME PROBABILITIES

```

```

INPUT "REGRESSION INTERCEPT, A = ", A
INPUT "REGRESSION SLOPE, B = ", B
INPUT "MEAN MAGNITUDE, MM = ", MM
INPUT "STANDARD DEVIATION OF MAGNITUDE, SM = ", SM

```

```

AE = 1.22157/SM
U = MM - (.56369/AE)

```

```

FOR M = -3# TO 6# STEP .1#
N = 10^(A + B*M)
PBI = 1 - (1 - N)^T
PEX = 1 - EXP(-T * EXP(-AE * (M - U)))
DBE = PBI - PEX
PRINT M,DBE
WRITE #1, M,DBE
NEXT M

```

```

GOTO 40

```

```

70 REM DIFFERENCE BETWEEN POISSON AND EXTREME PROBABILITIES

```

```

INPUT "REGRESSION INTERCEPT, A = ", A
INPUT "REGRESSION SLOPE, B = ", B
INPUT "MEAN MAGNITUDE, MM = ", MM
INPUT "STANDARD DEVIATION OF MAGNITUDE, SM = ", SM

```

```

AE = 1.22157/SM
U = MM - (.56369/AE)

```

```

FOR M = -3# TO 6# STEP .1#
N = 10^(A + B*M)
PPO = 1 - EXP(-N*T)
PEX = 1 - EXP(-T * EXP(-AE * (M - U)))
DPE = PPO - PEX
PRINT M,DPE
WRITE #1, M,DPE
NEXT M

```

```

40 CLOSE #1

```

```

STOP

```

Program MAGPRO.2

This program computes the value of sediment magnitude for given probabilities of occurrence, exposure times, and magnitude-frequency relationships.

```

REM PROGRAM "MAGPRO.2" J.R. KEATON 4 JULY 1988
REM THIS PROGRAM COMPUTES VALUES OF SEDIMENT MAGNITUDE
REM AS A FUNCTION OF EXPOSURE TIME, EXCEEDANCE PROBABILITY,
REM AND MAGNITUDE-FREQUENCY RELATIONSHIP FOR LOG-LINEAR
REM OR MEAN AND STANDARD DEVIATION FOR NON-LINEAR MAGNITUDE
REM DISTRIBUTIONS. HOLOCENE PERIOD OF RECORD IS TAKEN TO BE
REM 10 KA; HISTORIC PERIOD OF RECORD IS TAKEN TO BE 140 YR.

```

```

CALL TEXTFONT (4) 'MONACO FONT

```



```

CALL TEXTSIZE (9)      'SIZE 9 POINT

100  PRINT "COMPUTE MAGNITUDE (M) FOR SPECIFIED EXPOSURE TIME (T)"
      PRINT "AND EXCEEDANCE PROBABILITY (P) USING BINOMIAL (TYPE 1),"
      PRINT "POISSON (TYPE 2), OR EXTREME-VALUE (TYPE 3) ANALYSIS"

INPUT "SELECT TYPE OF ANALYSIS, TYPE = ", TYP
INPUT "FAN NAME = ", FAN$
INPUT "PERIOD OF RECORD (HOLOCENE, HO; HISTORIC, HI) = ", PR$

IF TYP = 3 GOTO 10

INPUT "REGRESSION INTERCEPT, A = ", A
INPUT "REGRESSION SLOPE, B = ", B
GOTO 15

10   INPUT "MEAN MAGNITUDE = ", MM
      INPUT "STANDARD DEVIATION = ", SD
15   INPUT "EXPOSURE TIME, T = ", T
      INPUT "EXCEEDANCE PROBABILITY, P = ", P

IF TYP = 1 GOTO 20
IF TYP = 2 GOTO 30

      GOSUB EXTREME

GOTO 40

20   GOSUB BINOMIAL

GOTO 40

30   GOSUB POISSON

40   LPRINT TAB(5);
      LPRINT FAN$;
      LPRINT "  FAN;  ";
      IF TYP = 1 GOTO 41
      IF TYP = 2 GOTO 42
      IF TYP = 3 GOTO 43
41   LPRINT "BINOMIAL ANALYSIS"
      GOTO 50
42   LPRINT "POISSON ANALYSIS"
      GOTO 50
43   LPRINT "EXTREME-VALUE ANALYSIS"
50   LPRINT TAB(15);
      LPRINT "EXPOSURE TIME = ";
      LPRINT T;
      LPRINT "  PROBABILITY = ";
      LPRINT P;
      LPRINT "  MAGNITUDE = ";
      LPRINT M

INPUT "PERFORM ANOTHER ANALYSIS FROM THE BEGINNING"; AN1$
IF LEFT$(AN1$,1) = "Y" GOTO 100

INPUT "CHANGE ANY PARAMETERS"; AN2$
IF LEFT$(AN2$,1) = "N" GOTO 200

```

```

PRINT "CHANGE P AND T, CH=1; CHANGE ONLY P, CH=2; CHANGE ONLY T, CH=3"
INPUT "SELECT ONE TYPE OF CHANGE, CH = ", CH
IF CH = 2 GOTO 60
IF CH = 3 GOTO 70

INPUT "NEW VALUE OF P = ", P
INPUT "NEW VALUE OF T = ", T
IF TYP = 1 GOTO 61
IF TYP = 2 GOTO 62
IF TYP = 3 GOTO 63

60   INPUT "NEW VALUE OF P = ", P
IF TYP = 1 GOTO 61
IF TYP = 2 GOTO 62
IF TYP = 3 GOTO 63

70   INPUT "NEW VALUE OF T = ", T
IF TYP = 1 GOTO 61
IF TYP = 2 GOTO 62
IF TYP = 3 GOTO 63

61   GOSUB BINOMIAL
      GOTO 50
62   GOSUB POISSON
      GOTO 50
63   GOSUB EXTREME
      GOTO 50

200  STOP

REM   SUBROUTINES

BINOMIAL:
  N = 1 - (1 - P)^(1/T)
  M = ((LOG(N)/LOG(10)) - A) / B
  RETURN

POISSON:
  N = (LOG(1 - P)) / (-T)
  M = ((LOG(N)/LOG(10)) - A) / B
  RETURN

EXTREME:
  AE = 1.22157/SD
  U = MM - (.56369/AE)
  M = ((LOG(LOG(1 - P) / (-T))) / (-AE)) + U
  RETURN

```

Program MAGPRO.3

This program is similar to MAGPRO.2 except the magnitude returned by this algorithm is based on the average value of the binomial distribution for the Holocene period of record and the extreme-value distribution for the historic period of record.

```

REM   PROGRAM "MAGPRO.3" J.R. KEATON 4 JULY 1988; REV 3 SEPT 88

```

```

REM      THIS PROGRAM COMPUTES VALUES OF SEDIMENT MAGNITUDE
REM      AS A FUNCTION OF EXPOSURE TIME, EXCEEDANCE PROBABILITY,
REM      AND MAGNITUDE-FREQUENCY RELATIONSHIP FOR THE AVERAGE
REM      OF LOG-LINEAR AND EXTREME-VALUE DISTRIBUTIONS. THIS IS
REM      TAKEN TO REPRESENT THE BEST APPROXIMATION OF REALITY
REM      GIVEN CURRENT STATE OF KNOWLEDGE.

CALL TEXTFONT (4)      'MONACO FONT
CALL TEXTSIZE (9)      'SIZE 9 POINT

100      PRINT "COMPUTE MAGNITUDE (M) FOR SPECIFIED EXPOSURE TIME (T)"
PRINT "AND EXCEEDANCE PROBABILITY (P) USING THE AVERAGE OF THE"
PRINT "BINOMIAL AND EXTREME-VALUE ANALYSIS"
INPUT "FAN NAME = ", FAN$
INPUT "REGRESSION INTERCEPT, A = ", A
INPUT "REGRESSION SLOPE, B = ", B
INPUT "MEAN MAGNITUDE = ", MM
INPUT "STANDARD DEVIATION = ", SD
INPUT "EXPOSURE TIME, T = ", T
INPUT "EXCEEDANCE PROBABILITY, P = ", P

120      GOSUB BINOMIAL

          GOSUB EXTREME

M = (MB + ME) / 2

      PRINT TAB(5);
      PRINT FAN$;
      PRINT "    FAN;    "
      PRINT "EXPOSURE TIME = ";
      PRINT T;
      PRINT "    PROBABILITY = ";
      PRINT P;
      PRINT "    MAGNITUDE = ";
      PRINT USING "##.##"; M

INPUT "PERFORM ANOTHER ANALYSIS FROM THE START"; AN1$
IF LEFT$(AN1$,1) = "Y" GOTO 100

INPUT "CHANGE EXPOSURE TIME ONLY"; AN2$
IF LEFT$(AN2$,1)="N" GOTO 110
INPUT "NEW EXPOSURE TIME, T= ", T
GOTO 120

110      INPUT "CHANGE PROBABILITY VALUE"; AN3$
          IF LEFT$(AN3$,1)="N" GOTO 130
          INPUT "NEW PROBABILITY VALUE, P = ", P
          GOTO 120

130      STOP

REM      SUBROUTINES

BINOMIAL:
      N = 1 - (1 - P)^(1/T)
      MB = ((LOG(N)/LOG(10)) - A) / B
      RETURN

```

EXTREME:

```

    AE = 1.22157/SD
    U = MM - (.56369/AE)
    ME = ((LOG(LOG(1 - P) / (-T))) / (-AE)) + U
    RETURN

```

Program MAGPRO.4

This program calculates the average value of magnitude returned by the binomial analysis of events based on the Holocene period of record and the extreme-value analysis of the historic period.

```

REM    MAGPRO.4, KEATON, 18 SEPT 88
REM    THIS PROGRAM CALCULATES AVERAGE MAGNITUDE USING
REM    BINOMIAL HOLOCENE RECORD AND EXTREME-VALUE HISTORIC
REM    RECORD.  INPUT PARAMETERS ARE EXPOSURE TIME (T),
REM    REGRESSION COEFFICIENTS (A AND B), MEAN AND STANDARD
REM    DEVIATION OF THE MAGNITUDE (MM AND SD).  THE REDUCED
REM    EXTREME VALUES FOR N = 140 ARE MEAN = 0.56369 AND
REM    STANDARD DEVIATION = 1.22157 (FROM GUMBEL, 1958)

CALL TEXTFONT (4)      'MONACO FONT
CALL TEXTSIZE (9)      'SIZE 9 POINT

100    PRINT "COMPUTE MAGNITUDES (M) FOR SPECIFIED EXPOSURE TIME (T)"
PRINT "FOR EXCEEDANCE PROBABILITIES (P) RANGING FROM 0.99 TO 0.01"
PRINT "USING THE AVERAGE OF BINOMIAL AND EXTREME-VALUE ANALYSES"
INPUT "FAN NAME = ", FAN$
INPUT "REGRESSION INTERCEPT, A = ", A
INPUT "REGRESSION SLOPE, B = ", B
INPUT "MEAN MAGNITUDE = ", MM
INPUT "STANDARD DEVIATION = ", SD
INPUT "EXPOSURE TIME, T = ", T

    AE = 1.22157/SD
    U = MM - (.56369/AE)

OPEN "CLIP:" FOR OUTPUT AS #1

FOR P = .99# TO .01# STEP -.01#

    N = 1 - (1 - P)^(1/T)
    MB = ((LOG(N)/LOG(10)) - A) / B
    ME = ((LOG(LOG(1 - P) / (-T))) / (-AE)) + U

M = (MB + ME) / 2

PRINT M, P
WRITE #1, M, P

NEXT P

CLOSE #1

STOP

```

Program HAZ.MOD

This program computes the scores for rating hazards at the proximal fan, middle fan, and distal fan areas. These scores are computed by comparing probabilistic sediment event magnitudes to the size of stream channels and existing debris basins, and the time since and size of historic sediment delivery events. The overall hazard on the fan is simply the average of the individual scores.

```

REM    PROGRAM "HAZ.MOD" 22 FEB 88 J.R. KEATON; REV. 8 JULY 88
REM    IT IS AN INTERACTIVE PROGRAM USING SCORES FOR ATTRIBUTES TO
REM    REPRESENT HAZARDS AT PROXIMAL, MIDDLE, AND DISTAL FAN LOCATIONS
REM    AND HAZARDS DUE TO ABSENCE OF HISTORIC SEDIMENT EVENTS.
REM    FAN HAZARD CLASSIFICATION IS THE AVERAGE OF INDIVIDUAL SCORES.

CALL TEXTFONT (4)      'MONACO FONT
CALL TEXTSIZE (9)      'SIZE 9 POINT

5      INPUT "FAN NAME = ", FAN$
      INPUT "FAN HEAD TRENCH AREA = ", FHT
      INPUT "MIDDLE FAN CHANNEL AREA = ", MFC
      INPUT "EXISTING DEBRIS BASIN VOLUME = ", EDB
      INPUT "YEARS SINCE LAST HISTORIC SEDIMENT EVENT = ", HSE
      INPUT "VOLUME OF LAST HISTORIC EVENT = ", HEV
6      INPUT "BASIS FOR SEDIMENT YIELD VALUE = ", SY$
      INPUT "AVERAGE SEDIMENT YIELD M^3/YR = ", ASY
10     INPUT "PERIOD OF RECORD AND TYPE OF PROBABILITY = ", PR$
      INPUT "MAGNITUDE OF 100-YR, 50% EVENT = ", M1005
      INPUT "MAGNITUDE OF 50-YR, 10% EVENT = ", M501
      INPUT "MAGNITUDE OF 100-YR, 10% EVENT = ", M1001

IF M1005 <= 0 THEN LET QP1005 = 0 : GOTO 11
IF M1005 > 0 AND M1005 <= 2.3 THEN LET QP1005 = 10.44*M1005 : GOTO 11
IF M1005 > 2.3 THEN LET QP1005 = (-28.08*M1005)+16.74*(M1005)^2 : GOTO 11

11     IF M501 <= 0 THEN LET QP501 = 0 : GOTO 12
IF M501 > 0 AND M501 <= 2.3 THEN LET QP501 = 10.44*M501 : GOTO 12
IF M501 > 2.3 THEN LET QP501 = (-28.08*M501) + 16.74*(M501)^2 : GOTO 12

12     IF M1001 <= 0 THEN LET QP1001 = 0 : GOTO 13
IF M1001 > 0 AND M1001 <= 2.3 THEN LET QP1001 = 10.44*M1001 : GOTO 13
IF M1001 > 2.3 THEN LET QP1001 = (-28.08*M1001) + 16.74*(M1001)^2 : GOTO
13

13     REM    FAN HEAD TRENCH SEGMENT
IF FHT < QP1005 THEN LET PFH = 4 : GOTO 20
IF FHT < QP501 THEN LET PFH = 3 : GOTO 20
IF FHT < QP1001 THEN LET PFH = 2 : GOTO 20
LET PFH = 1

20     REM    MIDDLE FAN CHANNEL SEGMENT
IF MFC < QP1005 THEN LET MFH = 4 : GOTO 30
IF MFC < QP501 THEN LET MFH = 3 : GOTO 30
IF MFC < QP1001 THEN LET MFH = 2 : GOTO 30
LET MFH = 1

30     REM    EXISTING DEBRIS BASIN SEGMENT

```

```

IF EDB < 10^M1005 THEN LET DFH = 4 : GOTO 40
IF EDB < 10^M501 THEN LET DFH = 3 : GOTO 40
IF EDB < 10^M1001 THEN LET DFH = 2 : GOTO 40
LET DFH = 1

```

```

40 REM HISTORIC SEDIMENT EVENT SEGMENT
IF HSE > 50 THEN LET HF = 4 : GOTO 50
IF HEV/ASY <= HSE THEN LET HF = 3 : GOTO 50
IF HEV/ASY <= 5*HSE THEN LET HF = 2 : GOTO 50
LET HF = 1

```

```

50 REM FAN HAZARD CLASSIFICATION
FHC = (PFH + MFH + DFH + HF) / 4
IF FHC > 3 THEN LET CL$ = "HIGH HAZARD" : GOTO 60
IF FHC > 2 THEN LET CL$ = "MODERATE HAZARD" : GOTO 60
IF FHC > 1.25 THEN LET CL$ = "LOW HAZARD" : GOTO 60
LET CL$ = "VERY LOW HAZARD"

```

```

60 LPRINT TAB(5);
LPRINT FAN$;
LPRINT " FAN";
LPRINT "; OVERALL ";
LPRINT CL$
LPRINT TAB(10);
LPRINT "BASED ON ";
LPRINT PR$;
LPRINT " PERIOD OF RECORD AND ";
LPRINT SY$;
LPRINT " SEDIMENT YIELD"
LPRINT TAB(10);
LPRINT "PROXIMAL: ";
LPRINT PFH;
LPRINT "; MEDIAL: ";
LPRINT MFH;
LPRINT "; DISTAL: ";
LPRINT DFH;
LPRINT "; LAST HISTORIC EVENT: ";
LPRINT HF
LPRINT TAB(10);
LPRINT "FAN HAZARD CLASSIFICATION = ";
LPRINT FHC
LPRINT

```

```

INPUT "CHANGE PERIOD OF RECORD BUT KEEP SEDIMENT YIELD"; AN$
IF LEFT$(AN$,1)="Y" GOTO 10

```

```

INPUT "CHANGE BOTH AVERAGE SEDIMENT YIELD AND PERIOD OF RECORD"; AN2$
IF LEFT$(AN2$,1)="Y" GOTO 6

```

```

INPUT "EVALUATE ANOTHER FAN"; RE$
IF LEFT$(RE$,1)="Y" GOTO 5

```

```

STOP

```